Université Fédérale
Toulouse Midi-Pyrénées

THÈSE

En vue de l'obtention du

DOCTORAT DE L'UNIVERSITÉ DE TOULOUSE

Délivré par :

Université Toulouse 3 Paul Sabatier (UT3 Paul Sabatier)

Présentée et soutenue par :
Colin VALET
le vendredi 10 mars 2017

Titre :

Rôles de la PI3 kinase de classe II alpha et de la PI3K de classe III, vps34, dans la production et les fonctions plaquettaires

---

École doctorale et discipline ou spécialité :

ED BSB : Physiopathologie

Unité de recherche :

INSERM UMR 1048 - Institut des Maladies Métaboliques et Cardiovasculaires

Directeur/trice(s) de Thèse :

Dr. Sonia SEVERIN
Pr. Bernard PAYRASTRE

Jury :

Pr. Thierry LEVADE, Président
Pr. Marie-Christine ALESSI, Rapporteur
Dr. Christilla BACHELOT-LOZA, Rapporteur
Dr. Catherine LEON, Examinateur
Dr. Sonia SEVERIN, Directrice de thèse
Pr. Bernard PAYRASTRE, Directeur de thèse

A mes parents sans qui rien de tout ça n'aurait été possible.

Je tiens en premier lieu à remercier mes rapporteurs de thèse, le **Pr. Marie-Christine Alessi** et le **Dr. Christilla Bachelot-Loza** pour leur investissement dans l'évaluation du manuscrit ainsi que pour leurs corrections pertinentes. Je remercie le **Dr. Catherine Léon** d'avoir accepté de participer au jury en qualité d'examinateur. Enfin, je remercie le **Pr. Thierry Levade** qui m'a fait l'honneur de présider ce jury.

Je souhaite également remercier l'Université Toulouse III Paul Sabatier et la Société Française d'Hématologie d'avoir financé mes travaux de thèse.

Je remercie aussi les membres de mon comité de thèse, le **Dr. Claire Racaud-Sultan** et le **Dr. Benoit Bilanges** pour leur enthousiasme, leur attitude très positive ainsi que pour les discussions constructives qui m'ont beaucoup aidé tout au long de la thèse.

Je remercie le **Pr. Bernard Payrastre** dans un premier temps de m'avoir accueilli en master 1 et m'avoir donné l'envie de travailler sur les mégacaryocytes et les PI3Ks. Je remercie le Pr. Bernard Payrastre dans un deuxième temps de m'avoir fait confiance et pour m'avoir permis de partir à Londres dans le laboratoire du Pr. Bart Vanhaesebroeck en master 2. Vous le savez Bernard pour moi ce master 2 à Londres a été une expérience géniale et très enrichissante qui m'a beaucoup apporté. Je remercie le Pr. Bernard Payrastre dans un troisième temps de m'avoir proposé cette bourse de thèse qui m'a permis de réaliser ma thèse dans un environnement scientifique et technique riche. Merci Bernard pour tous vos précieux conseils scientifiques, votre œil critique et votre faculté à calmer mes ardeurs dans les moments difficiles! Merci aussi Bernard de nous avoir fait confiance avec P.A dans l'élaboration du site internet de l'équipe. Enfin un grand merci pour ces discussions non-scientifiques toujours agréables qui ont beaucoup tourné autour du jeu du stade toulousain et du XV de France.

A ton tour **Knacki** (j'étais obligé So-nia)…Que dire ? Dans un premier temps je tiens à te remercier So de ton investissement à mes cotés depuis le master 1 jusqu'au départ en post-doc. Tu as toujours été là quoiqu'il advienne, d'une cheville tordue à un blot blanc tu ne m'as jamais laissé tomber (et pourtant il y en a eu des blots blancs !) et je ne saurais jamais te remercier assez. Dans un deuxième temps je tiens à te féliciter tout d'abord pour tout ce que tu as accompli (et oui finir 1ère de sa commission inserm, avoir 3 beaux papiers en dernier nom et être promue CR1 en moins de 4 ans il y a de quoi être fière, en tout cas moi je suis plus que fier que tu m'ais choisi pour travailler avec toi) et en suite d'avoir supporté mon caractère « blanc-noir », comme tu dis si bien, pendant 6 ans (tu remarqueras ton influence sur mes remerciements, je fais maintenant des phrases longues de 6 lignes, merci). Des hauts et des bas il y en a eu tout au long de ces 6 ans, mais je ne retiens que les super moments qu'on a pu vivre que ce soit au labo, en congrès ou hors travail quand tu faisais « l'avion » jusqu'à très tard par exemple…Plus qu'un mentor tu es une personne très chère pour moi et je croise les doigts pour qu'on retravaille un jour ensemble. Je te souhaite tout le meilleur au niveau professionnel et personnel car tu es quelqu'un d'exceptionnel et tu le mérites.

Même si la thèse est un accomplissement personnel, il serait impossible sans la collaboration de toute une équipe. Je remercie donc tous les membres actuels ou passés de l'équipe « PIMP-lab » que j'ai pu côtoyer.

Je commencerai par les Marie qui me supportent depuis quelques temps. En commençant par la plus vieille, je tiens à te remercier **Marie Levade** pour ta collaboration dans notre projet commun…on aura bien galéré avec ce projet n'est-ce pas ??? Merci pour ta bonne humeur et ta motivation inébranlable. Je te souhaite le meilleur en Australie avec ta petite famille! Maintenant la plus jeune, **Marie Bellio**, je te remercie pour ce souvenir inoubliable en TP… tu resteras ma « meurtrière » de souris préférée. Je te remercie aussi de toujours rire à mes blagues même quand elles ne sont pas drôles afin que je ne me sente pas trop seul. Merci aussi pour ta bonne humeur et ton aide au laboratoire! Bon courage pour la suite de la thèse, je suis sûr que tu vas gérer (ce sera surement grâce à ton régime hyper-raviolique).

P.A allias mon « crispy tender » je n'oublierai jamais ce stage de master 1 dans le laboratoire ainsi que ces manips dans l'animalerie la plus glauque du monde. Merci pour ton soutien infaillible tout au long de ces années, sans oublier Tata Jeannette bien-sur. Je n'oublierai pas non plus tous ces moments hors laboratoire, tu es un ami très proche et j'espère que la blanquette restera bonne encore de nombreuses années mon cher Hubert.

Un grand merci aux chercheuses de l'équipe, **Fred**, **Anne-Do** et **Marie-Pierre**, qui m'ont toutes les trois aidé à un moment ou à un autre. Je vous remercie donc toutes les trois, j'ai beaucoup aimé travailler à vos cotés pendant ces 4 années. Je vous souhaite le meilleur pour la suite.

Julien dit « le renard des surfaces » ou « carotte-man » merci pour ton aide au laboratoire, ton enthousiasme et pour tes bonnes blagues (qui ne font rire que moi…je crois qu'on a le même sens de l'humour pourri malheureusement…). Je garderai aussi en mémoire nos parties de foot en salle du jeudi soir et ton incroyable talent pour planter la tente devant le but adverse ainsi que ton superbe maillot des canaries nantais qui doit être collector à ce jour !

A toi **Gaëtan**, tu vois après 4 ans je n'oublie plus le tréma sur le E, c'est dire si j'ai bien évolué ;) . Je tiens dans un premier temps à te féliciter d'avoir réussi à supporter nos débats souvent « animés » avec Sonia, tu vas enfin pouvoir retrouver un bureau calme. Je te remercie dans un deuxième temps pour ta collaboration, toi le grand manitou des phosphoinositides, et ton aide tout au long de ces quatre années de thèse. Je te souhaite plein de bonheur avec ta petite famille et toute la réussite que tu mérites sur tes futures courses (j'attends avec impatience la sortie de l'intérieur sport à ton sujet).

Romain ou « l'homme qui met le feu à la paillotte », j'ai adoré maniper à tes cotés ainsi que discuter avec toi de tout et de rien. Je retiens aussi quelques unes de nos virées nocturnes d'anthologie ! Bonne chance à toi pour la suite.

Bien évidemment je ne peux pas oublier « l'oriental connexion » ! Merci **Rana** et **Abdul** pour votre bonne humeur dans le labo !! Sans oublier vos compagnons, **Laurie** et **Adrien**, merci à vous aussi pour les moments agréables passés au labo.

Ashraf alias « tonton Ash », merci pour tous ces gâteaux que tu m'as donné tout au long de la thèse et qui m'ont permis de tenir la distance. Merci aussi pour ta bonne humeur et ton soutien

inconditionnel. Je remercie aussi ton compère **Jean-Marie** alias « JMX » pour ton aide au laboratoire. Bonne suite à tous les deux.

Un grand merci aux compagnons du laboratoire d'hémato. Merci **Jennifer** pour ton sourire ainsi que pour tes boucles d'oreille perroquet qui m'ont beaucoup fait rire ! Merci à toi aussi **Cédric** allias « sérotonine-man » pour ton aide précieuse. Une grosse pensée pour **Fanny** qui en plus de gérer l'hôpital fait une thèse dans le laboratoire, courage !!!

Je ne peux pas écrire ces remerciements sans avoir une pensée pour l'**Adipolab**. Je pense qu'il n'ya pas une personne dans cette équipe qui ne m'a pas aidé au moins une fois durant ces 4 années. Vous avez tous un cœur gros comme ca ! Je ne peux que vous remercier. Un gros merci à **Aurélie** et **Alizée** (de la cambrousse) pour toute votre aide sur le projet adipo-méga qui, sans vous deux, n'en serait certainement pas là ou il en est aujourd'hui. Merci à **Simon** aussi toujours la pour prêter main forte ! Merci aux doctorants **Jean**, **Gwendo**, **Romain** qui ont toujours pris le temps de m'aider, bon courage pour la fin de la thèse. Merci **Isabelle** pour toute ton aide pour le monitorat ! Merci **Armelle** pour tes conseils avisés et pour ton aide avec ces fameuses OP9. Merci **Berni** (mon petit loukoum) pour ta bonne humeur, les fous rires qu'on a pu avoir et surtout pour tout le rêve que tu m'as vendu le jeudi soir au foot avec cette technique balle au pied qui fait cauchemarder Ronaldo (et Fred Lopez aussi haha). On finit par les plus beaux, les compères. Merci **JPP** et **Cédric** pour votre soutien et votre disponibilité que ce soit au labo ou en dehors. Merci aussi pour ces grands moments de football dont Thierry Roland et Jean-Michel Larqué ne se sont toujours pas remis…que ce soit un pointu/fracture du gros orteil 10 mètres au dessus de la barre par **JPP** ou une perte de balle de **Cédric** accompagnée de directives comme quoi il faut descendre défendre pendant que monsieur reste bien au chaud dans la surface de réparation adverse.

Un énorme merci à **Muriel** (qui se souviendra longtemps de l'édition 2016 de la NSFA je pense), à **Steph**, **Véro** (et oui les filles c'est la fin des « cassoss au labo »), **Nicole** et **Michel.** Bonne continuation à vous et comme dirait **Michel** « et b c'est bien ».

Merci à **Cendrine** pour sa collaboration et son expertise dans l'expérimentation animale *in vivo*.

Merci à **Childerick** de nous avoir ouvert les portes de ton microscope à force atomique et de nous l'avoir si bien fait comprendre !

Merci aussi aux plateformes avec qui j'ai eu un grand plaisir à travailler. Mon petit **Madjid** (System) merci pour ta bonne humeur et ton aide. Merci à **Justine**, **Pauline** et **Fabien** pour leur aide avec tous ces lipides ! Merci à **Jean-José** et **Fred** aussi pour votre aide. Merci aussi à **Christiane** (qui est remerciée sur les deux thèses familiales il me semble!) et **Alexia** pour votre soutien au cymomètre. Enfin je remercie chaleureusement les services de zootechnie de l'US006 pour leur aide et la gestion de nos élevages.

Merci **JJ** aussi pour ton aide sur les PC (on ne parlera pas ici de ton aide sur les Mac, je ne veux pas t'embarrasser…) ainsi que pour toute les distractions que tu as pu nous apporter que ce soit par ta coupe de cheveux ou par tes blagues. Je souhaite aussi remercie l'ensemble du

personnel administratif de l'Institut des Maladies Métaboliques et Cardiovasculaires avec une pensée pour **Jérôme**.

Je tiens aussi à remercier mes amis Londoniens **Samira** et **Benoit** pour leur super encadrement lors de mon stage de Master 2. Je n'oublierai jamais ces 6 super mois à Londres ni les week-ends qui suivirent. **Samira** ou « mamounette » je te souhaite tout le meilleur avec « Rocky » et votre petite fille. **Benoit** ou « papounet », en tant qu'ami proche tu sais déjà tout, merci, merci mais vraiment merci ! Je te souhaite toute la réussite que tu mérites !

Place aux footix du jeudi soir ! On a vécu de bons moments ensembles (et des engueulades aussi mais ca fait partie du jeu). **Hervé**, **Bruno**, **Nono**, **JPP**, **Cédric**, **JD**, **Lolo**, **David**, **Théo**, **Etienne**, **Fred**, **Valentin**, **Berni**, **Juju**, **Micha** je vous remercie et vous dis bon vent à tous ! J'espère qu'on se croisera à nouveau avenue de Larrieu ou ailleurs. Il faudra quand même bien dire à **Bruno** un jour que le foot est un sport collectif où les passes ne sont pas sanctionnées… je compte sur vous pour transmettre le message !

Amis **TUC**istes un grand merci pour votre soutien et tous ces bons moments qu'on a passé et qu'on passera ensemble ! **Juju**, **Jojo**, **Carole**, **JD**, **Camille**, **Julien**, **Titi**, **Luc**, **Olive**, **Cha**, **Mixou**, **Delphine**, **Beny** et **Guigui** je vous remercie les amis… non, non, non le TUC n'est pas mort !

Je n'oublie pas non plus mes collègues et amies **Fotine** et **Margaux** qui sont elles aussi plongées dans leur thèse à Paris et Bâle, bon courage à toutes les deux !

Robin alias « Dupond » mon compère de toujours. Il est long le chemin… mais avec toi à mes cotés il était juste génial ce chemin !

Je souhaite aussi remercie le groupe des **PhD killers** pour leur soutien, leur aide dans les moments difficiles ainsi que pour tous ces moments de bonheur partagés. Commençons par les filles ! Merci ma **Juju** pour ton énergie débordante, tes blagues vraiment pourries (personne n'oubliera le Giroud-phare de si tôt à mon avis !) et tes cours de danse à Barcelone, j'espère que tout ca continuera à Boston !!! Un grand merci à toi **Cecile** pour tous ces souvenirs mémorables, notamment cette bataille de gâteau dans le chalet (le plafond s'en souvient encore). Place aux gars ! Mon petit **P.A** j'ai déjà tout dit frère, que ça continue !!! **Adrien**, mon bouboule, de ces compte rendus de TP à la rédaction de la thèse on en a fait du chemin. Le labo, la moto, la rando, tout ce qui finit en « o » en somme ! Merci mon petit Enzo, mais ne t'inquiètes pas tout ça continuera outre-Atlantique ! **Guigui** mon petit barbu et coloc préféré, merci pour tous ces fous rires. Finalement on a réussi à te faire monter sur la moto (pas trop vite quand même). **Steven**, mon petit « steewi » on s'est quand même bien marré ! Merci à toi mon « grand » pour ton soutien, je te souhaite le meilleur pour la suite mais je ne m'en fais pas pour toi tu vas tout déchirer (comme ta chemise, que de toute façon tu devais jeter) ! Et on finit par le plus beau, ce sacré **David**. Merci à toi poulet, te côtoyer sur les terrains de rugby (ne serait-ce que 50 minutes) était une sacrée expérience, surtout pour mon pif. Te côtoyer en dehors aussi a été génial, surtout pour mon front ! J'espère que notre groupe restera soudé encore de nombreuses années.

Je tiens aussi à remercier chaleureusement mes grands-parents, **Papou**, **Mone**, **Papi** et **Mamie** qui m'ont toujours soutenu et qui ont toujours essayé de comprendre ce que je faisais au laboratoire. Je te remercie aussi **Mixou** pour ton soutien. Tu es un exemple, tu me pousses à ne rien lâcher et à me surpasser quand il le faut. Merci pour tout ça, je suis très fier de toi. Un gros gros merci à **Delphine** alias « dedel » pour tous ces bons moments passés ensemble ! Je veux aussi te remercier **Charlotte** pour ton soutien et d'être toujours là pour moi. En espérant que Boston soit une aventure inoubliable… Enfin je finis par les plus chers à mon cœur. **Papa**, **Maman** vous n'imaginez pas à quel point je vous suis reconnaissant. Sans votre amour et votre soutien je n'en serais pas là aujourd'hui. Vous êtes tous les deux des sources d'inspiration pour moi et ça va être dur de partir à Boston (même si l'aventure sera belle j'en suis sûr). Je vous remercie du fond du cœur pour tout.

Résumé

Les mégacaryocytes sont des cellules de la moelle osseuse qui par un processus complexe et encore mal caractérisé, mégacaryopoïèse/thrombopoïèse, donnent naissance, *in fine*, aux plaquettes sanguines. La différenciation mégacaryocytaire nécessite un intense remodelage nucléaire et cytoplasmique, guidé à la fois par des facteurs intrinsèques mais aussi par des facteurs extrinsèques provenant du microenvironnement médullaire. Les plaquettes sanguines sont des acteurs essentiels du maintien de l'intégrité vasculaire. Elles sont les premiers éléments cellulaires à intervenir dans l'arrêt du saignement lors d'une blessure vasculaire par la formation d'un thrombus *via* des mécanismes d'adhésion, de sécrétion et d'agrégation, trois étapes majeures de l'hémostase physiologique.

Dans un premier temps, mes travaux de thèse ont pour but de caractériser le rôle inconnu de l'isoforme α des PI3Ks de classe II (PI3KC2α), de la PI3K de classe III (Vps34) et de leur produit, le phosphatidylinositol 3-monophosphate (PtdIns3P), dans la production et les fonctions plaquettaires. Grâce à un modèle murin présentant une inactivation partielle de la PI3KC2α, j'ai mis en évidence son rôle clé dans la génération d'un « pool basal » de PtdIns3P dans les plaquettes. En effet, l'inactivation de la PI3KC2α affecte la composition du cortex sous-membranaire plaquettaire induisant une morphologie plaquettaire anormale, une accumulation de plaquettes à deux corps appelées « barbell-shaped proplatelets », un défaut de formation du thrombus *ex vivo* et un retard d'occlusion de la carotide après lésion *in vivo*. Ainsi, la PI3KC2α joue un rôle majeur dans le maintien de l'intégrité du squelette membranaire contrôlant la structure et la dynamique membranaire, processus critique à la production de plaquettes fonctionnelles. D'autre part, la délétion de Vps34 spécifiquement dans la lignée mégacaryocyte/plaquette se traduit par une microthrombopénie modérée associée à une migration anormale des mégacaryocytes liée à un défaut de trafic vésiculaire, d'autophagie et une diminution du taux de PtdIns3P. De façon intéressante, Vps34 joue aussi un rôle dans l'activation plaquettaire en régulant la production de PtdIns3P sous stimulation, la croissance du thrombus *ex vivo* et les capacités thrombotiques *in vivo*. Le rôle de Vps34 dans la plaquette indépendamment de son rôle dans le mégacaryocyte, a été confirmé *via* l'utilisation de nouveaux inhibiteurs spécifiques de Vps34, SAR405 et INH1, *ex vivo*. Vps34 est donc critique pour la régulation de la production plaquettaire par les mégacaryocytes ainsi que pour l'activation plaquettaire.

Dans un deuxième temps, je me suis intéressé à l'impact du microenvironnement médullaire sur la mégacaryopoïèse, et plus spécifiquement sur la communication entre adipocytes médullaires et progéniteurs hématopoïétiques lors de leur différenciation en mégacaryocytes. Grace à un système de co-culture *in vitro*, j'ai montré que les adipocytes améliorent la différenciation mégacaryocytaire *via* un transfert direct de lipides, dans un but non-énergétique. Dans un contexte d'obésité, nous observons *in vivo*, une macrothrombopénie modérée associée à une adiposité médullaire augmentée, une maturation mégacaryocytaire exacerbée, une production et une demi-vie plaquettaire défectueuses. Ainsi, le microenvironnement médullaire et plus particulièrement l'adipocyte impacte directement sur la mégacaryopoïèse et la production plaquettaire.

En conclusion, ces travaux de thèse contribuent à caractériser les mécanismes de production et de fonction plaquettaires régulés par des facteurs intrinsèques tels que le PI3KC2α et Vps34, ainsi que par des facteurs extrinsèques tels que l'adipocyte médullaire.

Abstract

Megakaryopoiesis is a highly specialised and complex process occurring in the bone marrow, by which megakaryocytes give rise to *de novo* circulating blood platelets. Megakaryocyte differentiation and platelet production imply megakaryocyte cytoplasmic and nuclear rearrangements regulated by intrinsic as well as extrinsic factors such as bone marrow microenvironment. Platelets play a critical role in preventing blood loss after vascular injury by orchestrating clot formation through mechanisms of both adhesion, secretion and aggregation. These mechanisms are the three major steps of physiological haemostasis leading to the maintenance of vascular integrity.

Firstly, my thesis work focused on characterizing the role of class II PI3K α isoform (PI3KC2α), class III PI3K (Vps34) and their common product the phosphatidylinositol 3 monophosphate (PtdIns3P) in platelet production and function. Using a unique mouse model partially inactivated for PI3KC2α, I highlighted its key role in the production of a basal PtdIns3P housekeeping pool in platelets. PI3KC2α partial inactivation affects platelet membrane skeleton composition leading to an abnormal platelet morphology, an enrichment of platelet with two cell bodies recently called "barbell-shaped proplatelets", an *ex vivo* defective thrombus formation and an *in vivo* delayed carotid occlusion following injury. Thus, PI3KC2α plays a major role in membrane structure and dynamics by maintaining membrane skeleton integrity, which is crucial in the production of functional platelets. On the other hand, Vps34 specific deletion in megakaryocyte/platelet lineage induced mild microthombopenia correlated to an abnormal megakaryocyte migration linked to an affected PtdIns3P production as well as vesicular trafficking and autophagy in megakaryocytes. In platelets, Vps34 plays a role in their activation by regulating PtdIns3P production under stimulation, *ex vivo* thrombus growth and *in vivo* thrombotic capacity. Vps34 role in platelet independently from its role in megakaryocyte was confirmed using two recently developed inhibitors, SAR405 and INH1, able to reproduce *ex vivo* thrombus growth defects. Therefore, Vps34 is critical for platelet production by megakaryocytes as well as platelet activation.

Secondly, I studied the impact of bone marrow microenvironment on megakaryopoiesis and more specifically the crosstalk between medullar adipocytes and hematopoietic progenitors differentiating towards the megakaryocyte lineage. Using an *in vitro* co-culture assay, I demonstrated that adipocytes enhanced megakaryocyte differentiation through a direct lipid transfer, in a non-energetic aim. In the context of obesity, increased marrow

adiposity is associated to enhanced megakaryocyte differentiation and defective platelet production and lifespan leading to mild macrothrombopenia. Thus, bone marrow microenvironment through adipocytes directly impacts on megakaryopoiesis and platelet production.

Altogether my thesis work contributes to better understand platelet production and function, mechanisms regulated by intrinsic factors such as PI3KC2α and Vps34 as well as extrinsic factors like medullar adipocytes.

Abréviations

A

ABP: Actin Binding Protein

ADP: Adénosine 5'-Diphosphate

AP3: Adaptator Protein 3

APPL1: Adaptator Protein, phosphotyrosine interaction, PH domain and Leucin zipper containing 1

AMPK: AMP-activated protein Kinase

ARC syndrom: Arthrogryposis, Renal dysfunction and Cholestasis syndrome

ARNm: Acide Ribo-Nucléique messager

Arp2/3: Actin related protein 2/3

Atg: Autophagy related-gene

ATP: Adénosine 5'-Triphosphate

B

BH: Breakpoint-cluster-region Homology domain

BLOC: Biogenesis of Lysosom-related Organelle Complexes

BSA: Bovine Serum Albumin

BTK: Bruton Tyrosine Kinase

C

CAR cell: CXCL12 Abundant Reticular cell

Cdc42: Cell division cycle 42

CD41: Intégrine αIIb

CDK1: Cyclin Dependent Kinase 1

CEBPα et β: CCAAT/Enhancer-Binding Protein α et β

CHS: Chediak-Higashi Syndrome

CIP4: Cdc42 Interacting Protein 4

CLP: Common Lymphoid Progenitor

cMAT: constitutive Medullar Adipose Tissue

CMP: Common Myeloid Progenitor

c-Mpl: Myeloproliferative leukemia protein

COX-1: Cyclooxygénases 1

CXCL12: voir SDF-1

CXCR4: C-X-C chemokine Receptor type 4, SDF-1 receptor

D

D3-PI: D3-Phosphoinositide

DAG: Diacylglyceérol

DFCP1: Double-FYVE-domain-Containing-Protein-1

DMS: Demarcation Membrane System

E

ECGF: Endothelial Cell Growth Factor

EEA1: Early Endosome Antigen 1

EGF: Endothelial Growth Factor

EPO: Erythropoietine

ESCRT: Endosomal Sorting Complex Required for Transport

F

F-BAR: F-Bin-Amphiphysin-Rvs

FcRγ : chaîne γ des récepteurs au fragment constant des immunoglobulines

FIG4 : SAC domain containing lipid phosphatase

FLI1: Friend Leukemia virus Integration 1

FOG1: Friend of GATA-1

FYVE: Fab-1 YGL023 Vps27 EEA1 domain

FYVE-CENT: FYVE domain-containing centrosomal protein

G

GAP1: GRB2-associated-binding-protein 1

GATA-1: Globin transcription factor 1

G-CSF: Granulocyte Colony Stimulating Factor

GEF: Guanosine nucleotide Exchange Factor

GM-CSF: Granulocyte Macrophage Colony Stimulating Factor

GMP: Granulocyte Macrophage Progenitor

GP: Glycoprotéine

H

HPC: Hematopoietic Progenitor Cell

HPS: Hermansky-Pudlak Syndrom

HSC: Hematopoietic Stem Cell

I

IGF1: Insulin Growth Factor 1

IL-3: Interleukine 3

IL-4: Interleukine 4

IL-6: Interleukine 6

$InsP_3$: Inositol 1,4,5-triphosphate

J

JAK2: Janus Kinase 2

L

LC3: microtubule-associated protein 1 Light Chain 3 beta

LT-HSC: Long Term Hematopoietic Stem Cell

LYST: Lysosomal Trafficking regulator

M

3MA: 3-Methyladenine

MAPK: Mitogen-Activated Protein Kinase

MAT: Medullar Adipose Tissue

M-CSF: Macrophage Colony Stimulating Factor

MEF: Mouse Embryonic Fibroblast

MEP: Megakaryocyte Erythrocyte Progenitor

MK: Megakaryocyte

MLC: Myosin Light Chain

MMP9: Matrix Metalloprotease 9

MPP: Multipotent Progenitor

MTM: Myotubularine

mTOR: mammalian Target Of Rapamycin

mTORC1: mammalian Target Of Rapamycin Complex 1

MVB: Multi-Vesicular Body

MYH9: non-muscle myosin IIA

MYH10: non-muscle myosin IIB

N

NADPH: Nicotinamide Adenine Dinucléotide Phosphate

NBEAL2: Neurobeachin-Like 2

NF-E2: Nuclear Factor Erythroid 2

NO: Monoxyde d'azote

P

PAI-1: Plasminogen Activator Inhibitor-1

PAK: p21-Associated Kinase

PAR: Protease-Activated Receptor

PARP: Poly-ADP-Ribose-Polymerase

PAS: PIKfyve/ArPIKfyve/SAC3

PDGF: Platelet Derived Growth Factor

PECAM-1: Platelet Endotehlial Cell Adhesion Molecule 1

PF4: Platelet Factor 4

PGI_2: Prostaglandin I_2

PH: Pleckstrin Homology domain

PI: Phosphoinositide

PI3K: Phosphoinositide 3-Kinase

PI4K: Phosphoinositide 4-Kinase

PI5K: Phosphoinositide 5-Kinase

PI3KC2α/β/γ: PI3K de classe II α/β/γ

PIKfyve: PtdIns 5-kinase

PLA_2: Phospholipase A_2

PLC: Phospholipase C

PPARγ: Peroxisome Proliferator-Activated Receptor γ

PPT: Proplaquette

PS: Phosphatidylsérine

PtdIns: Phosphatidylinositol

PtdIns3P: Phosphatidylinositol 3-monophosphate

PtdIns4P: Phosphatidylinositol 4-monophosphate

PtdIns5P: Phosphatidylinositol 5-monophosphate

$PtdIns(3,4)P_2$: Phosphatidylinositol 3,4-bisphosphate

$PtdIns(3,5)P_2$: Phosphatidylinositol 3,5-bisphosphate

$PtdIns(4,5)P_2$: Phosphatidylinositol 4,5-bisphosphate

$PtdIns(3,4,5)P_3$: Phosphatidylinositol 3,4,5-triphosphate

PTEN: Phosphatase and Tensin homologue deleted on chromosome 10

PX: Phox domain

R

RANTES: Reculated on Activation, Normal T cell Expression and Secreted

RBD: Ras Binding Domain

RCPG: Récepteur Couplé aux Protéines G

rMAT: regulated Medullar Adipose Tissue

RUN: RPIP8-UNC14-NESCA

Runx1: runt-related transcription factor 1

S

S6K1: S6 Kinase 1

SCF: Stem Cell Factor

SCO: Système Canaliculaire Ouvert

SDF-1: Stromal cell-Derived Factor 1

SH3: SRC Homology 3

Shh: Sonic Hedgehog

Shp 1 et 2: Src homology region 2 domain-containing phosphatase 1 et 2

SHIP1 et 2: SH2-containing inostol-5'-Phosphate 1 et 2

SKIP: Skeletal muscle and Kidney enriched Inositol Phosphatase

SNARE: Soluble NSF Attachment Protein

SNX: Sorting Nexin

SPG: Syndrome des Plaquettes Grises

STAT: Signal Transducers and Activators of Transcription

STD: Système Tubulaire Dense

ST-HSC: Short Term Hematopoietic Sstem Cell

T

TGFβ: Transforming Growth Factor β

TGFβR: Transforming Growth Factor β Receptor

TGN: Trans-Golgi Network

TPO: Thrombopoietine

TXA_2: Thromboxane A2

U

ULK1: Unc-51 Like autophagy activating Kinase 1

UVRAG: UV-adiation Resistance-Associated Gene

V

VAMP8: Vesicle Associated Membrane Protein 8

VEGF: Vascular Epidermal Growth Factor

Vps: Vacuolar protein sorting

Vps34: PI3K de classe III

vWF: von Willebrand Factor

W

WASp: Wiskott-Aldrich Syndrome protein

WAVE: Wiskott–Aldrich Syndrome protein family Verprolin homologous

WIPI 1 et 2: WD40 repeat protein Interactions with Phosphoinositides 1 et 2

Index des Figures

Revue Bibliographique

Chapitre I : La Mégacaryopoïèse

A) La moelle osseuse

1) Cellule souche hématopoïétique et microenvironnement médullaire

Chez l'adulte, l'hématopoïèse se déroule principalement dans la moelle osseuse et permet la production des cellules sanguines à partir d'une cellule précurseur, la cellule souche hématopoïétique (HSC).

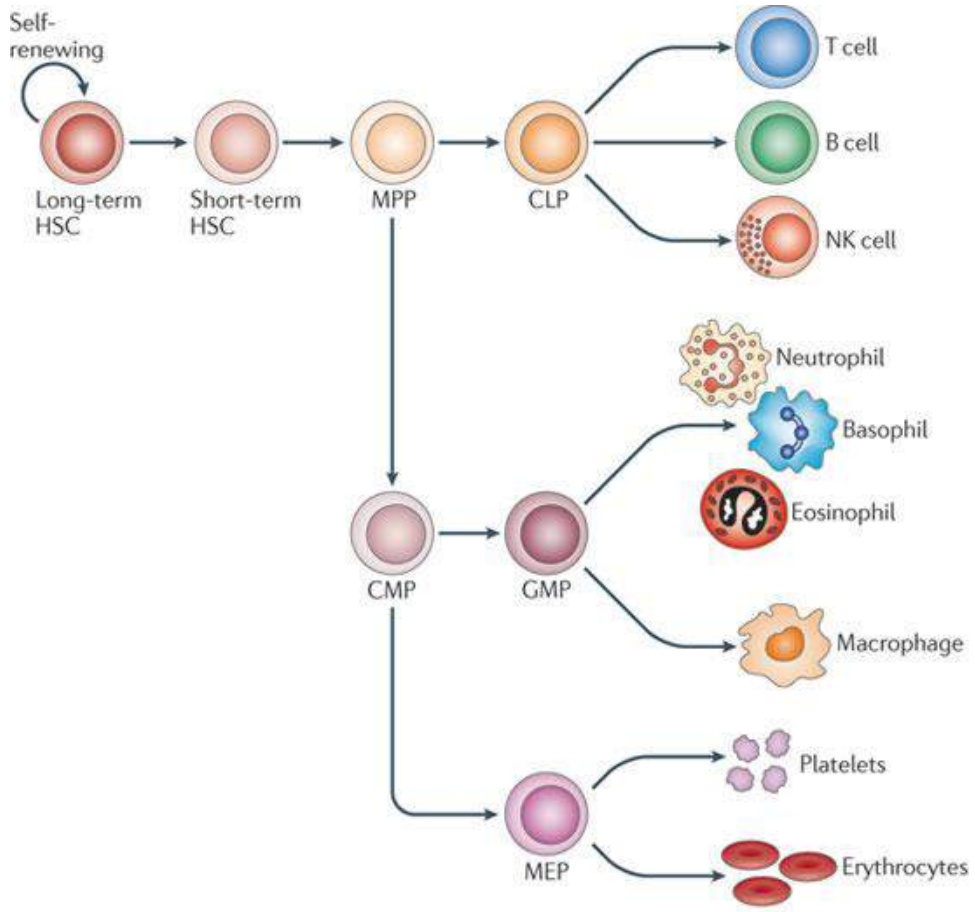

Figure 1: Le système hématopoïétique: Les LT-HSC ont une forte capacité d'auto-renouvellement tout au long de la vie de l'animal mais aussi la capacité de produire tous les types de cellules de la moelle osseuse et du sang. Les progéniteurs hématopoïétiques multipotents (MPP ou HPC) sont capables ensuite de se différencier en progéniteurs lymphoïdes (CLP) ou myéloïdes (CMP). Ces progéniteurs sont à l'origine du large spectre de cellules sanguines matures incapables de s'auto-renouveler et de durée de vie limitée (Lymphocytes T et B ; cellules NK ; neutrophile ; basophile ; éosinophile ; macrophage ; plaquette et érythrocyte). *D'après (King and Goodell, 2011)*

Les long-term HSC (LT-HSC) dont les propriétés d'auto-renouvellement sont importantes produisent les short-term HSC (ST-HSC) qui sont à la fois capables de s'auto-renouveler mais surtout de se différencier en cellules progénitrices hématopoïétiques multipotents (HPC ou

MPP) dont les capacités d'auto-renouvellement sont limitées. Sous l'influence de différents facteurs de croissance, ces progéniteurs s'engageront soit vers la lignée myéloïde soit vers la lignée lymphoïde (CMP et CLP respectivement) pour, *in fine*, produire les cellules sanguines. A l'âge adulte, la moelle osseuse est le siège de l'hématopoïèse qui, par la production de 10^{11} à 10^{12} cellules sanguines par jour, permet le renouvellement continu des cellules sanguines dont la durée de vie est limitée. Les CLP donneront naissance aux lymphocytes T et B ainsi qu'aux cellules « natural killers ». Les CMP produiront, soit les précurseurs granulocytes-macrophages (GMP), soit des précurseurs mégacaryocytes-érythrocytes (MEP) (Figure 1). Lors d'un stress aigu ou chronique tel un saignement ou une infection, le système hématopoïétique est capable d'augmenter significativement sa production de cellules sanguines pour palier soit à un déficit soit à une attaque de l'organisme (Cumano and Godin, 2007; Ho et al., 2015; King and Goodell, 2011; Manz and Boettcher, 2014).

La régulation de la différenciation d'une cellule HSC se fait sous le contrôle ordonné de différents facteurs de croissance, chacun étant spécifique d'une voie de différenciation amenant à une cellule sanguine mature (par exemples: IL3, IL6, GM-CSF, G-CSF, M-CSF, TPO, EPO, etc) (Cumano and Godin, 2007; Ho et al., 2015; Manz and Boettcher, 2014). Cependant, les facteurs de croissance ne sont pas les seuls à contrôler l'hématopoïèse: le microenvironnement médullaire est lui aussi critique dans ce processus. Au sein de la moelle osseuse, il existe différentes niches spécifiques de par leur localisation, les facteurs de croissance présents localement et leur composition en matrice extracellulaire. La localisation d'une cellule souche, au sein de la moelle osseuse, va déterminer son devenir. Ainsi, la niche ostéoblastique, composée majoritairement de LT-HSC, permet de maintenir un « pool » de cellules au fort potentiel d'auto-renouvellement. La niche périvasculaire, près des sinusoïdes sanguins médullaires, contient quant à elle des ST-HSC, prêtes à se différencier en progéniteurs, recrutées par l'intermédiaire de la chimiokine CXCL12 (ou stromal cell-derived factor 1 (SDF-1)) (Adams and Scadden, 2008; Ho et al., 2015; Morrison and Scadden, 2014) (Figure 2).

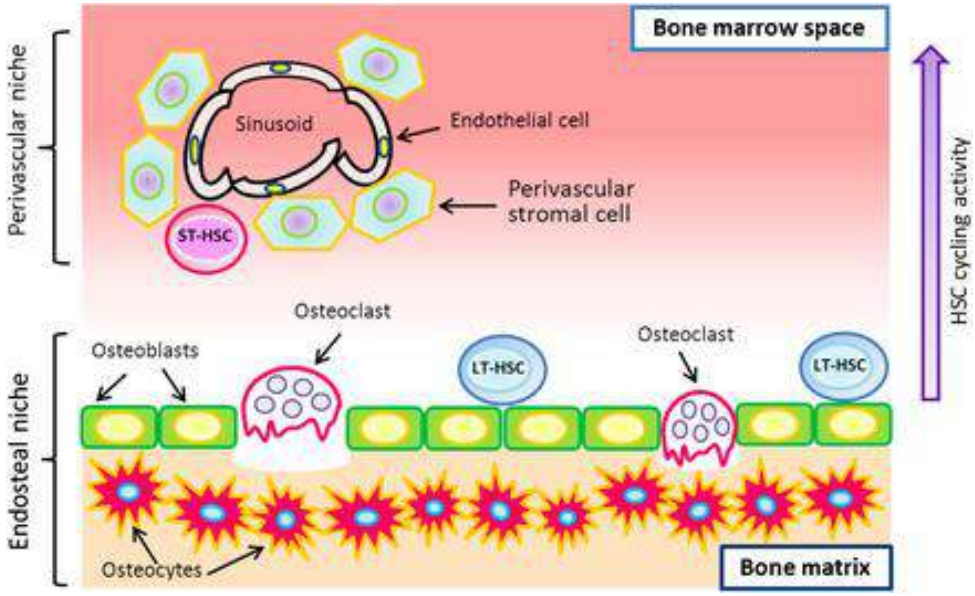

Figure 2: Représentation des différentes niches de HSC dans la moelle osseuse: Les HSC résident dans des microenvironnements spécifiques de la moelle osseuse. Les LT-HSC au fort potentiel d'auto-renouvellement se situent dans la niche ostéoblastique. Au contraire, les ST-HSC à faible potentiel prolifératrice se localisent prés des sinusoïdes sanguins. Cette niche périvasculaire est connue pour favoriser la différenciation des HSC et donner les progéniteurs des cellules sanguines. *D'après (Ho et al., 2015)*.

Au sein de l'environnement médullaire, il existe de plus en plus d'évidences que le tissu adipeux médullaire (MAT) joue un rôle important dans l'hématopoïèse. Cependant, le rôle du MAT reste encore assez mal connu mais suscite un intérêt grandissant et a été l'objet d'une partie de ma thèse.

2) Le tissu adipeux médullaire

Le tissu adipeux médullaire représente environ 5% de la masse adipeuse chez l'adulte et 50 à 70% du volume médullaire total. Son développement est dépendant du sexe et de l'âge. Tout comme le tissu adipeux extra-médullaire, le MAT est une glande endocrine capable de sécréter des adipokines, et plus particulièrement la leptine et l'adiponectine qui sont impliquées dans la régulation de la masse osseuse (Kawai et al., 2012; Naot and Cornish, 2014). Scheller *et al* proposent de distinguer le tissu adipeux médullaire constitutif (cMAT) du tissu adipeux médullaire régulé (rMAT) dont la distribution spatio-temporelle, la composition lipidique et l'expression génique diffèrent (Scheller et al., 2015). En effet, le cMAT, situé dans les zones distales des os, se développe rapidement après la naissance, est composé de grands adipocytes (38-39µm de diamètre) contenant des acides gras saturés et exprime peu les facteurs de transcription adipogéniques, CEBPα et CEBPβ. Contrairement au cMAT, le rMAT, localisé dans la zone proximale de l'os, se développe avec l'âge, est

composé de petits adipocytes (31-33μm de diamètre) contenant des acides gras insaturés et exprime largement les facteurs de transcription adipogéniques, CEBPα et CEBPβ (Scheller et al., 2015). Les rôles spécifiques de ces deux types de MAT restent encore méconnus (Hardouin et al., 2016; Scheller et al., 2016).

Le profil métabolique du MAT reste peu caractérisé. Cependant, les adipocytes médullaires expriment le récepteur à l'insuline et sont sensibles aux antidiabétiques augmentant la sensibilité à l'insuline (les thiazolidinediones). La question est de savoir si le rôle du MAT, comme les autres tissus adipeux, est de stocker et/ou mobiliser de l'énergie pour l'organisme selon les besoins. Il a été montré que, aussi bien lors d'une restriction calorique que lors d'un régime riche en gras, le MAT augmentait significativement, remettant ainsi en cause son potentiel rôle lié aux demandes énergétiques systémiques (Kim and Schafer, 2016).

Dans un contexte pathologique d'obésité, de diabète ou de vieillissement, il a été observé un accroissement du MAT et une corrélation positive avec la fragilité osseuse. De par le manque d'études et le fait que ces observations soient plus marquées chez le rongeur que chez l'humain, les points de vue de la littérature divergent. Malgré tout, la corrélation entre fragilité osseuse et accroissement du MAT semble admise. En effet, l'activité paracrine ainsi que les contraintes mécaniques imposées par une expansion du MAT diminuent significativement la masse osseuse (Cawthorn et al., 2014; Lecka-Czernik, 2012; Scheller et al., 2016).

L'impact du MAT sur l'hématopoïèse reste peu connu et controversé. Naveiras *et al* ont montré *in vivo* que le MAT inhibait l'hématopoïèse (Naveiras et al., 2009). L'irradiation de souris lipoatrophiques A-ZIP/F1 (incapables de former des adipocytes) (Moitra et al., 1998) ou de souris sauvages traitées par un inhibiteur de peroxysome proliferator-activated receptor-γ (PPAR γ) (Wright et al., 2000) (un facteur de transcription pro-adipogénique) a montré une accélération de la reconstitution hématopoïétique de la moelle osseuse (Naveiras et al., 2009), suggérant un rôle inhibiteur du MAT sur l'hématopoïèse. De plus, certaines équipes ont décrit que l'obésité induite par régime gras chez la souris, induisait d'un coté une perturbation de la lymphopoïèse (Adler et al., 2014a; Karlsson et al., 2010) et d'un autre l'amélioration de la myelopoïèse et de la lymphopoïèse (Adler et al., 2014b; Singer et al., 2014; Trottier et al., 2012; Yang et al., 2009). Décrire l'impact global du MAT reste une gageure de par le nombre et la diversité des cellules contenues dans la moelle osseuse, la diversité des facteurs

médullaires et extra-médullaires influençant le devenir des HSC ainsi que par les différentes régulations localisées de l'hématopoïèse au sein de la moelle osseuse.

B) Etapes précoces de la mégacaryopoïèse

La mégacaryopoïèse est un processus complexe et finement régulé de maturation du mégacaryocyte (MK) qui a lieu dans la moelle osseuse et qui aboutit à la production de plaquettes sanguines. Les MKs sont de grandes cellules de la moelle osseuse qui, lors de leur différenciation, vont devenir polyploïdes, produire des granules spécifiques et développer un large réseau de membranes interne appelé système de membrane de démarcation (DMS). Le DMS est indispensable à l'élongation des proplaquettes (PPT), étape finale de la production des plaquettes (Figure 3).

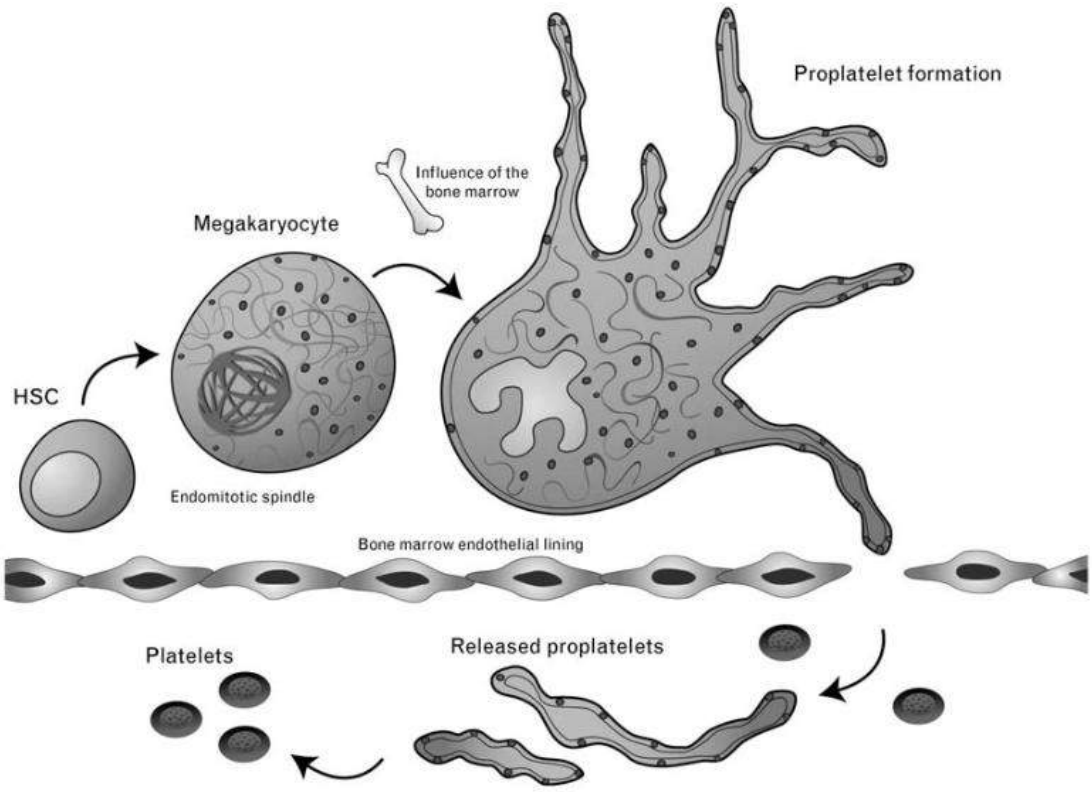

Figure 3: Représentation schématique de la différenciation du MK et de la production plaquettaire: Le MK se développe à partir d'une HSC en plusieurs étapes. Le MK subit des endomitoses, synthétise des organelles et forme son DMS. Le MK étend ensuite de longs prolongements cytoplasmiques, les PPT. Les PPT traversent l'endothélium avant de libérer les plaquettes dans la circulation sanguine. *D'après (Battinelli et al., 2007)*.

1) Cytokines

La thrombopoïétine (TPO) est le principal régulateur de la différenciation des MKs à partir des HSC. La TPO, glycoprotéine synthétisée constitutivement par le foie principalement, mais aussi par le rein, se lie spécifiquement sur son récepteur c-Mpl (Hitchcock and Kaushansky, 2014). c-Mpl est exprimé à la surface des MKs et des plaquettes. La génération de souris déficientes en TPO ou pour son récepteur a permis de mettre en évidence leur rôle majeur dans le développement des MKs et la production de plaquettes (Bartley et al., 1994; de Sauvage et al., 1994; Kaushansky et al., 1994; Lok et al., 1994; Wendling et al., 1994). En effet, ces souris présentent un nombre de MKs et un compte plaquettaire fortement réduits (Bunting et al., 1997; Gurney et al., 1994; Solar et al., 1998). Il a été montré que le taux plasmatique de TPO est inversement proportionnel au compte plaquettaire. En effet, c-Mpl plaquettaire fixe la TPO circulante, ce qui a pour conséquence de réguler le taux plasmatique de TPO (Kaushansky, 2006). Dans ce contexte, si le compte plaquettaire est élevé, davantage de TPO se fixera au c-Mpl plaquettaire, le taux de TPO plasmatique libre diminuera et inversement. Les plaquettes, *via* l'expression de c-Mpl, contrôlent ainsi elles-mêmes leur propre production (Nichol et al., 1995).

c-Mpl est un homodimère associé de façon constitutive à la tyrosine kinase Janus kinase 2 (Jak2). Lors de sa liaison à la TPO, c-Mpl change de conformation, permettant ainsi l'activation des Jak2 associées par trans-phosphorylation. Une fois Jak2 activée, celle-ci active à son tour diverses voies de signalisation cellulaire telles que (i) la voie des protéines de la famille STAT, qui stimule l'expression génique de p21, Bcl-xl et de la cycline D1 pour induire la différenciation et la survie du MK; (ii) la voie phosphoinositide-3-kinase (PI3K)-Akt qui induit la survie, la prolifération et la différenciation du MK et (iii) la voie des mitogen-activated protein kinase (MAPK) qui stimule la différenciation du MK (Geddis, 2010) (Figure 4).

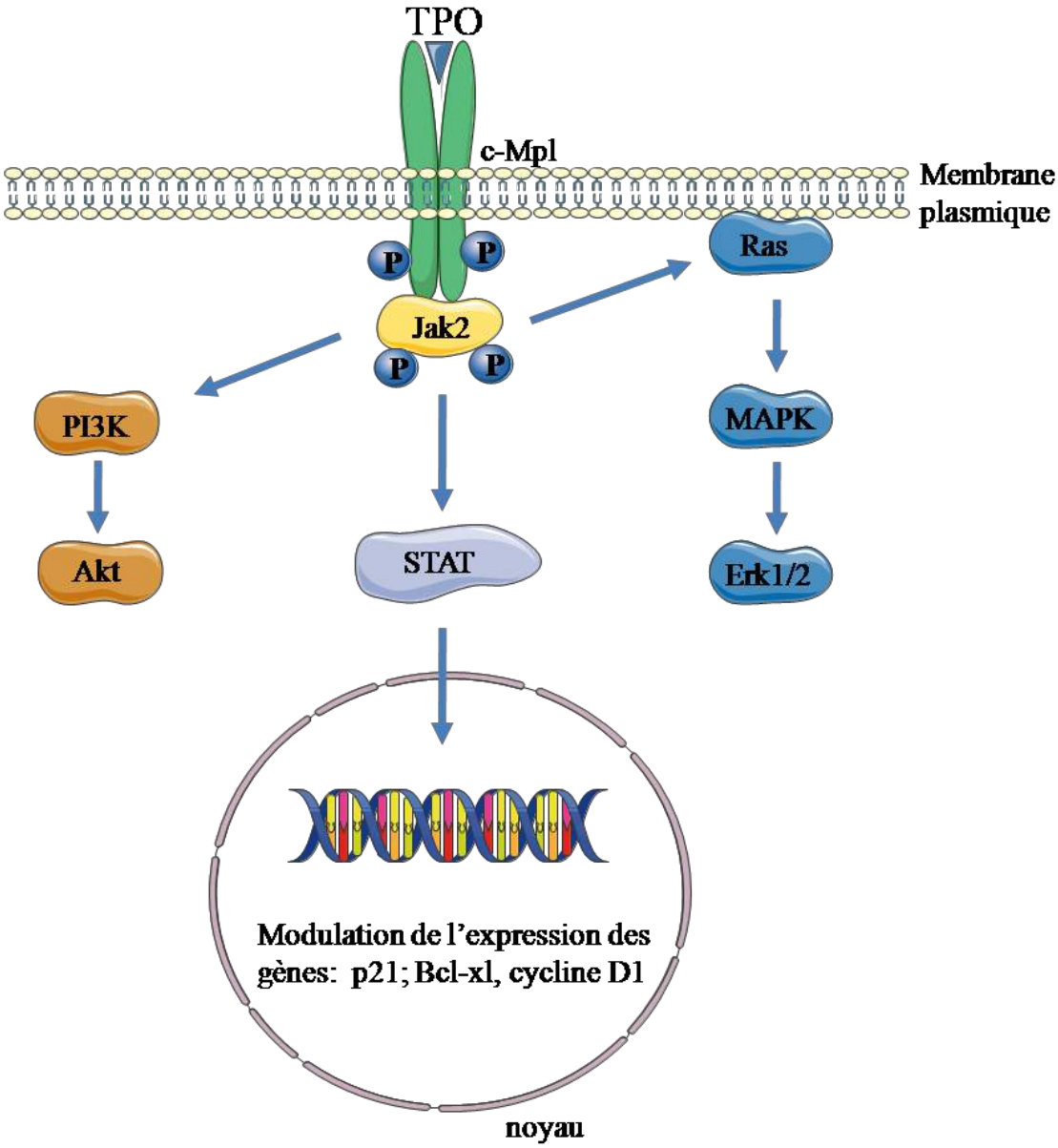

Figure 4: Voie de signalisation de la thrombopoïétine (TPO): Le récepteur de la TPO, c-Mpl est un homodimère associé à la tyrosine kinase Jak2. Lorsque la TPO active c-Mpl, celui-ci change de conformation, active Jak2 et *in fine* les voies de signalisation STAT, PI3K/Akt, Ras/MAPK.

Une autre chimiokine importante lors de la mégacaryopoïèse est le SDF-1 ou CXCL12. Cette dernière est synthétisée par les CXCL12-abundant reticular cells (cellules CAR), les ostéoblastes médullaires et les cellules endothéliales de la moelle osseuse (Niswander et al., 2014). Son récepteur au niveau du MK, CXCR4, est un récepteur à 7 domaines transmembranaires, couplé à une protéine Gi, dont l'expression augmente au cours de la différenciation du MK (Chatterjee and Gawaz, 2013; Riviere et al., 1999; Wang et al., 1998). Dans la moelle osseuse, grâce à un gradient de CXCL12, le progéniteur mégacaryocytaire en différenciation va migrer de la niche ostéoblastique vers la niche

vasculaire. CXCL12, en stimulant CXCR4, active différentes voies de signalisation telles que la voie PI3K-Akt et la voie des MAPK, comme montré dans la lignée mégacaryoblastique MO7e (Berthebaud et al., 2005; Pozzobon et al., 2016).

Certains facteurs comme le granulocyte-macrophage colony stimulating factor (GM-CSF), l'IL-3, l'IL-6, l'érythropoïétine (EPO) ou le stem cell factor (SCF) stimulent également la différenciation des mégacaryocytes (Broudy and Kaushansky, 1995; Bruno et al., 2003; Deutsch et al., 1995; Kaushansky, 1995). A l'inverse, certains inhibent le développement des MK tels que le TGF-β1 (Kuter et al., 1992) ou IL-4 (Han et al., 1991; Zauli and Catani, 1995).

2) Facteurs de transcription

La maturation du MK se fait en plusieurs étapes, contrôlées par des facteurs de transcription qui régulent l'expression de gènes impliqués dans la différenciation en MK mature. Globin transcription factor 1 (GATA-1) et Friend of GATA-1 (FOG) forment un complexe qui va, à la fois activer des gènes de la lignée mégacaryocytaire tels que GPIIb, PF4, GPIbα mais aussi réprimer la différenciation vers la lignée myéloïde dépendante de Pu.1 (Shivdasani et al., 1997; Tijssen and Ghevaert, 2013). Des mutations de GATA-1 ou de ses sites de liaison aux promoteurs de gènes cibles entrainent des dysfonctionnements plaquettaires, aboutissant à des pathologies comme, par exemple, une forme du syndrome de Bernard-Soulier induite par mutation du site de liaison de GATA-1 sur le promoteur de GPIbβ (Ludlow et al., 1996; Tijssen and Ghevaert, 2013). Runt-related transcription factor 1 (RUNX1) stimule lui aussi positivement la différenciation en MK en réprimant l'expression de la chaîne lourde de la myosine IIB non-musculaire (MYH10) et *in fine* en favorisant la polyploïdisation (Ichikawa et al., 2004; Tijssen and Ghevaert, 2013). RUNX1 et GATA-1 sont impliqués tout au long de la différenciation du MK. A l'inverse, certains facteurs ont plutôt un rôle lors de l'initiation ou de la terminaison de la mégacaryopoïese. Par exemple, Friend leukemia virus integration 1 (FLI1) stimule l'expression de gènes précoces de la différenciation (tels que GPIIb et c-Mpl) alors que Nuclear factor erythroid 2 (NF-E2) contrôle plutôt l'expression de gènes tardifs de la maturation des MKs (tels que β1-tubuline et caspase 12) permettant la formation du DMS et des PPT (Schulze and Shivdasani, 2004; Tijssen and Ghevaert, 2013) (Figure 5).

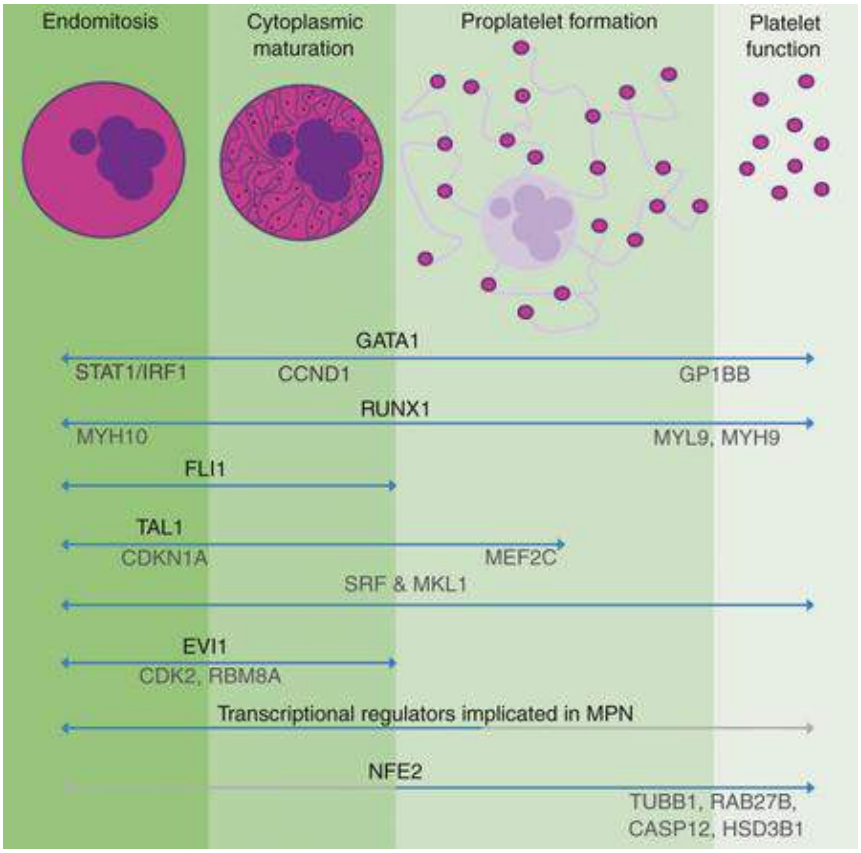

Figure 5: Résumé des différents facteurs de transcription et de leurs cibles en aval lors des différents stades de la mégacaryopoïèse. *D'après (Tijssen and Ghevaert, 2013).*

3) Endomitose

Une des caractéristiques du MK est sa polyploïdie. Le MK devient polyploïde par un processus dépendant de la TPO : l'endomitose (Machlus et al., 2014). L'endomitose est une succession de réplications de l'ADN sans aucune division cellulaire conduisant à la formation d'un noyau polylobé pouvant aller jusqu'à 128N, *in vitro* (Machlus et al., 2014; Zimmet and Ravid, 2000) (Figure 6). Ce phénomène, bien que mal caractérisé, est sous le contrôle de différents facteurs :

(i) L'absence de cycline B1, due à sa dégradation dépendante de l'ubiquitine, entraîne l'incapacité de former le complexe cyclin dependant kinase 1 (cdk1)/cycline B1. Sans ce complexe, la kinase de cdk1 est inactive, induisant une altération du cycle cellulaire lors de l'anaphase où a donc lieu une mitose abortive (Datta et al., 1996; Zhang et al., 1998; Zhang et al., 1996).

(ii) RUNX1, lors de la différenciation du MK, réprime l'expression de la chaîne lourde de la myosine IIB non-musculaire (MYH10), localisée spécifiquement dans l'anneau contractile composé de F-actine et de myosine II, et empêche ainsi la cytocinèse. La répression de

l'expression MYH10 par RUNX1 est donc responsable de la polyploïdisation du MK (Geddis et al., 2007; Lordier et al., 2012).

(iii) Les tyrosine phosphatases Shp1 et Shp2, *via* leurs rôles dans la signalisation en aval de c-Mpl et des intégrines ainsi que dans la formation de l'anneau contractile pour le passage de 2N à 4N, contrôlent aussi la polyploïdisation des MKs (Mazharian et al., 2013).

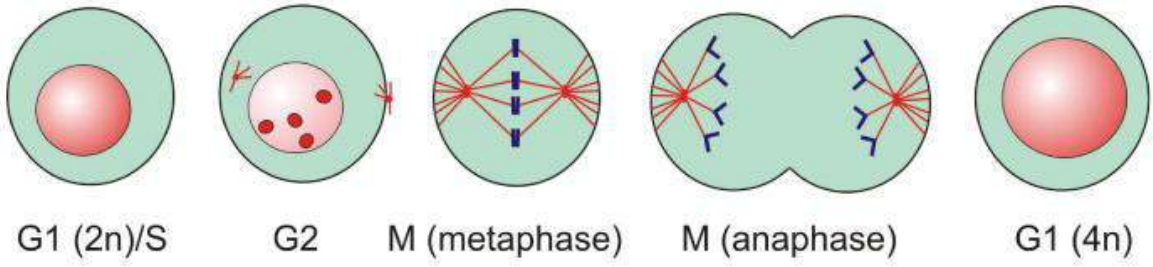

Figure 6: Endomitose: Le progéniteur mégacaryocytaire diploïde va subir la phase S et entrer en mitose. Bien que l'anaphase soit initiée, avec séparation des paires de chromosomes et formation du sillon de clivage, ce dernier régresse avant d'accomplir la cytocinèse résultant ainsi en une cellule tétraploïde qui recommence à nouveau la phase G1. *D'après (Geddis, 2010)*.

Quel intérêt a le MK à devenir polyploïde? Il semblerait que cela lui permette de produire les quantités d'ARNm et de protéines nécessaires à la production des granules et autres organites plaquettaires tout en gardant la capacité de produire le DMS et de former les PPT (Machlus and Italiano, 2013; Zimmet and Ravid, 2000).

4) Biogénèse des granules plaquettaires

La biogénèse des granules (α, denses ou δ) plaquettaires se produit dans le MK lors de sa différenciation. La sécrétion du contenu de ces granules est indispensable au bon fonctionnement plaquettaire (King and Reed, 2002). Le contenu et le rôle des granules dans la plaquette sera développé dans le chapitre II de l'introduction.

Les granules α proviennent à la fois du bourgeonnement de vésicules originaires du trans-golgi (TGN) mais aussi de l'endocytose (Hegyi et al., 1990; King and Reed, 2002). Ces vésicules vont, soit fusionner avec les granules α existants, soit être acheminées vers les corps multi-vésiculaires (MVB), qui sont des gares de triage primordiales dans la formation des granules α (Heijnen et al., 1998). Les granules α continuent à évoluer dans les plaquettes où l'endocytose est importante et contribue au remplissage des granules (zucker-franklin 1981). De façon très schématique, la Neurobeachin-like 2 (NBEAL2) permet le contrôle du contenu des granules (Gunay-Aygun et al., 2011) et les vacuolar protein sorting 33B (Vps33B) et 16B

(Vps16B) contrôlent la biogénèse des membranes des granules α (Lo et al., 2005; Urban et al., 2012) (Figure 7).

Des défauts de formation des granules α conduisent à des syndromes hémorragiques d'intensité variable chez l'homme. Il s'agit du syndrome des plaquettes grises (SPG) provenant d'une mutation sur le gène de *NBEAL2* (Albers et al., 2011) et de l'arthrogryposis, renal dysfunction and cholestasis (ARC) syndrome venant d'une mutation sur le gène *Vps33B* (Gissen et al., 2004). D'autres syndromes plaquettaires rares sont associés à des défauts de formation des granules α, tels que le syndrome de Paris-Trousseau qui provient d'une mutation de *FLI1* et dont les plaquettes présentent de très rares mais très gros granules α (Breton-Gorius et al., 1995; Veljkovic et al., 2009).

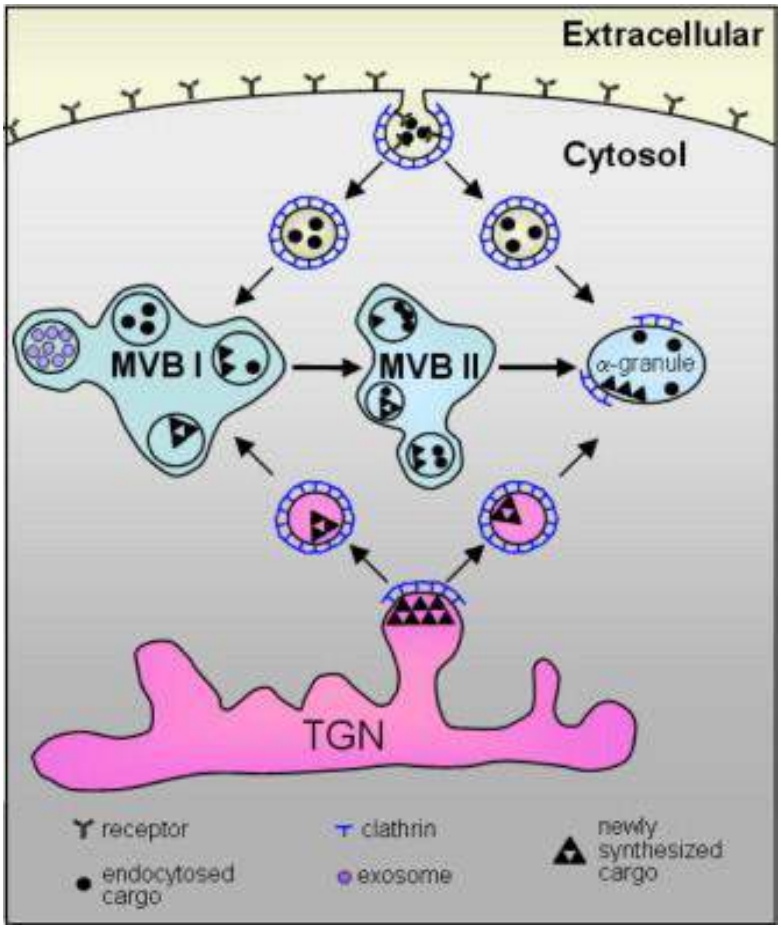

Figure 7: Modèle proposé de formation des granules α dans le mégacaryocyte: Les granules α proviennent de deux mécanismes dépendants de la clathrine: le bourgeonnement du TGN et l'endocytose au niveau de la membrane plasmique. Ces vésicules peuvent être triées au niveau des MVB ou directement fusionnées avec les granules α. Les MVB sont aussi capables de maturer pour produire des granules α. D'après (Blair and Flaumenhaft, 2009).

Les granules denses sont eux originaires des endosomes tardifs et des MVB du MK (Ambrosio et al., 2012; Meng et al., 2012; Youssefian and Cramer, 2000). La biogénèse des granules denses met en jeu plusieurs protéines dont les rôles sont encore mal caractérisés: adaptator protein 3 (AP3), lysosomal trafficking regulator (LYST), biogenesis of lysosom-related organelle complexes (BLOC) et le complexe Vps33A/Vps16A (Ambrosio et al., 2012; Huizing et al., 2008; Suzuki et al., 2003). Le syndrome d'Hermansky-Pudlak (HPS), provenant de mutations des gènes de *BLOC*, *HPS* et *AP3* (Feng et al., 1999; Huizing et al., 2009; Muller et al., 2009) et le syndrome Chediak-Higashi (CHS), provenant d'une mutation du gène *LYST* (Barbosa et al., 1996; Certain et al., 2000; Masliah-Planchon et al., 2013; Nagle et al., 1996), sont des pathologies héréditaires présentant entre autres des défauts de biogénèse des granules denses plaquettaires.

5) Développement du DMS

Une autre composante de la différenciation du MK est la formation du DMS. Le DMS est un réservoir de membranes, à l'intérieur même du MK, nécessaire à l'élongation des PPT et *in fine* à la production des plaquettes (Behnke, 1968, 1969).

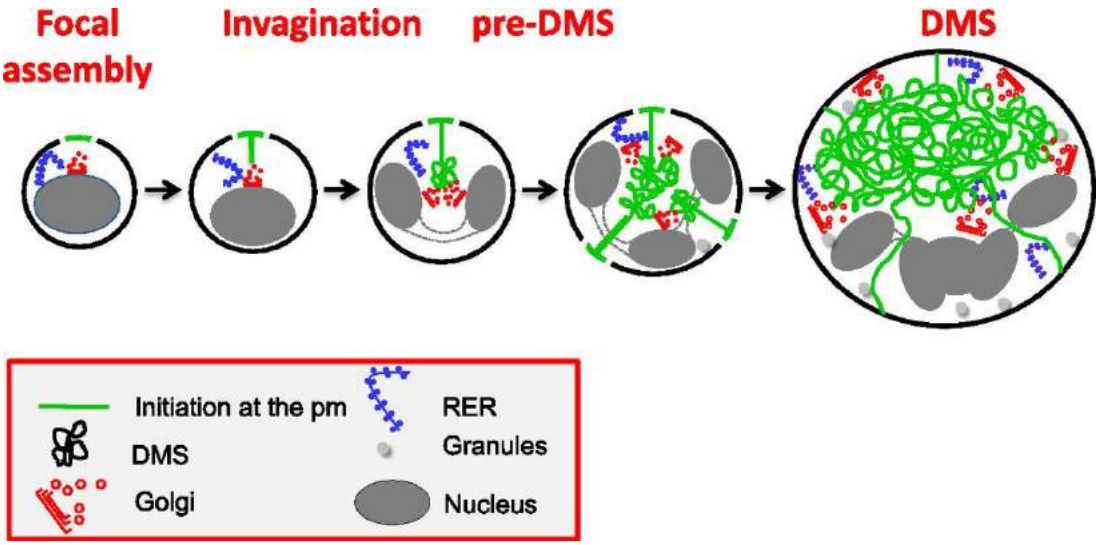

Figure 8: Modèle proposé de formation et de développement du DMS: L'initiation de la formation du DMS s'effectue au niveau de zones focales à la surface de la cellule. Pendant la différenciation du MK, un pré-DMS se forme dans la région péri-nucléaire, par invagination de la membrane plasmique selon un procédé ressemblant à un sillon de clivage. La suite du développement nécessite la fusion de vésicules, originaires des différentes structures du Golgi, avec le DMS en développement ainsi que potentiellement un transfert direct de lipides depuis le réticulum endoplasmique. *D'après (Eckly et al., 2014)*.

Eckly et collaborateurs ont montré, par microscopie confocale et électronique en 3 dimensions, les différents stades de formation du DMS au cours de la différenciation du MK.

Dans un premier temps, un pré-DMS rattaché à la membrane plasmique se forme dans la région péri-nucléaire du MK immature. Dans un deuxième et troisième temps, des vésicules provenant du Golgi puis du réticulum endoplasmique fusionnent avec le DMS pour permettre son expansion (Eckly et al., 2014) (Figure 8).

Afin de permettre l'invagination initiale nécessaire à la formation du DMS, la phosphatidylinositol-5phosphate 4 kinase α par sa production de phosphatidylinositol 4,5-bisphosphate (PtdIns(4,5)P_2) dans le DMS permettrait l'assemblage des fibres d'actine par la voie Wiskott-Aldrich syndrom/Wiskott–Aldrich Syndrome protein family verprolin homologous (WASp/WAVE) (Schulze et al., 2006). Le rôle des forces générées par le cytosquelette dans la formation du DMS reste encore peu caractérisé. Cependant, une étude de Chen *et al* montre que la Cdc42 interating protein 4 (CIP4), *via* son interaction avec le domaine SRC homology 3 (SH3) de WASp, fait le lien entre le cytosquelette et la membrane plasmique par son domaine F-bin-amphiphysin-rvs (F-BAR). Ceci permet la réorganisation du cytosquelette d'actine contribuant à la formation du DMS. La délétion de CIP4 induit une thrombopénie à cause d'une dynamique altérée de l'actine, entraînant une rigidité membranaire perturbée, ce qui affecte la formation du DMS et réduit le nombre de PPT formées (Chen et al., 2013a; Chen et al., 2013b). Dans le même sens, il a récemment été montré, notamment par notre équipe, que la régulation du cytosquelette d'actine spécifiquement par la GTPase Cdc42 et ses effecteurs PAK1/2/3 était indispensable à la bonne formation du DMS et l'émission des PPT (Antkowiak et al., 2016; Kosoff et al., 2015).

C) Etapes tardives de la mégacaryopoïèse

1) Migration vers la niche périvasculaire:

La différenciation du MK débute dans la niche ostéoblastique et se termine dans la niche périvasculaire où il va étendre de longs prolongements cytoplasmiques, les PPT, à travers les vaisseaux sinusoïdes de la moelle osseuse pour libérer les plaquettes directement dans la circulation sanguine. Pour cela, le MK va migrer en réponse à un gradient de CXCL12 (SDF1) mais aussi grâce à ses interactions avec la matrice extracellulaire et les cellules de la moelle osseuse. Hamada et collaborateurs ont montré qu'en bloquant CXCR4, la migration des MKs était fortement affectée, montrant un rôle majeur de l'axe CXCL12-CXCR4 dans la migration mégakaryocytaire (Chatterjee and Gawaz, 2013; Hamada et al., 1998). L'axe CXCL12-CXCR4 induit aussi une augmentation de l'adhésion et de la transmigration du MK

au travers des cellules endothéliales des sinusoïdes médullaires pour permettre le relargage des plaquettes dans la circulation sanguine (Chatterjee and Gawaz, 2013; Hamada et al., 1998; Niswander et al., 2014; Wang et al., 1998). Au niveau moléculaire, plusieurs protéines sont également mises en jeu lors de la migration du MK, telles que la glycoprotéine platelet-endothelial cell adhesion molecule 1 (PECAM-1), WASp ou encore la matrix métalloprotéase 9 (MMP9). L'absence de PECAM-1 dans les MKs est responsable d'une migration défectueuse du MK envers un gradient de CXCL12, ceci potentiellement dû à un défaut de polarisation de CXCR4 à la surface du MK (Dhanjal et al., 2007). Ceci a pour conséquence un retard du retour au compte plaquettaire normal suite à une thrombocytopénie immune induite chez des souris déficientes pour PECAM. Une autre protéine mise en jeu lors de la migration des MK est WASp. Les patients atteints du syndrome WAS présentent une microthrombopénie. L'analyse du modèle murin déficient pour WASp a permis de montrer que cette thrombopénie était due à (i) un défaut de migration des MKs vers un gradient de CXCL12 ainsi que (ii) une incapacité à former des podosomes riches en actine, (iii) un relargage ectopique par les MKs de plaquettes directement dans la moelle osseuse et (iv) une durée de vie plaquettaire diminuée (Falet et al., 2009; Sabri et al., 2006). Enfin, Lane et collaborateurs ont montré que la MMP9 sécrétée par le MK permettrait la migration de ce dernier envers un gradient de CXCL12 et que l'inhibition de MMP9 *in vivo* empêche l'augmentation du compte plaquettaire induit par injection de CXCL12 (Lane et al., 2000).

2) Libération de plaquettes

Une fois arrivé à la niche périvasculaire, le MK va étendre de longs prolongements cytoplasmiques, les PPT, dans les vaisseaux sinusoïdes de la moelle osseuse afin d'y libérer les plaquettes dans le flux sanguin. Grâce à la microscopie intravitale couplée à la fluorescence, Junt et collègues ont pu visualiser pour la première fois *in vivo* la formation de PPT, la traversée des PPT dans les microvaisseaux et la fragmentation des PPT sous l'influence du flux sanguin dans la moelle osseuse de crâne de souris vivantes (Junt et al., 2007). Ce travail a été réalisé grâce à un modèle de souris (Zhang et al., 2007) exprimant l'intégrine αIIb (ou CD41), spécifique de la lignée mégacaryocytaire, couplée a un fluorophore (Junt et al., 2007). Le mécanisme moléculaire par lequel les PPT traversent la paroi endothéliale des sinusoïdes restent encore à définir.

Le modèle de production des plaquettes aujourd'hui proposé comporte 3 étapes : (i) le MK forme des pseudopodes qui s'allongent en PPT grâce aux microtubules; (ii) la totalité du cytoplasme est convertie en PPT, ne laissant de coté que le noyau polylobé qui sera ensuite

éliminé par les macrophages (Gordge, 2005); (iii) dans la circulation sanguine, des pré-plaquettes allant de 2 à 10 µm de diamètre se transforment en plaquettes à 2 corps appelées « barbell-shaped proplatelets » qui, grâce à leur cortex sous-membranaire d'actine-spectrine-myosine et leur réseau de microtubules, se diviseront en 2 plaquettes distinctes (Italiano, 2013; Patel-Hett et al., 2011; Schwertz et al., 2010; Spinler et al., 2015; Thon et al., 2012; Thon et al., 2010). L'un des moteurs de la production des plaquettes est le cytosquelette du MK composé de microtubules-actine-myosine-spectrine (figure 9).

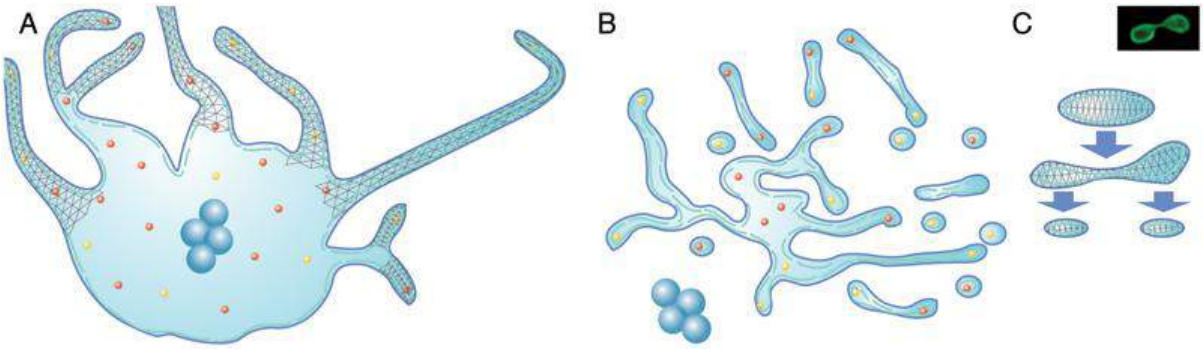

Figure 9: Modèle de production plaquettaire: (**A**) La formation des PPT débute par la formation de pseudopodes qui utilisent les microtubules pour s'étendre et former des PPT fines. (**B**) La totalité du cytoplasme est converti en une masse de PPT. (**C**) Les préplaquettes allant de 2 à 10 µm de diamètre relarguées par les PPT s'étirent pour former des plaquettes en forme d'altères (appelées « barbell-shaped proplatelets») qui, sous l'effet du flux sanguin et grâce à la dynamique de leur cortex sous-membranaire d'actine-spectrine-myosine finiront par donner deux plaquettes distinctes. *D'après (Italiano, 2013).*

- Etape 1 : Extension des PPT

La première étape est l'émission par le MK de pseudopodes à la base desquels des amas de microtubules sont formés. Dès le début de l'extension des pseudopodes, les microtubules vont développer un réseau linéaire tout le long des pseudopodes pour permettre l'extension de ces structures et en faire des PPT (Italiano et al., 1999). Les PPT constituent des prolongements cytoplasmiques contenant des bourgeons ressemblant à des plaquettes et reliés par des ponts cytoplasmiques (figure 10).

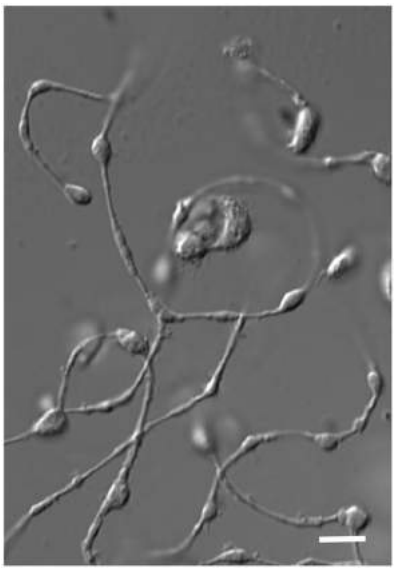

Figure 10: Architecture des PPT: Image en contraste de phase de PPT issues de MKs murins en culture. On peut observer la région terminale des PPT et les branchements cytoplasmiques entre les structures ressemblant aux plaquettes. Echelle : 5µm. *D'après (Italiano, 2013)*.

Les microtubules servent aussi « d'autoroute » le long des PPT pour l'acheminement des organelles plaquettaires (granules, mitochondries) après que la myosine IIA, *via* la structuration de l'actine dans le MK, ait correctement positionné les granules (Pertuy et al., 2014; Richardson et al., 2005). L'élongation des PPT est associée à la sortie massive du DMS qui sert de réservoir de membranes dans ce processus. A l'extrémité des PPT seulement, les microtubules forment une boucle sous la membrane plasmique. Cette structure est similaire au cytosquelette retrouvé dans les plaquettes, suggérant ainsi que les plaquettes ne pourraient être générées que dans la région terminale des PPT (Italiano et al., 1999).

- Etape 2 : Ramification des PPT

La deuxième étape est la ramification de la région terminale des PPT permettant d'augmenter la production plaquettaire. Pendant que les microtubules permettent l'allongement des PPT, l'actine permet la ramification du bout de ces mêmes PPT. En effet, l'utilisation d'inhibiteurs de la polymérisation de l'actine a permis de montrer que cette ramification est dépendante de l'actine (Italiano et al., 1999). Cependant, le mécanisme moléculaire exact n'a toujours pas été caractérisé. Il est néanmoins suggéré qu'une forte connexion entre l'actine et les microtubules permette la mise en place de forces nécessaires à la formation des ramifications. Une hypothèse propose que l'association de l'actine avec la myosine soit le moteur suffisant pour permettre la ramification. Cette hypothèse est appuyée par une étude montrant que l'inactivation de *myh9* (le gène codant pour la myosine IIA ;

MYH9Δ) spécifiquement dans la lignée mégacaryocytaire chez la souris induit une morphologie anormale des MKs avec un DMS moins abondant et dilaté avec pour conséquence une formation des PPT défectueuse (diminution du nombre de MK formant des PPT et de l'aire des PPT). Les PPT provenant des MK MYH9Δ ont des « platelet-like » particules plus grosses, ce qui explique la macrothrombopénie des souris MYH9Δ. L'ensemble de ces données suggère un rôle important de la myosine IIA dans le phénomène de ramification des PPT et la production des plaquettes (Eckly et al., 2010; Eckly et al., 2009; Leon et al., 2007).

La spectrine, quant à elle, a été très peu étudiée dans ce phénomène. Cependant, une étude par Patel-hett et collaborateurs a montré que l'assemblage de tétramères de spectrine est indispensable à la formation du DMS mais aussi que la spectrine stabilise la morphologie des PPT (Patel-Hett et al., 2011) (Figure 11).

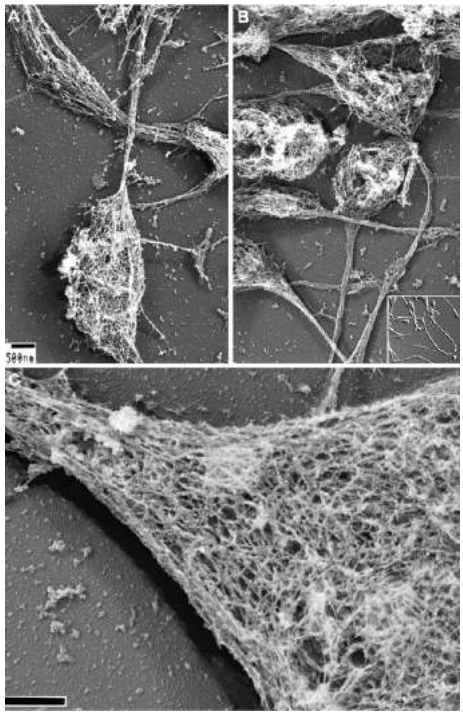

Figure 11: Structure du squelette sous-membranaire des proplaquettes: (**A-B**) Image en microscopie électronique à balayage du cytosquelette insoluble au détergent (permettant de préserver le squelette sous-membranaire). L'observation des PPT révèle un squelette sous-membranaire intact qui s'étend tout le long des PPT. Echelle : 500nm. (**C**) Image en 3D de microscopie électronique montrant un long réseau filamenteux ressemblant au réseau de spectrine des érythrocytes et des plaquettes. Echelle : 200nm. *D'après (Patel-Hett et al., 2011)*.

Récemment, Bury et collaborateurs ont suggéré que la macrothrombopénie observée chez les patients souffrant d'un variant de la Thrombasthénie de Glanzmann (mutation gain de

fonction induisant une réduction de l'expression de surface de l'intégrine $\alpha_{IIb}\beta_3$ et aussi son activation constitutive à la surface des MK et des plaquettes) était due à un défaut de réorganisation de l'actine au niveau du MK avec un impact sur la ramification des PPT et la libération de « barbell-shaped proplatelets asymétriques » (Bury et al., 2016).

- Etape 3 : « Division plaquettaire »

La libération des plaquettes à partir des PPT du MK n'est pas le seul stade final de la production plaquettaire. En effet, plusieurs études ont montré la présence ou la libération dans la circulation sanguine de fragments du MK de tailles plus importantes que les plaquettes, suggérant l'existence d'une étape ultime de production plaquettaire pouvant se réaliser directement dans la circulation sanguine (Behnke and Forer, 1998; Junt et al., 2007). Ce concept étant nouveau, peu de choses sont connues à ce jour.

En 2010, Shwertz et collaborateurs ont « cultivé » (mise en rotation à 37°C) pendant 6 ou 24 heures, du plasma riche en plaquettes et ont observé une production de « corps cellulaires » ressemblant à des plaquettes, contenant des organelles tels que des mitochondries ou des granules α, exprimant à leur surface des récepteurs plaquettaires tels que la P-selectine et capables d'adhérer et de s'étaler sur matrice extracellulaire (Schwertz et al., 2010). Cette étude suggère donc une division des plaquettes dans le sang.

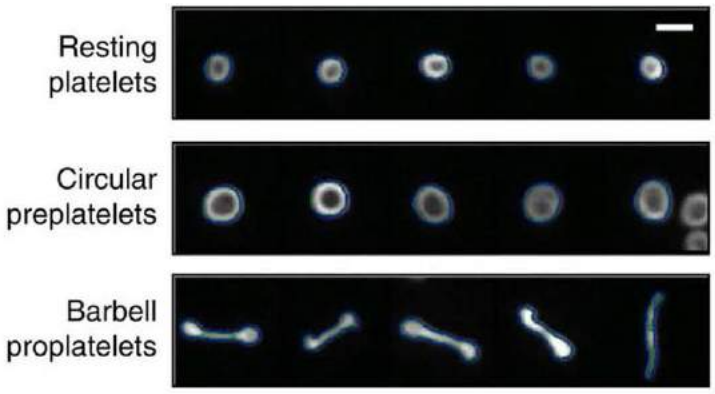

Figure 12: Galerie d'images de plaquettes au repos, de préplaquettes et de « barbell-shaped proplatelets ». *D'après (Thon et al., 2012).*

En 2011, Thon *et al* ont réussi à isoler des PPT provenant de MKs de souris par une succession de centrifugation et de gradients d'albumine bovine sérique (BSA). Ils ont pu observer les différentes étapes amenant à la production de 2 ou plusieurs plaquettes à partir d'une PPT. Cette étude a aussi mis en évidence un stade intermédiaire de production de plaquettes directement dans la circulation, appelé préplaquette (grosse plaquette faisant 2 à 10

µm de large), capable de se transformer de façon réversible en plaquette à deux corps appelée « barbell-shaped proplatelet » (Figure 9). Cette transformation est possible grâce aux forces des microtubules qui, par torsion, permettront la formation de ces fragments à deux corps cellulaires, puis d'un site de clivage et amenant *in fine* à la production de 2 plaquettes. Les forces de cisaillement du flux sanguin participent aussi à ce phénomène en promouvant la scission. Thon *et al* ont aussi démontré la présence de MVB (plateforme de tri des granules plaquettaires) dans les préplaquettes et « barbell-shaped proplatelets ». A l'aide de fibrinogène couplé à un fluorophore, ils ont observé le trafic des granules, *in vivo*, pendant la conversion des préplaquettes en « barbell-shaped proplatelets », démontrant ainsi que la biogénèse des granules se produit aussi pendant ce stade terminal de production plaquettaire (Thon et al., 2010) (Figure 13).

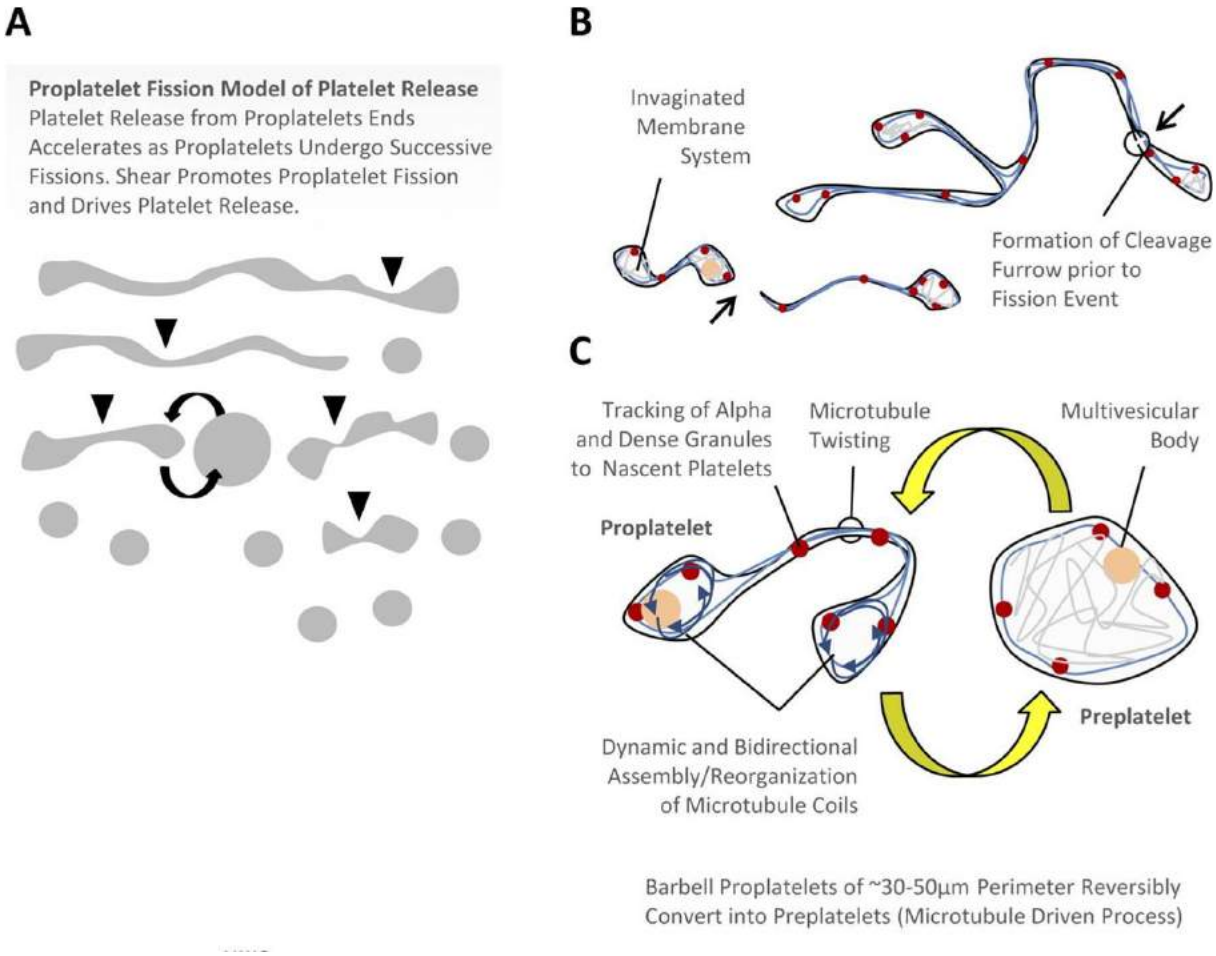

Figure 13: Modèle proposé de relargage de plaquettes par scission de PPT: (**A-B**) Une PPT libérée subit des scissions tour à tour à son niveau médian et terminal. Ce phénomène est dû à la formation d'un sillon de clivage et aboutit à la libération d'une plaquette du bout de la PPT. Les forces de cisaillement stimulent la scission et la libération de plaquettes. (**C**) Les « barbell-shaped proplatelets » de 30 à 50 µm de périmètre se transforment de manière réversible en préplaquettes. Ce

processus est emmené par les forces de torsion des microtubules et pourrait représenter un nouveau mécanisme de réorganisation des microtubules et de la redistribution des granules après chaque scission. Lors de la formation des « barbell-shaped proplatelets », la réorganisation du cytosquelette est médiée par l'assemblage dynamique et bidirectionnel des microtubules ainsi que leur réorganisation. En parallèle, les granules α et denses (en rouge) sont délivrés aux régions terminales des « barbell-shaped proplatelets ». Les plaquettes sont en suite relarguées après chaque scission. *D'après (Thon et al., 2010).*

En 2011, Patel-Hett et collègues se sont intéressés au rôle du squelette sous-membranaire riche en spectrine et actine dans la production des « barbell-shaped proplatelets » et des plaquettes. Ce squelette sous-membranaire maintient la structure et la dynamique des plaquettes (Fox et al., 1988; Fox et al., 1987; Hartwig and DeSisto, 1991). La transfection d'un rétrovirus exprimant une forme de dominant négatif de spectrine (inhibant la tétramérisation de la spectrine) dans des « barbell-shaped proplatelets », provoque leur réversion en préplaquettes et leur incapacité à se diviser en plaquettes. Cette étude révèle donc le rôle primordial du squelette sous-membranaire riche en spectrine dans la formation des plaquettes à partir des « barbell-shaped proplatelets » (Patel-Hett et al., 2011) (Figure 14).

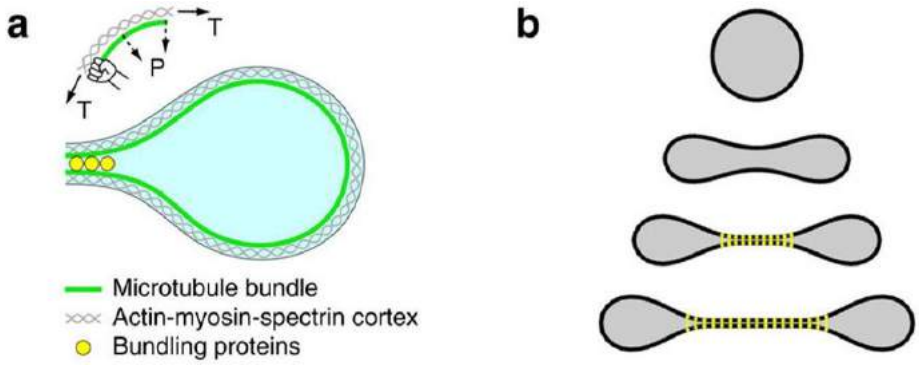

Figure 14: Modèle proposé de formation des « barbell-shaped proplatelets »: (**a**) Schéma représentatif de l'équilibre des forces. (**b**) Simulation des formes lors des différentes étapes de conversion de préplaquette en « barbell-shaped proplatelet ». En jaune la force de torsion/compression des microtubules. *D'après (Thon et al., 2012).*

En 2012, Thon *et al* ont tout d'abord quantifié la proportion de plaquettes (96,31%), préplaquettes (3,63%) et « barbell-shaped proplatelets » (0.05%) dans le sang humain. Cette étude vient compléter celle de 2011 qui démontre que la conversion des préplaquettes en « barbell-shaped proplatelets » puis en plaquettes est régulée (i) par le diamètre et l'épaisseur des boucles de microtubules (ce qui permet l'augmentation des forces de torsion au niveau du pont entre les deux futures plaquettes mais aussi l'augmentation des forces permettant la courbure des « barbell-shaped proplatelets » par les microtubules périphériques) et (ii) par le squelette sous-membranaire actine-spectrine-myosine (Thon et al., 2012).

Enfin, en 2015, Spinler *et al* ont montré que l'inhibition pharmacologique ou la mutation myh9 inhibe la mécano-activation de la myosine IIA entrainant la libération de larges fragments CD41 positifs ressemblants à des préplaquettes. De plus, les patients portant la mutation du gène myh9 ont une macrothrombopénie suggérant une accumulation de ces préplaquettes dans la circulation sanguine (Spinler et al., 2015).

En résumé, il semble que la formation de « barbell-shaped proplatelets » provienne d'une perte de cet équilibre entre les forces des microtubules plutôt favorables à la scission et les forces du cortex actine-spectrine-myosine, plutôt favorables au maintien de la structure discoïde de la plaquette. Dans un modèle si dynamique et mettant en jeu autant de facteurs, les 0,05% de « barbell-shaped proplatelets » quantifiées dans la circulation sanguine suggèrent une imperfection du système global (Italiano, 2013; Patel-Hett et al., 2011; Schwertz et al., 2010; Spinler et al., 2015; Thon et al., 2012; Thon et al., 2010).

Chapitre II : Les plaquettes sanguines

Les plaquettes sanguines sont des cellules anucléées de forme discoïde, de 2 à 3 μm de diamètre, libérées dans la circulation sanguine par le MK. Chez l'adulte, on trouve entre 150 000 à 400 000 plaquettes par μl de sang. Les plaquettes ont une durée de vie d'une dizaine de jours puis sont phagocytées et éliminées par les macrophages de la rate et du foie.

Le rôle majeur des plaquettes est le maintien de l'intégrité vasculaire. En effet, lors d'une lésion vasculaire, les plaquettes vont interagir avec le sous-endothélium mis à nu, s'activer et s'agréger pour former un thrombus qui va arrêter le saignement.

A) Morphologie des plaquettes sanguines

Une plaquette est constituée de trois zones principales qui ont chacune des spécificités fonctionnelles et biochimiques : le système membranaire, les organelles et le cytosquelette.

1) Le système membranaire

a) La membrane plasmique

La membrane plasmique plaquettaire est une bicouche de phospholipides distribués de façon asymétrique et dont les charges négatives sont présentes dans le feuillet interne (phosphatidylsérine ou PS et phosphatidylinositol ou PtdIns) des plaquettes au repos. Lors de l'activation des plaquettes, les PS sont transloqués vers le feuillet externe de la membrane plasmique dans le but de fournir une surface propice à l'interaction avec des protéines de la coagulation (Chap et al., 1979; Lhermusier et al., 2011; Shattil and Bennett, 1981). Sont aussi retrouvés des microdomaines riches en sphingomyéline et en cholestérol, appelés « rafts », qui constituent des plateformes de signalisation contribuant à l'activation plaquettaire (Bodin et al., 2005; Bodin et al., 2003).

Une autre composante essentielle de la membrane plasmique plaquettaire sont les glycoprotéines (GP) de surface. Celles-ci sont ancrées dans la bicouche phospholipidique et la traverse grâce à leurs domaines transmembranaires hydrophobes. Leur partie cytoplasmique se lie avec le cytosquelette plaquettaire en interagissant soit directement avec l'actine soit avec des protéines liant l'actine: les actin binding proteins (ABP). Cette interaction assure la liaison entre les molécules adhésives de la matrice extracellulaire et le système contractile plaquettaire sous-membranaire. Ceci est indispensable pour promouvoir les modifications morphologiques plaquettaires inhérentes à leur activation (Fox, 1985; Painter et al., 1985).

Grâce aux GPs, véritables récepteurs de molécules extracellulaires, les plaquettes adhèrent au sous-endothélium vasculaire: le complexe GPIb-IX-V lie le Facteur de von Willebrand (vWF) ; la GPIc-IIa (ou intégrine $\alpha_5\beta_1$) lie la fibronectine ; GPIa-IIa (ou intégrine $\alpha_2\beta_1$), GPIV et GPVI lient le collagène ; la GPIIb-IIIa (ou intégrine $\alpha_{IIb}\beta_3$) se lie au fibrinogène, au vWF et à la fibronectine.

b) Le système canaliculaire ouvert

Le système canaliculaire ouvert (SCO) est un réservoir de membranes provenant d'invaginations de la membrane plasmique plaquettaire dans le cytoplasme (van Nispen tot Pannerden et al., 2010). Le SCO est impliqué dans l'endocytose de molécules plasmatiques et dans la sécrétion du contenu des granules plaquettaires par fusion du SCO avec les granules pendant l'activation plaquettaire. Ce réservoir de membranes est également mis à profit lors du changement de forme des plaquettes, de la formation des filopodes, de l'étalement et de l'agrégation plaquettaire *via* l'augmentation de la surface membranaire et de l'exposition des GPs d'adhésion à la surface plaquettaire.

c) Le système tubulaire dense

Le système tubulaire dense (STD) est en réalité ce qu'il reste du réticulum endoplasmique du MK. Ce STD contient du calcium intracellulaire ainsi que des enzymes du métabolisme lipidique telles que les cyclooxygénases, responsables de la production de thromboxane A2 (TXA2) à partir d'acide arachidonique, mécanisme indispensable à l'amplification de l'activation plaquettaire.

2) Les organelles plaquettaires

Le cytoplasme plaquettaire contient des granules (granules α et granules denses) et des lysosomes sécrétés lors de l'activation plaquettaire, des mitochondries et des grains de glycogène.

a) Les granules α et denses

Les plaquettes contiennent 3 à 9 petits granules sécrétoires d'environ 150nm de diamètre, les granules denses (ou granules δ). Dans ces granules sont retrouvés de fortes concentrations d'adénosine 5'-diphosphate (ADP), d'adénosine 5'-triphosphate (ATP), de pyrophosphate, de sérotonine et de calcium (Golebiewska and Poole, 2015).

Les granules α quant à eux mesurent entre 300 et 500 nm de diamètre et sont abondants dans les plaquettes (entre 50 et 80 par plaquette) (Golebiewska and Poole, 2015). Les granules α contiennent:

- des protéines d'adhésion: fibrinogène, vWF, fibronectine, vitronectine, thrombospondine.

- des facteurs de croissance: platelet derived growth factor (PDGF), endothelial growth factor (EGF), endothelial cell growth factor (ECGF), vascular epidermal growth factor (VEGF), insulin growth factor 1 (IGF1), transforming growth factor β (TGF β).

- des protéines impliquées dans la cascade de la coagulation et la régulation de la fibrinolyse: facteurs V, XI, XIII, VIII, kininogène de haut poids moléculaire, plasminogène, protéinase S, plasminogen activator inhibitor-1 (PAI-1), α2-antiplasmine.

- des cytokines comme interleukine 1β (IL-1β) et des chimiokines comme RANTES.

- des GPs de surface: GPIb-IX-V, $\alpha_{IIb}\beta_3$, PECAM, P-selectine, CD40L.

- des protéines spécifiques des plaquettes: platelet factor 4 (PF4), β-thromboglobuline.

b) Les lysosomes

Les lysosomes (ou granules λ) sont connus pour leur fonction de dégradation intracellulaire. Pour cela, ils contiennent des enzymes digestives actives à pH acide telles que des hydrolases acides, les cathepsines D et E, des proélastases et des collagénases (Dangelmaier and Holmsen, 1980; Golebiewska and Poole, 2015). Les lysosomes ne sont sécrétés que lors d'une activation maximale de la plaquette où les hydrolases jouent un rôle dans la destruction et l'élimination des agrégats plaquettaires.

c) Les mitochondries

Les plaquettes au repos sont des cellules métaboliquement actives, qui ont une production d'ATP plus élevée que des cellules musculaires au repos par exemple. Le rôle principal des mitochondries plaquettaires est la production d'énergie sous forme d'ATP indispensable au bon fonctionnement des plaquettes (Detwiler, 1972; Garcia-Souza and Oliveira, 2014). Les mitochondries plaquettaires jouent aussi un rôle lors de l'activation plaquettaire. En effet, lors d'une activation forte, les taux de calcium intra-mitochondriaux augmentent ce qui induit la production d'espèces réactives de l'oxygène (ROS) et contribue à l'exposition des PS à la surface des plaquettes (Choo et al., 2012; Garcia-Souza and Oliveira, 2014).

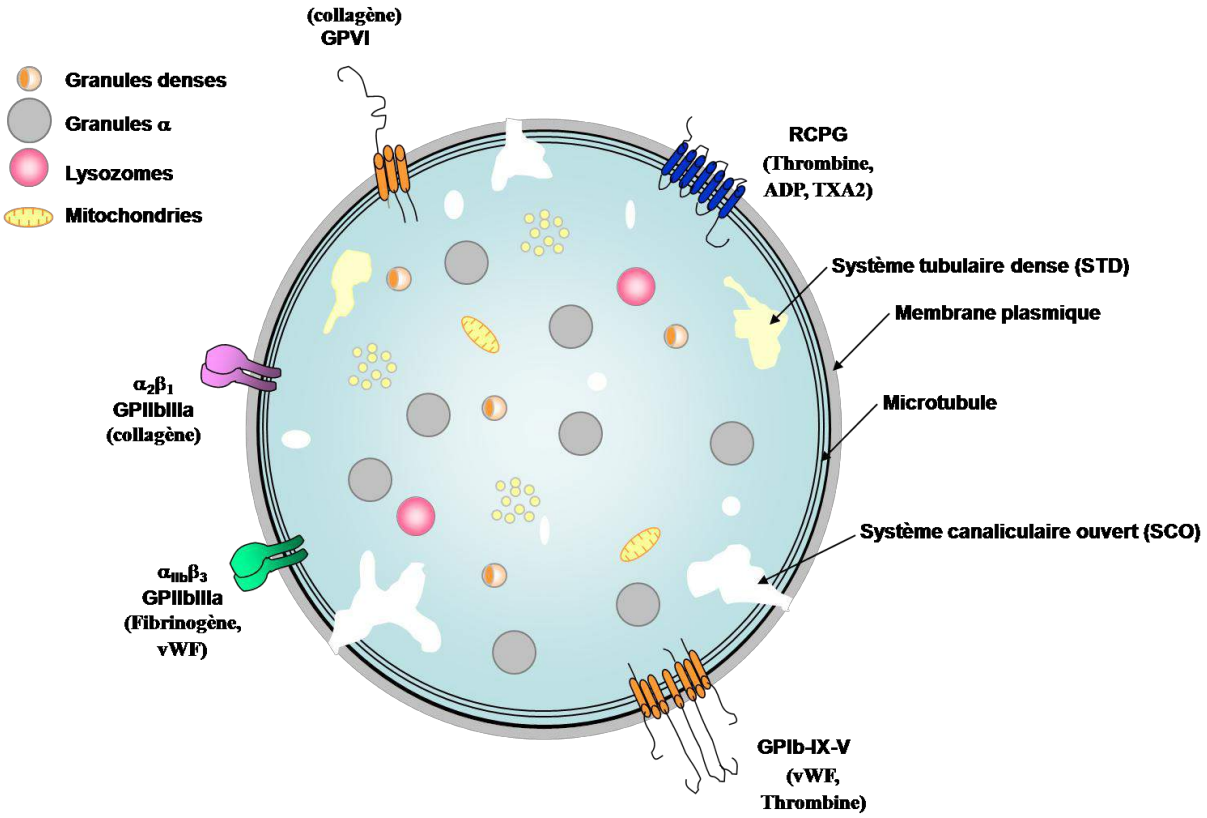

Figure 15: Représentation schématique de la structure de la plaquette et des principaux récepteurs membranaires: GP : glycoprotéine ; FcRγ : chaîne γ des récepteurs aux fragments constants des immunoglobulines ; RCPGs : récepteurs couplés aux protéines G hétérotrimériques ; vWF : facteur de von Willebrand ; ADP : adénosine 5'-disphosphate ; TXA_2 : thromboxane A_2 ; STD : sytème tubulaire dense ; SCO : système canaliculaire ouvert.

3) Le cytosquelette plaquettaire

Le cytosquelette plaquettaire (très riche) est composé d'un microtubule, d'un système de filaments d'actine, de complexes d'acto-myosine important pour la contraction plaquettaire et de filaments intermédiaires au rôle mal connu. Le cytosquelette plaquettaire permet le maintien de la forme discoïde des plaquettes au repos mais aussi leur changement de forme lors de l'activation où les plaquettes deviennent sphériques, émettent des filopodes et adhèrent au sous-endothélium.

a) Le microtubule

Le microtubule est généré à l'extrémité des PPT lors de la production plaquettaire. Ce microtubule est un polymère composé d'hétérodimères de tubuline α et β enroulé sur lui-même 7-8 fois en forme d'anneau appelé bande marginale. Il est localisé sous la membrane plasmique et permet le maintien de la forme discoïde des plaquettes au repos (Diagouraga et al., 2014; White and Rao, 1998). Lors de l'activation plaquettaire, la dynéine liée à l'actine

corticale va étendre cette bande marginale en faisant glisser l'anneau de microtubule le long de la membrane plasmique. Cet allongement de la bande marginale suivi de son enroulement associée à l'action de l'acto-myosine va permettre la contraction des plaquettes qui les rendra sphériques (Diagouraga et al., 2014; Sadoul, 2015) (figure 16).

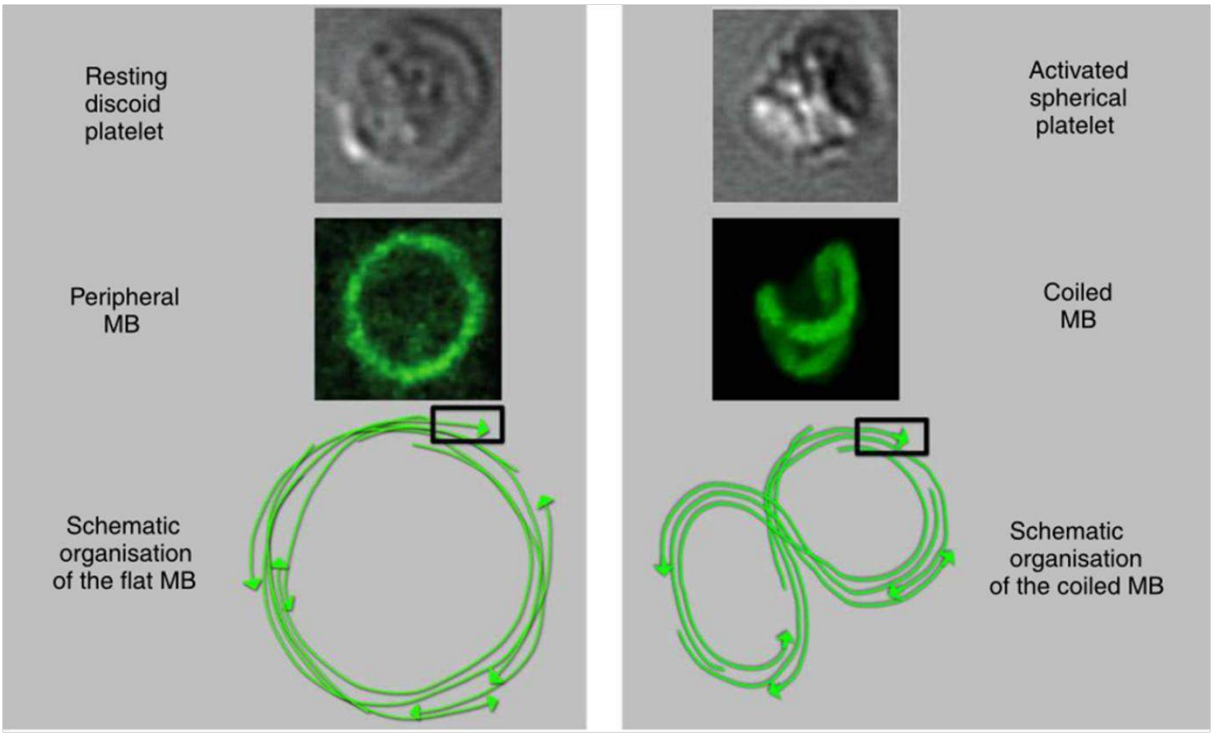

Figure 16: Représentation schématique de l'organisation du microtubule dans la plaquette au repos et activée: (**A**) Organisation du microtubule dans la plaquette au repos: microtubule enroulé sur lui-même forme la bande marginale qui maintient la forme discoïde de la plaquette (photo du haut: image par transmission ; photo du milieu: marquage de la tubuline ; schéma du bas: représentation de l'organisation du microtubule). (**B**) Organisation du microtubule dans la plaquette activée: le microtubule enroulé induit la forme sphérique de la plaquette (photo du haut: image par transmission ; photo du milieu: marquage de la tubuline ; schéma du bas: représentation de l'organisation du microtubule). *D'après (Sadoul, 2015)*.

b) Le cytosquelette d'actine

L'actine, protéine la plus abondante dans les plaquettes, représente 20% des protéines totales (Burkhart et al., 2012). Dans les plaquettes au repos, le rôle du cytosquelette d'actine est de servir de support structural. Pendant l'activation des plaquettes, ce dernier va permettre le rapide changement de forme des plaquettes inhérent à leur fonction.

Au repos, l'actine est, soit sous forme de monomères (G-actine), soit sous forme de filaments (F-actine). Ces monomères d'actine, forme majoritaire dans la plaquette, permettent l'assemblage et le désassemblage en filaments. Les filaments d'actine s'organisent en deux structures distinctes dans les plaquettes au repos:

- Le squelette sous-membranaire: est constitué de courts filaments parallèles reliés entre eux par la spectrine et recouvre la face interne de la membrane plasmique (Hartwig and DeSisto, 1991). Il est lié à la membrane plasmique par des ABPs (telles que filamine, taline, vinculine) et des GPs (tels que le complexe GPIb-IX-V, les intégrines $\alpha_{IIb}\beta_3$ et $\alpha_2\beta_1$). Le maintien de la forme discoïde des plaquettes est en partie du à l'interaction entre la filamine et la GPIbα du complexe GPIb-IX-V qui stabilise la membrane plasmique (Berrou et al., 2013; Jurak Begonja et al., 2011) (Figure 17).

- Le squelette cytoplasmique: est constitué de filaments d'actine plus ou moins longs formant un réseau à travers le cytoplasme et est associé à trois ABPs: la filamine, l'α-actinine et la tropomyosine.

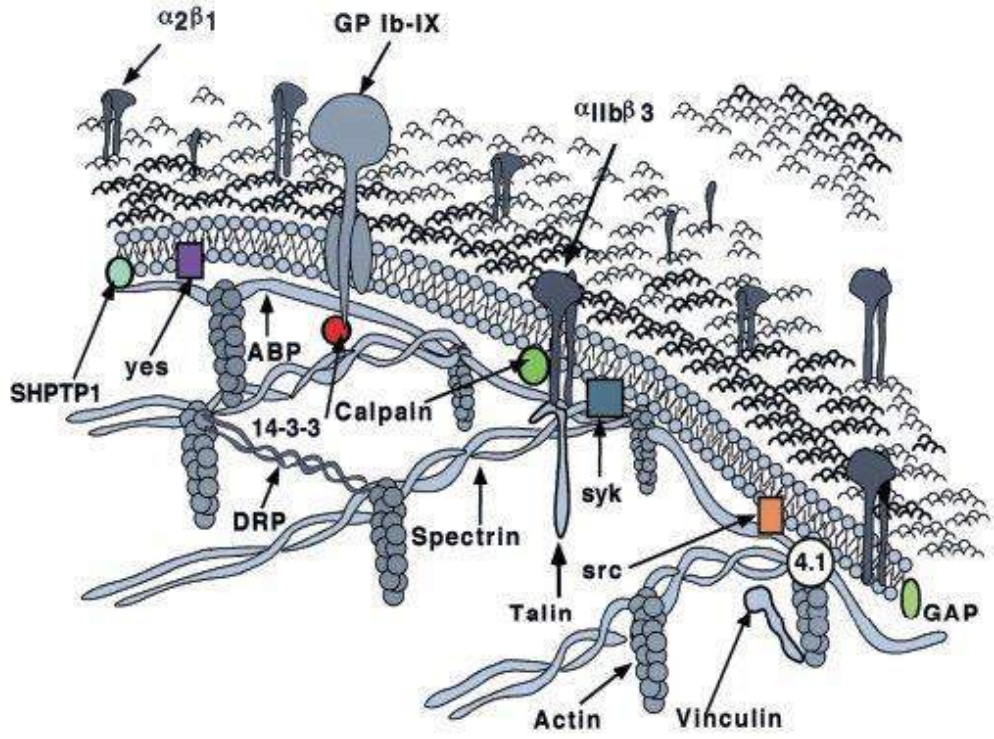

Figure 17: Représentation schématique du squelette sous-membranaire plaquettaire. *D'après (Fox, 2001).*

Lors de leur activation, les plaquettes vont changer de forme et devenir sphérique avant d'émettre des filopodes. Pour cela, le cytosquelette d'actine va se réorganiser de façon très dynamique. En effet, les filaments d'actine existant vont être fragmentés en néo-filaments grâce à l'activation de la gelsoline par augmentation des concentrations calciques intracellulaires (Barkalow et al., 1996; Fujita et al., 1997). Ensuite, les protéines de coiffage telles que la gelsoline et CapZ, par leur intéraction avec le PtdIns(4,5)P_2, vont libérer les

extrémités des néofilaments, permettant ainsi leur élongation avec des monomères d'actine non séquestrés par la thymosine β4 et la profiline (Barkalow et al., 1996; Goldschmidt-Clermont et al., 1992; Schafer et al., 1996). Le complexe actin related protein 2/3 (Arp2/3) va lui servir de site de nucléation des nouveaux filaments d'actine (Falet et al., 2002). Enfin, l'association des filaments d'actine à la myosine permettra la formation de filaments contractiles d'acto-myosine (ou « fibres de stress ») indispensables pour la contraction des plaquettes (Hartwig et al., 1999; Stossel et al., 2006) mise en jeu lors de l'agrégation forte et la rétraction du clou plaquettaire.

c) Filopodes, lamellipodes et zones d'adhésion focale

Lors de leur adhésion, les plaquettes changent de forme, s'arrondissent, émettent des filopodes, des lamellipodes, forment des zones d'adhésion focales et s'étalent fermement sur la matrice extracellulaire. L'activation de l'intégrine $\alpha_{IIb}\beta_3$ va favoriser l'association du squelette sous-membranaire avec les filaments d'actine cytoplasmiques et induire le regroupement des intégrines dans des structures spécifiques appelées complexes focaux. Ces complexes focaux, grâce aux intégrines, aux protéines du cytosquelette et aux protéines de la signalisation, vont permettre l'extension (i) de filopodes par polymérisation de nouveaux filaments d'actine, (ii) de lamellipodes par incorporation de filaments d'actine au squelette sous-membranaire (de Mali et al 2003 ; Johnson et al 2015) et (iii) de zones d'adhésion focales formées par liaison de filaments contractiles d'acto-myosine (« fibres de stress ») avec les intégrines.

Les GTPases de la famille Rho contribuent fortement à la dynamique du cytosquelette plaquettaire (figure 18) :

- Cdc42 contrôle la formation de protrusions riches en actine, les filopodes, *via* les voies de signalisation PAK, WASp et PI3K mais ses fonctions dans les plaquettes restent controversées (Goggs et al., 2015).

- Rac1 stimule la formation des lamellipodes *via* son interaction avec WASp. Le complexe Rac1/WASp active Arp2/3 qui entraine la nucléation et la polymérisation de l'actine en nouveaux filaments et ainsi la formation de lamellipodes (Goggs et al., 2015; Nobes and Hall, 1995; Price et al., 1998).

- RhoA induit la formation des fibres de stress. RhoA active la Rho-kinase du squelette sous-membranaire qui va alors inhiber, en la phosphorylant, la phosphatase de la chaîne légère de

myosine (MLC). Ceci entraîne l'augmentation de la phosphorylation de la MLC (qui est aussi phosphorylée directement par la MLC kinase). Une fois phosphorylée, la MLC s'associe avec l'actine et permet la formation de filaments contractiles d'acto-myosine ou fibres de stress. Ces fibres de stress génèrent les forces de tension nécessaires pour la contraction plaquettaire (Amano et al., 1997; Burridge and Chrzanowska-Wodnicka, 1996; Goggs et al., 2015).

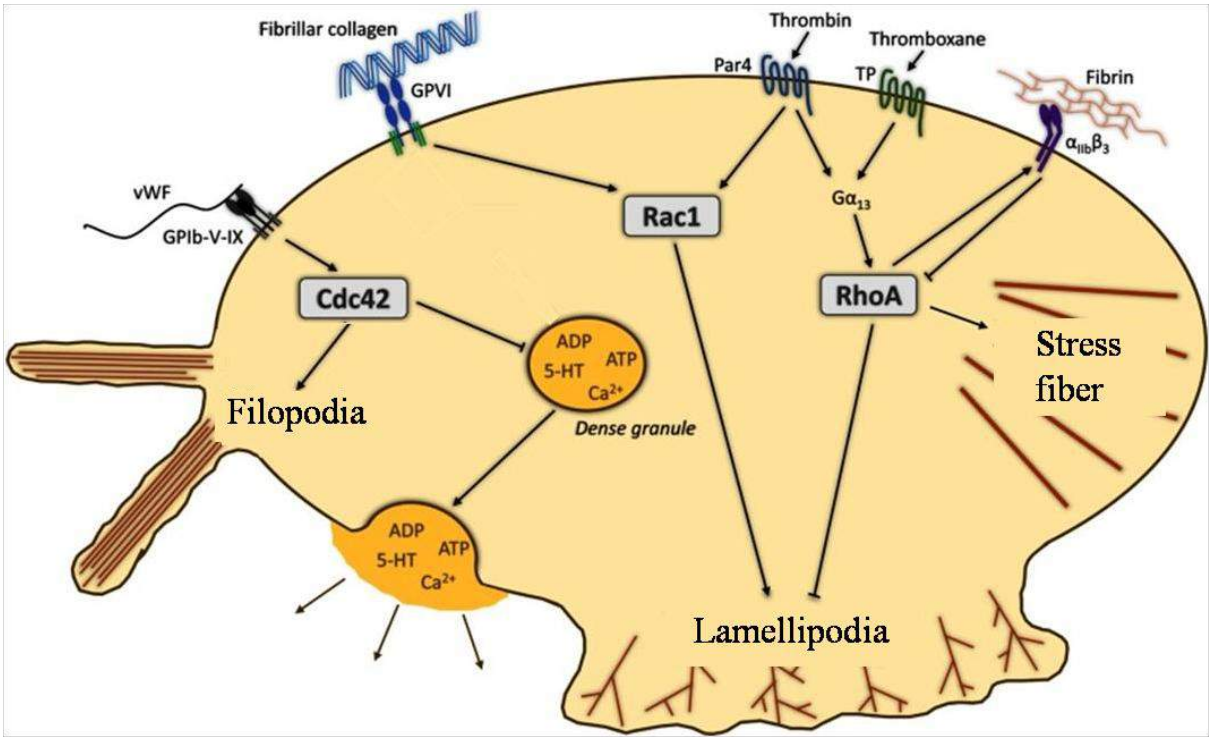

Figure 18: Représentation schématique des rôles connus de Cdc42, Rac1 et RhoA dans la formation des filopodes, lamellipodes et fibres de stress. Cdc42 contrôle la sécrétion des granules denses et est en partie responsable de la formation des filopodes plaquettaires. Rac est impliquée dans la formation de lamellipodes. RhoA est aussi impliquée dans la formation de fibres de stress, l'activation de l'intégrine $\alpha_{IIb}\beta_3$ et contrôlerait la formation de lamellipodes. *D'après (Goggs et al., 2015)*.

B) L'activation plaquettaire

La paroi vasculaire est recouverte de cellules endothéliales qui forment une surface non-thrombogène notamment grâce à la synthèse de molécules comme la prostaglandine I_2 (PGI_2) et le monoxyde d'azote (NO). Suite à une lésion vasculaire dévoilant le sous-endothélium, les plaquettes vont s'activer dans le but de former un thrombus plaquettaire afin d'obturer la brèche vasculaire et d'arrêter le saignement. Aussi, un dysfonctionnement des cellules endothéliales provoqué par la modification du débit sanguin ou l'apparition de molécules

bioactives dans la circulation sanguine peut être à l'origine d'une activation intempestive des plaquettes.

La formation du thrombus est un processus très dynamique qui se réalise en plusieurs étapes (Figure 19) :

- Recrutement et adhésion transitoire des plaquettes
- Adhésion ferme des plaquettes
- Amplification de l'activation plaquettaire
- Activation de l'intégrine $\alpha_{IIb}\beta_3$ et agrégation plaquettaire

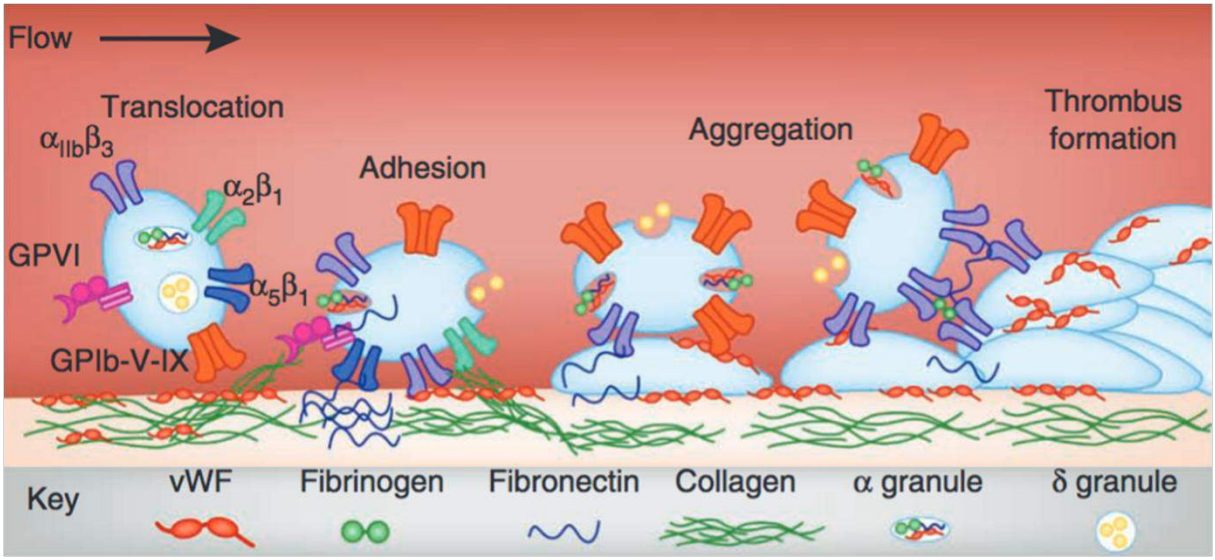

Figure 19: Schéma représentatif de l'activation plaquettaire suite à une lésion vasculaire. Les plaquettes se lient au vWF fixé au collagène grâce au complexe GPIb-IX-V, induisant l'adhésion transitoire des plaquettes (translocation) au niveau de la lésion vasculaire. La liaison du récepteur GPVI et de l'intégrine $\alpha_2\beta_1$ plaquettaires au collagène ainsi que l'engagement de l'intégrine $\alpha_5\beta_1$ avec la fibronectine permettent ensuite une adhésion plaquettaire stable. L'adhésion ferme des plaquettes permet l'activation de l'intégrine $\alpha_{IIb}\beta_3$ induisant sa liaison de haute affinité avec des protéines adhésives: le vWF, le fibrinogène et la fibronectine. Ces interactions adhésives sont indispensables à la formation d'agrégats plaquettaires stables et à la croissance du thrombus. *D'après (Jackson, 2011)*.

1) Recrutement et adhésion transitoire des plaquettes

Lorsque le sous-endothélium est mis à nu consécutivement à une lésion vasculaire, le collagène, la fibrine, les laminines et la fibronectine exposés vont lier rapidement le vWF circulant. Le vWF est une protéine plasmatique synthétisée par les MK et les cellules endothéliales et libérée dans le sang majoritairement (80%) des corps de Weibel-Palade des cellules endothéliales et de façon minoritaire (20%) des granules α plaquettaires (Schmugge

et al., 2003; Sporn et al., 1989). Une fois immobilisé, le vWF change de conformation et devient capable de se lier à son récepteur plaquettaire: le complexe GPIb-IX-V.

Le complexe GPIb-IX-V est un récepteur d'adhésion unique, exclusivement exprimé à la surface des MKs et des plaquettes, composé de deux GPIbα, deux GPIbβ, deux GPIX et un GPV associé selon la stœchiométrie 2:2:2:1. Il est exprimé de façon constitutive à la surface des plaquettes à hauteur de 25 000 copies par plaquette. La liaison du vWF à la sous-unité GPIbα du complexe GPIb-IX-V permet les premiers contacts entre les plaquettes et la paroi vasculaire lésée et va permettre le ralentissement des plaquettes ou adhésion transitoire des plaquettes (phénomène de « rolling »). Il est considéré comme un mécano-récepteur permettant la première liaison des plaquettes à la paroi vasculaire lésée. Malgré une activation faible et transitoire, il met en jeu des cascades de signalisation permettant la sécrétion des granules, la production de thromboxane A_2 (TXA_2), la mobilisation calcique, l'activation de l'intégrine $\alpha_{IIb}\beta_3$ et la réorganisation du cytosquelette plaquettaire pour le changement de forme et la formation de filopodes et lamellipodes (Bryckaert et al., 2015) (Figure 20).

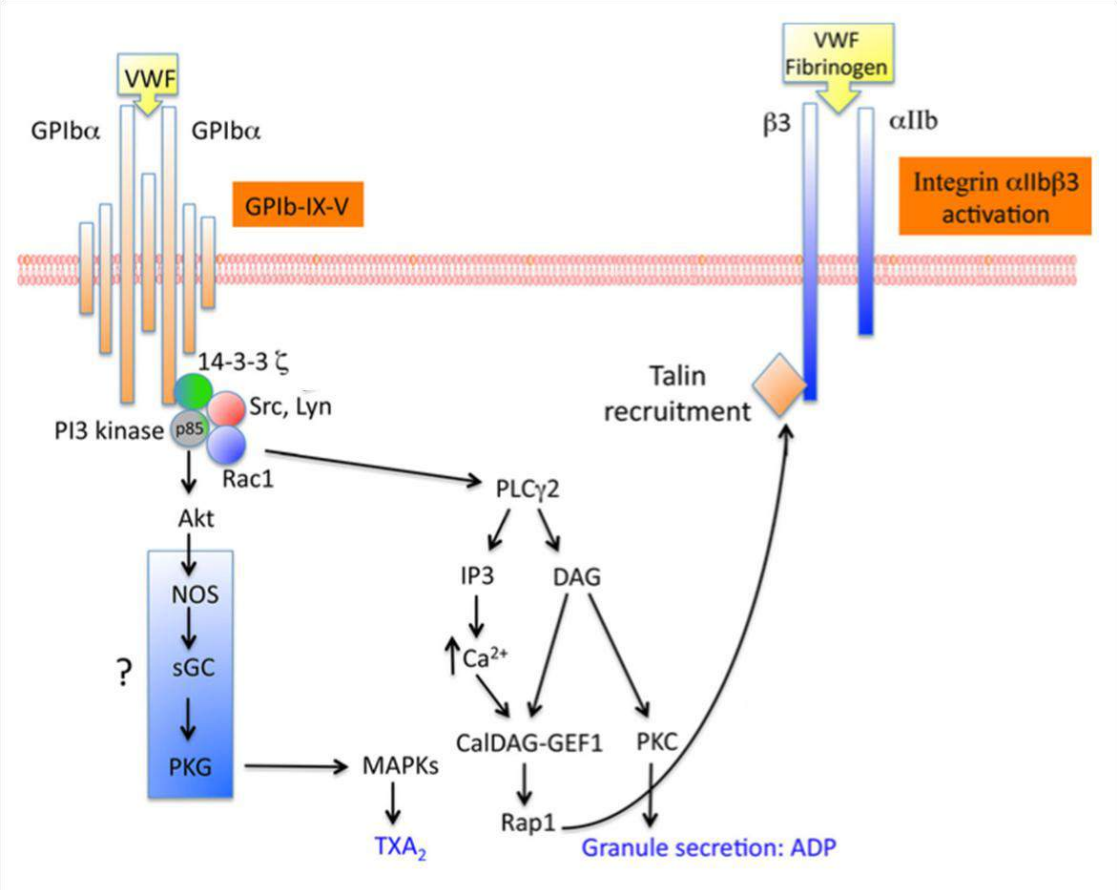

Figure 20: Représentation schématique de l'activation du complexe GPIb-IX-V par le vWF. La liaison du vWF au complexe GPIb-V-IX déclenche plusieurs voies de signalisation, la voie PI3K/Akt et la voie de la PLCγ2, permettant l'adhésion stable des plaquettes *via* notamment l'activation de l'intégrine $\alpha_{IIb}\beta_3$ mais aussi la production de TXA2 et la sécrétion d'ADP. La voie de la PLCγ2 induit l'activation de la petite protéine G, Rap1, ce qui permet le recrutement de la taline à l'intégrine β_3. Ce recrutement est essentiel à l'activation de l'intégrine $\alpha_{IIb}\beta_3$. Alors que l'implication de la PLCγ2 est bien décrite, la voie de signalisation impliquant le NO et l'activation de la PKG en aval de la voie PI3K/Akt est controversée. *D'après (Bryckaert et al., 2015)*.

La maladie de vWF est la plus fréquente des pathologies hémorragiques constitutionelles. Elle est due soit à une quantité insuffisante de vWF soit à une altération de sa fonctionnalité. Il en existe 3 catégories : la maladie de vWF de type 1, la plus fréquente, et de type 3, plus rare, sont dues à des déficiences quantitatives. La maladie de vWF de type 2 est causée par un défaut qualitatif du vWF provenant d'altérations de sa structure (Nurden, 2007). D'autre part, le syndrome de Bernard-Soulier se caractérise par une macrothrombopénie et des troubles hémorragiques provenant de mutations des différentes sous-unités du récepteur GPIb-IX-V, ce qui affecte son expression dans les plaquettes (Kunishima et al., 2002).

2) Adhésion ferme des plaquettes

Le collagène est un élément thrombogène du sous-endothélium permettant l'adhésion et l'activation des plaquettes sur le site de la lésion vasculaire. Suite au ralentissement des plaquettes par l'interaction vWF-GPIb-IX-V, les plaquettes vont pouvoir se fixer au collagène par l'intermédiaire du récepteur GPVI et de l'intégrine $\alpha_2\beta_1$ (Nieswandt and Watson, 2003).

GPVI est un récepteur transmembranaire exprimé exclusivement à la surface des MKs et des plaquettes (Berlanga et al., 2000). Il est exprimé à la surface des plaquettes à hauteur de 1000 à 5000 copies par plaquette sous forme d'un complexe constitutif et non-covalent avec la chaine γ des récepteurs aux fragments constants des immunoglobulines (FcRγ). Par ses deux domaines IgG extracellulaires, il est capable de lier le collagène fibrillaire de type I et III (Moroi and Jung, 2004).

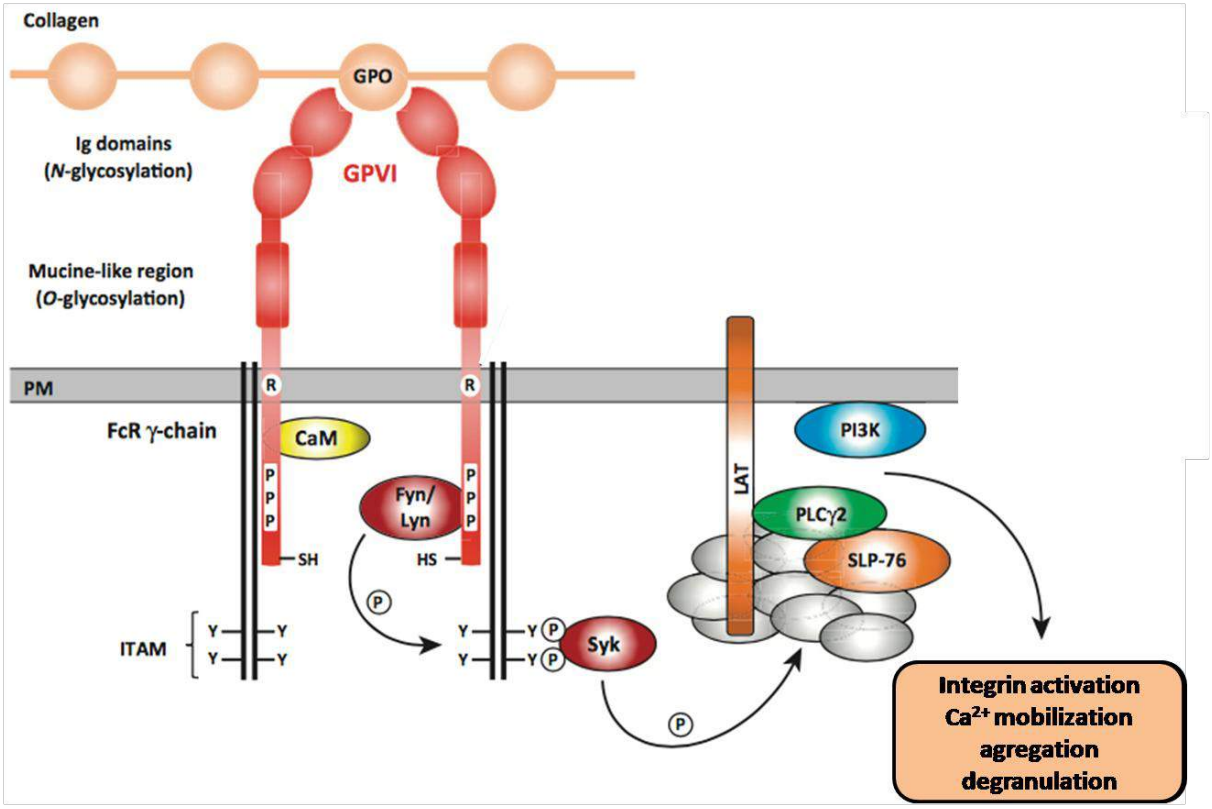

Figure 21: Représentation schématique des voies de signalisation après activation de GPVI par le collagène. GPVI est composée de deux domaines immunoglobuline extracellulaires avec un site *N*-glycosylation lié à une région riche en mucine qui présente des sites d'*O*-glycosylation. Le domaine transmembranaire contient un résidu arginine (R) requis pour l'association avec la chaîne FcRγ. La queue cytosolique de GPVI contient un site de liaison à la calmoduline et une région riche en proline qui recrute constitutivement les kinases de la famille de Src, Lyn et Fyn, à la membrane plasmique. La chaine FcRγ est un homodimère qui a deux tyrosines dans une séquence conservée : un immunoreceptor tyrosine-based activation motif (ITAM). La liaison de GPVI aux motifs répétés glycine-proline-hydroxyproline du collagène permet la phosphorylation de la chaîne FcRγ-ITAMs par Fyn/Lyn. Ceci induit une cascade de signalisation dépendante de Syk amenant à la formation de signalosome qui comprend plusieurs protéines adaptatrices telle que *linker of activated T cells* (LAT) et signalisantes telles que la PI3K qui *in fine* résulte en l'activation de la PLCγ2 et déclenche l'activation de l'intégrine $\alpha_{IIb}\beta_3$, la mobilisation calcique, l'agrégation et la dégranulation. *D'après (Dutting et al., 2012)*.

Suite à sa liaison au collagène, le regroupement des complexes GPVI-FcRγ va permettre la mise en place des voies de signalisation intra-plaquettaires (figure 21). Ces voies de signalisation entrainent la synthèse de TXA_2, la mobilisation calcique intracellulaire, l'activation de l'intégrine $\alpha_{IIb}\beta_3$ et la sécrétion des granules plaquettaires (Watson et al., 2005).

$\alpha_2\beta_1$, premier récepteur au collagène identifié, est un hétérodimère constitué d'une sous-unité α_2 et d'une sous-unité β_1 (Saelman et al., 1994). Elle est présente à la surface des

plaquettes à une densité d'environ 900 à 3500 par plaquette. Il a été montré que l'affinité d'$\alpha_2\beta_1$ pour le collagène était augmentée par des agonistes plaquettaires comme l'ADP, le TXA_2 et la stimulation spécifique de GPVI (Jung and Moroi, 2000, 2001). La signalisation découlant de la liaison du collagène à $\alpha_2\beta_1$ induit une mobilisation calcique intracellulaire, l'activation de l'intégrine $\alpha_{IIb}\beta_3$ et la formation de filopodes et lamellipodes indispensables à l'étalement des plaquettes (Inoue et al., 2003).

Ainsi, la mise en place des voies de signalisation en aval des récepteurs d'adhésion (le complexe GPIb-IX-V, GPVI et $\alpha_2\beta_1$) permet à la fois l'amplification de l'activation plaquettaire *via* la synthèse du TXA_2 et la sécrétion des granules mais aussi l'activation de l'intégrine $\alpha_{IIb}\beta_3$ qui permet, avec $\alpha_2\beta_1$, l'adhésion ferme et l'arrêt des plaquettes sur le sous-endothélium ainsi que la formation des contacts stables entre plaquettes.

3) Amplification de l'activation plaquettaire

L'amplification de l'activation plaquettaire se traduit par le recrutement de plaquettes circulantes au niveau de celles déjà fermement adhérées au sous-endothélium exposé ou au niveau du thrombus permettant la croissance et la stabilisation de ce dernier. Ce processus nécessite, entre autres, les agonistes solubles plaquettaires: l'ADP, le TXA_2 et la thrombine.

L'ADP est stockée dans les granules denses des plaquettes au repos. Comme mentionné ci-dessus, lors de l'activation plaquettaire, les granules sont sécrétés. L'ADP ainsi libéré, va pouvoir activer deux récepteurs purinergiques : P2Y1 et P2Y12. Ces récepteurs, exprimés dans la membrane plasmique des plaquettes (presque exclusivement pour le P2Y12), sont des récepteurs à sept domaines transmembranaires. P2Y1, couplé à la protéine $G\alpha_q$, va induire le changement de forme des plaquettes et initier l'agrégation. P2Y12, couplé à la protéine $G\alpha_i$, va amplifier l'agrégation initiée par P2Y1 ainsi que l'agrégation et la sécrétion induites par d'autres agonistes tels que la thrombine, le TXA_2 ou le collagène (Gachet, 2008, 2012; Offermanns, 2006). La coactivation des deux récepteurs est indispensable pour une agrégation induite par l'ADP. Les patients ayant une anomalie de P2Y12 souffrent d'hémorragies (Cattaneo, 2011). Les inhibiteurs de P2Y12 (Clopidogrel, Prasugrel, Ticagrelor) sont largement utilisés en clinique pour prévenir et traiter la thrombose artérielle. Cependant ces traitements augmentent le risque de saignement (Yousuf and Bhatt, 2011) (Figure 22).

Le TXA_2 est un prostanoïde produit par la cyclooxygénase-1 (COX-1) à partir de l'acide arachidonique. Il est synthétisé pendant l'activation plaquettaire, après activation de la

phospholipase A_2 (PLA_2), avant d'être libéré par diffusion à travers la membrane plasmique. Son action reste très localisée car il est rapidement hydrolysé en thromboxane B2 qui est un métabolite inactif. Néanmoins, le TXA_2 stimule ses deux récepteurs couplés aux protéines $G\alpha_q$ et $G_{12/13}$: TPα et TPβ et induit le changement de forme des plaquettes et l'agrégation (Offermanns, 2006). Les rares patients atteints d'une mutation du gène codant pour le récepteur du TXA_2 souffrent de saignements modérés (Okuma et al., 1996) (Figure 22).

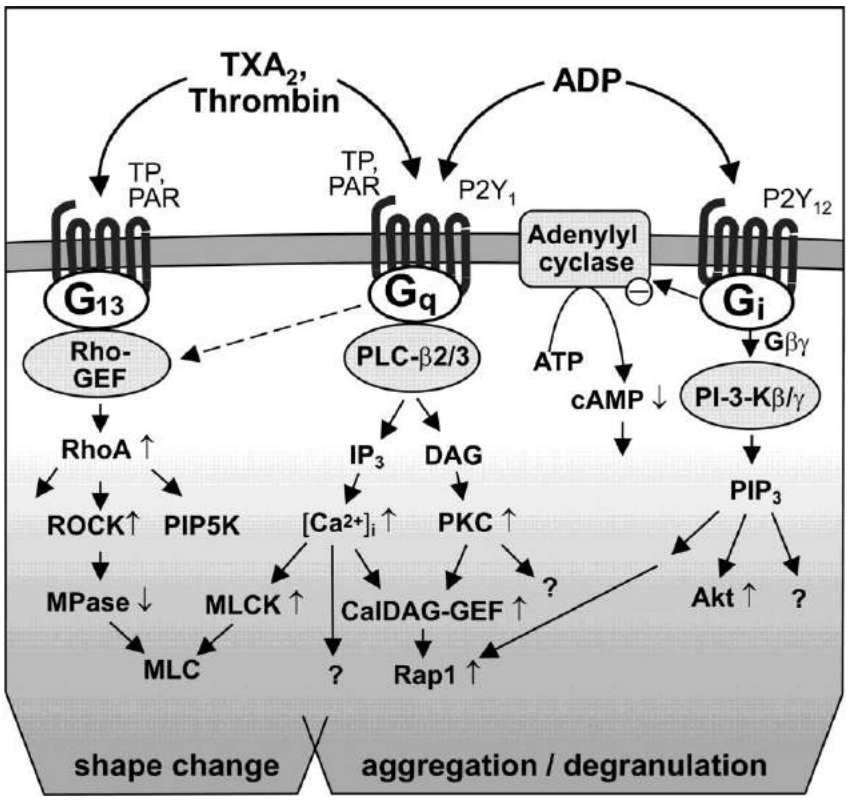

Figure 22: Représentation schématique des voies de signalisation activées par les protéines G hétérotrimériques dans les plaquettes. Sont représentées les voies de signalisation en aval des récepteurs couplés aux protéines G de l'ADP, du TXA_2 et de la thrombine. L'activation des protéines G_{13}, G_q et G_i induit le changement de forme plaquettaire, la signalisation « inside-out » d'activation des intégrines et la dégranulation. *D'après (Offermanns, 2006)*.

Issue de la cascade de la coagulation, la thrombine est l'activateur le plus puissant des plaquettes. C'est une sérine protéase capable d'induire le changement de forme, la sécrétion et l'agrégation des plaquettes. Elle active les plaquettes en agissant sur ses récepteurs couplés à des protéines $G\alpha_q$ et $G_{12/13}$: PAR1 et PAR4 chez l'humain et PAR3 et PAR4 chez la souris (Kahn et al., 1999; Kahn et al., 1998; Offermanns, 2006). En parallèle, la thrombine est un élément clef de la cascade de la coagulation. Grâce à son activité enzymatique, elle va cliver le fibrinogène induisant sa polymérisation en fibrine et permettre la consolidation du thrombus (Crawley et al., 2007) (Figure 22).

4) Activation de l'intégrine $\alpha_{IIb}\beta_3$ et agrégation plaquettaire

Toutes les voies de signalisation décrites ci-dessus amènent à l'activation de l'intégrine $\alpha_{IIb}\beta_3$. Une fois activée, elle permet la formation de contacts stables entre les plaquettes favorisant ainsi la croissance et la stabilisation du thrombus ainsi que la rétraction du clou plaquettaire.

L'intégrine $\alpha_{IIb}\beta_3$ n'est exprimée que dans les plaquettes et les MKs. A la surface des plaquettes au repos elle est retrouvée à hauteur de 80 000 copies par plaquette et son expression augmente sous activation par translocation à partir des membranes du SCO et des granules de sécrétion. C'est un hétérodimère constitué d'une sous-unité α_{IIb} et d'une sous-unité β_3 associées de façon non-covalente. Dans les plaquettes au repos, l'intégrine $\alpha_{IIb}\beta_3$ est dans une conformation ne lui permettant de se lier ni au fibrinogène ni à ces autres ligands solubles avec une bonne affinité. Lors de l'activation plaquettaire, se mettent en place des voies d'amplification de signalisations intra-plaquettaires en aval des récepteurs couplés à des protéines G (récepteurs de l'ADP, du TXA et de la thrombine) ou des récepteurs d'adhésion (GPIb, GPVI et $\alpha_2\beta_1$). Ces voies de signalisation aboutissent à l'activation de l'intégrine $\alpha_{IIb}\beta_3$ grâce à sa liaison à la taline ou la kindline (Calderwood et al., 2013; Nieswandt et al., 2009; Tadokoro et al., 2003). Cette voie d'activation de l'intégrine $\alpha_{IIb}\beta_3$ constitue la signalisation « inside-out ». La finalité de cette signalisation « inside-out » est le changement de conformation de l'intégrine $\alpha_{IIb}\beta_3$ lui conférant ainsi une haute affinité pour le fibrinogène et le vWF (Coller, 2015). L'intégrine $\alpha_{IIb}\beta_3$ activée joue un rôle primordial dans l'agrégation et la formation du thrombus : (i) en connectant 2 plaquettes adjacentes grâce au fibrinogène en condition de faibles forces de cisaillement et au vWF circulants en condition de hautes forces de cisaillement, qui forment des « ponts » entre les plaquettes (ii) en liant la fibronectine ou la vitronectine de la matrice du sous-endothélium permettant ainsi l'adhésion ferme et l'étalement des plaquettes. La liaison de l'intégrine $\alpha_{IIb}\beta_3$ avec le fibrinogène, le vWF ou la fibronectine va induire la signalisation « outside-in ». Cette signalisation va entrainer le remodelage du cytosquelette d'actine et la formation de filaments d'acto-myosine générant des forces de tension et des zones d'adhésion focales nécessaires à l'étalement et la rétraction du clou plaquettaire (Gruner et al., 2003; Nieswandt et al., 2011) (Figure 23).

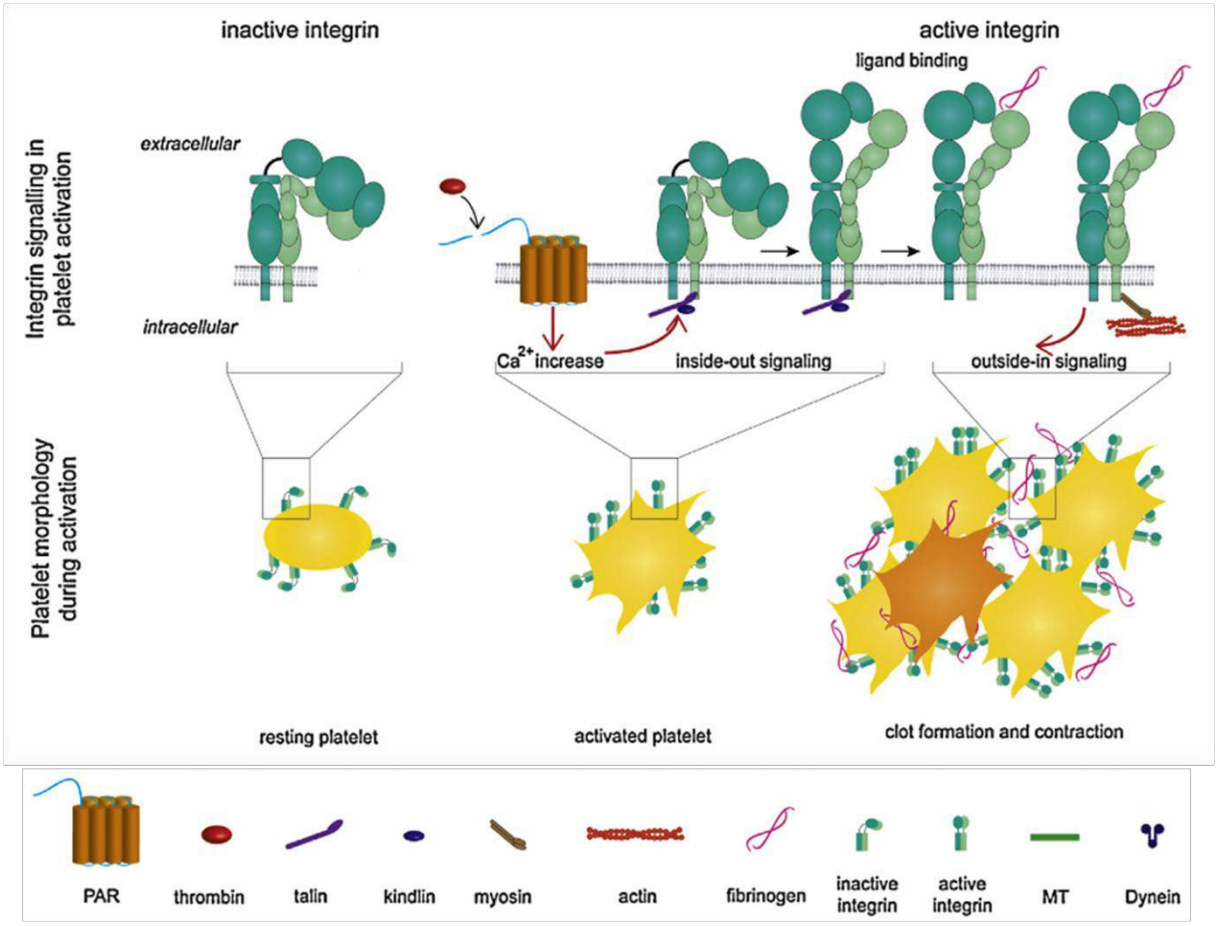

Figure 23: Représentation schématique de l'activation de l'intégrine $\alpha_{IIb}\beta_3$. Dans les plaquettes au repos, l'intégrine $\alpha_{IIb}\beta_3$ est dans une conformation inactive. La signalisation « inside-out » induite par la liaison d'un agoniste plaquettaire à son récepteur permet l'activation de l'intégrine $\alpha_{IIb}\beta_3$. Est représenté ici un exemple de l'activation du récepteur PAR *via* la thrombine qui déclenche une augmentation de Ca^{2+} cytosolique. Cette libération de Ca^{2+} cytosolique permet la liaison de la taline à la queue cytoplasmique de la chaine β_3. Ceci induit le changement conformationnel de l'intégrine $\alpha_{IIb}\beta_3$ dans un état activé. Ainsi la liaison de l'intégrine $\alpha_{IIb}\beta_3$ activée à son ligand soluble, le fibrinogène, induit la signalisation « outside-in » et permet la formation du clou plaquettaire. *D'après (Sorrentino et al., 2015).*

La thrombasthénie de Glanzmann est une maladie autosomique récessive rare due à une mutation sur les gènes codant pour l'intégrine $\alpha_{IIb}\beta_3$ et induisant un déficit qualitatif ou quantitatif de cette dernière. Les symptômes sont variables allant de quelques ecchymoses à des hémorragies fréquentes pouvant être fatales (Nurden et al., 2013).

C) Un rôle de l'autophagie dans la production et la fonction plaquettaire

L'autophagie est un processus biologique indispensable aux fonctions cellulaires, dont le but est la dégradation d'une partie des constituants du cytoplasme (protéines et organelles) en acides aminés, lipides ou sucres. Un des rôles de l'autophagie est de protéger la cellule, dans

un contexte de stress, en dégradant des agrégats protéiques ou des organelles et en les recyclant à des fins énergétiques. L'autophagie intervient donc dans l'homéostasie, la survie et le développement cellulaire ainsi que dans certaines pathologies telles que le cancer, le diabète et les maladies neurodégénératives (Lamb et al., 2013; White et al., 2015). Pendant l'autophagie, les constituants cytoplasmiques vont être séquestrés dans une vésicule à double membrane, l'autophagosome. Cet autophagosome fusionne ensuite avec un lysosome où a lieu la dégradation de ces constituants (Kobayashi, 2015) (Figure 24).

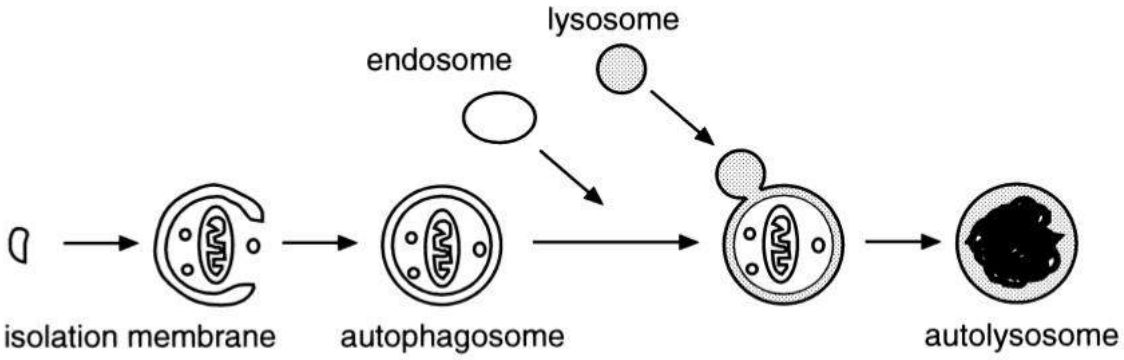

Figure 24: Schéma représentatif de l'autophagie dans une cellule de mammifère: Une partie du cytoplasme est englobée par la membrane d'isolation avant de former un autophagosome. La membrane externe de l'autophagosome fusionne avec un lysosome dans le but de dégrader le contenu de l'autophagosome. Cette voie peut aussi dégrader des organelles tel qu'une mitochondrie. *D'après (Mizushima et al., 2002)*.

L'autophagie est un procédé dynamique comportant plusieurs étapes contrôlées principalement par les 37 protéines « autophagy related-genes » (Atg). Le développement de souris déficientes pour ces protéines a permis de révéler leurs rôles (Mizushima et al., 2011) et récemment de mettre en avant l'implication de l'autophagie dans la mégacaryopoïèse et la thrombose.

En 2014, Feng *et al* ont mis en évidence que les plaquettes au repos expriment les protéines de l'autophagie Atg5, Atg7, LC3 et Beclin1 et que l'autophagie pouvait y être induite. Les souris hétérozygotes déficientes pour la Beclin1, une protéine majeure de l'autophagie, présentent un défaut d'agrégation *in vitro* en réponse à des agonistes plaquettaires et ont un temps de saignement à la queue allongé (Feng et al., 2014), montrant un rôle de l'autophagie dans l'activation plaquettaire. L'utilisation du 3-methyladenine (3MA) comme inhibiteur de la PI 3-kinase de classe III (Vps34), bien que remis en cause par

différents experts du domaine, laisse suggérer que l'autophagie dans les plaquettes est dépendante de Vps34.

En 2015, Ouseph et collègues ont montré une augmentation de l'autophagie lors de l'activation plaquettaire. Les souris déficientes pour Atg7 spécifiquement dans les mégacaryocytes et les plaquettes ($Atg7^{f/f}$; PF4-Cre/+) ont un temps de saignement après section de l'extrémité de la queue et un temps d'occlusion après lésion au chlorure ferrique ($FeCl_3$) *in vivo* significativement augmentés (Ouseph et al., 2015). Cao *et al* ont montré que les souris déficientes pour Atg7 spécifiquement dans le système hématopoïétique ($Atg7^{f/f}$;Vav-Cre) ont aussi un temps de saignement après section de l'extrémité de la queue significativement augmenté. Les plaquettes de ces souris ont une agrégation diminuée *in vitro* en réponse à la thrombine. Contrairement à ce qu'a pu montrer Ouseph *et al* avec le modèle $Atg7^{f/f}$; PF4-Cre/+, les souris ($Atg7^{f/f}$;Vav-Cre) de l'étude de Cao *et al* présentent une diminution significative du compte plaquettaire et un volume plaquettaire augmenté associés à une diminution du nombre de MKs matures dans la moelle osseuse ainsi qu'une capacité réduite de différenciation des progéniteurs hématopoïétiques en MKs matures (Cao et al., 2015).

Ces données montrent le rôle important de l'autophagie dans les mécanismes de thrombose et d'hémostase. L'autophagie semble requise pour la mégacaryopoïèse et la production de plaquettes ainsi que pour leur bon fonctionnement. Cependant, la façon dont l'autophagie régule ces processus reste encore méconnue.

Chapitre III : Les phosphoinositide 3-kinases

A) Le métabolisme des phosphoinositides

Les phosphoinositides (PI) sont des glycérophospholipides anioniques membranaires composés d'un squelette sn-1,2-diacylglycérol couplé au groupement hydroxyl D1 d'un myo-inositol par une liaison phosphodiester. Les deux acides gras qui les constituent sont majoritairement l'acide stéarique (C18:0) en position 1 et l'acide arachidonique (C20 :4) en position 2 du squelette glycérol (Mauco et al., 1984; Viaud et al., 2016) (cf. Annexe 1) (Figure 25).

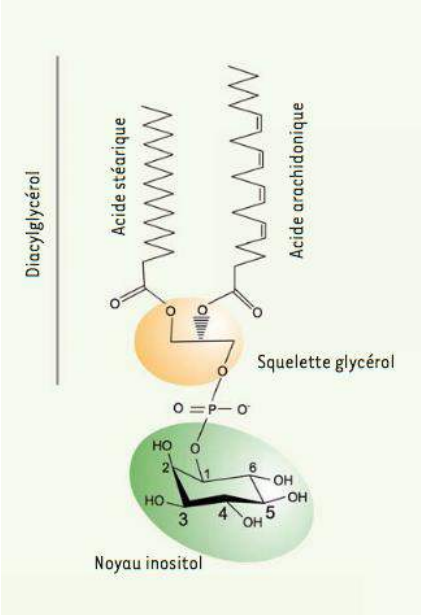

Figure 25: Structure du phosphatidylinositol: Le phosphatidylinositol, précurseur des autres PI, est composé d'un squelette sn-1,2-diacyllglycérol couplé à un myo-inositol par une liaison phosphodiester et de deux acides gras : l'acide stéarique et l'acide arachidonique en majorité. *D'après (Viaud et al., 2016)*.

Le noyau inositol du phosphatidylinositol (PtdIns) est phosphorylable en position 3, 4 et 5 par des lipide kinases spécifiques permettant ainsi la génération de 7 PI différents :

- Les phosphatidylinositol-monophosphates : phosphatidylinositol 3-monophosphate (PtdIns3P), phosphatidylinositol 4-monophosphate (PtdIns4P) et le phosphatidylinositol 5-monophosphate (PtdIns5P)

- Les phosphatidylinositol-bisphosphates : phosphatidylinositol 3,4-bisphosphate (PtdIns(3,4)P_2), le phosphatidylinositol 3,5-bisphosphate (PtdIns(3,5)P_2) et le phosphatidylinositol 4,5-bisphosphate (PtdIns(4,5)P_2)
- Le phosphatidylinositol 3,4,5-trisphosphate (PtdIns(3,4,5)P_3)

Dans la cellule, le PtdIns est l'inositol lipide le plus abondant (80% des PI totaux et 5 à 8% des phospholipides totaux) devant le PtdIns4P et le PtdIns(4,5)P_2 qui n'atteignent que 1 à 3% des phospholipides totaux. Les autres PI comptent pour 2% des phospholipides totaux.

Les premières bases du « cycle des phosphoinositides » proviennent de la découverte par Hokin en 1964 montrant que les phosphoinositides pouvaient être hydrolysés (Hokin and Hokin, 1964). A partir de là, l'implication des PI dans la signalisation cellulaire a pu être mise en évidence, permettant de découvrir la voie « canonique » conduisant à la production des seconds messagers, inositol 1,4,5-trisphosphate ($InsP_3$) et diacylglycerol (DAG) (Berridge, 1984; Michell, 1975). Enfin, la découverte des D3-phosphoinositides (D3-PI) et des PI 3-kinases (PI3K), a ouvert un domaine très important de la signalisation cellulaire avec des retombées récentes dans le traitement de certaines pathologies (Balla, 2013; Viaud et al., 2016).

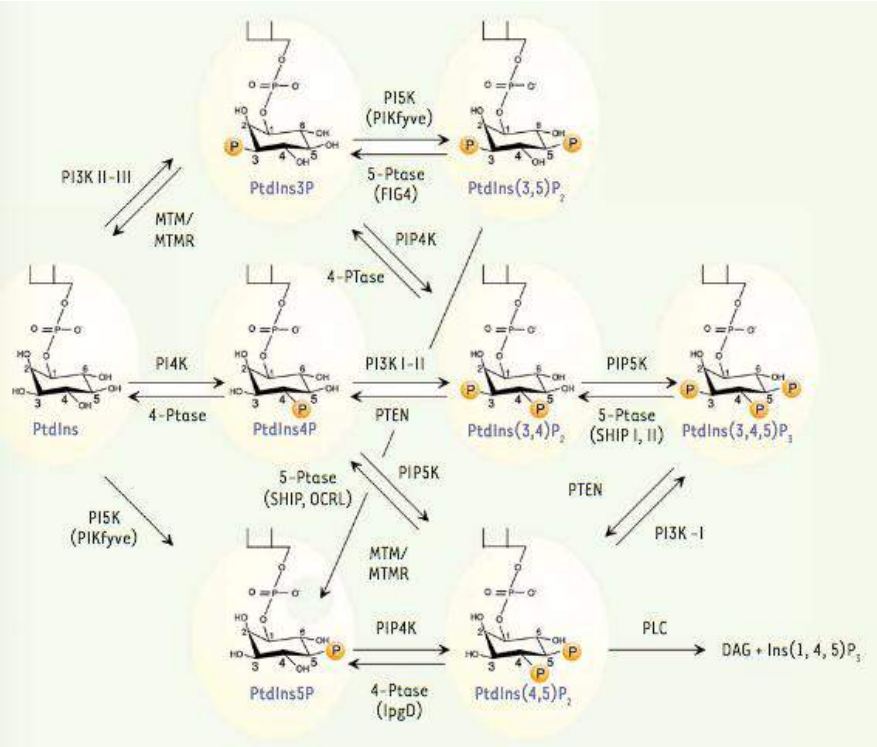

Figure 26: Métabolisme des phosphoinositides: Le PtdIns et les sept PI produits par les kinases et les phosphatases sont représentés schématiquement. La production d'$InsP_3$ et de DAG à partir de PtdIns(4,5)P_2 par la PLC est également indiquée. L'action des trois classes de PI3K, des 3-

phosphatases (PTEN et les myotubularines) et de la 4-phosphatase bactérienne IpgD est également présentée. *D'après (Viaud et al., 2016)*.

Le métabolisme des PI est très actif et met en jeu différentes PI-kinases et phosphatases spécifiques (Figure 26). Ce métabolisme peut être présenté sous la forme de 3 voies (Balla, 2013):

- La voie « canonique »: à partir du PtdIns, l'action d'une PtdIns 4-kinase (PI4K) puis d'une 5-kinase (PI5K) conduit à la production du PtdIns(4,5)P_2, le substrat de la phospholipase C (PLC) qui va l'hydrolyser en InsP_3 et DAG. Ces deux seconds messagers sont des intervenants essentiels de la mobilisation du calcium et de l'activation des PKC.
- Les voies de génération du PtdIns5P: (i) soit directement par phosphorylation du PtdIns par la 5-kinase (PIKfyve), (ii) soit par l'action concertée de PIKfyve et des 3-phosphatases de la famille des myotubularines (MTM) sur la voie PtdIns3P/PtdIns(3,5)P_2/PtdIns5P, (iii) soit enfin par la déphosphorylation du PtdIns(4,5)P_2 par une 4-phosphatase. Le PtdIns5P intervient dans différents processus intracellulaires tels que le remodelage du cytosquelette, le trafic intracellulaire ou encore l'expression des gènes.
- La voie des D3-PI: le PtdIns, le PtdIns4P et le PtdIns(4,5)P_2 peuvent être phosphorylés en position 3 du noyau inositol par une activité PI3K spécifique pour produire le PtdIns3P, le PtdIns(3,4)P_2 et le PtdIns(3,4,5)P_3. Leur synthèse par les PI3Ks est contrebalancée par différentes 3-phosphatases (MTM et phosphatase and tensin homologue deleted on chromosome 10 (PTEN)). Le PtdIns(3,4,5)P_3 est également hydrolysé par les 5-phosphatases SH2-containing inostol-5'-phosphate 1 et 2 (SHIP1 et SHIP2). Les D3-PI sont considérés comme des seconds messagers importants qui contrôlent de nombreux processus cellulaires notamment lors de l'activation plaquettaire (Jackson et al., 2004; Payrastre et al., 2001; Toker and Cantley, 1997).

B) Les D3-phosphoinositides (D3-PI)

Les D3-PI sont capables d'interagir directement avec des domaines protéiques fonctionnels tels que les domaines pleckstrin homology (PH), Fab-1-YGL023-Vps27-EEA1 (FYVE) et phox (PX). La localisation spécifique de chacun de ces D3-PI et la nature réversible de leur phosphorylation les positionnent en tant qu'éléments clés des processus liés aux membranes intracellulaires allant de l'activation de voies de signalisation en aval de

récepteurs spécifiques à la régulation du trafic vésiculaire (Balla, 2013; Raiborg et al., 2013; Viaud et al., 2016) (Figure 27).

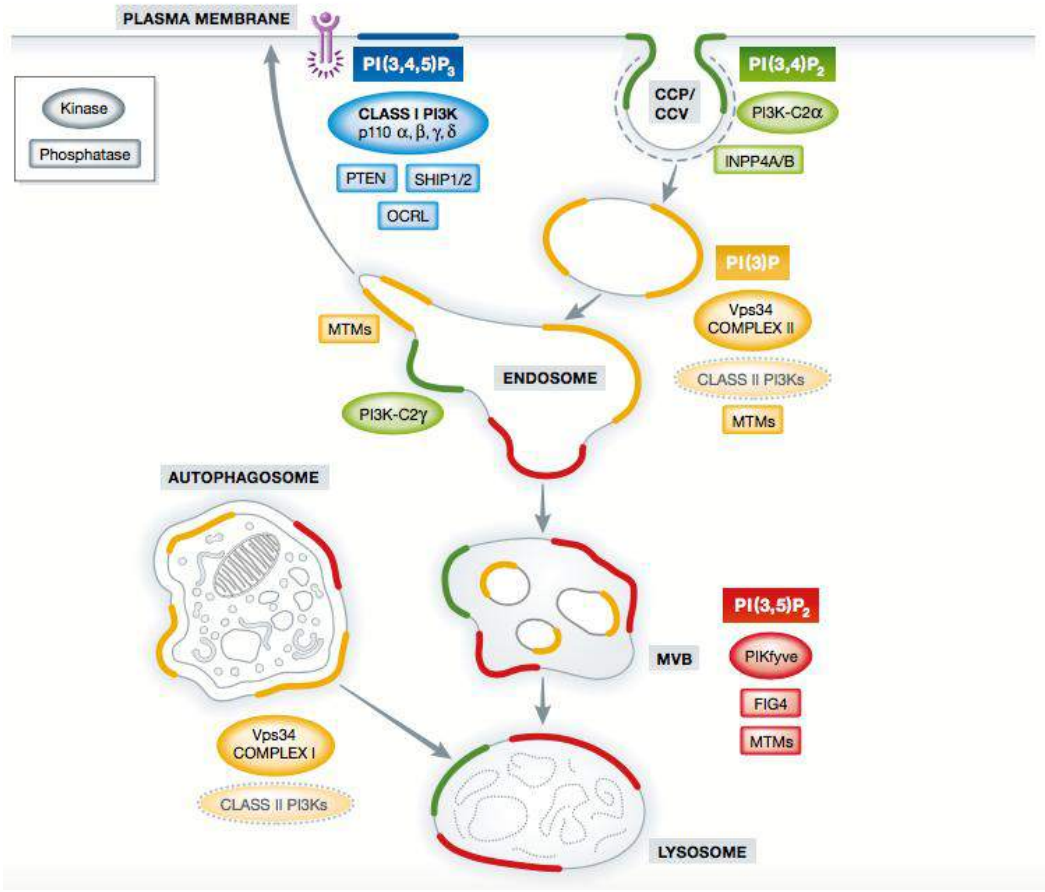

Figure 27: Localisation cellulaire des D3-PI et des kinases et phosphatases mises en jeu dans leur métabolisme: A la membrane plasmique, l'activation d'un récepteur à activité tyrosine kinase résulte en la production de PtdIns(3,4,5)P_3 par les PI3Ks de classe I (isoformes α, β, γ et δ). Ce second messager lipidique est un substrat de la 3-phosphatase PTEN et des 5-phosphatases SHIP1/2. L'isoforme α des PI3Ks de classe II est capable de produire du PtdIns(3,4)P_2 à la membrane plasmique permettant la maturation des puits couverts de clathrine et la formation des vésicules couvertes de clathrine lors de l'endocytose. Le PtdIns3P est essentiel à la fonction des endosomes précoces et est produit par la PI3K de classe III (Vps34), par les PI3Ks de classe II, par la 4-phosphatase INPP4A/B qui déphosphoryle le PtdIns(3,4)P_2 et par la 5-phosphatase FIG4. PIKfyve produit du PtdIns(3,5)P_2 à partir de PtdIns3P lors de la maturation des endosomes précoces en endosomes tardifs/corps multivésiculaires (MVB). Vps34 produit aussi du PtdIns3P lors de la formation de l'autophagosome. Le recyclage endosomal à la membrane plasmique nécessite l'hydrolyse du PtdIns3P par les MTM ainsi que la génération de PtdIns4P pour l'exocytose. *D'après (Marat and Haucke, 2016).*

1) Le PtdIns3P

Le PtdIns3P, présent en faible quantité dans les cellules eucaryotes, est généré soit par les PI3Ks de classe II et la PI3K de classe III à partir du PtdIns, soit par une 4-phosphatase de

type Iα à partir du PtdIns(3,4)P_2, soit enfin par une 5-phosphatase (FIG4) à partir du PtdIns(3,5)P_2.

Le rôle du PtdIns3P est dépendant de sa localisation dans la cellule (Figure 28). Le maintien de son taux de base est indispensable pour l'homéostasie cellulaire car il joue, entre autre, un rôle majeur dans la régulation du trafic intracellulaire, en recrutant des effecteurs protéiques ayant des domaines d'interaction FYVE ou PX. En effet, le PtdIns3P régule la voie de l'endocytose par interaction avec le domaine FYVE des protéines early endosomes antigen 1 (EEA1) ou Rab5 (Simonsen et al., 1998). Le PtdIns3P recrute également la protéine HRS par son domaine FYVE qui, par interaction avec des protéines séquestrant les protéines membranaires ubiquitinylées (endosomal sorting complex required for transport (ESCRT)), guide les protéines membranaires vers la dégradation par les lysosomes (Schink et al., 2013; Viaud et al., 2016). En interagissant avec le domaine PX des protéines sorting nexin (SNX), le PtdIns3P contrôle le recyclage à la membrane plasmique ainsi que le transport rétrograde d'endosomes vers le *trans*-Golgi (Schink et al., 2013; Viaud et al., 2016). Lors d'une déprivation en nutriments, la PI3K de classe III (Vps34), produit du PtdIns3P au niveau de l'autophagosome naissant, le phagophore, permettant le recrutement de protéines telles que double-FYVE-domain-containing-protein-1 (DFCP1) ou encore WD40 repeat protein interactions with phosphoinositides 1 and 2 (WIPI-1 et 2) qui sont indispensables à l'initiation de l'autophagie (Proikas-Cezanne et al., 2015; Schink et al., 2013; Viaud et al., 2016). Il a été montré que PtdIns3P joue aussi un rôle dans l'exocytose des granules d'insuline (Dominguez et al., 2011) , dans l'activation d'un domaine de la NADPH oxydase ($p40^{phox}$) (Ellson et al., 2006) et dans la cytocinèse au niveau du pont intracellulaire en recrutant la protéine centrosomale FYCE-CENT (FYVE domain-containing centrosomal protein) indispensable a la division cellulaire (Sagona et al., 2010).

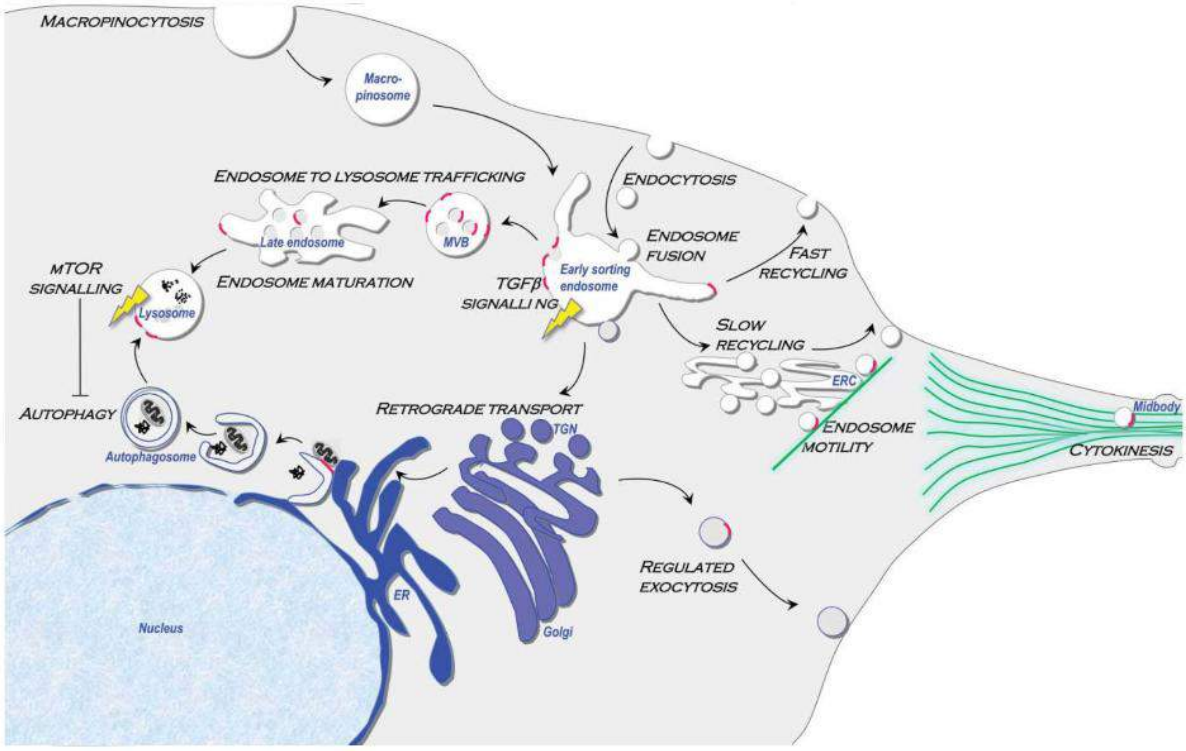

Figure 28: Représentation schématique des processus cellulaires contrôlés par le PtdIns3P: Les processus cellulaires contrôlés par le PtdIns3P sont illustrés sur le schéma. En rouge sont représentées les localisations membranaires suggérées du PtdIns3P. *D'aprés (Schink et al., 2013)*.

2) Le PtdIns(3,4)P_2

Le PtdIns(3,4)P_2 est synthétisé par l'isoforme α des PI3K de classe II, à partir de PtdIns4P, pour contrôler l'endocytose dépendante de la clathrine *via* le recrutement de la SNX9 par son domaine PX (Posor et al., 2013). Le PtdIns(3,4)P_2 provient aussi de la déphosphorylation du PtdIns(3,4,5)P_3 par les 5-phosphatases SHIP1 et 2 et skeletal muscle and kidney enriched inositol phosphatase (SKIP). Les rôles du PtdIns(3,4)P_2 sont encore peu connus. Cependant, il est capable d'interagir avec des domaines PH de certaines protéines comme la lamellipodine et serait ainsi impliqué dans la formation de lamellipodes et de podosomes (Bae et al., 2010; Li and Marshall, 2015). Dans les plaquettes, une part importante du PtdIns(3,4)P_2 est produit en aval de l'intégrine $\alpha_{IIb}\beta_3$ par déphosphorylation du PtdIns(3,4,5)P_3 par SHIP1 lors de l'agrégation plaquettaire (Giuriato et al., 2000).

3) Le PtdIns(3,5)P_2

Le PtdIns(3,5)P_2, généré majoritairement par la 5-kinase PIKfyve à partir de PtdIns3P, est peu abondant dans les cellules eucaryotes. PIKfyve fonctionne au sein d'un complexe de kinases/phosphatases, PIKfyve/ArPIKfyve/SAC3 (PAS), localisé au niveau des endosomes grâce à son domaine FYVE liant le PtdIns3P. Ce complexe PAS est capable de produire du

PtdIns(3,5)P_2 mais aussi du PtdIns3P. Le PtdIns(3,5)P_2 et les enzymes du PAS contrôleraient l'homéostasie du trafic endosomal en régulant la fission et la fusion endosomale, le transport rétrograde des endosomes vers le *trans*-Golgi et le tri vésiculaire vers l'endosome tardif. Cependant, le manque d'outils permettant la localisation et le dosage précis du PtdIns(3,5)P_2 limite son étude (McCartney et al., 2014; Viaud et al., 2016).

4) Le PtdIns(3,4,5)P_3

Le PtdIns(3,4,5)P_3 est présent en très faible quantité dans des cellules au repos, notamment dans les plaquettes. Il est produit de façon rapide et transitoire par phosphorylation du PtdIns(4,5)P_2 par les PI3K de classe I et est indispensable à l'organisation de plusieurs voies de signalisation. On le retrouve majoritairement dans le feuillet interne de la membrane plasmique où il recrute des protéines via leur domaine PH comme par exemple la protéine kinase Akt, des facteurs d'échange (GEF) des GTPases Arf ou Rac, des tyrosines kinases (Bruton tyrosine kinase (BTK)) et des protéines adaptatrices comme GRB2-associated-binding-protein 1 (GAB1). Ainsi, le PtdIns(3,4,5)P_3 participe au contrôle de différents processus tels que la prolifération et la survie cellulaire, l'homéostasie glucidique ou encore les processus de mobilité cellulaire (Salamon and Backer, 2013; Viaud et al., 2016). Dans les plaquettes, il est produit de façon rapide lors de l'activation par la plupart des agonistes physiologiques et également lors de l'engagement de l'intégrine $\alpha_{IIb}\beta_3$ (Gratacap et al., 2011).

C) Généralités sur les PI3Ks

Les PI3Ks sont une famille d'enzyme catalysant l'ajout d'un phosphate en position 3 du noyau inositol des PI. A ce jour, huit isoformes de PI3K, divisées en trois classes, ont été caractérisées en fonction de leur substrat lipidique, leur mode de régulation et leur structure protéique (Vanhaesebroeck et al., 2010).

1) Les PI3Ks de classe I

Les PI3Ks de classe I sont divisées en deux sous-classes. Les isoformes α, β et δ forment la classe IA et sont composées d'une sous-unité catalytique p110, dont il existe trois isoformes (p110α, p110β et p110δ) et d'une sous-unité régulatrice composée de cinq isoformes (p85α, p85β, p55γ, p55α et p50α). La classe IB ne contient qu'un seul isoforme composé de la sous-unité catalytique p110γ et d'une sous-unité régulatrice (p101 ou p87). Les isoformes p110α et β sont exprimés de façon ubiquiste, l'isoforme δ est retrouvé dans les leucocytes et les plaquettes et enfin l'isoforme γ est exprimé dans les cellules

hématopoïétiques mais aussi les cellules endothéliales, les cardiomyocytes, les ilôts pancréatiques et les cellules musculaires lisses (Vanhaesebroeck et al., 2010).

Les sous-unités catalytiques p110 contiennent un domaine N-terminal de liaison à la sous-unité régulatrice (p85-BD pour p110α, β, δ), un domaine de liaison à Ras (RBD), un domaine C2 de liaison à la membrane plasmique, un domaine lipide kinase en C-terminal et un domaine en super-hélice au rôle non caractérisé. Les sous-unités régulatrices de classe IA contiennent un domaine iSH2 (flanqué de part et d'autre d'un domaine SH2) de liaison à p110, de domaines riches en proline, d'un domaine SH3 (pour p85α et β) et d'un domaine « breakpoint-cluster-region homology » (BH ; pour p85α et β). Les sous-unités régulatrices de classe IB, quant à elles, n'ont aucune homologie de séquences avec les sous-unités régulatrices de classe IA mais possèdent un domaine de liaison aux sous-unités β et γ des protéines G hétérotrimériques (Thorpe et al., 2015) (Figure 29).

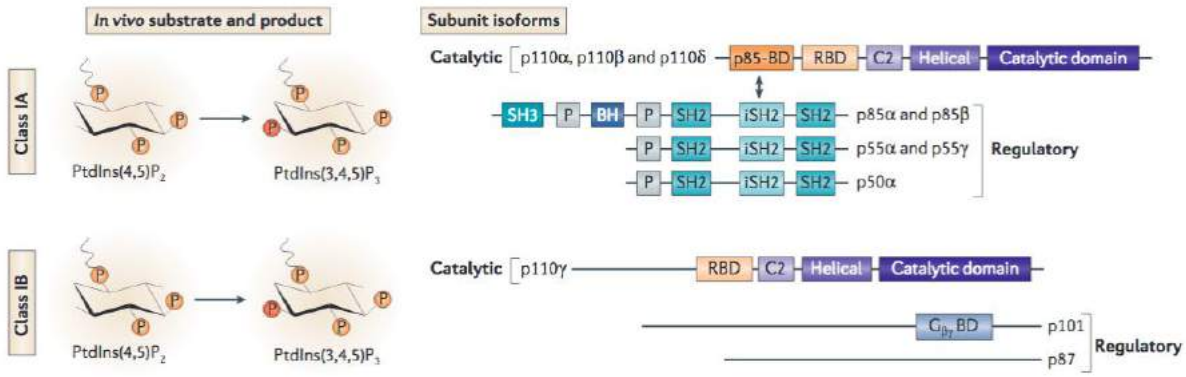

Figure 29: Isoformes de classe I des PI3Ks: Les PI3Ks de classe I phosphorylent le PtdIns(4,5)P_2 en position 3 du noyau inositol pour donner du PtdIns(3,4,5)P_3. La classe IA est composée d'hétérodimères contenant une sous-unité catalytique p110 (α, β ou δ) et d'une sous-unité régulatrice « p85-like » (p85α et β, p55α et δ et p50α). La classe IB est composée d'hétérodimères avec une sous-unité catalytique p110γ et une sous-unité régulatrice p101 ou p87. *D'après (Thorpe et al., 2015).*

Suite à l'activation d'un récepteur à activité tyrosine kinase ou couplé aux protéines G, les PI3Ks de classe I sont recrutées à proximité de leur substrat lipidique dans la membrane plasmique. S'en suit la phosphorylation du PtdIns(4,5)P_2 en PtdIns(3,4,5)P_3 qui organise de façon spatio-temporelle certaines voies de signalisation comme évoqué précédemment (Thorpe et al., 2015; Vanhaesebroeck et al., 2010) (Figure 30) .

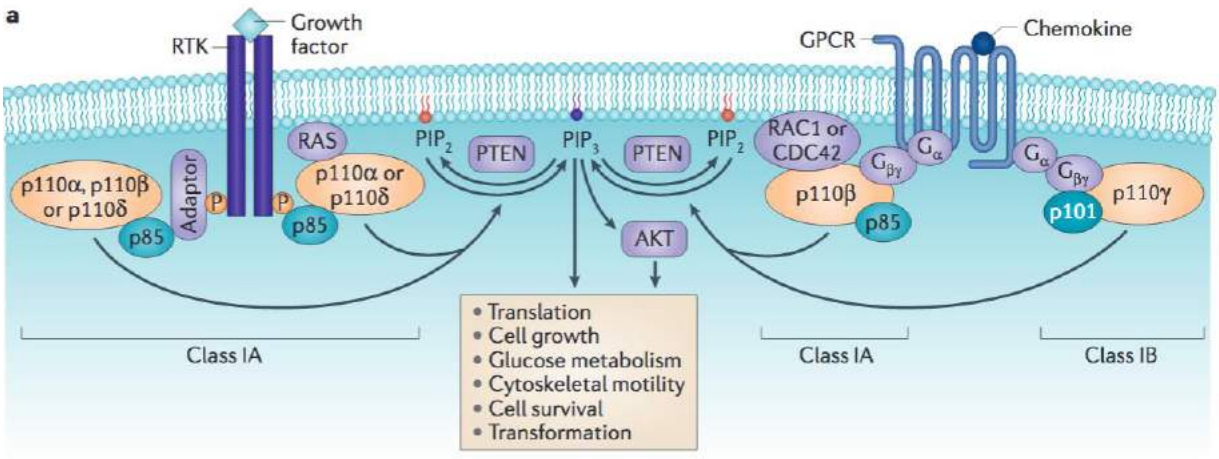

Figure 30: Voies de signalisation contrôlées par les PI3Ks de classe I: Après activation d'un récepteur à activité tyrosine kinase ou couplé à une protéine G, les PI3Ks de classe I sont recrutées à la membrane plasmique par interaction avec les motifs YXXM phosphorylés des récepteurs à activité tyrosine kinase ou par interaction avec les protéines $G_{\beta\gamma}$. Ensuite, elles phosphorylent le PtdIns(4,5)P_2 en PtdIns(3,4,5)P_3, un second messager lipidique qui active des voies de signalisation notamment les voies dépendantes d'Akt pour contrôler différents processus cellulaires : transcription, croissance, métabolisme glucidique, dynamique du cytosquelette, survie cellulaire et traduction. *D'après (Thorpe et al., 2015)*.

2) Les PI3Ks de classe II (PI3KC2)

Il existe trois isoformes de PI3KC2: α, β et γ. Les isoformes α et β sont exprimés de façon ubiquiste alors que l'isoforme γ a une expression restreinte (foie, prostate, glandes salivaires et mammaires). Les PI3KC2 sont des lipide kinases monomériques qui ne possèdent pas de sous-unité régulatrice connue à ce jour. Ces monomères sont composés d'un domaine catalytique, d'un domaine en super-hélice au rôle non caractérisé, d'un domaine RBD, d'un domaine PX et deux domaines C2 de liaison à la membrane plasmique. Les trois isoformes divergent par le nombre de séquences riche en prolines en N-terminal. Les PI3KC2 sont capables de phosphoryler le PtdIns et le PtdIns4P en position 3 du noyau inositol pour générer du PtdIns3P et du PtdIns(3,4)P_2 respectivement (Falasca et al., 2016; Thorpe et al., 2015; Vanhaesebroeck et al., 2010) (Figure 31).

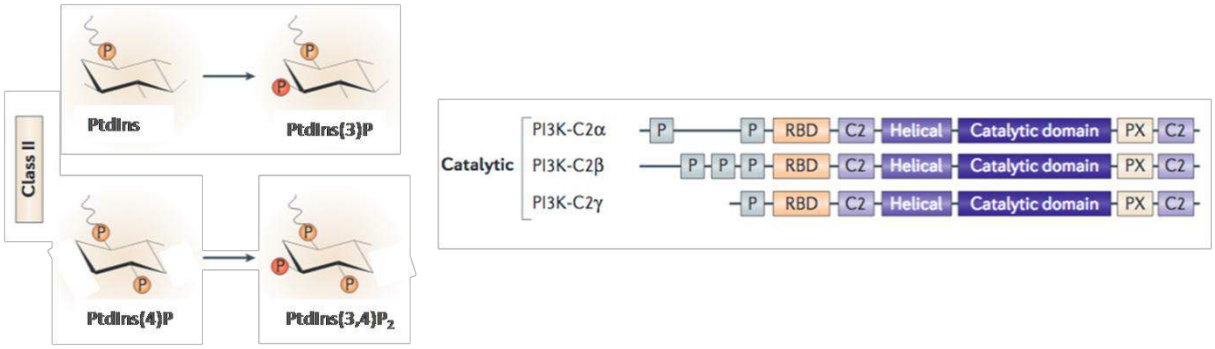

Figure 31: Isoformes de classe II des PI3Ks: La classe II des PI3Ks est composée de 3 isoformes, α, β et γ. Ce sont des monomères contenant un domaine catalytique mais sans sous-unité régulatrice identifiée à ce jour. *D'après (Thorpe et al., 2015)*.

a) La PI3K de classe II α (PI3KC2α)

In vitro, il a été montré que la PI3KC2α est activée par des cytokines, des chimiokines, l'insuline et certains facteurs de croissance (Falasca et al., 2016; Ktori et al., 2003; Turner et al., 1998). Sa particularité par rapport aux autres PI3KC2 est de posséder en sa région N-terminale un domaine de liaison à la clathrine. Son interaction avec la clathrine entraîne son activation et la production de PtdIns(3,4)P_2 ce qui permet la scission des puits à clathrine lors de l'endocytose grâce au recrutement de la SNX9 (Falasca et al., 2016; Gaidarov et al., 2001; Posor et al., 2013). La PI3KC2α est aussi impliquée dans le transport de vésicules vers la membrane plasmique tel que la translocation de Glut4 en réponse à l'insuline (Maffucci et al., 2003) et l'exocytose. En effet, la PI3KC2α est impliquée dans la sécrétion d'insuline, la libération de granules neurosécrétoires et la dégranulation des basophiles (Dominguez et al., 2011; Meunier et al., 2005; Nigorikawa et al., 2014). Il a été montré dans des expériences *in vitro* que la PI3KC2α régule d'autres voies, en particulier la survie cellulaire par régulation de la voie caspase 9/poly-ADP-ribose-polymerase (PARP) ou encore la contraction des cellules musculaire lisses induite par la noradrénaline, la ionomycine ou le KCl en régulant la voie RhoA/MLC (Elis et al., 2008; Eun et al., 2010; Falasca et al., 2016; Wang et al., 2006) (Figure 32).

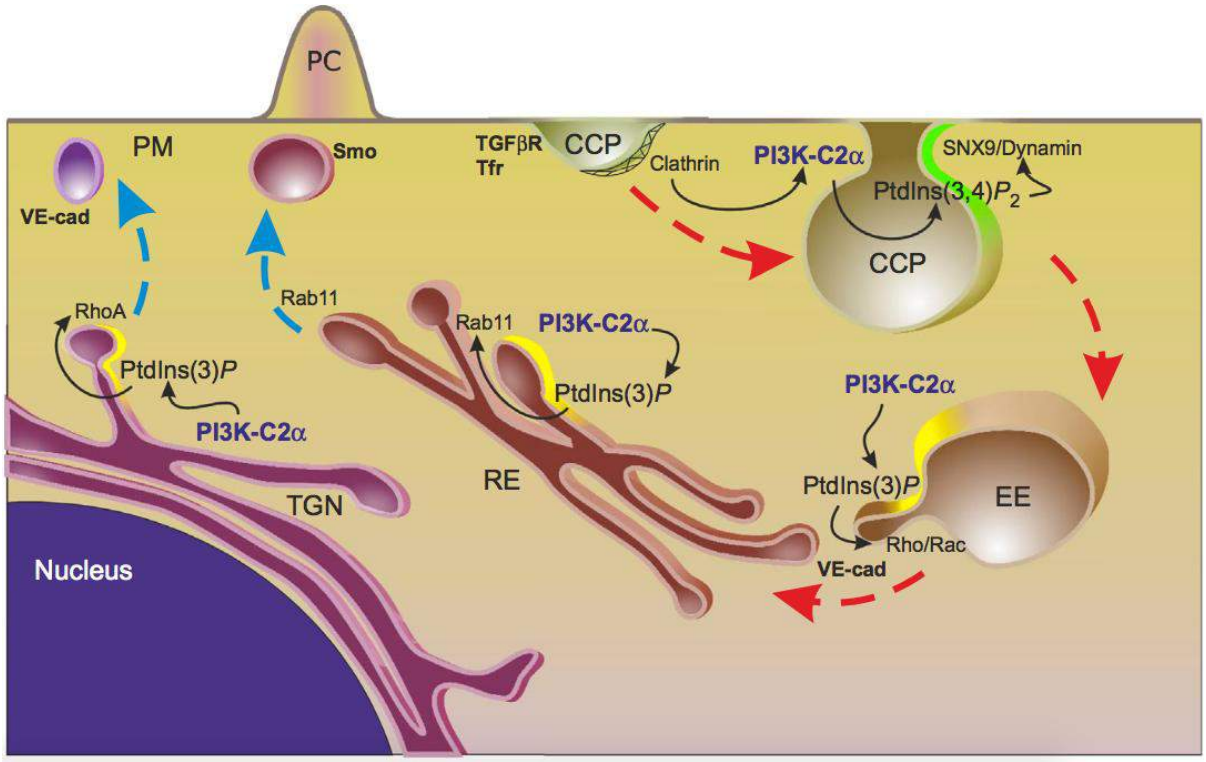

Figure 32: Rôles de la PI3KC2α dans les différents compartiments cellulaires: La PI3KC2α est localisée dans différents compartiments cellulaires et son activité contrôle à la fois la voie de l'endocytose (flèche rouge) et la voie de l'exocytose (flèche bleue). Après activation de récepteurs tels que celui du transforming growth factor β (TGFβR) ou de la transferrine (Tfr), la PI3KC2α est recrutée à la membrane plasmique (PM) au niveau de puits à clathrine (CCP) nouvellement formés pour y produire du PtdIns(3,4)P_2 (en vert) qui est essentiel au recrutement de SNX9 pour la scission des CCPs. La PI3KC2α est nécessaire à la maturation des vésicules endocytés en endosomes précoces. La PI3KC2α produit du PtdIns3P (en jaune) dans les endosomes et permet l'activation de GTPases impliquées dans le réarrangement de l'actine et le trafic vésiculaire. RhoA est indispensable pour le transport des VE-cadherines (VE-cadh) des endosomes de recyclage (RE) et du *trans*-Golgi (TGN) vers la membrane plasmique. De plus, la PI3KC2α produit du PtdIns3P à la base du cil primaire (PC) indispensable pour son élongation. *D'après (Campa et al., 2015)*.

Le développement de modèles animaux déficients ou inactivés pour la PI3KC2α a permis de mieux caractériser son rôle dans différents processus cellulaires (Tableau 1). La délétion ou l'inactivation totale de la PI3KC2α dans l'animal entier est létale au stade embryonnaire (Alliouachene et al., 2016; Franco et al., 2014; Mountford et al., 2015; Yoshioka et al., 2012). En effet, la délétion totale de la PI3KC2α est létale pour différentes raisons comme des défauts de vasculogénèse (Yoshioka et al., 2012) et de formation du cil primaire (Franco et al., 2014).

Modèle murin	Phénotype	Références
PI3KC2α tronquée	Défaillances rénales, survie diminuée, retard de croissance	(Harris et al., 2011)
Délétion totale	Létalité embryonnaire	(Yoshioka et al., 2012) (Franco et al., 2014) (Mountford et al., 2015)
Délétion spécifique cellules endothéliales	Létalité embryonnaire	(Yoshioka et al., 2012)
Mutation inactivatrice homozygote	Létalité embryonnaire	(Alliouachene et al., 2016)
Délétion spécifique cellules endothéliales inductible	Défaut revascularisation après ischémie, diminution de l'angiogénèse de la rétine	(Yoshioka et al., 2012)
Délétion hétérozygote Délétion totale inductible	Défaut des fonctions plaquettaires	(Mountford et al., 2015)
Mutation inactivatrice hétérozygote	Défaut des fonctions plaquettaires Résistance à la leptine dépendante du sexe	(Valet et al., 2015) (Alliouachene et al., 2016)

Tableau 1: Modèles murins déficients pour PI3KC2α et leurs phénotypes. *D'après (Falasca et al., 2016).*

En 2013, Yoshioka *et al*, en délétant spécifiquement l'expression de la PI3KC2α dans les cellules endothéliales, ont mis en évidence une diminution du nombre d'endosomes riches en PtdIns3P et un transport des VE-cadherines aux jonctions entre cellules endothéliales défectueux. Ceci a pour conséquence un défaut d'assemblage des jonctions entre cellules endothéliales responsable d'une perméabilité vasculaire accrue et d'une angiogénèse altérée. En effet, en réponse au vascular endothelial growth factor (VEGF), la PI3KC2α produit du PtdIns3P, au niveau des endosomes et du TGN, permettant l'activation de la GTPase RhoA et le transport des VE-cadherines aux jonctions cellulaires. La PI3KC2α est donc indispensable pour la migration, la prolifération, la tubulogénèse et l'intégrité de la barrière endothéliale.

Après greffe de tumeur solide sur les souris déficientes pour la PI3KC2α spécifiquement dans les cellules endothéliales, Yoshioka *et al* ont observé une diminution de la densité de micro-vaisseaux et du volume global de la tumeur, faisant de la PI3KC2α une potentielle cible thérapeutique dans le cancer (Yoshioka et al., 2012).

En 2014, Franco et collaborateurs ont montré que la PI3KC2α générait un pool de PtdIns3P à la base du cil primaire dans les endosomes de recyclage péricentriolaires. Ce pool de PtdIns3P permet la relocalisation de Rab11 à la base du cil primaire, et son activation ainsi que celle de Rab8. Ceci est indispensable à l'élongation du cil primaire et à l'activation de la voie Sonic Hedgehog (Shh) et *in fine* au développement embryonnaire (Franco et al., 2014).

En 2016, Alliouachène *et al* ont montré, grâce à un modèle hétérozygote d'inactivation de la PI3KC2α (par mutation ponctuelle dans un exon codant pour son site catalytique), un rôle de la PI3KC2α dans la sensibilité à la leptine et dans l'homéostasie glucidique dépendant du sexe. En effet, les souris mâles inactivées partiellement pour la PI3KC2α développent une résistance à la leptine au niveau hypothalamique corrélée à une obésité dépendante de l'âge, une insulino-résistance et une intolérance au glucose (Alliouachene et al., 2016).

Nous verrons dans la partie "résultats" que la PI3KC2α est également impliquée dans la structuration des membranes, notamment au cours de la production plaquettaire.

b) La PI3K de classe II β (PI3KC2β)

Le rôle de la PI3KC2β a été moins étudié que celui de la PI3KC2α. *In vitro*, des études ont montré son rôle dans la régulation de la migration cellulaire. En effet, en réponse à l'acide lysophosphatidique et à la sphingosine-1-phosphate ou suite à l'activation du récepteur à l'EGF, la PI3KC2β produit du PtdIns3P à la membrane plasmique et contribue à la migration cellulaire (Domin et al., 2005; Katso et al., 2006; Maffucci et al., 2005; Tibolla et al., 2013). La PI3KC2β est aussi impliquée dans la régulation de la morphologie et la survie cellulaire. En effet, lors d'une surexpression de la PI3KC2β dans des fibroblastes, la PI3KC2β forme, en réponse au PDGF, un complexe avec un RhoGef, Dbl, qui va activer RhoA et Rac1 induisant la formation de fibres de stress et l'étalement des cellules (Blajecka et al., 2012).

In vivo, l'inactivation ou la délétion totale de la PI3KC2β dans l'animal entier n'est pas létale et n'entraine pas de phénotype évident (Harada et al., 2005; Mountford et al., 2015). La surexpression ainsi que la délétion totale de la PI3KC2β n'a aucun effet sur la différenciation

de l'épiderme. Afin de savoir si la PI3KC2α compensait la perte de la PI3KC2β, Harada *et al* ont délété la PI3KC2α avec des ARN interférents dans le modèle de délétion totale de la PI3KC2β. Ceci n'impacte pas la différenciation de l'épiderme suggérant que PI3KC2α ne compense pas la perte de la PI3KC2β (Harada et al., 2005).

En 2015, Alliouachène *et al* ont montré, grâce à un modèle homozygote d'inactivation de la PI3KC2β (par mutation ponctuelle dans un exon codant pour son site catalytique), une meilleure sensibilité à l'insuline et tolérance au glucose de ces souris. En effet, les hépatocytes primaires de ces souris ont un taux basal de PtdIns3P significativement diminué ainsi qu'une accumulation d'endosomes très précoces APPL1 positifs associée à une diminution des endosomes précoces EEA1 positifs. Le trafic endosomal du récepteur à l'insuline est affecté et ces mêmes hépatocytes stimulés à l'insuline, présentent une augmentation de la signalisation Akt. Il semble que le récepteur à l'insuline dans les endosomes très précoces APPL1 positifs soit encore actif ce qui explique la meilleure sensibilité à l'insuline de ces souris (Figure 33). Ces souris inactivées pour la PI3KC2β sont aussi protégées contre la stéatose hépatique suite à un régime gras, ce qui confirme que la PI3KC2β pourrait être une cible potentielle dans le diabète de type 2 (Alliouachene et al., 2015) (travaux auxquels j'ai participé au cours de mon Master 2 ; cf. Annexe 2).

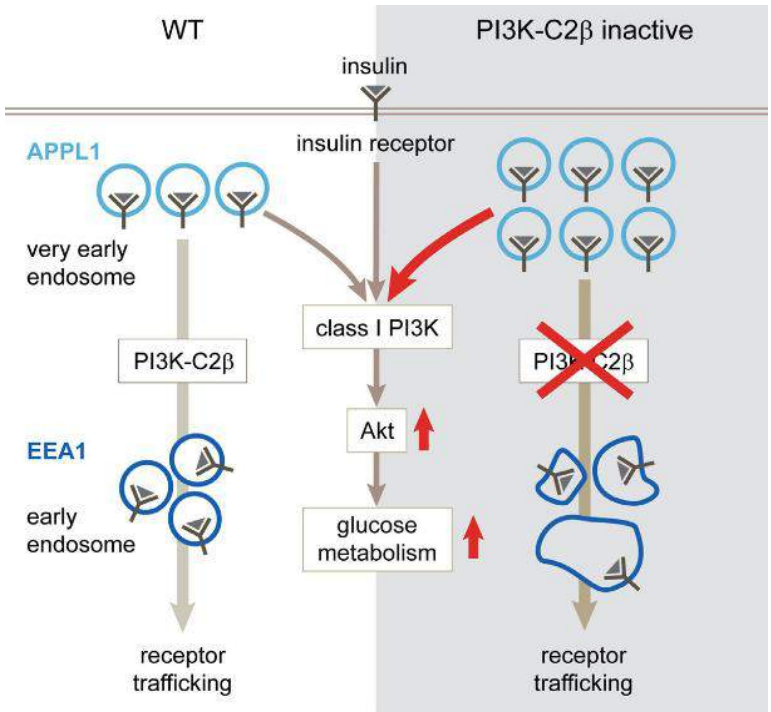

Figure 33: Modèle proposé du rôle de la PI3KC2β en aval du récepteur à l'insuline dans les hépatocytes. *D'après (Alliouachene et al., 2015).*

Lors du séquençage du génome de différents échantillons de cancer du poumon, le gène de la PI3KC2β a été retrouvé muté, suggérant l'implication potentielle de la PI3KC2β dans le cancer. (Falasca et al., 2016; Falasca and Maffucci, 2012; Maffucci and Falasca, 2014).

c) La PI3K de classe II γ (PI3KC2γ)

La PI3KC2γ est exprimée de façon restreinte dans le foie, la prostate et les glandes salivaires et mammaires (Rozycka et al., 1998). Son rôle a très peu été étudié mais il a été montré qu'*in vitro*, elle produit du PtdIns3P et du PtdIns(3,4)P_2 (Misawa et al., 1998). Récemment, le premier modèle murin de délétion totale de la PI3KC2γ a été caractérisé par Braccini *et al*. (Braccini et al., 2015). Ces souris, à l'inverse du modèle inactivé pour la PI3KC2β, présentent une diminution du taux de glycogène hépatique, deviennent hyperlipidémiques et insulino-résistantes en réponse à un régime gras. En effet, en réponse à l'insuline, la PI3KC2γ s'associe avec Rab5-GTP et est recrutée sur les endosomes précoces Rab5 positifs. Dans ces compartiments, elle génère du PtdIns(3,4)P_2 qui retarde l'avancée du trafic endosomal et ainsi augmente l'activation de la voie Akt2, spécifiquement, amenant à la synthèse de glycogène. La PI3KC2γ semble donc importante pour l'amplification du signal Akt2 en réponse à l'insuline qui permet le stockage de glucose sous forme de glycogène et protège de la mise en place de la résistance à l'insuline (Braccini et al., 2015).

3) La PI3K de classe III (Vps34)

La classe III des PI3Ks est composée d'un seul isoforme: Vps34. Celle-ci est composée d'un domaine catalytique, un domaine en super-hélice et un domaine C2. Elle forme un hétérodimère avec Vps15, sa sous-unité régulatrice. Son expression est ubiquiste et elle produit du PtdIns3P à partir de PtdIns. Sa sous-unité régulatrice Vps15 est myristoylée ce qui lui permet d'être localisée aux membranes intracellulaires (Backer, 2016) (Figure 34).

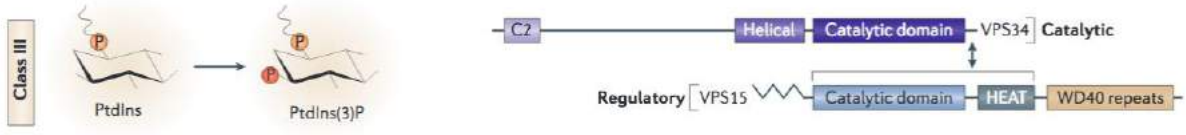

Figure 34: Vps34, isoforme de classe III des PI3Ks: Vps34 forme un hétérodimère avec Vps15, sa sous-unité régulatrice. Vps34 est constituée d'un domaine catalytique, un domaine en super-hélice et un domaine C2. *D'après (Thorpe et al., 2015)*.

Vps34 intervient dans divers processus cellulaires en fonction des protéines auxquelles elle est associée. Il existe plusieurs complexes dans lesquels Vps34 intervient:

- Le premier complexe est composé de Vps34 et sa sous-unité régulatrice Vps15 et peut être associé à Beclin1.
- Le complexe I est constitué de Vps34, Vps15, Beclin1 et Atg14.
- Le complexe II est composé de Vps34, Vps15, Beclin1 et UVRAG (UV-radiation resistance-associated gene).

L'activité de Vps34 peut être régulée par des modifications post-traductionnelles touchant directement Vps34 ou ses partenaires de complexes. Parmi ses modifications, nous retrouvons la phosphorylation, l'ubiquitination, la sumoylation ou encore l'acétylation. Par exemple, lors de l'induction de l'autophagie par déprivation en acide aminés, la Beclin1 des complexes I et II est phosphorylée sur sa sérine 14 par Unc-51 like autophagy activating kinase 1 (ULK1) ce qui va entrainer l'activation de l'activité lipide kinase de Vps34 (Backer, 2016; Russell et al., 2013). L'activité de Vps34 peut aussi être contrôlée par des modifications de l'assemblage des complexes I et II ou par la liaison à d'autres protéines ou inhibiteurs. En effet, la protéine Rubicon est capable de lier Vps34 par son domaine RPIP8-UNC14-NESCA (RUN) ou de lier UVRAG par son domaine FYVE et d'inhiber l'activité lipide kinase de Vps34 dans l'autophagie (Backer, 2016; Zhong et al., 2009). Vps34 est aussi contrôlée par régulation de sa localisation intracellulaire et par dégradation sélective des constituants de ses complexes. Par exemple, la localisation de Vps34 au pré-autophagosome requiert Atg14 et permet ainsi son activation (Backer, 2016; Obara et al., 2006). Lors d'une déprivation en acide aminés prolongée, l'ubiquitine-ligase Cul3-KLHL20 va ubiquitinyler Beclin1, Vps34 et ULK1 par association directe et induire leur dégradation (Backer, 2016; Liu et al., 2016). Enfin, le dernier mode de régulation de Vps34 est une régulation transcriptionnelle sur le long terme (Backer, 2016; Sandri et al., 2004; Yamada et al., 2012).

Par sa production de PtdIns3P au niveau de membranes intracellulaires, Vps34 est fortement impliquée dans la gestion du trafic vésiculaire. Vps15 recrute Vps34, par son domaine WD40, à proximité de Rab5 activé où elle va générer du PtdIns3P ce qui permettra le recrutement d'EEA1 et la formation des endosomes précoces. De même, Vps34-Vps15 vont se lier à Rab7 lors de la maturation des endosomes tardifs. Vps34 intervient aussi au niveau des corps multivésiculaires (MVB) où sa production de PtdIns3P permet le recrutement des protéines ESCRT (Henne et al., 2011). Ces protéines ESCRT, qui possèdent un domaine FYVE de liaison au PtdIns3P, se lient aux protéines membranaires ubiquitinylées et permet leur internalisation dans les MVB (Henne et al., 2011). Vps34 régule aussi le transport rétrograde de cargos endocytés vers le Golgi grâce au complexe rétromère formé de

quatre protéines SNX (1, 2, 5 et 6) par leur domaine PX de liaison au PtdIns3P (Bonifacino and Hurley, 2008). Vps34 intervient également lors de la formation et de la maturation des phagosomes (Figure 35). Vps34 du complexe II intervient dans la cytocinèse où, par la production de PtdIns3P, il recruterait des protéines nécessaires à la scission (Backer, 2016; Boularan et al., 2014). Vps34 est impliquée dans l'autophagie induite par déprivation en nutriments. Cette déprivation entraîne la production de PtdIns3P, par le complexe I, qui va recruter DFCP1, *via* son domaine FYVE, au niveau de la membrane du réticulum endoplasmique et permettre la formation du précurseur de l'autophagosome, l'omégasome. Vps34 dans le complexe II est également indispensable à l'étape finale de l'autophagie pour la fusion de l'autophagosome avec le lysosome. Ainsi, le complexe I intervient lors du processus d'initiation de l'autophagie alors que le complexe II intervient à l'étape finale de l'autophagie ainsi que dans la régulation du trafic endosomal (Backer, 2016; Kihara et al., 2001; Lamb et al., 2013; McKnight et al., 2014; Thoresen et al., 2010) (figure 35). En effet, la présence d'Atg14 dans le complexe I permet son recrutement (et activation) au niveau de l'omégasome alors que la présence d'UVRAG dans le complexe II permet son recrutement (et activation) au niveau des endosomes *via* Rab5 et Rab7 permettant leur maturation et la fusion des endosomes ou des autophagosomes avec les lysosomes (Backer, 2016; Liang et al., 2008).

De façon intéressante, la déprivation en nutriments stimule l'activité de Vps34 dans les complexes I et II (comme décrit précédemment) mais inhibe aussi l'activité de Vps34 dans les complexes avec Vps15 et avec Vps15-Beclin1. En effet, la déprivation en nutriments va entraîner la phosphorylation inhibitrice de Vps34 des complexes Vps34-Vps15 et Vps34-Vps15-Beclin1 par l'AMPK et par mTORC1 (Backer, 2016; Yuan et al., 2013). A l'inverse, l'apport de nutriments va activer le complexe Vps34-Vps15 qui va à son tour stimuler le complexe 1 de mTOR (mTORC1) et permettre la synthèse protéique, *via* la S6 kinase 1 (S6K1) augmentant ainsi la croissance, la prolifération et la survie cellulaire. De plus, l'activation de mTORC1 inhibe Vps34 du complexe I par phosphorylation d'Atg14 (Backer, 2016; Yuan et al., 2013). En fin de compte, Vps34, selon le complexe, joue des rôles qui semblent contradictoires mais cette régulation fine permet l'adaptation de la cellule aux modifications de son environnement.

A ce jour, on ne connait pas de pathologies humaines issues de mutations du gène codant pour Vps34. Cependant, chez un patient atteint de déficit mental et un patient atteint de déficit d'apprentissage ont été trouvées une microdélétion du gène *PIK3C3* (de Vps34) et une

délétion dans l'exons 5-23 de *PIK3C3* respectivement (Inaguma et al., 2016; Vulto-van Silfhout et al., 2013). Il semblerait aussi que Vps34 soit impliqué dans des troubles psychiatriques tels que la schizophrénie et la bipolarité (Stopkova et al., 2004; Tang et al., 2008).

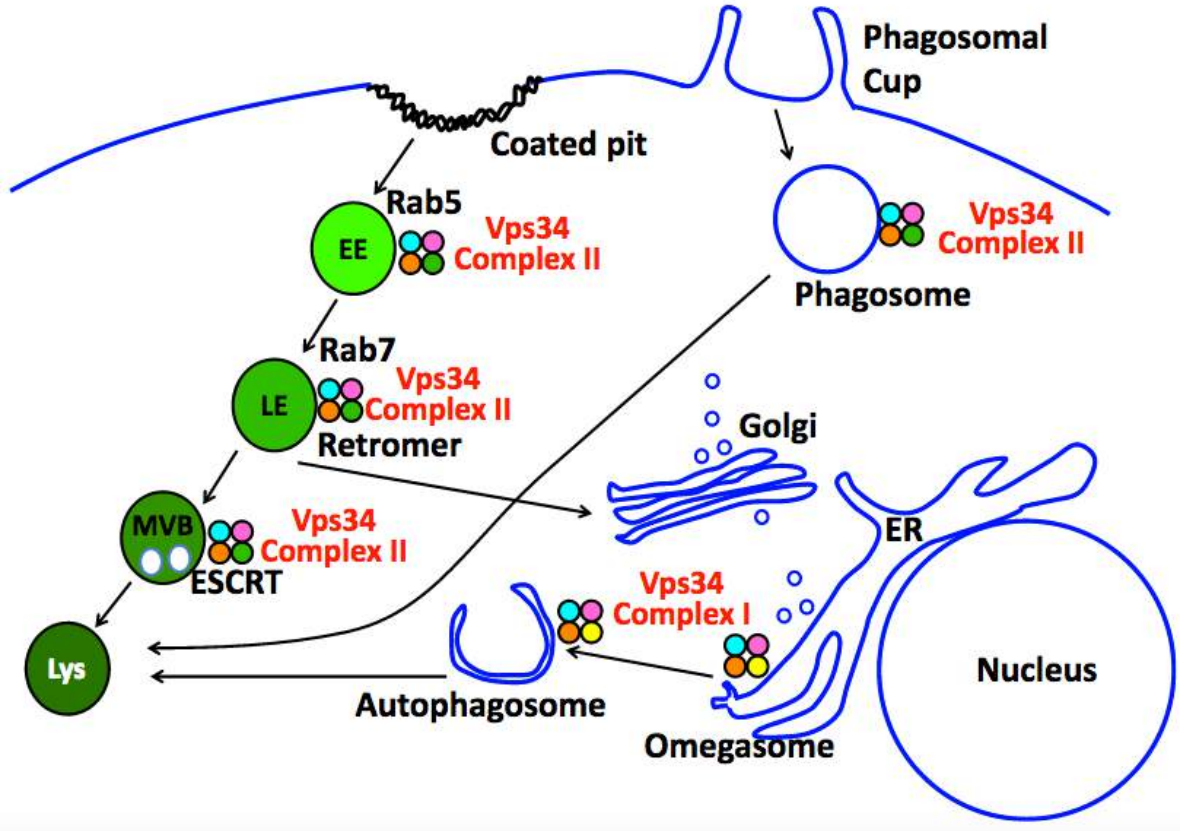

Figure 35: Les fonctions cellulaires de Vps34: Vps34 agit dans des complexes tétramériques en formant du PtdIns3P. Elle régule la maturation des endosomes précoces Rab5-positifs (EE) et des endosomes tardifs Rab7-positifs (LE). Le PtdIns3P produit recrute le complexe rétromère dans le cadre du transport rétrograde vers le Golgi et le complexe ESCRT dans la maturation des MVBs. Enfin, Vps34 est indispensable à l'initiation de l'omégasome au niveau du réticulum endoplasmique (ER) et aussi pour la fusion de l'autophagosome avec le lysosome. *D'après (Backer, 2016)*.

La délétion totale dans l'animal entier de Vps34 est létale au niveau embryonnaire et s'accompagne d'une inhibition de « mammalian target of rapamycin » (mTOR) ainsi que de la prolifération cellulaire (Zhou et al., 2011). Pour éviter cette létalité, ont été générées des souris délétées pour Vps34 spécifiquement dans certains tissus grâce au système Cre recombinase placé derrière des promoteurs tissus-spécifiques. Les souris délétées pour Vps34 dans le foie ont un renouvellement protéique pauvre et développent une hépatomégalie et une

stéatose hépatique. Les souris délétées spécifiquement dans le cœur ont des défauts de contractilité cardiaque et développent une cardiomégalie. De plus, l'ablation de Vps34 dans des « mouse embryonic fibroblastes » (MEFs) entraîne un défaut de flux autophagique, de production de PtdIns3P et de signalisation de mTOR. Cela a pour conséquence une accumulation de protéines, phénomène aussi observé dans le foie et le cœur délétés pour Vps34 et pouvant être à l'origine des défaillances de ces organes lorsque Vps34 est absent (Jaber et al., 2012).

La délétion spécifique de Vps34 dans les lymphocytes T, grâce au système Cre recombinase placé en aval du promoteur CD4 ou Lck, a mis en évidence le rôle primordial de Vps34 dans l'homéostasie des lymphocytes T. En effet, les lymphocytes T délétés pour Vps34 ont des défauts de flux autophagiques entraînant une augmentation significative de l'apoptose ainsi qu'un défaut de transport du récepteur α de l'interleukine 7 à la surface cellulaire, récepteur indispensable à la survie des lymphocytes (McLeod et al., 2011; Parekh et al., 2013; Willinger and Flavell, 2012).

Vps34 joue aussi un rôle dans le développement du muscle squelettique. Les souris délétées pour Vps34 spécifiquement dans le muscle, meurent de cardiomyopathie en moyenne deux mois après la naissance. Ceci est du à un défaut du système lysosomal provoquant l'accumulation de protéines dans les fibres musculaires induisant une dystrophie musculaire (Reifler et al., 2014). De manière intéressante, la délétion spécifique de Vps15 dans les muscles entraîne un phénotype similaire (Nemazanyy et al., 2013).

Au niveau du système nerveux central, il semble que Vps34 soit impliquée dans le trafic endosomal. En effet, la délétion de Vps34 spécifiquement dans les neurones hippocampiques ou sensoriels ou du système pyramidal engendre une dégénérescence progressive des neurones à cause d'un trafic endosomal défectueux (Backer, 2016; Wang et al., 2011; Zhou et al., 2010).

Enfin, la génération de souris déficientes pour Vps34 spécifiquement dans les podocytes a mis en évidence son rôle au niveau rénal. Ces souris décèdent 3 à 9 semaines après leur naissance à cause d'une protéinurie, d'une dégénérescence rapide des podocytes et de la mise en place d'une sclérose glomérulaire. La voie endocytique est indispensable au bon fonctionnement des podocytes car elle permettrait la régulation de la réabsorption de protéines ou d'urine. Les podocytes déficients pour Vps34 ont un trafic endosomal perturbé avec une inhibition du captage de la phase-fluide, de l'endocyose médiée par les récepteurs et de la

maturation des endosomes précoces en endosomes tardifs (Backer, 2016; Bechtel et al., 2013).

IC_{50} in vitro (μM)								
Inhibiteur	p110α	p110β	p110δ	p110γ	PI3KC2α	PI3KC2α	PI3KC2α	**Vps34**
Vps34-IN1	**>10**	**>10**	**>10**	**>10**	**>10**	**>10**	**>10**	**0.025**
SAR405	**>10**	**>10**	**>10**	**>10**	**>10**	**>10**	**>10**	**0.0012**
Compound31	**2.7**	**4.5**	**2.5**	**>10**	**>10**	**>10**	**>10**	**0.002**
3-MA	0.039	0.590	0.120	0.004	ND	ND	ND	0.036
PI-103	0.026	0.045	0.048	0.560	>10	0.490	0.250	0.488
GDC0941	0.003	0.033	0.003	0.075	ND	0.670	ND	>10
PIK-III	3.96	>9	1.2	3.04	ND	ND	ND	0.018

Tableau 2: Tableau comparatif des IC50 des inhibiteurs de Vps34 récemment développés. *D'après (Backer, 2016)*.

Récemment, des inhibiteurs spécifiques de Vps34 actifs *in vitro* ont été développés (SAR405 par Sanofi et Vps34-IN1 par Novartis par Sanofi) et *in vivo* (Compound 31) dont les IC50 sont très faibles comparés à celle du 3-MA précédemment utilisé comme inhibiteur de Vps34 et dont la spécificité est très controversée (tableau 2). Grâce à l'utilisation de Vps34-IN1, Bago *et al* ont montré que Vps34, par sa production de PtdIns3P, entraine l'activation de la SGK3 (grâce à son domaine PX se liant au PtdIns3P) et induit la survie et la prolifération cellulaire. Ce phénomène serait mis en place par les cellules cancéreuses dans le but de contourner l'inhibition prolongée de la voie PI3K-Akt par des inhibiteurs de PI3K de classe I afin de continuer à proliférer (Bago et al., 2014; Bago et al., 2016; Bilanges and Vanhaesebroeck, 2014). Ronan *et al* ont décrit l'effet du deuxième inhibiteur de Vps34, le SAR405, sur la fusion endosome-lyososome et le flux autophagique. De plus, ils ont montré qu'en traitant des cellules tumorales de rein avec SAR405 en combinaison de l'inhibiteur de mTOR (everolimus), la prolifération cellulaire est significativement diminuée (Ronan et al., 2014). Enfin, le développement récent par le même groupe d'un inhibiteur de Vps34 actif *in vivo* (Compound 31) permettra de tester son efficacité directement sur le modèle animal (Pasquier et al., 2015).

D) Rôles des PI3Ks dans les plaquettes

Au cours de ma thèse j'ai eu l'opportunité de rédiger une revue générale qui résume la place des PI3Ks dans les plaquettes (Valet et al., 2016).

Publication n°1

The role of class I, II and III PI 3-kinases in platelet production and activation and their implication in thrombosis.

Colin Valet[a], Sonia Severin[a], Gaetan Chicanne[a], Pierre-Alexandre Laurent[a], Frederique Gaits-Iacovoni[a], Marie-Pierre Gratacap[a], Bernard Payrastre[a,b]

[a]Inserm U1048, I2MC and Universite Paul Sabatier, 31432, Toulouse Cedex 04, France
[b]CHU de Toulouse, Laboratoire d'Hematologie, 31059, Toulouse Cedex 03, France

Review in Advances in Biological Regulation 2016; 61: 33-41

Advances in Biological Regulation xxx (2015) 1–9

Contents lists available at ScienceDirect

Advances in Biological Regulation

journal homepage: www.elsevier.com/locate/jbior

The role of class I, II and III PI 3-kinases in platelet production and activation and their implication in thrombosis

Colin Valet [a], Sonia Severin [a], Gaëtan Chicanne [a], Pierre Alexandre Laurent [a], Frédérique Gaits-Iacovoni [a], Marie-Pierre Gratacap [a], Bernard Payrastre [a, b, *]

[a] Inserm U1048, I2MC and Université Paul Sabatier, 31432, Toulouse Cedex 04, France
[b] CHU de Toulouse, Laboratoire d'Hématologie, 31059, Toulouse Cedex 03, France

ARTICLE INFO

Article history:
Received 7 October 2015
Received in revised form 23 November 2015
Accepted 25 November 2015
Available online xxx

Keywords:
PI 3-kinase isoforms
Platelets
Thrombosis
Signal transduction

ABSTRACT

Blood platelets play a pivotal role in haemostasis and are strongly involved in arterial thrombosis, a leading cause of death worldwide. Besides their critical role in pathophysiology, platelets represent a valuable model to investigate, both in vitro and in vivo, the biological roles of different branches of the phosphoinositide metabolism, which is highly active in platelets. While the phospholipase C (PLC) pathway has a crucial role in platelet activation, it is now well established that at least one class I phosphoinositide 3-kinase (PI3K) is also mandatory for proper platelet functions. Except class II PI3Kγ, all other isoforms of PI3Ks (class I α, β, γ, δ; class II α, β and class III) are expressed in platelets. Class I PI3Ks have been extensively studied in different models over the past few decades and several isoforms are promising drug targets to treat cancer and immune diseases. In platelet activation, it has been shown that while class I PI3Kδ plays a minor role, class I PI3Kβ has an important function particularly in thrombus growth and stability under high shear stress conditions found in stenotic arteries. This class I PI3K is a potentially interesting target for antithrombotic strategies. The role of class I PI3Kα remains ill defined in platelets. Herein, we will discuss our recent data showing the potential impact of inhibitors of this kinase on thrombus formation.

The role of class II PI3Kα and β as well as class III PI3K (Vps34) in platelet production and function is just emerging. Based on our data and those very recently published in the literature, we will discuss the impact of these three PI3K isoforms in platelet production and functions and in thrombosis.

Contents

* Corresponding author. Inserm U1048, I2MC and Université Paul Sabatier, 31432, Toulouse Cedex 04, France.
E-mail address: bernard.payrastre@inserm.fr (B. Payrastre).

http://dx.doi.org/10.1016/j.jbior.2015.11.008
2212-4926/

1. Introduction

Platelet plug formation at sites of vascular damage is essential to prevent bleeding. However, formation of a platelet thrombus can be detrimental following atherosclerotic plaque rupture leading to atherothrombosis and eventually to ischemic complications, a major cause of death and disability worldwide (Jackson, 2011). Besides their critical role in haemostasis and thrombosis platelets have long been used as a model to investigate the different aspects of the phosphoinositide (PIs) metabolism in the regulation of various primary cell functions. Accumulating evidence indicates that PIs are crucial molecules in platelet signaling (Min and Abrams, 2013). Several data also suggest that these bioactive lipids are strongly involved in the production of normal platelets by megakaryocytes (Mountford et al., 2015; Valet et al., 2015; Wang et al., 2008).

Platelet plug formation is a highly regulated process involving multistep adhesion mechanisms and the coordination of complex intracellular signaling mechanisms (Furie and Furie, 2008; Jackson et al., 2009). Briefly, following a vascular injury, platelets tether to von Willebrand factor (vWF) and collagen leading to integrin-dependent stable adhesion to the subendothelial matrix. The soluble agonists secreted by activated platelets, including adenosine diphosphate (ADP) and thromboxane A_2 (TXA_2), or agonist generated by the coagulation cascade such as thrombin, will amplify platelet activation leading to aggregation between platelets and stabilization of the thrombus (Ruggeri, 2007; Ruggeri and Mendolicchio, 2007; Smyth et al., 2009; Varga-Szabo et al., 2008).

It is well established that phospholipases C (PLC) activation, leading to the production of the second messengers inositol trisphosphate (IP3) and diacylglycerol (DAG), is crucial for platelet activation (Harper and Poole, 2010; Varga-Szabo et al., 2009). Accumulating evidence indicates that phosphoinositide 3-kinases (PI3Ks) are also strongly involved in different aspects of platelet production and activation. All class I PI3K isoforms, class II PI3Kα and β as well as class III PI3K are expressed in platelets. Class I PI3Ks generate the lipid second messenger phosphatidylinositol 3,4,5 trisphosphate (PtdIns(3,4,5)P_3) at the plasma membrane upon cell stimulation. This lipid has the remarkable property to interact with several proteins to organize, in a spatio-temporal manner, functional intracellular signaling complexes. One of the best characterized PtdIns(3,4,5)P_3-dependent signaling pathway involves the activation of the protein kinase Akt (or protein kinase B, PKB). Using biochemical and genetic approaches, several groups have shown that class I PI3Kβ is an important player in platelet signaling (Bodin et al., 2003; Canobbio et al., 2009; Jackson et al., 2005; Martin et al., 2010). Since its inhibition prevents occlusive thrombus formation in mouse, rat and dog with a limited increase in bleeding risk and acceptable safety in humans, this lipid kinase is proposed as a potential target for antithrombotic therapy (Jackson et al., 2005; Nylander et al., 2012, 2015). However, the implication of class I PI3Kβ in thrombus stability at high shear rate raises the question of potential secondary ischemic events in the microcirculation due to possible formation of platelet emboli following inhibition of this kinase (Laurent et al., 2015). Class I PI3Kδ is minimally implicated in platelet activation processes. Class I PI3Kγ is mainly activated downstream the ADP receptor and contributes to platelet activation (Hirsch et al., 2006). The role of class I PI3Kα remains poorly characterized although recent data suggest an implication of this kinase in platelet priming and activation by collagen.

Class II and III PI3Ks do not produce PtdIns(3,4,5)P_3 but are thought to synthesize PtdIns3P and, in addition for class II, PtdIns(3,4)P_2. PtdIns3P is implicated in the regulation of vesicular trafficking, especially in the endosomal system and in autophagy. Presently, these kinases are the subject of intense studies but their role in megakaryocytes and platelets remains poorly understood. However, two very recent studies have revealed an unexpected role of class II PI3Kα in the control of the membrane structure of megakaryocytes and platelets (Mountford et al., 2015, Valet et al., 2015). Moreover, a recent publication suggests that, through the regulation of autophagy, class III PI3K plays an important role in platelets (Feng et al., 2014).

In this review, we will briefly discuss the contribution of the different class I PI3K isoforms in platelet activation, thrombus growth and stability and will comment the recent findings demonstrating an important biochemical and physiological role of class II PI3Kα in platelet production and functions. The potential contribution of class III PI3K in these processes will also be discussed.

2. Class I PI3Ks in platelets

Class I enzymes are best characterized and further subdivided into class IA (p110α, p110β and p110δ) and class IB (p110γ). Class I PI3K subunits have a relatively broad tissue distribution with however an enrichment of p110γ and p110δ in leukocytes.

Please cite this article in press as: Valet, C., et al., The role of class I, II and III PI 3-kinases in platelet production and activation and their implication in thrombosis, Advances in Biological Regulation (2015), http://dx.doi.org/10.1016/j.jbior.2015.11.008

At the cellular level, class I PI3K contribute to many processes ranging from cell proliferation and survival to immunity, cancer, metabolism and cardiovascular control through their activation by cell surface receptors, inducing synthesis of the phosphoinositide lipid signal, PIP_3. PIP_3 influences the function of numerous direct PIP_3-binding proteins such as Akt and PDK1 kinases, GTPase exchange factors such as P-REX and cytohesin family of ARF-GAP proteins. Both p110α and p110β play important and distinct roles in angiogenesis and thrombosis and in insulin metabolism, growth and development whereas p110γ and p110δ are implicated in immune functions (Kriplani et al., 2015).

Class IA PI3Ks are composed of a catalytic subunit (p110α, β or δ) associated with a SH2-containing regulatory subunit (p85, p50 or p55). Following cell stimulation, the regulatory subunit binds to phosphorylated tyrosine residues with a preference for a Y(P)xxM motifs (where x is any amino acid) leading to activation of the catalytic subunit downstream of receptor tyrosine-kinase (Fruman, 2010). In contrast, the catalytic subunit of class IB PI3K (p110γ) associates with p101 or p84 regulatory subunits which bind Gβγ subunits allowing activation of p110γ by G-protein coupled receptors (Hawkins et al., 2006; Vanhaesebroeck et al., 2010). It is noteworthy that class IA p110β can directly bind Gβγ subunits (Dbouk et al., 2012) and by doing so be activated by G-protein coupled receptors including in platelets (Martin et al., 2010). Moreover, the catalytic subunits of class I PI3K isoforms have a Ras-binding domain (RBD) and the Ras GTPase has been shown to activate several of these isoforms (Vanhaesebroeck et al., 2010).

All class I PI3Ks are expressed in platelets (Jackson et al., 2004) and form the lipid second messenger PtdIns(3,4,5)P_3 at the plasma membrane upon cell stimulation (Anderson and Jackson, 2003). This lipid recruits signaling proteins, mainly through their PH domain, to generate a steric environment favorable for protein interactions and activation. Hence, classes I PI3Ks are key spatio-temporal organizers of specific signalosomes at the plasma membrane in response to cell activation. This critical role of class I PI3Ks is downregulated by the action of specific PtdIns(3,4,5)P_3 phosphatases such as PTEN and SHIP1. It is important to note that class I PI3Ks have also protein scaffolding properties that may contribute to their signaling function (Ciraolo et al., 2008; Hirsch et al., 2009; Jia et al., 2008; Patrucco et al., 2004).

Since this review focuses on summarize the role of the different isoforms of class I PI3K in platelet activation and thrombosis, more detailed description can be found in recent reviews (Gratacap et al., 2011; Guidetti et al., 2015; Jackson and Schoenwaelder, 2010; Laurent et al., 2014).

2.1. PI3Kδ

P110δ-deficient mice are viable, have a normal platelet count and do not exhibit a bleeding disorder. PI3Kδ is highly expressed in leucocytes but much less in platelets. Mouse platelets expressing a catalytically inactive form of the enzyme or deficient for this enzyme have only a slight spreading defect in static conditions on fibrinogen or vWF (Senis et al., 2005; Zhang et al., 2002). Thus, PI3Kδ is thought to have a very weak implication in the regulation of platelet functions. Consistent with this conclusion, no side effect related to bleeding has been so far reported in patients with B-cell malignancies treated with a selective inhibitor of this enzyme (idelalisib).

2.2. PI3Kγ

Mice deficient for PI3Kγ or expressing an inactive form of p110γ have a normal platelet count and no bleeding phenotype but are protected against ADP-induced platelet-dependent thromboembolic vascular occlusion (Hirsch et al., 2001). In platelets, PI3Kγ appears mainly involved downstream of the $P2Y_{12}$ receptor for ADP, a G-protein coupled receptor also able to activate PI3Kβ (Canobbio et al., 2009; Cosemans et al., 2006; Martin et al., 2010; Schoenwaelder et al., 2007; van der Meijden et al., 2008; Woulfe et al., 2002). PI3Kγ may regulate the adhesive function of the integrin αIIbβ3 downstream of $P2Y_{12}$ through a catalytic and a non-catalytic mechanism (Schoenwaelder et al., 2007). A combined catalytic function of PI3Kβ and non-catalytic function of PI3Kγ may contribute to ADP receptor $P2Y_{12}$/Gi signaling (Schoenwaelder et al., 2007).

2.3. PI3Kβ

As shown by the development of different mouse models and the use of selective inhibitors, the catalytic activity of PI3Kβ is critical for platelet function (Canobbio et al., 2009; Jackson et al., 2005; Martin et al., 2010; Nylander et al., 2012). PI3Kβ is essential downstream of the collagen receptor GPVI as it allows an efficient activation of PLCγ2 and Ca^{2+} mobilization. An optimal mode of activation of p110β in platelets appears to involve βγ subunits from Gi (mainly downstream of $P2Y_{12}$) and tyrosine kinases (through the ITAM-signaling). Different groups have shown that PI3Kβ is essential for the sustained activation of the integrin αIIbβ3 and for the αIIbβ3 outside-in signaling through complex mechanisms involving Rap1b and other signaling actors that remain to be fully characterized (Canobbio et al., 2009; Guidetti and Torti, 2012). Recent studies have reported an important role for a PI3K in the Rasa3/Rap1b signaling which is important for megakaryocyte development and platelet activation downstream of $P2Y_{12}$ (Schurmans et al., 2015; Stefanini et al., 2015). PI3Kβ is also important downstream of other integrins such as α2β1 where its activation requires the tyrosine kinase PYK2 (Consonni et al., 2012). The implication of PI3Kβ in the outside-in signaling of platelet integrins is particularly important under the high shear stress situation that is found in stenotic arteries. Indeed, we recently demonstrated that invalidation or pharmacological inhibition of PI3Kβ leads to a high instability of the thrombus formed at high shear rate (Laurent et al., 2015). Interestingly, in the absence of PI3Kβ, inhibition of GSK3 can restore thrombus stability suggesting that the control of platelet thrombus stability at high shear rate

Please cite this article in press as: Valet, C., et al., The role of class I, II and III PI 3-kinases in platelet production and activation and their implication in thrombosis, Advances in Biological Regulation (2015), http://dx.doi.org/10.1016/j.jbior.2015.11.008

requires the PI3Kβ/Akt/GSK3 signaling axis. These observations are important since PI3Kβ is proposed as an antithrombotic drug target having modest effect on bleeding but significantly decreasing the risk of occlusive arterial thrombosis (Jackson et al., 2005; Martin et al., 2010; Nylander et al., 2012). A phase I clinical trial with the selective PI3Kβ inhibitor AZD6482 has shown a reduction in shear-induced human platelet activation ex vivo without increasing skin bleeding time and no major drug-induced adverse events (Nylander et al., 2012). A second study has recently shown the advantage of combining AZD6482 and aspirin compared with the current classical antithrombotic treatment associating clopidogrel with aspirin (Nylander et al., 2015). Indeed, this combination provides a potential for greater overall antiplatelet effect with significantly less bleeding potential. However, our data concerning the role of PI3Kβ in thrombus stability point to a potential risk of distal embolization of thrombotic material on treatment with PI3Kβ inhibitors (Laurent et al., 2015). Whether a combination with aspirin will reduce platelet emboli shedding at high shear rate or dissolve released platelet emboli preventing potential occlusion of downstream microvessels remains to be investigated. Thus, while a series of convergent studies suggest that inhibition of PI3Kβ represents an interesting new potential antithrombotic strategy, the benefit-risk ratio remains to be further evaluated.

2.4. PI3Kα

A role for PI3Kα in the potentiating effect of IGF-1 on platelet aggregation induced by low doses of agonists including ADP, thrombin or collagen has been suggested (Blair et al., 2014; Hers, 2007; Kim et al., 2007; Motani et al., 1996). Inhibition of PI3Kα also partly affects Akt phosphorylation downstream of GPVI (Kim et al., 2009). It appears that PI3Kα and PI3Kβ are involved downstream of GPVI in a non-redundant way since both isoforms are required for full PLCγ2 activation, IP_3 formation, Ca^{2+} mobilization and Rap1b activation (Gilio et al., 2009; Kim et al., 2009; Larson et al., 2003). Recently, we have generated a mouse model in which PI3Kα (p110α) is selectively deleted in the megakaryocyte lineage (Laurent et al., 2015) and obtained data suggesting that the absence of PI3Kα in platelets does not increase the tail bleeding time of the animals but leads to a consistent decrease in thrombus formation in vivo, possibly due to a reduced adhesion of platelets on collagen and vWF. However, in contrast to PI3Kβ, our data clearly show that PI3Kα is not required for thrombus stability even at very high pathological shear rate.

PI3Kα is an important target in cancer therapy and several selective inhibitors are under development as anticancer drugs (Sabbah et al., 2015). The results of our experimental studies suggest that such inhibitors, used alone, should have moderated effects on haemostasis and on the bleeding risk.

3. Class II PI3Ks and their role in platelets

The class II PI3Ks (PI3KC2) is composed of three isoforms called α, β and γ. While the α and β isoforms are ubiquitously expressed, the γ isoform has a more restrictive tissue expression (mainly liver, prostate, breast, salivary glands) (El Sheikh et al., 2003). Class II PI3Ks are unique monomers and so far no regulatory subunit able to modulate their activity has been identified. Class II PI3Ks phosphorylate the position 3 of the inositol ring of phosphatidylinositol (PtdIns) and/or PtdIns4P to produce PtdIns3P and PtdIns(3,4)P_2, respectively (Maffucci and Falasca, 2014). Because of the lack of selective pharmacological inhibitors and the recent development of relevant mouse models, the organismal role of class II PI3Ks remains unclear. The majority of the studies on PI3KC2 have been performed in vitro, revealing a role for this kinase in a variety of processes, depending on the cellular context.

3.1. PI3KC2α

In vitro studies have shown that PI3KC2α is involved in many different aspects of cell biology. Its activity is enhanced by clathrin and plays a major role in endocytosis by regulating clathrin-coated pits maturation and scission through PtdIns(3,4)P_2 production (Gaidarov et al., 2001; Posor et al., 2013). In addition, PI3KC2α has been shown to contribute to exocytosis, particularly to insulin secretion, neurosecretory granule release and antigen-induced degranulation (Dominguez et al., 2011; Meunier et al., 2005; Nigorikawa et al., 2014). PI3KC2α, via PtdIns3P production and subsequent activation of the small GTPase TC10, is also involved in glucose transport by regulating GLUT4 translocation to the plasma membrane upon insulin stimulation (Maffucci et al., 2003). PI3KC2α mRNA level have been found decreased in islets from type 2 diabetic patients (Dominguez et al., 2011) suggesting a potential role of this kinase in type 2 diabetes development. In vascular smooth muscle cells, PI3KC2α regulates the KCl, noradrenaline and ionomycin induced contraction by regulating the RhoA/Myosin Light Chain pathway (Wang et al., 2006). An increased PI3KC2α activity has been described in aorta and mesenteric arteries following KCl stimulation, associated to increased RhoA activation and MYPT1 phosphorylation (Seok et al., 2010). A role of PI3KC2α in cell survival, through caspase 9 and PARP (poly-ADP-ribose-polymerase) regulation and independently of the Akt/GSK3 pathway, has also been proposed (Elis et al., 2008; Eun et al., 2010) suggesting a potential implication of this kinase in cancer.

The recent generation of mouse models, genetically modified on the endogenous PI3KC2α gene, has shed some light on the in vivo physiological role of PI3KC2α. The first mouse model was generated by gene-trapping strategy targeting PI3KC2α PX and C2 domains inducing significant reduction of PI3KC2α protein expression and activity with a residual truncated form still detectable in brain and liver (Harris et al., 2011). These mice have a decreased survival curves along with a reduced body

Please cite this article in press as: Valet, C., et al., The role of class I, II and III PI 3-kinases in platelet production and activation and their implication in thrombosis, Advances in Biological Regulation (2015), http://dx.doi.org/10.1016/j.jbior.2015.11.008

weight at 6 weeks. Blood and urine parameters of these mice demonstrated a chronic renal failure associated to histological lesions revealing a glomerulonephropathy (Harris et al., 2011). Following this study, three laboratories have generated different mouse models with total deletions of PI3KC2α. They all found that total deletion of PI3KC2α leads to an embryonic lethality between E10.5 and 12.5 (Franco et al., 2014; Mountford et al., 2015, Yoshioka et al., 2012). Franco et al. have reported that the role of PI3KC2α in embryonic development is related to the production of PtdIns3P at the base of the primary cilium. This PtdIns3P pool appears essential for Rab11 relocation at the pericentriolar recycling compartment and the subsequent Rab11 and Rab8 activation, leading to primary cilium elongation, Smo ciliary translocation and Sonic Hedgehog signaling. Yoshioka et al. have shown a key role for PI3KC2α in endothelial cells in the context of normal angiogenesis and vascular barrier integrity, which are crucial during embryonic development. Loss of PI3KC2α-derived PtdIns3P leads to a defective endosomal trafficking inducing the loss of vascular endothelial-cadherine recruitment at the endothelial cell junctions. Thus, these reports highlight a crucial role for PtdIns3P produced by PI3KC2α in embryogenesis through its role in the spatio-temporal control of protein trafficking. Overall, in vitro and in vivo data point to a crucial role of this kinase in the regulation of critical cell functions but they are still incomplete and a clear idea of the role of PI3KC2α is lacking.

What can be the role of PI3KC2α in platelet production and functions?

Until very recently, the only report suggesting a potential role of class II PI3Ks in platelets was published 17 years ago by the group of S. Rittenhouse (Zhang et al., 1998). However, two independent laboratories have just published data describing the in vivo role of PI3KC2α in megakaryocytes and platelets (Mountford et al., 2015; Valet et al., 2015). To override the embryonic lethality of PI3KC2α deletion, two different mouse models were developed in these studies. Mountford et al. (Mountford et al., 2015) developed an inducible PI3KC2α global deletion by shRNA gene targeting, while our group used a model of partial inactivation of PI3KC2α kinase activity by point mutation in the endogenous PI3KC2α gene (Valet et al., 2015). Overall, the data obtained with theses mouse models point to a novel role for PI3KC2α in membrane structure and remodeling with consequences on platelet production and functions. Mountford et al. have reported that PI3KC2α-deficient platelets have an enlarged open canalicular system leading to an enhanced membrane tether formation when platelets are perfused over a vWF matrix. Moreover, using the model of partial inactivation of PI3KC2α kinase activity, our group has also observed the enlarged open canalicular system and a significant percentage of platelets with tortuous and invaginated plasma membrane. This major defect in membrane ultrastructure is associated with changes in the biophysical properties of platelet membranes including reduced platelet elasticity, as shown by atomic force microscopy, and membrane dynamics, as highlighted by a deficiency in filopodia formation. This platelet membrane phenotype was associated with a significant enrichment of the so-called barbell-shaped proplatelets in the bloodstream (Valet et al., 2015). This recently discovered intermediate stage of platelet formation is normally hardly detectable in the circulation (<1% of total platelets). In the two studies, platelet membrane alterations were correlated to abnormal demarcation membrane system in megakaryocytes, showing that membrane defects in platelets are inherited from megakaryocytes and are not only intrinsic to platelets. Interestingly, these membrane defects were associated with a reduced recruitment of several membrane skeleton proteins including spectrin and myosin and a defective link between plasma membrane and cytoskeleton (Valet et al., 2015). Thus, these two studies reveal a novel role for PI3KC2α in membrane structure and dynamics. They also show that PI3KC2α is not responsible for the agonist-inducible pools of PtdIns3P and PtdIns(3,4)P_2. However, while Mountford et al. concluded that PI3KC2α was acting on membrane structure by a mechanism independent of phosphoinositides, our group could show, by using a specific mass assay (Chicanne et al., 2012), that PI3KC2α was necessary for the production of a housekeeping pool of PtdIns3P in platelets. How this housekeeping pool of PtdIns3P can regulate membrane skeleton integrity remains an open question. A PtdIns3P interactome study on colorectal cancer cell line has revealed that spectrin, myosin and filamin can interact with PtdIns3P (Catimel et al., 2013). It is thus tempting to speculate that the housekeeping pool of PtdIns3P produced by PI3KC2α is involved in the recruitment of important proteins of the membrane skeleton. PtdIns3P is known to regulate early endosome maturation and vesicular trafficking, which may indirectly contribute to the adequate localization of membrane skeleton proteins.

What are the consequences of this defect of platelet membrane structure and dynamics on platelet functions? Mountford et al. (Mountford et al., 2015) have shown the formation of large and unstable thrombi in the absence of platelet PI3KC2α in vivo. The tail bleeding time of their mouse model was normal but following hirudin treatment, to prevent the effect of thrombin produced through the coagulation cascade, the tail bleeding time increased as PI3KC2α protein expression decreased. In contrast, in our mouse model, where PI3KC2α is expressed but 50% of it is inactive, we observed a decreased thrombus formation with smaller but stable thrombi in ex vivo flow assays. Moreover, a delayed arterial thrombus formation was observed in vivo, without affecting the tail bleeding time. These discrepancies may be explained by the use of two quite different mouse models. In contrast to the model used by Mountford et al. where the protein is not or minimally expressed, the kinase-inactivated PI3KC2α mouse model, which mimics a treatment with low doses of an inhibitor, may limit the emergence of compensatory mechanisms by other PI3Ks that could happen in deficient mouse models. Importantly, this model prevents the loss of a potential scaffolding role of the PI3KC2α.

Thus, overall, these two recent studies show that PI3KC2α plays a critical role in the production of platelets and impacts on their prothrombotic functions. PI3KC2α appears to control the production of a housekeeping pool of PtdIns3P, the regulation of membrane skeleton organization and in turn the membrane structure and dynamics. These studies shed new light on the role of this class II PI3K and will stimulate further studies to better understand the molecular mechanisms involving PIs in the production of mature platelets.

Please cite this article in press as: Valet, C., et al., The role of class I, II and III PI 3-kinases in platelet production and activation and their implication in thrombosis, Advances in Biological Regulation (2015), http://dx.doi.org/10.1016/j.jbior.2015.11.008

3.2. PI3KC2β

PI3KC2β has been less studied than PI3KC2α and its organismal role remains unknown. The knock-out of PI3KC2β in mouse has no impact on viability and fertility and these mice have normal epidermal growth, differentiation and wound healing (Harada et al., 2005). However, evidence is accumulating that PI3KC2β plays a role in cell migration. Down-regulation of PI3KC2β decreases LPA-dependent migration of ovarian and cervical cancer line (Maffucci et al., 2005), while its over-expression enhances cell motility, lamellipodia and filopodia formation and decreases cell adhesion (Domin et al., 2005). These studies have pointed to a role of PI3KC2β-derived PtdIns3P production in cell migration (Domin et al., 2005; Maffucci et al., 2005). Overexpression of PI3KC2β also increases proliferation of epidermoid carcinoma cell line cells and inhibits apoptosis in neuroblastoma cells (Das et al., 2007; Katso et al., 2006). Amplification of PI3KC2β mRNA has been observed in glioblastomas (Knobbe and Reifenberger, 2003) suggesting a potential implication of PI3KC2β in cancer.

In platelets, the study from S. Rittenhouse laboratory indirectly suggested that PI3KC2β could act downstream of $\alpha_{IIb}\beta_3$ integrin (Zhang et al., 1998). Recently, Mountford et al. (Mountford et al., 2015) have shown that the global deletion of PI3KC2β has no impact on platelet count and size and on platelet morphology and functions. Accordingly, PI3KC2β-depleted mice have a normal tail bleeding time. Biochemical analysis did not reveal an implication of PI3KC2β in basal or agonist-induced pools of PtdIns3P or PtdIns(3,4)P_2. The question of a potential redundancy between the α and β isoform of PI3KC2 in platelets remains open since some data obtained by Mountford and al (Mountford et al., 2015) suggest that the role of the β isoform may only be revealed when the α isoform is absent. Although this isoforms appears less important than PI3KC2α, further investigations are needed to fully understand its role in platelets and megakaryocytes.

4. Class III PI3K (Vps34) and its role in platelets

Class III PI3K, also known as Vps34, is the most ancient form of PI3Ks and the only PI3K found in yeast where it plays an essential role in vacuolar trafficking (Herman and Emr, 1990). It is thought that Vps34 phosphorylates PtdIns to generate PtdIns3P, a central phospholipid for the regulation of membrane trafficking. In mammalian cells, Vps34 has been found to regulate endocytic trafficking, autophagosome formation and mTOR activation (Backer, 2008; Vanhaesebroeck et al., 2010). The organismal role of mammalian Vps34 has been investigated recently by the development of mouse gene targeting studies. Loss of Vps34 expression in mouse causes early embryonic lethality (between E7.5 and E8.5) (Zhou et al., 2011). Using the cre-lox system an important role for Vps34 was revealed in heart and liver functions (Jaber et al., 2012), in T cells (Willinger and Flavell, 2012), in podocytes (Bechtel et al., 2013), in skeletal muscle homeostasis (Reifler et al., 2014) and in sensory, cortical and hippocampal neurons integrity (Wang et al., 2011; Zhou et al., 2010). In most cases, dysregulation of multiples aspects of the endocytic/endosomal and/or the autophagic pathways were proposed.

As shown these last years, intra-cellular vesicular trafficking and autophagy are important processes in megakaryocytes and platelets (Feng et al., 2014; Ouseph et al., 2015; Zucker-Franklin, 1981). Using the poorly specific Vps34 inhibitor, 3-methyladenine (3-MA), Feng et al. have recently suggested that autophagy is Vps34 activity-dependent in platelets and that this inhibitor can inhibit collagen and thrombin-induced platelet aggregation (Feng et al., 2014). These data should stimulate further research to decipher the still elusive role of Vps34 in megakaryocyte and platelet biology. The use of highly potent and specific Vps34 inhibitors that have been recently developed (Bago et al., 2014; Ronan et al., 2014) and/or mice models targeting Vps34 specifically in megakaryocyte/platelet lineage will be essential in this quest.

5. Concluding remarks

The class I PI3Ks, particularly the β, α and γ isoforms, plays an important role in the regulation of platelet signaling downstream of various receptors and integrins. PI3Kβ is especially involved in the complex mechanisms of thrombus formation and stability under high shear stress. Targeting this lipid kinase may be relevant to develop a new antithrombotic strategy since class I PI3Kβ inhibitors reduce the risk of occlusive thrombosis in the arterial circulation without increasing the bleeding risk. Further work should tell us if this strategy might be more efficient and safer than the currently used antithrombotic agents. A particularly important point will be to show that the risk of distal embolization, due to platelet emboli shedding at high shear rate, is not a potential consequence of such a treatment. A combination of class I PI3Kβ inhibitors with other antithrombotic agents such as aspirin may be of interest to reduce this potential risk and reach an efficient antithrombotic effect. This strategy may be helpful in certain pathological or surgical situations. The role of class I PI3Kα in platelets remains to be fully understood, particularly since this isoforms is a major target in cancer therapy. The effects of drugs targeting signaling enzymes on platelet activation have to be considered in clinical practice. This is exemplified by dasatinib (Gratacap et al., 2009) or more recently by ibrutinib, the inhibitor of the tyrosine kinase Btk (one of the class I PI3K downstream effector), which affects platelet activation and induces bleeding in patients (Levade et al., 2014). The bleeding risk is particularly important when these drugs are used in combination with commonly used antithrombotic agents such as aspirin and $P2Y_{12}$ antagonists. The role of class II and III PI3K in platelets is just emerging and further work will be necessary to understand the mechanisms they regulate. These kinases are thought to be less specialized in signaling compared to class I PI3Ks but they contribute to membrane dynamics, vesicular trafficking and autophagy, which are very important processes during megakaryocyte differentiation and platelet maturation. The results of recent studies on class II and class III PI3K

Please cite this article in press as: Valet, C., et al., The role of class I, II and III PI 3-kinases in platelet production and activation and their implication in thrombosis, Advances in Biological Regulation (2015), http://dx.doi.org/10.1016/j.jbior.2015.11.008

isoforms in megakaryocytes/platelets open a new field for platelet biology research with many exciting questions that will help understanding the complex mechanisms regulating platelet production, maturation and functions.

Conflict of interest

The authors declare no competing financial interests.

Acknowledgments

Our work is funded by grants from INSERM, Fondation de France (Cardiovasculaire 2015) and Fondation pour la Recherche Médicale (grant number DPC20111122988 to M.-P.G.). B.P. is a scholar of the Institut Universitaire de France.

References

Anderson, K.E., Jackson, S.P., 2003. Class I phosphoinositide 3-kinases. Int. J. Biochem. Cell Biol. 35, 1028–1033.
Backer, J.M., 2008. The regulation and function of class III PI3Ks: novel roles for Vps34. Biochem. J. 410, 1–17.
Bago, R., Malik, N., Munson, M.J., Prescott, A.R., Davies, P., Sommer, E., et al., 2014. Characterization of VPS34-IN1, a selective inhibitor of Vps34, reveals that the phosphatidylinositol 3-phosphate-binding SGK3 protein kinase is a downstream target of class III phosphoinositide 3-kinase. Biochem. J. 463, 413–427.
Bechtel, W., Helmstadter, M., Balica, J., Hartleben, B., Kiefer, B., Hrnjic, F., et al., 2013. Vps34 deficiency reveals the importance of endocytosis for podocyte homeostasis. J. Am. Soc. Nephrol. JASN 24, 727–743.
Blair, T.A., Moore, S.F., Williams, C.M., Poole, A.W., Vanhaesebroeck, B., Hers, I., 2014. Phosphoinositide 3-kinases p110alpha and p110beta have differential roles in insulin-like growth factor-1-mediated Akt phosphorylation and platelet priming. Arterioscler. Thromb. Vasc. Biol. 34, 1681–1688.
Bodin, S., Viala, C., Ragab, A., Payrastre, B., 2003. A critical role of lipid rafts in the organization of a key FcgammaRIIa-mediated signaling pathway in human platelets. Thromb. Haemost. 89, 318–330.
Canobbio, I., Stefanini, L., Cipolla, L., Ciraolo, E., Gruppi, C., Balduini, C., et al., 2009. Genetic evidence for a predominant role of PI3K{beta} catalytic activity in ITAM- and integrin-mediated signaling in platelets. Blood 114, 2193–2196.
Catimel, B., Kapp, E., Yin, M.X., Gregory, M., Wong, L.S., Condron, M., et al., 2013. The PI(3)P interactome from a colon cancer cell. J. Proteom. 82, 35–51.
Chicanne, G., Severin, S., Boscheron, C., Terrisse, A.D., Gratacap, M.P., Gaits-Iacovoni, F., et al., 2012. A novel mass assay to quantify the bioactive lipid PtdIns3P in various biological samples. Biochem. J. 447, 17–23.
Ciraolo, E., Iezzi, M., Marone, R., Marengo, S., Curcio, C., Costa, C., et al., 2008. Phosphoinositide 3-kinase p110beta activity: key role in metabolism and mammary gland cancer but not development. Sci. Signal. 1, ra3.
Consonni, A., Cipolla, L., Guidetti, G., Canobbio, I., Ciraolo, E., Hirsch, E., et al., 2012. Role and regulation of phosphatidylinositol 3-kinase beta in platelet integrin alpha2beta1 signaling. Blood 119, 847–856.
Cosemans, J.M., Munnix, I.C., Wetzker, R., Heller, R., Jackson, S.P., Heemskerk, J.W., 2006. Continuous signaling via PI3K isoforms beta and gamma is required for platelet ADP receptor function in dynamic thrombus stabilization. Blood 108, 3045–3052.
Das, M., Scappini, E., Martin, N.P., Wong, K.A., Dunn, S., Chen, Y.J., et al., 2007. Regulation of neuron survival through an intersectin-phosphoinositide 3'-kinase C2beta-AKT pathway. Mol. Cell. Biol. 27, 7906–7917.
Dbouk, H.A., Vadas, O., Shymanets, A., Burke, J.E., Salamon, R.S., Khalil, B.D., et al., 2012. G protein-coupled receptor-mediated activation of p110beta by gbetagamma is required for cellular transformation and invasiveness. Sci. Signal. 5, ra89.
Domin, J., Harper, L., Aubyn, D., Wheeler, M., Florey, O., Haskard, D., et al., 2005. The class II phosphoinositide 3-kinase PI3K-C2beta regulates cell migration by a PtdIns3P dependent mechanism. J. Cell. Physiol. 205, 452–462.
Dominguez, V., Raimondi, C., Somanath, S., Bugliani, M., Loder, M.K., Edling, C.E., et al., 2011. Class II phosphoinositide 3-kinase regulates exocytosis of insulin granules in pancreatic beta cells. J. Biol. Chem. 286, 4216–4225.
El Sheikh, S.S., Domin, J., Tomtitchong, P., Abel, P., Stamp, G., Lalani, E.N., 2003. Topographical expression of class IA and class II phosphoinositide 3-kinase enzymes in normal human tissues is consistent with a role in differentiation. BMC Clin. Pathol. 3, 4.
Elis, W., Triantafellow, E., Wolters, N.M., Sian, K.R., Caponigro, G., Borawski, J., et al., 2008. Down-regulation of class II phosphoinositide 3-kinase alpha expression below a critical threshold induces apoptotic cell death. Mol. Cancer Res. MCR 6, 614–623.
Eun, L.Y., Song, B.W., Cha, M.J., Song, H., Kim, I.K., Choi, E., et al., 2010. Overexpression of phosphoinositide-3-kinase class II alpha enhances mesenchymal stem cell survival in infarcted myocardium. Biochem. Biophys. Res. Commun. 402, 272–279.
Feng, W., Chang, C., Luo, D., Su, H., Yu, S., Hua, W., et al., 2014. Dissection of autophagy in human platelets. Autophagy 10, 642–651.
Franco, I., Gulluni, F., Campa, C.C., Costa, C., Margaria, J.P., Ciraolo, E., et al., 2014. PI3K class II alpha controls spatially restricted endosomal PtdIns3P and Rab11 activation to promote primary cilium function. Dev. Cell 28, 647–658.
Fruman, D.A., 2010. Regulatory subunits of class IA PI3K. Curr. Top. Microbiol. Immunol. 346, 225–244.
Furie, B., Furie, B.C., 2008. Mechanisms of thrombus formation. N. Engl. J. Med. 359, 938–949.
Gaidarov, I., Smith, M.E., Domin, J., Keen, J.H., 2001. The class II phosphoinositide 3-kinase C2alpha is activated by clathrin and regulates clathrin-mediated membrane trafficking. Mol. Cell 7, 443–449.
Gilio, K., Munnix, I.C., Mangin, P., Cosemans, J.M., Feijge, M.A., van der Meijden, P.E., et al., 2009. Non-redundant roles of phosphoinositide 3-kinase isoforms alpha and beta in glycoprotein VI-induced platelet signaling and thrombus formation. J. Biol. Chem. 284, 33750–33762.
Gratacap, M.P., Guillermet-Guibert, J., Martin, V., Chicanne, G., Tronchere, H., Gaits-Iacovoni, F., et al., 2011. Regulation and roles of PI3Kbeta, a major actor in platelet signaling and functions. Adv. Enzyme Regul. 51, 106–116.
Gratacap, M.P., Martin, V., Valera, M.C., Allart, S., Garcia, C., Sie, P., et al., 2009. The new tyrosine-kinase inhibitor and anticancer drug dasatinib reversibly affects platelet activation in vitro and in vivo. Blood 114, 1884–1892.
Guidetti, G.F., Canobbio, I., Torti, M., 2015. PI3K/Akt in platelet integrin signaling and implications in thrombosis. Adv. Biol. Regul. 59, 36–52.
Guidetti, G.F., Torti, M., 2012. The small GTPase Rap1b: a bidirectional regulator of platelet adhesion receptors. J. Signal Transduct. 2012, 412089.
Harada, K., Truong, A.B., Cai, T., Khavari, P.A., 2005. The class II phosphoinositide 3-kinase C2beta is not essential for epidermal differentiation. Mol. Cell. Biol. 25, 11122–11130.
Harper, M.T., Poole, A.W., 2010. Diverse functions of protein kinase C isoforms in platelet activation and thrombus formation. J. Thromb. Haemost. 8, 454–462.
Harris, D.P., Vogel, P., Wims, M., Moberg, K., Humphries, J., Jhaver, K.G., et al., 2011. Requirement for class II phosphoinositide 3-kinase C2alpha in maintenance of glomerular structure and function. Mol. Cell. Biol. 31, 63–80.
Hawkins, P.T., Anderson, K.E., Davidson, K., Stephens, L.R., 2006. Signalling through class I PI3Ks in mammalian cells. Biochem. Soc. Trans. 34, 647–662.
Herman, P.K., Emr, S.D., 1990. Characterization of VPS34, a gene required for vacuolar protein sorting and vacuole segregation in Saccharomyces cerevisiae. Mol. Cell. Biol. 10, 6742–6754.
Hers, I., 2007. Insulin-like growth factor-1 potentiates platelet activation via the IRS/PI3Kalpha pathway. Blood 110, 4243–4252.

Please cite this article in press as: Valet, C., et al., The role of class I, II and III PI 3-kinases in platelet production and activation and their implication in thrombosis, Advances in Biological Regulation (2015), http://dx.doi.org/10.1016/j.jbior.2015.11.008

Hirsch, E., Bosco, O., Tropel, P., Laffargue, M., Calvez, R., Altruda, F., et al., 2001. Resistance to thromboembolism in PI3Kgamma-deficient mice. Faseb J. 15, 2019–2021.
Hirsch, E., Braccini, L., Ciraolo, E., Morello, F., Perino, A., 2009. Twice upon a time: PI3K's secret double life exposed. Trends Biochem. Sci. 34, 244–248.
Hirsch, E., Lembo, G., Montrucchio, G., Rommel, C., Costa, C., Barberis, L., 2006. Signaling through PI3Kgamma: a common platform for leukocyte, platelet and cardiovascular stress sensing. Thromb. Haemost. 95, 29–35.
Jaber, N., Dou, Z., Chen, J.S., Catanzaro, J., Jiang, Y.P., Ballou, L.M., et al., 2012. Class III PI3K Vps34 plays an essential role in autophagy and in heart and liver function. Proc. Natl. Acad. Sci. U. S. A. 109, 2003–2008.
Jackson, S.P., 2011. Arterial thrombosis–insidious, unpredictable and deadly. Nat. Med. 17, 1423–1436.
Jackson, S.P., Nesbitt, W.S., Westein, E., 2009. Dynamics of platelet thrombus formation. J. Thromb. Haemost. 7 (Suppl. 1), 17–20.
Jackson, S.P., Schoenwaelder, S.M., 2010. PI 3-Kinase p110beta regulation of platelet integrin alpha(IIb)beta3. Curr. Top. Microbiol. Immunol. 346, 203–224.
Jackson, S.P., Schoenwaelder, S.M., Goncalves, I., Nesbitt, W.S., Yap, C.L., Wright, C.E., et al., 2005. PI 3-kinase p110beta: a new target for antithrombotic therapy. Nat. Med. 11, 507–514.
Jackson, S.P., Yap, C.L., Anderson, K.E., 2004. Phosphoinositide 3-kinases and the regulation of platelet function. Biochem. Soc. Trans. 32, 387–392.
Jia, S., Liu, Z., Zhang, S., Liu, P., Zhang, L., Lee, S.H., et al., 2008. Essential roles of PI(3)K-p110beta in cell growth, metabolism and tumorigenesis. Nature 454, 776–779.
Katso, R.M., Pardo, O.E., Palamidessi, A., Franz, C.M., Marinov, M., De Laurentiis, A., et al., 2006. Phosphoinositide 3-Kinase C2beta regulates cytoskeletal organization and cell migration via rac-dependent mechanisms. Mol. Biol. Cell 17, 3729–3744.
Kim, S., Garcia, A., Jackson, S.P., Kunapuli, S.P., 2007. Insulin-like growth factor-1 regulates platelet activation through PI3-Kalpha isoform. Blood 110, 4206–4213.
Kim, S., Mangin, P., Dangelmaier, C., Lillian, R., Jackson, S.P., Daniel, J.L., et al., 2009. Role of phosphoinositide 3-kinase beta in glycoprotein VI-mediated Akt activation in platelets. J. Biol. Chem. 284, 33763–33772.
Knobbe, C.B., Reifenberger, G., 2003. Genetic alterations and aberrant expression of genes related to the phosphatidyl-inositol-3'-kinase/protein kinase B (Akt) signal transduction pathway in glioblastomas. Brain Pathol. 13, 507–518.
Kriplani, N., Hermida, M.A., Brown, E.R., Leslie, N.R., Class, I.P.I., 2015. 3-kinases: function and evolution. Adv. Biol. Regul. 59, 53–64.
Larson, M.K., Chen, H., Kahn, M.L., Taylor, A.M., Fabre, J.E., Mortensen, R.M., et al., 2003. Identification of P2Y12-dependent and -independent mechanisms of glycoprotein VI-mediated Rap1 activation in platelets. Blood 101, 1409–1415.
Laurent, P.A., Severin, S., Gratacap, M.P., Payrastre, B., 2014. Class I PI 3-kinases signaling in platelet activation and thrombosis: PDK1/Akt/GSK3 axis and impact of PTEN and SHIP1. Adv. Biol. Regul. 54C, 162–174.
Laurent, P.A., Severin, S., Hechler, B., Vanhaesebroeck, B., Payrastre, B., Gratacap, M.P., 2015. Platelet PI3Kbeta and GSK3 regulate thrombus stability at a high shear rate. Blood 125, 881–888.
Levade, M., David, E., Garcia, C., Laurent, P.A., Cadot, S., Michallet, A.S., et al., 2014. Ibrutinib treatment affects collagen and von Willebrand factor-dependent platelet functions. Blood 124, 3991–3995.
Maffucci, T., Brancaccio, A., Piccolo, E., Stein, R.C., Falasca, M., 2003. Insulin induces phosphatidylinositol-3-phosphate formation through TC10 activation. EMBO J. 22, 4178–4189.
Maffucci, T., Cooke, F.T., Foster, F.M., Traer, C.J., Fry, M.J., Falasca, M., 2005. Class II phosphoinositide 3-kinase defines a novel signaling pathway in cell migration. J. Cell Biol. 169, 789–799.
Maffucci, T., Falasca, M., 2014. New insight into the intracellular roles of class II phosphoinositide 3-kinases. Biochem. Soc. Trans. 42, 1378–1382.
Martin, V., Guillermet-Guibert, J., Chicanne, G., Cabou, C., Jandrot-Perrus, M., Plantavid, M., et al., 2010. Deletion of the p110beta isoform of phosphoinositide 3-kinase in platelets reveals its central role in Akt activation and thrombus formation in vitro and in vivo. Blood 115, 2008–2013.
Meunier, F.A., Osborne, S.L., Hammond, G.R., Cooke, F.T., Parker, P.J., Domin, J., et al., 2005. Phosphatidylinositol 3-kinase C2alpha is essential for ATP-dependent priming of neurosecretory granule exocytosis. Mol. Biol. Cell 16, 4841–4851.
Min, S.H., Abrams, C.S., 2013. Regulation of platelet plug formation by phosphoinositide metabolism. Blood 122, 1358–1365.
Motani, A.S., Anggard, E.E., Ferns, G.A., 1996. Recombinant insulin-like growth factor-1 modulates aggregation in human platelets via extracellular calcium. Life Sci. 58. PL269–74.
Mountford, J.K., Petitjean, C., Putra, H.W., McCafferty, J.A., Setiabakti, N.M., Lee, H., et al., 2015. The class II PI 3-kinase, PI3KC2alpha, links platelet internal membrane structure to shear-dependent adhesive function. Nat. Commun. 6, 6535.
Nigorikawa, K., Hazeki, K., Guo, Y., Hazeki, O., 2014. Involvement of class II phosphoinositide 3-kinase alpha-isoform in antigen-induced degranulation in RBL-2H3 cells. PLoS One 9, e111698.
Nylander, S., Kull, B., Bjorkman, J.A., Ulvinge, J.C., Oakes, N., Emanuelsson, B.M., et al., 2012. Human target validation of phosphoinositide 3-kinase (PI3K) beta: effects on platelets and insulin sensitivity, using AZD6482 a novel PI3Kbeta inhibitor. J. Thromb. Haemost. 10, 2127–2136.
Nylander, S., Wagberg, F., Andersson, M., Skarby, T., Gustafsson, D., 2015. Exploration of efficacy and bleeding with combined phosphoinositide 3-kinase beta inhibition and aspirin in man. J. Thromb. Haemost. 13, 1494–1502.
Ouseph, M.M., Huang, Y., Banerjee, M., Joshi, S., MacDonald, L., Zhong, Y., et al., 2015. Autophagy is induced upon platelet activation and is essential for hemostasis and thrombosis. Blood 126, 1224–1233.
Patrucco, E., Notte, A., Barberis, L., Selvetella, G., Maffei, A., Brancaccio, M., et al., 2004. PI3Kgamma modulates the cardiac response to chronic pressure overload by distinct kinase-dependent and -independent effects. Cell 118, 375–387.
Posor, Y., Eichhorn-Gruenig, M., Puchkov, D., Schoneberg, J., Ullrich, A., Lampe, A., et al., 2013. Spatiotemporal control of endocytosis by phosphatidylinositol-3,4-bisphosphate. Nature 499, 233–237.
Reifler, A., Li, X., Archambeau, A.J., McDade, J.R., Sabha, N., Michele, D.E., et al., 2014. Conditional knockout of pik3c3 causes a murine muscular dystrophy. Am. J. Pathol. 184, 1819–1830.
Ronan, B., Flamand, O., Vescovi, L., Dureuil, C., Durand, L., Fassy, F., et al., 2014. A highly potent and selective Vps34 inhibitor alters vesicle trafficking and autophagy. Nat. Chem. Biol. 10, 1013–1019.
Ruggeri, Z.M., 2007. The role of von Willebrand factor in thrombus formation. Thromb. Res. 120 (Suppl. 1), S5–S9.
Ruggeri, Z.M., Mendolicchio, G.L., 2007. Adhesion mechanisms in platelet function. Circ. Res. 100, 1673–1685.
Sabbah, D.A., Hu, J., Zhong, H.A., 2015. Advances in the development of class I phosphoinositide 3-Kinase (PI3K) inhibitors. Curr. Top. Med. Chem.
Schoenwaelder, S.M., Ono, A., Sturgeon, S., Chan, S.M., Mangin, P., Maxwell, M.J., et al., 2007. Identification of a unique co-operative phosphoinositide 3-kinase signaling mechanism regulating integrin alpha IIb beta 3 adhesive function in platelets. J. Biol. Chem. 282, 28648–28658.
Schurmans, S., Polizzi, S., Scoumanne, A., Sayyed, S., Molina-Ortiz, P., 2015. The Ras/Rap GTPase activating protein RASA3: from gene structure to in vivo functions. Adv. Biol. Regul. 57, 153–161.
Senis, Y.A., Atkinson, B.T., Pearce, A.C., Wonerow, P., Auger, J.M., Okkenhaug, K., et al., 2005. Role of the p110delta PI 3-kinase in integrin and ITAM receptor signalling in platelets. Platelets 16, 191–202.
Seok, Y.M., Azam, M.A., Okamoto, Y., Sato, A., Yoshioka, K., Maeda, M., et al., 2010. Enhanced Ca2+-dependent activation of phosphoinositide 3-kinase class IIalpha isoform-Rho axis in blood vessels of spontaneously hypertensive rats. Hypertension 56, 934–941.
Smyth, S.S., Woulfe, D.S., Weitz, J.I., Gachet, C., Conley, P.B., Goodman, S.G., et al., 2009. G-protein-coupled receptors as signaling targets for antiplatelet therapy. Arterioscler. Thromb. Vasc. Biol. 29, 449–457.
Stefanini, L., Paul, D.S., Robledo, R.F., Chan, E.R., Getz, T.M., Campbell, R.A., et al., 2015. RASA3 is a critical inhibitor of RAP1-dependent platelet activation. J. Clin. Investig. 125, 1419–1432.

Please cite this article in press as: Valet, C., et al., The role of class I, II and III PI 3-kinases in platelet production and activation and their implication in thrombosis, Advances in Biological Regulation (2015), http://dx.doi.org/10.1016/j.jbior.2015.11.008

Valet, C., Chicanne, G., Severac, C., Chaussade, C., Whitehead, M.A., Cabou, C., et al., 2015. Essential role of class II PI3K-C2alpha in platelet membrane morphology. Blood 126, 1128–1137.
van der Meijden, P.E., Schoenwaelder, S.M., Feijge, M.A., Cosemans, J.M., Munnix, I.C., Wetzker, R., et al., 2008. Dual P2Y 12 receptor signaling in thrombin-stimulated platelets—involvement of phosphoinositide 3-kinase beta but not gamma isoform in Ca2+ mobilization and procoagulant activity. FEBS J. 275, 371–385.
Vanhaesebroeck, B., Guillermet-Guibert, J., Graupera, M., Bilanges, B., 2010. The emerging mechanisms of isoform-specific PI3K signalling. Nat. Rev. 11, 329–341.
Varga-Szabo, D., Braun, A., Nieswandt, B., 2009. Calcium signaling in platelets. J. Thromb. Haemost. 7, 1057–1066.
Varga-Szabo, D., Pleines, I., Nieswandt, B., 2008. Cell adhesion mechanisms in platelets. Arterioscler. Thromb. Vasc. Biol. 28, 403–412.
Wang, L., Budolfson, K., Wang, F., 2011. Pik3c3 deletion in pyramidal neurons results in loss of synapses, extensive gliosis and progressive neurodegeneration. Neuroscience 172, 427–442.
Wang, Y., Litvinov, R.I., Chen, X., Bach, T.L., Lian, L., Petrich, B.G., et al., 2008. Loss of PIP5KIgamma, unlike other PIP5KI isoforms, impairs the integrity of the membrane cytoskeleton in murine megakaryocytes. J. Clin. Investig. 118, 812–819.
Wang, Y., Yoshioka, K., Azam, M.A., Takuwa, N., Sakurada, S., Kayaba, Y., et al., 2006. Class II phosphoinositide 3-kinase alpha-isoform regulates Rho, myosin phosphatase and contraction in vascular smooth muscle. Biochem. J. 394, 581–592.
Willinger, T., Flavell, R.A., 2012. Canonical autophagy dependent on the class III phosphoinositide-3 kinase Vps34 is required for naive T-cell homeostasis. Proc. Natl. Acad. Sci. U. S. A. 109, 8670–8675.
Woulfe, D., Jiang, H., Mortensen, R., Yang, J., Brass, L.F., 2002. Activation of Rap1B by G(i) family members in platelets. J. Biol. Chem. 277, 23382–23390.
Yoshioka, K., Yoshida, K., Cui, H., Wakayama, T., Takuwa, N., Okamoto, Y., et al., 2012. Endothelial PI3K-C2alpha, a class II PI3K, has an essential role in angiogenesis and vascular barrier function. Nat. Med. 18, 1560–1569.
Zhang, J., Banfic, H., Straforini, F., Tosi, L., Volinia, S., Rittenhouse, S.E., 1998. A type II phosphoinositide 3-kinase is stimulated via activated integrin in platelets. A source of phosphatidylinositol 3-phosphate. J. Biol. Chem. 273, 14081–14084.
Zhang, J., Vanhaesebroeck, B., Rittenhouse, S.E., 2002. Human platelets contain p110delta phosphoinositide 3-kinase. Biochem. Biophys. Res. Commun. 296, 178–181.
Zhou, X., Takatoh, J., Wang, F., 2011. The mammalian class 3 PI3K (PIK3C3) is required for early embryogenesis and cell proliferation. PLoS One 6, e16358.
Zhou, X., Wang, L., Hasegawa, H., Amin, P., Han, B.X., Kaneko, S., et al., 2010. Deletion of PIK3C3/Vps34 in sensory neurons causes rapid neurodegeneration by disrupting the endosomal but not the autophagic pathway. Proc. Natl. Acad. Sci. U. S. A. 107, 9424–9429.
Zucker-Franklin, D., 1981. Endocytosis by human platelets: metabolic and freeze-fracture studies. J. Cell Biol. 91, 706–715.

Please cite this article in press as: Valet, C., et al., The role of class I, II and III PI 3-kinases in platelet production and activation and their implication in thrombosis, Advances in Biological Regulation (2015), http://dx.doi.org/10.1016/j.jbior.2015.11.008

***

L'objectif de ma thèse a été d'étudier les rôles de facteurs intrinsèques et extrinsèques au MK sur la production et l'activation plaquettaire. Dans un premier temps, je me suis intéressé au rôle de la PI3KC2α grâce à un modèle original de souris muté ponctuellement, de façon hétérozygote, sur un exon codant pour son activité kinase et résultant en son inactivation partielle. En parallèle, j'ai étudié le rôle de la classe III des PI3Ks, Vps34, en générant un modèle de souris délété pour Vps34 spécifiquement dans la lignée mégacaryocytaire et les plaquettes. Ces deux isoformes de PI3Ks représentent les facteurs intrinsèques au MK sur lesquels j'ai travaillé et dont le rôle reste méconnu. Enfin, je me suis intéressé à l'influence, non caractérisée, de l'adipocyte, facteur extrinsèque au MK mais très présent dans la moelle osseuse, sur la mégacaryopoïèse et la production plaquettaire *in vitro* ainsi que *in vivo* grâce à des souris obèses. Les résultats obtenus seront décrits dans le chapitre « Résultats expérimentaux » de cette thèse.

Résultats expérimentaux

A) PI3KC2α et Vps34 : rôles de deux facteurs intrinsèques au MK dans la régulation de la mégacaryopoïèse, la production et l'activation plaquettaire

Une caractérisation moléculaire détaillée de la biologie du MK et des mécanismes de production et d'activation des plaquettes apparait nécessaire pour une meilleure compréhension de ces processus complexes et la mise à jour de nouvelles cibles pharmacologiques potentielles afin de lutter contre les complications cardiovasculaires liées à des défauts de production et / ou d'activation plaquettaire.

Dans les plaquettes, le rôle des PI3Ks de classe I a largement été étudié ces dernières années, en particulier par notre équipe. Dans ce contexte, l'équipe a contribué à montrer que l'isoforme β des PI3Ks de classe I contrôle les étapes clés de l'activation plaquettaire et la stabilité du thrombus à haute force de cisaillement, ce qui en fait une potentielle cible anti-thrombotique d'intérêt (Laurent et al., 2014; Laurent et al., 2015; Martin et al., 2010).

Contrairement aux PI3Ks de classe I, le rôle des PI3KC2 et de la PI3K de classe III (Vps34) est encore très peu caractérisé. Les PI3KC2 et Vps34 sont plutôt spécialisées dans la production du PtdIns3P. Ce lipide est particulièrement enrichi dans les membranes des endosomes et des autophagosomes et ainsi joue un rôle critique dans les processus de trafic vésiculaire. Nous avons émis l'hypothèse que les PI3KC2, Vps34 et leur produit commun, le PtdIns3P, pourraient jouer un rôle important dans la production et l'activation plaquettaire pour plusieurs raisons: (i) la mégacaryopoïèse et la production plaquettaire font appel à un intense remodelage du cytosquelette et des membranes et un trafic vésiculaire très actif, qui sont des processus régulés par les PI3KC2, Vps34 et le PtdIns3P, (ii) les travaux anciens de l'équipe de S. Rittenhouse ont suggéré un rôle pour les PI3KC2 dans l'activation plaquettaire et (iii) nos données récentes montrent une production de PtdIns3P lors de l'activation plaquettaire (Chicanne et al., 2012).

1) Rôle essentiel de la PI3KC2α dans le contrôle de la morphologie membranaire des plaquettes

Pour ce travail, nous avons étudié le rôle de la PI3KC2α dans la production et les fonctions plaquettaires en utilisant un modèle de souris original muté de façon ponctuelle sur un exon codant pour l'activité kinase de la PI3KC2α (Alliouachene et al., 2016). Alors que la mutation homozygote dans l'animal entier est létale, les souris portant une mutation hétérozygote (PI3KC2α$^{WT/D1268A}$) qui entraîne une inactivation partielle de la PI3KC2α sont viables et fertiles.

Publication n°2

Essential role of class II PI3K-C2α in platelet membrane morphology.

Colin Valet[1], Gaetan Chicanne[1], Childeric Severac[2], Claire Chaussade[3], Maria Whitehead[3], Cendrine Cabou[1], Marie-Pierre Gratacap[1], Frederique Gaits-Iacovoni[1], Bart Vanhaesebroeck[3*], Bernard Payrastre[1,4*], Sonia Severin[1*]

[1] Inserm U1048, I2MC and Universite Paul Sabatier, 31432, Toulouse Cedex 04, France

[2] CNRS, ITAV-USR3505, Toulouse, France ; Universite de Toulouse, ITAV-USR3505, Toulouse, France

[3] UCL Cancer Institute, Paul O'Gorman Building, University College London, London, United Kingdom

[4] CHU de Toulouse, Laboratoire d'Hematologie, 31059, Toulouse Cedex 03, France

[*] These authors share senior authorship

Article in Blood 2015; 126: 1128-37

Regular Article

PLATELETS AND THROMBOPOIESIS

Essential role of class II PI3K-C2α in platelet membrane morphology

Colin Valet,[1] Gaëtan Chicanne,[1] Childerick Severac,[2,3] Claire Chaussade,[4] Maria A. Whitehead,[4] Cendrine Cabou,[1] Marie-Pierre Gratacap,[1] Frederique Gaits-Iacovoni,[1] Bart Vanhaesebroeck,[4] Bernard Payrastre,[1,5] and Sonia Severin[1]

[1]Inserm, U1048-Université Toulouse III, Institut des Maladies Métaboliques et Cardiovasculaires, Toulouse, France; [2]CNRS, ITAV-USR3505, Toulouse, France; [3]Université de Toulouse, ITAV-USR3505, Toulouse, France, [4]UCL Cancer Institute, Paul O'Gorman Building, University College London, London, United Kingdom; [5]Centre Hospitalier Universitaire de Toulouse, Laboratoire d'Hématologie, Toulouse, France

Key Points

- PI3K-C2α controls platelet membrane structure and remodeling.
- PI3K-C2α is a key regulator of a basal housekeeping PI3P pool in platelets.

The physiologic roles of the class II phosphoinositide 3-kinases (PI3Ks) and their contributions to phosphatidylinositol 3-monophosphate (PI3P) and PI(3,4)P_2 production remain elusive. Here we report that mice heterozygous for a constitutively kinase-dead PI3K-C2α display aberrant platelet morphology with an elevated number of barbell-shaped proplatelets, a recently discovered intermediate stage in the final process of platelet production. Platelets with heterozygous PI3K-C2α inactivation have critical defects in α-granules and membrane structure that are associated with modifications in megakaryocytes. These platelets are more rigid and unable to form filopodia after stimulation. Heterozygous PI3K-C2α inactivation in platelets led to a significant reduction in the basal pool of PI3P and a mislocalization of several membrane skeleton proteins known to control the interactions between the plasma membrane and cytoskeleton. These alterations had repercussions on the performance of platelet responses with delay in the time of arterial occlusion in an in vivo model of thrombosis and defect in thrombus formation in an ex vivo blood flow system. These data uncover a key role for PI3K-C2α activity in the generation of a basal housekeeping PI3P pool and in the control of membrane remodeling, critical for megakaryocytopoiesis and normal platelet production and function. (*Blood*. 2015;126(9):1128-1137)

Introduction

Phosphoinositide 3-kinases (PI3Ks) are lipid kinases that produce D3-phosphorylated phosphoinositides, which are able to interact with proteins to organize functional complexes regulating various biological processes including signal transduction, cytoskeletal organization, and vesicular trafficking.[1,2] After stimulation, class I PI3Ks produce phosphatidylinositol 3,4,5 trisphosphate [PI(3,4,5)P_3], a short-lived second messenger involved in signal transduction. In contrast, class II and III PI3Ks are thought to generate phosphatidylinositol 3-monophosphate (PI3P), a lipid that is present at relatively low amounts in cells and that controls vesicular trafficking. Whether class II and III PI3Ks produce both basal and inducible pools of PI3P remain unclear. In addition to PI3P, class II PI3Ks can also produce phosphatidylinositol 3,4 bisphosphate [PI(3,4)P_2].[3] Class II α PI3K (PI3K-C2α), 1 of the 3 members of the class II PI3K subfamily, has become the focus of recent studies, but its exact physiological role still remains enigmatic.[3-8] In vitro studies have implicated PI3K-C2α in intracellular membrane trafficking, endocytosis, exocytosis, and autophagy.[3-5] Recently, loss of the *Pik3c2a* gene in mouse was shown to cause early embryonic lethality (between embryonic day 10.5 and embryonic day 11.5) as a result of severe defects in angiogenesis and vascular barrier function, together with primary cilium organization.[6-8]

More than 15 years ago, the group of Susan Rittenhouse suggested that a class II PI3K could be implicated in blood platelet activation,[9] but to our knowledge, no work has followed since then. Platelets are small, anucleated blood cells that play a vital role in hemostasis and thrombosis. After vascular injury and exposure of the subendothelial matrix, platelets adhere and form an hemostatic plug to prevent excessive blood loss.[10,11] Platelets are produced by megakaryocytes after a highly regulated process of maturation of hematopoietic stem cells into giant polyploid cells, characterized by intense membrane and cytoskeleton remodeling.[12] Mature megakaryocytes extend long, branched structures designated as proplatelets, which cross the endothelial barrier and, under hemodynamic flow, split into young "reticulated" platelets in the bloodstream. Platelet shaping and sizing resulting from reversible conversion of round-shaped platelets into barbell-shaped proplatelets also occurs in the bloodstream, where they undergo successive rounds of fission via membrane and cytoskeleton remodeling to produce mature platelets.[13-20]

To gain insight into the physiological role of PI3K-C2α in platelet production and function, we used a mouse line heterozygous for a germ-line kinase-inactive knock-in (KI) mutation (D1268A) in the endogenous *Pik3c2a* gene. These mice with a heterozygous inactivation of PI3K-C2α were viable and fertile but showed aberrant platelet formation with critical defect in platelet membrane morphology and dynamics and an enrichment of barbell-shaped proplatelets in the bloodstream. Our data demonstrate that PI3K-C2α regulates an agonist-independent pool of PI3P and is important for organizing the membrane skeleton to allow normal platelet production and functions.

Submitted March 24, 2015; accepted June 15, 2015. Prepublished online as *Blood* First Edition paper, June 24, 2015; DOI 10.1182/blood-2015-03-636670.

B.V., B.P., and S.S. share senior authorship of this study.

The online version of this article contains a data supplement.

There is an Inside *Blood* Commentary on this article in this issue.

The publication costs of this article were defrayed in part by page charge payment. Therefore, and solely to indicate this fact, this article is hereby marked "advertisement" in accordance with 18 USC section 1734.

Methods

Animals

Wild-type (WT) and heterozygous mutant mice with inactive PI3K-C2α (WT/D1268A) were of C57BL/6 genetic background and housed in the Anexplo (Toulouse) vivarium according to institutional guidelines. For all experiments, 8- to 14-week-old mice were used. Ethical approval for animal experiments was obtained from the French Ministry of Research in agreement with European Union guidelines.

Preparation of murine platelets, flow assay on collagen, carotid artery thrombosis, and tail bleeding time are described in detail in the supplemental *Methods*.

In vitro PI 3-kinase assay

Platelets (4×10^8) were lysed at 4°C in 20 mM Tris·HCl (pH 7.7), 150 mM NaCl, 4 mM EDTA, 1 mM Na_3VO_4, 10 μg/mL leupeptin and aprotinin, 1 mM phenylmethylsulfonyl fluoride, and 0.5% Triton X-100. Lysates were centrifuged at 16 000*g*, and the supernatants were incubated for 2 hours with anti-PI3K-C2α antibody and protein A-Sepharose beads. Immunoprecipitate was resuspended in kinase assay buffer (20 mM Tris·HCl at pH 7.4, 100 mM NaCl, 0.5 mM EGTA, 10 mM $MgCl_2$, and 100 μM ATP). Then, 10 μg phosphatidylinositol vesicles and 10 μCi γ-[^{32}P] ATP were added, and after 20 minutes at 37°C, under gentle shaking, reaction was terminated and lipids were extracted using the Bligh and Dyer procedure.

Electron microscopy

Platelets were fixed in 2.5% glutaraldehyde in 0.1 M sodium cacodylate buffer at 4°C overnight. After 2 washes in the same buffer, platelets were allowed to adhere on poly-lysine-coated cover glasses and then dehydrated in a graded ethanol series (scanning electron microscopy) or embedded in resin and sectioned (transmission electron microscopy) according to standard procedures for electron microscopy imaging. Tibia bone marrow was flushed and fixed in 2.5% glutaraldehyde in 0.1 M sodium cacodylate buffer at 4°C overnight, embedded in resin, and sectioned (transmission electron microscopy) according to standard procedures for electron microscopy imaging. Samples were analyzed with HT 7700 Hitachi transmission electron microscope or FEG FEI Quanta 250 scanning electron microscope.

Platelet morphology

Freshly isolated platelets were fixed with formalin (2% final), either immediately to assess baseline morphology or after 24 hours of suspension culture in M199 medium (Gibco, Invitrogen). Fixed platelets were subsequently layered onto poly-L-Lysine-coated microscope slides, using a cytospin centrifuge (Shandon Cytospin; Thermo Fisher Scientific). To determine the number of platelets with extensions and distinct cell bodies, fixed cells were counterstained with an anti-α-tubulin antibody and an AlexaFluor488 secondary antibody. Ten random fields were captured, using Zeiss LSM780 confocal and Zen Zeiss software, from each independent experiment, and platelets with two or more distinct cell bodies on the total platelet count were counted. Round platelet diameter was evaluated by line-scan analysis, using Zen Zeiss software, as previously described.[21]

Lipid analysis

PI3P mass assay and phosphoinositide labeling were performed on washed platelets, as previously described.[22,23] To analyze phospholipid and cholesterol, washed platelets were homogenized in 2 mL of a mixture of methanol:5 mM EGTA (2:1, volume to volume ratio [v/v]) and were extracted according to Bligh and Dyer in a chloroform/methanol/water mixture (2.5:2.5:2.1, v/v/v) in the presence of the internal standard (15 μg stigmasterol, phosphatidylethanolamine, 12:0/12:0; phosphatidylcholine, 13:0/13:0; phosphatidylinositol (PI), 16:0/17:0; and phosphatidylserine, 12:0/12:0). Cholesterol quantification was obtained after gas chromatography analysis. To simultaneously separate phospholipids liquid chromatography-tandem mass spectrometry, the previous extract was analyzed on an ultrahigh-performance liquid chromatography system (Agilent LC1290 Infinity) HYLIC column coupled to Agilent 6460 triple quadrupole MS (Agilent Technologies) equipped with electrospray ionization operating in negative and positive mode.

Flow assay on von Willebrand factor

Murine von Willebrand factor (vWF; 10 μg/mL) was immobilized overnight on a surface precoated for 4 hours with a polyclonal anti-human vWF antibody (31 μg/mL; Dako). Washed platelets were perfused in vWF-coated microcapillaries at a shear rate of 18 dynes/cm^2. Real-time adhesion was observed in 3 microscopic fields at ×40 magnification during a 35-minute period, starting 4 minutes after the onset of perfusion (1 frame every 5 seconds).

Atomic force microscopy

A NanoWizard II atomic force microscope (JPK Instruments) mounted on an inverted optical microscope (Axiovert 200; Carl Zeiss MicroImaging) was used to localize platelets, image them, and measure their membrane mechanical forces (Young Modulus). Silicon Nitride cantilevers (MLCT, Bruker) with nominal spring constant of 0.1 N/m, a pyramidal shaped tip, and a half cone angle $\alpha = 17.5°$.

The thermal tune method[24] was systematically used to measure the cantilevers spring constants, which were all found in the range from 0.14 to 0.16 N/m.

Elasticity measurements. All experiments were conducted in N-2-hydroxyethylpiperazine-N′-2-ethanesulfonic acid liquid media and maintained at 37°C, using a temperature-controlled sample holder (BioCell; JPK Instruments). Washed platelets were placed on a fibrinogen-coated surface and left to adhere for 45 minutes in the presence of thrombin (0.5 IU/mL) before any experiments. Force (F) vs displacement curves were recorded according to a 16×16 matrix over a 1.5×1.5 μm^2 area for each platelet, with a maximum load of 4 nN to preserve membrane integrity. These curves were then converted into indentation (δ) curves and fitted using JPK Instruments data processing software with the conical hertz model[25] of Equation 1 with a Poisson ratio (ν) arbitrary fixed to 0.5:

$$F = \frac{2\ E\ tan\ \alpha}{\pi(1-\upsilon^2)}\delta^2 \quad (1)$$

For each force curve, the Young's modulus (E) is calculated and plotted on histograms.

Atomic force microscopy imaging. After adhesion, platelets were fixed in 1.5% formalin solution for 30 minutes and then washed and imaged in air at room temperature. The atomic force microscopy (AFM) scanner has a maximum range of 100 μm in XY directions and 15 μm in the vertical direction. Images were acquired at 512 × 512 pixel resolution at a line rate of 1 to 2 Hz with a maximum applied force of 4 nN. All images were analyzed using JPK data processing software. Linear plan fit was used to remove sample tilt from height images, using the glass slide as the zero reference plan.

Isolation of membrane skeleton

Platelets were lysed by the addition of ice-cold cytoskeleton buffer (100 mM Tris·HCl at pH 7.4, 20 mM EGTA, 2 mM Na_3VO_4, 4 μg/mL each of aprotinin and leupeptin, 2 mM phenylmethylsulfonyl fluoride, and 2% Triton X-100) for 10 minutes at 4°C. Platelet membrane skeleton (Triton X-100 insoluble fraction) was isolated from the 16 000*g* supernatant by centrifugation at 100 000*g* overnight and then solubilized and prepared for sodium dodecyl sulfate-polyacrylamide gel electrophoresis.

Statistical analysis

Data are expressed as mean ± standard error of the mean. Significance of differences was determined using 2-tailed Student t test or 2-way analysis of variance or 1-sample t test. P values $< .05$ were considered significant ($^*P < .05$, $^{**}P < .01$, $^{***}P < .001$).

Results

PI3K-C2α$^{WT/D1268A}$ mice display defects in platelet formation and membrane morphology

To investigate the role of PI3K-C2α in platelets, we used a mouse line with a germline kinase-inactivating KI mutation in the PI3K-C2α protein, further referred to as PI3K-C2α^{D1268A}. Whereas homozygous KI mice are embryonic lethal, heterozygous mice (hereafter called PI3K-C2α$^{WT/D1268A}$ mice) are born at the expected Mendelian ratio, are viable and fertile, and develop normally, with no apparent morphological abnormalities (B.V., manuscript in preparation). PI3K-C2α$^{WT/D1268A}$ mice showed no signs of spontaneous bleeding compared with littermate WT mice and had comparable levels of *Pik3c2a* mRNA level in megakaryocytes and unaltered protein expression of PI3K-C2α and other class I, II, and III PI3K isoforms in platelets (Figure 1A-B). PI3K-C2α immunoprecipitates from PI3K-C2α$^{WT/D1268A}$ platelets displayed a 50% reduction in lipid kinase activity (Figure 1B), in line with heterozygous inactivation of PI3K-C2α.

Except for hematocrit, which was slightly enhanced, basic blood parameters such as red/white blood cell count, hemoglobin concentration, and mean globular volume, as well as immune cell populations (B cells, T cells, granulocytes), were unaltered in PI3K-C2α$^{WT/D1268A}$ mice (Table 1). PI3K-C2α$^{WT/D1268A}$ mice displayed a normal platelet count (Figure 1C). However, although the mean volume of platelet population was not significantly different (7.70 $\mu m^3 \pm 0.27$ μm^3 for PI3K-C2α$^{WT/D1268A}$ vs 7.16 $\mu m^3 \pm 0.25$ μm^3 for WT; n = 30 mice), platelets were heterogeneous in size, as reflected by increased platelet distribution width in PI3K-C2α$^{WT/D1268A}$ mice compared with in WT mice (3.76% ± 0.41% vs 2.82% ± 0.22%; n = 30 mice; $P < .05$) and confirmed by tubulin ring diameter measurement (Figure 1C; supplemental Figure 1, available on the *Blood* Web site). Expression levels of major platelet surface receptors were comparable in PI3K-C2α$^{WT/D1268A}$ and WT platelets (Figure 1C). Transmission electron microscopy analysis revealed an abnormal ultrastructure of resting PI3K-C2α$^{WT/D1268A}$ platelets, with major defects in membrane morphology including an aberrant invaginated and tortuous shape of the plasma membrane as compared with the smooth plasma membrane from WT platelets (Figure 1D). The open canalicular system, which represents invaginations of the plasma membrane and constitutes a reservoir of membranes necessary for platelet shape change during activation, appeared altered in PI3K-C2α$^{WT/D1268A}$ platelets (Figure 1D). Quantification indicated that 31% ± 5.4% of PI3K-C2α$^{WT/D1268A}$ platelets have an invaginated and rough morphology compared with 4.2% ± 2.2% of WT platelets. The winding plasma membrane shape of PI3K-C2α$^{WT/D1268A}$ platelets was confirmed by scanning electron microscopy (Figure 1D). Strikingly, an enrichment of platelets with 2 cell bodies, recently named barbell-shaped proplatelets,[19] which are normally very rare, was observed in PI3K-C2α$^{WT/D1268A}$ platelet suspension (Figure 1D). In addition, PI3K-C2α$^{WT/D1268A}$ platelets displayed an abnormal α-granule distribution characterized by 46.0% ± 1.2% reduction in number and 60.5% ± 3.7% increase in size compared with WT platelets (Figure 1E). Global platelet α-granule content such as vWF and fibrinogen was, however, not altered. Transmission electron microscopy, mepacrine uptake, and serotonin quantification showed no substantial difference in the number, size, and content of dense granules between WT and PI3K-C2α$^{WT/D1268A}$ platelets (supplemental Figure 2). Despite membrane and α-granule defects, but consistent with a normal platelet count, the in vivo life span of PI3K-C2α$^{WT/D1268A}$ platelets and their count recovery after immune-induced thrombocytopenia was similar to that of WT platelets (supplemental Figure 3).

The defects in membrane and α-granules were already observed in PI3K-C2α$^{WT/D1268A}$ megakaryocytes, as shown by transmission electron microscopy analysis of the native bone marrow. The demarcation membrane system was less developed and delineated compared with WT megakaryocytes (Figure 1F). Fewer α-granules, heterogeneous in shape and bigger than in WT, were also observed in PI3K-C2α$^{WT/D1268A}$ megakaryocytes (Figure 1F).

Altogether, these data point to a critical role for PI3K-C2α in the organization of membrane structure and platelet morphology, already detectable in megakaryocytes.

PI3K-C2α$^{WT/D1268A}$ platelets have a reduction in the basal, agonist-insensitive, pool of PI3P

Whether class II PI3Ks control a basal or a stimulation-sensitive pool of PI3P, or both, remains unclear. Emerging evidence suggests class II PI3Ks can also generate PI(3,4)P_2 under certain conditions.[3] We used 3 complementary methods to analyze phosphoinositide levels in PI3K-C2α$^{WT/D1268A}$ platelets: high-performance liquid chromatography analysis after short-term (45 minutes) ^{32}P-labeling of platelets, efficient in determining the fast turnover of phosphoinositides and their acute changing after stimulation[26]; a PI3P-specific mass assay to measure the total amount of PI3P[22]; and imaging using the PI3P-binding FYVE^{HRS} domain as a probe. High-performance liquid chromatography analysis of the short-lived phosphoinositide pools did not show any significant differences in the basal or agonist-stimulated levels of PI3P or other phosphoinositides, including PI(3,4)P_2 and PI(3,4,5)P_3 (Figure 2A; supplemental Figure 4). However, as PI3P also exists in a pool with slow turnover time, we next used a PI3P-specific mass assay and found a 29.7% ± 3.3% decrease in PI3P in resting PI3K-C2α$^{WT/D1268A}$ platelets compared with WT (Figure 2B). This decrease was highly significant, given that only 50% of the PI3K-C2α was inactivated, suggesting PI3K-C2α contributes to about half of the basal PI3P level in WT platelets. The decrease in basal PI3P pool in resting PI3K-C2α$^{WT/D1268A}$ platelets was confirmed by immunofluorescence staining with the FYVE^{HRS} probe (40.3% ± 3.3% decrease in PI3K-C2α$^{WT/D1268A}$ platelets compared with WT platelets; Figure 2C). In platelets stimulated with collagen-related peptide (CRP) or thrombin, the amount of PI3P was found to increase and reach comparable levels in WT and PI3K-C2α$^{WT/D1268A}$ platelets (Figure 2A-B). Overall, these data show that PI3K-C2α does not significantly contribute to the agonist-inducible pool of PI3P in platelets, but interestingly, it produces a major fraction (~50%) of the basal, housekeeping, pool of PI3P. This pool of PI3P likely has a slow turnover, as short-term (45 minutes) ^{32}P-labeling did not reveal significant differences between WT and PI3K-C2α$^{WT/D1268A}$ platelets.

PI3K-C2α$^{WT/D1268A}$ mice display an enrichment of barbell proplatelets in the bloodstream and a decrease in platelet filopodia formation

To further investigate the enrichment of barbell-shaped proplatelets observed in PI3K-C2α$^{WT/D1268A}$ mice by transmission electron microscopy (Figure 1D), we analyzed freshly obtained washed platelets or washed platelets cultured in suspension for 24 hours, which is known to increase the level of barbell-shaped proplatelets.[17] The percentage of platelets with 2 cell bodies was dramatically increased in PI3K-C2α$^{WT/D1268A}$ samples compared with in WT samples (Figure 3A). A similar increase was observed after perfusion

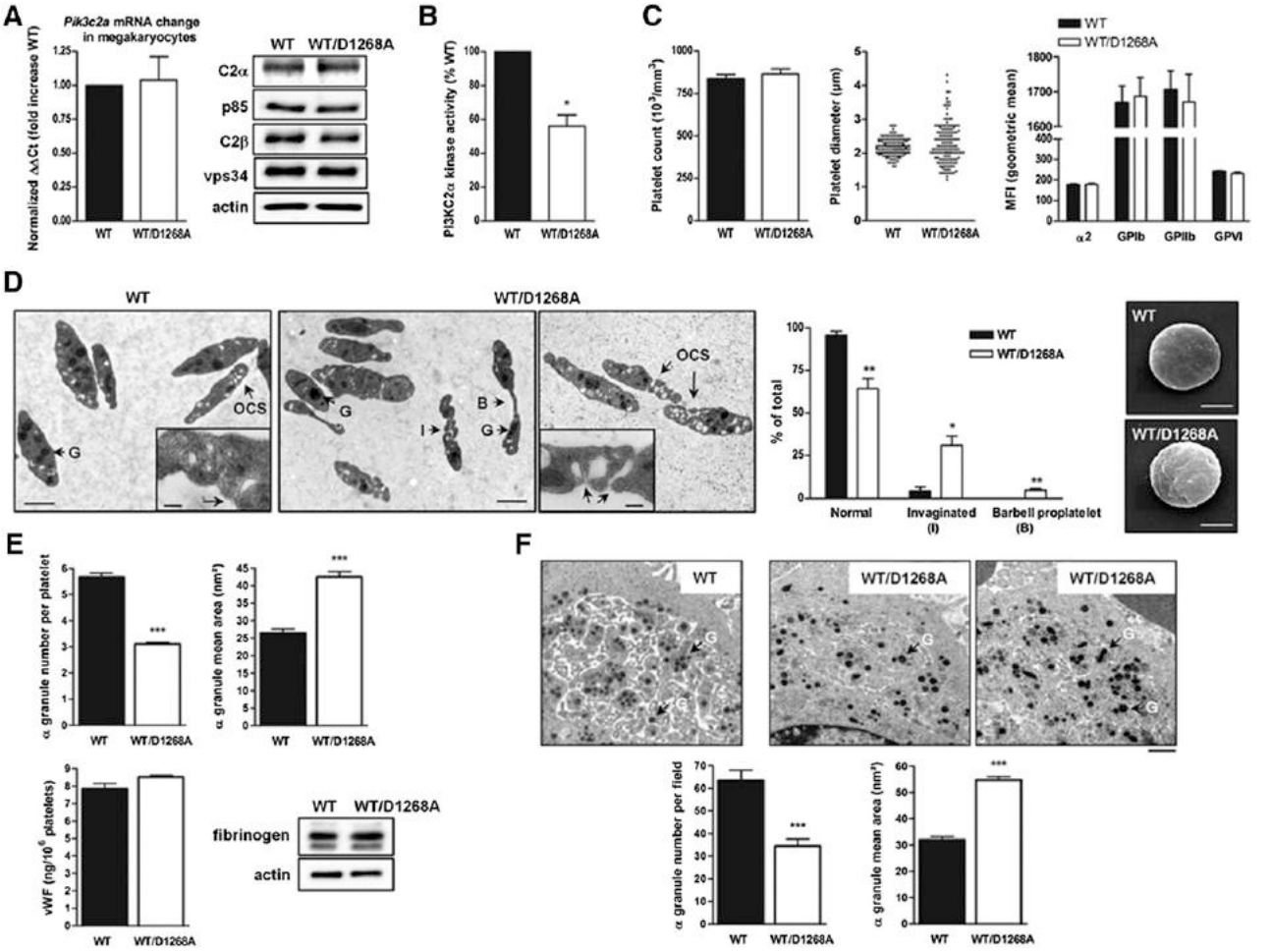

Figure 1. PI3K-C2α regulates platelet biogenesis. (A) Megakaryocyte relative *Pik3c2a* mRNA expression normalized to β-actin cDNA (mean ± standard error of the mean [SEM]; n = 4). Western blot analysis for PI3K-C2α, p85, PI3K-C2β, and vps34 in platelet lysates. (B) In vitro platelet PI3K-C2α lipid kinase activity (mean ± SEM; n = 4; $^*P < .05$ vs WT according to 1 sample *t* test). (C) Whole-blood platelet count (mean ± SEM; n = 30 mice), measured using Micros60 (Horiba ABX Diagnostics). Platelet diameter measured using line-scan analysis after α-tubulin staining on fixed resting platelets (mean ± SEM; n = 150 platelets). Surface glycoprotein expression on resting platelets (MFI, mean fluorescence intensity; mean ± SEM; n = 4). (D) Transmission and scanning electron microscopy on resting platelets. Images are representative of 5 mice of each genotype. Scale bar: 1 μm. Enlarged pictures of OCS from WT and PI3K-C2α$^{WT/D1268A}$ platelets are shown. Scale bar: 200 nm. I, invaginated platelet; B, barbell shaped-proplatelets; G, α-granule; OCS, open canalicular system. Quantification on transmission electron microscopy images of normal platelets, aberrant platelets (A), and barbell shaped-proplatelets (B) (mean ± SEM; n > 400 platelets; $^*P < .05$ and $^{**}P < .01$ vs WT, according to 2-tailed Student *t* test. (E) α-granule number and mean area quantified on transmission electron microscopy images using ImageJ software (mean ± SEM; n = 100 platelets; $^{***}P < .001$ vs WT, according to 2-tailed Student *t* test). Quantification of vWF by enzyme-linked immunosorbent assay test and fibrinogen by western blotting on resting platelets (mean ± SEM; n = 3). (F) Transmission electron microscopy of mice bone marrow section (n = 3). Scale bar: 2 μm. G; α-granule. α-granule number and mean area quantified as (E) (mean ± SEM, n = 20 megakaryocytes, $^{***}P < .001$ vs WT, according to 2-tailed Student *t* test).

of platelets over a vWF-coated microcapillary for 30 minutes at 18 dynes/cm^2, which is another mean to increase the percentage of barbell-shaped proplatelets[16] (Figure 3B; supplemental Videos 1 and 2). These data reveal a significant increase in the amount of platelets with 2 cell bodies upon heterozygous inactivation of PI3K-C2α, suggesting a defect in the scission required to produce mature platelets, possibly related to the abnormal membrane structure observed in PI3K-C2α$^{WT/D1268A}$ megakaryocytes and platelets. To make sure the observed phenotype was not a result of defects of the vascular endothelium during delivery of platelets into vessel sinusoids, we performed bone marrow transplantation experiments. As shown in Figure 3C, a similar accumulation of platelets with 2 cell bodies was observed when hematopoietic cells carrying the PI3K-C2α$^{WT/D1268A}$ mutation were grafted into a WT or a PI3K-C2α$^{WT/D1268A}$ recipient, and conversely. Thus, the enrichment in barbell-shaped proplatelets observed in PI3K-C2α$^{WT/D1268A}$ mice is a result of a defect of hematopoietic cells.

To further analyze the membrane abnormalities of PI3K-C2α$^{WT/D1268A}$ platelets, we investigated the platelet shape change mechanism by scanning electron microscopy. Although PI3K-C2α$^{WT/D1268A}$ platelets were able to exhibit shape change after

Table 1. Blood parameters

	WT (n = 28)	WT/D1628A (n = 31)
WBC, 10^3/mm^3	3.8 ± 0.3	4.4 ± 0.4
RBC, 10^6 /mm^3	7.2 ± 0.2	7.6 ± 0.2
HGB, g/dL	9.1 ± 0.3	9.6 ± 0.2
HCT, %	31.8 ± 0.9	34.2 ± 0.5*
MGV, μm^3	47 ± 0.2	47.8 ± 0.3

Whole-blood parameters were analyzed with an automated blood analyzer Micros60 (Horiba ABX diagnostics). Mean ± SEM; $^*P < .05$ vs WT according to 2-tailed Student *t* test.

HCT, hematocrit; HGB, hemoglobin; MGV, mean globular volume; RBC, red blood cells; WBC, white blood cells.

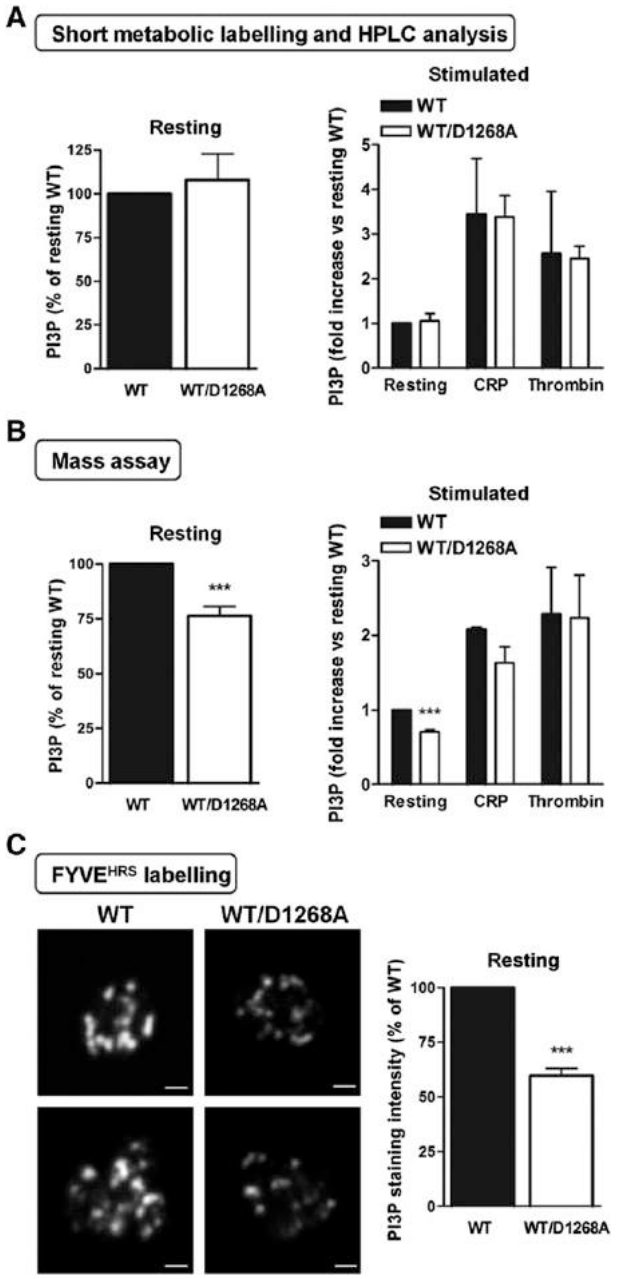

Figure 2. PI3K-C2α is critical for the regulation of basal PI3P level in platelets. (A) High-performance liquid chromatography analysis of PI3P levels in resting and stimulated (10 μg/mL CRP and 0.5 IU/mL thrombin for 3 minutes) ^{32}P-labeled platelets (mean ± SEM; n = 4). (B) PI3P mass assay in resting and stimulated (10 μg/mL CRP and 0.5 IU/mL thrombin for 3 minutes) platelets. The assay was performed as previously described.[22] Briefly, platelet phosphatidylinositol monophosphate (PIP) fraction purified by lipid extraction and thin-layer chromatography was submitted to specific phosphorylation by recombinant PIKfyve, in the presence of [γ-^{32}P]ATP. PIKfyve only phosphorylates PI3P to produce [^{32}P]-PI(3,5)P_2, which reflects the amount of PI3P present in the sample. (mean ± SEM; n = 4; ***$P < .001$ vs WT, according to 1 sample *t* test). (C) Resting platelets were fixed and stained with simple FYVE^{HRS} probe coupled to 647-AlexaFluor. Representative confocal images of FYVE^{HRS}-647 AlexaFluor labeled platelets are shown. Scale bar: 1 μm. Staining intensity in platelets were quantified by ImageJ software (mean ± SEM; n = 3; ***$P < .001$ vs WT, according to 1-sample *t* test).

stimulation by CRP or thrombin in suspension, they showed a dramatic defect in filopodia extension (Figure 4A). The decrease in scission highlighted by the elevated percentage of barbell-shaped proplatelets, the defect in filopodia extension, and the winding plasma membrane shape of resting PI3K-C2α$^{WT/D1268A}$ platelets suggested a reduction in platelet elasticity. Therefore, we used AFM operating in force distance mode to measure platelet compliance by quantifying the Young's modulus. WT and PI3K-C2α$^{WT/D1268A}$ platelets were stimulated by thrombin and allowed to adhere and to spread on fibrinogen to similar extent (supplemental Figure 5). AFM height images revealed numerous membrane invaginations (Figure 4B, see arrows), leading to a tortuous and rough aspect of PI3K-C2α$^{WT/D1268A}$ platelets compared with the homogeneous smooth WT platelet surface (Figure 4B). In line with the electron microscopy analysis, these data indicated an inhomogeneity in PI3K-C2α$^{WT/D1268A}$ platelet membrane. Interestingly, PI3K-C2α$^{WT/D1268A}$ platelets displayed a significantly higher Young's modulus (40.7 kPa ± 3.7 kPa for WT platelets and 62.2 kPa ± 5.4 kPa for PI3K-C2α$^{WT/D1268A}$ platelets) showing an increased rigidity of the latter (Figure 4B). Altogether, these results demonstrate an important role of PI3K-C2α in the control of membrane morphology and biophysical properties.

PI3K-C2α$^{WT/D1268A}$ platelets have normal major lipid composition but aberrant membrane skeleton with repercussion for thrombosis

To gain insight into the mechanisms leading to the observed platelet phenotype, we analyzed potential modifications in the membrane major lipid composition and the spectrin-based membrane skeleton that can affect both membrane structure and dynamics. We first performed a targeted mass-spectrometry-based lipidomic analysis of WT and PI3K-C2α$^{WT/D1268A}$ platelets. No difference in cholesterol, phospholipid, and fatty acid content was observed (Figure 5A), indicating that heterozygous inactivation of PI3K-C2α had no effect on the composition of major membrane lipids. The spectrin-based membrane skeleton is critical for biophysical membrane properties, both in platelets and megakaryocytes,[27,28] and is essential for the conversion from preplatelets to barbell-shaped proplatelets and to mature platelets.[15,19] The membrane skeleton of WT and PI3K-C2α$^{WT/D1268A}$ platelets was isolated, and its composition analyzed by immunoblotting. Although the level of cortical polymerized actin was normal, a significant decrease of cortical spectrin and myosin was observed in PI3K-C2α$^{WT/D1268A}$ platelets compared with in WT platelets (Figure 5B). The presence of proteins known to link plasma membrane to the cytoskeleton such as moesin, filamin, GPIbα, and GPIIb was also decreased in the membrane skeleton of PI3K-C2α$^{WT/D1268A}$ platelets, whereas vinculin levels were not affected (Figure 5B). These differences were not a result of a decrease in the whole-cell lysates expression level of these proteins (Figure 5B; supplemental Figure 6), nor a decrease in the surface expression of GPIb and GPIIb (Figure 1C). Therefore, PI3K-C2α activity appears to be critical for the recruitment and/or stabilization of several membrane skeleton proteins that are required for normal membrane shape and dynamics in platelets.

We next tested whether the morphological defects observed in PI3K-C2α$^{WT/D1268A}$ platelets affected platelet functions in vitro, ex vivo, and in vivo. The in vitro platelet aggregation in response to thrombin, thromboxane A2 analog, or adenosine diphosphate was normal. A decreased aggregation response to low doses of collagen or CRP was observed, but increasing the doses of agonists restored a normal response (supplemental Figure 7). Analysis of acute signaling through Akt or myosin light chain phosphorylation did not point to a role for PI3K-C2α in these events, even in response to low doses of GPVI agonists (supplemental Figure 7), suggesting the platelet aggregation defect was related to changes in membrane structure, rather than signaling defect. In vivo, no significant effect on tail bleeding was observed of PI3K-C2α$^{WT/D1268A}$ mice, suggesting primary hemostasis was spared (Figure 6A). To investigate the potential effect of the

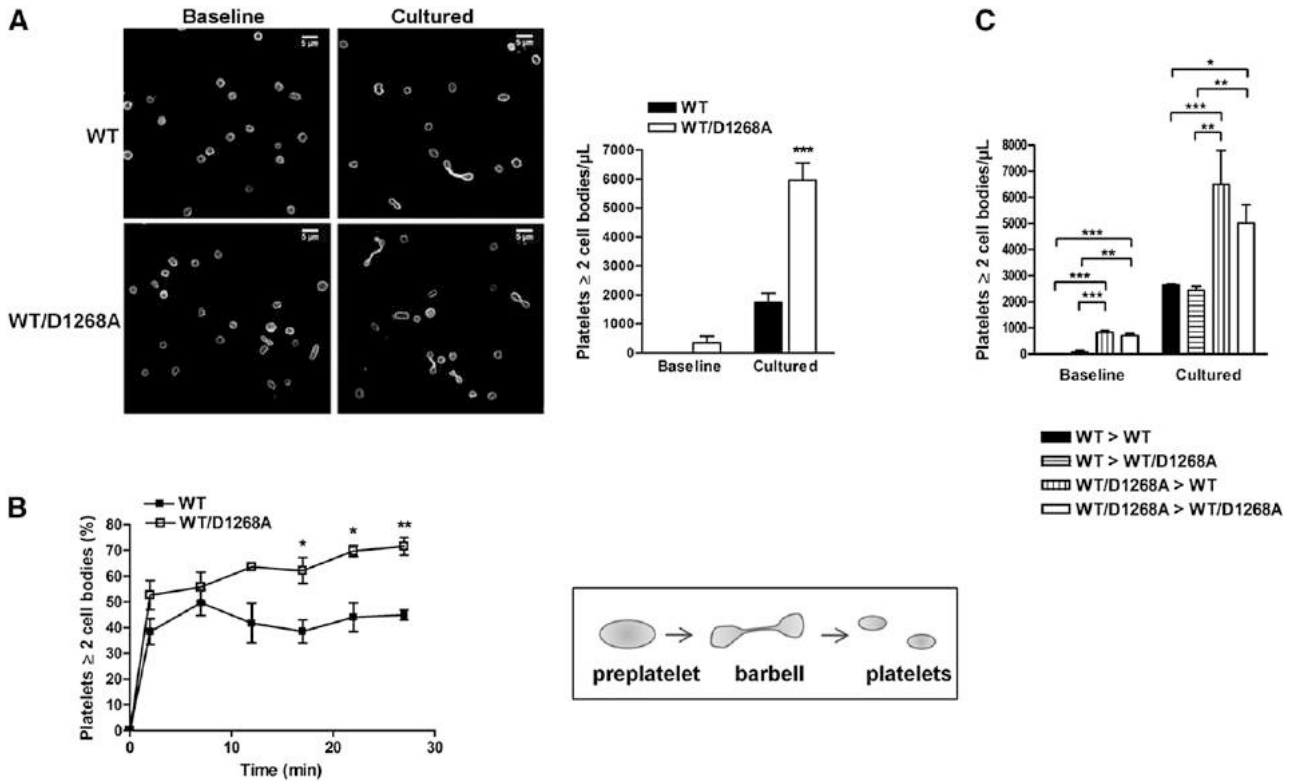

Figure 3. Barbell-shaped proplatelet enrichment in PI3K-C2α$^{WT/D1268A}$ mice. (A) Washed platelets were immediately fixed (baseline) or cultured in suspension for 24 hours (cultured). Panels display a representative example where the platelets were stained for α-tubulin. Scale bar: 5 μm. The bar graph indicates the number of platelets with at least 2 cell bodies per microliter (mean ± SEM; n = 4; ***$P < .001$ vs WT according to 2-tailed Student *t* test). (B) Washed platelets were perfused on murine vWF-coated microcapillaries at 18 dynes/cm^2. 2 cell bodies platelets and discoid platelets were visualized by real-time videomicroscopy. The percentage of 2 cell bodies platelets on total platelets was calculated (mean ± SEM; n = 3; *$P < .05$ and **$P < .01$ vs WT according to 2-tailed Student *t* test). Schematic representation of dynamic platelet release from preplatelets through barbell-shaped proplatelets. (C) Washed platelets from WT mice transplanted with WT bone marrow (WT > WT), PI3K-C2α$^{WT/D1268A}$ mice transplanted with WT bone marrow (WT > WT/D1268A), WT mice transplanted with PI3K-C2α$^{WT/D1268A}$ bone marrow (WT/D1268A > WT), and PI3K-C2α$^{WT/D1268A}$ mice transplanted with PI3K-C2α$^{WT/D1268A}$ bone marrow (WT/D1268A > WT/D1268A) mice were treated as described in A (mean ± SEM; n = 3; *$P < .05$, **$P < .01$, and ***$P < .001$, according to 2-way ANOVA).

PI3K-C2α inactivation on the prothrombotic function of platelets, we analyzed arterial thrombus formation after injury of the mouse carotid with ferric chloride. A significant delay in artery occlusion was observed in PI3K-C2α$^{WT/D1268A}$ mice compared with WT mice (Figure 6B). Ex vivo thrombus formation assay performed on a collagen matrix at arterial shear rate also showed a significant reduction in the prothrombotic capacity of PI3K-C2α$^{WT/D1268A}$ platelets (Figure 6C). These data indicate that the membrane defects arising from PI3K-C2α inactivation have little effect on platelet aggregation in vitro but affect the prothrombotic platelet function observed under arterial shear stress.

Discussion

Using a mouse model of partial inactivation of PI3K-C2α, we show that the kinase activity of this class II isoform of PI3K is essential for normal platelet formation. The most striking phenotype is a defect in membrane morphology and dynamics in platelets and megakaryocytes. PI3K-C2α$^{WT/D1268A}$ platelets are heterogeneous in size with a winding and wrinkled aspect plasma membrane, altered open canalicular system, and defects in α-granules. We show, for the first time, a role for a lipid kinase in the mechanism of terminal platelet production in the bloodstream, with an effect on the generation of barbell-shaped proplatelets. Megakaryocytes release into the sinusoid blood vessels large preplatelet intermediates that convert into barbell-shaped proplatelets and further fragment into platelets in the circulation.[13,17,29,30] Barbell-shaped proplatelet conversion, as well as platelet shape and size, are determined by the balance of microtubule bundling, elastic bending forces linked to membrane biophysical properties, and compressive pressure of the membrane skeleton.[19] In agreement with the profound defect on membrane morphology, PI3K-C2α$^{WT/D1268A}$ platelets are more rigid than normal platelets, as determined by atomic force microscopy. As a consequence, partial inactivation of PI3K-C2α decreases the performance of barbell-shaped proplatelets when undergoing scission, which leads to an accumulation of 2 cell bodies' platelets in the circulation. The membrane dynamics are also affected, as PI3K-C2α$^{WT/D1268A}$ platelets hardly form filopodia after stimulation, despite a normal phosphorylation of myosin light chain. The less developed and structured demarcation membrane system observed in PI3K-C2α$^{WT/D1268A}$ megakaryocytes suggests the membrane defects come from megakaryocytes and are not intrinsic to platelets.

Depending on the cell context, PI3K-C2α has been shown to produce PI3P and PI(3,4)P_2,[3,7,8,31] but whether this enzyme controls a housekeeping pool of these lipids or a pool generated after acute signaling is unknown. We show that in platelets, PI3K-C2α controls a basal PI3P pool that has a slow turnover but is not involved in the agonist-induced pool of PI3P. We did not find an implication of PI3K-C2α in the increased production of other phosphoinositides, including D3-phosphoinositides, after platelet activation. For instance, when PI3K-C2α is half inactivated, the production of PI(3,4)P_2

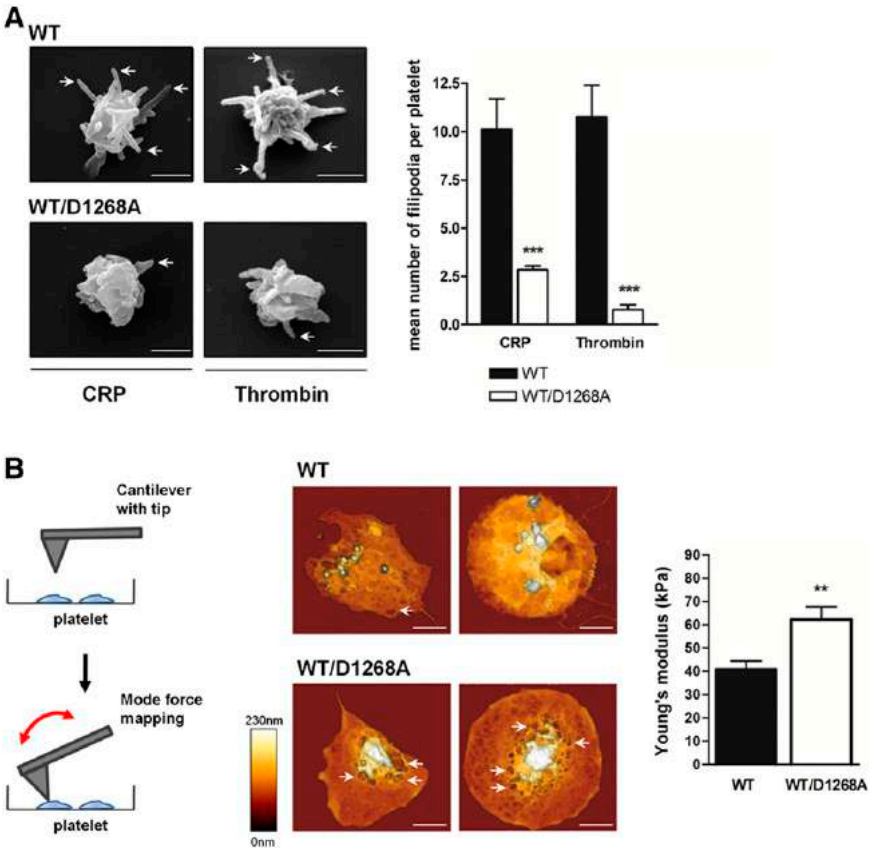

Figure 4. PI3K-C2α controls membrane dynamics and mechanical forces. (A) Washed platelets stimulated in suspension with CRP (10 μg/mL) and thrombin (0.5 IU/mL) were visualized by scanning electron microscopy. Images of 2 WT and PI3K-C2α$^{WT/D1268A}$ platelets are representative of 5 mice. Scale bar: 1 μm. Arrows show filopodia. Filopodia mean number was quantified per platelet (mean ± SEM; n = 3; *$P < .05$ and **$P < .01$ vs WT according to 2-tailed Student *t* test). (B) Schematic representation of AFM technique "force mapping mode," using a cantilever with tip to record platelet topography and measure the Young's modulus, inverse reflection of platelet elasticity. Washed platelets were placed on a fibrinogen-coated surface for 45 minutes in the presence of thrombin (0.5 IU/mL). Representative AFM images are shown and arrows indicate membrane invaginations. Scale bar: 1 μm. Quantitative determination of the local mechanical properties of live platelets was carried out by atomic force microscopy (JPK NWII), operating in force distance mode in liquid buffer solution at 37°C. The bar graph represents the platelet mean Young's modulus (mean ± SEM; n = 3; **$P < .01$, according to 2-tailed Student *t* test).

was not affected in platelets, which is in agreement with previous reports showing that a large part of PI(3,4)P_2 in platelets comes from the dephosphorylation of PI(3,4,5)P_3 by the 5-phosphatase SHIP1.[23] Thus, our results show that PI3K-C2α regulates a housekeeping pool of PI3P in platelets.

How can a defect in a particular pool of PI3P explain the membrane defect observed in PI3K-C2α$^{WT/D1268A}$ platelets? Our data show no differences in the major lipid composition and in microtubule thickness in these platelets but, rather, a deficiency in the membrane skeleton. The composition of the spectrin-based-membrane skeleton appears affected as spectrin itself, myosin, and filamin, moesin, GPIbα, and GPIIb are less abundant in this compartment. Spectrin-based membrane skeleton controls plasma membrane organization, stability, and shape and provides mechanical forces for the increment of elasticity and rigidity, which are needed to withstand the turbulence of blood circulation. Discontinuities in the skeleton may favor local inhomogeneities, creating specialized plasma membrane microdomains that may affect curvature and shape variation.[32] The spectrin-based membrane skeleton is critical for platelet membrane properties and has a strong effect on membrane shape and regulates the lateral distribution of the membrane glycoproteins to which it is attached.[27] It has recently been shown that the cortical actin-myosin-spectrin system brings external compressive forces during barbell-shaped proplatelet formation and determines platelet size.[15,19,33] This is important in the context of nonmuscle myosin MYH9-related diseases affecting platelets,[33] and possibly Bernard-Soulier syndrome, and may explain the large size and decreased number of platelets of these patients. Interestingly, membrane skeleton proteins such as β-spectrin and filamin, as well as myosin IIA and moesin, were identified in a screen of proteins able to interact with PI3P.[34,35] Conversely, vinculin that localizes to the membrane skeleton is normal in PI3K-C2α$^{WT/D1268A}$ platelets and was found not to bind PI3P.[36] Thus, loss of a PI3K-C2α-derived pool of PI3P with low turnover may induce a mislocalization/stabilization of proteins at the membrane skeleton, leading to modifications in membrane biophysical properties. PI3K-C2α has been shown to regulate clathrin-dependent endocytosis[3] and to play an important role in cargo delivery to the primary cilium.[7] In endothelial cells, deletion of PI3K-C2α leads to defective delivery of VE-cadherin to cell junctions, leading to impaired assembly of endothelial junctions.[8] The class II PI3K homolog in flies regulates endosomal sorting from the endocytic compartment to the plasma membrane.[37,38] Thus, PI3K-C2α is a central spatiotemporal player of membrane dynamics by acting at several levels, including membrane skeleton organization, clathrin-dependent endocytosis, and endocytic recycling.

In megakaryocytes and platelets, which require intense membrane plasticity and remodeling, partial inactivation of the kinase activity of PI3K-C2α has profound consequences. In addition to a disorganization of the membrane skeleton, defects in vesicular trafficking may also take place as suggested by α-granule defects. Although these structural defects have a minor effect on primary hemostasis, they are associated with a marked alteration in the function of platelets in arterial thrombosis. Interestingly, a very recent study by Mountford et al,[39] using knock-down mice models of PI3K-C2α, also highlights the key role of PI3K-C2α in the regulation of membrane structure and dynamics in platelets. In addition to similarities in the phenotypes of our KI and their knock-down models, several differences exist, including α-granule defects and thrombus stability, that may come from the putative scaffolding role of PI3K-C2α. In addition, by using a sensitive method to measure PI3P pools, we

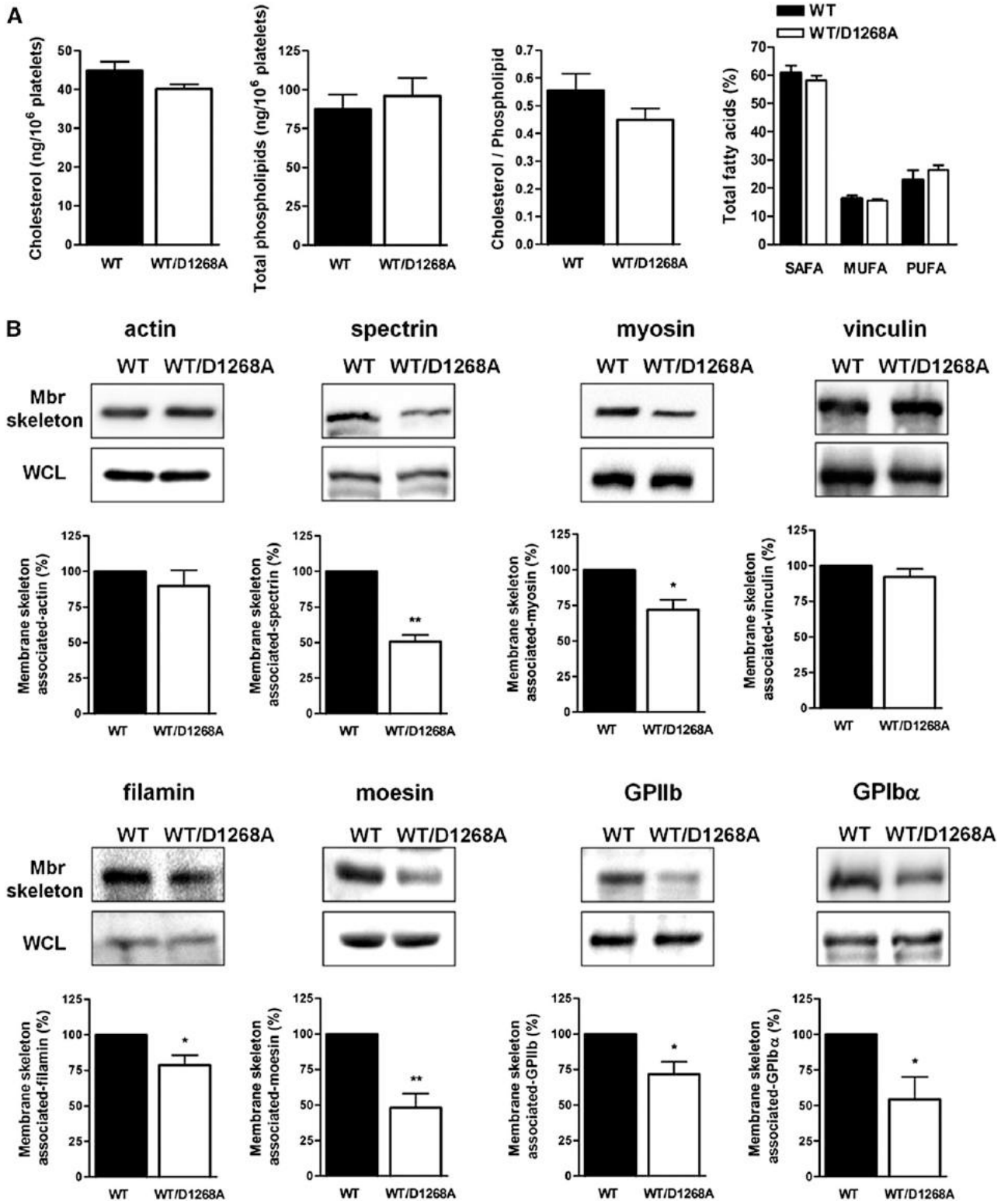

Figure 5. PI3K-C2α is a key regulator of plasma membrane/skeleton integrity. (A) Cholesterol, phospholipids, and fatty acids from resting platelets were analyzed as described in *Methods*. MUFA, monounsaturated fatty acids; PUFA, polyunsaturated fatty acids; SAFA, saturated fatty acids. (B) Western blot analysis of actin, spectrin, myosin, vinculin, filamin, moesin, GPIIb, and GPIbα from isolated membrane skeleton (Mbr skeleton) and whole lysates (WCL) of resting platelets (mean ± SEM; n = 4–7; $^*P < .05$, $^{**}P < .01$ vs WT according 1 sample *t* test).

provide evidence that defects in platelet biogenesis are linked to PI3K-C2α regulation of a PI3P housekeeping pool that was not observed by Mountford et al.

In conclusion, our study points to a new function of PI3K-C2α as a critical regulator of normal platelet ultrastructure through the control of membrane morphology and association with the cortical

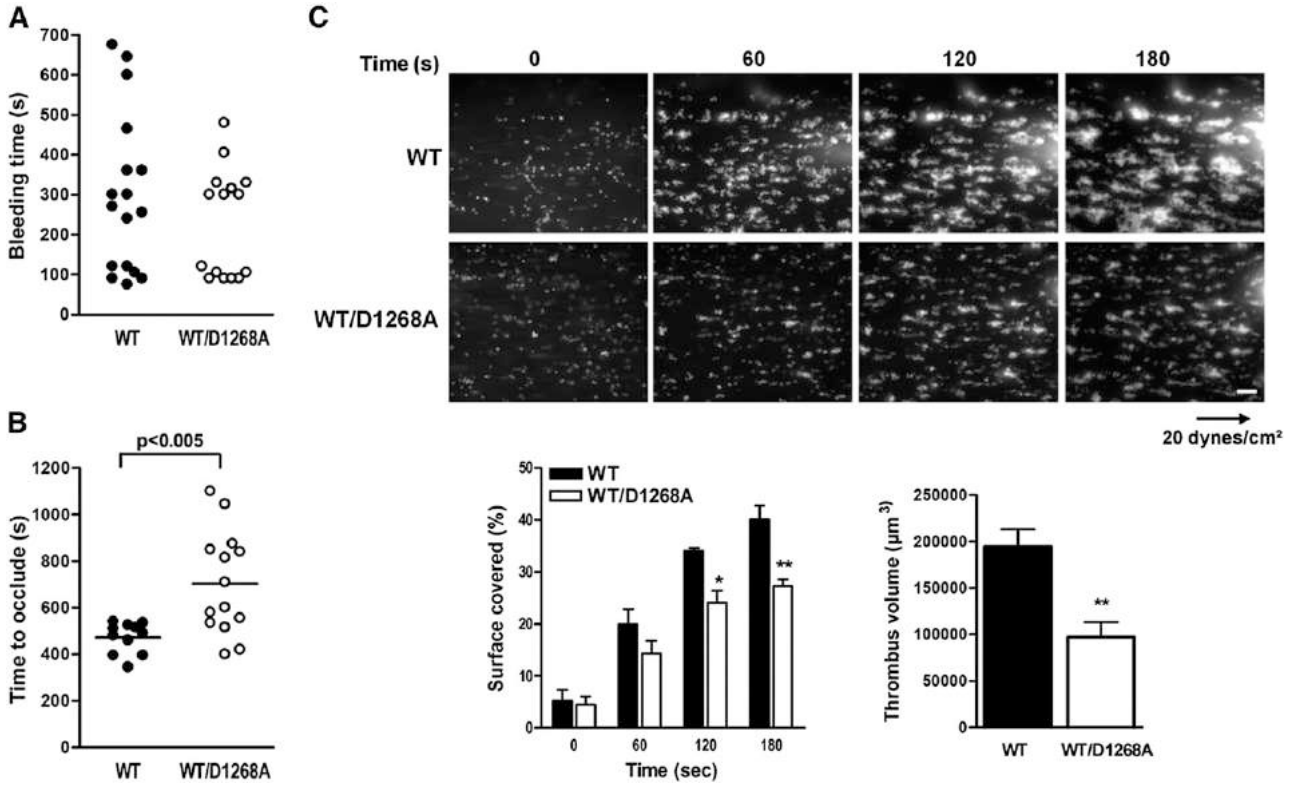

Figure 6. PI3K-C2α$^{WT/D1268A}$ mice exhibit defective platelet activation and prothrombotic capacity. (A) Tail bleeding time of WT (n = 17) and PI3K-C2α$^{WT/D1268A}$ (n = 18) mice was measured as described in *Methods*. (B) Thrombotic response of mice to ferric chloride injury of the carotid artery. Time to occlude (blood flow arrest) was measured in the carotid artery after exposure to 7.5% $FeCl_3$ for 3 minutes (mean ± SEM; n = 14 mice; $P < .005$ according to 2-tailed Student *t* test). (C) $DiOC_6$-labeled platelets in whole blood were perfused through a collagen-coated microcapillary at a shear rate of 20 dynes/cm^2 during 3 minutes. Thrombus formation was visualized in real time. Scale bar: 20 μm. Area covered by platelet thrombi and thrombus volume were measured using Image J software (mean ± SEM; n = 3; *$P < .05$, **$P < .01$ vs WT according to 2-tailed Student *t* test and 2-way ANOVA).

skeleton, with consequences on the level of circulating barbell-shaped proplatelets and on the arterial thrombosis function of platelets.

Acknowledgments

We thank the personnel of Anexplo animal facilities (US006/Centre Régional d'Exploration Fonctionnelle et de Ressources Expérimentales Inserm / Université Toulouse III) for animal handling and the Non-Invasive Exploration Service (US006/Centre Régional d'Exploration Fonctionnelle et de Ressources Expérimentales Inserm / Université Toulouse III) for the use of their irradiator, Genotoul Imaging facilities (INSERM U1048, R. D'angelo and M. Zanoun; Centre de Microscopie Electronique Appliqué à la Biologie/Université Toulouse III, B. Payre and I. Fourqaux), the cytometry facility of Inserm U1048 (A. Zakaroff-Girard and C. Pecher), the genomic and transcriptomic platform of Inserm U1048 (J. J. Maoret and F. Martins), and the lipidomic facility of Inserm U1048 (J. Bertrand-Michel). We thank J. Viaud for providing the FYVE^{HRS} probe and P. Valet for *Pik3c2a* gene RT-PCR primers. We also thank all members of the B.P. laboratory.

C.V. was supported by a PhD grant from Université Toulouse III. C.C. was supported by an EU Marie Curie fellowship (PIIF-GA-2009-252846). Work in the laboratory of B.P. was supported by Inserm (U104815B and SPDOTSEVERI) and the Fondation pour la Recherche Médicale (R13059BB). Work in the laboratory of B.V. was supported by the Medical Research Council (G0700755), the UK Biotechnology and Biological Sciences Research Council (BB/I007806/1), Cancer Research UK (C23338/A15965), the Ludwig Institute for Cancer Research, and the National Institute for Health Research University College London Hospitals Biomedical Research Centre. B.P. is a scholar of the Institut Universitaire de France.

Authorship

Contribution: C.V. and S.S. designed and performed most experiments and analyzed the data; C.C., M.A.W., and B.V. generated and carried out the basic characterization of the PI3K-C2α^{D1268A} mice; G.C. and B.P. designed and performed phosphoinositide analysis; C.S. performed AFM experiments; C.C. performed arterial thrombosis in vivo; F.G.-I. and M.-P.G. analyzed data; and B.P., B.V., and S.S. analyzed data and wrote the article.

Conflict-of-interest disclosure: B.V. is a consultant to Retroscreen (London, United Kingdom) and Karus Therapeutics (Oxford, United Kingdom).

Correspondence: Sonia Severin, INSERM, U1048-Université Toulouse III, Institut des Maladies Métaboliques et Cardiovasculaires, 1 Avenue Jean Poulhes, BP 84225, 31432 Toulouse Cedex 04, France; e-mail: sonia.severin@inserm.fr.

References

1. Di Paolo G, De Camilli P. Phosphoinositides in cell regulation and membrane dynamics. *Nature.* 2006;443(7112):651-657.
2. Vanhaesebroeck B, Guillermet-Guibert J, Graupera M, Bilanges B. The emerging mechanisms of isoform-specific PI3K signalling. *Nat Rev Mol Cell Biol.* 2010;11(5):329-341.
3. Posor Y, Eichhorn-Gruenig M, Puchkov D, et al. Spatiotemporal control of endocytosis by phosphatidylinositol-3,4-bisphosphate. *Nature.* 2013;499(7457):233-237.
4. Devereaux K, Dall'Armi C, Alcazar-Roman A, et al. Regulation of mammalian autophagy by class II and III PI 3-kinases through PI3P synthesis. *PLoS One.* 2013;8(10):e76405.
5. Falasca M, Maffucci T. Regulation and cellular functions of class II phosphoinositide 3-kinases. *Biochem J.* 2012;443(3):587-601.
6. Fan CW, Chen B, Franco I, et al. The Hedgehog pathway effector smoothened exhibits signaling competency in the absence of ciliary accumulation. *Chem Biol.* 2014;21(12): 1680-1689.
7. Franco I, Gulluni F, Campa CC, et al. PI3K class II α controls spatially restricted endosomal PtdIns3P and Rab11 activation to promote primary cilium function. *Dev Cell.* 2014;28(6):647-658.
8. Yoshioka K, Yoshida K, Cui H, et al. Endothelial PI3K-C2α, a class II PI3K, has an essential role in angiogenesis and vascular barrier function. *Nat Med.* 2012;18(10):1560-1569.
9. Zhang J, Banfić H, Straforini F, Tosi L, Volinia S, Rittenhouse SE. A type II phosphoinositide 3-kinase is stimulated via activated integrin in platelets. A source of phosphatidylinositol 3-phosphate. *J Biol Chem.* 1998;273(23): 14081-14084.
10. George JN. Platelets. *Lancet.* 2000;355(9214): 1531-1539.
11. Hartwig JH. The platelet: form and function. *Semin Hematol.* 2006;43(1 Suppl 1):S94-S100.
12. Chang Y, Bluteau D, Debili N, Vainchenker W. From hematopoietic stem cells to platelets. *J Thromb Haemost.* 2007;5(Suppl 1):318-327.
13. Behnke O, Forer A. From megakaryocytes to platelets: platelet morphogenesis takes place in the bloodstream. *Eur J Haematol Suppl.* 1998; 61:3-23.
14. Junt T, Schulze H, Chen Z, et al. Dynamic visualization of thrombopoiesis within bone marrow. *Science.* 2007;317(5845):1767-1770.
15. Patel-Hett S, Wang H, Begonja AJ, et al. The spectrin-based membrane skeleton stabilizes mouse megakaryocyte membrane systems and is essential for proplatelet and platelet formation. *Blood.* 2011;118(6):1641-1652.
16. Poirault-Chassac S, Nguyen KA, Pietrzyk A, et al. Terminal platelet production is regulated by von Willebrand factor. *PLoS One.* 2013;8(5):e63810.
17. Schwertz H, Köster S, Kahr WH, et al. Anucleate platelets genere progeny. *Blood.* 2010;115(18): 3801-3809.
18. Thon JN, Italiano JE Jr. Does size matter in platelet production? *Blood.* 2012;120(8): 1552-1561.
19. Thon JN, Macleod H, Begonja AJ, et al. Microtubule and cortical forces determine platelet size during vascular platelet production. *Nat Commun.* 2012;3:852.
20. Thon JN, Montalvo A, Patel-Hett S, et al. Cytoskeletal mechanics of proplatelet maturation and platelet release. *J Cell Biol.* 2010;191(4): 861-874.
21. Severin S, Gaits-Iacovoni F, Allart S, Gratacap MP, Payrastre B. A confocal-based morphometric analysis shows a functional crosstalk between the actin filament system and microtubules in thrombin-stimulated platelets. *J Thromb Haemost.* 2013;11(1):183-186.
22. Chicanne G, Severin S, Boscheron C, et al. A novel mass assay to quantify the bioactive lipid PtdIns3P in various biological samples. *Biochem J.* 2012;447(1):17-23.
23. Giuriato S, Pesesse X, Bodin S, et al. SH2-containing inositol 5-phosphatases 1 and 2 in blood platelets: their interactions and roles in the control of phosphatidylinositol 3,4,5-trisphosphate levels. *Biochem J.* 2003;376(Pt 1):199-207.
24. Hutter JL, Bechhoefer J. Calibration of atomic-force microscope tips. *Rev Sci Instrum.* 1993; 64(7):1868-1873.
25. Sneddon IN. The relation between load and penetration in the axisymmetric problem for a punch of arbitrary profile. *Int J Eng Sci.* 1965; 3(1):47-57.
26. Payrastre B. Phosphoinositides: lipid kinases and phosphatases. *Methods Mol Biol.* 2004;273: 201-212.
27. Fox JE, Boyles JK. The membrane skeleton– a distinct structure that regulates the function of cells. *BioEssays.* 1988;8(1):14-18.
28. Italiano JE Jr. Unraveling mechanisms that control platelet production. *Semin Thromb Hemost.* 2013; 39(1):15-24.
29. Hartwig J, Italiano J Jr. The birth of the platelet. *J Thromb Haemost.* 2003;1(7):1580-1586.
30. Thon JN, Italiano JE. Platelets: production, morphology and ultrastructure. *Handb Exp Pharmacol.*2012(210):3-22.
31. Mazza S, Maffucci T. Class II phosphoinositide 3-kinase C2alpha: what we learned so far. *Int J Biochem Mol Biol.* 2011;2(2):168-182.
32. De Matteis MA, Morrow JS. Spectrin tethers and mesh in the biosynthetic pathway. *J Cell Sci.* 2000;113(Pt 13):2331-2343.
33. Spinler KR, Shin JW, Lambert MP, Discher DE. Myosin-II repression favors pre/proplatelets but shear activation generates platelets and fails in macrothrombocytopenia. *Blood.* 2015;125(3): 525-533.
34. Catimel B, Kapp E, Yin MX, et al. The PI(3)P interactome from a colon cancer cell. *J Proteomics.* 2013;82:35-51.
35. Gunn-Moore FJ, Welh GI, Herron LR, et al. A novel 4.1 ezrin radixin moesin (FERM)-containing protein, 'Willin'. *FEBS Lett.* 2005;579(22): 5089-5094.
36. Steimle PA, Hoffert JD, Adey NB, Craig SW. Polyphosphoinositides inhibit the interaction of vinculin with actin filaments. *J Biol Chem.* 1999; 274(26):18414-18420.
37. Jean S, Cox S, Schmidt EJ, Robinson FL, Kiger A. Sbf/MTMR13 coordinates PI(3)P and Rab21 regulation in endocytic control of cellular remodeling. *Mol Biol Cell.* 2012; 23(14):2723-2740.
38. Velichkova M, Juan J, Kadandale P, et al. Drosophila Mtm and class II PI3K coregulate a PI(3)P pool with cortical and endolysosomal functions. *J Cell Biol.* 2010;190(3):407-425.
39. Mountford JK, Petitjean C, Putra HW, et al. The class II PI 3-kinase, PI3KC2α, links platelet internal membrane structure to shear-dependent adhesive function. *Nat Commun.* 2015;6:6535.

SUPPLEMENTAL DATA

SUPPLEMENTAL METHODS

Materials: Anti–GPIbα, α2-FITC, GPVI-FITC and GPIb-FITC antibodies were from Emfret Analytics. Anti-GPIIb and anti-p-MLC^{S19} antibodies were obtained from Santa Cruz Technologies. Anti-moesin, anti-vps34 and anti-p-Akt^{S473} antibodies were purchased from Cell Signaling Technology. AlexaFluor secondary antibodies and streptavidin-PE were obtained from Invitrogen. Biochips with microcapillaries (Vena8Fluoro+) were obtained from Cellix. Anti-human von Willebrand factor, anti-human von Willebrand factor HRP and anti-human fibrinogen antibodies were purchased from Dako. Mouse von Willebrand factor was a gift from Dr. Cécile Denis (Inserm U770, Le Kremlin-Bicêtre, Paris, France). Anti- GPIIb-FITC, anti-PI3K-C2α and anti-PI3K-C2β antibodies were from BD Pharmingen. Anti-p85 and anti-filamin antibodies were from Merck Millipore and anti-spectrin antibody was from Abcam. Lipids were from Avanti Polar Lipids (Coger, Paris, France). CRP was from Pr. Richard Farndale laboratory (Cambridge, UK). Collagen Reagent HORM® (equine) suspension was purchased from Takeda, $DIOC_6$ from Life Technologies. All other reagents were purchased from Sigma-Aldrich.

Quantitative real-time polymerase chain reaction (PCR) determination of transcript levels: Total RNA was isolated from megakaryocytes using GeneJet RNA purification kit (Thermo Scientific) according to the manufacturer's instructions. Reverse transcription and cDNA pre-amplification were performed with Single Cell-to-CT Kit (Ambion, Life Technologies) according to manufacturer's instructions. Quantitative PCR were performed with MESA BLUE qPCR MasterMix (Eurogentec) in a ViiA 7 Real-Time PCR System (Life Technologies) according to manufacturer's instructions.

Preparation of murine platelets: Whole blood was drawn from the inferior *vena cava* of anesthetized mice into a syringe containing acid citrate dextrose (1 volume anticoagulant / 9 volumes blood). Platelet-rich plasma was obtained by mixing blood with 1 volume of modified HEPES-Tyrode's buffer (140 mM NaCl, 2 mM KCl, 12 mM $NaHCO_3$, 0.3 mM NaH_2PO_4, 1 mM $MgCl_2$, 5.5 mM glucose, 5 mM HEPES, pH 6.7) containing 0.35 % BSA followed by a 300 x *g* centrifugation for 4 min. After PGI_2 addition at a final concentration of 500 nM to the PRP, platelets were pelleted by centrifugation at 1,000 x *g* for 6 min, resuspended in modified HEPES-Tyrode's buffer (pH 7.38) in the presence of 0.02 IU/ml of the ADP scavenger apyrase (adenosine-5′-triphosphate diphosphohydrolase), and rested for 45 min at 37°C.

Bone marrow transplantation: Recipient mice were lethally irradiated (9.2 Gy, γ source) and then reconstituted with an intravenous injection of freshly isolated mice bone marrow cells. Chimera mice were used 6 weeks after injection. The genotype of reconstituted bone marrow cells was assessed by PCR.

Flow cytometry: Platelets were stained with FITC-conjugated anti–mouse α2, anti–mouse GPVI, anti–mouse GPIIb, anti–mouse GPIb antibodies for 30 min and analyzed using an LSRFortessa^{TM} Cell analyser flow cytometer and Diva software (Becton Dickinson). For mepacrine uptake, washed platelets were incubated with 100 nM mepacrine in the dark at 37°C. After 30 min, stained platelets were analyzed using an LSRFortessa^{TM} Cell analyser flow cytometer and Diva software (Becton Dickinson).

ELISA assays: Serotonin quantification of washed platelets was performed using the IBL Serotonin ELISA test (RE59121, IBL) according to manufacturer's instructions. Washed platelet VWF levels were quantified by a previously described immunosorbent assay using -human von Willebrand factor, anti-human von Willebrand factor HRP antibodies (1).

Gel electrophoresis and immunoblotting: Proteins were resuspended in electrophoresis sample buffer containing 100 mM Tris-HCl (pH 6.8), 15% (v/v) glycerol, 25 mM DTT, and 3% SDS, boiled for 5 min, separated on SDS-PAGE, transferred onto a nitrocellulose membrane (Gelman Sciences), and analyzed using the relevant antibody.

Flow assay on collagen: Biochips microcapillaries (Vena8Fluoro+, Cellix) were coated with a collagen fibril suspension (50 µg/ml) for 1 h and saturated with a solution of 0.5 % BSA. Blood was drawn into heparin (10 IU/ml), and platelets were labeled with $DIOC_6$ (2 µM) in whole blood. Using a syringe pump (PHD-2000, Harvard Apparatus) labelled blood was then perfused through a microcapillary for 3 min at a wall shear rate of 20 dynes/cm^2. Platelet adhesion and thrombus formation was visualized with a 40x oil immersion objective for both fluorescent and transmitted light microscopy and recorded in real time (1 frame every 5 sec) with ORCA Camera (Zeiss). Image sequences of the time lapse recording and analysis of surface coverage were performed offline on single frame by quantification of pixel surface after manual thresholding using ImageJ. Thrombi volumes are calculated by thresholding of surface covered by thrombi on slice of Z-stack images and addition of voxel (automatically converted into μm^3 by Zen® Zeiss software).

Carotid artery thrombosis: Right and left carotids were dissected from surrounding tissues. A 1 × 4-mm strip of paper saturated with 7.5 % $FeCl_3$ solution (Mallinckrodt Chemical) was applied to the adventitial surface of the right carotid for 3 min. Left carotid was used as an internal control. Flow probes connected to a Transonic model T403 flow meter (Transonic System; Emka Technologies) were used to record carotid blood flow (milliliters per min) continuously throughout the procedure (IOX software). The time for total occlusion (no more blood flow) was recorded.

Tail bleeding time: Bleeding was measured by 3-mm tail-tip transection mice anesthetized by an i.p. injection of a mixture of ketamine (25 mg/kg) and xylazine (10 mg/kg). A stopwatch was started immediately upon transection to determine the time required for the bleeding to stop. Blood drops were removed every 15 sec with the use of a paper filter. If bleeding did not recur within 30 sec of cessation, it was considered stopped.

REFERENCE

1. Romijn RA, *et al*. (2003) Mapping the collagen-binding site in the von Willebrand factor-A3 domain. *The Journal of biological chemistry* 278(17):15035-15039.

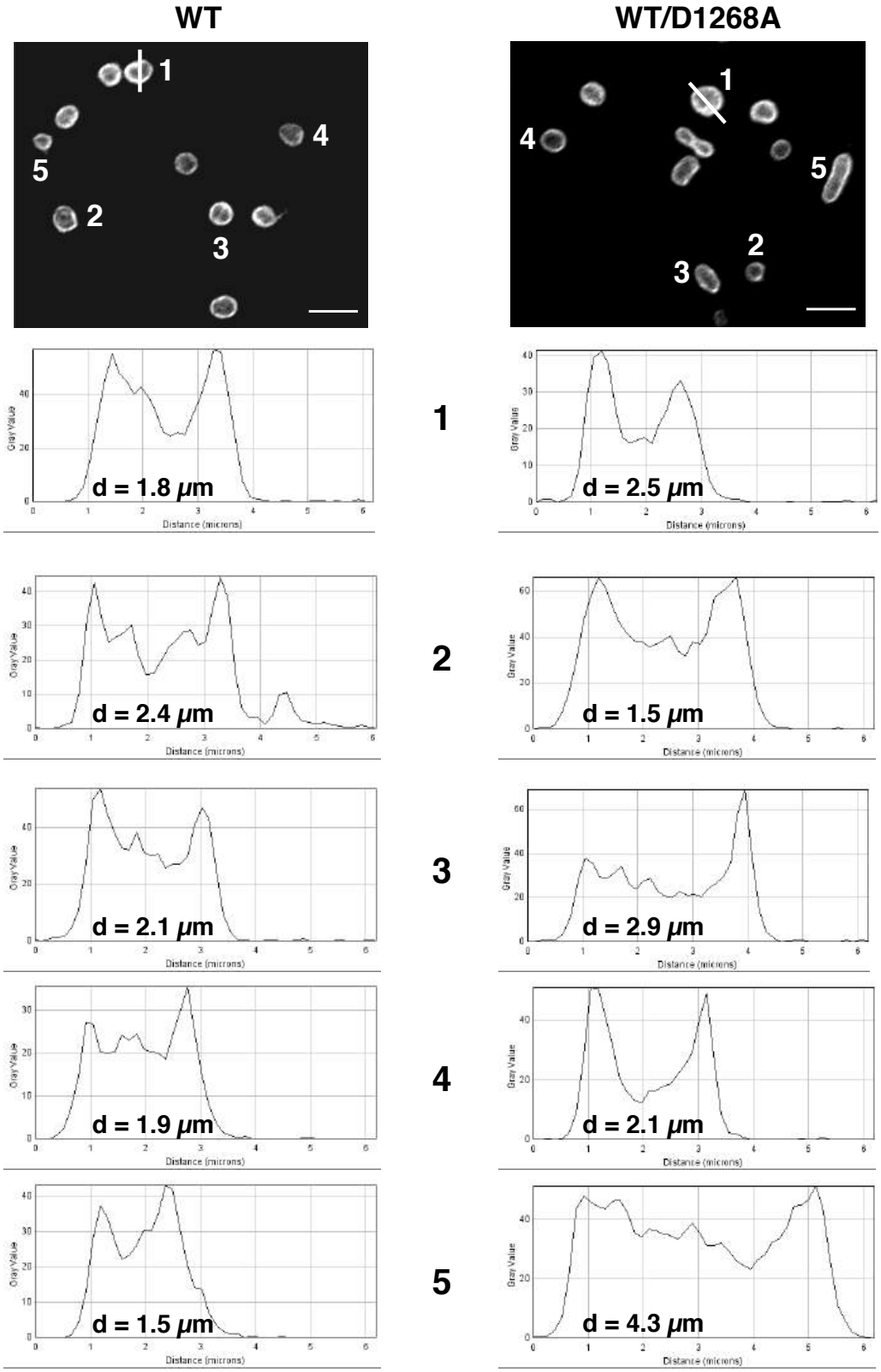

Supplemental Figure 1: PI3K-C2α$^{WT/D1268A}$ mice display platelet size heterogeneity. Resting washed platelets were fixed and labelled with an anti-α-tubulin and AlexaFluor secondary antibodies. Tubulin ring diameter (d = distance between the two peaks and reflect of platelet diameter) was measured by linescan analysis using a Carl Zeiss LSM 780 confocal microscope and Image J software.[21] Five exemples of WT and PI3K-C2α$^{WT/D1268A}$ platelet linescan analysis are shown, barbell-shaped proplatelets were excluded for the analysis of platelet size.

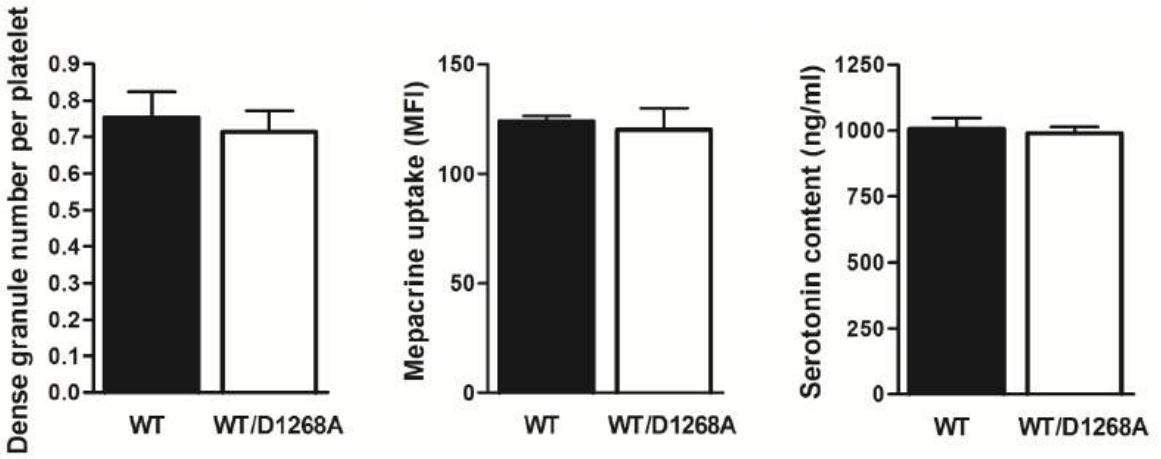

Supplemental Figure 2: Platelet dense granule content. Dense granule number were quantified on transmission electron microscopy images by ImageJ software (mean ± SEM, n=100 platelets). Dense granule content (mepacrine uptake and serotonin) was quantified on resting platelets as described in methods (mean ± SEM; n=3)

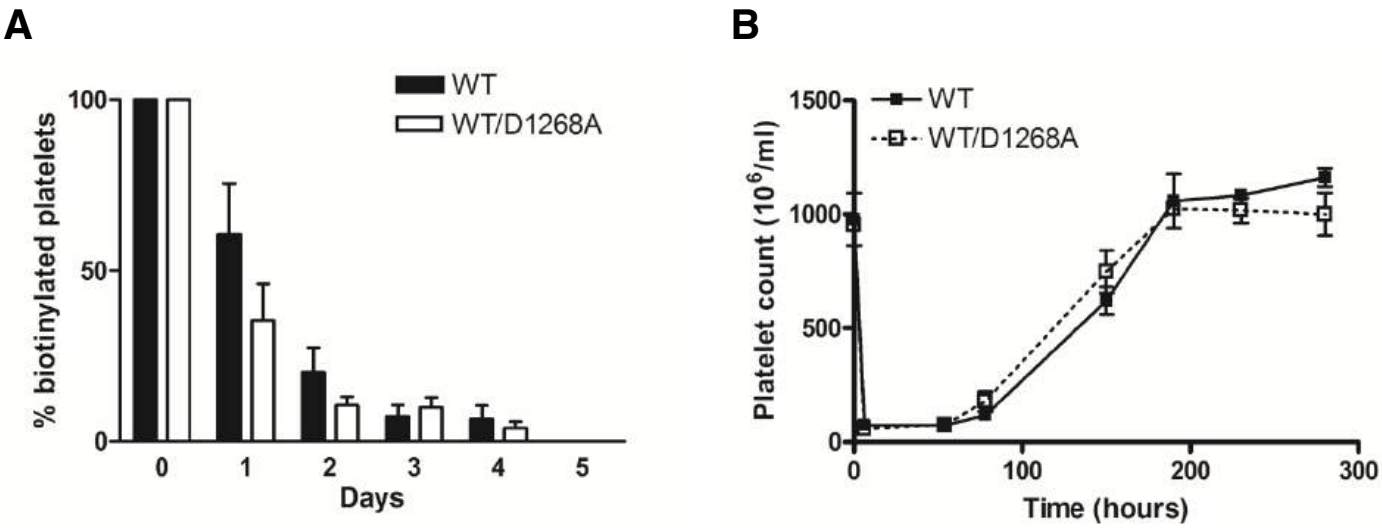

Supplemental Figure 3: PI3K-C2α$^{WT/D1268A}$ mice exhibit a normal platelet life span and platelet count recovery after immune induced thrombocytopenia. (**A**) Mice were injected intravenously with 150 µl of 4 mg/ml biotin-NHS on day 0. At various time points after injection, the percentage of biotinylated platelets (GPIIb$^+$biotin$^+$) was determined by flow cytometry by staining whole blood with anti–mouse GPIIb-FITC and streptavidin-PE for 30 min. Platelet survival was estimated from the decay curve of the percentage of biotinylated platelets over time. (**B**) Thrombocytopenia was induced in 8- to 12-week-old mice by intraperitoneal injection of anti-mouse GPIbα antibody (2 µg/g body weight). Blood samples were collected before injection (time=0) and then at 6, 54, 78, 150, 190, 230, and 280 h after injection by tail bleeding. Platelet counts were measured using a Micros60 (Horiba ABX Diagnostics).

Resting

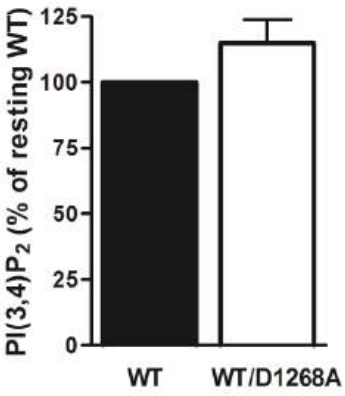

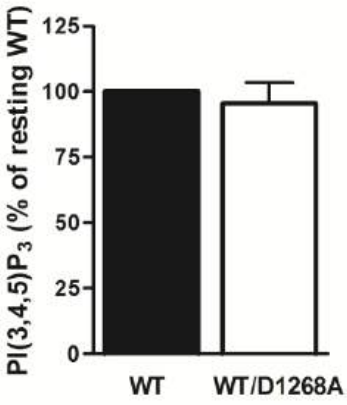

Stimulated

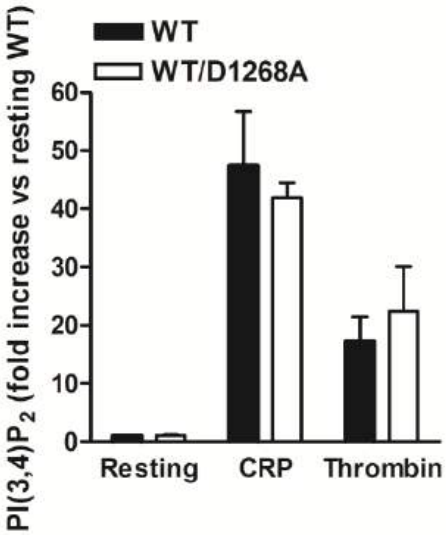

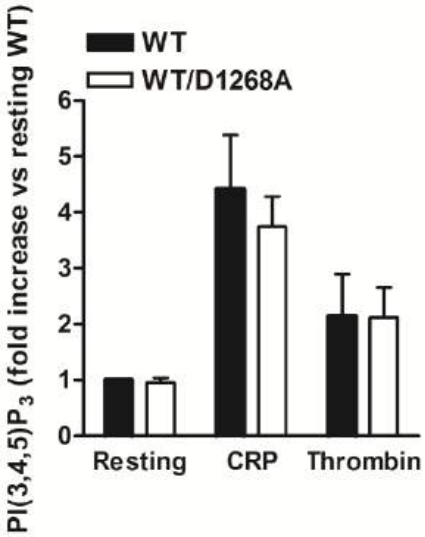

Supplemental Figure 4: Normal basal and inducible PI(3,4)P_2 and PI(3,4,5)P_3 levels in PI3K-C2α$^{WT/D1268A}$ platelets. HPLC analysis of PI(3,4)P_2 and PI(3,4,5)P_3 of resting and stimulated (10 µg/ml CRP and 0.5 IU/ml thrombin) ^{32}Pi-labelled platelets (mean ± SEM; n=3).

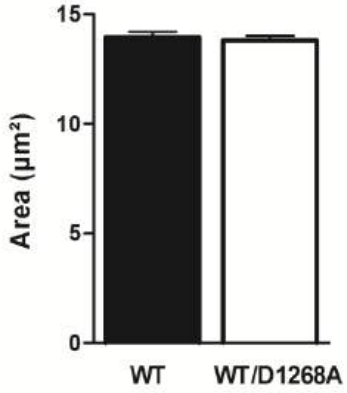

Supplemental Figure 5: WT and PI3K-C2α$^{WT/D1268A}$ platelets spread to similar extent onto fibrinogen. Washed platelets were placed on a fibrinogen-coated surface (100 µg/mL) in the presence of thrombin (0.5 IU/ml) during 45 min, fixed and labeled with phalloidin. Platelet area per condition were measured using ImageJ software (mean ± SEM; n>1000 platelets).

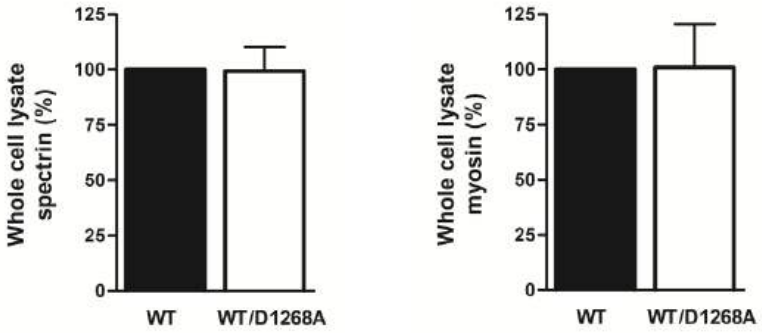

Supplemental Figure 6: Normal expression of spectrin and myosin in WT and PI3K-C2α$^{WT/D1268A}$ platelets. Western blot analysis of spectrin and myosin from whole cell lysates of resting platelets (mean ± SEM; n=6 and n=4 respectively).

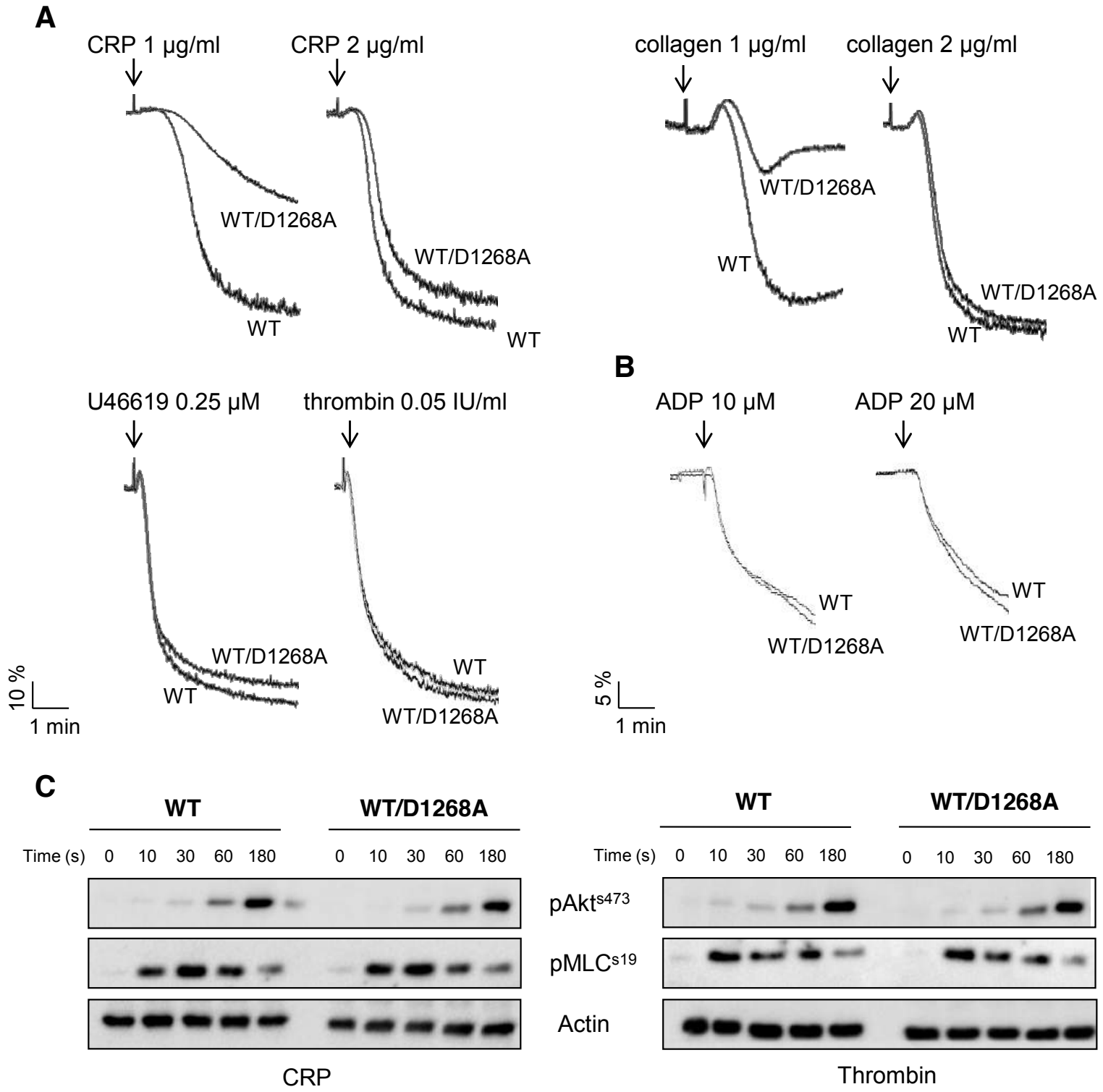

Supplemental Figure 7: PI3K-C2α$^{WT/D1268A}$ platelet aggregation and signalling. (**A**) Washed platelets were stimulated at indicated concentration of CRP, collagen, thromboxane A_2 analogue (U46619) and thrombin. (**B**) Whole blood was stimulated at indicated concentration of ADP. Aggregation was assessed with a Chrono-log dual-channel aggregometer under stirring at 1000 rpm for 5 minutes. Representative aggregation curves of 4 independent experiments are shown. (**C**) Washed platelets were stimulated with CRP (1 µg/ml) or thrombin (0.05 IU/ml) for the indicated times. Lysates were then immunoblotted with the indicated antibody. Data are representatives from 3 independent experiments.

- **Conclusions**

Grâce à un modèle original d'inactivation partielle de la PI3KC2α, nous avons mis en évidence le rôle majeur de la PI3KC2α dans la production plaquettaire. Tout d'abord, nous montrons que la PI3KC2α est un régulateur de la production basale du PtdIns3P plaquettaire et n'est pas impliquée dans la synthèse du pool de PtdIns3P induit par stimulation avec des agonistes plaquettaires. De plus, nous observons que la PI3KC2α contrôle la morphologie membranaire des MKs et des plaquettes. En effet, les plaquettes partiellement inactivées pour la PI3KC2α présentent des membranes tortueuses et invaginées, un SCO altéré et un défaut de biogénèse des granules α. L'inactivation de la PI3KC2α entraîne aussi une augmentation nette de « barbell-shaped proplatelets » dans la population plaquettaire. L'augmentation de la rigidité des plaquettes inactivées pour la PI3KC2α, mesurée par microscopie à force atomique, associée à leur incapacité d'étendre des filopodes démontre que la PI3KC2α contrôle la dynamique et les forces mécaniques membranaires des plaquettes. Le squelette sous-membranaire d'actine-spectrine-myosine joue un rôle important dans le maintien de la structure et de la dynamique membranaire des plaquettes ainsi que dans la scission des « barbell-shaped proplatelets » en deux plaquettes matures (Italiano, 2013). Or, nous avons mis en évidence un défaut de relocalisation de différentes protéines telles que la spectrine et la myosine au squelette sous-membranaire des plaquettes inactivées pour la PI3KC2α, ce qui montre un défaut d'intégrité du squelette sous-membranaire plaquettaire. Enfin, les défauts de structure et de dynamique membranaire des plaquettes inactivées pour la PI3KC2α ont des répercussions sur leur potentiel prothrombotique. Celles-ci forment des thrombi plus petits *ex vivo* et le temps d'occlusion de la carotide après lésion au chlorure ferrique des souris inactivées pour la PI3KC2α *in vivo* est augmenté sans pour autant altérer le temps de saignement à la queue.

En conclusion, les travaux de Mountford *et al* (Mountford et al., 2015) et l'ensemble de nos résultats montrent que la PI3KC2α joue un rôle clé dans la structuration des membranes plaquettaires. Nos travaux montrent, en outre, que la PI3KC2α régule : (i) la production d'un « pool » basal de PtdIns3P plaquettaire et (ii) l'intégrité du squelette sous-membranaire et de fait la structure et la dynamique membranaire nécessaire à la production de plaquettes fonctionnelles.

Ces travaux ont fait l'objet d'un commentaire dans le journal *Blood* en 2015 (cf. Annexe 3).

2) Le double jeu de la PI3K de classe III, Vps34, dans la production plaquettaire et la croissance du thrombus

Afin d'étudier le rôle de Vps34 dans la production et les fonctions plaquettaires, nous avons généré un modèle de souris original présentant une délétion de Vps34 spécifiquement dans la lignée mégacaryocytaire et les plaquettes (Pf4-Cre-*Pik3c3*$^{lox/lox}$). Nous avons également utilisé deux inhibiteurs spécifiques de Vps34, SAR405 et Vps34-IN1, récemment développés (Bago et al., 2014; Ronan et al., 2014).

Publication n°3

The double game of class III PI3K, Vps34, in platelet production and thrombus growth.

Colin Valet[1*], Marie Levade[1,2*], Gaetan Chicanne[1], Cendrine Cabou[1,3], Marie-Pierre Gratacap[1], Frederique Gaits-Iacovoni[1], Bart Vanhaesebroeck[4], Bernard Payrastre[1,4$], Sonia Severin[1$]

[1] Inserm U1048, I2MC and Universite Paul Sabatier, 31432, Toulouse Cedex 04, France

[2] CHU de Toulouse, Laboratoire d'Hematologie, 31059, Toulouse Cedex 03, France

[3] Faculte de Pharmacie, Chemin des maraîchers, Toulouse, France

[4] UCL Cancer Institute, Paul O'Gorman Building, University College London, London, United Kingdom

[*] The authors contribute equally to this work

[$] These authors share senior authorship

The double game of class III PI3K, Vps34, in platelet production and thrombus growth

Colin Valet[1*], Marie Levade[1,2*], Gaëtan Chicanne[1], Cendrine Cabou[1,3], Marie-Pierre Gratacap[1], Frédérique Gaits-Iacovoni[1], Bart Vanhaesebroeck[4], Bernard Payrastre[1,2$] and Sonia Severin[1$]

[1] *Inserm U1048 and Universite Toulouse 3, I2MC, Toulouse, France*

[2] *CHU de Toulouse, Laboratoire d'Hematologie, Toulouse, France*

[3] *Faculte de Pharmacie, Chemin des maraichers, Toulouse, France*

[4] *UCL Cancer Institute, Paul O'Gorman Building, University College London, 72 Huntley Street London WC1E 6DD, UK*

[*] *The authors contribute equally to this work*
[$] *These authors share senior authorship*

Address correspondence to:

Sonia Severin, Inserm U1048 and Universite Toulouse 3, I2MC, 31432 Toulouse Cedex4, France. Phone: +33-531224143; Email: sonia.severin@inserm.fr

Text word count : 4474
Abstract word count : 223
Number of figures and tables : 7
Number of references : 39

ABSTRACT

To uncover the physiological role of the class III phosphoinositide 3-kinase, Vps34, in MKs and platelets, which remains enigmatic, we have generated a mouse model with Vps34 deletion specifically in the megakaryocyte (MK)/platelet lineage (*PF4*-Cre/Vps34$^{lox/lox}$). Absence of Vps34 leads to a microthrombocytopenia associated to granule defects. Vps34 deficiency had no effect on MK polyploidisation or proplatelet formation but affected directional cues for MK migration toward SDF1α gradient linked to a significant reduction of PI3P associated to trafficking and autophagy defects. Surprisingly, in platelets, we show that Vps34 weakly contributes to the production of the basal pool of PI3P but is rather involved in the synthesis of the stimulation-dependent pool of PI3P. Absence of Vps34 has no effect on platelet lifespan but affects *ex vivo* thrombus growth at arterial shear rate. *Ex vivo* treatment of platelets with the recently developed Vps34 specific inhibitors, SAR405 or INH1, reproduced these defects, highlighting the role of Vps34 kinase activity in platelet activation, independently from its role in MKs. *In vivo*, Vps34 deletion has no impact on the tail bleeding time but significantly reduced the thrombotic capacity of platelets following carotid injury. This study shows for the first time a dual role for Vps34 as an important regulator of platelet production by MKs and as an unexpected player in the dynamics of platelet activation and arterial thrombus formation.

INTRODUCTION

Phosphoinositide 3-kinases (PI3Ks) are important lipid kinases producing D3-phosphorylated phosphoinositides that organize functional protein complexes regulating various biological processes [1, 2]. Class III PI3K, Vps34, represents the most ancient form of PI3Ks and was initially identified in yeast with an essential role in vacuolar trafficking [3]. Vps34 specifically catalyzes the phosphorylation of phosphatidylinositol to generate phosphatidylinositol 3-monophosphate (PI3P), a lipid present at relatively low amounts in cells which plays a central role in vesicular trafficking. In mammals, Vps34 has first been studied in cell lines where it regulates endocytic trafficking, autophagosome formation and mTOR activation [4, 5]. Recently, the organismal role of mammalian Vps34 has been investigated using mouse gene targeting strategies. Loss of the *Pik3c3* gene in mouse causes early embryonic lethality (between E7.5 and E8.5) due to severe decreased cell proliferation capacity [6]. *In vivo* studies using the tissue-specific cre-lox system have shown an important role for Vps34 in heart and liver functions [7] as well as in T cells [8], podocytes [9, 10] and skeletal muscles homeostasis and in sensory, cortical and hippocampal neuron integrity [11, 12] by regulating multiples aspects of endocytic/endosomal and/or autophagic pathways.

Nowadays, the role of Vps34 and its product, PI3P, in megakaryocytes (MKs) and platelets remains unknown. Platelets are small anucleate blood cells that play a vital role in preventing excessive blood loss in response to vascular injury by adhering to exposed extracellular matrix and forming an hemostatic plug. To efficiently produce around 10^{11} platelets each days into the circulation, MKs strategically locate close to bone marrow (BM) sinusoids and protrude long cytoplasmic extensions called proplatelets through the endothelium into the sinusoidal lumen to release *de novo* circulating platelets [13]. In MKs and platelets, intra-cellular trafficking is crucial in several processes such as platelet secretory granule biogenesis, receptor and organelles trafficking [14, 15, 16] for normal platelet production and responses.

Defining the role of Vps34 in these highly dynamic processes is important not only to gain insights into these complex mechanisms but also to bring new informations about this still poorly characterized kinase. Moreover, as inhibitors of Vps34 have been recently developed to increase the efficiency of chemotherapy [17, 18], it will be critical to characterize the effects of these new molecules on platelet production and functions. In this study, we have created a new mouse line with specific deletion of Vps34 in the MK/platelet lineage by *Pik3c3* gene targeting through tissue-specific expression of *Pf4*-Cre recombinase. We report that Vps34 is critical for platelet production as well as platelet granule biogenesis in MKs through the regulation of endosomal trafficking- and autophagy-related mechanisms including MK migration. Interestingly, we show that Vps34 has also a role in platelet activation where it controls the production of a stimulation-dependent pool of PI3P as well as thrombus growth under arterial shear stress. Our study provides new insights into the importance of Vps34 as a regulator of both platelet production by MKs and platelet activation/arterial thrombus growth.

METHODS

Animals: Mice were of C57BL/6 genetic background and housed in the Anexplo (Toulouse) vivarium according to institutional guidelines. For all experiments, 8 to 14 week-old mice were used. Ethical approval for animal experiments was obtained from the French Ministry of Research in agreement with European Union guidelines.

MK purification and culture: Bone marrow cells were obtained from femora and tibiae of C57BL/6 mice by flushing, and cells expressing one or more of the following surface proteins, CD16/CD32$^+$, Gr1$^+$, B220$^+$, CD11b$^+$, were depleted using immunomagnetic beads (sheep anti-rat IgG Dynabeads; Invitrogen, Paisley, UK). The remaining population was cultured in 2.6% serum-supplemented Stempro medium with 2 mM l-glutamine, penicillin/streptomycin, 20 ng/mL murine stem cell factor (SCF) and 50 ng/mL murine TPO at 37°C under 5% CO_2 for 3 days.

Immunofluorescence: MKs were allowed to adhere on a fibronectin-coated coverslip (20µg/mL) for 1 h. For EEA1 and LC3 staining, MKs were fixed and permeabilized in one step for 45 min in PBS (phosphate buffered saline) with 3.7% formaldehyde and 0.05% Triton X100. Samples were saturated in 3% fatty acid free BSA in PBS for 20 min and incubated with primary antibody, relevant Alexa Fluor®^{488} secondary antibody and DAPI for 2 h at room temperature. PI3P labeling using specific anti-PI3P antibody was performed as previously described [19]. For lysosome content analysis, MKs were stained with LysoTracker® Deep Red (100nM) for 30 min, washed and fixed with 3.7% formaldehyde for 30 min. For endocytosis assay, MKs were incubated for 20 min at 4°C with 20 µg/mL transferrin-Alexa Fluor®^{546}, washed and incubated for the indicated time periods at 37°C before being fixed with 3.7% formaldehyde for 30 min. Confocal images were captured with a LSM780 operated with Zen software (Carl Zeiss). Image analysis was performed using ImageJ software.

Platelet lifespan: Circulating platelets were labelled *in vivo* by intravenous injection of Dylight^{488}-anti-GPIbβ Ig derivative (0.1µg/g body weight). 2 h after antibody injection and every 24 h for 4 days, the percentage of the Dylight^{488}-positive platelet population in whole blood was determined using an LSRFortessa^{TM} Cell analyser flow cytometer (BD Biosciences).

Immune induced thrombocytopenia: Thrombocytopenia was induced in 8- to 12-week-old mice by intraperitoneal injection of anti-mouse GPIbα antibody (2 µg/g of mouse). Blood samples were collected at indicated times. Platelet counts were measured using Micros60 (Horiba ABX Diagnostics).

MK migration assay: Chemotaxis was assessed using the Dunn chamber (Chemotaxis Dunn, Hawksley). MKs were allowed to adhere on fibronectin-coated (20 µg/mL) coverslips in complete medium at 37°C for 1h. The coverslip was then placed directly onto the Dunn chamber where the inner well is filled with serum free medium and the outer well with serum free medium containing 300 ng/mL SDF1α. The Dunn chamber was placed into a 5% humidified CO_2 atmosphere at 37°C. Videomicroscopy was performed with an Axio Observer.Z1 inverted microscope operated by the Zen software (Carl Zeiss), in controlled atmosphere for 6h. Images were taken every 5 min with an ORCA R2 camera (Hamamatsu, Japan) using a 10x, 0.30 EC Plan Neofluar objective lens (Carl Zeiss). Migration analysis were performed using ImageJ software and Chemotaxis tool plug-in.

CXCR4 surface expression: MKs were fixed with 3.7% formaldehyde for 30 min and stained with FITC-conjugated anti-CXCR4 for 45 min at room temperature. Samples were analyzed using an LSRFortessa^{TM} Cell analyser flow cytometer and Diva software (Becton Dickinson).

Scanning and Transmission electron microscopy were performed on washed platelets and freshly isolated bone marrow from tibiae as previously described [20].

Platelet aggregation and α-granule (P-selectin) and dense granule secretion (ATP): Aggregation and adenosine triphosphate (ATP) secretion were measured simultaneously under continuous stirring at 1000 rpm at 37°C using a Born lumi-aggregometer (Chrono-Log). Resting and stimulated washed platelets (1×10^6) were incubated with 1 μg/μl FITC-labeled anti–P-selectin antibody for 30 minutes, and fixed with 1% formalin for 10 minutes. Samples were analyzed with LSRFortessa^{TM} Cell analyser flow cytometer and Diva software (Becton Dickinson).

αIIbβ3 integrin function assays: For integrin activation, washed platelets (1×10^6) were stimulated with agonists at 37°C for 15 min in presence of 1mM Ca^{2+} and incubated subsequently with PE-conjugated JON/A antibody for 30 min at room temperature before being analyzed using an LSRFortessa^{TM} Cell analyser flow cytometer and Diva software (Becton Dickinson). For spreading experiments under static condition, coverslips were coated with 100μg/ml of human fibrinogen and blocked with 1% BSA. Washed platelets (1×10^7 platelets) were allowed to adhere and spread on fibrinogen for 20 min at 37°C. Platelets were either fixed with 1.5% formaldehyde for 30 min, permeabilsed with 0.1% Triton X100 for 10 min and labelled with phalloidin Alexa Fluor®^{488} for confocal analysis with a LSM780 operated with Zen software (Carl Zeiss) and with ImageJ software.

Flow assay on collagen, carotid artery thrombosis and tail bleeding time were performed as described previously [20, 21]. For assay of new platelets incorporation into an existing thrombus, unlabelled whole blood was perfused through a collagen-coated microcapillary at 60 dynes/cm^2. After 1 min of flow, blood was replaced by $DiOC_6$-labelled whole blood and

perfused for 1 min at 60 dynes/cm^2. The surface covered (%) by fluorescent platelets was then analyzed using ImageJ software.

Statistical analysis: Data are expressed as mean ± SEM. Significance of differences was determined using two-tailed Student's test or two-way ANOVA or one sample *t* test. P values < 0.05 were considered significant. (*p<0.05, **p<0.01, ***p<0.001).

RESULTS

Conditional genetic deletion of Vps34 in the MK/platelet lineage

We generated a mouse model with a conditional specific deletion of Vps34 in the MK/platelet lineage by *Pik3c3* gene targeting. Exon 21 of the kinase domain of the *Pik3c3* gene was flanked by *LoxP* sites (*Pik3c3*$^{lox/lox}$) to enable its excision by Cre recombinase. Deletion of exon 21 of the kinase domain of the *Pik3c3* gene specifically in the MK/platelet lineage was obtained by breeding *Pik3c3*$^{flox/flox}$ mice with *Pf4*-Cre transgenic mice to generate *Pf4*-Cre-*Pik3c3*$^{lox/lox}$ mice (referred as Vps34). Littermate *Pik3c3*$^{lox/lox}$ (referred as WT) mice were used as controls. Western blot analysis shows a severe deficiency of the full-length Vps34 protein in MKs and platelets from *Pf4*-Cre-*Pik3c3*$^{lox/lox}$ mice (- 84.3% ± 2.6% and - 87.8% ± 1.5% of WT for MKs and platelets respectively, Supplemental Figure 1A). The amount of Vps34 regulatory protein kinase, Vps15, was also strongly decreased in MKs and platelets from *Pf4*-Cre-*Pik3c3*$^{lox/lox}$ mice when compared to WT mice (Supplemental Figure 1A). Vps34 deletion has no impact on the expression of class I PI3K catalytic or regulatory subunits or class II PI3Ks (Supplemental Figure 1A) and is, as expected, MK/platelet lineage specific (Supplemental Figure 1B). Consistent with the low level of remaining Vps34 and Vps15 protein expression (~15%), a residual lipid-kinase activity (17.1% ± 4.1%) was detected in Vps34 immunoprecipitated from Vps34-deficient platelets (Supplemental Figure 1C). *Pf4*-Cre-*Pik3c3*$^{lox/lox}$ mice are viable and fertile, develop normally with no apparent morphological abnormalities and showed no signs of spontaneous bleeding.

Mild microthrombopenia and platelet granule abnormalities in absence of Vps34

Platelets (150 to 400 × 10^3 platelets/µl in humans and 700 to 1500 × 10^3 platelets/µl in mice) circulate in blood with a short lifespan (7 to 10 days in humans and 3 to 5 days in mice). Deletion of Vps34 in the MK/platelet lineage resulted in a moderated microthrombocytopenia

as shown by a significant decreased in median platelet count (- 19.3 % ± 0.5 %) and in mean platelet size (Figure 1A). The decrease in size is outlined by a significant increased percentage of *Pf4*-Cre-*Pik3c3*$^{lox/lox}$ mice with a mean platelet volume <7 μm^3 compared to WT mice and a mean platelet volume of 6.18 μm^3 ± 0.24 μm^3 for *Pf4*-Cre-*Pik3c3*$^{lox/lox}$ mice versus 7.39 μm^3 ± 0.22 μm^3 for WT mice (n=30, $p<0.05$). Expression levels of major platelet surface receptors were comparable in *Pf4*-Cre-*Pik3c3*$^{lox/lox}$ and WT platelets (Supplemental Figure 1D).

Circulating platelet count and size are the net result of a balance between platelet clearance and platelet production. To determine the cause of this microthrombocytopenia, we measured *in vivo* platelet lifespan and platelet count recovery after immune-induced platelet depletion. Platelet lifespan was normal in *Pf4*-Cre-*Pik3c3*$^{lox/lox}$ mice (Figure 1B) whereas platelet production was affected (Figure 1C). Indeed, despite a normal platelet recovery kinetic following anti-GPIbα antibody-induced thrombocytopenia, a reduced number of platelets was produced in *Pf4*-Cre-*Pik3c3*$^{lox/lox}$ mice (Figure 1C). Accordingly, serum TPO levels, which are inversely proportional to platelet count, were significantly elevated in *Pf4*-Cre-*Pik3c3*$^{lox/lox}$ (Figure 1C). Overall, these findings show that *Pf4*-Cre-*Pik3c3*$^{lox/lox}$ mice thrombocytopenia is due to a reduced rate of platelet production by MKs.

Morphological analysis by transmission electron microscopy (TEM) revealed an abnormal granule distribution in Vps34-depleted platelets (Figure 1D). These platelets display a 33.2% ± 3.1% reduction in the number and 44.5 % ± 3.2% increase in the size of α-granules compared to WT platelets (Figure 1D). Abnormality of dense granules in Vps34-depleted platelets is also observed (Figure 1D). The global platelet α- or dense- granule content of von Willebrand factor (VWF), fibrinogen and serotonin was however not affected (Supplemental Figure 2A). Of note, mitochondria content and activity (investigated by TEM, MitoTracker® labeling and mitoSOX® staining) (Supplemental Figure 2B) as well as lysosome content and activity (investigated by levels of the lysosomal protein LAMP-1 (lysosomal-associated

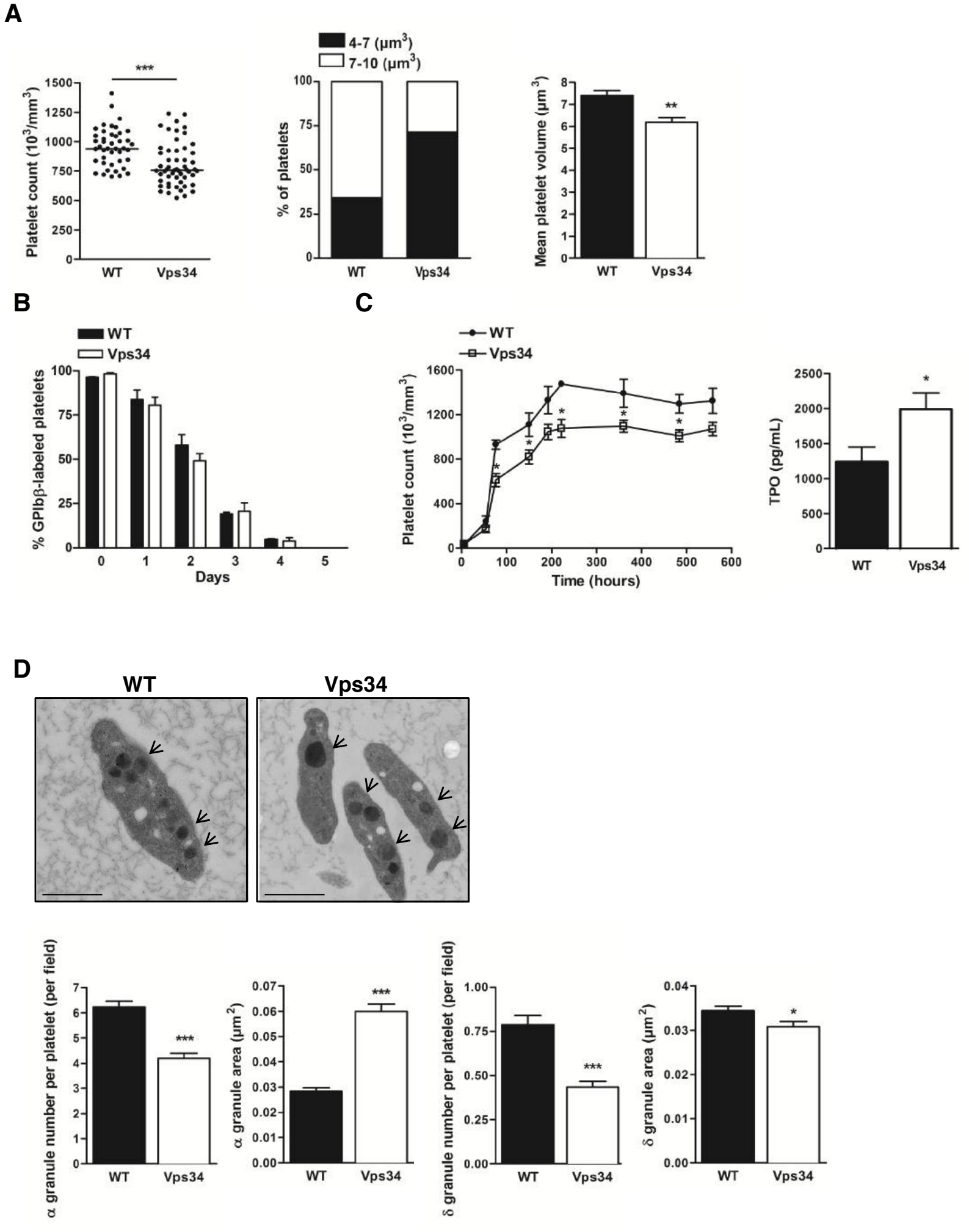
A
Platelet count (10^3/mm^3)
***
WT
Vps34
4-7 (μm^3)
7-10 (μm^3)
% of platelets
Mean platelet volume (μm^3)
**
B
WT
Vps34
% GPIbβ-labeled platelets
Days
C
Platelet count (10^3/mm^3)
Time (hours)
TPO (pg/mL)
*
D
WT
Vps34
α granule number per platelet (per field)
α granule area (μm^2)
δ granule number per platelet (per field)
δ granule area (μm^2)

Figure 1

E

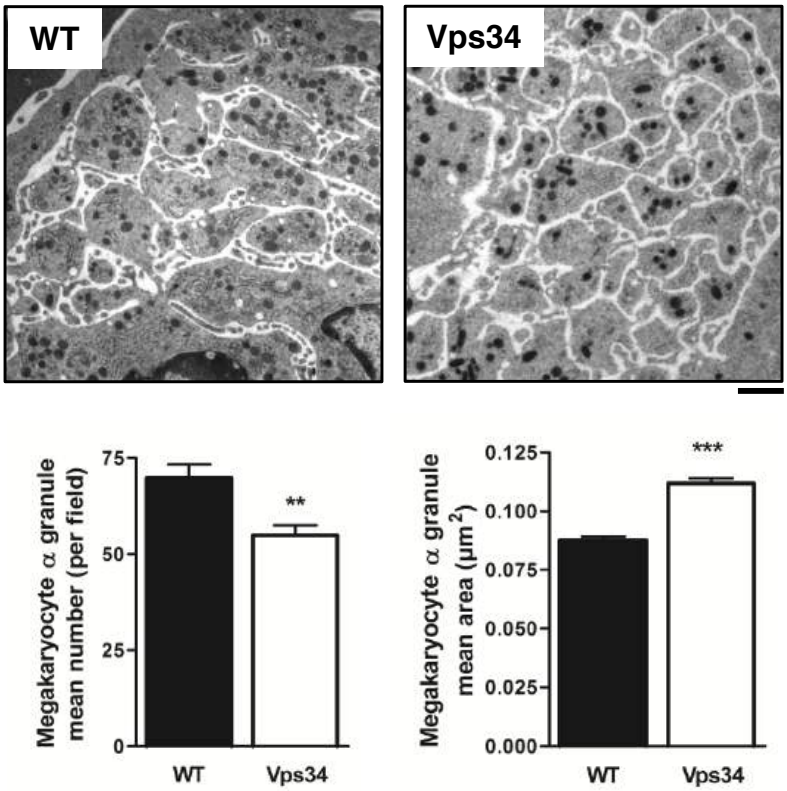

Figure 1: Defective platelet production and granule distribution in platelets in absence of Vps34. (**A**) Whole blood platelet count (left graph) and volume (right graph) were measured using HORIBA ABX Micros 60 hematology analyser (median ± SEM; n=47 WT and 54 Vps34 mice; **p<0.01, ***p<0.001 versus WT according to two-tailed Student's *t* test). Percentage of platelets with a volume range from 4 to 7μm^3 and from 7 to 10μm^3 were quantified (middle graph) (mean ± SEM; n=150 platelets). (**B**) Mice were injected intravenously with a derivative anti-GPIbβ (0.1 μg/g body weight) coupled to an AlexaFluor^{488}. At various time points after injection, the percentage of labelled platelets was measured by flow cytometry. (**C**) Thrombocytopenia in mice was induced by intraperitoneal injection of anti-mouse GPIbα antibody (2 μg/g body weight). Platelet count in blood samples collected 6h after injection (time=0) and at various time points by tail bleeding was measured using HORIBA ABX Micros 60 hematology analyser (mean ± SEM; n=50 blood samples; *p<0.05 versus WT according to two-tailed Student's *t* test). Mice plasma TPO level was quantified by immunoassay (mean ± SEM, n=4, *p<0.05 versus WT according to two-tailed Student's *t* test). (**D**) Transmission electron microscopy on resting platelets. Images are representative of 5 mice of each genotype. Scale bar: 1.5 μm. Arrows indicate α granules. Platelet α-granule number and mean area were measured on transmission electron microscopy images using ImageJ software (mean ± SEM; n=109 WT and 142 Vps34-deficient platelets; ***p<0.001 versus WT according to two-tailed Student's *t* test). Dense (δ) granule number was quantified on transmission electron microscopy images using ImageJ software (mean ± SEM; n= 260 WT and 310 Vps34-deficient platelets; *p<0.05, ***p<0.001 versus WT according to two-tailed Student's *t* test). (**E**) Transmission electron microscopy of bone marrow section (n=3). Scale bar: 1 μm. α-granule number and mean area were quantified on transmission electron microscopy images using ImageJ software (mean ± SEM; n=9 mice per genotype; **p<0.01, ***p<0.001 versus WT according to two-tailed Student's *t* test).

membrane protein 1) and activity of the β-galactosidase lysosomal enzyme respectively) (Supplemental Figure 2C) were normal in Vps34-deficient platelets, showing that Vps34 specifically acts on α- and dense- platelet granule homeostasis. TEM analysis of the native bone marrow showed that Vps34-depleted MKs display less (21.4% ± 3.7% reduction in number) but bigger (26.5% ± 2.4% increase in size) α-granules compared to WT MKs (Figure 1E) indicating that platelet granule defects originate from an abnormal granule biogenesis in MKs.

Vps34 and PI3P are required for MK endosomal trafficking and autophagy

To gain insight into the molecular mechanisms explaining the defect of platelet production and granule biogenesis by MKs, we first analyzed the contribution of Vps34 on PI3P levels in MKs using a specific mass assay [22] and a specific anti-PI3P antibody analysed by confocal microscopy. Both methods showed a significant reduction in the amount of PI3P in Vps34-depleted MKs, from 30 to 40% compared to WT MKs (Figure 2A and 2B), indicating a significant contribution of Vps34 in PI3P production in MKs. However, the degree of reduction is not proportional to the loss of Vps34 protein (Supplemental Figure 1C) suggesting that Vps34 is not the sole enzyme responsible for PI3P production in MKs.

Vps34/Vps15 complex and PI3P are known to interact with a growing list of proteins to form distinct multiprotein complexes controlling endocytic/endosomal/lysosomal trafficking processes and autophagy [4, 23]. Firstly, we analyze endocytosis by examinating the ability of MKs to internalise transferrin at early time point (20 min) and we show that Vps34-deficient MKs display a significant decrease in transferrin labelling intensity compared to WT MKs, despite a normal surface expression level of transferrin receptor (Figure 2C and Supplemental Figure 3A). This finding indicates that the absence of Vps34 in MKs results in a defective transferrin internalisation, a reflect of an altered endocytosis. Secondly, we observed that

Vps34-deficient MKs display a significant accumulation of large early endosomes as shown by an increased number (+ 22.6% ± 2.7%) and size (+ 24.8% ± 4.5%) of EEA1-positive structures (Figure 2D). One important function of early endosomes is sorting of internalized receptor either for delivery to lysosomes for degradation or recycling to the plasma membrane. The significant decreased number (- 36.8% ± 0.1%) and size (- 27.8% ± 1.3%) of lysotracker labelled structures point to a defective endosome to lysosome pathway (Figure 2E). In addition, we observe a significant higher transferrin staining at late time point (60 and 120 min) in Vps34-deficient MKs compared to WT MKs, showing that Vps34 deficiency in MKs delays the kinetics of transferrin recycling (Figure 2C). Normal expression of the early/recycling endosomes GTPase Rab5 and late endosomal Rab7, which directly interacts with Vps15, discard the hypothesis of an abnormal endosomal pathway due to defective protein expression in MKs (Figure 2F). Altogether, these results highlight a requirement for Vps34 and its product, PI3P, for a normal megakaryocytic endocytic/recycling/lysosomal trafficking. Thirdly, we quantified the conversion of LC3-I to its lipidated form, LC3-II, a specific marker for autophagosomes by western blot. LC3-positive structures corresponding to autophagosomes [24] were also analysed by confocal microscopy. Interestingly, mature MKs produce LC3-II in steady-state conditions, accumulate LC3-II after chloroquine treatment (Figure 2G) and present steady-state LC3B-positive structures corresponding to mature autophagosomes (Figure 2H) indicating a constitutive autophagic flux in MKs. A significant decrease in LC3-II (- 29.8% ± 11.3% for steady-state and - 40.3% ± 3.9% for chloroquine treatment, Figure 2H) and in steady-state LC3-positive structure number (- 32.3% ± 7.4%, Figure 2H) were observed in Vps34-deficient MKs, showing a defective autophagy in absence of Vps34 in MKs. Vps34-deficient MKs also expressed less beclin-1, a protein with a central role in autophagy (Figure 2F). These results show that Vps34 is required for a normal beclin-1

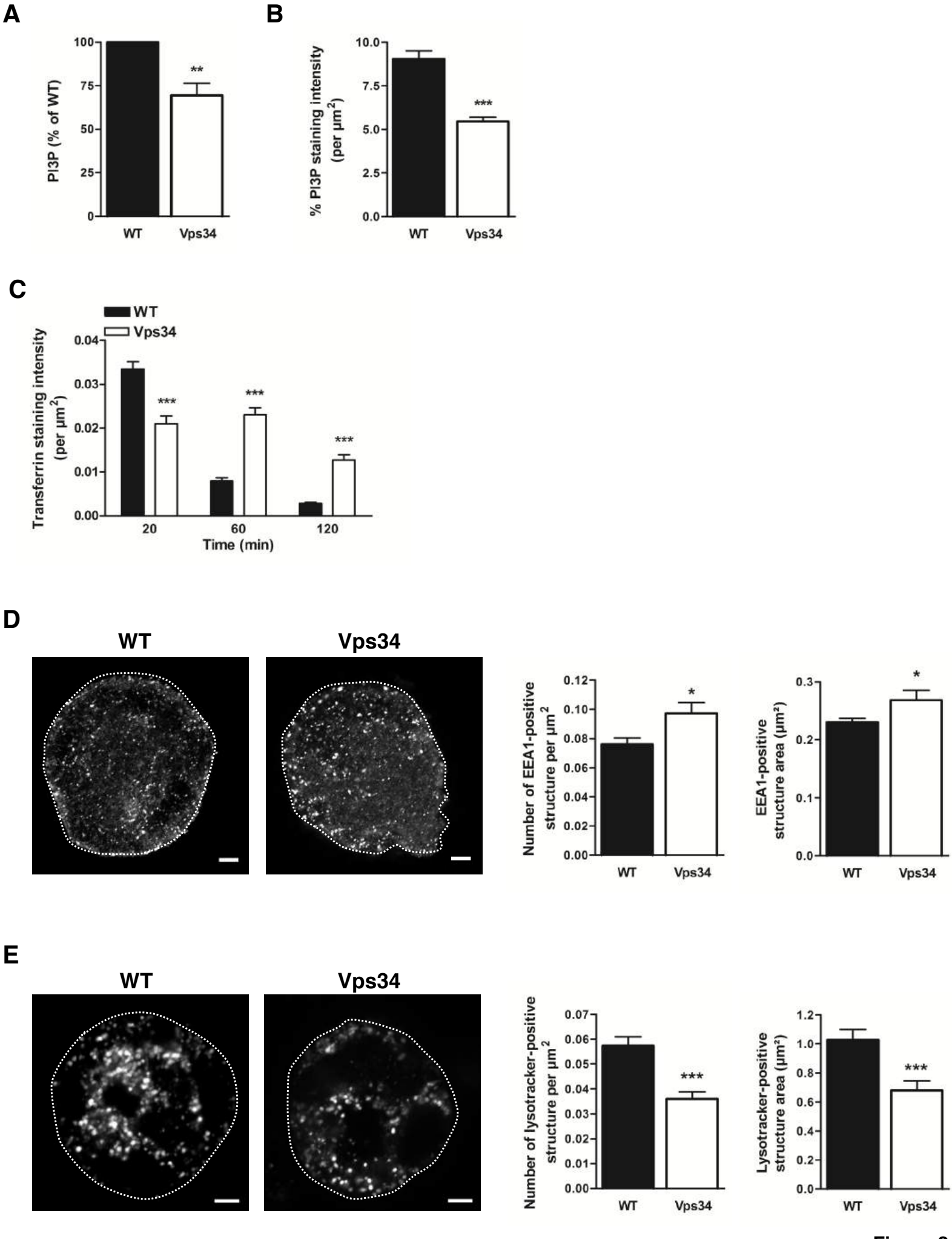
A
PI3P (% of WT)
100
75
50
25
0
**
WT
Vps34
B
% PI3P staining intensity (per µm²)
10.0
7.5
5.0
2.5
0.0
***
WT
Vps34
C
WT
Vps34
Transferrin staining intensity (per µm²)
0.04
0.03
0.02
0.01
0.00
***
***
***
20
60
120
Time (min)
D
WT
Vps34
Number of EEA1-positive structure per µm²
0.12
0.10
0.08
0.06
0.04
0.02
0.00
*
WT
Vps34
EEA1-positive structure area (µm²)
0.3
0.2
0.1
0.0
*
WT
Vps34
E
WT
Vps34
Number of lysotracker-positive structure per µm²
0.07
0.06
0.05
0.04
0.03
0.02
0.01
0.00
***
WT
Vps34
Lysotracker-positive structure area (µm²)
1.2
1.0
0.8
0.6
0.4
0.2
0.0
***
WT
Vps34

Figure 2

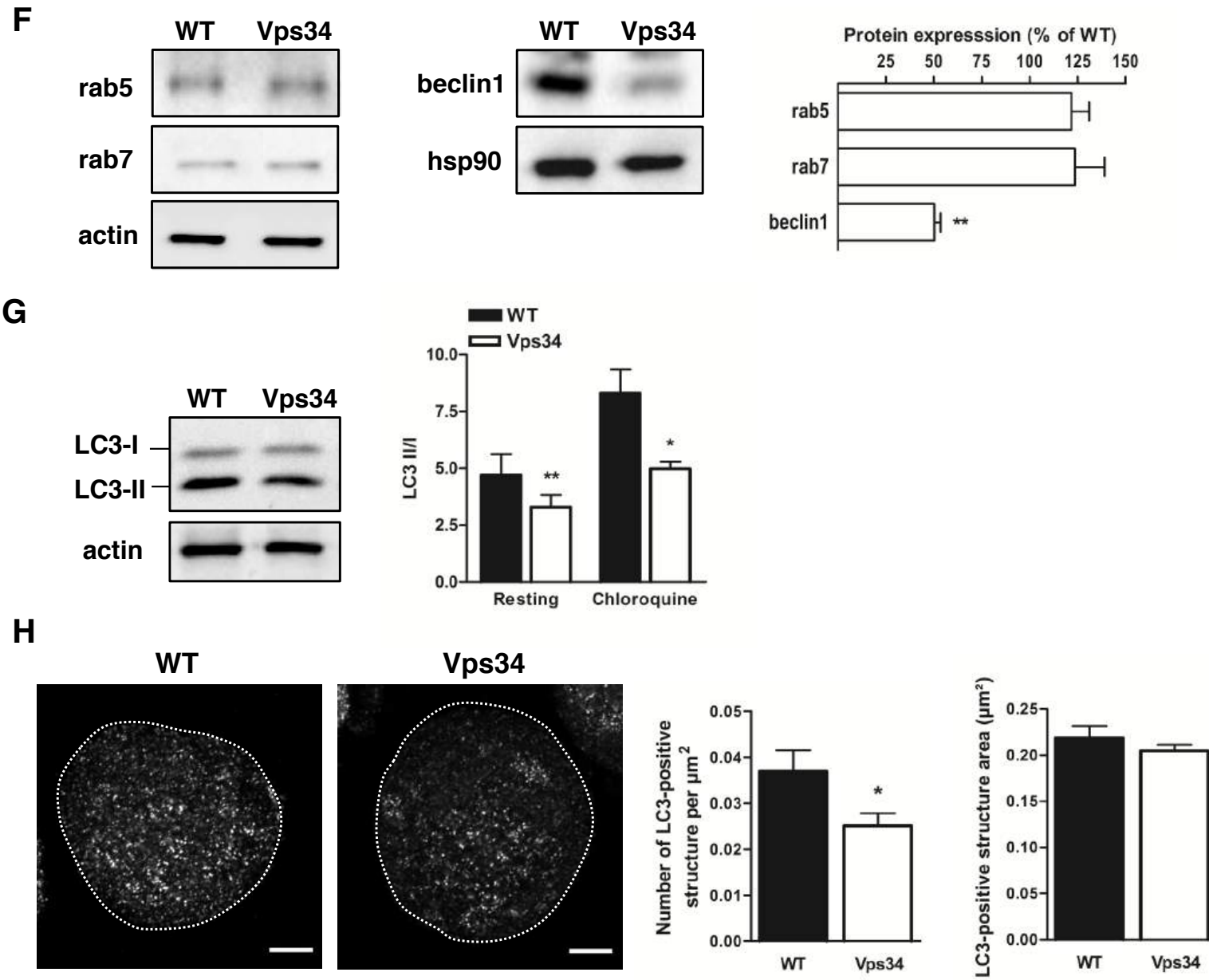

Figure 2: Vps34 and PI3P are required for MK endosomal trafficking and autophagy. (**A**) PI3P mass assay was performed on MKs as previously described (mean ± SEM; n=5; **p<0.01 versus WT according one sample *t* test). (**B**) MKs were stained with anti-PI3P and secondary Alexa Fluor®^{488} antibodies, observed by confocal microscopy and fluorescence intensity was quantified using ImageJ software (mean ± SEM; n=40 MKs/genotype; ***p<0.001 versus WT according to two-tailed Student's *t* test). (**C**) MKs were incubated with transferrin-Alexa Fluor®^{546} and its internalisation was observed by confocal microscopy 20, 60 and 120 min after incubation and quantified using ImageJ software (mean ± SEM; n=60 MKs; ***p<0.001 versus WT according to two-way ANOVA test). (**D**) Fixed MKs were stained with anti-EEA1 and secondary Alexa Fluor®^{488} antibodies and observed by confocal microscopy. Graphs represent EEA1 positive structure number and area analysed with ImageJ software (mean ± SEM; n=50 MKs; *p<0.05 versus WT according to two-tailed Student's *t* test). Scale: 5µm. (**E**) MKs were stained with LysoTracker® Deep Red and observed by confocal microscopy. Graphs represent lysotracker positive structure number and area analysed with ImageJ software (mean ± SEM; n=50 MKs; ***p<0.001 versus WT according to two-tailed Student's *t* test). Scale: 5µm (**F**) Western blot analysis of rab5, rab7 and beclin1 in MK lysates. Representative western blot of 6 independent experiments are shown. Graph represents mean ± SEM (n=6; **p<0.01 versus WT according one sample *t* test). (**G**) Western blot analysis of LC3-I and LC3-II of resting and chloroquine treated MK lysates (mean ± SEM; n=15 and 5 respectively; *p<0.05, **p<0.01 versus WT according according to two-tailed Student's *t* test). (**H**) Fixed MKs were stained with anti-LC3 and secondary Alexa Fluor®^{488} antibodies and observed by confocal microscopy. Graphs represent LC3-positive structure number and area quantified using ImageJ software (mean ± SEM; n=50 MKs; *p<0.05 versus WT according to two-tailed Student's *t* test). Scale: 5µm.

Figure 2

protein expression in MKs and autophagic flux in MKs. Altogether, these results show a role for Vps34 and its product, PI3P, for a normal autophagic flux in MKs.

Vps34 is critical for MK migration

What is the functional impact of Vps34-dependent defective endocytic/recycling/lysosomal trafficking and autophagy on MK functions remains an open question. *Pf4*-Cre-*Pik3c3*$^{lox/lox}$ mice have normal MK number and size in the bone marrow (Supplemental Figure 3B) and bone marrow-derived MKs exhibited normal ploidy levels (Supplemental Figure 3C)demarcation membrane system (Supplemental Figure 3D) and proplatelet-producing capacity (Supplemental Figure 3E). A critical stage of megakaryopoiesis for platelet release is MK migration from the proliferative osteoblastic niche to the capillary-rich vascular niche in response to SDF1α gradient [25]. We found that MK migration toward SDF1α gradient on fibronectin, a major extracellular matrix component in bone marrow [26], is significantly affected in the absence of Vps34. Interestingly, Vps34-depleted MKs are able to migrate equal distance than WT MKs but show a significant reduced directionality toward SDF1α gradient (Figure 3A). The migration paths demonstrate that Vps34-depleted MKs move relatively short distances before changing direction due to a lack of directional persistence toward SDF1α gradient (Figure 3A). This abnormal migration is associated to a significant increase in the SDF1α receptor, CXCR4, at the MK surface (Figure 3B). As the total expression of CXCR4 was normal (Figure 3B), these data suggest that CXCR4 trafficking is affected when Vps34 is invalidated in MKs. Altogether, these findings are consistent with a critical role for Vps34 in regulating MK migration.

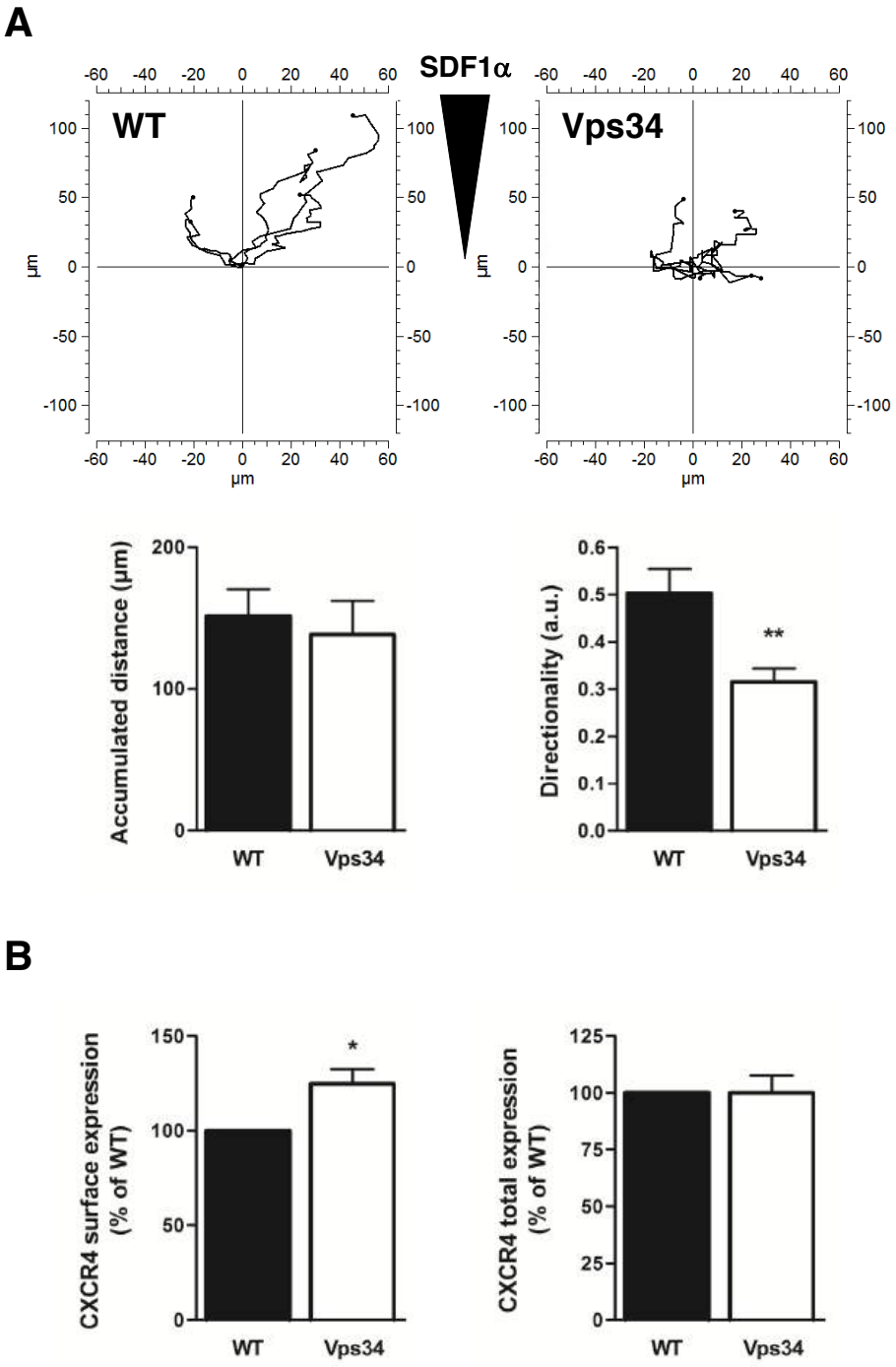

Figure 3: Vps34 is critical for MK migration and granule biogenesis. (**A**) MKs were exposed to an SDF1α gradient within the Dunn chamber. Migration paths over 6 hours of 5 representative MKs from 9 mice in each graph were traced. The intersection of the x- and y-axis was taken to be the starting point of each cell path, whereas the source of the SDF1α was at the top. MKs accumulated distance and directionality were analysed using ImageJ manual tracking plug-in (mean ± SEM; n=9; **p<0.01 versus WT according to two-tailed Student's *t* test). (**B**) Surface CXCR4 was labelled using an anti-CXCR4 antibody coupled to an Alexa Fluor®^{488} and analysed by flow cytometry (mean ± SEM; n=6; *p<0.05 versus WT according one sample *t* test). Western blot analysis of CXCR4 total expression in MK lysates was assessed (mean ± SEM; n=3).

Vps34 is involved in the stimulation-dependent PI3P pool in platelets

An important question was then to know whether Vps34-deficient platelets have a normal or an altered function. We first analyzed the impact of Vps34 in the production of PI3P in platelets by using a specific mass assay to quantify the total amount of PI3P [22] and HPLC analysis following short term ^{32}Pi-labelling to determine the fast turnover of phosphoinositides and their acute changes following platelet stimulation [27]. The PI3P specific mass assay demonstrated a weak but significant decrease in the basal level of PI3P (10.1% ± 1.3%). Following CRP or thrombin stimulation the inducible pool of PI3P decreased by 41.1% ± 5.8% and 40.2% ± 7.9%, respectively (Figure 4A). HPLC analysis confirmed these results and did not show any significant differences in the basal or agonist-stimulated levels of $PI(3,4)P_2$, $PI(3,4,5)P_3$ and phosphatidic acid (Figure 4B and Supplemental Figure 4). Furthermore, we revealed that platelet stimulation resulted in 1.5-fold increase in Vps34 lipid kinase activity (Figure 4C). Overall, these data indicate that Vps34 weakly contributes to the production of the basal pool of PI3P but is important for the synthesis of the stimulation-dependent pool of PI3P in platelets. These data provide the demonstration of a role for Vps34 activity in acute stimulation of platelets and suggest its involvement in their activation.

Vps34 plays an important role in arterial thrombosis *via* its kinase activity

In vitro platelet aggregation in response to low doses of CRP, collagen, thrombin or thromboxane A2 analogue was normal (Supplemental Figure 5A) as well as shape change (Supplemental Figure 5B). Similar results were obtained in human platelets treated with a specific inhibitor of Vps34, INH1 [17] (Supplemental Figure 5C).

We then examined platelet thrombus formation under physiological arterial or arteriolar wall shear rate (500 and 1500 s^{-1} respectively) over a collagen surface. As expected, blood from WT mice exhibited robust formation of densely packed platelets on collagen (Figure 5A). In

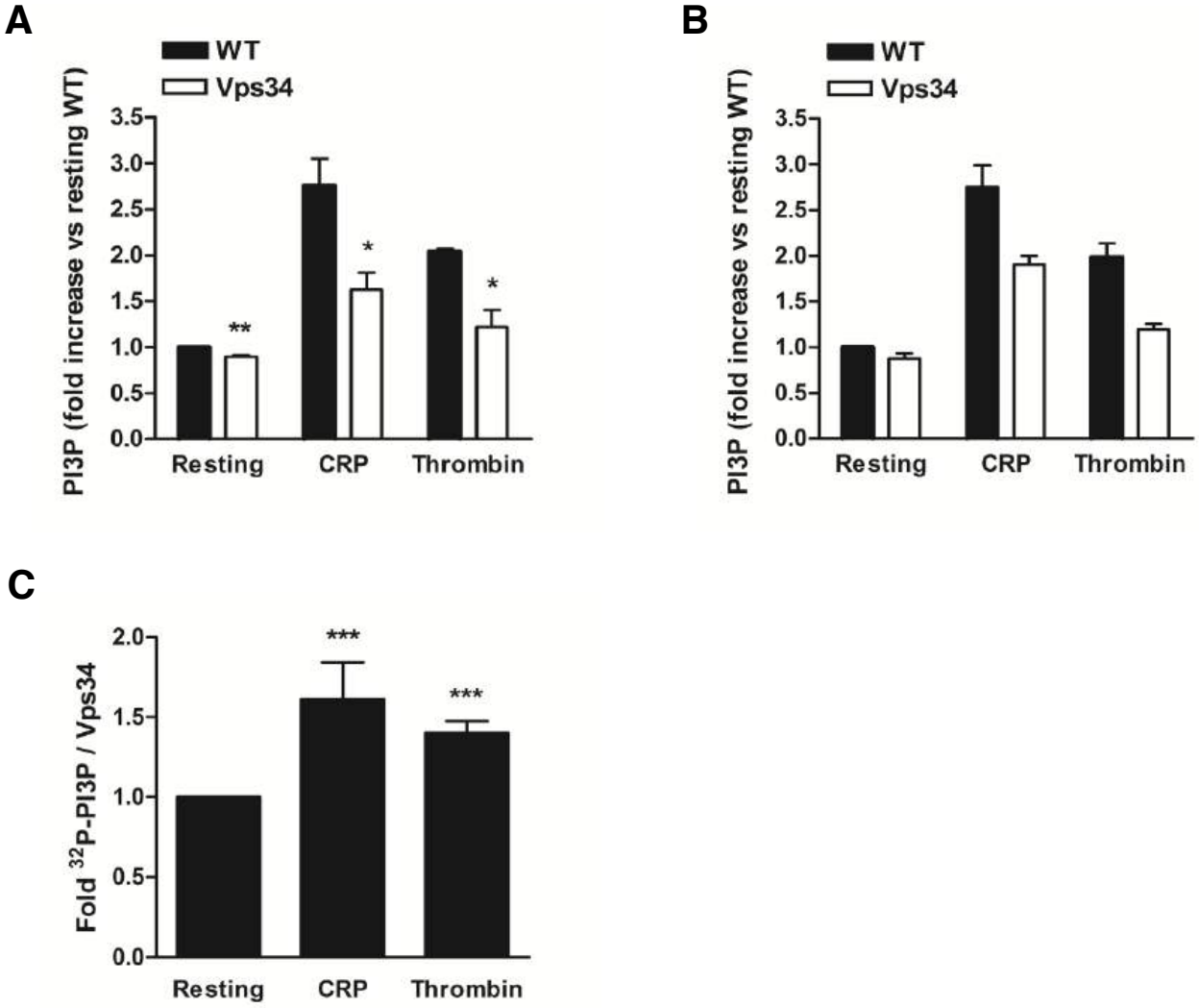

Figure 4: Role of Vps34 in induced PI3P production in platelets. PI3P content of washed platelets under resting or stimulated (CRP, 10 µg/ml; thrombin, 0.5 UI/ml) conditions was assessed as described in methods by (**A**) mass assay (mean ± SEM; n=5; *p<0.05; **p<0.01 versus WT according to two-way ANOVA test) and (**B**) HPLC analysis (mean ± SD; n=2). (**C**) Vps34 was immunoprecipitated from resting or activated (CRP, 10 µg/ml; thrombin, 0.5 UI/ml) washed platelets and assayed for lipid kinase activity *in vitro* (mean ± SEM; n=5; ***p<0.001 *versus* resting according to one sample *t* test).

Figure 4

contrast, Vps34-depleted platelets attached along the collagen fibres (Supplemental Figure 5D) but formed significantly smaller thrombi as shown by a 50 % significant decrease in surface covered by platelets and thrombus volume at all shear rates tested (Figure 5A and B). Interestingly, when labelled whole blood from *Pf4*-Cre-*Pik3c3*$^{lox/lox}$ was perfused over preexisting WT thrombi under a physiological shear rate, we observed a significantly decreased surface covered by fluorescent Vps34 lacking platelets, showing that Vps34 is important for the recruitment and incorporation of new circulating platelets to the growing thrombus (Figure 5C).

Importantly, *in vivo*, using the $FeCl_3$-induced carotid injury model, we observed that 50% of *Pf4*-Cre-*Pik3c3*$^{lox/lox}$ mice were protected against occlusive arterial thrombus formation (Figure 5D). However, *Pf4*-Cre-*Pik3c3*$^{lox/lox}$ mice underwent normal primary haemostasis as shown by tail bleeding times comparable to those of WT mice (Figure 5E).

To get further insights into the mechanisms regulated by Vps34 in platelets, we analysed secretion and $\alpha_{IIb}\beta_3$ integrin activation. We showed that Vps34-deficient platelets displayed a dysregulated release of granules upon *in vitro* stimulation. In the absence of Vps34, P-selectin surface exposure (for α-granule release) significantly increased in response to CRP (Figure 6A) as well as ATP secretion (for dense-granule release) in response to all agonists tested (Figure 6B). Reactive oxygen species production was unaffected in Vps34-depleted platelets, showing that Vps34-dependent PI3P production in platelets is not mandatory for NADPH oxydase activity in our experimental conditions (Supplemental Figure 5E and 5F). Moreover, thromboxane A2 production was not affected as its stable derivative, thromboxane B2, was normally produced in CRP- and thrombin-stimulated Vps34-depleted platelets. Thrombin and CRP-induced JON/A binding, reflecting αIIbβ3 integrin activation, was not strongly affected in Vps34-depleted platelets compared to WT platelets (Figure 6C). Vps34-depleted platelets displayed an enhanced spreading on fibrinogen (Figure 6D). However, this was counteracted

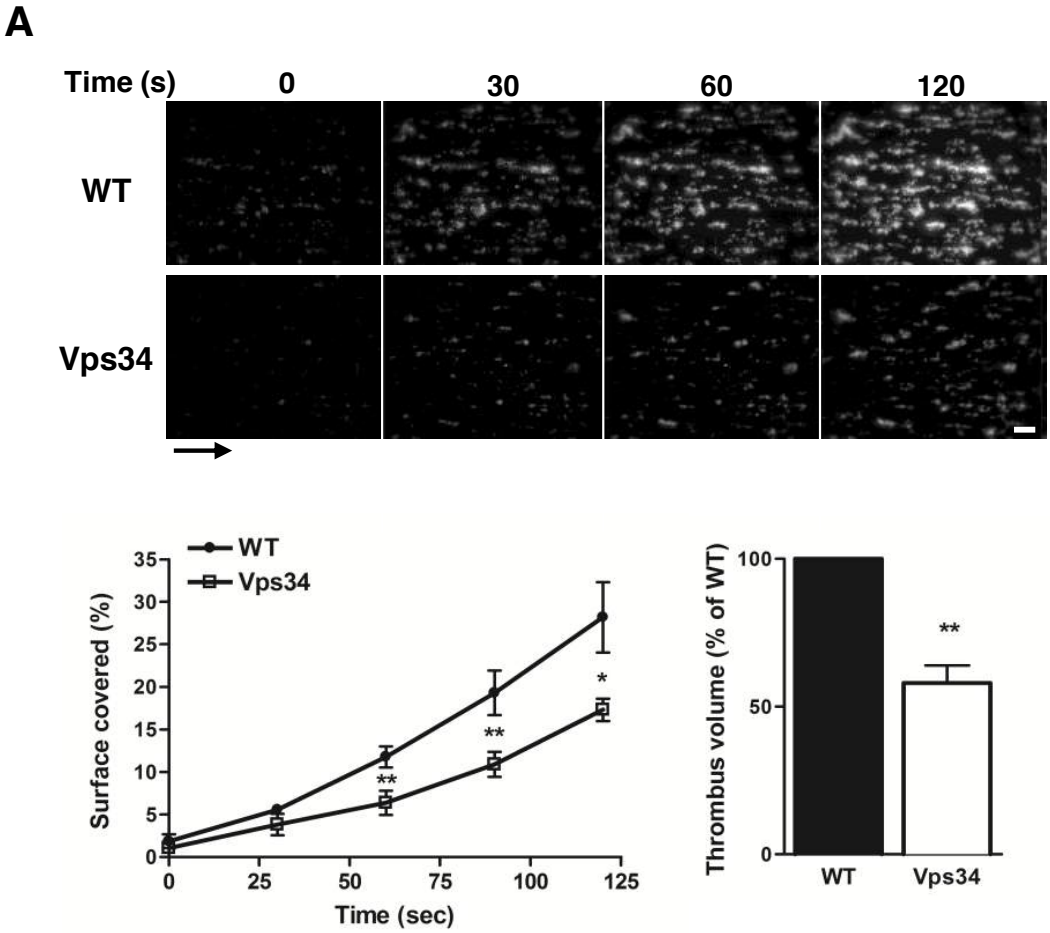
A
Time (s)
0
30
60
120
WT
Vps34
Surface covered (%)
Time (sec)
Thrombus volume (% of WT)
B
C
Surface coverage of fluorescent platelets (%)

Figure 5

D

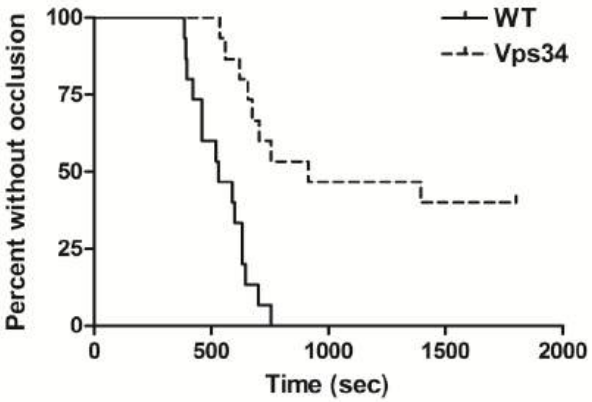

E

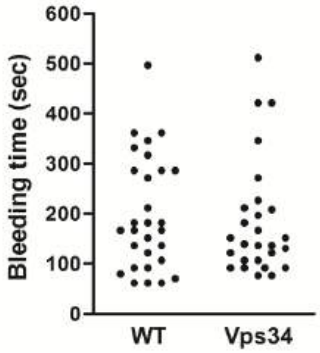

Figure 5: Vps34 plays an important role in thrombosis. $DiOC_6$-labelled platelets in whole blood were perfused through a collagen-coated microcapillary at a physiological arterial shear rate of 500 s^{-1} (**A**) or 1500 s^{-1} (**B**). Scale bar: 20 µm. Surface covered by fluorescent platelets and thrombus volume were analysed using ImageJ software (mean ± SEM; n=8; *p<0.05; **p<0.01 versus WT according to two-tailed Student's *t* test). (**C**) Unlabelled whole blood from WT mice were perfused through a collagen-coated microcapillary at 1500 s^{-1} during 1 minute. Control blood was then replaced by $DiOC_6$-labelled platelets in whole blood from WT or Vps34 mice perfused at the same shear rate. Surface covered by fluorescent platelets was analysed using ImageJ software (mean ± SEM; n=3 WT and 4 Vps34 mice; *p<0.05; **p<0.01 versus WT according to two-tailed Student's *t* test). (**D**) Thrombotic response of mice to carotid injury after exposure to 7.5 % $FeCl_3$ for 3 min was measured using a flow probe. Graph represents percentage of mice without occlusion 30 minutes after injury (n=15 mice of each genotype; p=0.0002 according to one sample *t* test). (**E**) Tail bleeding time (n=30 mice of each genotype) mice was measured as described in methods.

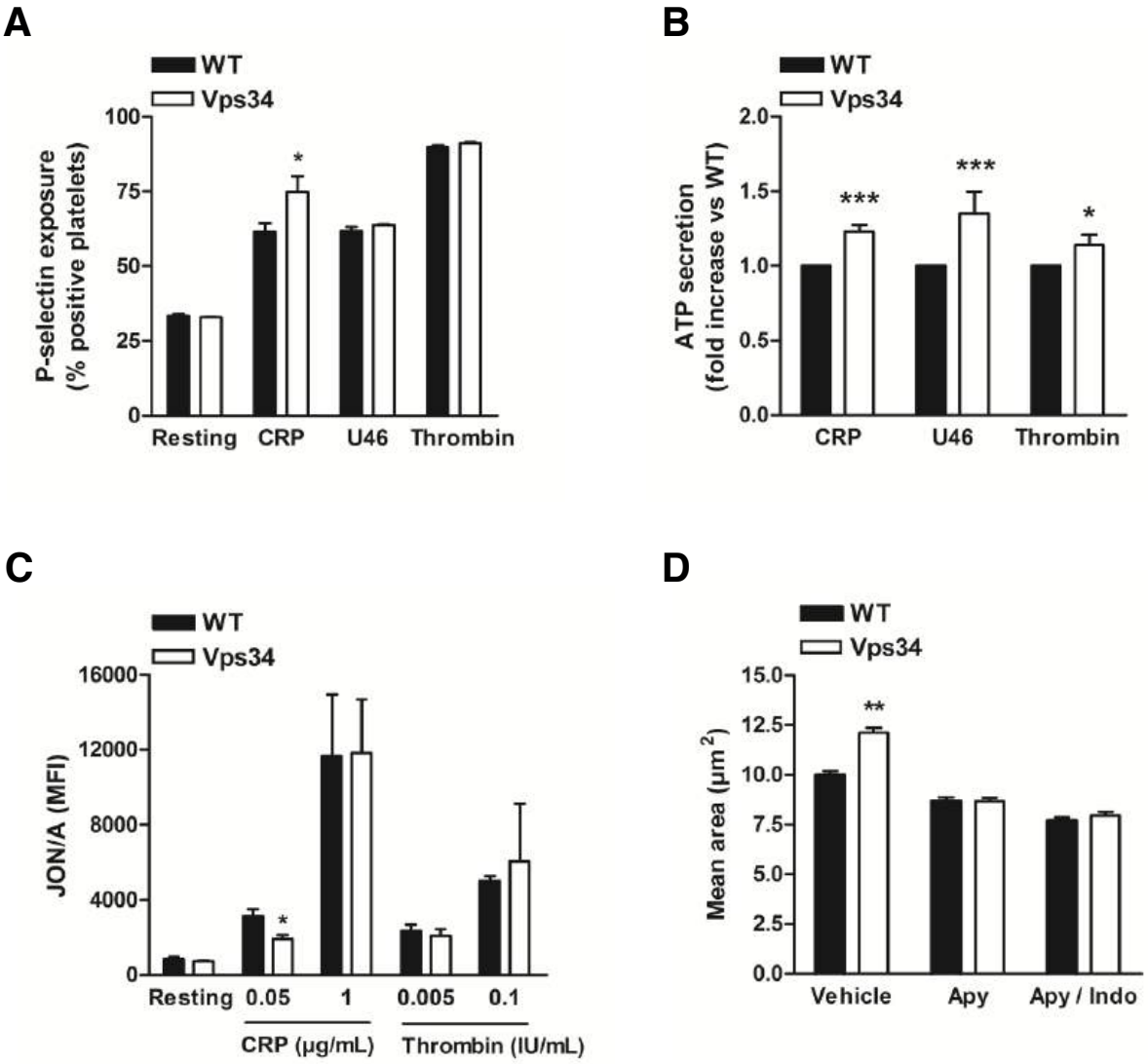

Figure 6: Secretion dysregulation in Vps34 depleted platelets. (**A**) P-selectin exposure at the platelet surface was analysed by flow cytometry under resting and stimulated conditions (CRP, 1 µg/ml; U46619, 0.25µM; thrombin, 0.05 UI/ml) (mean ± SEM; n=3; *p<0.05 versus resting WT according to two-way ANOVA). (**B**) ATP secretion of washed platelets under stimulated conditions (CRP, 1 µg/ml; U46619, 0.5µM; thrombin, 0.1 UI/ml) (mean ± SEM; n=3) was recorded by measuring the luminescence from the firefly luciferin-luciferase reaction by lumiaggregometry using the Chrono-log aggregometer (mean ± SEM; n=6-15 depending the agonist; *p<0.05, ***p<0.001 versus WT according to two-tailed Student's *t* test). (**C**) Flow cytometry analysis of JON/A-PE antibody binding to platelets at resting or stimulated state. Results are cumulative data from 6 independent experiments and are presented as mean fluorescence intensity (MFI) ± SEM (*p<0.05 versus WT according to two-way ANOVA). (**D**) Washed platelets were spread on a fibrinogen-coated surface for 20 minutes after pre-inbubation or not with apyrase (2 IU/ml) alone or in combinaison with indomethacine (10µM) for 15 min (mean ± SEM; n=3 mice per genotype; **p<0.01 versus WT according to two-way ANOVA).

by hydrolysis of released ATP/ADP with apyrase (Figure 6D), strongly suggesting that increased secretion of platelets when Vps34 is absent impacts on αIIbβ3 integrin-dependent platelet adhesion capacity.

To know whether thrombus growth defects were due to the direct inhibition of Vps34 in platelets we took advantage of two specific inhibitors, SAR405 and INH1 [17, 18] that we used to treat blood *ex vivo*. Interestingly, thrombus formation on collagen matrix under physiological shear rate was affected to the same extent as *Pf4*-Cre-*Pik3c3*$^{lox/lox}$ blood mice (Figure 7A and B). These data demonstrate a direct role for Vps34 activity on thrombus growth, independently of its impact on MKs.

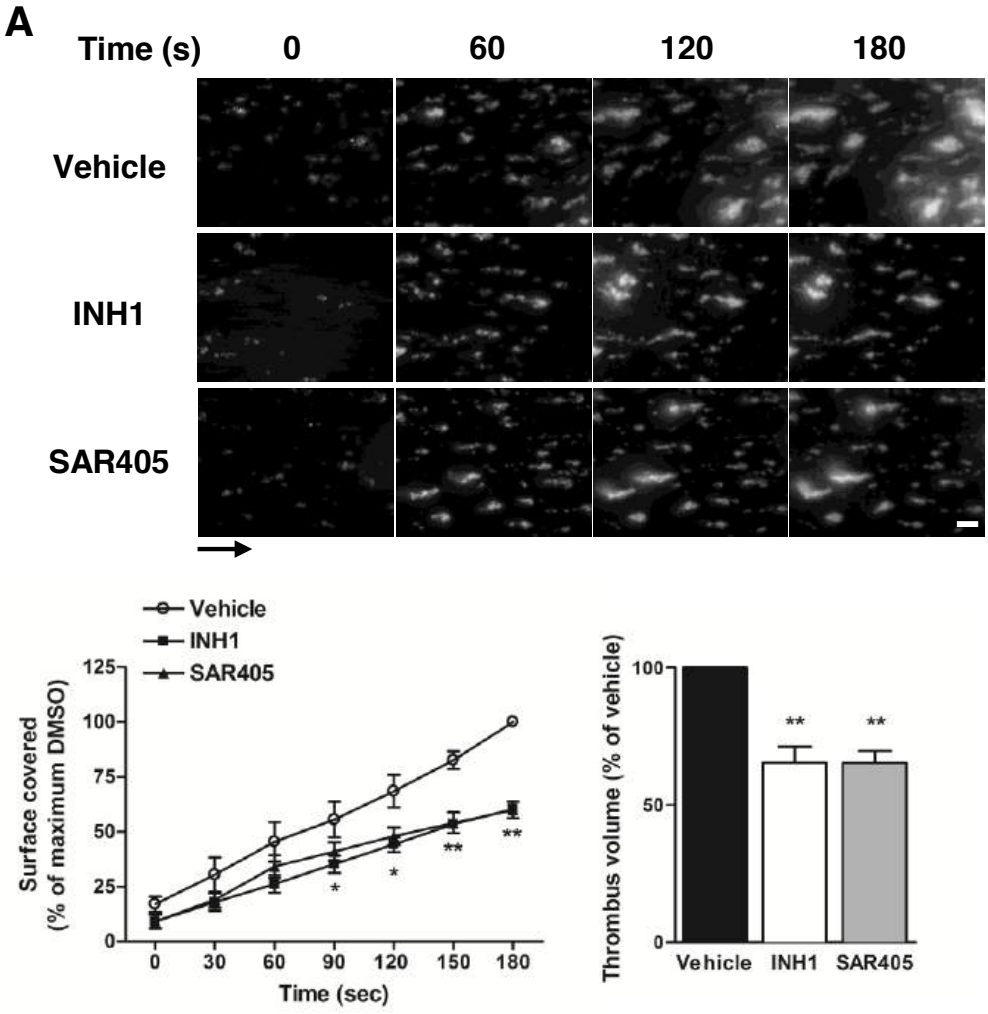

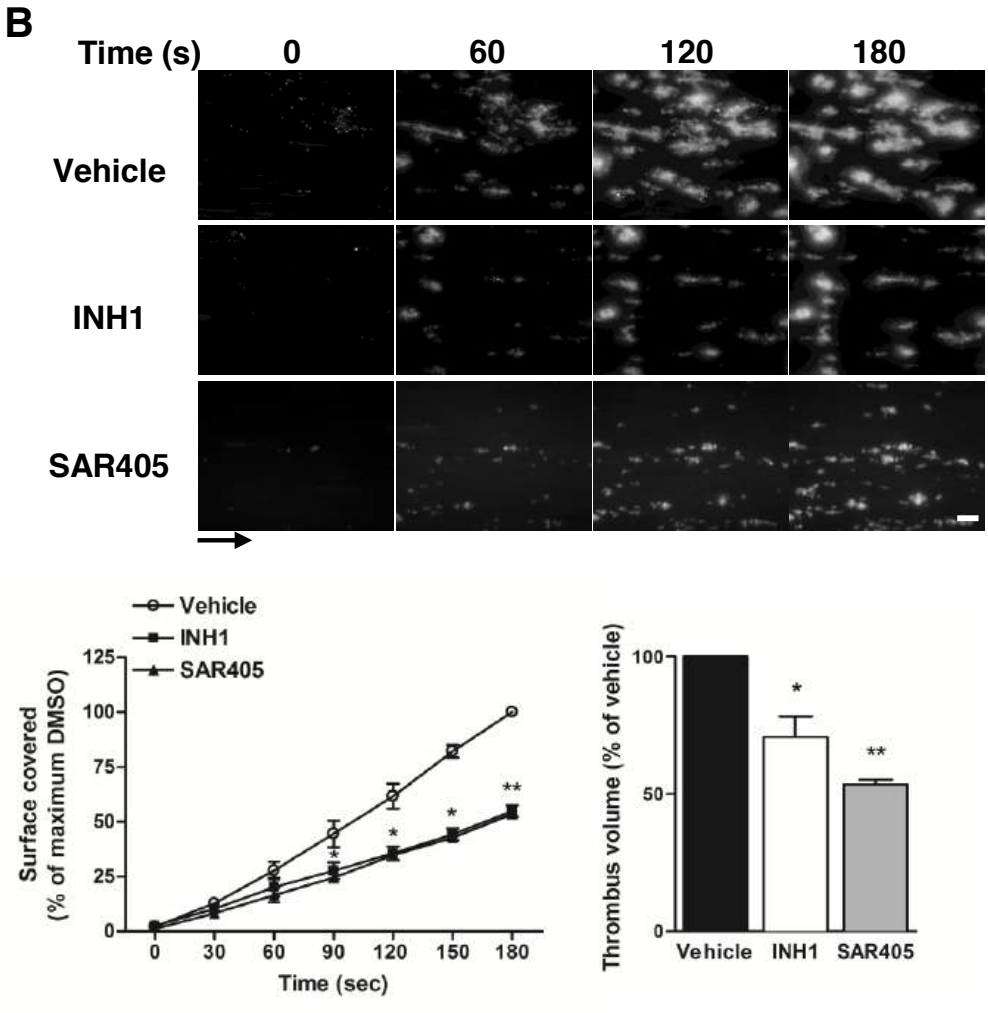

Figure 7: Role of Vps34 in thrombosis *via* its kinase activity. Whole blood from WT mice (**A**) or healthy human donors (**B**) were treated with Vps34 inhibitors (INH1; 1µM or SAR405; 1µM) or vehicle (DMSO) for 1 h. Then, $DiOC_6$-labelled platelets in treated whole blood were perfused through a collagen-coated microcapillary at a physiological arterial shear rate of 500 s^{-1} (mice) or 1500 s^{-1} (human). Scale bar: 20 µm. Surface covered by fluorescent platelets and thrombus volume were analysed using ImageJ software (mean ± SEM; n=3-5 depending on the inhibitor and support; *p<0.05; **p<0.01 versus WT according to one sample *t* test).

Figure 7

DISCUSSION

In this study, we have generated a mouse model of MK/platelet lineage-specific deletion allowing the first phenotypic description of Vps34 in MKs and platelets. Vps34 deficiency in MKs and platelets results in three major outcomes: (i) moderated microthrombocytopenia correlated to defective MK migration, (ii) abnormal platelet granule biogenesis and (iii) decreased thrombotic responses with no impact on tail bleeding time.

Vps34 has been proposed as the major PI3P producing kinase in mammalian cells. Here, we show that Vps34 contributes for 40% of PI3P level production in MKs. In platelets, the contribution of Vps34 to the production of the basal pool of PI3P is weak (~10%). This is consistent with our recent study showing a significant contribution of PI3KC2α to the basal production of platelet PI3P pool [20]. Contrariwise, we show a rapid increase in Vps34 kinase activity in platelets following activation either by G-protein coupled receptors or ITAM receptors. Consistent with this activation, we show that Vps34 regulates a significant part of the stimulation-dependent PI3P production. Our data showing a rapid Vps34 activation and PI3P production in activated platelets and a recent study in insulin-stimulated hepatocytes [28] strongly suggest that this lipid kinase can be activated during acute cellular responses.

Our data indicate that the moderated microthrombocytopenia observed in *Pf4*-Cre-*Pik3c3*$^{lox/lox}$ mice derives from a defective platelet production rather than an abnormal platelet lifespan pointing to a role for Vps34 in MK biology. While MK nuclear and membrane maturation as well as proplatelet extension were normal in the absence of Vps34, MK migration and directionality toward SDF1α gradient were particularly affected. Such a defect in MK migration toward SDF1α gradient has been reported in a case of thrombocytopenia due to WASP defects and in a case of decreased platelet production after immune induced-thrombopenia in PECAM knock-out mice [29, 30]. SDF1α drives MK movement from the proliferative osteoblastic niche to the vascular niche where platelets are released. The

increased surface expression of its receptor, CXCR4 and the defective endosomal trafficking due to the absence of Vps34 in MKs strongly suggest that CXCR4 trafficking dynamics are altered. As CXCR4 polarization is important for MK migration toward SDF1α gradient [29], the lack of persistence of Vps34-deficient MK directionality might be the result of a defective CXCR4 polarization. Likewise, a defective trafficking of the fibronectin receptor α5β1 integrin may also contribute as integrin trafficking is a polarized process in migrating cells to ensure normal directionality [31]. The defect in vesicular trafficking observed in Vps34-depleted MKs might be at the origin of abnormalities in the number and size of secretory granules in MKs. Indeed, α and dense granules originate in MKs from a multivesicular bodies (MVBs)/late endosomes compartment where cargos derive from both regulated secretory and endocytic pathways after a highly regulated molecular sorting [15, 16]. Thus, the present observations support a model in which the defect in platelet production observed is due, at least in part, to altered endosomal trafficking in Vps34-depleted MKs. Recent studies show that autophagy is also essential for MK maturation and platelet production [32, 33] but the precise mechanisms by which autophagy regulates these processes are still unclear. It has recently been shown that autophagy facilitates focal adhesion turnover by promoting their dynamic disassembly [34, 35]. Focal adhesion turnover is important to direct cell migration. In particular disassembly of focal adhesion enables efficient displacement of the advancing cell [36]. Thus, defective autophagy in Vps34-depleted MKs may contribute to the impaired directionality during their migration due to impeded focal adhesion turnover.

This study reveals a role for Vps34 in platelet function by controlling *ex vivo* thrombus growth under flow condition and *in vivo* after ferric chloride injury without any effects on bleeding. The integrin αIIbβ3 and granule secretion are two processes that are essential for thrombus growth [37, 38]. We observed an increased platelet secretion in Vps34-depleted platelets in response to several agonists. We also show normal αIIbβ3 integrin activation in

platelets when Vps34 is absent but exacerbated platelet spreading on fibrinogen surface. When secretion was counteracted, Vps34-depleted platelets spread to the same extent than WT platelets indicated that dysregulated secretion impacts on integrin αIIbβ3 adhesive capacity. In line with a recent study from Eckly *et al* demonstrating different mechanisms and kinetics of secretion in platelets depending of activation rate [39], further investigation is needed to better understand how platelet secretion dysregulation in absence of Vps34 impact on thrombus growth. We can hypothesize that, when Vps34 is absent in platelets, at the site of vascular lesion, massive and rapid platelet granule release allows local platelet activation but might be insufficient for the recruitment of new platelets in a growing thrombus.

Interestingly, we demonstrate an important role for Vps34 in platelets *via* its kinase activity by controlling thrombus growth. Two specific Vps34 inhibitors allowed us to conclude that decreased thrombus growth in *Pf4*-Cre-*Pik3c3*$^{lox/lox}$ blood mice is not a direct consequence of Vps34 implication in MKs and platelet production but is due to a platelet specific role of Vps34 *via* its kinase activity and thus its agonist inducible pool of PI3P.

In conclusion, our study points to a new function for Vps34 and its product, PI3P, in platelet production by regulating MK migration and granule biogenesis but also in platelet activation by controlling thrombus growth in response to vascular injury with no impact on haemostasis.

REFERENCES

1. Di Paolo G, De Camilli P. Phosphoinositides in cell regulation and membrane dynamics. *Nature* **443**, 651-657 (2006).

2. Vanhaesebroeck B, Guillermet-Guibert J, Graupera M, Bilanges B. The emerging mechanisms of isoform-specific PI3K signalling. *Nature reviews Molecular cell biology* **11**, 329-341 (2010).

3. Herman PK, Emr SD. Characterization of VPS34, a gene required for vacuolar protein sorting and vacuole segregation in Saccharomyces cerevisiae. *Molecular and cellular biology* **10**, 6742-6754 (1990).

4. Backer JM. The regulation and function of Class III PI3Ks: novel roles for Vps34. *The Biochemical journal* **410**, 1-17 (2008).

5. Vanhaesebroeck B, Guillermet-Guibert J, Graupera M, Bilanges B. The emerging mechanisms of isoform-specific PI3K signalling. *Nature reviews* **11**, 329-341.

6. Zhou X, Takatoh J, Wang F. The mammalian class 3 PI3K (PIK3C3) is required for early embryogenesis and cell proliferation. *PloS one* **6**, e16358 (2011).

7. Jaber N, *et al*. Class III PI3K Vps34 plays an essential role in autophagy and in heart and liver function. *Proceedings of the National Academy of Sciences of the United States of America* **109**, 2003-2008 (2012).

8. Willinger T, Flavell RA. Canonical autophagy dependent on the class III phosphoinositide-3 kinase Vps34 is required for naive T-cell homeostasis. *Proceedings of the National Academy of Sciences of the United States of America* **109**, 8670-8675 (2012).

9. Bechtel W, *et al*. Vps34 deficiency reveals the importance of endocytosis for podocyte homeostasis. *Journal of the American Society of Nephrology : JASN* **24**, 727-743 (2013).

10. Bechtel W, Helmstadter M, Balica J, Hartleben B, Schell C, Huber TB. The class III phosphatidylinositol 3-kinase PIK3C3/VPS34 regulates endocytosis and autophagosome-autolysosome formation in podocytes. *Autophagy* **9**, 1097-1099 (2013).

11. Wang L, Budolfson K, Wang F. Pik3c3 deletion in pyramidal neurons results in loss of synapses, extensive gliosis and progressive neurodegeneration. *Neuroscience* **172**, 427-442 (2011).

12. Zhou X, Wang F. Effects of neuronal PIK3C3/Vps34 deletion on autophagy and beyond. *Autophagy* **6**, 798-799 (2010).

13. Machlus KR, Italiano JE, Jr. The incredible journey: From megakaryocyte development to platelet formation. *The Journal of cell biology* **201**, 785-796 (2013).

14. Huang Y, *et al*. Arf6 controls platelet spreading and clot retraction via integrin alphaIIbbeta3 trafficking. *Blood* **127**, 1459-1467 (2016).

15. Ambrosio AL, Boyle JA, Di Pietro SM. Mechanism of platelet dense granule biogenesis: study of cargo transport and function of Rab32 and Rab38 in a model system. *Blood* **120**, 4072-4081 (2012).

16. Blair P, Flaumenhaft R. Platelet alpha-granules: basic biology and clinical correlates. *Blood reviews* **23**, 177-189 (2009).

17. Bago R, *et al*. Characterization of VPS34-IN1, a selective inhibitor of Vps34, reveals that the phosphatidylinositol 3-phosphate-binding SGK3 protein kinase is a downstream target of class III phosphoinositide 3-kinase. *The Biochemical journal* **463**, 413-427 (2014).

18. Ronan B, *et al*. A highly potent and selective Vps34 inhibitor alters vesicle trafficking and autophagy. *Nat Chem Biol* **10**, 1013-+ (2014).

19. Posor Y, *et al*. Spatiotemporal control of endocytosis by phosphatidylinositol-3,4-bisphosphate. *Nature* **499**, 233-237 (2013).

20. Valet C, *et al*. Essential role of class II PI3K-C2alpha in platelet membrane morphology. *Blood* **126**, 1128-1137 (2015).

21. Laurent PA, Severin S, Hechler B, Vanhaesebroeck B, Payrastre B, Gratacap MP. Platelet PI3Kbeta and GSK3 regulate thrombus stability at a high shear rate. *Blood* **125**, 881-888 (2015).

22. Chicanne G, *et al*. A novel mass assay to quantify the bioactive lipid PtdIns3P in various biological samples. *The Biochemical journal* **447**, 17-23 (2012).

23. Simonsen A, Tooze SA. Coordination of membrane events during autophagy by multiple class III PI3-kinase complexes. *The Journal of cell biology* **186**, 773-782 (2009).

24. Mizushima N, Yoshimori T, Levine B. Methods in mammalian autophagy research. *Cell* **140**, 313-326 (2010).

25. Hattori K, Heissig B, Rafii S. The regulation of hematopoietic stem cell and progenitor mobilization by chemokine SDF-1. *Leukemia & lymphoma* **44**, 575-582 (2003).

26. Nilsson SK, Debatis ME, Dooner MS, Madri JA, Quesenberry PJ, Becker PS. Immunofluorescence characterization of key extracellular matrix proteins in murine bone marrow in situ. *The journal of histochemistry and cytochemistry : official journal of the Histochemistry Society* **46**, 371-377 (1998).

27. Giuriato S, *et al*. SH2-containing inositol 5-phosphatases 1 and 2 in blood platelets: their interactions and roles in the control of phosphatidylinositol 3,4,5-trisphosphate levels. *The Biochemical journal* **376**, 199-207 (2003).

28. Nemazanyy I, *et al*. Class III PI3K regulates organismal glucose homeostasis by providing negative feedback on hepatic insulin signalling. *Nature communications* **6**, 8283 (2015).

29. Dhanjal TS, *et al*. A novel role for PECAM-1 in megakaryocytokinesis and recovery of platelet counts in thrombocytopenic mice. *Blood* **109**, 4237-4244 (2007).

30. Sabri S, *et al*. Deficiency in the Wiskott-Aldrich protein induces premature proplatelet formation and platelet production in the bone marrow compartment. *Blood* **108**, 134-140 (2006).

31. Paul NR, Jacquemet G, Caswell PT. Endocytic Trafficking of Integrins in Cell Migration. *Current biology : CB* **25**, R1092-1105 (2015).

32. Cao Y, *et al*. Loss of autophagy leads to failure in megakaryopoiesis, megakaryocyte differentiation, and thrombopoiesis in mice. *Experimental hematology* **43**, 488-494 (2015).

33. Ouseph MM, *et al*. Autophagy is induced upon platelet activation and is essential for hemostasis and thrombosis. *Blood* **126**, 1224-1233 (2015).

34. Kenific CM, *et al*. NBR1 enables autophagy-dependent focal adhesion turnover. *The Journal of cell biology* **212**, 577-590 (2016).

35. Sharifi MN, *et al*. Autophagy Promotes Focal Adhesion Disassembly and Cell Motility of Metastatic Tumor Cells through the Direct Interaction of Paxillin with LC3. *Cell reports* **15**, 1660-1672 (2016).

36. Gardel ML, Schneider IC, Aratyn-Schaus Y, Waterman CM. Mechanical integration of actin and adhesion dynamics in cell migration. *Annual review of cell and developmental biology* **26**, 315-333 (2010).

37. Coller BS, Shattil SJ. The GPIIb/IIIa (integrin alphaIIbbeta3) odyssey: a technology-driven saga of a receptor with twists, turns, and even a bend. *Blood* **112**, 3011-3025 (2008).

38. Golebiewska EM, Poole AW. Platelet secretion: From haemostasis to wound healing and beyond. *Blood reviews* **29**, 153-162 (2015).

39. Eckly A, *et al*. Respective contributions of single and compound granule fusion to secretion by activated platelets. *Blood* **128**, 2538-2549 (2016).

Acknowledgements

We thank the personnel of Anexplo animal facilities (US006/CREFRE Inserm/UPS) for animal handling, Genotoul Imaging facilities (INSERM U1048, R. D'angelo and M. Zanoun ; CMEAB, B. Payre and I. Fourqaux), the Cytometry facility of Inserm U1048 (A. Zakaroff-Girard and C. Pecher), and the Lipidomic facility of Inserm U1048 (J. Bertrand-Michel). The authors thank all members from the B.P. laboratory. C.V. was supported by the MNRT and the Société Francaise d'Hématologie fellowships. SS was supported by the Fondation pour la Recherche Médicale (grant number DPC20111122988 to M.-P.G.) Work in the laboratory of B.P. was supported by Inserm and the Fondation pour la Recherche Médicale (grant number DPC20111122988 to M.-P.G.). Work in the laboratory of B.V. was supported by the Medical Research Council [G0700755], the UK Biotechnology and Biological Sciences Research Council [BB/I007806/1], Cancer Research UK [C23338/A15965], the Ludwig Institute for Cancer Research and the National Institute for Health Research (NIHR) University College London Hospitals Biomedical Research Centre. B.P. is a scholar of the Institut Universitaire de France.

Author contributions

C.V., M.L. and S.S. designed and performed most experiments and analyzed data; B.V. generated *Pik3c3*$^{flox/flox}$ mice; G.C. and B.P. designed and performed phosphoinositide analysis, C.C. performed arterial thrombosis *in vivo*; M.P.G analysed data; B.P and S.S. wrote the article.

Disclosure of conflicts of interest

B.V. is consultant to Retroscreen (London, UK) and Karus Therapeutics (Oxford, UK).

SUPPLEMENTAL DATA

Supplemental Methods

Materials: Anti–mouse dylight-488-anti-GPIbβ Ig derivative, GPIb-FITC, α2-FITC, JON/A-PE and GPVI-FITC antibodies and anti–mouse GPIbα antibody for platelet depletion were from Emfret Analytics. Anti-p110α, anti-p110β, anti-hsp90, anti-LC3 and anti-vps34 antibodies for western blotting were purchased from Cell Signaling Technology. Anti-vps34 antibody for immunioprecipitation and anti-PI3P was from Echelon Biosciences Inc. Anti-vps15 and anti-Beclin antibodies were from Bethyl Laboratories Inc. Anti-p85 antibody was from Merck Millipore. Anti-mCXCR4-FITC and anti-mCXCR4 antibodies were from RnDSystems. Serotonin ELISA test was from IBL International. Anti-human von Willebrand factor, anti-human von Willebrand factor HRP and anti-human fibrinogen antibodies were purchased from Dako. Lysotracker® Deep Red, MitoTracker® Deep Red FM, MitoSOX™ Red mitochoindrial superoxide indicator, transferrin-Alexa Fluor®^{546} and Propidium iodide were obtained from Molecular Probes™. Biochips with microcapillaries (Vena8Fluoro+) were obtained from Cellix. Anti-GPIIb-FITC, anti-EEA1, anti-Rab5, anti-Rab7, anti-P selectin-FITC, anti-LAMP1 and anti-PI3K-C2β antibodies were from BD Pharmingen. Lipids were from Avanti Polar Lipids (Coger, Paris, France). CRP was from Pr. Richard Farndale laboratory (Cambridge, UK). Collagen Reagent HORM® (equine) suspension was purchased from Takeda, $DIOC_6$ and AlexaFluor secondary antibodies from Life Technologies. Thrombopoietin and SDF1α were obtained from Peprotech. All other reagents were purchased from Sigma-Aldrich.

Washed murine platelets were prepared as previously described [1].

***In vitro* PI 3-kinase assay:** Vps34 immunoprecipitation and *in vitro* kinase assay were performed on washed platelets as previously described [2].

Gel electrophoresis and immunoblotting: MKs or washed platelets were lysed in Laemmli electrophoresis sample buffer containing 100 mM Tris-HCl (pH 6.8), 15% (v/v) glycerol, 25 mM DTT, and 3% SDS, boiled for 5 min, separated on SDS-PAGE, transferred onto a nitrocellulose membrane (Gelman Sciences) and analyzed using the relevant antibody.

Flow cytometry on platelets: Platelets in whole blood were stained with FITC-conjugated anti–mouse α2, anti–mouse GPVI, anti–mouse GPIIb or anti–mouse GPIb antibodies for 30 min at room temperature. For mitochondria content, washed platelets were incubated with a specific mitochondria fluorescent-probe (MitoTracker® Deep Red^{FM} and MitoSOX^{TM} Red mitochondrial superoxide indicator) for 30 min at 37°C. For ROS content, washed platelets were incubated with Dichloro-dihydro-fluorescein diacetate (DCFH-DA) for 30 min at 37°C. Samples were analyzed using an LSRFortessa^{TM} Cell analyser flow cytometer and Diva software (Becton Dickinson).

Lipid analysis: PI3P mass assay and phosphoinositide labelling were performed as previously described [3,4].

ELISA assays: Washed platelet serotonin content was measured using IBL Serotonin ELISA test (RE59121, IBL) according to manufacturer instructions. Plasma TPO quantification was performed using RnDSystems Mouse Thrombopoietin Immunoassay (MTP00, RnDSystems) according to manufacturer instructions. Washed platelet VWF levels were quantified by a previously described immunosorbent assay using anti-human VWF and anti-human VWF HRP antibodies [5].

TXB2 were analyzed by mass spectrometry as described previously [6].

Lysosomal β-galactosidase activity was quantified by spectrofluorometry using the fluorogenic 4-methylumbelliferyl (Muf)-glycoside derivatives as substrate.

Polyploidy of mature MKs isolated by BSA gradient was analyzed after MK fixation with 0.5% formalin and subsequent DNA staining with propidium iodide. Samples were analyzed using an LSRFortessa^{TM} Cell analyser flow cytometer and Diva software (Becton Dickinson).

Proplatelet formation assay from bone marrow explants were performed as previously described [7].

References

1. Valet C, Chicanne G, Severac C, et al. Essential role of class II PI3K-C2alpha in platelet membrane morphology. *Blood*. 2015;126(9):1128-1137.

2. Russell RC, Tian Y, Yuan H, et al. ULK1 induces autophagy by phosphorylating Beclin-1 and activating VPS34 lipid kinase. *Nat Cell Biol*. 2013;15(7):741-750.

3. Chicanne G, Severin S, Boscheron C, et al. A novel mass assay to quantify the bioactive lipid PtdIns3P in various biological samples. *Biochem J*. 2012;447(1):17-23.

4. Giuriato S, Pesesse X, Bodin S, et al. SH2-containing inositol 5-phosphatases 1 and 2 in blood platelets: their interactions and roles in the control of phosphatidylinositol 3,4,5-trisphosphate levels. *Biochem J*. 2003;376(Pt 1):199-207.

5. Romijn RA, Westein E, Bouma B, et al. Mapping the collagen-binding site in the von Willebrand factor-A3 domain. *J Biol Chem*. 2003;278(17):15035-15039.

6. Le Faouder P, Baillif V, Spreadbury I, et al. LC-MS/MS method for rapid and concomitant quantification of pro-inflammatory and pro-resolving polyunsaturated fatty acid metabolites. *J Chromatogr B Analyt Technol Biomed Life Sci*. 2013;932:123-133.

7. Antkowiak A, Viaud J, Severin S, et al. Cdc42-dependent F-actin dynamics drive structuration of the demarcation membrane system in megakaryocytes. *J Thromb Haemost*. 2016;14(6):1268-1284.

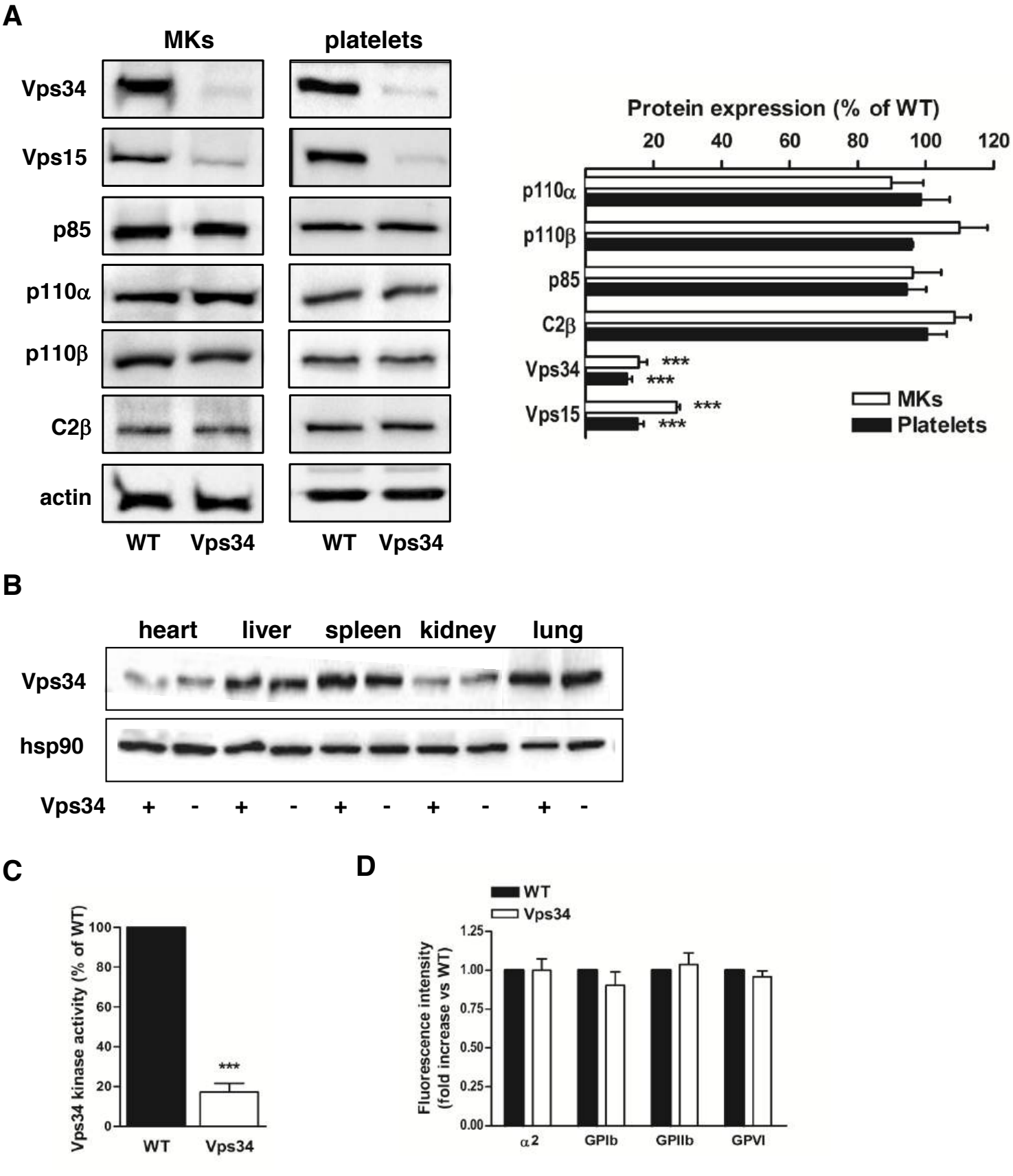

Supplemental Figure 1: Conditional genetic deletion of Vps34 in the MK/platelet lineage. (**A**) Western blot analysis for p110α, p110β, p85, PI3K-C2β, Vps34 and Vps15 in platelet and MK lysates (mean ± SEM; n=3; ***p<0.001 versus WT according one sample *t* test). (**B**) Western blot analysis for Vps34 in heart, liver, spleen, kidney and lung lysates. (**C**) Vps34 was immunoprecipitated from resting washed platelets and assayed for lipid kinase activity *in vitro* (mean ± SEM; n=5; ***p<0.001 *versus* WT according to one sample *t* test). (**D**) Surface glycoprotein expression was assessed on resting platelets (MFI: mean fluorescence intensity; mean ± SEM; n=4) by flow cytometry.

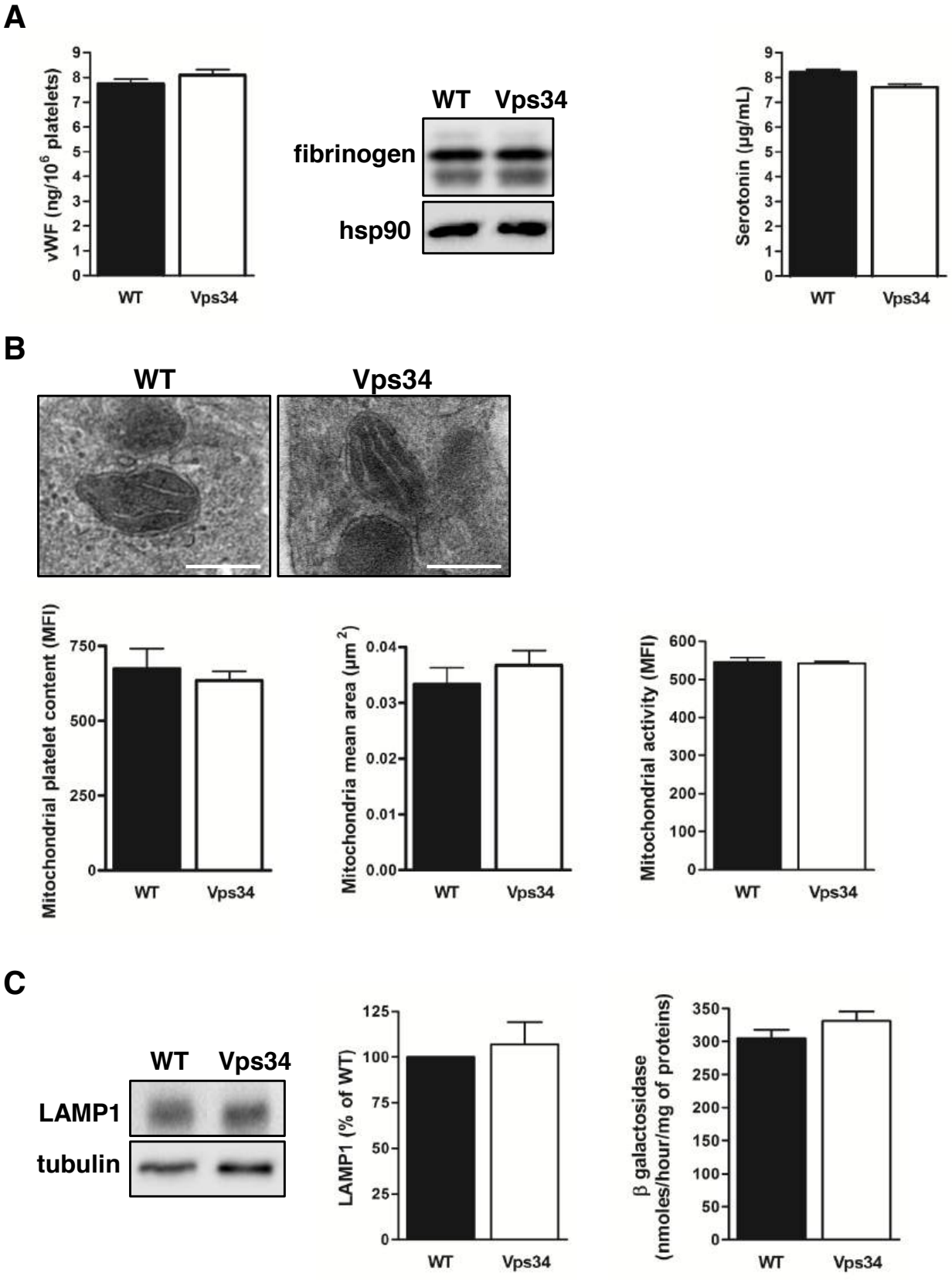

Supplemental Figure 2: Normal granule content and mitochondria / lysosome homoeostasis in Vps34-deficient platelets. (**A**) Platelet VWF, fibrinogen and serotonin content were quantified by immunoassay or western blot (mean ± SEM; n=6). (**B**) Transmission electron microscopy images of MK mitochondria representative from 3 mice of each genotype. Scale bar: 200 nm. Mitochondria area was quantified using ImageJ software (mean ± SEM; n=3 mice/genotype). Platelet mitochondrial content and activity were assessed by flow cytometry using MitoTracker® Red FM and MitoSOX™ Red mitochondrial superoxide indicator staining respectively (mean ± SEM; n=3). (**C**) Platelet lysosomal content and activity were assessed by western blotting using anti-LAMP1 antibody and by β galactosidase activity using a fluorogenic substrate (mean ± SEM; n=5).

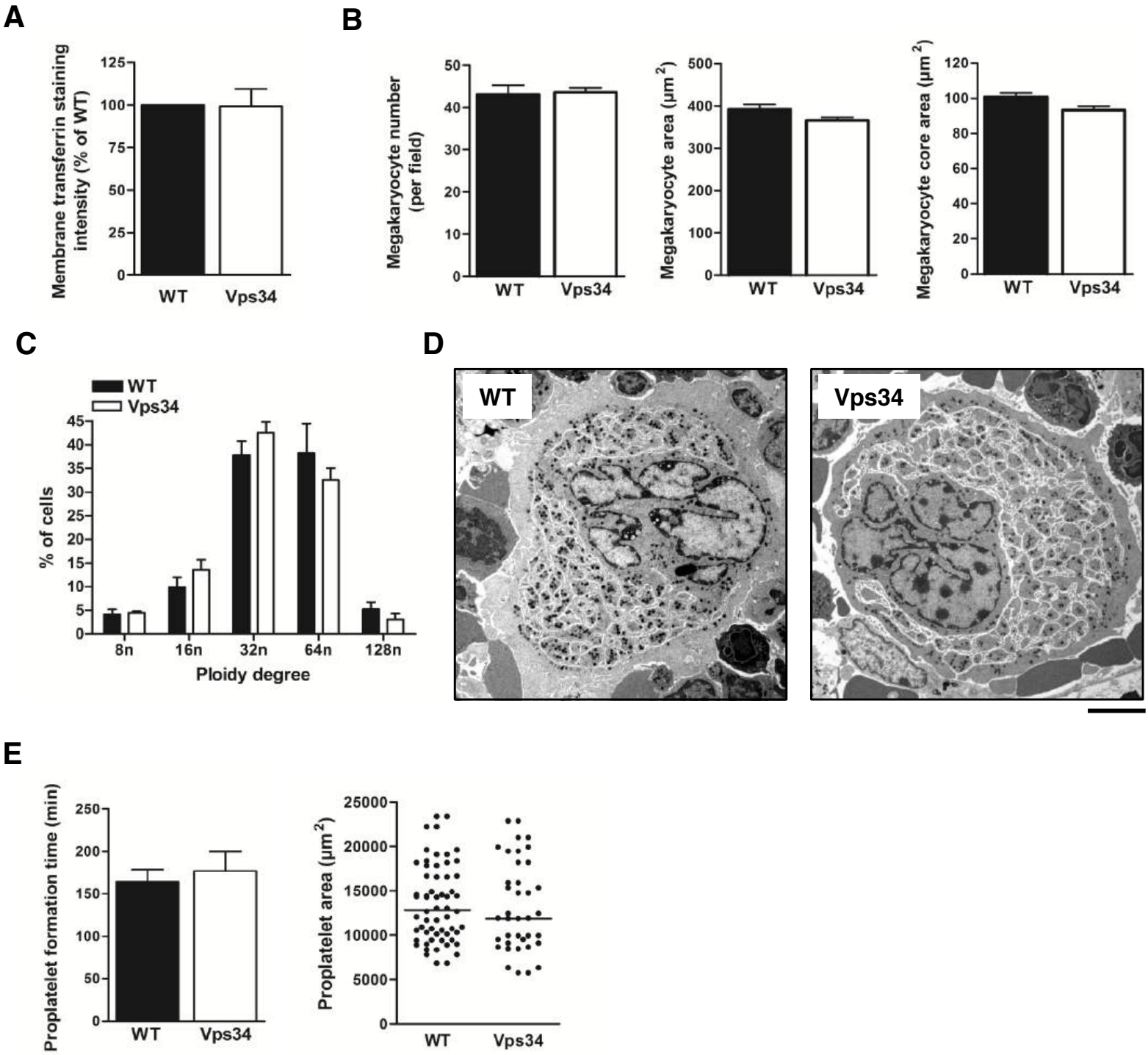

Supplemental Figure 3: No role for Vps34 in MK nuclear and cytoplasmic maturation and in proplatelet formation. (**A**) MKs were stained with transferrin-Alexa Fluor®^{546} and transferrin-Alexa Fluor®^{546} MK surface labeling was analysed by flow cytometry (mean ± SEM; n=3). (**B**) Analysis of bone marrow sections from WT and Vps34 mouse tibias. MK number, area and core area were quantified using NDP view software (mean ± SEM; n=6 mice/genotype and 50 MKs/mouse). (**C**) After three days of *in vitro* maturation, MKs were stained with propidium iodide and ploidy degree was evaluated by flow cytometry (mean ± SEM; n=4). (**D**) Transmission electron microscopy of MKs from bone marrow section. Images are representative of 5 mice of each genotype. Scale bar: 5 µm. (**E**) After bone marrow dissection, MKs were imaged for 15 hours by videomicroscopy. Time to proplatelet formation and proplatelet area was quantified using Zen software (mean ± SEM; n=16 MKs).

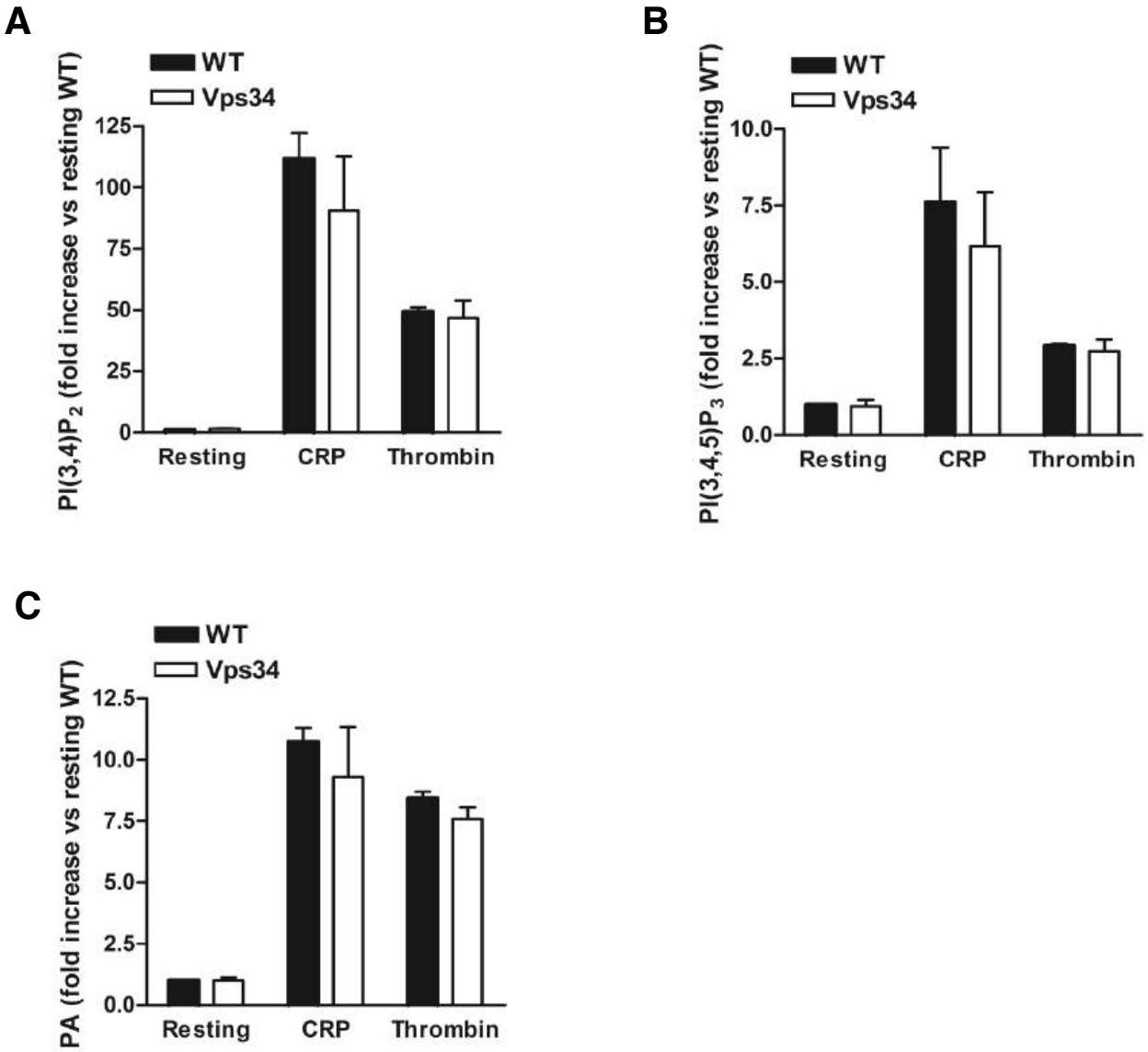

Supplemental Figure 4: Normal basal and inducible $PI(3,4)P_2$, $PI(3,4,5)P_3$ and phosphatidic acid levels in platelets. HPLC analysis of $PI(3,4)P_2$ (**A**) and $PI(3,4,5)P_3$ (**B**) and phosphatidic acid (PA) (**C**) of resting and stimulated (CRP, 10 µg/ml; thrombin, 0.5 UI/ml) ^{32}Pi-labelled platelets (mean ± SD; n=2).

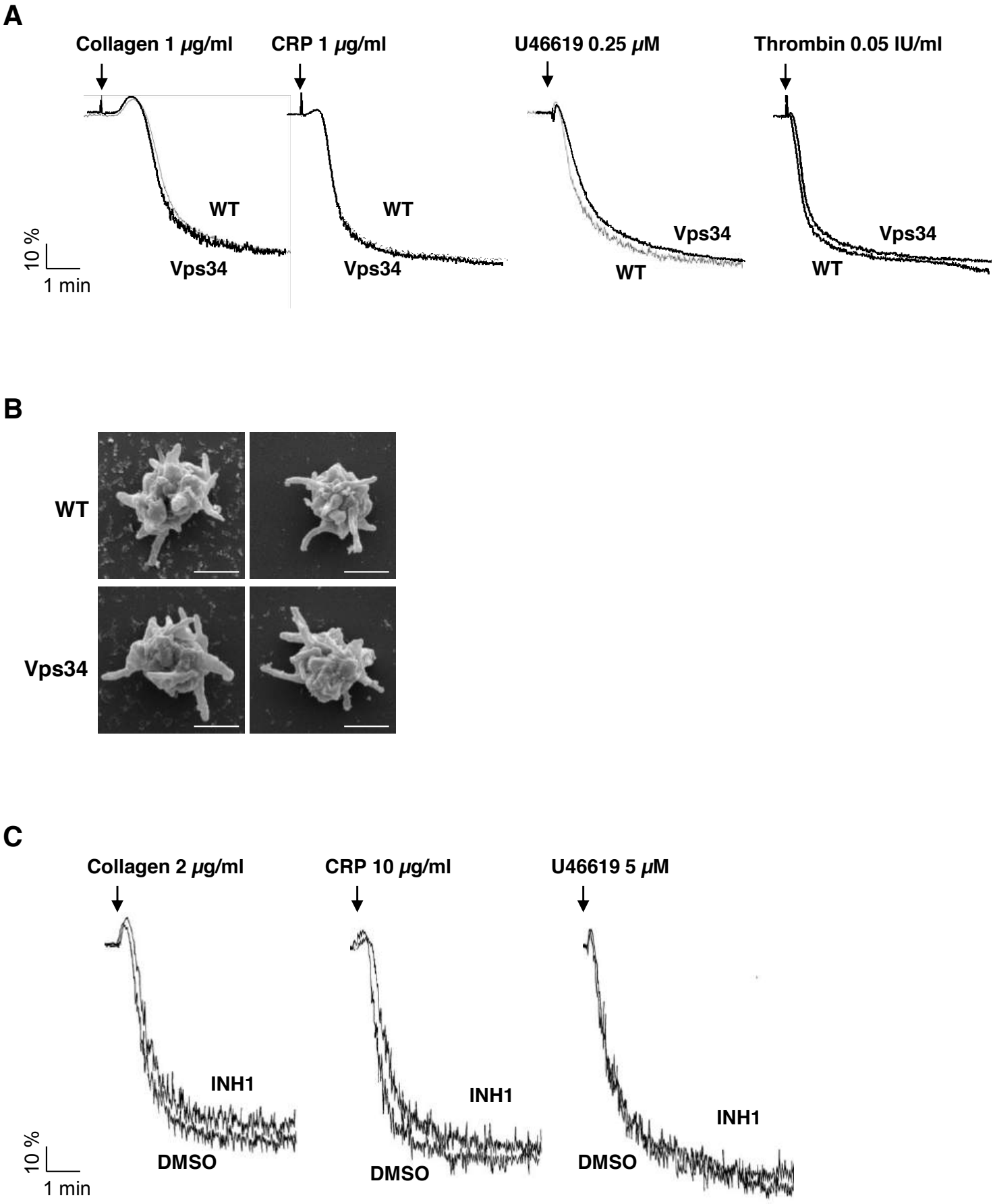

Supplemental Figure 5

D

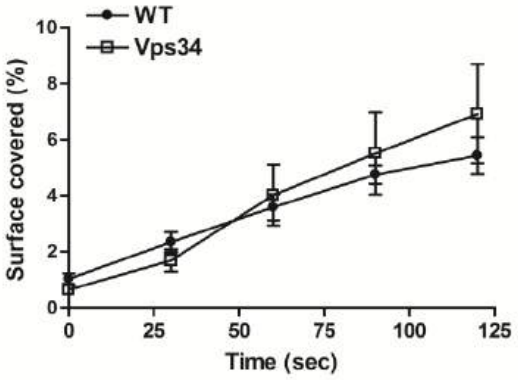

E

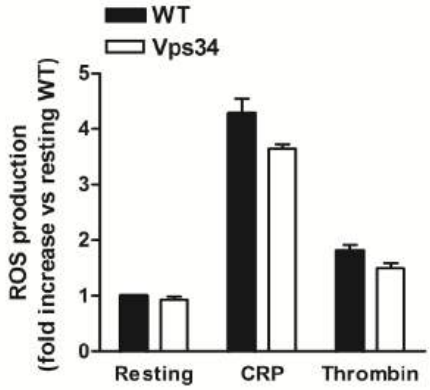

F

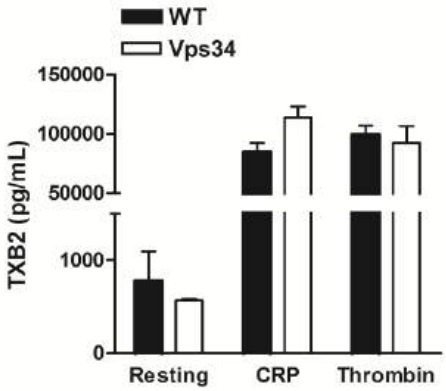

Supplemental Figure 5: Normal *in vitro* platelet activation when Vps34 is deleted or inactivated. (**A**) Representative curves of washed platelet aggregation in response to various agonists (2.10^8 platelets/ml, n=6-15 mice) analysed by light transmission aggregometry. (**B**) Washed platelets stimulated in suspension with CRP (1 µg/ml) were visualized by scanning electron microscopy. Two representative images of each phenotype are representative of 5 mice. Scale bar: 1 µm. (**C**) Platelet-rich plasma from human healthy donors was pre-incubated with DMSO or 1 µM INH1 during 1 hour at 37°C. Then, platelet aggregation in response to agonists was assessed by light transmission aggregometry. Aggregation curves are representative of 3 independent experiments. (**D**) Platelet adhesion on collagen-coated microcapillary after αIIbβ3 blockage. Mice whole blood were pre-incubated with Integrilin® (40 µg/ml) for 10 minutes. Then, $DiOC_6$-labelled platelets in treated whole blood were perfused through a collagen-coated microcapillary at a physiological arterial shear rate of 1500 s^{-1}. Surface covered by fluorescent platelets and thrombus volume were analysed using ImageJ software (mean ± SEM; n=3). (**E**) Reactive oxygen species (ROS) production in resting or stimulated (CRP, 1 µg/ml; thrombin, 0.1 UI/ml) platelets was analysed by flow cytometry using DCFDA compound (mean ± SEM; n=3). (**F**) TXB_2 production in resting or stimulated (CRP, 1 µg/ml; thrombin, 0.1 UI/ml) platelets was analysed by mass spectrometry (mean ± SEM; n=3).

- **Conclusions**

De façon intéressante, nous observons que la délétion de Vps34 dans la lignée mégacaryocyte-plaquettes se traduit par une microthrombopénie modérée associée à une production plaquettaire défectueuse suite à une thrombocytopénie immune induite. Ce résultat ne s'explique pas par un défaut de polyploidisation, de formation/structure du DMS ou d'extension des PPT des MKs mais semble être dû à un défaut de directionnalité de migration des MKs en réponse à un gradient de CXCL12. L'analyse morphologique des plaquettes et des MKs déficients en Vps34 a aussi révélé des anomalies de granules plaquettaires. La diminution du nombre de granules α et l'augmentation de leur taille, à la fois dans les plaquettes et les MKs, montrent un défaut de biogénèse des granules. De plus, nous mettons en évidence une diminution nette de la production de PtdIns3P dans les MKs délétés pour Vps34 ainsi qu'un trafic endosomal et une autophagie perturbés, ce qui pourrait expliquer le défaut de migration et de biogénèse des granules dans le MK.

Au niveau plaquettaire, de façon inattendue, nous montrons que Vps34 régule la production de PtdIns3P en réponse à une stimulation plaquettaire. *In vitro,* nous ne mettons pas en évidence de modification de l'agrégation des plaquettes de souris déficientes en Vps34 ou des plaquettes humaines traitées avec l'inhibiteur Vps34-IN1. Par contre, e*x vivo*, l'inhibition de Vps34 entraîne un défaut de croissance du thrombus sur matrice de collagène. Ce défaut est reproduit par l'utilisation des inhibiteurs de Vps34 sur des plaquettes humaines ou de souris sauvages, montrant que l'activité catalytique de Vps34 joue un rôle dans l'activation plaquettaire, indépendamment des défauts hérités du MK. *In vivo*, malgré un temps de saignement normal à la queue, un retard significatif d'occlusion de la carotide après lésion au chlorure ferrique est observé.

L'ensemble de ces résultats met en évidence un rôle de Vps34 dans la production plaquettaire au niveau du MK et dans la dynamique d'activation plaquettaire et de formation du thrombus en condition de flux.

B) L'adipocyte : rôle d'un facteur extrinsèque au MK dans la régulation de la mégacaryopoïèse et la production plaquettaire

1) Contexte scientifique

Les adipocytes constituent un élément essentiel du microenvironnement médullaire, cependant leur rôle reste à ce jour peu étudié. Récemment, les adipocytes médullaires ont été proposés comme régulateurs négatifs de l'hématopoïèse (Naveiras et al., 2009). Le nombre d'adipocytes varie considérablement au cours du développement, ainsi que dans différentes situations pathologiques au cours desquelles se produisent des modifications de l'hématopoïèse. En effet, dans un contexte d'obésité et de diabète de type II, il a été décrit une expansion de l'adiposité médullaire (Adler et al., 2014b) associée à une lymphopoïèse et une myèlopoïèse perturbées (Adler et al., 2014a; Karlsson et al., 2010; Singer et al., 2014; Trottier et al., 2012; Yang et al., 2009). Par ailleurs, les patients atteints d'obésité et de diabète de type II présentent un renouvellement plaquettaire plus rapide, un volume moyen plaquettaire augmenté et une hyperactivabilité plaquettaire (Morange and Alessi, 2013; Santilli et al., 2012). Ces modifications constituent des facteurs de risque importants dans la survenue d'événements thrombotiques chez ces patients.

A ce jour, rien n'est connu concernant l'impact des adipocytes sur la mégacaryopoiëse et la production plaquettaire. Pour étudier cela, nous avons mis en place un système de co-culture où des adipocytes adhérents sont mis en présence de progéniteurs hématopoïétiques en suspension, sans aucun contact physique possible entre les deux types cellulaires. Des souris sauvages sous régime riche en lipides pendant douze semaines (contexte d'adiposité médullaire augmentée) nous ont également permis d'étudier l'impact de l'obésité et du diabète de type II sur la mégacaryopoïèse et la production plaquettaire.

Publication n°4

Adipocyte influences megakaryopoiesis and platelet production: a link with obesity.

Colin Valet[1], Aurelie Batut[1], Alize Dortignac[1], Bernard Payrastre[1,2*], Philippe Valet[1*], Sonia Severin[1*]

[1] Inserm U1048, I2MC and Universite Paul Sabatier, 31432, Toulouse Cedex 04, France

[2] CHU de Toulouse, Laboratoire d'Hematologie, 31059, Toulouse Cedex 03, France

[*] These authors share senior authorship

Adipocyte influences megakaryopoiesis and platelet production: a link with obesity

Short title : Adipocyte role in megakaryopoiesis

Colin Valet[1], Aurelie Batut[1], Alizee Dortignac[1], Bernard Payrastre[1,2*], Philippe Valet[1*] and Sonia Severin[1*]

[1] *Inserm U1048 and Université Toulouse 3, I2MC, 31432 Toulouse Cedex 4, France*

[2] *Laboratoire d'Hématologie CHU de Toulouse, Toulouse, France*

[*] *These authors share senior authorship*

Address correspondence to:

Sonia Severin, Inserm U1048 and Université Toulouse 3, I2MC, 31432 Toulouse Cedex 4, France. Phone: +33-531224143; Email: sonia.severin@inserm.fr

Scientific section heading : Platelets and Thrombopoiesis

Text word count: 1406

Abstract word count: 157

Number of figures and tables: 2

Number of references: 17

Key points

- Adipocytes directly influence megakaryocyte maturation through lipid transfer.
- High-fat diet induced obesity affects medullar megakaryocyte maturation and decreases platelet production in mouse.

Abstract

Megakaryocytes (MKs) come from a highly complex and specialized hematopoietic progenitor maturation process within the bone marrow (BM) and give rise to *de novo* circulating platelets. BM microenvironment is composed of different cell types including a large number of adipocytes which medullar role is still ill defined. Co-culture of freshly isolated hematopoietic progenitors with differentiated adipocytes shows that adipocytes directly impact MK maturation by enhancing their size and ploidy levels. Hematopoietic progenitors induce adipocyte delipidation in order to uptake fatty acids / lipids to reinforce their maturation into MKs in a non-energetic aim. In the context of obesity in mouse, marrow adiposity increases and is associated to enhanced MK maturation but defective platelet production and lifespan leading to moderate macrothrombopenia. Altogether, these data uncover an unsuspected crosstalk between adipocytes and MKs *via* a fatty acid / lipid transfer from adipocytes to MKs. Obesity has a direct impact on BM adipocyte content and influences MK and platelet homeostasis.

Introduction

In adult, megakaryopoiesis and platelet production occur within the complex bone marrow (BM) microenvironment. Megakaryocytes (MKs) are highly specialized BM cells releasing up to 10^{11} platelets every day with a turnover every 8–9 days in humans and 4-5 days in mice to maintain an appropriate circulating platelet count. MK maturation is a multi-step process where MKs increase in size, become polyploid, expand their cytoplasmic content and develop a highly invaginated membrane system allowing proplatelet projections at the origin of *de novo* circulating platelets.[1,2] Within the central cavities of axial and long bones, BM consists of hematopoietic tissue islands and adipose cells surrounded by vascular sinuses.[3] Marrow adipocytes have been firstly characterized as negative regulators of BM hematopoietic microenvironment *in vivo* but their role appear more complex.[4] It has recently been shown that high-fat diet (HFD) increases marrow adipocyte content and can modify BM lymphopoiesis and myelopoiesis[5-9] suggesting a potential impact of diet-induced obesity on the hematopoietic system.[10] Considering the critical role of BM niche in hematopoiesis and the vulnerability of BM microenvironment to obesity, we addressed the question whether adipocytes and diet-induced obesity could impact on both megakaryopoiesis and platelet production. Interestingly, co-cultivating hematopoietic progenitors with adipocytes improve their maturation toward MK lineage directly through a fatty acid / lipid transfer from adipocytes to MKs. Obese mice display an enhanced MK maturation within the BM associated to increased adiposity. However this physiopathological context dampens platelet production and increases platelet clearance leading to macrothrombopenia. Thus, these findings demonstrate an unsuspected effect of adipocytes and obesity on MK and platelet homeostasis.

Methods

Animals: C57Bl6/J male mice (obtained from Harlan, Gannat, France) were fed with a normal diet (ND) from weaning until 9 weeks aged and then either maintained on ND or fed with a high-fat diet (HFD) containing 20% protein, 20% carbohydrate, 60% fat (ResearchDiets, NJ, US) for 12 weeks. All procedures were performed in accordance with institutional guidelines for animal research and were approved by the French Ministry of Research in agreement with European Union guidelines.

Differentiation into adipocytes: Mouse 3T3-F442A pre-adipocyte cell line was grown to confluence and differentiated in DMEM with 10% FBS in presence of 50 nM insulin for 10 days as previously described.[11] OP9 mouse BM mesenchymal stem cells were grown to confluence and differentiated for 7 days in MEM-α with 15% KnockOut^{TM} SR (Invitrogen).[12]

MK purification and co-culture with 3T3-F442A or OP9 differentiated adipocytes: BM hematopoietic progenitor cells ($2x10^6$ cells) were obtained from femora and tibiae of C57Bl/6J mice after CD16/CD32$^+$, Gr1$^+$, B220$^+$ or CD11b$^+$ cell depletion. Cells were then seeded for 3 days in the upper chamber of the 0.4 μm Transwell system over adherent 3T3-F442A or OP9 differentiated adipocytes (no direct contact) in 10% serum-supplemented DMEM medium with 2 mM l-glutamine and penicillin/streptomycin at 37°C under 5% CO_2 in the presence or absence of the megakaryocytic differentiation cytokine (thrombopoietin (TPO, 50ng/mL)) (Figure 1A).

Materials, **[^{14}C] palmitate labeling**, **triglyceride measurement**, **flow cytometry, immune thrombocytopenia**, **platelet lifespan, plasma TPO quantification, proplatelet formation assay from bone marrow explants** are described in details in the supplemental Methods.

Statistical analysis: Data are expressed as mean ± SEM. Significance of differences was determined using two-tailed Student's test and two-way ANOVA. p values < 0.05 were considered significant (*p<0.05, **p<0.01, ***p<0.001).

Results and Discussion

Adipocyte directly improves MK maturation

To investigate whether adipocytes can directly influence MK maturation, we set up an *in vitro* adipocyte/hematopoietic progenitor co-culture assay (Figure 1A). Interestingly, co-culture caused a decreased apoptotic level (supplemental Figure 1) and a significant increased expression of MK lineage differentiation markers (CD41 and CD42) in the hematopoietic progenitor cell/MK population (Figure 1B). Co-culture significantly enhanced MK size (+ 62.5 % ± 4.86 %, n= 60, p< 0.001) and polyploidisation in presence of TPO (Figure 1C). Modal ploidy was significantly higher (26.52 ± 2.5 for co-culture *vs* 16.07 ± 2.2 for non-coculture, n=8, p< 0.01) with a marked increase in cells with ploidy levels equal or higher than 32n associated to a decrease in cells with lower polyploidy levels (Figure 1C). Even in absence of TPO, co-culture induced a marked increase in MK polyploidisation (Figure 1D). Co-culture with non-differentiated 3T3-F442A had no impact on MK differentiation (data not shown). Altogether, these data show that adipocytes are able to dramatically enhance hematopoietic progenitor differentiation toward MK lineage. The effect of adipocytes on MKs occurs during the whole maturation process as polyploidisation enhancement was observed either when hematopoietic progenitors were cultivated during one day with adipocytes at early time (supplemental Figure 2A) or during two days at a later stage of differentiation (supplemental Figure 2B).

Interestingly, either in presence or absence of TPO, enhanced MK maturation caused by adipocytes was associated with adipocyte delipidation as shown by a significant decrease in adipocyte triglyceride content and red oil labeling (Figure 1E). Thus, *in vitro* co-culture of adipocytes/hematopoietic progenitors induced a net increase in the overall MK maturation associated to adipocyte delipidation, highlighting a crosstalk between MKs and adipocytes.

When [^{14}C] palmitate-labeled adipocytes were co-cultivated with hematopoietic progenitors, [^{14}C] palmitate was detected in the MK population after 3 days of differentiation in presence or absence of TPO (Figure 1F). This finding demonstrates a fatty acid / lipid transfer from adipocytes to MKs. Importantly, this transfer has a direct impact on MK maturation since interfering with the fatty acid / lipid transfer and uptake by adding albumin and free fatty acid uptake inhibitor, phloretin, to co-culture medium, prevented adipocyte-induced MK maturation enhancement (Figure 1G). Inhibiting β-oxydation using etomoxir, a selective inhibitor of the carnitine palmitoyltransferase 1, had no consequences on the enhanced MK polyploidization (supplemental Figure 3A), therefore excluding an energetic contribution of this fatty acid / lipid uptake by MKs. Adding a blocking anti-TPO antibody during the co-culture allowed to exclude that adipocyte-secreted TPO[13] causes MK maturation enhancement (supplemental Figure 3B). More investigation is needed to highlight the precise mechanism and role of fatty-acid and lipids transferred from adipocytes to MKs. We can hypothesize that this could be achieved *via* phospholipid-containing membrane vesicles called adiposomes[14] whose phospholipid and fatty acids might contribute to the development of the MK extensive membrane demarcation system and whose cargo proteins such as transcriptional and translational regulators[15] might amplify MK polyploidy.

Adipocytes derived from BM mesenchymal stem cells (OP9) have the same effect on MK maturation than 3T3-F442A-derived adipocytes (Figure 1H), showing that marrow adipocytes influence MK maturation.

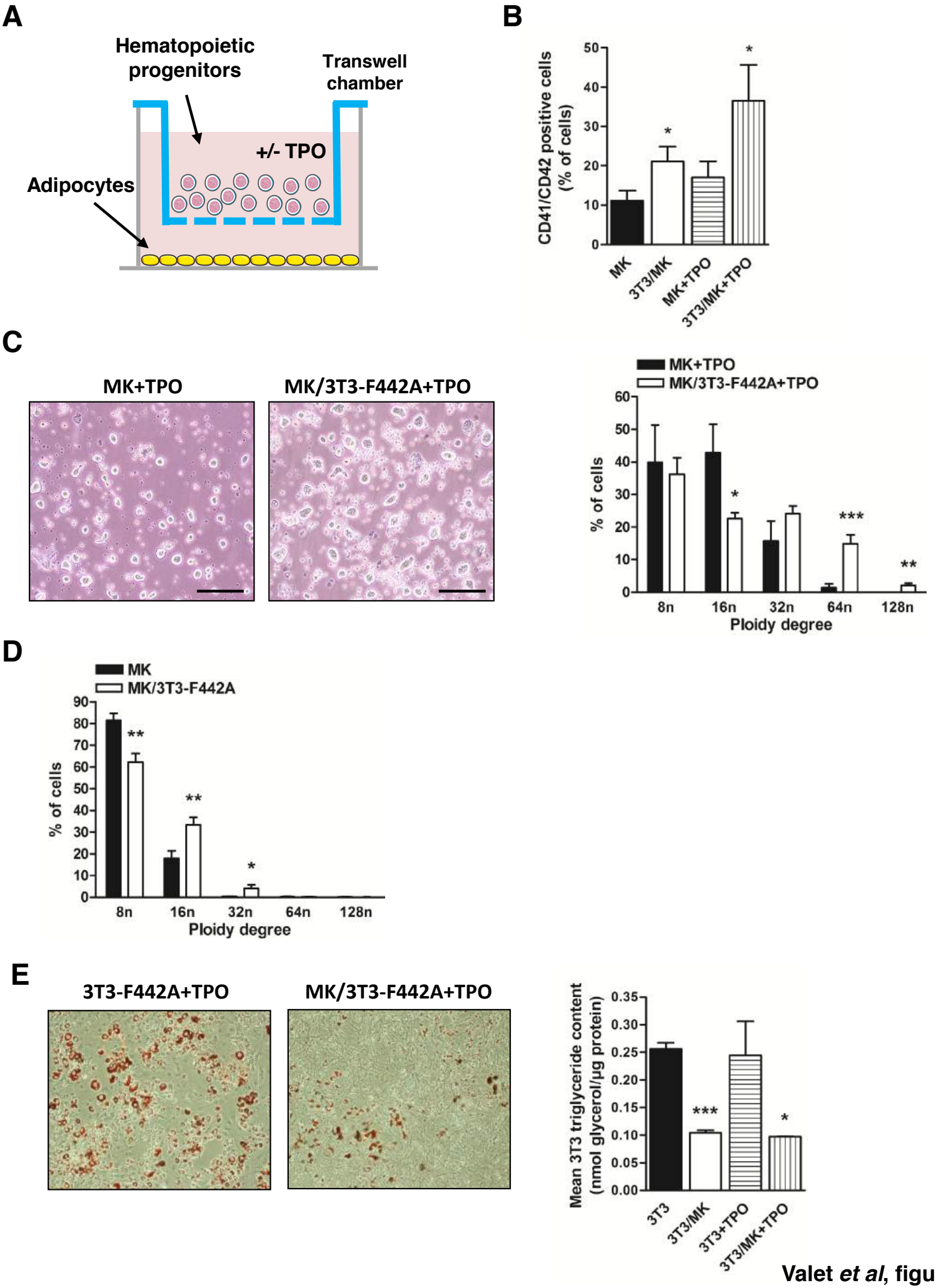

Valet *et al*, figure 1

F

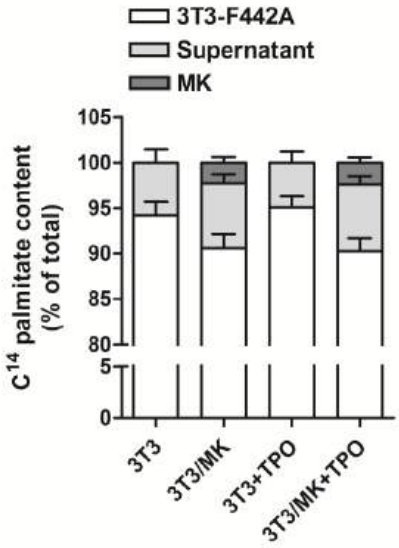

G

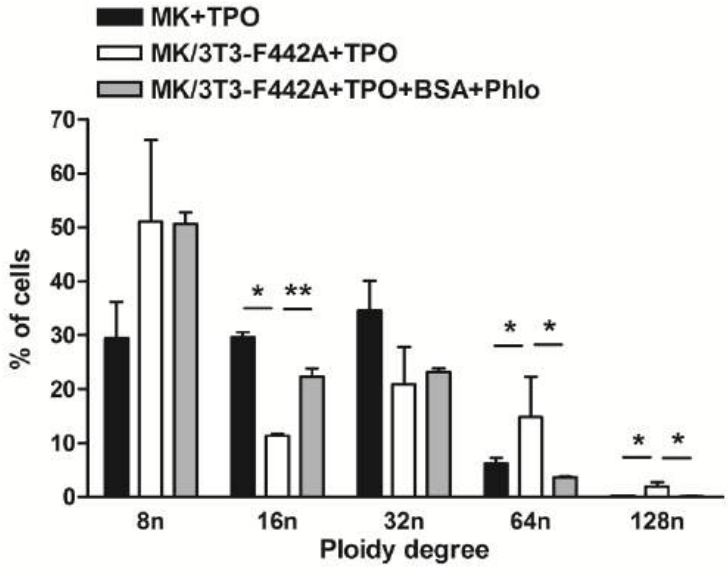

H

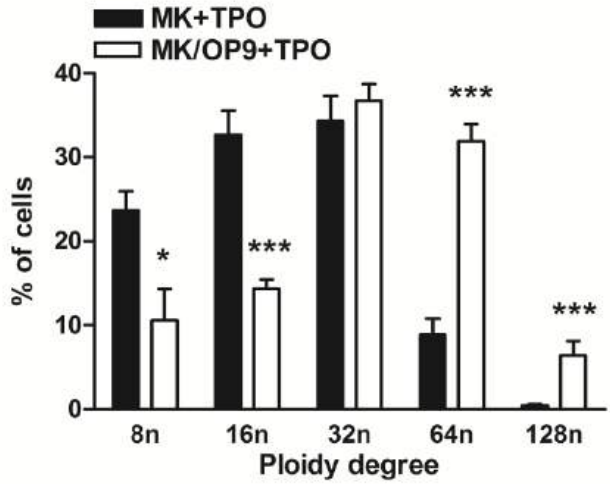

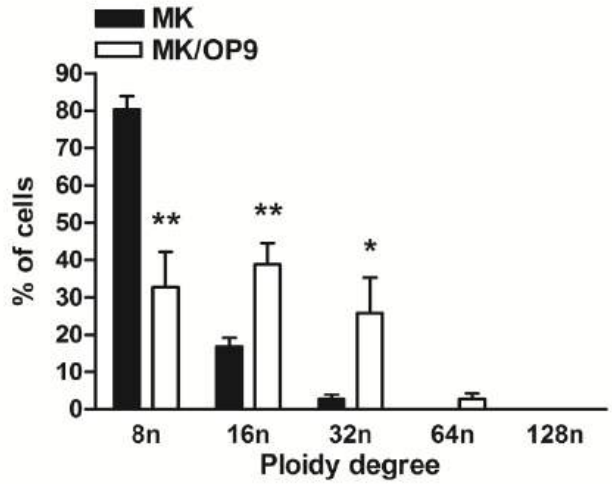

Valet *et al*, figure 1

Figure 1. Reciprocal communication between MKs and adipocytes. (**A**) Hematopoietic progenitor cells isolated from murine BM were seeded for 3 days in the upper chamber of the 0.4 µm Transwell system over adherent mouse 3T3-F442A pre-adipocyte cells or OP9 mesenchymal stem cells differentiated into adipocytes in the presence or not of TPO (50ng/mL). (**B**) Surface glycoprotein expression was assessed by flow cytometry on hematopoietic progenitor cell / MK population cultivated for 3 days in different conditions (mean ± SEM; n=3 independent experiments; *p<0.05 versus non-cocultivated MKs according to two-tailed Student's t test). (**C**) Representative images of MKs co-cultivated or not with 3T3-F442A differentiated adipocytes in presence of TPO for 3 days; scale bar: 100µm. MK DNA ploidy was analyzed after 3 days of co-culture or not with 3T3-F442A differentiated adipocytes in presence of TPO by flow cytometry after propidium iodide labeling. Quantification of the percentage of cells with different levels of ploidy equal or greater to 8n was assessed (mean ± SEM; n=7 independent experiments; *p<0.05, **p<0.01 and ***p<0.001 versus non-co-cultivated MKs according to two-tailed Student's t test). (**D**) MK DNA ploidy was analyzed after 3 days of co-culture or not with 3T3-F442A differentiated adipocytes in absence of TPO by flow cytometry after propidium iodide labeling. Quantification of the percentage of cells with different levels of ploidy equal or greater to 8n was assessed (mean ± SEM; n=7 independent experiments; *p<0.05 and **p<0.01 versus non-co-cultivated MKs according to two-tailed Student's t test). (**E**) Representative Red-Oil labeling images of 3T3-F442A differentiated adipocytes co-cultivated or not with MKs in presence of TPO for 3 days; magnification: 100x. 3T3-F442A differentiated adipocyte triglyceride content were measured after 3 days of co-culture in the presence or not of hematopoietic progenitors and TPO (50ng/mL) (mean ± SEM; n=3 independent experiments; *p<0.05 and ***p<0.001 versus non-co-cultivated 3T3-F442A with or without TPO according to two-tailed Student's t test). (**F**) [^{14}C] palmitate labeled 3T3-F442A differentiated adipocytes were co-cultivated in presence or not of hematopoietic progenitors and TPO (50ng/mL) in a non-containing [^{14}C] palmitate medium for 3 days. Radioactivity in 3T3-F442A differentiated adipocytes, MKs and co-culture supernatant was quantified (mean ± SEM; n=3 independent experiments). (**G**) Hematopoietic progenitor cells isolated from murine BM were cultivated with or without 3T3-F442A differentiated adipocytes, TPO (50ng/mL), phloretin (400µM) and 2% BSA for 3 days. MK DNA ploidy was then analyzed by flow cytometry after propidium iodide labeling. Quantification of the percentage of cells with different levels of ploidy equal or greater to 8n was assessed (mean ± SEM; n=3 independent experiments; *p<0.05 and **p<0.01 according to two-way ANOVA). MK: megakaryocyte; TPO: thrombopoïetin; BSA: Bovine Serum Albumin; Phlo: phloretin. (**H**) MK DNA ploidy was analyzed after 3 days of co-culture or not with OP9 differentiated adipocytes in presence (left) or absence (right) of TPO by flow cytometry after propidium iodide labeling. Quantification of the percentage of cells with different levels of ploidy equal or greater to 8n was assessed (mean ± SEM; n=5 independent experiments; *p<0.05, **p<0.01 and ***p<0.001 versus non-cocultivated MKs according to two-tailed Student's t test).

Valet *et al*, figure 1

Abnormal medullar MK maturation and platelet production in obese mice

Having shown that marrow adipocytes directly influence MK maturation, we investigated megakaryopoiesis in a context of marrow adipocyte accumulation such as HFD-induced obesity. As expected, HFD resulted in a significant increase in mouse body weight, fasted glyceamia, marrow adipose tissue content and blood monocyte count (Figure 2A and supplemental Figure 4A, 4B and 4C).[7,16] Alike our adipocyte/MK co-culture assay (Figure 1C), histomorphometric analysis of BM from HFD-fed mice revealed a significant increase in MK total size (+ 26.1% ± 2.6%) and in MK nucleus size (+ 33.6% ± 4.0%), with a normal medullar MK count (Figure 2B) and normal plasma TPO level (supplemental Figure 4D). Thus, HFD-induced obesity has a direct impact on medullar MK maturation *in vivo*.

HFD-induced obesity also resulted in a significant decrease in the platelet count (- 17.6% ± 2%, Figure 2C) associated to an increased platelet volume (+ 8.6% ± 2%, Figure 2C). We also observed that obesity altered platelet production (Figure 2D), accelerated MK proplatelet formation (Figure 2E) and increased platelet clearance (Figure 2F). These data suggest that decreased platelet count is associated to a quicker MK proplatelet formation and a potential release of ectopic platelets in the BM. Likewise increased platelet volume is linked to the youth of platelets, as previously suggested in obese patients[17], due to their decreased lifespan.

Overall, these data show that diet induced-obesity and increased marrow adiposity has a direct impact on both marrow MK homeostasis and platelet production / turn-over.

These findings clearly demonstrate an interplay between adipocytes and MKs, with adipocyte delipidation associated to improved MK maturation through a direct fatty acid / lipid transfer from adipocytes to MKs in a non-energetic aim. In addition to the growing list of marrow cellularity dysregulation known to be associated with obesity as lymphopoiesis and myelopoiesis[10], we show that HFD-induced obesity and increased marrow adiposity directly

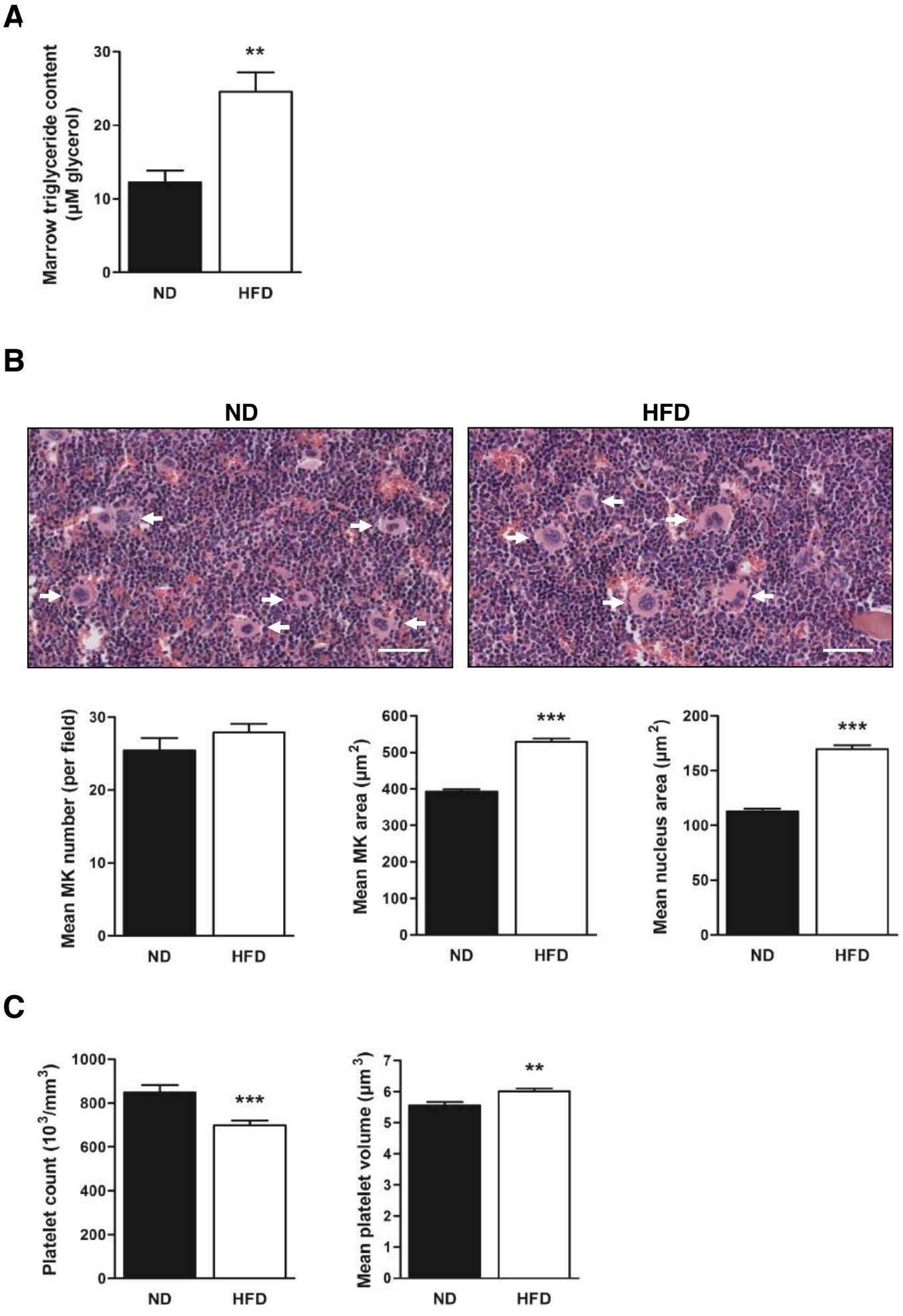

Valet *et al*, figure 2

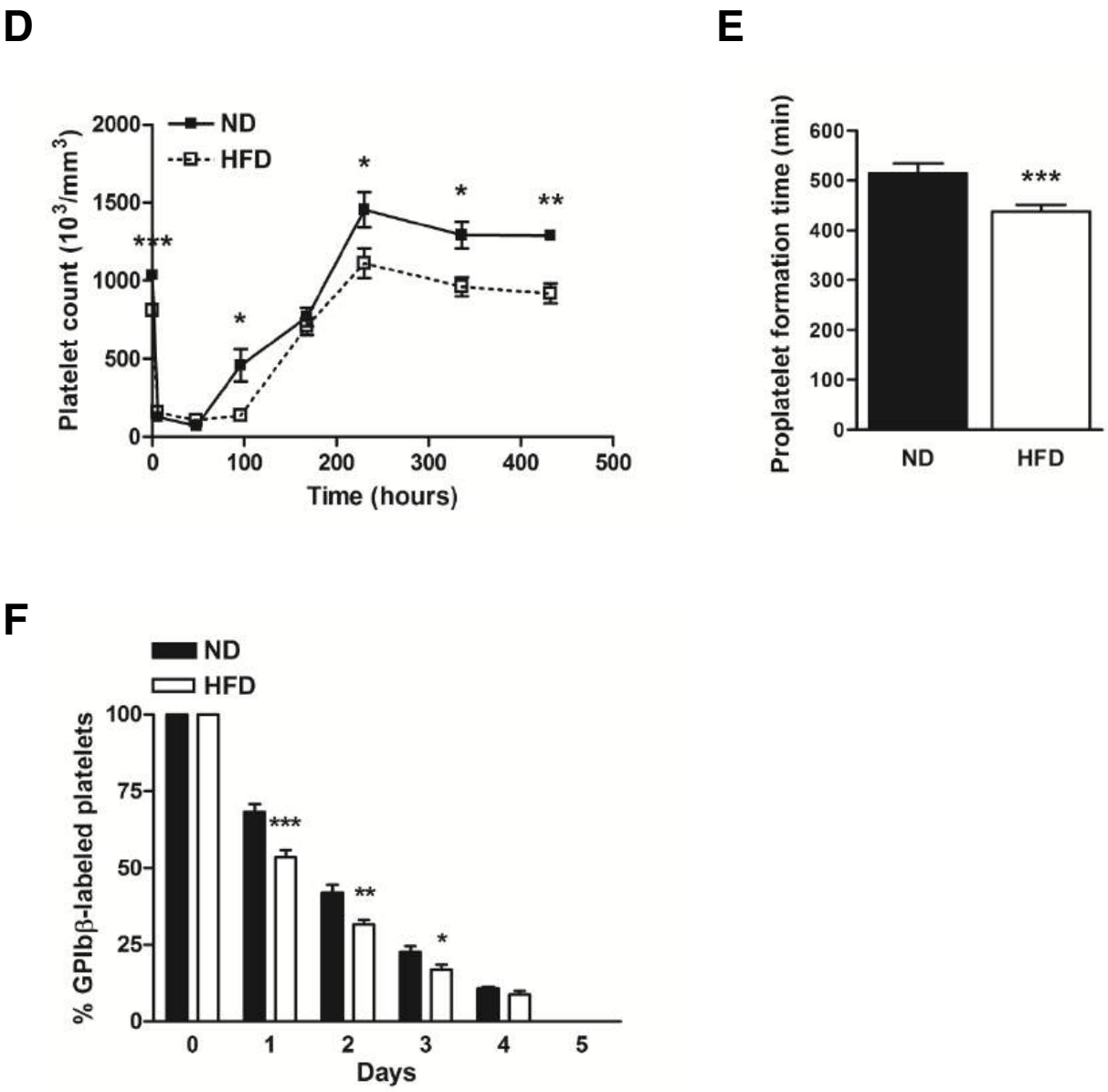

Figure 2. Impact of diet-induced obesity on MK homeostasis and platelet production. (**A**) BM triglyceride content of ND- and HFD- fed mice (mean ± SEM; n=14 mice; ***p*<0.01 versus ND-fed mice according to two-tailed Student's *t* test). (**B**) BM hematoxylin/eosin staining of ND- and HFD-fed mice; scale bar: 50µm. Mean MK total area, nucleus area and number were quantified using NDPview software (mean ± SEM; n=350 MKs from 4 mice; ***p<0.001 versus ND-fed mice according to two-tailed Student's *t* test). (**C**) Whole blood platelet count and volume (mean ± SEM; n=25 mice; ***p*<0.01 and ***p<0.001 versus ND-fed mice according to two-tailed Student's *t* test) were measured using Micros60 (Horiba ABX Diagnostics). (**D**) Thrombocytopenia was induced in 21 week-old mice by intraperitoneal injection of anti-mouse GPIbα antibody (1.5 µg/g body weight). Platelet counts were measured using a Micros60 (Horiba ABX Diagnostics) from blood samples collected before injection (time=0) and then 6, 48, 96, 168, 230, 336 and 432 hours after injection (mean ± SEM; n=4 mice; **p*<0.05, ***p*<0.01 and ***p<0.001 versus ND-fed mice according to two-tailed Student's *t* test). (**E**) After BM dissection, megakaryocytes were imaged for 15 hours by videomicroscopy. Time to proplatelet formation was quantified using Zen software (mean ± SEM; n=130 MKs from 4 mice; ***p*<0.01 versus ND-fed mice according to two-tailed Student's *t* test). (**F**) Mice were injected intravenously with a derivative anti-GPIbb (0.1 µg/g body weight) coupled to an AlexaFluor-488. At various time points after injection, the percentage of labeled platelets was measured by flow cytometry (mean ± SEM; n=4 mice; **p*<0.05, ***p*<0.01 and ***p<0.001 versus ND-fed mice according to two-tailed Student's *t* test). ND: normal diet; HFD: high fat diet; MK: megakaryocyte.

impact on megakaryopoieis by enhancing this process and altering platelet production / turn-over. This study contributes to the ongoing discussion on the impact of obesity in the marrow homeostasis and platelet biology.

Acknowledgements

We thank the personnel of Anexplo animal facilities (UMS US006/ Inserm) for animal handling, of experimental histopathology (UMS US006/ Inserm), of Cytometry core facility of Inserm UMR1048 (A. Zakaroff-Girard and C. Pecher), of imaging core facility of INSERM UMR1048 (R. D'Angelo, M. Zanoun) and of MetaToul-Lipidomic core facility (Inserm U1048), MetaboHUB-ANR-11-INBS-0010 (A. Dupuy and J. Bertrand-Michel). The authors thank all members from the B.P. and P.V laboratories and A. Mairal for helpful discussions. C.V. was supported by a Université Paul Sabatier scolarship. Work in B.P. laboratory was supported by Inserm and Fondation de France (grant 00056850). B.P. is a scholar of the Institut Universitaire de France. Work in P.V. laboratory was supported by Inserm and the Fondation pour la Recherche Médicale (grant ING20121226373).

Authorship contributions

C.V. and S.S. designed and performed experiments, analyzed data and wrote the article; A.B. and A.D performed experiments and analyzed data; B.P. and P.V. designed experiments and wrote the article.

Disclosure of conflicts of interest

The authors declare no conflicts of interest.

REFERENCES

1. Machlus KR, Thon JN, Italiano JE, Jr. Interpreting the developmental dance of the megakaryocyte: a review of the cellular and molecular processes mediating platelet formation. *Br J Haematol*. 2014;165(2):227-236.

2. Machlus KR, Italiano JE, Jr. The incredible journey: From megakaryocyte development to platelet formation. *J Cell Biol*. 2013;201(6):785-796.

3. Travlos GS. Normal structure, function, and histology of the bone marrow. *Toxicol Pathol*. 2006;34(5):548-565.

4. Naveiras O, Nardi V, Wenzel PL, Hauschka PV, Fahey F, Daley GQ. Bone-marrow adipocytes as negative regulators of the haematopoietic microenvironment. *Nature*. 2009;460(7252):259-263.

5. Adler BJ, Green DE, Pagnotti GM, Chan ME, Rubin CT. High fat diet rapidly suppresses B lymphopoiesis by disrupting the supportive capacity of the bone marrow niche. *PLoS One*. 2014;9(3):e90639.

6. Karlsson EA, Sheridan PA, Beck MA. Diet-induced obesity in mice reduces the maintenance of influenza-specific CD8+ memory T cells. *J Nutr*. 2010;140(9):1691-1697.

7. Singer K, DelProposto J, Morris DL, et al. Diet-induced obesity promotes myelopoiesis in hematopoietic stem cells. *Mol Metab*. 2014;3(6):664-675.

8. Trottier MD, Naaz A, Li Y, Fraker PJ. Enhancement of hematopoiesis and lymphopoiesis in diet-induced obese mice. *Proc Natl Acad Sci U S A*. 2012;109(20):7622-7629.

9. Yang H, Youm YH, Vandanmagsar B, et al. Obesity accelerates thymic aging. *Blood*. 2009;114(18):3803-3812.

10. Adler BJ, Kaushansky K, Rubin CT. Obesity-driven disruption of haematopoiesis and the bone marrow niche. *Nat Rev Endocrinol*. 2014;10(12):737-748.

11. Boucher J, Masri B, Daviaud D, et al. Apelin, a newly identified adipokine up-regulated by insulin and obesity. *Endocrinology*. 2005;146(4):1764-1771.

12. Wolins NE, Quaynor BK, Skinner JR, et al. OP9 mouse stromal cells rapidly differentiate into adipocytes: characterization of a useful new model of adipogenesis. *J Lipid Res*. 2006;47(2):450-460.

13. Ge Q, Ryken L, Noel L, Maury E, Brichard SM. Adipokines identified as new downstream targets for adiponectin: lessons from adiponectin-overexpressing or -deficient mice. *Am J Physiol Endocrinol Metab*. 2011;301(2):E326-335.

14. Muller G, Jung C, Straub J, Wied S, Kramer W. Induced release of membrane vesicles from rat adipocytes containing glycosylphosphatidylinositol-anchored microdomain and lipid droplet signalling proteins. *Cell Signal*. 2009;21(2):324-338.

15. Ung TH, Madsen HJ, Hellwinkel JE, Lencioni AM, Graner MW. Exosome proteomics reveals transcriptional regulator proteins with potential to mediate downstream pathways. *Cancer Sci*. 2014;105(11):1384-1392.

16. Doucette CR, Horowitz MC, Berry R, et al. A High Fat Diet Increases Bone Marrow Adipose Tissue (MAT) But Does Not Alter Trabecular or Cortical Bone Mass in C57BL/6J Mice. *J Cell Physiol*. 2015;230(9):2032-2037.

17. Coban E, Ozdogan M, Yazicioglu G, Akcit F. The mean platelet volume in patients with obesity. *Int J Clin Pract*. 2005;59(8):981-982.

SUPPLEMENTAL DATA

Supplemental Methods

Materials: Thrombopoietin was obtained from Peprotech. Anti-GPIbα, PE-conjugated anti–mouse CD42 and dylight-488-anti-GPIbβ Ig derivative antibodies were obtained from EMFRET analytics. FITC-conjugated anti–mouse CD41 antibody or PE-conjugated Annexin V were from BD Pharmingen. Transwell system was from Merck Millipore. Mouse TPO Immunoassay and b locking anti-TPO antibody were from RnDSystems. DMEM, MEM-α, Propidium iodide and KnockOut^{TM} SR were from Invitrogen. All other reagents were purchased from Sigma-Aldrich.

Flow cytometry: Cells were stained with FITC-conjugated anti–mouse CD41 and PE-conjugated anti–mouse CD42 antibodies or PE-conjugated Annexin V for 30 min at room temperature. Polyploidy of MKs isolated by BSA gradient was analyzed after DNA staining with propidium iodide. Samples were analyzed using an LSRFortessa^{TM} Cell analyser flow cytometer and Diva software (Becton Dickinson).

Palmitate [^{14}C] labeling: Once 3T3-F442A preadipocytes reached confluence, they were incubated in presence of 50 nM insulin and [^{14}C] palmitate acid (0.12 µCi/ml; PerkinElmer) to label lipids. After 8 days of culture, radiolabeled 3T3-F442A adipocytes were washed and freshly isolated hematopoietic progenitors were then seeded in the upper chamber of Transwell system. After 3 days, radioactivity was counted in MKs, adipocytes and adipocyte supernatant.

Triglyceride measurement: 3T3-F442A and BM triglyceride content were measured by colorimetric technique using F6428 and T2449 kits according to manufacturer instructions (Sigma, France).

Immune thrombocytopenia: Thrombocytopenia was induced in 21 weeks-old ND- and HFD-fed mice by intraperitoneal injection of anti-mouse GPIbα antibody (1.5 µg/g of mouse). Platelet count was measured using Micros60 (Horiba ABX Diagnostics) from blood samples collected at different times for 18 days.

Platelet lifespan: Circulating platelets were labelled *in vivo* by intravenous injection of Dylight-488-anti-GPIbβ Ig derivative antibody (0.1µg/g body weight). 2 h after antibody injection and every 24 h for 5 days, the percentage of the Dylight-488-positive platelet population in whole blood was determined using an LSRFortessa^{TM} Cell analyser flow cytometer and Diva software (Becton Dickinson).

Plasma TPO quantification was performed using RnDSystems Mouse Thrombopoietin Immunoassay (MTP00, RnDSystems) according to manufacturer instructions.

Proplatelet formation assay from bone marrow explants was performed as previously described.[1]

References

1. Antkowiak A, Viaud J, Severin S, et al. Cdc42-dependent F-actin dynamics drive structuration of the demarcation membrane system in megakaryocytes. *J Thromb Haemost*. 2016;14(6):1268-1284.

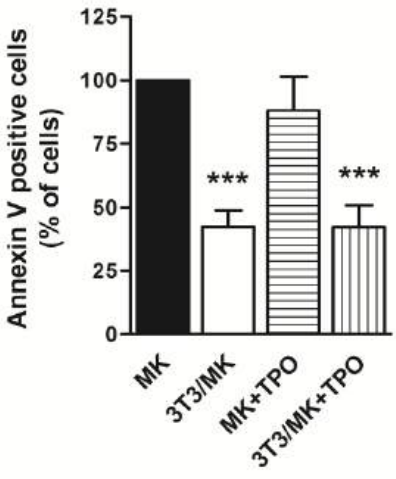

Supplemental Figure 1. Decreased apoptotic level of hematopoietic progenitor cell / MK population in co-culture condition. Hematopoietic progenitor cells isolated from murine BM were cultivated with or without 3T3-F442A differentiated adipocytes and TPO (50ng/mL) for 3 days. Annexin V labeling was assessed by flow cytometry on total cell population after 3 days of culture in different conditions (mean ± SEM; n=6 independent experiments; ***p<0.001 versus non-co-cultivated MKs with or without TPO according to two-tailed Student's *t* test).

Valet *et al*, supplemental figure 1

A

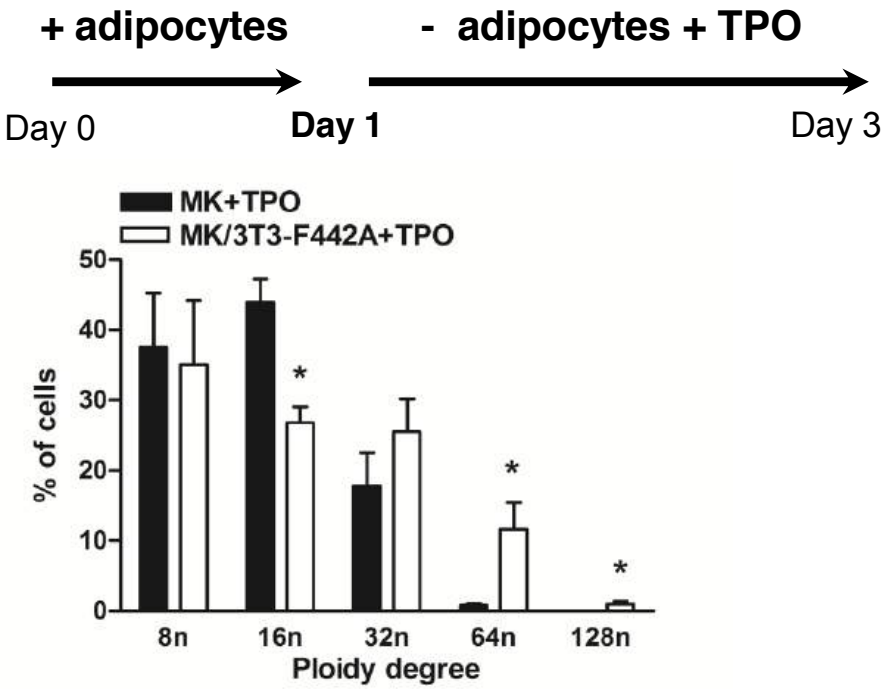

B

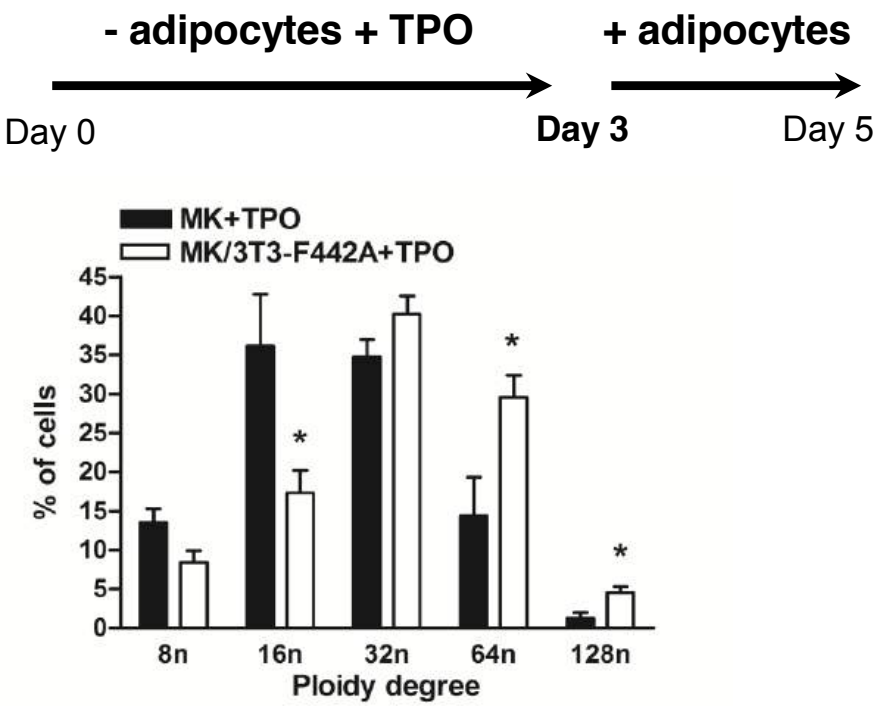

Supplemental Figure 2. Adipocyte-enhanced polyploidization in early and late stages of MK differentiation. (**A**) Hematopoietic progenitor cells isolated from murine BM were cultivated for one day with 3T3-F442A differentiated adipocytes and for the following two days with TPO (50ng/mL). MK DNA ploidy was then analyzed in presence of TPO by flow cytometry after propidium iodide labeling. Quantification of the percentage of cells with different levels of ploidy equal or greater to 8n was assessed (mean ± SEM; n=3 independent experiments, *p<0.05 versus non-co-cultivated MKs according to two-tailed Student's t test). (**B**) Hematopoietic progenitor cells isolated from murine BM were cultured for three day with TPO (50ng/mL) and for the following two days with 3T3-F442A differentiated adipocytes. MK DNA ploidy was then analyzed by flow cytometry after propidium iodide labeling. Quantification of the percentage of cells with different levels of ploidy equal or greater to 8n was assessed (mean ± SEM; n=3 independent experiments, *p<0.05 versus MKs non-co-cultivated according to two-tailed Student's t test). MK: megakaryocyte; TPO: thrombopoietin.

Valet *et al*, supplemental figure 2

A

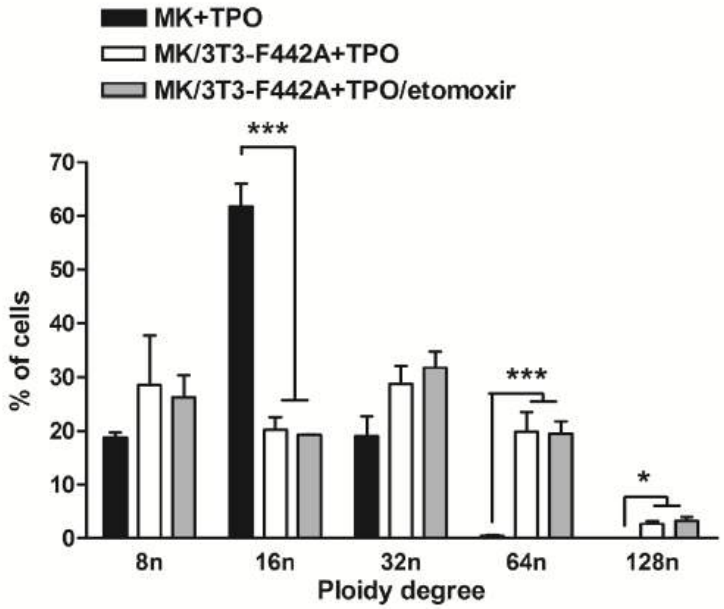

B

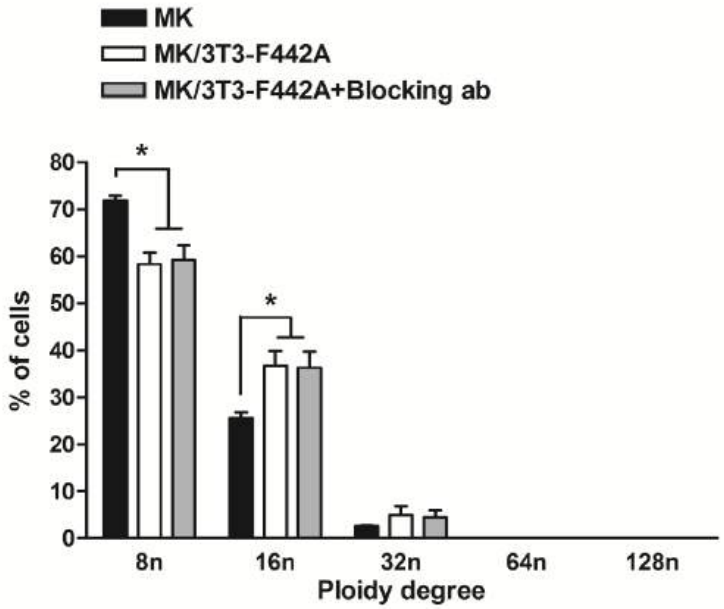

Supplemental Figure 3. Adipocyte-enhanced polyploidisation neither *via* an energetic transfer nor TPO secretion. (**A**) Hematopoietic progenitor cells isolated from murine BM were cultivated with or without 3T3-F442A differentiated adipocytes, TPO (50ng/mL) and etomoxir (30µM) for 3 days. MK DNA ploidy was then analyzed by flow cytometry after propidium iodide labeling. Quantification of the percentage of cells with different levels of ploidy equal or greater to 8n was assessed (mean ± SEM; n=7 independent experiments; *p<0.05 and ***p<0.001 according to two-way ANOVA). (**B**) Hematopoietic progenitor cells isolated from murine BM were cultured with or without 3T3-F442A differentiated adipocytes and blocking anti-TPO antibody (0.3µg/mL) for 3 days. MK DNA ploidy was then analyzed by flow cytometry after propidium iodide labeling. Quantification of the percentage of cells with different levels of ploidy equal or greater to 8n was assessed (mean ± SEM; n=3 independent experiments; *p<0.05 according to two-way ANOVA). MK: megakaryocyte; TPO: thrombopoietin; Blocking ab: anti-TPO blocking antibody.

Valet *et al*, supplemental figure 3

A

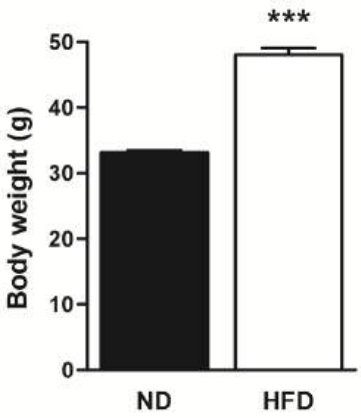

B

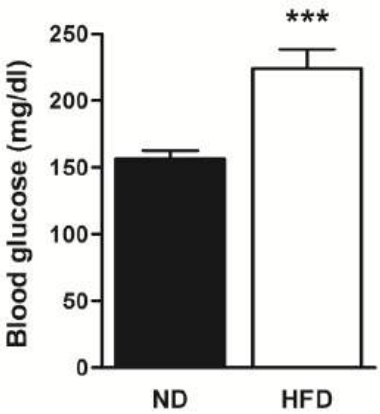

C

	ND (n=24)	HFD (n=25)
Rbc, 10^6 /mm^3	8.3 ± 0.3	8.6 ± 0.1
Lym, 10^3 /mm^3	9.0 ± 0.6	9.7 ± 0.7
Mon,10^3 /mm^3	0.9 ± 0.1	1.5 ± 0.1***
Gra, 10^3 /mm^3	0.9 ± 0.9	1.0 ± 0.5

D

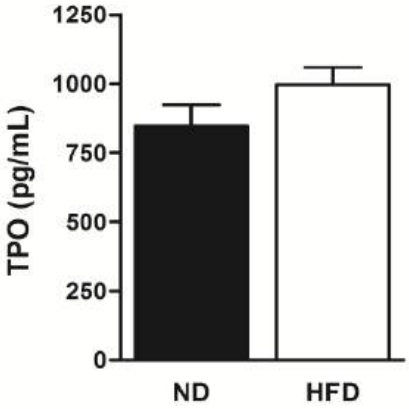

Supplemental Figure 4. HFD-induced obese mice characteristics. (**A**) Whole body weight and (**B**) blood glucose were measured in 21 week-old mice after 12 weeks under normal diet (ND) or high fat diet (HFD) (mean ± SEM; n=25 mice; ***p<0.001 versus ND-fed mice according to two-tailed Student's t test). (**C**) Whole blood parameters were analysed using a Micros60 (Horiba ABX Diagnostics) (mean ± SEM; ***p<0.001 versus ND-fed mice according to two-tailed Student's t test). Rbc, Red blood cells; Lym, Lymphocytes; Mon, Monocytes; Gra, Granulocytes. (**D**) Mice plasma thrombopoietin (TPO) level was quantified by immunoassay (mean ± SEM, n=10 mice).

Valet *et al*, supplemental figure 4

2) Conclusions

Grâce à la co-culture *in vitro* d'adipocytes avec des progéniteurs hématopoïétiques, nous montrons que les adipocytes, qu'ils proviennent d'une lignée pré-adipocytaire (3T3-F442A) ou de cellules souches médullaires (OP9), potentialisent la différenciation des mégacaryocytes (augmentation de l'expression des marqueurs de différenciation mégacaryocytaire, de la taille des MKs et de la proportion de MKs à haut niveau de ploïdie). Nous mettons en évidence une communication réciproque entre les deux types cellulaires. En effet, lors de la co-culture, les adipocytes se délipident et les MKs captent ces acides gras / lipides. Ce transfert d'acides gras / lipides est indispensable à l'amélioration de la différenciation mégacaryocytaire mais ne constitue pas un apport énergétique pour la différenciation en MKs.

Chez des souris rendues obèses-diabétiques par un régime riche en lipides, nous observons une augmentation de l'adiposité médullaire associée à une augmentation de la taille des MKs et de leur noyau *in vivo*. De plus, ces souris obèses-diabétiques présentent une thrombopénie associée à une augmentation du volume moyen plaquettaire, un défaut de production plaquettaire après une thrombocytopénie immune induite *in vivo*, une demi-vie plaquettaire diminuée et une extension de PPTs par les MKs *ex vivo* plus rapides.

Ces résultats démontrent une communication réciproque entre adipocytes et MKs qui contrôle la mégacaryopoïèse ainsi que l'influence de l'obésité sur la mégacaryopoïèse et la production plaquettaire.

Discussion - Perspectives

Au cours de ma thèse, je me suis intéressé, dans un premier temps, à deux lipide kinases intrinsèques au MK et à la plaquette, l'isoforme α des PI3Ks de classe II et la PI3K de classe III, Vps34, et leurs rôles sur la production et la fonction plaquettaires. Dans les plaquettes, les PI3Ks de classe I ont été largement étudiées et jouent un rôle important dans les mécanismes de signalisation mis en jeu en aval de différents récepteurs plaquettaires, en particulier, l'isoforme β des PI3Ks de classe I (Laurent et al., 2014). Par contre, rien n'était connu, lorsque j'ai commencé ma thèse des rôles des PI3Ks de classe II et III dans la production et la fonction plaquettaire. Cependant, leur caractérisation comme régulateurs majeurs du trafic intracellulaire grâce à leur produit commun, le PtdIns3P, laissait à penser qu'elles pouvaient jouer un rôle important dans ces phénomènes.

La moelle osseuse est formée de microenvironnements spécifiques définis par différents types cellulaires, composants de la matrice extracellulaire et autres facteurs qui impactent directement le devenir des cellules médullaires (Figure 36). Un de ces facteurs est le tissu adipeux médullaire, dont le rôle reste encore peu décrit. Le tissu adipeux est connu pour être un lieu de stockage d'énergie mais aussi pour sécréter de multiples adipokines contrôlant différents mécanismes tels que la satiété, le métabolisme lipidique, la sensibilité à l'insuline, l'inflammation ou encore l'angiogénèse (Lafontan, 2012; Trayhurn and Wood, 2004). Le tissu adipeux est une part importante de la composition de la moelle osseuse (Hardouin et al., 2016; Scheller et al., 2016) et la différenciation du MK étant sujette à des régulations par des facteurs solubles, je me suis intéressé, dans un deuxième temps, à l'influence que pourrait avoir sur la différenciation mégacaryocytaire et la production plaquettaire, un facteur extrinsèque au MK: le tissu adipeux médullaire.

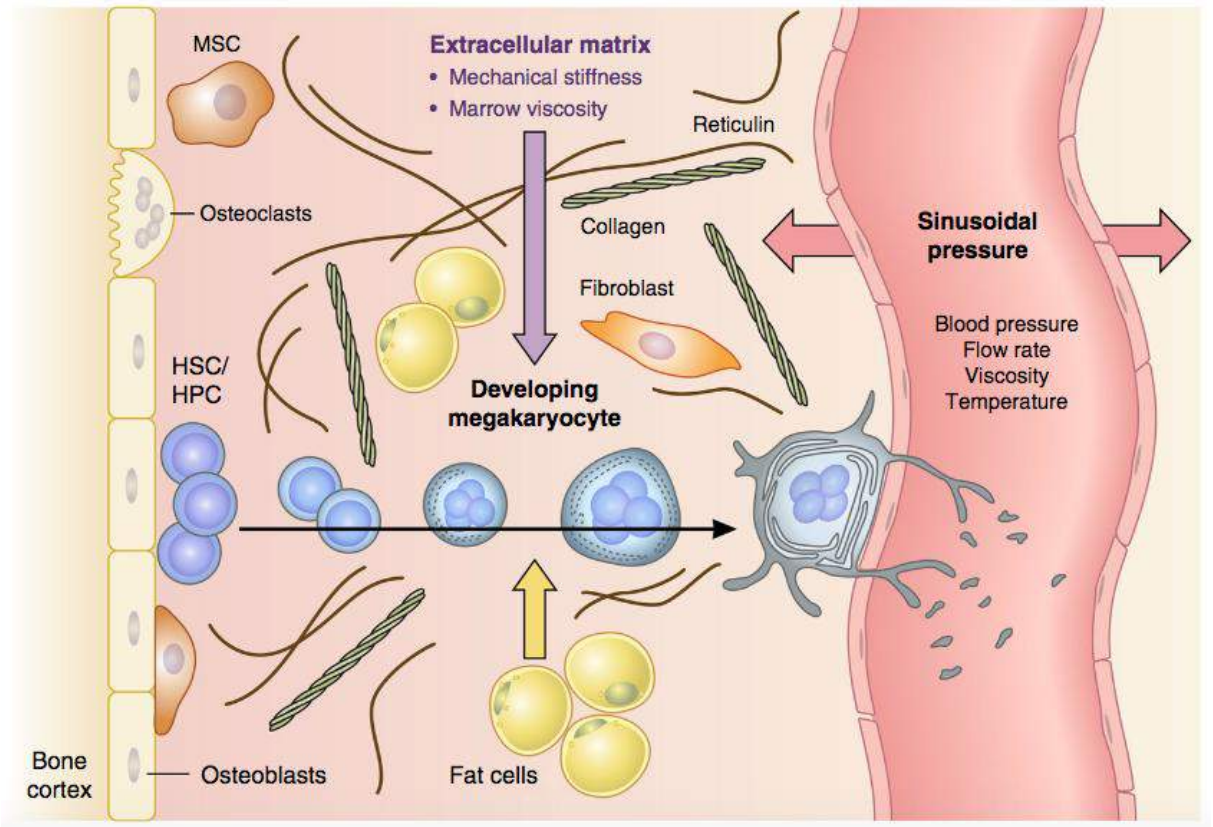

Figure 36: Représentation schématique des éléments influençant le microenvironnement médullaire: Le modèle proposé montre un MK en différenciation migrant de la niche ostéoblastique vers un sinusoïde médullaire. La croissance, la polyploïdisation et la formation du DMS sont représentées ainsi que la libération des plaquettes, à l'extrémité des PPT, dans la circulation sanguine. Différents facteurs peuvent influencer les forces mécaniques au sein de la moelle osseuse (larges flèches): le tissu adipeux médullaire, les composants de la matrice extracellulaire (collagène, fibronectine et vitronectine) et la pression hydrostatique des sinusoïdes qui est elle-même contrôlée par la pression sanguine, le débit sanguin, la viscosité du sang et la température. *D'après (Psaila, 2016)*.

A) PI3KC2α et son produit, le PtdIns3P: régulateur de la structuration des membranes plaquettaires

Grâce à un modèle original de souris présentant une inactivation partielle de la PI3KC2α, nous avons mis en évidence le rôle primordial de cette kinase dans la production des plaquettes. En effet, les plaquettes de ces souris présentent des défauts de morphologie membranaire et une proportion significative de cette population plaquettaire est composée de plaquettes à deux corps appelées « barbell-shaped proplatelets ». Naturellement, ces entités représentent 0.05 % de la population plaquettaire, or dans notre modèle d'inactivation partielle de la PI3KC2α, nous comptabilisons ces entités à hauteur de 4,2 %. Dans le même sens, le volume moyen plaquettaire de ces souris est très hétérogène et 31 % des plaquettes

présentent des membranes invaginées et tortueuses. Ces résultats corroborent une étude récente du laboratoire de Shaun Jackson dans laquelle les auteurs observent des plaquettes présentant une morphologie membranaire anormale (SCO dilaté) dans différents modèles de souris de délétion de la PI3KC2α (Mountford et al., 2015). De plus, l'incapacité des plaquettes partiellement inactivées pour la PI3KC2α à émettre des filopodes sous stimulation par des agonistes plaquettaires montre un défaut de dynamique des membranes plaquettaires, en plus de leur défaut de structure.

D'un point de vue moléculaire, l'isolement du squelette sous-membranaire des plaquettes partiellement inactivées pour la PI3KC2α a mis en évidence un défaut de localisation de protéines composant le squelette sous-membranaire (spectrine et myosine) et de protéines faisant le lien avec la membrane plasmique (filamine, moesine, GPIb et GPIIb). Ainsi, la PI3KC2α, en régulant l'intégrité du squelette sous-membranaire, contrôle la structure et la dynamique membranaire des plaquettes et la scission des « barbell-shaped proplatelets » en plaquettes matures (Patel-Hett et al., 2011; Spinler et al., 2015). Nous montrons aussi que le DMS des MKs inactivés pour la PI3KC2α est fortement altéré, or il a été décrit que la spectrine est essentielle à sa formation (Patel-Hett et al., 2011). Ces résultats suggèrent que ces protéines ont un défaut d'adressage au squelette sous-membranaire lors de l'assemblage de ce dernier dans les MKs.

Parallèlement, grâce à une technique de dosage en masse de PtdIns3P développée au sein de l'équipe, nous avons mis en évidence, pour la première fois, que la PI3KC2α était responsable de la production basale (pool à métabolisme lent) de PtdIns3P dans les plaquettes. Une seule étude s'est intéressée à l'interactome du PtdIns3P dans une lignée de cellules de cancer de colon (LIM1215) en utilisant des billes recouvertes de PtdIns3P. Cette étude a permis d'identifier, par spectrométrie de masse, 681 protéines capables de lier directement le PtdIns3P. Parmi elles, ont été retrouvées : la spectrine, la myosine, la filamine et la moesine (Catimel et al., 2013), des protéines du squelette sous-membranaire plaquettaire. Or, ces mêmes protéines sont significativement moins présentes dans le squelette sous-membranaire des plaquettes partiellement inactivées pour la PI3KC2α. De façon intéressante, la vinculine qui n'est pas retrouvée dans cet interactome du PtdIns3P n'est pas non plus diminuée dans le squelette sous-membranaire des plaquettes partiellement inactivées pour la PI3KC2α. Dans le but de caractériser le rôle du PtdIns3P produit par la PI3KC2α dans la localisation des protéines au squelette sous-membranaire des plaquettes, il serait donc intéressant d'identifier

les protéines capables de lier le PtdIns3P dans les MKs et les plaquettes après précipitation grâce à des billes recouvertes de PtdIns3P suivi d'analyses de spectrométrie de masse. Ceci permettrait de savoir si, dans les MKs et les plaquettes, le PtdIns3P lie directement la spectrine, la myosine, la filamine et la moesine.

En 2007, Falasca *et al* ont montré que la PI3KC2α était recrutée à la membrane plasmique et activée grâce à la GTPase TC10 sous stimulation à l'insuline. Cette localisation cellulaire est indispensable à la translocation du transporteur de glucose, GLUT-4, à la membrane plasmique (Falasca et al., 2007). Une autre étude, par Takuwa *et al* a montré que lors d'une stimulation par le VEGF, la PI3KC2α était responsable de l'activation de la GTPase RhoA au niveau d'endosomes riches en PtdIns3P et que cette activation était indispensable à l'adressage des VE-cadherines au niveau des jonctions entre cellules (Yoshioka et al., 2012). Ces études montrent donc que la PI3KC2α est impliquée dans la relocalisation à la membrane plasmique de protéines transmembranaires. Il serait intéressant de localiser la PI3KC2α et le PtdIns3P qu'elle produit par imagerie de haute résolution dans les MKs et les plaquettes afin de définir si leurs localisations sont plutôt à la membrane plasmique à proximité du squelette sous-membranaire ou plutôt à la membrane de vésicules intracellulaires. Cette étude permettrait de révéler comment la PI3KC2α permet la relocalisation au squelette sous-membranaire de ces protéines par liaison directe avec le PtdIns3P soit à la membrane plasmique directement soit en régulant le trafic vésiculaire d'adressage au squelette sous-membranaire.

Au niveau du MK des souris déficientes en PI3KC2α, nous avons observé des granules α moins nombreux et plus gros. La biogénèse des granules dans le MK, que ce soit α ou denses, fait intervenir un intense trafic vésiculaire au niveau de l'endocytose, des MVB, des endosomes précoces et tardifs ou encore du TGN (Blair and Flaumenhaft, 2009). Or, le PtdIns3P, le PtdIns(3,4)P_2 et la PI3KC2α sont connus pour contrôler le trafic vésiculaire (Campa et al., 2015). Dans le but de comprendre ce défaut de biogénèse des granules, le suivi par microscopie confocale de la formation des granules et la distribution du PtdIns3P et du PtdIns(3,4)P_2 à différentes étapes de la différenciation du MK pourrait aider à comprendre le rôle de la PI3KC2α dans ce phénomène. Dans le même sens, doser le PtdIns3P et le PtdIns(3,4)P_2 dans des MKs partiellement inactivés pour la PI3KC2α aidera à une meilleure compréhension de ce défaut de granules. Ce défaut de biogénèse des granules observé au

niveau du MK est un argument dans notre hypothèse d'un trafic vésiculaire altéré qui serait responsable du défaut d'adressage des protéines au squelette sous-membranaire.

Par marquage métabolique des plaquettes au ^{32}Pi, nous montrons que la PI3KC2α n'est pas impliquée dans la production rapide de PtdIns3P, de PtdIns(3,4)P_2 ou de PtdIns(3,4,5)P_3 induite par des agonistes plaquettaires. De plus, *in vitro*, *ex vivo* et *in vivo*, les réponses thrombotiques de nos souris partiellement inactivées pour la PI3KC2α sont affectées, sans défaut majeur d'activation des voies de signalisation induite par des agonistes plaquettaires. Ces données montrent que (i) contrairement aux PI3Ks de classe I, la PI3KC2α n'intervient pas dans les voies de signalisation en aval de récepteurs plaquettaires et (ii) que les défauts de structure et de dynamique membranaire sont vraisemblablement responsables des perturbations d'efficacité des réponses thrombotiques. A l'inverse, les plaquettes du modèle de souris de l'équipe de Shaun Jackson (délétion hétérozygote) ont des réponses thrombotiques *ex vivo* plus efficaces, cependant *in vivo* les thrombi formés sont instables et créent des emboles (Mountford et al., 2015). Ces différences entre ces deux modèles de souris peuvent s'expliquer par le fait que, dans notre modèle, l'inactivation de la PI3KC2α mime l'effet d'un agent inhibiteur où la protéine est toujours présente alors que, dans le modèle de délétion hétérozygote, la protéine n'est plus exprimée qu'à 50%. Ce défaut d'expression pourrait, de fait, perturber la formation de complexes protéiques autour de la kinase et entrainer la mise en place de phénomènes de compensations par d'autres PI3Ks. Ces mêmes auteurs ont également générés un modèle de souris déficientes à la fois pour la PI3KC2α et pour la PI3KC2β. Dans ce modèle de double déficience, les auteurs ne révèlent pas d'aggravation du phénotype montrant ainsi que la PI3KC2β ne compense pas la perte de la PI3KC2α. De façon surprenante, une nouvelle étude venant du même laboratoire rapporte une augmentation de l'expression protéique de Vps34 et suggère une potentielle compensation de la perte de PI3KC2α par Vps34 (Petitjean et al., 2016).

B) Production plaquettaire et croissance du thrombus: double rôle pour Vps34 et son produit, le PtdIns3P

Notre modèle de souris délété pour Vps34 présente une microthrombopénie modérée due à un défaut de production plaquettaire mis en évidence après thrombopénie immune induite. Ce phénotype plaquettaire n'est pas la conséquence d'un défaut de maturation nucléaire ou membranaire des MKs ni d'un défaut de formation des PPT. Par contre, la migration des

MKs, mécanisme mis en jeu lors de la mégacaryopoïèse, est affectée. En effet, les MKs déficients pour Vps34 sont capables de migrer la même distance que les MKs sauvages mais leur directionnalité de migration envers le gradient de CXCL12 est altérée.

Des défauts de migration de MKs ont déjà été associés à des thrombopénies ou des défauts de production plaquettaire. Il s'agit entre autres des cas de délétion de PECAM ou de WASP (Dhanjal et al., 2007; Sabri et al., 2006).

- La délétion de WASP est caractérisée entre autres par une thrombopénie due à un défaut de migration des MKs envers le gradient de CXCL12, amenant à la libération ectopique de plaquettes dans la moelle osseuse, et à une durée de vie plaquettaire diminuée (Falet et al., 2009; Sabri et al., 2006). La durée de vie des plaquettes déficientes en Vps34 étant normale, il sera donc intéressant, dans la suite de notre étude, de rechercher la présence de plaquettes dans la moelle osseuse en dehors des sinusoïdes médullaires par immunohistochimie sur coupe de moelle de fémur de souris déficientes en Vps34. Ceci permettrait de montrer clairement que la thrombopénie induite par la délétion de Vps34 est la conséquence d'un défaut de migration des MKs induisant le relarguage prématuré de plaquettes dans la moelle osseuse.

- La délétion de PECAM induit un défaut de polarisation de CXCR4 qui engendre un défaut de migration des MKs (Dhanjal et al., 2007). A la surface des MKs délétés pour Vps34, nous observons une expression augmentée du récepteur au CXCL12, CXCR4. Parallèlement à ça, nous montrons que la production de PtdIns3P, l'endocytose et le trafic endosomal dans les MKs déficients pour Vps34 sont altérés. Nous observons des endosomes précoces plus gros et plus nombreux impactant sur la voie de recyclage et de dégradation avec des lysosomes plus petits et moins nombreux. Des études récentes ont décrit le rôle de Vps34 dans la régulation du trafic vésiculaire de récepteurs. En 2015, Nemazanyy *et al* ont montré que, dans des hépatocytes primaires, l'insuline stimule l'activité de Vps34 dans le complexe II (Vps34-Vps15-Beclin1-UVRAG) et induit son association avec le récepteur à l'insuline ce qui permet de l'amener à travers la voie endosomale de dégradation et ainsi réguler la réponse à l'insuline (Nemazanyy et al., 2013). En 2016, Jaber *et al* ont montré que la délétion de Vps34 dans des MEFs entraine l'accumulation d'endosomes tardifs et la diminution de la dégradation du récepteur à l'EGF (Jaber et al., 2016). L'ensemble de ces données suggère fortement que le trafic de CXCR4 est défectueux dans les MKs déficients en Vps34 ce qui pourrait expliquer le manque de directionnalité des MKs envers CXCL12.

Nous observons le défaut de migration des MKs délétés pour Vps34 sur matrice de fibronectine, une composante majeure de la matrice extracellulaire de la moelle osseuse. Le récepteur liant la fibronectine est l'intégrine $\alpha_5\beta_1$ (Paul et al., 2015). Récemment, il a été mis en évidence que l'Ankyrine-B se lie aux endosomes riches en PtdIns3P, y recrute la Rab GTPase Activating Protein 1-like qui inactive Rab22A et permet le trafic endosomal polarisé au front de migration de fibroblastes en migration. Dans ces endosomes spécifiques, l'Ankyrin-B coordonne le transport polarisé de l'intégrine $\alpha_5\beta_1$ ce qui permet la migration des fibroblastes (Qu et al., 2016). Nous pouvons donc penser que la diminution de PtdIns3P observée dans les MKs déficients en Vps34 impacte sur le trafic endosomal polarisé de l'intégrine $\alpha_5\beta_1$ entrainant une migration anormale des MKs. L'autophagie est un autre mode de régulation du recyclage d'intégrines à la membrane plasmique. En effet, l'inhibition de l'autophagie ou la délétion de certains Atg (3 ou 5 ou 7) dans des cellules HeLa augmente le potentiel de migration de ces cellules, diminue la dégradation de l'intégrine β1 et augmente son recyclage à la surface cellulaire (Tuloup-Minguez et al., 2013). De plus, des études récentes ont montré que l'autophagie permet le désassemblage des adhésions focales afin de permettre une migration dirigée (Kenific et al., 2016; Sharifi et al., 2016). Nous pouvons donc penser que le flux autophagique altéré des MKs déficients en Vps34 pourrait directement impacter sur leur potentiel migratoire en régulant le recyclage de l'intégrine β1 et la dynamique des adhésions focales.

Au niveau des MKs, si l'on associe la diminution de PtdIns3P, le défaut d'endocytose, de trafic endosomal et d'autophagie avec l'augmentation de CXCR4 à la membrane plasmique, on peut proposer que la polarisation de l'intégrine $\alpha_5\beta_1$ ou de CXCR4 au front de migration des MKs délétés pour Vps34 ou la dynamique des adhésions focales est défectueuse et entraine ce défaut de directionnalité envers le gradient de CXCL12. Suivre le trafic de l'intégrine $\alpha_5\beta_1$ et de CXCR4 dans les différents endosomes et analyser la dynamique en conditions de migration par immunofluorescence nous permettraient de comprendre le défaut de directionnalité des MKs déficients en Vps34. Nous pourrons aussi étudier la dynamique des adhésions focales par marquage en immunofluorescence de la paxilline.

Les MKs délétés pour Vps34 contiennent significativement moins de granules sécrétoires mais ceux-ci sont plus gros, phénotype que l'on retrouve aussi au niveau des plaquettes. Ces données montrent que la biogénèse des granules dans les MKs est défectueuse. La biogénèse des granules dans les MKs fait intervenir différents aspects du trafic vésiculaire tels que le bourgeonnement de vésicules originaires du TGN, l'endocytose et les MVB (Ambrosio et al.,

2012; Hegyi et al., 1990; King and Reed, 2002; Meng et al., 2012; Youssefian and Cramer, 2000). Or, le trafic vésiculaire dans les MKs délétés pour Vps34 est fortement perturbé. Afin de caractériser précisément à quel niveau Vps34 intervient lors de la biogénèse des granules, il serait intéressant de suivre par vidéomicroscopie la dynamique des granules α et denses (par marquage avec du fibrinogène et de la mépacrine respectivement) tout au long de la différenciation du MK.

Grâce au modèle de souris présentant une délétion de Vps34 spécifiquement dans les MKs et les plaquettes et l'utilisation de deux inhibiteurs spécifiques de Vps34 récemment développés, nous montrons que Vps34 contrôle l'activation plaquettaire, indépendamment de son rôle dans le MK. En effet, sur matrice de collagène, les plaquettes déficientes en Vps34 ou traitées avec les inhibiteurs de Vps34 forment des thrombi plus petits en condition de flux *ex vivo*. La perfusion de plaquettes déficientes en Vps34 sur des thrombi déjà formés par des plaquettes normales révèle un rôle de Vps34 dans la croissance du thrombus. De même, *in vivo*, nous observons un défaut majeur de thrombose occlusive après lésion de la carotide au chlorure ferrique. Un défaut de croissance du thrombus peut s'expliquer par au moins deux mécanismes moléculaires: (i) une signalisation défectueuse de l'intégrine $\alpha_{IIb}\beta_3$ entrainant ainsi l'incapacité des plaquettes à adhérer fermement ou (ii) une sécrétion des granules plaquettaires dérégulée empêchant ainsi l'amplification de l'activation plaquettaire et le recrutement de plaquettes circulantes. En réponse à différents agonistes, la signalisation « inside-out » de l'intégrine $\alpha_{IIb}\beta_3$ est normale dans les plaquettes déficientes en Vps34 alors que leur sécrétion est significativement augmentée. Sur matrice de fibrinogène (reflet de la signalisation « outside-in » de l'intégrine $\alpha_{IIb}\beta_3$), nous observons une augmentation significative de l'aire moyenne d'adhésion des plaquettes déficientes en Vps34 par rapport aux plaquettes sauvages. Cependant, en présence d'inhibiteurs de la sécrétion, l'aire moyenne des plaquettes déficientes en Vps34 est similaire à celle des plaquettes sauvages. L'ensemble de ces données est en faveur d'une signalisation normale de l'intégrine $\alpha_{IIb}\beta_3$ et suggère fortement que la dérégulation de la sécrétion plaquettaire impacte sur les capacités adhésives des plaquettes, ce qui pourrait être la cause d'une moindre croissance du thrombus en condition de flux *ex vivo* ou *in vivo*.

Récemment, Eckly *et al* ont révélé deux mécanismes de sécrétion plaquettaire en réponse à des agonistes: (i) les plaquettes sécrètent le contenu de granules individuels ou (ii) les granules fusionnent en une seule entité au sein de la plaquette avant d'être sécrétés. Eckly *et*

al ont mis en évidence le rôle majeur de la protéine vesicle associated membrane protein 8 (VAMP8) lors de la fusion et de la sécrétion de granules sous stimulation plaquettaire (Eckly et al., 2016). De façon intéressante, une étude par Dai *et al* a montré que l'infection d'une cellule par la bactérie pathogène *Salmonella enterica* entraîne la production de PtdIns3P au niveau de la membrane plasmique qui à son tour recrute, par liaison directe, VAMP8 afin d'induire sa propre macropinocytose par la cellule hôte (Dai et al., 2007). Nous pouvons donc imaginer que lors d'une activation plaquettaire, le PtdIns3P produit par Vps34 permettrait le recrutement de VAMP8 et la fusion puis sécrétion normale des granules. Or, en cas de délétion de Vps34, la perte de cette production de PtdIns3P sous activation pourrait expliquer le phénotype observé de sécrétion dérégulée, probablement par défaut de recrutement de VAMP8 et de fusion homotypique des granules entre eux puis avec la membrane plasmique. Ceci impacterait l'activation fine, *ex vivo* et *in vivo,* des plaquettes déficientes en Vps34 car comme le montre Eckly *et al,* la formation du thrombus *in vivo* met en jeu la sécrétion de granules fusionnés. Cette hypothèse est appuyée par le fait que lors d'une forte activation telle que l'agrégation *in vitro,* nous n'observons pas de défaut car VAMP8 n'intervient pas dans des conditions de forte activation comme montré par Eckly *et al*. Il serait donc intéressant d'observer la dynamique de fusion et de sécrétion des granules des plaquettes déficientes en Vps34 à fortes et faibles doses d'agonistes et selon différentes cinétiques par microscopie électronique à transmission. Parallèlement, l'étude d'interactome du PtdIns3P avec les protéines plaquettaires (proposée dans l'étude sur la PI3KC2α) nous permettra de savoir si le PtdIns3P est capable de lier directement VAMP8 afin d'expliquer notre phénotype plaquettaire observé en l'absence de Vps34. Ensuite, nous analyserons si le défaut de fusion / sécrétion granulaire est propre à la plaquette ou si le défaut de biogénèse des granules plaquettaires hérité du MK a un rôle dans la dérégulation de la fusion / sécrétion des granules plaquettaires lorsque Vps34 est absent. Pour ce faire, il serait intéressant de caractériser cette dynamique de fusion / sécrétion par l'utilisation d'inhibiteurs de Vps34 sur des plaquettes sauvages.

C) Régulation de la production de PtdIns3P dans les plaquettes

La production de PtdIns3P dans les plaquettes au repos et lors de l'activation plaquettaire reste encore mal caractérisée. Grâce au modèle d'inactivation partielle de la PI3KC2α, nous avons montré que celle-ci était responsable d'une part du « pool » basal de PtdIns3P et qu'elle n'est pas impliquée dans la production de ce lipide dépendante de la stimulation plaquettaire.

Grâce au modèle de délétion totale de Vps34, nous montrons que Vps34 produit une partie du PtdIns3P en réponse à l'activation plaquettaire par des agonistes. Ainsi, mon étude montre que la PI3KC2α et Vps34 produisent différents pools de PtdIns3P contrôlant *in fine* différents processus plaquettaires. Une étude de notre équipe en 2012 montre que la wortmaninne à des doses inhibant les classes I et III des PI3Ks empêche la production de PtdIns3P dépendante de la stimulation par des agonistes plaquettaires (Chicanne et al., 2012). Des données non publiées de l'équipe montrent que la PI3KC2β ne produit pas de PtdIns3P au repos ou lors d'une stimulation par des agonistes plaquettaires. L'ensemble de ces résultats suggère fortement une implication des PI3Ks de classe I dans la production de PtdIns3P sous stimulation plaquettaire. A l'aide des techniques biochimiques de dosage de PtdIns3P utilisées en routine dans le laboratoire et l'utilisation d'inhibiteurs et de modèles de souris déficientes pour différents isoformes de PI3Ks de classe I disponibles au laboratoire, nous identifierons quels isoformes de PI3Ks de classe I produit le PtdIns3P dans la plaquette que ce soit au repos et sous stimulation. Cette étude, en plus des résultats obtenus au cours de ma thèse, permettra de définir avec précision la régulation de la production du PtdIns3P dans la plaquette.

D) Dialogues entre adipocytes et mégacaryocytes

Grâce à la mise en place d'un système de co-culture sans contact physique entre adipocytes (différenciés à partir de pré-adipocytes (3T3-F442A) ou de cellules souches mésenchymateuses médullaires (OP9)) et progéniteurs hématopoïétiques, nous avons montré que l'adipocyte potentialisait la différenciation mégacaryocytaire. En effet, en présence d'adipocytes, les MKs sont plus gros, expriment davantage les marqueurs de différenciation et le degré de polyploidisation des MKs augmente significativement. Parallèlement à cette potentialisation de la différenciation des MKs, les adipocytes perdent une partie de leur contenu lipidique. De façon intéressante, il existe un transfert direct d'acide gras des adipocytes vers les MKs. Ces résultats montrent donc une communication réciproque entre les deux types cellulaires. Lorsque le captage d'acide gras / lipides est bloqué pharmacologiquement, la différenciation des MKs n'est plus améliorée. Par ailleurs, lorsque le captage de la TPO par le MK est bloqué, la différenciation des MKs reste améliorée. Ces données montrent que l'adipocyte ne stimule pas la différenciation du MK par la TPO, cytokine majeure de la différenciation mégacaryocytaire et pouvant être sécrétée par l'adipocyte (Ge et al., 2011) mais que le transfert de d'acide gras / lipides est le facteur induisant l'amélioration de la différenciation mégacaryocytaire par les adipocytes.

Plusieurs études ont montré que des adipocytes co-cultivés avec des cellules cancéreuses sécrètent des exosomes contenant des protéines impliquées dans l'oxydation des acides gras et que les cellules cancéreuses captent ces exosomes à des fins énergétiques. Ce captage d'exosomes par les cellules cancéreuses augmente leur agressivité (Dirat et al., 2011; Laurent et al., 2016; Lazar et al., 2016). La différenciation du MK est un processus très dynamique et très consommateur d'énergie. Ainsi, nous avons cherché à savoir si le transfert de lipides des adipocytes aux MKs était à but énergétique afin de favoriser la différenciation mégacaryocytaire. L'inhibition de l'utilisation d'acides gras par la chaîne respiratoire permettant la production d'énergie sous forme d'ATP n'a pas empêché l'effet amplificateur de la co-culture d'adipocytes sur la différenciation des MKs. Ces résultats ont permis de conclure que le transfert direct d'acide gras / lipides de l'adipocyte vers le MK n'est pas à but énergétique. Sachant que la différenciation mégacaryocytaire nécessite un apport lipidique important afin de développer son système dense de membranes, le DMS, on peut suggérer que ce transfert de lipides participe à ce processus. Il sera donc intéressant, dans un premier temps, de mieux caractériser comment se réalise ce transfert de lipides (présence ou non d'exosomes et / ou d'acides gras libres dans le surnageant de culture). Les exosomes pourraient contenir des facteurs capables d'influencer la mégacaryopoïèse (lipides, protéines, facteurs de transcription, miRNA). Deux études récentes ont montré que des fibroblastes 3T3-L1 ou des cellules souches médullaires OP9 expriment des gènes codant pour des facteurs de transcription capables d'induire la mégacaryopoïèse tels que GATA2, RUNX1 ou FLI1 (Matsubara et al., 2013; Ono et al., 2012). Parallèlement, une étude protéomique d'exosomes dérivés de medulloblastome a révélé la présence de facteurs de transcription au sein de ces exosomes (Ung et al., 2014). On peut imaginer que les adipocytes, par la sécrétion d'exosomes contenant des facteurs de transcription de la mégacaryopoiëse, pourraient amplifier la différenciation des MKs. Il sera donc intéressant, dans un deuxième temps, d'isoler les exosomes du surnageant de co-culture et d'analyser leur contenu protéique (notamment des facteurs de transcription) afin d'identifier des molécules capables de contrôler la différenciation en MK. Par ailleurs, il sera intéressant d'analyser le contenu global du surnageant avant, pendant et après co-culture par analyse protéomique afin de caractériser quel(s) facteur(s) sécrété(s) par les MKs influent sur l'adipocyte.

Je me suis ensuite intéressé à la mégacaryopoïèse dans un contexte pathologique d'obésité et/ou de diabète, où l'adiposité médullaire est augmentée. Pour ce faire, des souris ont été rendues obèses par un régime riche en lipides. Ces souris présentent une thrombopénie

associée à une augmentation du volume moyen plaquettaire due à une production plaquettaire défectueuse et une demi-vie plaquettaire diminuée. Les MKs des souris sous régime gras sont significativement plus gros et les taux de triglycérides médullaires (qui reflètent l'adiposité médullaire) significativement augmentés. La mise en perspectives de ces résultats avec les résultats de co-culture *in vitro* permet de penser que l'accroissement de l'adiposité médullaire augmente le transfert de lipides (ou exosomes) des adipocytes vers les MKs. Cependant, de façon paradoxale, cette mégacaryopoïèse augmentée *in vivo* est associée à une moins bonne production plaquettaire, comme en attestent la thrombopénie et le retour au compte plaquettaire altéré après thrombocytopénie immune induite. Des expériences de formation de PPT *ex vivo* sur explants de moelle osseuse de souris obèses montrent que les MKs de ces souris étendent leurs PPT plus rapidement que les MKs de souris non-obèses, laissant penser que la thrombopénie de ces souris pourrait provenir d'une libération précoce des plaquettes dans la moelle osseuse et non dans les sinusoïdes sanguins. Il serait donc intéressant de visualiser, sur coupes de moelle osseuse par immunohistochimie, la présence de plaquettes en dehors des sinusoïdes médullaires ou la fragmentation précoce de MKs loin des sinusoïdes dans la moelle osseuse de souris obèses.

Des données récentes et non publiées du laboratoire de Bart Vanhaesebroeck montrent que l'inactivation partielle de Vps34 dans l'animal entier (stratégie similaire au modèle d'inactivation partielle de la PI3KC2α) entraîne une amélioration de la sensibilité générale à l'insuline et une meilleure tolérance au glucose chez des souris obèses-diabétiques. En effet, au niveau hépatique, l'autophagie est significativement diminuée, réduisant l'apport d'acides aminés et donc inhibant la respiration mitochondriale ainsi que la néoglucogenèse hépatique. Au niveau musculaire, l'inactivation partielle de Vps34 a pour effet d'augmenter la glycolyse et *in fine* le captage de glucose. Ces effets au niveau hépatique et musculaire permettent une diminution générale de la glycémie. De plus, l'utilisation de l'inhibiteur actif *in vivo* de Vps34, Compound31, reproduit l'amélioration de la sensibilité à l'insuline observée chez les souris partiellement inactivées pour Vps34 (Bilanges B *et al* en préparation ; travail auquel j'ai participé lors de mon Master 2). L'obésité est l'élément clé du syndrome métabolique qui désigne l'ensemble des facteurs de risques pour le développement du diabète de type 2 et des pathologies cardiovasculaires. Le syndrome métabolique est défini par plusieurs facteurs de risque : obésité, diminution de la tolérance au glucose, dyslipidémie, hypertension, état pro-inflammatoire et état pro-thrombotique. Il a été observé chez les patients présentant un syndrome métabolique, une hyperactivité plaquettaire due à plusieurs phénomènes tels que

l'élévation des concentrations calciques cytosoliques, l'augmentation de la production d'isoprostane et de TXA_2, la résistance aux effets anti-agrégants du NO et de la PGI_2 ou encore l'augmentation de l'expression de surface de la P-selectine et de l'intégrine $\alpha_{IIb}\beta_3$ (Grundy et al., 2004; Morange and Alessi, 2013). Nos données sur les plaquettes démontrent que la délétion totale de Vps34 dans les plaquettes entraîne un défaut de croissance du thrombus *ex vivo* et *in vivo* sans pour autant induire de saignement. Il semble donc que l'inhibition de Vps34 améliore la sensibilité à l'insuline d'un coté et retarde la formation de thrombus de l'autre. Si l'on combine donc ces deux études et les données concernant la résistance à l'insuline et l'hyperactivabilité plaquettaire observée chez les patients obèses, il sera donc très intéressant d'étudier l'effet de l'inhibition de Vps34 chez des souris obèses diabétiques sur l'activité plaquettaire. Dans ce cas, Vps34 deviendrait une cible de choix dans le traitement de la sensibilité à l'insuline et de l'hyperactivité plaquettaire chez le patient obèse-diabétique, si les effets secondaires potentiels sont acceptables pour un traitement au long cours (notamment l'apparition de la microthrombopénie modérée).

A travers mon travail de thèse, j'ai pu révéler une partie du contrôle intrinsèque et extrinsèque au MK de la production et de l'activation plaquettaire à travers le rôle d'acteurs tels que certaines PI3Ks et l'adipocyte médullaire. La poursuite de l'étude du rôle de ces facteurs dans un contexte pathologique d'obésité-diabète bien que peu connu apparaît important d'un point de vue à la fois physiopathologique mais aussi dans la perspective de l'identification de nouvelles cibles thérapeutiques.

Bibliographie

AAdams, G.B., and Scadden, D.T. (2008). A niche opportunity for stem cell therapeutics. Gene therapy *15*, 96-99.

Adler, B.J., Green, D.E., Pagnotti, G.M., Chan, M.E., and Rubin, C.T. (2014a). High fat diet rapidly suppresses B lymphopoiesis by disrupting the supportive capacity of the bone marrow niche. PloS one *9*, e90639.

Adler, B.J., Kaushansky, K., and Rubin, C.T. (2014b). Obesity-driven disruption of haematopoiesis and the bone marrow niche. Nature reviews Endocrinology *10*, 737-748.

Albers, C.A., Cvejic, A., Favier, R., Bouwmans, E.E., Alessi, M.C., Bertone, P., Jordan, G., Kettleborough, R.N., Kiddle, G., Kostadima, M.*, et al.* (2011). Exome sequencing identifies NBEAL2 as the causative gene for gray platelet syndrome. Nature genetics *43*, 735-737.

Alliouachene, S., Bilanges, B., Chaussade, C., Pearce, W., Foukas, L.C., Scudamore, C.L., Moniz, L.S., and Vanhaesebroeck, B. (2016). Inactivation of class II PI3K-C2alpha induces leptin resistance, age-dependent insulin resistance and obesity in male mice. Diabetologia *59*, 1503-1512.

Alliouachene, S., Bilanges, B., Chicanne, G., Anderson, K.E., Pearce, W., Ali, K., Valet, C., Posor, Y., Low, P.C., Chaussade, C.*, et al.* (2015). Inactivation of the Class II PI3K-C2beta Potentiates Insulin Signaling and Sensitivity. Cell reports *13*, 1881-1894.

Amano, M., Chihara, K., Kimura, K., Fukata, Y., Nakamura, N., Matsuura, Y., and Kaibuchi, K. (1997). Formation of actin stress fibers and focal adhesions enhanced by Rho-kinase. Science *275*, 1308-1311.

Ambrosio, A.L., Boyle, J.A., and Di Pietro, S.M. (2012). Mechanism of platelet dense granule biogenesis: study of cargo transport and function of Rab32 and Rab38 in a model system. Blood *120*, 4072-4081.

Antkowiak, A., Viaud, J., Severin, S., Zanoun, M., Ceccato, L., Chicanne, G., Strassel, C., Eckly, A., Leon, C., Gachet, C.*, et al.* (2016). Cdc42-dependent F-actin dynamics drive structuration of the demarcation membrane system in megakaryocytes. Journal of thrombosis and haemostasis : JTH *14*, 1268-1284.

Backer, J.M. (2016). The intricate regulation and complex functions of the Class III phosphoinositide 3-kinase Vps34. The Biochemical journal *473*, 2251-2271.

Bae, Y.H., Ding, Z., Das, T., Wells, A., Gertler, F., and Roy, P. (2010). Profilin1 regulates PI(3,4)P2 and lamellipodin accumulation at the leading edge thus influencing motility of MDA-MB-231 cells. Proceedings of the National Academy of Sciences of the United States of America *107*, 21547-21552.

Bago, R., Malik, N., Munson, M.J., Prescott, A.R., Davies, P., Sommer, E., Shpiro, N., Ward, R., Cross, D., Ganley, I.G.*, et al.* (2014). Characterization of VPS34-IN1, a selective inhibitor of Vps34, reveals that the phosphatidylinositol 3-phosphate-binding SGK3 protein kinase is a downstream target of class III phosphoinositide 3-kinase. The Biochemical journal *463*, 413-427.

Bago, R., Sommer, E., Castel, P., Crafter, C., Bailey, F.P., Shpiro, N.,

Baselga, J., Cross, D., Eyers, P.A., and Alessi, D.R. (2016). The hVps34-SGK3 pathway alleviates sustained PI3K/Akt inhibition by stimulating mTORC1 and tumour growth. The EMBO journal *35*, 2263.

Balla, T. (2013). Phosphoinositides: tiny lipids with giant impact on cell regulation. Physiological reviews *93*, 1019-1137.

Barbosa, M.D., Nguyen, Q.A., Tchernev, V.T., Ashley, J.A., Detter, J.C., Blaydes, S.M., Brandt, S.J., Chotai, D., Hodgman, C., Solari, R.C.*, et al.* (1996). Identification of the homologous beige and Chediak-Higashi syndrome genes. Nature *382*, 262-265.

Barkalow, K., Witke, W., Kwiatkowski, D.J., and Hartwig, J.H. (1996). Coordinated regulation of platelet actin filament barbed ends by gelsolin and capping protein. The Journal of cell biology *134*, 389-399.

Bartley, T.D., Bogenberger, J., Hunt, P., Li, Y.S., Lu, H.S., Martin, F., Chang, M.S., Samal, B., Nichol, J.L., Swift, S.*, et al.* (1994). Identification and cloning of a megakaryocyte growth and development factor that is a ligand for the cytokine receptor Mpl. Cell *77*, 1117-1124.

Battinelli, E.M., Hartwig, J.H., and Italiano, J.E., Jr. (2007). Delivering new insight into the biology of megakaryopoiesis and thrombopoiesis. Current opinion in hematology *14*, 419-426.

Bechtel, W., Helmstadter, M., Balica, J., Hartleben, B., Kiefer, B., Hrnjic, F., Schell, C., Kretz, O., Liu, S., Geist, F.*, et al.* (2013). Vps34 deficiency reveals the importance of endocytosis for podocyte homeostasis. Journal of the American Society of Nephrology : JASN *24*, 727-743.

Behnke, O. (1968). An electron microscope study of the megacaryocyte of the rat bone marrow. I. The development of the demarcation membrane system and the platelet surface coat. Journal of ultrastructure research *24*, 412-433.

Behnke, O. (1969). An electron microscope study of the rat megacaryocyte. II. Some aspects of platelet release and microtubules. Journal of ultrastructure research *26*, 111-129.

Behnke, O., and Forer, A. (1998). From megakaryocytes to platelets: platelet morphogenesis takes place in the bloodstream. European journal of haematology Supplementum *61*, 3-23.

Berlanga, O., Bobe, R., Becker, M., Murphy, G., Leduc, M., Bon, C., Barry, F.A., Gibbins, J.M., Garcia, P., Frampton, J.*, et al.* (2000). Expression of the collagen receptor glycoprotein VI during megakaryocyte differentiation. Blood *96*, 2740-2745.

Berridge, M.J. (1984). Inositol trisphosphate and diacylglycerol as second messengers. The Biochemical journal *220*, 345-360.

Berrou, E., Adam, F., Lebret, M., Fergelot, P., Kauskot, A., Coupry, I., Jandrot-Perrus, M., Nurden, A., Favier, R., Rosa, J.P.*, et al.* (2013). Heterogeneity of platelet functional alterations in patients with filamin A mutations. Arteriosclerosis, thrombosis, and vascular biology *33*, e11-18.

Berthebaud, M., Riviere, C., Jarrier, P., Foudi, A., Zhang, Y., Compagno, D., Galy, A., Vainchenker, W., and Louache, F. (2005). RGS16 is a negative regulator of SDF-1-CXCR4 signaling in megakaryocytes. Blood *106*, 2962-2968.

Bilanges, B., and Vanhaesebroeck, B. (2014). Cinderella finds her shoe: the first Vps34 inhibitor uncovers a new PI3K-AGC protein kinase connection. The Biochemical journal *464*, e7-10.

Blair, P., and Flaumenhaft, R. (2009). Platelet alpha-granules: basic biology and clinical correlates. Blood reviews *23*, 177-189.

Blajecka, K., Marinov, M., Leitner, L., Uth, K., Posern, G., and Arcaro, A. (2012). Phosphoinositide 3-kinase C2beta regulates RhoA and the actin cytoskeleton through an interaction with Dbl. PloS one *7*, e44945.

Bodin, S., Soulet, C., Tronchere, H., Sie, P., Gachet, C., Plantavid, M., and Payrastre, B. (2005). Integrin-dependent interaction of lipid rafts with the actin cytoskeleton in activated human platelets. Journal of cell science *118*, 759-769.

Bodin, S., Tronchere, H., and Payrastre, B. (2003). Lipid rafts are critical membrane domains in blood platelet activation processes. Biochimica et biophysica acta *1610*, 247-257.

Bonifacino, J.S., and Hurley, J.H. (2008). Retromer. Current opinion in cell biology *20*, 427-436.

Boularan, C., Kamenyeva, O., Cho, H., and Kehrl, J.H. (2014). Resistance to inhibitors of cholinesterase (Ric)-8A and Galphai contribute to cytokinesis abscission by controlling vacuolar protein-sorting (Vps)34 activity. PloS one *9*, e86680.

Braccini, L., Ciraolo, E., Campa, C.C., Perino, A., Longo, D.L., Tibolla, G., Pregnolato, M., Cao, Y., Tassone, B., Damilano, F.*, et al.* (2015). PI3K-C2gamma is a Rab5 effector selectively controlling endosomal Akt2 activation downstream of insulin signalling. Nature communications *6*, 7400.

Breton-Gorius, J., Favier, R., Guichard, J., Cherif, D., Berger, R., Debili, N., Vainchenker, W., and Douay, L. (1995). A new congenital dysmegakaryopoietic thrombocytopenia (Paris-Trousseau) associated with giant platelet alpha-granules and chromosome 11 deletion at 11q23. Blood *85*, 1805-1814.

Broudy, V.C., and Kaushansky, K. (1995). Thrombopoietin, the c-mpl ligand, is a major regulator of platelet production. Journal of leukocyte biology *57*, 719-725.

Bruno, S., Gunetti, M., Gammaitoni, L., Dane, A., Cavalloni, G., Sanavio, F., Fagioli, F., Aglietta, M., and Piacibello, W. (2003). In vitro and in vivo megakaryocyte differentiation of fresh and ex-vivo expanded cord blood cells: rapid and transient megakaryocyte reconstitution. Haematologica *88*, 379-387.

Bryckaert, M., Rosa, J.P., Denis, C.V., and Lenting, P.J. (2015). Of von Willebrand factor and platelets. Cellular and molecular life sciences : CMLS *72*, 307-326.

Bunting, S., Widmer, R., Lipari, T., Rangell, L., Steinmetz, H., Carver-Moore, K., Moore, M.W., Keller, G.A.,

and de Sauvage, F.J. (1997). Normal platelets and megakaryocytes are produced in vivo in the absence of thrombopoietin. Blood *90*, 3423-3429.

Burkhart, J.M., Vaudel, M., Gambaryan, S., Radau, S., Walter, U., Martens, L., Geiger, J., Sickmann, A., and Zahedi, R.P. (2012). The first comprehensive and quantitative analysis of human platelet protein composition allows the comparative analysis of structural and functional pathways. Blood *120*, e73-82.

Burridge, K., and Chrzanowska-Wodnicka, M. (1996). Focal adhesions, contractility, and signaling. Annual review of cell and developmental biology *12*, 463-518.

Bury, L., Falcinelli, E., Chiasserini, D., Springer, T.A., Italiano, J.E., Jr., and Gresele, P. (2016). Cytoskeletal perturbation leads to platelet dysfunction and thrombocytopenia in variant forms of Glanzmann thrombasthenia. Haematologica *101*, 46-56.

Calderwood, D.A., Campbell, I.D., and Critchley, D.R. (2013). Talins and kindlins: partners in integrin-mediated adhesion. Nature reviews Molecular cell biology *14*, 503-517.

Campa, C.C., Franco, I., and Hirsch, E. (2015). PI3K-C2alpha: One enzyme for two products coupling vesicle trafficking and signal transduction. FEBS letters *589*, 1552-1558.

Cao, Y., Cai, J., Zhang, S., Yuan, N., Li, X., Fang, Y., Song, L., Shang, M., Liu, S., Zhao, W.*, et al.* (2015). Loss of autophagy leads to failure in megakaryopoiesis, megakaryocyte differentiation, and thrombopoiesis in mice. Experimental hematology *43*, 488-494.

Catimel, B., Kapp, E., Yin, M.X., Gregory, M., Wong, L.S., Condron, M., Church, N., Kershaw, N., Holmes, A.B., and Burgess, A.W. (2013). The PI(3)P interactome from a colon cancer cell. Journal of proteomics *82*, 35-51.

Cattaneo, M. (2011). The platelet P2Y(1)(2) receptor for adenosine diphosphate: congenital and drug-induced defects. Blood *117*, 2102-2112.

Cawthorn, W.P., Scheller, E.L., Learman, B.S., Parlee, S.D., Simon, B.R., Mori, H., Ning, X., Bree, A.J., Schell, B., Broome, D.T.*, et al.* (2014). Bone marrow adipose tissue is an endocrine organ that contributes to increased circulating adiponectin during caloric restriction. Cell metabolism *20*, 368-375.

Certain, S., Barrat, F., Pastural, E., Le Deist, F., Goyo-Rivas, J., Jabado, N., Benkerrou, M., Seger, R., Vilmer, E., Beullier, G.*, et al.* (2000). Protein truncation test of LYST reveals heterogenous mutations in patients with Chediak-Higashi syndrome. Blood *95*, 979-983.

Chap, H., Perret, B., Mauco, G., Simon, M.F., and Douste-Blazy, L. (1979). Organization and role of platelet membrane phospholipids as studied with purified phospholipases. Agents and actions *9*, 400-406.

Chatterjee, M., and Gawaz, M. (2013). Platelet-derived CXCL12 (SDF-1alpha): basic mechanisms and clinical implications. Journal of thrombosis and haemostasis : JTH *11*, 1954-1967.

Chen, Y., Aardema, J., and Corey, S.J. (2013a). Biochemical and functional significance of F-BAR domain proteins interaction with WASP/N-WASP. Seminars in cell & developmental biology *24*, 280-286.

Chen, Y., Aardema, J., Kale, S., Whichard, Z.L., Awomolo, A., Blanchard, E., Chang, B., Myers, D.R., Ju, L., Tran, R.*, et al.* (2013b). Loss of the F-BAR protein CIP4 reduces platelet production by impairing membrane-cytoskeleton remodeling. Blood *122*, 1695-1706.

Chicanne, G., Severin, S., Boscheron, C., Terrisse, A.D., Gratacap, M.P., Gaits-Iacovoni, F., Tronchere, H., and Payrastre, B. (2012). A novel mass assay to quantify the bioactive lipid PtdIns3P in various biological samples. The Biochemical journal *447*, 17-23.

Choo, H.J., Saafir, T.B., Mkumba, L., Wagner, M.B., and Jobe, S.M. (2012). Mitochondrial calcium and reactive oxygen species regulate agonist-initiated platelet phosphatidylserine exposure. Arteriosclerosis, thrombosis, and vascular biology *32*, 2946-2955.

Coller, B.S. (2015). alphaIIbbeta3: structure and function. Journal of thrombosis and haemostasis : JTH *13 Suppl 1*, S17-25.

Crawley, J.T., Zanardelli, S., Chion, C.K., and Lane, D.A. (2007). The central role of thrombin in hemostasis. Journal of thrombosis and haemostasis : JTH *5 Suppl 1*, 95-101.

Cumano, A., and Godin, I. (2007). Ontogeny of the hematopoietic system. Annual review of immunology *25*, 745-785.

Dai, S., Zhang, Y., Weimbs, T., Yaffe, M.B., and Zhou, D. (2007). Bacteria-generated PtdIns(3)P recruits VAMP8 to facilitate phagocytosis. Traffic *8*, 1365-1374.

Dangelmaier, C.A., and Holmsen, H. (1980). Determination of acid hydrolases in human platelets. Analytical biochemistry *104*, 182-191.

Datta, N.S., Williams, J.L., Caldwell, J., Curry, A.M., Ashcraft, E.K., and Long, M.W. (1996). Novel alterations in CDK1/cyclin B1 kinase complex formation occur during the acquisition of a polyploid DNA content. Molecular biology of the cell *7*, 209-223.

de Sauvage, F.J., Hass, P.E., Spencer, S.D., Malloy, B.E., Gurney, A.L., Spencer, S.A., Darbonne, W.C., Henzel, W.J., Wong, S.C., Kuang, W.J.*, et al.* (1994). Stimulation of megakaryocytopoiesis and thrombopoiesis by the c-Mpl ligand. Nature *369*, 533-538.

Detwiler, T.C. (1972). Control of energy metabolism in platelets. The effects of thrombin and cyanide on glycolysis. Biochimica et biophysica acta *256*, 163-174.

Deutsch, V.R., Olson, T.A., Nagler, A., Slavin, S., Levine, R.F., and Eldor, A. (1995). The response of cord blood megakaryocyte progenitors to IL-3, IL-6 and aplastic canine serum varies with gestational age. British journal of haematology *89*, 8-16.

Dhanjal, T.S., Pendaries, C., Ross, E.A., Larson, M.K., Protty, M.B., Buckley, C.D., and Watson, S.P. (2007). A novel role for PECAM-1 in megakaryocytokinesis and recovery of platelet counts in thrombocytopenic mice. Blood *109*, 4237-4244.

Diagouraga, B., Grichine, A., Fertin, A., Wang, J., Khochbin, S., and Sadoul, K. (2014). Motor-driven marginal band coiling promotes cell shape change during platelet activation. The Journal of cell biology *204*, 177-185.

Dirat, B., Bochet, L., Dabek, M., Daviaud, D., Dauvillier, S., Majed, B., Wang, Y.Y., Meulle, A., Salles, B., Le Gonidec, S.*, et al.* (2011). Cancer-associated adipocytes exhibit an activated phenotype and contribute to breast cancer invasion. Cancer research *71*, 2455-2465.

Domin, J., Harper, L., Aubyn, D., Wheeler, M., Florey, O., Haskard, D., Yuan, M., and Zicha, D. (2005). The class II phosphoinositide 3-kinase PI3K-C2beta regulates cell migration by a PtdIns3P dependent mechanism. Journal of cellular physiology *205*, 452-462.

Dominguez, V., Raimondi, C., Somanath, S., Bugliani, M., Loder, M.K., Edling, C.E., Divecha, N., da Silva-Xavier, G., Marselli, L., Persaud, S.J.*, et al.* (2011). Class II phosphoinositide 3-kinase regulates exocytosis of insulin granules in pancreatic beta cells. The Journal of biological chemistry *286*, 4216-4225.

Dutting, S., Bender, M., and Nieswandt, B. (2012). Platelet GPVI: a target for antithrombotic therapy?! Trends in pharmacological sciences *33*, 583-590.

Eckly, A., Heijnen, H., Pertuy, F., Geerts, W., Proamer, F., Rinckel, J.Y., Leon, C., Lanza, F., and Gachet, C. (2014). Biogenesis of the demarcation membrane system (DMS) in megakaryocytes. Blood *123*, 921-930.

Eckly, A., Rinckel, J.Y., Laeuffer, P., Cazenave, J.P., Lanza, F., Gachet, C., and Leon, C. (2010). Proplatelet formation deficit and megakaryocyte death contribute to thrombocytopenia in Myh9 knockout mice. Journal of thrombosis and haemostasis : JTH *8*, 2243-2251.

Eckly, A., Rinckel, J.Y., Proamer, F., Ulas, N., Joshi, S., Whiteheart, S.W., and Gachet, C. (2016). Respective contributions of single and compound granule fusion to secretion by activated platelets. Blood *128*, 2538-2549.

Eckly, A., Strassel, C., Freund, M., Cazenave, J.P., Lanza, F., Gachet, C., and Leon, C. (2009). Abnormal megakaryocyte morphology and proplatelet formation in mice with megakaryocyte-restricted MYH9 inactivation. Blood *113*, 3182-3189.

Elis, W., Triantafellow, E., Wolters, N.M., Sian, K.R., Caponigro, G., Borawski, J., Gaither, L.A., Murphy, L.O., Finan, P.M., and Mackeigan, J.P. (2008). Down-regulation of class II phosphoinositide 3-kinase alpha expression below a critical threshold induces apoptotic cell death. Molecular cancer research : MCR *6*, 614-623.

Ellson, C., Davidson, K., Anderson, K., Stephens, L.R., and Hawkins, P.T. (2006). PtdIns3P binding to the PX domain of p40phox is a physiological signal in NADPH oxidase activation. The EMBO journal *25*, 4468-4478.

Eun, L.Y., Song, B.W., Cha, M.J., Song, H., Kim, I.K., Choi, E., Chang, W., Lim, S., Choi, E.J., Ham, O.*, et al.* (2010). Overexpression of phosphoinositide-3-kinase class II alpha enhances mesenchymal stem cell survival in infarcted myocardium. Biochemical and biophysical research communications *402*, 272-279.

Falasca, M., Hamilton, J.R., Selvadurai, M., Sundaram, K., Adamska, A., and Thompson, P.E. (2016). Class II Phosphoinositide 3-Kinases as Novel Drug Targets. Journal of medicinal chemistry.

Falasca, M., Hughes, W.E., Dominguez, V., Sala, G., Fostira, F., Fang, M.Q., Cazzolli, R., Shepherd, P.R., James, D.E., and Maffucci, T. (2007). The role of phosphoinositide 3-kinase C2alpha in insulin signaling. The Journal of biological chemistry *282*, 28226-28236.

Falasca, M., and Maffucci, T. (2012). Regulation and cellular functions of class II phosphoinositide 3-kinases. The Biochemical journal *443*, 587-601.

Falet, H., Hoffmeister, K.M., Neujahr, R., and Hartwig, J.H. (2002). Normal Arp2/3 complex activation in platelets lacking WASp. Blood *100*, 2113-2122.

Falet, H., Marchetti, M.P., Hoffmeister, K.M., Massaad, M.J., Geha, R.S., and Hartwig, J.H. (2009). Platelet-associated IgAs and impaired GPVI responses in platelets lacking WIP. Blood *114*, 4729-4737.

Feng, L., Seymour, A.B., Jiang, S., To, A., Peden, A.A., Novak, E.K., Zhen, L., Rusiniak, M.E., Eicher, E.M., Robinson, M.S.*, et al.* (1999). The beta3A subunit gene (Ap3b1) of the AP-3 adaptor complex is altered in the mouse hypopigmentation mutant pearl, a model for Hermansky-Pudlak syndrome and night blindness. Human molecular genetics *8*, 323-330.

Feng, W., Chang, C., Luo, D., Su, H., Yu, S., Hua, W., Chen, Z., Hu, H., and Liu, W. (2014). Dissection of autophagy in human platelets. Autophagy *10*, 642-651.

Fox, J.E. (1985). Identification of actin-binding protein as the protein linking the membrane skeleton to glycoproteins on platelet plasma membranes. The Journal of biological chemistry *260*, 11970-11977.

Fox, J.E. (2001). Cytoskeletal proteins and platelet signaling. Thrombosis and haemostasis *86*, 198-213.

Fox, J.E., Boyles, J.K., Berndt, M.C., Steffen, P.K., and Anderson, L.K. (1988). Identification of a membrane skeleton in platelets. The Journal of cell biology *106*, 1525-1538.

Fox, J.E., Reynolds, C.C., Morrow, J.S., and Phillips, D.R. (1987). Spectrin is associated with membrane-bound actin filaments in platelets and is hydrolyzed by the Ca2+-dependent protease during platelet activation. Blood *69*, 537-545.

Franco, I., Gulluni, F., Campa, C.C., Costa, C., Margaria, J.P., Ciraolo, E., Martini, M., Monteyne, D., De Luca, E., Germena, G.*, et al.* (2014). PI3K class II alpha controls spatially restricted endosomal PtdIns3P and Rab11 activation to promote primary cilium function. Developmental cell *28*, 647-658.

Fujita, H., Allen, P.G., Janmey, P.A., Azuma, T., Kwiatkowski, D.J., Stossel,

T.P., Furu-uchi, K., and Kuzumaki, N. (1997). Characterization of gelsolin truncates that inhibit actin depolymerization by severing activity of gelsolin and cofilin. European journal of biochemistry *248*, 834-839.

Gachet, C. (2008). P2 receptors, platelet function and pharmacological implications. Thrombosis and haemostasis *99*, 466-472.

Gachet, C. (2012). P2Y(12) receptors in platelets and other hematopoietic and non-hematopoietic cells. Purinergic signalling *8*, 609-619.

Gaidarov, I., Smith, M.E., Domin, J., and Keen, J.H. (2001). The class II phosphoinositide 3-kinase C2alpha is activated by clathrin and regulates clathrin-mediated membrane trafficking. Molecular cell *7*, 443-449.

Garcia-Souza, L.F., and Oliveira, M.F. (2014). Mitochondria: biological roles in platelet physiology and pathology. The international journal of biochemistry & cell biology *50*, 156-160.

Ge, Q., Ryken, L., Noel, L., Maury, E., and Brichard, S.M. (2011). Adipokines identified as new downstream targets for adiponectin: lessons from adiponectin-overexpressing or -deficient mice. American journal of physiology Endocrinology and metabolism *301*, E326-335.

Geddis, A.E. (2010). Megakaryopoiesis. Seminars in hematology *47*, 212-219.

Geddis, A.E., Fox, N.E., Tkachenko, E., and Kaushansky, K. (2007). Endomitotic megakaryocytes that form a bipolar spindle exhibit cleavage furrow ingression followed by furrow regression. Cell cycle *6*, 455-460.

Gissen, P., Johnson, C.A., Morgan, N.V., Stapelbroek, J.M., Forshew, T., Cooper, W.N., McKiernan, P.J., Klomp, L.W., Morris, A.A., Wraith, J.E.*, et al.* (2004). Mutations in VPS33B, encoding a regulator of SNARE-dependent membrane fusion, cause arthrogryposis-renal dysfunction-cholestasis (ARC) syndrome. Nature genetics *36*, 400-404.

Giuriato, S., Bodin, S., Erneux, C., Woscholski, R., Plantavid, M., Chap, H., and Payrastre, B. (2000). pp60c-src associates with the SH2-containing inositol-5-phosphatase SHIP1 and is involved in its tyrosine phosphorylation downstream of alphaIIbbeta3 integrin in human platelets. The Biochemical journal *348 Pt 1*, 107-112.

Goggs, R., Williams, C.M., Mellor, H., and Poole, A.W. (2015). Platelet Rho GTPases-a focus on novel players, roles and relationships. The Biochemical journal *466*, 431-442.

Goldschmidt-Clermont, P.J., Furman, M.I., Wachsstock, D., Safer, D., Nachmias, V.T., and Pollard, T.D. (1992). The control of actin nucleotide exchange by thymosin beta 4 and profilin. A potential regulatory mechanism for actin polymerization in cells. Molecular biology of the cell *3*, 1015-1024.

Golebiewska, E.M., and Poole, A.W. (2015). Platelet secretion: From haemostasis to wound healing and beyond. Blood reviews *29*, 153-162.

Gordge, M.P. (2005). Megakaryocyte apoptosis: sorting out the signals. British journal of pharmacology *145*, 271-273.

Gratacap, M.P., Guillermet-Guibert, J., Martin, V., Chicanne, G., Tronchere, H., Gaits-Iacovoni, F., and Payrastre, B. (2011). Regulation and roles of PI3Kbeta, a major actor in platelet signaling and functions. Advances in enzyme regulation *51*, 106-116.

Grundy, S.M., Brewer, H.B., Jr., Cleeman, J.I., Smith, S.C., Jr., Lenfant, C., American Heart, A., National Heart, L., and Blood, I. (2004). Definition of metabolic syndrome: Report of the National Heart, Lung, and Blood Institute/American Heart Association conference on scientific issues related to definition. Circulation *109*, 433-438.

Gruner, S., Prostredna, M., Schulte, V., Krieg, T., Eckes, B., Brakebusch, C., and Nieswandt, B. (2003). Multiple integrin-ligand interactions synergize in shear-resistant platelet adhesion at sites of arterial injury in vivo. Blood *102*, 4021-4027.

Gunay-Aygun, M., Falik-Zaccai, T.C., Vilboux, T., Zivony-Elboum, Y., Gumruk, F., Cetin, M., Khayat, M., Boerkoel, C.F., Kfir, N., Huang, Y.*, et al.* (2011). NBEAL2 is mutated in gray platelet syndrome and is required for biogenesis of platelet alpha-granules. Nature genetics *43*, 732-734.

Gurney, A.L., Carver-Moore, K., de Sauvage, F.J., and Moore, M.W. (1994). Thrombocytopenia in c-mpl-deficient mice. Science *265*, 1445-1447.

Hamada, T., Mohle, R., Hesselgesser, J., Hoxie, J., Nachman, R.L., Moore, M.A., and Rafii, S. (1998). Transendothelial migration of megakaryocytes in response to stromal cell-derived factor 1 (SDF-1) enhances platelet formation. The Journal of experimental medicine *188*, 539-548.

Han, Z.C., Bellucci, S., and Caen, J.P. (1991). Megakaryocytopoiesis: characterization and regulation in normal and pathologic states. International journal of hematology *54*, 3-14.

Harada, K., Truong, A.B., Cai, T., and Khavari, P.A. (2005). The class II phosphoinositide 3-kinase C2beta is not essential for epidermal differentiation. Molecular and cellular biology *25*, 11122-11130.

Hardouin, P., Rharass, T., and Lucas, S. (2016). Bone Marrow Adipose Tissue: To Be or Not To Be a Typical Adipose Tissue? Frontiers in endocrinology *7*, 85.

Harris, D.P., Vogel, P., Wims, M., Moberg, K., Humphries, J., Jhaver, K.G., DaCosta, C.M., Shadoan, M.K., Xu, N., Hansen, G.M.*, et al.* (2011). Requirement for class II phosphoinositide 3-kinase C2alpha in maintenance of glomerular structure and function. Molecular and cellular biology *31*, 63-80.

Hartwig, J.H., Barkalow, K., Azim, A., and Italiano, J. (1999). The elegant platelet: signals controlling actin assembly. Thrombosis and haemostasis *82*, 392-398.

Hartwig, J.H., and DeSisto, M. (1991). The cytoskeleton of the resting human blood platelet: structure of the membrane skeleton and its attachment to actin filaments. The Journal of cell biology *112*, 407-425.

Hegyi, E., Heilbrun, L.K., and Nakeff, A. (1990). Immunogold probing of platelet factor 4 in different ploidy classes of rat

megakaryocytes sorted by flow cytometry. Experimental hematology *18*, 789-793.

Heijnen, H.F., Debili, N., Vainchencker, W., Breton-Gorius, J., Geuze, H.J., and Sixma, J.J. (1998). Multivesicular bodies are an intermediate stage in the formation of platelet alpha-granules. Blood *91*, 2313-2325.

Henne, W.M., Buchkovich, N.J., and Emr, S.D. (2011). The ESCRT pathway. Developmental cell *21*, 77-91.

Hitchcock, I.S., and Kaushansky, K. (2014). Thrombopoietin from beginning to end. British journal of haematology *165*, 259-268.

Ho, M.S., Medcalf, R.L., Livesey, S.A., and Traianedes, K. (2015). The dynamics of adult haematopoiesis in the bone and bone marrow environment. British journal of haematology *170*, 472-486.

Hokin, L.E., and Hokin, M.R. (1964). The Incorporation of 32p from Triphosphate into Polyphosphoinositides (Gamma-32p)Adenosine and Phosphatidic Acid in Erythrocyte Membranes. Biochimica et biophysica acta *84*, 563-575.

Huizing, M., Helip-Wooley, A., Westbroek, W., Gunay-Aygun, M., and Gahl, W.A. (2008). Disorders of lysosome-related organelle biogenesis: clinical and molecular genetics. Annual review of genomics and human genetics *9*, 359-386.

Huizing, M., Pederson, B., Hess, R.A., Griffin, A., Helip-Wooley, A., Westbroek, W., Dorward, H., O'Brien, K.J., Golas, G., Tsilou, E.*, et al.* (2009). Clinical and cellular characterisation of Hermansky-Pudlak syndrome type 6. Journal of medical genetics *46*, 803-810.

Ichikawa, M., Asai, T., Saito, T., Seo, S., Yamazaki, I., Yamagata, T., Mitani, K., Chiba, S., Ogawa, S., Kurokawa, M.*, et al.* (2004). AML-1 is required for megakaryocytic maturation and lymphocytic differentiation, but not for maintenance of hematopoietic stem cells in adult hematopoiesis. Nature medicine *10*, 299-304.

Inaguma, Y., Matsumoto, A., Noda, M., Tabata, H., Maeda, A., Goto, M., Usui, D., Jimbo, E.F., Kikkawa, K., Ohtsuki, M.*, et al.* (2016). Role of Class III phosphoinositide 3-kinase in the brain development: possible involvement in specific learning disorders. Journal of neurochemistry *139*, 245-255.

Inoue, O., Suzuki-Inoue, K., Dean, W.L., Frampton, J., and Watson, S.P. (2003). Integrin alpha2beta1 mediates outside-in regulation of platelet spreading on collagen through activation of Src kinases and PLCgamma2. The Journal of cell biology *160*, 769-780.

Italiano, J.E., Jr. (2013). Unraveling mechanisms that control platelet production. Seminars in thrombosis and hemostasis *39*, 15-24.

Italiano, J.E., Jr., Lecine, P., Shivdasani, R.A., and Hartwig, J.H. (1999). Blood platelets are assembled principally at the ends of proplatelet processes produced by differentiated megakaryocytes. The Journal of cell biology *147*, 1299-1312.

Jaber, N., Dou, Z., Chen, J.S., Catanzaro, J., Jiang, Y.P., Ballou, L.M., Selinger, E., Ouyang, X., Lin, R.Z., Zhang, J.*, et al.* (2012). Class III PI3K

Vps34 plays an essential role in autophagy and in heart and liver function. Proceedings of the National Academy of Sciences of the United States of America *109*, 2003-2008.

Jaber, N., Mohd-Naim, N., Wang, Z., DeLeon, J.L., Kim, S., Zhong, H., Sheshadri, N., Dou, Z., Edinger, A.L., Du, G.*, et al.* (2016). Vps34 regulates Rab7 and late endocytic trafficking through recruitment of the GTPase activating protein Armus. Journal of cell science.

Jackson, S.P. (2011). Arterial thrombosis--insidious, unpredictable and deadly. Nature medicine *17*, 1423-1436.

Jackson, S.P., Yap, C.L., and Anderson, K.E. (2004). Phosphoinositide 3-kinases and the regulation of platelet function. Biochemical Society transactions *32*, 387-392.

Jung, S.M., and Moroi, M. (2000). Signal-transducing mechanisms involved in activation of the platelet collagen receptor integrin alpha(2)beta(1). The Journal of biological chemistry *275*, 8016-8026.

Jung, S.M., and Moroi, M. (2001). Platelet collagen receptor integrin alpha2beta1 activation involves differential participation of ADP-receptor subtypes P2Y1 and P2Y12 but not intracellular calcium change. European journal of biochemistry *268*, 3513-3522.

Junt, T., Schulze, H., Chen, Z., Massberg, S., Goerge, T., Krueger, A., Wagner, D.D., Graf, T., Italiano, J.E., Jr., Shivdasani, R.A.*, et al.* (2007). Dynamic visualization of thrombopoiesis within bone marrow. Science *317*, 1767-1770.

Jurak Begonja, A., Hoffmeister, K.M., Hartwig, J.H., and Falet, H. (2011). FlnA-null megakaryocytes prematurely release large and fragile platelets that circulate poorly. Blood *118*, 2285-2295.

Kahn, M.L., Nakanishi-Matsui, M., Shapiro, M.J., Ishihara, H., and Coughlin, S.R. (1999). Protease-activated receptors 1 and 4 mediate activation of human platelets by thrombin. The Journal of clinical investigation *103*, 879-887.

Kahn, M.L., Zheng, Y.W., Huang, W., Bigornia, V., Zeng, D., Moff, S., Farese, R.V., Jr., Tam, C., and Coughlin, S.R. (1998). A dual thrombin receptor system for platelet activation. Nature *394*, 690-694.

Karlsson, E.A., Sheridan, P.A., and Beck, M.A. (2010). Diet-induced obesity in mice reduces the maintenance of influenza-specific CD8+ memory T cells. The Journal of nutrition *140*, 1691-1697.

Katso, R.M., Pardo, O.E., Palamidessi, A., Franz, C.M., Marinov, M., De Laurentiis, A., Downward, J., Scita, G., Ridley, A.J., Waterfield, M.D.*, et al.* (2006). Phosphoinositide 3-Kinase C2beta regulates cytoskeletal organization and cell migration via Rac-dependent mechanisms. Molecular biology of the cell *17*, 3729-3744.

Kaushansky, K. (1995). Thrombopoietin: the primary regulator of platelet production. Blood *86*, 419-431.

Kaushansky, K. (2006). Lineage-specific hematopoietic growth factors. The New

England journal of medicine *354*, 2034-2045.

Kaushansky, K., Lok, S., Holly, R.D., Broudy, V.C., Lin, N., Bailey, M.C., Forstrom, J.W., Buddle, M.M., Oort, P.J., Hagen, F.S.*, et al.* (1994). Promotion of megakaryocyte progenitor expansion and differentiation by the c-Mpl ligand thrombopoietin. Nature *369*, 568-571.

Kawai, M., de Paula, F.J., and Rosen, C.J. (2012). New insights into osteoporosis: the bone-fat connection. Journal of internal medicine *272*, 317-329.

Kenific, C.M., Stehbens, S.J., Goldsmith, J., Leidal, A.M., Faure, N., Ye, J., Wittmann, T., and Debnath, J. (2016). NBR1 enables autophagy-dependent focal adhesion turnover. The Journal of cell biology *212*, 577-590.

Kihara, A., Noda, T., Ishihara, N., and Ohsumi, Y. (2001). Two distinct Vps34 phosphatidylinositol 3-kinase complexes function in autophagy and carboxypeptidase Y sorting in Saccharomyces cerevisiae. The Journal of cell biology *152*, 519-530.

Kim, T.Y., and Schafer, A.L. (2016). Diabetes and Bone Marrow Adiposity. Current osteoporosis reports *14*, 337-344.

King, K.Y., and Goodell, M.A. (2011). Inflammatory modulation of HSCs: viewing the HSC as a foundation for the immune response. Nature reviews Immunology *11*, 685-692.

King, S.M., and Reed, G.L. (2002). Development of platelet secretory granules. Seminars in cell & developmental biology *13*, 293-302.

Kobayashi, S. (2015). Choose Delicately and Reuse Adequately: The Newly Revealed Process of Autophagy. Biological & pharmaceutical bulletin *38*, 1098-1103.

Kosoff, R.E., Aslan, J.E., Kostyak, J.C., Dulaimi, E., Chow, H.Y., Prudnikova, T.Y., Radu, M., Kunapuli, S.P., McCarty, O.J., and Chernoff, J. (2015). Pak2 restrains endomitosis during megakaryopoiesis and alters cytoskeleton organization. Blood *125*, 2995-3005.

Ktori, C., Shepherd, P.R., and O'Rourke, L. (2003). TNF-alpha and leptin activate the alpha-isoform of class II phosphoinositide 3-kinase. Biochemical and biophysical research communications *306*, 139-143.

Kunishima, S., Kamiya, T., and Saito, H. (2002). Genetic abnormalities of Bernard-Soulier syndrome. International journal of hematology *76*, 319-327.

Kuter, D.J., Gminski, D.M., and Rosenberg, R.D. (1992). Transforming growth factor beta inhibits megakaryocyte growth and endomitosis. Blood *79*, 619-626.

Lafontan, M. (2012). Historical perspectives in fat cell biology: the fat cell as a model for the investigation of hormonal and metabolic pathways. American journal of physiology Cell physiology *302*, C327-359.

Lamb, C.A., Yoshimori, T., and Tooze, S.A. (2013). The autophagosome: origins unknown, biogenesis complex. Nature reviews Molecular cell biology *14*, 759-774.

Lane, W.J., Dias, S., Hattori, K., Heissig, B., Choy, M., Rabbany, S.Y., Wood, J., Moore, M.A., and Rafii, S. (2000). Stromal-derived factor 1-induced megakaryocyte migration and platelet production is dependent on matrix metalloproteinases. Blood *96*, 4152-4159.

Laurent, P.A., Severin, S., Gratacap, M.P., and Payrastre, B. (2014). Class I PI 3-kinases signaling in platelet activation and thrombosis: PDK1/Akt/GSK3 axis and impact of PTEN and SHIP1. Advances in biological regulation *54*, 162-174.

Laurent, P.A., Severin, S., Hechler, B., Vanhaesebroeck, B., Payrastre, B., and Gratacap, M.P. (2015). Platelet PI3Kbeta and GSK3 regulate thrombus stability at a high shear rate. Blood *125*, 881-888.

Laurent, V., Guerard, A., Mazerolles, C., Le Gonidec, S., Toulet, A., Nieto, L., Zaidi, F., Majed, B., Garandeau, D., Socrier, Y.*, et al.* (2016). Periprostatic adipocytes act as a driving force for prostate cancer progression in obesity. Nature communications *7*, 10230.

Lazar, I., Clement, E., Dauvillier, S., Milhas, D., Ducoux-Petit, M., LeGonidec, S., Moro, C., Soldan, V., Dalle, S., Balor, S.*, et al.* (2016). Adipocyte Exosomes Promote Melanoma Aggressiveness through Fatty Acid Oxidation: A Novel Mechanism Linking Obesity and Cancer. Cancer research *76*, 4051-4057.

Lecka-Czernik, B. (2012). Marrow fat metabolism is linked to the systemic energy metabolism. Bone *50*, 534-539.

Leon, C., Eckly, A., Hechler, B., Aleil, B., Freund, M., Ravanat, C., Jourdain, M., Nonne, C., Weber, J., Tiedt, R.*, et al.* (2007). Megakaryocyte-restricted MYH9 inactivation dramatically affects hemostasis while preserving platelet aggregation and secretion. Blood *110*, 3183-3191.

Lhermusier, T., Chap, H., and Payrastre, B. (2011). Platelet membrane phospholipid asymmetry: from the characterization of a scramblase activity to the identification of an essential protein mutated in Scott syndrome. Journal of thrombosis and haemostasis : JTH *9*, 1883-1891.

Li, H., and Marshall, A.J. (2015). Phosphatidylinositol (3,4) bisphosphate-specific phosphatases and effector proteins: A distinct branch of PI3K signaling. Cellular signalling *27*, 1789-1798.

Liang, C., Lee, J.S., Inn, K.S., Gack, M.U., Li, Q., Roberts, E.A., Vergne, I., Deretic, V., Feng, P., Akazawa, C.*, et al.* (2008). Beclin1-binding UVRAG targets the class C Vps complex to coordinate autophagosome maturation and endocytic trafficking. Nature cell biology *10*, 776-787.

Liu, C.C., Lin, Y.C., Chen, Y.H., Chen, C.M., Pang, L.Y., Chen, H.A., Wu, P.R., Lin, M.Y., Jiang, S.T., Tsai, T.F.*, et al.* (2016). Cul3-KLHL20 Ubiquitin Ligase Governs the Turnover of ULK1 and VPS34 Complexes to Control Autophagy Termination. Molecular cell *61*, 84-97.

Lo, B., Li, L., Gissen, P., Christensen, H., McKiernan, P.J., Ye, C., Abdelhaleem, M., Hayes, J.A., Williams, M.D., Chitayat, D.*, et al.* (2005). Requirement of VPS33B, a member of the Sec1/Munc18 protein family, in

megakaryocyte and platelet alpha-granule biogenesis. Blood *106*, 4159-4166.

Lok, S., Kaushansky, K., Holly, R.D., Kuijper, J.L., Lofton-Day, C.E., Oort, P.J., Grant, F.J., Heipel, M.D., Burkhead, S.K., Kramer, J.M.*, et al.* (1994). Cloning and expression of murine thrombopoietin cDNA and stimulation of platelet production in vivo. Nature *369*, 565-568.

Lordier, L., Bluteau, D., Jalil, A., Legrand, C., Pan, J., Rameau, P., Jouni, D., Bluteau, O., Mercher, T., Leon, C.*, et al.* (2012). RUNX1-induced silencing of non-muscle myosin heavy chain IIB contributes to megakaryocyte polyploidization. Nature communications *3*, 717.

Ludlow, L.B., Schick, B.P., Budarf, M.L., Driscoll, D.A., Zackai, E.H., Cohen, A., and Konkle, B.A. (1996). Identification of a mutation in a GATA binding site of the platelet glycoprotein Ibbeta promoter resulting in the Bernard-Soulier syndrome. The Journal of biological chemistry *271*, 22076-22080.

Machlus, K.R., and Italiano, J.E., Jr. (2013). The incredible journey: From megakaryocyte development to platelet formation. The Journal of cell biology *201*, 785-796.

Machlus, K.R., Thon, J.N., and Italiano, J.E., Jr. (2014). Interpreting the developmental dance of the megakaryocyte: a review of the cellular and molecular processes mediating platelet formation. British journal of haematology *165*, 227-236.

Maffucci, T., Brancaccio, A., Piccolo, E., Stein, R.C., and Falasca, M. (2003). Insulin induces phosphatidylinositol-3-phosphate formation through TC10 activation. The EMBO journal *22*, 4178-4189.

Maffucci, T., Cooke, F.T., Foster, F.M., Traer, C.J., Fry, M.J., and Falasca, M. (2005). Class II phosphoinositide 3-kinase defines a novel signaling pathway in cell migration. The Journal of cell biology *169*, 789-799.

Maffucci, T., and Falasca, M. (2014). New insight into the intracellular roles of class II phosphoinositide 3-kinases. Biochemical Society transactions *42*, 1378-1382.

Manz, M.G., and Boettcher, S. (2014). Emergency granulopoiesis. Nature reviews Immunology *14*, 302-314.

Marat, A.L., and Haucke, V. (2016). Phosphatidylinositol 3-phosphates-at the interface between cell signalling and membrane traffic. The EMBO journal *35*, 561-579.

Martin, V., Guillermet-Guibert, J., Chicanne, G., Cabou, C., Jandrot-Perrus, M., Plantavid, M., Vanhaesebroeck, B., Payrastre, B., and Gratacap, M.P. (2010). Deletion of the p110beta isoform of phosphoinositide 3-kinase in platelets reveals its central role in Akt activation and thrombus formation in vitro and in vivo. Blood *115*, 2008-2013.

Masliah-Planchon, J., Darnige, L., and Bellucci, S. (2013). Molecular determinants of platelet delta storage pool deficiencies: an update. British journal of haematology *160*, 5-11.

Matsubara, Y., Ono, Y., Suzuki, H., Arai, F., Suda, T., Murata, M., and Ikeda, Y. (2013). OP9 bone marrow stroma cells differentiate into megakaryocytes and platelets. PloS one *8*, e58123.

Mauco, G., Dangelmaier, C.A., and Smith, J.B. (1984). Inositol lipids, phosphatidate and diacylglycerol share stearoylarachidonoylglycerol as a common backbone in thrombin-stimulated human platelets. The Biochemical journal *224*, 933-940.

Mazharian, A., Mori, J., Wang, Y.J., Heising, S., Neel, B.G., Watson, S.P., and Senis, Y.A. (2013). Megakaryocyte-specific deletion of the protein-tyrosine phosphatases Shp1 and Shp2 causes abnormal megakaryocyte development, platelet production, and function. Blood *121*, 4205-4220.

McCartney, A.J., Zhang, Y., and Weisman, L.S. (2014). Phosphatidylinositol 3,5-bisphosphate: low abundance, high significance. BioEssays : news and reviews in molecular, cellular and developmental biology *36*, 52-64.

McKnight, N.C., Zhong, Y., Wold, M.S., Gong, S., Phillips, G.R., Dou, Z., Zhao, Y., Heintz, N., Zong, W.X., and Yue, Z. (2014). Beclin 1 is required for neuron viability and regulates endosome pathways via the UVRAG-VPS34 complex. PLoS genetics *10*, e1004626.

McLeod, I.X., Zhou, X., Li, Q.J., Wang, F., and He, Y.W. (2011). The class III kinase Vps34 promotes T lymphocyte survival through regulating IL-7Ralpha surface expression. Journal of immunology *187*, 5051-5061.

Meng, R., Wang, Y., Yao, Y., Zhang, Z., Harper, D.C., Heijnen, H.F., Sitaram, A., Li, W., Raposo, G., Weiss, M.J.*, et al.* (2012). SLC35D3 delivery from megakaryocyte early endosomes is required for platelet dense granule biogenesis and is differentially defective in Hermansky-Pudlak syndrome models. Blood *120*, 404-414.

Meunier, F.A., Osborne, S.L., Hammond, G.R., Cooke, F.T., Parker, P.J., Domin, J., and Schiavo, G. (2005). Phosphatidylinositol 3-kinase C2alpha is essential for ATP-dependent priming of neurosecretory granule exocytosis. Molecular biology of the cell *16*, 4841-4851.

Michell, R.H. (1975). Inositol phospholipids and cell surface receptor function. Biochimica et biophysica acta *415*, 81-47.

Misawa, H., Ohtsubo, M., Copeland, N.G., Gilbert, D.J., Jenkins, N.A., and Yoshimura, A. (1998). Cloning and characterization of a novel class II phosphoinositide 3-kinase containing C2 domain. Biochemical and biophysical research communications *244*, 531-539.

Mizushima, N., Ohsumi, Y., and Yoshimori, T. (2002). Autophagosome formation in mammalian cells. Cell structure and function *27*, 421-429.

Mizushima, N., Yoshimori, T., and Ohsumi, Y. (2011). The role of Atg proteins in autophagosome formation. Annual review of cell and developmental biology *27*, 107-132.

Moitra, J., Mason, M.M., Olive, M., Krylov, D., Gavrilova, O., Marcus-Samuels, B., Feigenbaum, L., Lee, E.,

Aoyama, T., Eckhaus, M.*, et al.* (1998). Life without white fat: a transgenic mouse. Genes & development *12*, 3168-3181.

Morange, P.E., and Alessi, M.C. (2013). Thrombosis in central obesity and metabolic syndrome: mechanisms and epidemiology. Thrombosis and haemostasis *110*, 669-680.

Moroi, M., and Jung, S.M. (2004). Platelet glycoprotein VI: its structure and function. Thrombosis research *114*, 221-233.

Morrison, S.J., and Scadden, D.T. (2014). The bone marrow niche for haematopoietic stem cells. Nature *505*, 327-334.

Mountford, J.K., Petitjean, C., Putra, H.W., McCafferty, J.A., Setiabakti, N.M., Lee, H., Tonnesen, L.L., McFadyen, J.D., Schoenwaelder, S.M., Eckly, A.*, et al.* (2015). The class II PI 3-kinase, PI3KC2alpha, links platelet internal membrane structure to shear-dependent adhesive function. Nature communications *6*, 6535.

Muller, F., Mutch, N.J., Schenk, W.A., Smith, S.A., Esterl, L., Spronk, H.M., Schmidbauer, S., Gahl, W.A., Morrissey, J.H., and Renne, T. (2009). Platelet polyphosphates are proinflammatory and procoagulant mediators in vivo. Cell *139*, 1143-1156.

Nagle, D.L., Karim, M.A., Woolf, E.A., Holmgren, L., Bork, P., Misumi, D.J., McGrail, S.H., Dussault, B.J., Jr., Perou, C.M., Boissy, R.E.*, et al.* (1996). Identification and mutation analysis of the complete gene for Chediak-Higashi syndrome. Nature genetics *14*, 307-311.

Naot, D., and Cornish, J. (2014). Cytokines and Hormones That Contribute to the Positive Association between Fat and Bone. Frontiers in endocrinology *5*, 70.

Naveiras, O., Nardi, V., Wenzel, P.L., Hauschka, P.V., Fahey, F., and Daley, G.Q. (2009). Bone-marrow adipocytes as negative regulators of the haematopoietic microenvironment. Nature *460*, 259-263.

Nemazanyy, I., Blaauw, B., Paolini, C., Caillaud, C., Protasi, F., Mueller, A., Proikas-Cezanne, T., Russell, R.C., Guan, K.L., Nishino, I.*, et al.* (2013). Defects of Vps15 in skeletal muscles lead to autophagic vacuolar myopathy and lysosomal disease. EMBO molecular medicine *5*, 870-890.

Nichol, J.L., Hokom, M.M., Hornkohl, A., Sheridan, W.P., Ohashi, H., Kato, T., Li, Y.S., Bartley, T.D., Choi, E., Bogenberger, J.*, et al.* (1995). Megakaryocyte growth and development factor. Analyses of in vitro effects on human megakaryopoiesis and endogenous serum levels during chemotherapy-induced thrombocytopenia. The Journal of clinical investigation *95*, 2973-2978.

Nieswandt, B., Pleines, I., and Bender, M. (2011). Platelet adhesion and activation mechanisms in arterial thrombosis and ischaemic stroke. Journal of thrombosis and haemostasis : JTH *9 Suppl 1*, 92-104.

Nieswandt, B., Varga-Szabo, D., and Elvers, M. (2009). Integrins in platelet activation. Journal of thrombosis and haemostasis : JTH *7 Suppl 1*, 206-209.

Nieswandt, B., and Watson, S.P. (2003). Platelet-collagen interaction: is GPVI the central receptor? Blood *102*, 449-461.

Nigorikawa, K., Hazeki, K., Guo, Y., and Hazeki, O. (2014). Involvement of class II phosphoinositide 3-kinase alpha-isoform in antigen-induced degranulation in RBL-2H3 cells. PloS one *9*, e111698.

Niswander, L.M., Fegan, K.H., Kingsley, P.D., McGrath, K.E., and Palis, J. (2014). SDF-1 dynamically mediates megakaryocyte niche occupancy and thrombopoiesis at steady state and following radiation injury. Blood *124*, 277-286.

Nobes, C.D., and Hall, A. (1995). Rho, rac and cdc42 GTPases: regulators of actin structures, cell adhesion and motility. Biochemical Society transactions *23*, 456-459.

Nurden, A.T. (2007). Interesting variations on how a disease is defined: comparisons of von Willebrand disease and Glanzmann thrombasthenia. Journal of thrombosis and haemostasis : JTH *5*, 647-649; author reply 649-651.

Nurden, A.T., Pillois, X., and Wilcox, D.A. (2013). Glanzmann thrombasthenia: state of the art and future directions. Seminars in thrombosis and hemostasis *39*, 642-655.

Obara, K., Sekito, T., and Ohsumi, Y. (2006). Assortment of phosphatidylinositol 3-kinase complexes--Atg14p directs association of complex I to the pre-autophagosomal structure in Saccharomyces cerevisiae. Molecular biology of the cell *17*, 1527-1539.

Offermanns, S. (2006). Activation of platelet function through G protein-coupled receptors. Circulation research *99*, 1293-1304.

Okuma, M., Hirata, T., Ushikubi, F., Kakizuka, A., and Narumiya, S. (1996). Molecular characterization of a dominantly inherited bleeding disorder with impaired platelet responses to thromboxane A2. Polish journal of pharmacology *48*, 77-82.

Ono, Y., Wang, Y., Suzuki, H., Okamoto, S., Ikeda, Y., Murata, M., Poncz, M., and Matsubara, Y. (2012). Induction of functional platelets from mouse and human fibroblasts by p45NF-E2/Maf. Blood *120*, 3812-3821.

Ouseph, M.M., Huang, Y., Banerjee, M., Joshi, S., MacDonald, L., Zhong, Y., Liu, H., Li, X., Xiang, B., Zhang, G.*, et al.* (2015). Autophagy is induced upon platelet activation and is essential for hemostasis and thrombosis. Blood *126*, 1224-1233.

Painter, R.G., Prodouz, K.N., and Gaarde, W. (1985). Isolation of a subpopulation of glycoprotein IIb-III from platelet membranes that is bound to membrane actin. The Journal of cell biology *100*, 652-657.

Parekh, V.V., Wu, L., Boyd, K.L., Williams, J.A., Gaddy, J.A., Olivares-Villagomez, D., Cover, T.L., Zong, W.X., Zhang, J., and Van Kaer, L. (2013). Impaired autophagy, defective T cell homeostasis, and a wasting syndrome in mice with a T cell-specific deletion of Vps34. Journal of immunology *190*, 5086-5101.

Pasquier, B., El-Ahmad, Y., Filoche-Romme, B., Dureuil, C., Fassy, F.,

Abecassis, P.Y., Mathieu, M., Bertrand, T., Benard, T., Barriere, C.*, et al.* (2015). Discovery of (2S)-8-[(3R)-3-methylmorpholin-4-yl]-1-(3-methyl-2-oxobutyl)-2-(trifluoromethyl)- 3,4-dihydro-2H-pyrimido[1,2-a]pyrimidin-6-one: a novel potent and selective inhibitor of Vps34 for the treatment of solid tumors. Journal of medicinal chemistry *58*, 376-400.

Patel-Hett, S., Wang, H., Begonja, A.J., Thon, J.N., Alden, E.C., Wandersee, N.J., An, X., Mohandas, N., Hartwig, J.H., and Italiano, J.E., Jr. (2011). The spectrin-based membrane skeleton stabilizes mouse megakaryocyte membrane systems and is essential for proplatelet and platelet formation. Blood *118*, 1641-1652.

Paul, N.R., Jacquemet, G., and Caswell, P.T. (2015). Endocytic Trafficking of Integrins in Cell Migration. Current biology : CB *25*, R1092-1105.

Payrastre, B., Missy, K., Giuriato, S., Bodin, S., Plantavid, M., and Gratacap, M. (2001). Phosphoinositides: key players in cell signalling, in time and space. Cellular signalling *13*, 377-387.

Pertuy, F., Eckly, A., Weber, J., Proamer, F., Rinckel, J.Y., Lanza, F., Gachet, C., and Leon, C. (2014). Myosin IIA is critical for organelle distribution and F-actin organization in megakaryocytes and platelets. Blood *123*, 1261-1269.

Petitjean, C., Setiabakti, N.M., Mountford, J.K., Arthur, J.F., Ellis, S., and Hamilton, J.R. (2016). Combined deficiency of PI3KC2alpha and PI3KC2beta reveals a nonredundant role for PI3KC2alpha in regulating mouse platelet structure and thrombus stability. Platelets *27*, 402-409.

Posor, Y., Eichhorn-Gruenig, M., Puchkov, D., Schoneberg, J., Ullrich, A., Lampe, A., Muller, R., Zarbakhsh, S., Gulluni, F., Hirsch, E.*, et al.* (2013). Spatiotemporal control of endocytosis by phosphatidylinositol-3,4-bisphosphate. Nature *499*, 233-237.

Pozzobon, T., Goldoni, G., Viola, A., and Molon, B. (2016). CXCR4 signaling in health and disease. Immunology letters *177*, 6-15.

Price, L.S., Leng, J., Schwartz, M.A., and Bokoch, G.M. (1998). Activation of Rac and Cdc42 by integrins mediates cell spreading. Molecular biology of the cell *9*, 1863-1871.

Proikas-Cezanne, T., Takacs, Z., Donnes, P., and Kohlbacher, O. (2015). WIPI proteins: essential PtdIns3P effectors at the nascent autophagosome. Journal of cell science *128*, 207-217.

Psaila, B. (2016). Tense your megas! Structural rigidity is key. Blood *128*, 1997-1999.

Qu, F., Lorenzo, D.N., King, S.J., Brooks, R., Bear, J.E., and Bennett, V. (2016). Ankyrin-B is a PI3P effector that promotes polarized alpha5beta1-integrin recycling via recruiting RabGAP1L to early endosomes. eLife *5*.

Raiborg, C., Schink, K.O., and Stenmark, H. (2013). Class III phosphatidylinositol 3-kinase and its catalytic product PtdIns3P in regulation of endocytic membrane traffic. The FEBS journal *280*, 2730-2742.

Reifler, A., Li, X., Archambeau, A.J., McDade, J.R., Sabha, N., Michele, D.E., and Dowling, J.J. (2014). Conditional knockout of pik3c3 causes a murine muscular dystrophy. The American journal of pathology *184*, 1819-1830.

Richardson, J.L., Shivdasani, R.A., Boers, C., Hartwig, J.H., and Italiano, J.E., Jr. (2005). Mechanisms of organelle transport and capture along proplatelets during platelet production. Blood *106*, 4066-4075.

Riviere, C., Subra, F., Cohen-Solal, K., Cordette-Lagarde, V., Letestu, R., Auclair, C., Vainchenker, W., and Louache, F. (1999). Phenotypic and functional evidence for the expression of CXCR4 receptor during megakaryocytopoiesis. Blood *93*, 1511-1523.

Ronan, B., Flamand, O., Vescovi, L., Dureuil, C., Durand, L., Fassy, F., Bachelot, M.F., Lamberton, A., Mathieu, M., Bertrand, T.*, et al.* (2014). A highly potent and selective Vps34 inhibitor alters vesicle trafficking and autophagy. Nature chemical biology *10*, 1013-1019.

Rozycka, M., Lu, Y.J., Brown, R.A., Lau, M.R., Shipley, J.M., and Fry, M.J. (1998). cDNA cloning of a third human C2-domain-containing class II phosphoinositide 3-kinase, PI3K-C2gamma, and chromosomal assignment of this gene (PIK3C2G) to 12p12. Genomics *54*, 569-574.

Russell, R.C., Tian, Y., Yuan, H., Park, H.W., Chang, Y.Y., Kim, J., Kim, H., Neufeld, T.P., Dillin, A., and Guan, K.L. (2013). ULK1 induces autophagy by phosphorylating Beclin-1 and activating VPS34 lipid kinase. Nature cell biology *15*, 741-750.

Sabri, S., Foudi, A., Boukour, S., Franc, B., Charrier, S., Jandrot-Perrus, M., Farndale, R.W., Jalil, A., Blundell, M.P., Cramer, E.M.*, et al.* (2006). Deficiency in the Wiskott-Aldrich protein induces premature proplatelet formation and platelet production in the bone marrow compartment. Blood *108*, 134-140.

Sadoul, K. (2015). New explanations for old observations: marginal band coiling during platelet activation. Journal of thrombosis and haemostasis : JTH *13*, 333-346.

Saelman, E.U., Nieuwenhuis, H.K., Hese, K.M., de Groot, P.G., Heijnen, H.F., Sage, E.H., Williams, S., McKeown, L., Gralnick, H.R., and Sixma, J.J. (1994). Platelet adhesion to collagen types I through VIII under conditions of stasis and flow is mediated by GPIa/IIa (alpha 2 beta 1-integrin). Blood *83*, 1244-1250.

Sagona, A.P., Nezis, I.P., Pedersen, N.M., Liestol, K., Poulton, J., Rusten, T.E., Skotheim, R.I., Raiborg, C., and Stenmark, H. (2010). PtdIns(3)P controls cytokinesis through KIF13A-mediated recruitment of FYVE-CENT to the midbody. Nature cell biology *12*, 362-371.

Salamon, R.S., and Backer, J.M. (2013). Phosphatidylinositol-3,4,5-trisphosphate: tool of choice for class I PI 3-kinases. BioEssays : news and reviews in molecular, cellular and developmental biology *35*, 602-611.

Sandri, M., Sandri, C., Gilbert, A., Skurk, C., Calabria, E., Picard, A., Walsh, K., Schiaffino, S., Lecker, S.H., and Goldberg, A.L. (2004). Foxo

transcription factors induce the atrophy-related ubiquitin ligase atrogin-1 and cause skeletal muscle atrophy. Cell *117*, 399-412.

Santilli, F., Vazzana, N., Liani, R., Guagnano, M.T., and Davi, G. (2012). Platelet activation in obesity and metabolic syndrome. Obesity reviews : an official journal of the International Association for the Study of Obesity *13*, 27-42.

Schafer, D.A., Jennings, P.B., and Cooper, J.A. (1996). Dynamics of capping protein and actin assembly in vitro: uncapping barbed ends by polyphosphoinositides. The Journal of cell biology *135*, 169-179.

Scheller, E.L., Cawthorn, W.P., Burr, A.A., Horowitz, M.C., and MacDougald, O.A. (2016). Marrow Adipose Tissue: Trimming the Fat. Trends in endocrinology and metabolism: TEM *27*, 392-403.

Scheller, E.L., Doucette, C.R., Learman, B.S., Cawthorn, W.P., Khandaker, S., Schell, B., Wu, B., Ding, S.Y., Bredella, M.A., Fazeli, P.K.*, et al.* (2015). Region-specific variation in the properties of skeletal adipocytes reveals regulated and constitutive marrow adipose tissues. Nature communications *6*, 7808.

Schink, K.O., Raiborg, C., and Stenmark, H. (2013). Phosphatidylinositol 3-phosphate, a lipid that regulates membrane dynamics, protein sorting and cell signalling. BioEssays : news and reviews in molecular, cellular and developmental biology *35*, 900-912.

Schmugge, M., Rand, M.L., and Freedman, J. (2003). Platelets and von Willebrand factor. Transfusion and apheresis science : official journal of the World Apheresis Association : official journal of the European Society for Haemapheresis *28*, 269-277.

Schulze, H., Korpal, M., Hurov, J., Kim, S.W., Zhang, J., Cantley, L.C., Graf, T., and Shivdasani, R.A. (2006). Characterization of the megakaryocyte demarcation membrane system and its role in thrombopoiesis. Blood *107*, 3868-3875.

Schulze, H., and Shivdasani, R.A. (2004). Molecular mechanisms of megakaryocyte differentiation. Seminars in thrombosis and hemostasis *30*, 389-398.

Schwertz, H., Koster, S., Kahr, W.H., Michetti, N., Kraemer, B.F., Weitz, D.A., Blaylock, R.C., Kraiss, L.W., Greinacher, A., Zimmerman, G.A.*, et al.* (2010). Anucleate platelets generate progeny. Blood *115*, 3801-3809.

Sharifi, M.N., Mowers, E.E., Drake, L.E., Collier, C., Chen, H., Zamora, M., Mui, S., and Macleod, K.F. (2016). Autophagy Promotes Focal Adhesion Disassembly and Cell Motility of Metastatic Tumor Cells through the Direct Interaction of Paxillin with LC3. Cell reports *15*, 1660-1672.

Shattil, S.J., and Bennett, J.S. (1981). Platelets and their membranes in hemostasis: physiology and pathophysiology. Annals of internal medicine *94*, 108-118.

Shivdasani, R.A., Fujiwara, Y., McDevitt, M.A., and Orkin, S.H. (1997). A lineage-selective knockout establishes the critical role of transcription factor GATA-1 in megakaryocyte growth and platelet development. The EMBO journal *16*, 3965-3973.

Simonsen, A., Lippe, R., Christoforidis, S., Gaullier, J.M., Brech, A., Callaghan, J., Toh, B.H., Murphy, C., Zerial, M., and Stenmark, H. (1998). EEA1 links PI(3)K function to Rab5 regulation of endosome fusion. Nature *394*, 494-498.

Singer, K., DelProposto, J., Morris, D.L., Zamarron, B., Mergian, T., Maley, N., Cho, K.W., Geletka, L., Subbaiah, P., Muir, L.*, et al.* (2014). Diet-induced obesity promotes myelopoiesis in hematopoietic stem cells. Molecular metabolism *3*, 664-675.

Solar, G.P., Kerr, W.G., Zeigler, F.C., Hess, D., Donahue, C., de Sauvage, F.J., and Eaton, D.L. (1998). Role of c-mpl in early hematopoiesis. Blood *92*, 4-10.

Sorrentino, S., Studt, J.D., Medalia, O., and Tanuj Sapra, K. (2015). Roll, adhere, spread and contract: structural mechanics of platelet function. European journal of cell biology *94*, 129-138.

Spinler, K.R., Shin, J.W., Lambert, M.P., and Discher, D.E. (2015). Myosin-II repression favors pre/proplatelets but shear activation generates platelets and fails in macrothrombocytopenia. Blood *125*, 525-533.

Sporn, L.A., Marder, V.J., and Wagner, D.D. (1989). Differing polarity of the constitutive and regulated secretory pathways for von Willebrand factor in endothelial cells. The Journal of cell biology *108*, 1283-1289.

Stopkova, P., Saito, T., Papolos, D.F., Vevera, J., Paclt, I., Zukov, I., Bersson, Y.B., Margolis, B.A., Strous, R.D., and Lachman, H.M. (2004). Identification of PIK3C3 promoter variant associated with bipolar disorder and schizophrenia. Biological psychiatry *55*, 981-988.

Stossel, T.P., Fenteany, G., and Hartwig, J.H. (2006). Cell surface actin remodeling. Journal of cell science *119*, 3261-3264.

Suzuki, T., Oiso, N., Gautam, R., Novak, E.K., Panthier, J.J., Suprabha, P.G., Vida, T., Swank, R.T., and Spritz, R.A. (2003). The mouse organellar biogenesis mutant buff results from a mutation in Vps33a, a homologue of yeast vps33 and Drosophila carnation. Proceedings of the National Academy of Sciences of the United States of America *100*, 1146-1150.

Tadokoro, S., Shattil, S.J., Eto, K., Tai, V., Liddington, R.C., de Pereda, J.M., Ginsberg, M.H., and Calderwood, D.A. (2003). Talin binding to integrin beta tails: a final common step in integrin activation. Science *302*, 103-106.

Tang, R., Zhao, X., Fang, C., Tang, W., Huang, K., Wang, L., Li, H., Feng, G., Zhu, S., Liu, H.*, et al.* (2008). Investigation of variants in the promoter region of PIK3C3 in schizophrenia. Neuroscience letters *437*, 42-44.

Thon, J.N., Macleod, H., Begonja, A.J., Zhu, J., Lee, K.C., Mogilner, A., Hartwig, J.H., and Italiano, J.E., Jr. (2012). Microtubule and cortical forces determine platelet size during vascular platelet production. Nature communications *3*, 852.

Thon, J.N., Montalvo, A., Patel-Hett, S., Devine, M.T., Richardson, J.L., Ehrlicher, A., Larson, M.K., Hoffmeister, K., Hartwig, J.H., and Italiano, J.E., Jr. (2010). Cytoskeletal mechanics of proplatelet maturation and

platelet release. The Journal of cell biology *191*, 861-874.

Thoresen, S.B., Pedersen, N.M., Liestol, K., and Stenmark, H. (2010). A phosphatidylinositol 3-kinase class III sub-complex containing VPS15, VPS34, Beclin 1, UVRAG and BIF-1 regulates cytokinesis and degradative endocytic traffic. Experimental cell research *316*, 3368-3378.

Thorpe, L.M., Yuzugullu, H., and Zhao, J.J. (2015). PI3K in cancer: divergent roles of isoforms, modes of activation and therapeutic targeting. Nature reviews Cancer *15*, 7-24.

Tibolla, G., Pineiro, R., Chiozzotto, D., Mavrommati, I., Wheeler, A.P., Norata, G.D., Catapano, A.L., Maffucci, T., and Falasca, M. (2013). Class II phosphoinositide 3-kinases contribute to endothelial cells morphogenesis. PloS one *8*, e53808.

Tijssen, M.R., and Ghevaert, C. (2013). Transcription factors in late megakaryopoiesis and related platelet disorders. Journal of thrombosis and haemostasis : JTH *11*, 593-604.

Toker, A., and Cantley, L.C. (1997). Signalling through the lipid products of phosphoinositide-3-OH kinase. Nature *387*, 673-676.

Trayhurn, P., and Wood, I.S. (2004). Adipokines: inflammation and the pleiotropic role of white adipose tissue. The British journal of nutrition *92*, 347-355.

Trottier, M.D., Naaz, A., Li, Y., and Fraker, P.J. (2012). Enhancement of hematopoiesis and lymphopoiesis in diet-induced obese mice. Proceedings of the National Academy of Sciences of the United States of America *109*, 7622-7629.

Tuloup-Minguez, V., Hamai, A., Greffard, A., Nicolas, V., Codogno, P., and Botti, J. (2013). Autophagy modulates cell migration and beta1 integrin membrane recycling. Cell cycle *12*, 3317-3328.

Turner, S.J., Domin, J., Waterfield, M.D., Ward, S.G., and Westwick, J. (1998). The CC chemokine monocyte chemotactic peptide-1 activates both the class I p85/p110 phosphatidylinositol 3-kinase and the class II PI3K-C2alpha. The Journal of biological chemistry *273*, 25987-25995.

Ung, T.H., Madsen, H.J., Hellwinkel, J.E., Lencioni, A.M., and Graner, M.W. (2014). Exosome proteomics reveals transcriptional regulator proteins with potential to mediate downstream pathways. Cancer science *105*, 1384-1392.

Urban, D., Li, L., Christensen, H., Pluthero, F.G., Chen, S.Z., Puhacz, M., Garg, P.M., Lanka, K.K., Cummings, J.J., Kramer, H.*, et al.* (2012). The VPS33B-binding protein VPS16B is required in megakaryocyte and platelet alpha-granule biogenesis. Blood *120*, 5032-5040.

Valet, C., Chicanne, G., Severac, C., Chaussade, C., Whitehead, M.A., Cabou, C., Gratacap, M.P., Gaits-Iacovoni, F., Vanhaesebroeck, B., Payrastre, B.*, et al.* (2015). Essential role of class II PI3K-C2alpha in platelet membrane morphology. Blood *126*, 1128-1137.

Valet, C., Severin, S., Chicanne, G., Laurent, P.A., Gaits-Iacovoni, F., Gratacap, M.P., and Payrastre, B. (2016). The role of class I, II and III PI 3-kinases in platelet production and activation and their implication in thrombosis. Advances in biological regulation *61*, 33-41.

van Nispen tot Pannerden, H., de Haas, F., Geerts, W., Posthuma, G., van Dijk, S., and Heijnen, H.F. (2010). The platelet interior revisited: electron tomography reveals tubular alpha-granule subtypes. Blood *116*, 1147-1156.

Vanhaesebroeck, B., Guillermet-Guibert, J., Graupera, M., and Bilanges, B. (2010). The emerging mechanisms of isoform-specific PI3K signalling. Nature reviews Molecular cell biology *11*, 329-341.

Veljkovic, D.K., Rivard, G.E., Diamandis, M., Blavignac, J., Cramer-Borde, E.M., and Hayward, C.P. (2009). Increased expression of urokinase plasminogen activator in Quebec platelet disorder is linked to megakaryocyte differentiation. Blood *113*, 1535-1542.

Viaud, J., Mansour, R., Antkowiak, A., Mujalli, A., Valet, C., Chicanne, G., Xuereb, J.M., Terrisse, A.D., Severin, S., Gratacap, M.P., *et al.* (2016). Phosphoinositides: Important lipids in the coordination of cell dynamics. Biochimie *125*, 250-258.

Vulto-van Silfhout, A.T., Hehir-Kwa, J.Y., van Bon, B.W., Schuurs-Hoeijmakers, J.H., Meader, S., Hellebrekers, C.J., Thoonen, I.J., de Brouwer, A.P., Brunner, H.G., Webber, C., *et al.* (2013). Clinical significance of de novo and inherited copy-number variation. Human mutation *34*, 1679-1687.

Wang, J.F., Liu, Z.Y., and Groopman, J.E. (1998). The alpha-chemokine receptor CXCR4 is expressed on the megakaryocytic lineage from progenitor to platelets and modulates migration and adhesion. Blood *92*, 756-764.

Wang, L., Budolfson, K., and Wang, F. (2011). Pik3c3 deletion in pyramidal neurons results in loss of synapses, extensive gliosis and progressive neurodegeneration. Neuroscience *172*, 427-442.

Wang, Y., Yoshioka, K., Azam, M.A., Takuwa, N., Sakurada, S., Kayaba, Y., Sugimoto, N., Inoki, I., Kimura, T., Kuwaki, T., *et al.* (2006). Class II phosphoinositide 3-kinase alpha-isoform regulates Rho, myosin phosphatase and contraction in vascular smooth muscle. The Biochemical journal *394*, 581-592.

Watson, S.P., Auger, J.M., McCarty, O.J., and Pearce, A.C. (2005). GPVI and integrin alphaIIb beta3 signaling in platelets. Journal of thrombosis and haemostasis : JTH *3*, 1752-1762.

Wendling, F., Maraskovsky, E., Debili, N., Florindo, C., Teepe, M., Titeux, M., Methia, N., Breton-Gorius, J., Cosman, D., and Vainchenker, W. (1994). cMpl ligand is a humoral regulator of megakaryocytopoiesis. Nature *369*, 571-574.

White, E., Mehnert, J.M., and Chan, C.S. (2015). Autophagy, Metabolism, and Cancer. Clinical cancer research : an official journal of the American Association for Cancer Research *21*, 5037-5046.

White, J.G., and Rao, G.H. (1998). Microtubule coils versus the surface membrane cytoskeleton in maintenance and restoration of platelet discoid shape. The American journal of pathology *152*, 597-609.

Willinger, T., and Flavell, R.A. (2012). Canonical autophagy dependent on the class III phosphoinositide-3 kinase Vps34 is required for naive T-cell homeostasis. Proceedings of the National Academy of Sciences of the United States of America *109*, 8670-8675.

Wright, H.M., Clish, C.B., Mikami, T., Hauser, S., Yanagi, K., Hiramatsu, R., Serhan, C.N., and Spiegelman, B.M. (2000). A synthetic antagonist for the peroxisome proliferator-activated receptor gamma inhibits adipocyte differentiation. The Journal of biological chemistry *275*, 1873-1877.

Yamada, E., Bastie, C.C., Koga, H., Wang, Y., Cuervo, A.M., and Pessin, J.E. (2012). Mouse skeletal muscle fiber-type-specific macroautophagy and muscle wasting are regulated by a Fyn/STAT3/Vps34 signaling pathway. Cell reports *1*, 557-569.

Yang, H., Youm, Y.H., Vandanmagsar, B., Rood, J., Kumar, K.G., Butler, A.A., and Dixit, V.D. (2009). Obesity accelerates thymic aging. Blood *114*, 3803-3812.

Yoshioka, K., Yoshida, K., Cui, H., Wakayama, T., Takuwa, N., Okamoto, Y., Du, W., Qi, X., Asanuma, K., Sugihara, K.*, et al.* (2012). Endothelial PI3K-C2alpha, a class II PI3K, has an essential role in angiogenesis and vascular barrier function. Nature medicine *18*, 1560-1569.

Youssefian, T., and Cramer, E.M. (2000). Megakaryocyte dense granule components are sorted in multivesicular bodies. Blood *95*, 4004-4007.

Yousuf, O., and Bhatt, D.L. (2011). The evolution of antiplatelet therapy in cardiovascular disease. Nature reviews Cardiology *8*, 547-559.

Yuan, H.X., Russell, R.C., and Guan, K.L. (2013). Regulation of PIK3C3/VPS34 complexes by MTOR in nutrient stress-induced autophagy. Autophagy *9*, 1983-1995.

Zauli, G., and Catani, L. (1995). Human megakaryocyte biology and pathophysiology. Critical reviews in oncology/hematology *21*, 135-157.

Zhang, J., Varas, F., Stadtfeld, M., Heck, S., Faust, N., and Graf, T. (2007). CD41-YFP mice allow in vivo labeling of megakaryocytic cells and reveal a subset of platelets hyperreactive to thrombin stimulation. Experimental hematology *35*, 490-499.

Zhang, Y., Wang, Z., Liu, D.X., Pagano, M., and Ravid, K. (1998). Ubiquitin-dependent degradation of cyclin B is accelerated in polyploid megakaryocytes. The Journal of biological chemistry *273*, 1387-1392.

Zhang, Y., Wang, Z., and Ravid, K. (1996). The cell cycle in polyploid megakaryocytes is associated with reduced activity of cyclin B1-dependent cdc2 kinase. The Journal of biological chemistry *271*, 4266-4272.

Zhong, Y., Wang, Q.J., Li, X., Yan, Y., Backer, J.M., Chait, B.T., Heintz, N., and Yue, Z. (2009). Distinct regulation of autophagic activity by Atg14L and Rubicon associated with Beclin 1-phosphatidylinositol-3-kinase complex. Nature cell biology *11*, 468-476.

Zhou, X., Takatoh, J., and Wang, F. (2011). The mammalian class 3 PI3K (PIK3C3) is required for early embryogenesis and cell proliferation. PloS one *6*, e16358.

Zhou, X., Wang, L., Hasegawa, H., Amin, P., Han, B.X., Kaneko, S., He, Y., and Wang, F. (2010). Deletion of PIK3C3/Vps34 in sensory neurons causes rapid neurodegeneration by disrupting the endosomal but not the autophagic pathway. Proceedings of the National Academy of Sciences of the United States of America *107*, 9424-9429.

Zimmet, J., and Ravid, K. (2000). Polyploidy: occurrence in nature, mechanisms, and significance for the megakaryocyte-platelet system. Experimental hematology *28*, 3-16.

Annexes

Annexe n°1

Phosphoinositides: important lipids in the coordination of cell dynamics.

Julien Viaud[1], Rana Mansour[2], Adrien Antkowiak[2], Abdulrahman Mujalli[2], Colin Valet[2],Jean-Marie Xuereb[2], Anne-Dominique Terrisse[2], Sonia Severin[2], Marie-Pierre Gratacap[2], Frédérique Gaits-Iacovoni[2], Bernard Payrastre[3]

[1] Inserm U1048, I2MC and Universite Paul Sabatier, 31432, Toulouse Cedex 04, France. Electronic address: julien.viaud@inserm.fr

[2] Inserm U1048, I2MC and Universite Paul Sabatier, 31432, Toulouse Cedex 04, France

[3] Inserm U1048, I2MC and Universite Paul Sabatier, 31432, Toulouse Cedex 04, France. Centre Hospitalier Universitaire de Toulouse, Laboratoire d'Hématologie, Toulouse, France. Electronic address: bernard.payrastre@inserm.fr

Review in Biochimie 2016; 125: 250-8

Biochimie 125 (2016) 250–258

Contents lists available at ScienceDirect

Biochimie

journal homepage: www.elsevier.com/locate/biochi

Review

Phosphoinositides: Important lipids in the coordination of cell dynamics

Julien Viaud [a, *], Rana Mansour [a], Adrien Antkowiak [a], Abdulrahman Mujalli [a], Colin Valet [a], Gaëtan Chicanne [a], Jean-Marie Xuereb [a], Anne-Dominique Terrisse [a], Sonia Séverin [a], Marie-Pierre Gratacap [a], Frédérique Gaits-Iacovoni [a], Bernard Payrastre [a, b, *]

[a] INSERM UMR 1048, Institut des Maladies Métaboliques et Cardiovasculaires (I2MC), Université Toulouse III Paul Sabatier, 1 Avenue Jean Poulhès, BP84225, 31432 Toulouse Cedex 04, France
[b] Centre Hospitalier Universitaire de Toulouse, Laboratoire d'Hématologie, 31059 Toulouse Cedex 03, France

ARTICLE INFO

Article history:
Received 10 July 2015
Accepted 2 September 2015
Available online 25 September 2015

Keywords:
Phosphoinositides
Cell signaling
Lipids
Pathologies
Phosphoinositide-metabolizing enzymes
PI3K

ABSTRACT

By interacting specifically with proteins, phosphoinositides organize the spatiotemporal formation of protein complexes involved in the control of intracellular signaling, vesicular trafficking and cytoskeleton dynamics. A set of specific kinases and phosphatases ensures the production, degradation and interconversion of phosphoinositides to achieve a high level of precision in the regulation of cellular dynamics coordinated by these lipids. The direct involvement of these enzymes in cancer, genetic or infectious diseases, and the recent arrival of inhibitors targeting specific phosphoinositide kinases in clinic, emphasize the importance of these lipids and their metabolism in the biomedical field.

Contents

* Corresponding authors. INSERM UMR 1048, Institut des Maladies Métaboliques et Cardiovasculaires (I2MC), Université Toulouse III Paul Sabatier, 1 Avenue Jean Poulhès, BP84225, 31432 Toulouse Cedex 04, France.
E-mail addresses: julien.viaud@inserm.fr (J. Viaud), bernard.payrastre@inserm.fr (B. Payrastre).

http://dx.doi.org/10.1016/j.biochi.2015.09.005

1. Introduction

Phosphoinositides (PIs), also called inositol lipids, are glycerophospholipids that account for about 10–15% of membrane phospholipids. They are composed of two fatty acids, predominantly stearic acid (C18:0) in position 1 and arachidonic acid (C20:4) in position 2, but other minor molecular species coexist in most cells. These fatty acids are attached to a glycerol backbone, which is connected to an inositol ring by a phosphodiester bond (Fig. 1, **top left**). Despite the presence of five free

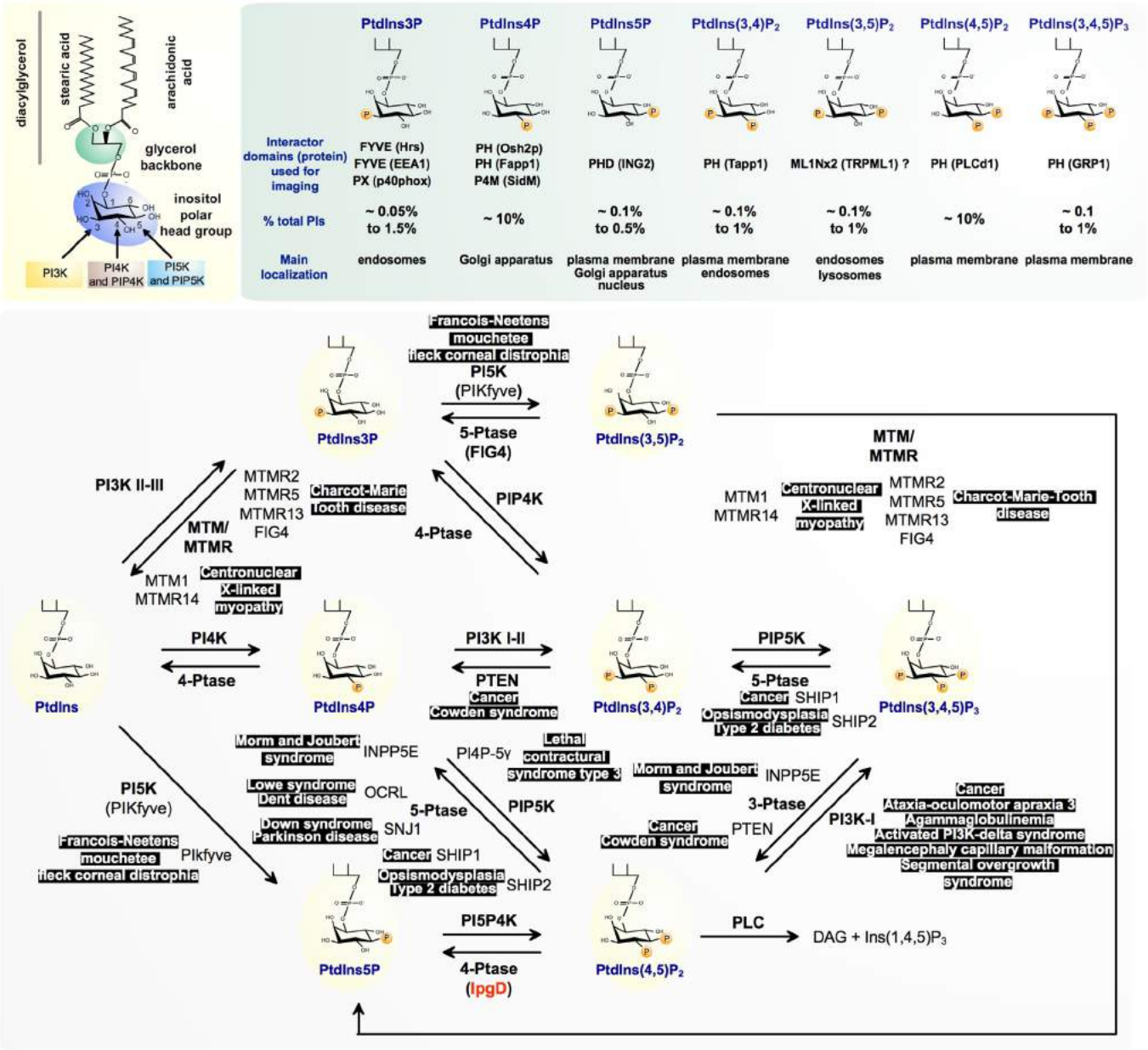

Fig. 1. Phosphoinositides: structure, localization, metabolism and pathophysiology.

hydroxyl groups in the inositol ring, only the positions 3, 4 and 5 are phosphorylated by specific kinases. Steric hindrance likely prevents access to positions 1 and 6 by the kinases. Thus, in addition to phosphatidylinositol (PtdIns) representing 80% of the total level of PIs, 7 other PIs were identified, corresponding to the various combinations of phosphorylation of the inositol ring (Fig. 1, **top right**). PtdIns4P and PtdIns(4,5)P_2 represent ~10% of total PIs while the remaining species do not represent more than 1%–2% (Fig. 1, **top right**). PIs are characterized by an highly active metabolism involving a set of tightly regulated specific kinases and phosphatases (Fig. 1, bottom), a reflection of their role as second messengers. These lipids can directly interact with protein domains including PH (Pleckstrin Homology), FYVE (Fab-1, YGL023, Vps27 and EEA1), PX (phox) or ENTH (Epsin N-Terminal Homology) domains. Following various stimuli (hormones, growth factors, adhesion molecules, chemoattractants, stresses, etc …), PI-kinases and -phosphatases are relocalized, activated or inhibited to allow the spatio-temporal formation of membrane territories with specific PIs content. PIs can then coordinate the recruitment of specific signaling proteins to control cellular events. The use of PI-interacting domains to locate these lipids by imaging has generated much interest in recent years. Using these approaches, it has been shown that PtdIns(4,5)P_2, PtdIns(3,4)P_2 and PtdIns(3,4,5)P_3 are predominantly localized at the plasma membrane [1,2] while PtdIns3P is preferentially found on early endosomes [3] and PtdIns4P is present both at the plasma membrane and at the Golgi apparatus [4]. In some cells, the distribution of PIs is essential to maintain cell polarity [5]. In this review we will discuss the role of the different PIs and the implication of PI-metabolic enzymes in pathologies such as cancer and arterial thrombosis. We will emphasize on the role of class I PI3-kinases (PI3K) and their recent therapeutic use in the treatment of cancer.

2. Phosphoinositides: different roles for different species

2.1. PtdIns3P [3]

This lipid is present in small amounts in eukaryotic cells and is mainly generated from PtdIns by class II and class III PI3Ks (protein domains are shown in Fig. 2). It is also produced by dephosphorylation of PtdIns(3,4)P_2 by a type Iα 4-phosphatase, and of PtdIns(3,5)P_2 by a 5-phosphatase called Fig4 (or Sac3). Class II PI3Ks [6,7] and type Iα 4-phosphatase [8] may generate a pool of PtdIns3P at the plasma membrane while the class III PI3K (also called Vps34) and Fig4 could be responsible for the control of the endosomal pool [9]. It is noteworthy that class III PI3K also plays a major role in autophagy by producing PtdIns3P in autophagosomes [10]. Except in cells infected by the pathogen *Plasmodium falciparum,* which exhibit an important increase in PtdIns3P levels [11], literature does not report example of major modifications of PtdIns3P levels. However, a number of cellular stimuli can induce modest increases in the amount of PtdIns3P. This the case in platelets following thrombin or collagen-related peptide (CRP) situlation [7,12]. However, the maintenance of a basal, housekeeping, pool of PtdIns3P appears to be essential for cellular homeostasis, particularly in the control of intracellular trafficking and membrane dynamics and structuration [6,7]. PtdIns3P recruits protein effectors through FYVE or PX domains (FYVE domains are widely used to locate this lipid by imaging) and, according to its location, regulates: i) intracellular trafficking (endosomal fusion, vesicle recycling to the plasma membrane and to the trans-Golgi, vesicular sorting to lysosomal compartments) [3]; ii) autophagosome maturation by recruiting proteins from the Atg-18 family (WIPI1 and 2) [13]; iii) exocytosis of insulin granules by an unknown mechanism [14]; iv) activation of p40phox, a component of the NADPH oxidase [15]; v) cytokinesis as it recruits the protein FYVE-HUNDRED to cytokinetic bridges [16]. PtdIns3P is also an important intermediate in the biosynthesis of PtdIns(3,5)P_2 through phosphorylation by the 5-kinase PIKfyve. Thus, PtdIns3P has many roles but its involvement in the regulation of intracellular trafficking (endosomal pathway and autophagy) is the best characterized.

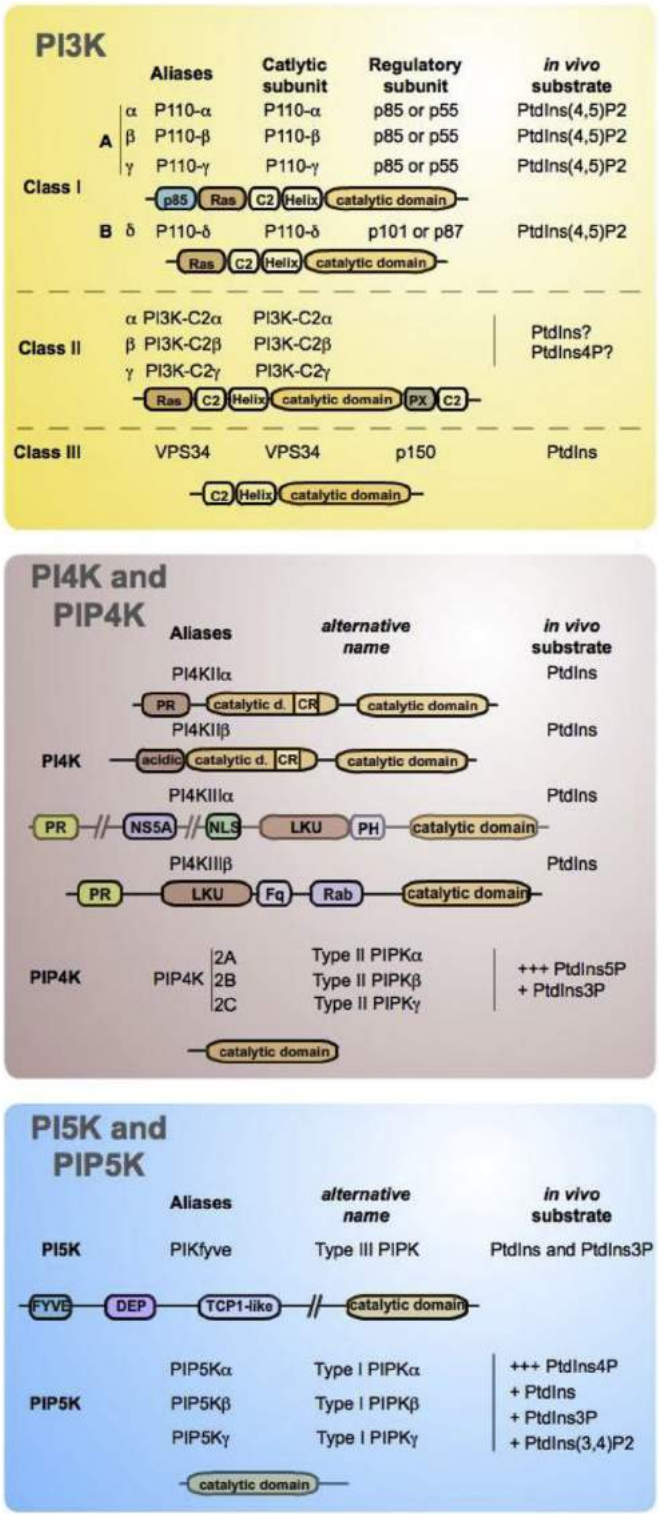

Fig. 2. Protein domain organization and *in vivo* substrates of phosphoinositide kinases.

2.2. PtdIns4P [4]

This is one of the most abundant PI. It is mainly present at the Golgi apparatus and at the plasma membrane, but it is also found in endosomal compartments and in the trans-Golgi. Its production is ensured in mammals by two class II PI4K (PI4KII α and β) and two class III PI4K (PI4KIII α and β) (protein domains are shown in Fig. 2). PI4KIIα is predominantly found in the endosomal system, the trans-Golgi and the plasma membrane [17] while PI4KIIβ is mainly present at the plasma membrane [18]. The regulation of these kinases is still unclear. PI4KIIIα is present at the plasma membrane, at the endoplasmic reticulum (ER) and at the Golgi apparatus. PI4KIIIβ is described as the enzyme responsible for the synthesis of PtdIns4P at the Golgi apparatus following its interaction with the small G protein Arf1 and the NCS-1 (neuronal calcium sensor-1) protein [19]. It is activated by phosphorylation and maintained active by interactions with 14-3-3 proteins that prevent its dephosphorylation [20]. Another enzyme involved in the metabolism of PtdIns4P is the 4-phosphatase Sac1 which is localized at the ER and at the plasma membrane. Following nutrient deprivation, Sac1 relocates at the Golgi apparatus to decrease the local pool of PtdIns4P [21]. Recently, it has been shown that proteins from the OSBP family are able to transfer the PtdIns4P from the trans-Golgi or the plasma membrane to the RE in a cholesterol-dependent way [22]. PtdIns4P regulates vesicular transport from the Golgi apparatus to the plasma membrane and the endosomal compartments. Thus, this lipid ensures several functions including: i) location of enzymes resident in the Golgi apparatus; ii) vesicle formation by inducing membrane deformations [23]; iii) sorting of proteins to endosomes (by interacting with the clathrin adapter protein, GGA2, which in turn interacts with Arf1 for an efficient recruitment) [24] and iv) proteins transport from the trans-Golgi to the plasma membrane (which involves the recruitment and activation of Sec2, an exchange factor of Rab proteins) [25]. In addition, PtdIns4P is a key intermediate in the biosynthesis of PtdIns(4,5)P_2 at the plasma membrane.

2.3. PtdIns5P [26]

This is the last identified PI, which is present in low amounts in quiescent cells. This lipid can be synthesized by phosphorylation of PtdIns by the 5-kinase PIKfyve but also by dephosphorylation of PtdIns(3,5)P_2 by 3-phosphatases of the myotubularins family. Although it has never been clearly demonstrated, it can also be generated by mammalian type II 4-phosphatases acting on PtdIns(4,5)P_2. Conversely, it has been shown that PtdIns5P is specifically phosphorylated by PIP4K A, B and C (also called type II PIPKα, β and γ) to produce PtdIns(4,5)P_2 (protein domains are shown in Fig. 2). The level of PtdIns5P increases following specific stimuli (thrombin, insulin, FGF-1, some oncogenes, osmotic stress, H_2O_2, UV, bacterial infection) [26]. It is located at the plasma membrane and in intracellular compartments (including endosomes, ER and Golgi apparatus) [27]. The functions associated to PtdIns5P increase are different regarding the location of this lipid. The best characterized correspond to nuclear PtdIns5p which has been described as a stress-response element. In the nucleus, PtdIns5P modulates gene expression by interacting with proteins involved in chromatin remodeling. PtdIns5P interacts especially with the PHD domain of ING2, which is commonly used as a probe to image this lipid [28]. Our team pioneered a body of work, starting from 2002, that demonstrated that the virulence factor of *Shigella flexneri*, IpgD (Invasion plasmid gene D), is a powerful PtdIns(4,5)P_2 4-phosphatase producing significant amounts of PtdIns5P in the host cell upon infection. Subsequently, PtdIns5P generated at the entry sites of the bacteria, modulates membrane dynamics and intracellular signals of the host cell [29]. It induces clustering, ligand-free activation and stabilization of the EGF receptor by impairing lysosomal trafficking, thereby activating survival signaling of the host cell for the benefit of bacteria [30,31]. Interestingly, this blockade of EGFR degradation seems to involve TOM1 [32]. Moreover, this increase in PtdIns5P at the plasma membrane leads to the closure of connexin hemichannels, which normally release ATP in the extracellular medium to activate the inflammatory reaction against the pathogen [33]. Thus, the bacterial pathogen uses PtdIns5P to hijack host cell molecular machinery and responses for its benefit. Besides this pathological situation, the role of PtdIns5P in physiology remains largely unknown. It has been shown that the engagement of the T receptor (TCR) in T cells induces an increase in PtdIns5P, which in turns recruits DOK (Downstream of Tyrosine Kinases) family proteins to promote their phosphorylation and to activate a negative feedback loop [34]. Stimulation of adipocytes with insulin also induces a peak production of PtdIns5P resulting in the loss of actin stress fibers and the acceleration of the translocation of the glucose transporter GLUT4 to the plasma membrane [35]. Recently, we have shown that PtdIns5P was coordinating membrane dynamics and actin cytoskeleton reorganization. Indeed, an increase in PtdIns5P levels resulting from either ectopic expression of the bacterial phosphatase IpgD, stimulation of cells with FGF-1 or expression of the NPM-ALK oncogene, leads to the recruitment and the activation of the guanine nucleotide factor exchange (GEF) Tiam1 by direct interaction of the lipid with its C-terminal PH domain. This interaction leads to Rac1 activation and induces a strong membrane dynamics associated with the loss of actin fibers promoting cell motility and invasion [36]. Recruitment and local activation of the Tiam1/Rac1 module happens to be restricted to endosomes and dorsal ruffles, and to regulate recycling of receptors and secretion of metalloproteinases involved in PtdIns5P-dependent invasion. Recent work demonstrated that PtdIns5P regulates autophagy independently of the canonical pathway involving Vps34 and PtdIns3P, strongly suggesting that non-nuclear PtdIns5P could be a central regulator of vesicular trafficking with different outcomes depending on the way of production [37].

2.4. PtdIns(3,4)P_2 [38]

This PI is produced at the plasma membrane upon cell stimulation by dephosphorylation of PtdIns(3,4,5)P_3 by the 5 phosphatase SHIP1, SHIP2 and SKIP whose expression varies according to tissues. Class II PI3Ks have been reported to produce a pool of PtdIns(3,4)P_2 that controls clathrin-dependent endocytosis from PtdIns4P [39] (protein domains are shown in Fig. 2). Specific functions of PtdIns(3,4)P_2 are still poorly understood and only few effectors have been identified [40]. However, some publications ascribe important functions to this lipid in diverse cellular processes in addition to its role in endocytosis. Those include: i) downregulation of insulin signaling by direct interaction with the PH domain of TAPP1 and 2 [41]; ii) ligand-dependent G protein-coupled receptors endocytosis through a process involving SHIP1, SHIP2, the recruitment of Lamellipodin via its PH domain, and the subsequent recruitment of Endophilin to mediate endocytosis [42]; iii) formation of lamellipodia, possibly throught its interaction with Lamellipodin [43]; and iv) formation of podosomes [44].

2.5. PtdIns(3,5)P_2 [45]

This scarce PI is synthesized mainly through phosphorylation of PtdIns3P by the 5-kinase PIKfyve (protein domains are shown in Fig. 2). PIKfyve operates within a protein complex called PAS (for PIKfyve/ArPIKfyve/Sac3). PAS has the capacity to reversibly produce

PtdIns(3,5)P_2 because of the presence of the 5-phosphatase Sac3 (or Fig4 in mammals), which hydrolyses PtdIns(3,5)P_2 into PtdIns3P [45]. This kinase/phosphatase complex is localized to endosomes, due to the interaction of the FYVE domain of PIKfyve with PtdIns3P [46]. Another important route of PtdIns(3,5)P_2 metabolism implicates the 3-phosphatases of the myotubularins family, which produce PtdIns5P by dephosphorylating PtdIns(3,5)P_2 [47]. RNA silencing and/or inhibition of the enzymes of the PAS complex has shown that these enzymes and PtdIns(3,5)P_2 is involved in homeostasis of endosomal trafficking. PtdIns(3,5)P_2 may regulate endosomal fission and fusion, the retrograde transport of endosomes to the trans-Golgi and vesicle sorting to the late endosome [48–50]. These effects are mediated through effectors having for the majority a β-propeller domain capable to bind this lipid [51,52]. However, the lack of tools to precisely locate PtdIns(3,5)P_2 and specifically block its downstream signaling are major limitations to get a better knowledge of its functions. Current data suggest that PtdIns3P, PtdIns5P and PtdIns(3,5)P_2 are highly connected and that the interconversion between these lipids could be at the basis of the tight regulation and coordination of vesicular trafficking and cytoskeleton dynamics.

2.6. PtdIns(4,5)P_2 [1]

As abundant as PtdIns4P, this lipid is predominantly present in the inner leaflet of the plasma membrane. PtdIns(4,5)P_2 has also been found in the Golgi apparatus, in endosomes, in the endoplasmic reticulum and in the nucleus. Six different kinases control its biosynthesis in a spatiotemporal manner. PIP5Ks α, β and γ (also called type I PIPK (α, β, and γ)) use PtdIns4P as a substrate and produce the majority of PtdIns(4,5)P_2 (protein domains are shown in Fig. 2). PIP4K2 A, B and C (also called type II PIP4K α, β and γ) phosphorylate PtdIns5P at the position 4 to produce a quantitatively minor (but probably very localized) pool of PtdIns(4,5)P_2 (protein domains are shown in Fig. 2).

Historically, the first reports concerning this lipid highlighted the fact that it is the preferred substrate of phospholipase C (PLC) which, upon cellular activation, produce the second messengers inositol trisphosphate (Ins(1,4,5)P_3) and diacylglycerol (DAG). Few years later, it was shown that Class I PI3Ks also use PtdIns(4,5)P_2 as a substrate to produce the second messenger PtdIns(3,4,5)P_3. Thus, PtdIns(4,5)P_2 is at the origin of three fundamental intracellular second messengers. Moreover, it is now well established that PtdIns(4,5)P_2 directly interacts with proteins through specific domain (PH, ENTH, FERM (Four-point-one, Ezrin, Radixin, Moesin)). Through these interactions, it modulates several regulators of the actin cytoskeleton, but also some ion channels. PtdIns(4,5)P_2 is thus a very important lipid directly or indirectly involved in various biological functions.

2.7. PtdIns(3,4,5)P_3 [2]

This PI is a typical lipid second messenger. It is present in trace amounts in quiescent cells and is rapidly and transiently produced by Class I PI3K activation following membrane receptors triggering (protein domains are shown in Fig. 2). PtdIns(3,4,5)P_3 is produced mainly in the inner leaflet of the plasma membrane where it recruits and activates PH domain-containing proteins including the well known protein kinase Akt [53]. Among the different PH domain-containing proteins recruited by this lipid one can note exchange factors of Arf (ARNO and GRP1) or Rac (PREX1 and Vav) [54], tyrosine kinases such as Btk and adapter proteins like GAB1. Some of these PH domains are used to localize PtdIns(3,4,5)P_3 by imaging. In summary, this lipid is highly involved in the formation and the organization of intracellular signaling complexes and thus regulates cell proliferation and survival but also glucose homeostasis, and other processes such as cell polarization [55] and motility [56].

3. How to quantify and localize phosphoinositides?

3.1. Quantification

Different approaches have been developed to quantify PIs including [^{32}Pi] or [^{3}H]-*myo*-inositol metabolic labeling followed by HPLC analysis, mass assay using specific recombinant kinases and more recently mass spectrometry-based measurements.

3.1.1. [^{32}Pi] or [^{3}H]-myo-inositol metabolic labeling

The general procedure of this approach is as follows: i) extract PIs from [^{32}Pi] or [^{3}H]-*myo*-inositol-labeled cells (after stimulation with an agonist for example); ii) separate the different families of PIs by thin layer chromatography (this step is optional) and iii) deacetylate them and separate the resulting glycero-inositol phosphates by anion-exchange HPLC [57]. Separations between each species can be easily performed using a single column except for PtdIns5P, which efficient separation from PtdIns4P requires two anion-exchange HPLC columns mounted in series [27]. One major drawback of this assay is that it does not allow quantification of PIs from biological samples such as tissues biopsies. Furthermore, to detect an increase in mass rather than a change in the turn-over, it is essential to reach the isotopic equilibrium, which is not always possible, for example when primary cells are used. Moreover, this assay requires relatively high amounts of radioactivity and large number of cells.

3.1.2. Mass assay

These assays are based on the phosphorylation of the PI to be quantified by a recombinant specific lipid kinase in the presence of [γ-^{32}P]ATP to generate a new radioactive polyphosphorylated PI. For example, PtdIns5P can be transformed into PtdIns(4,5)P_2 using recombinant PIP4K2α [58] and PtdIns3P into PtdIns(3,5)P_2 by using recombinant PIKfyve [12]. It is important to note that, *in vitro*, an enzyme may not be strictly specific for one lipid and the nature of the radioactive product of the kinase reaction must be clearly identified (using HPLC) to define the best experimental conditions. It is noteworthy that these assays require less radioactivity than the metabolic labeling described above, but generally a large number of cells is needed.

3.1.3. Mass spectrometry

Recently, a mass spectrometry method has been developed to quantify PtdIns(3,4,5)P_3 [59]. It is based on the methylation of the phosphate groups of PIs with TMS-diazomethane coupled to HPLC-mass spectrometry analysis. This very efficient and sensitive method allows the quantification of the different molecular species of PtdIns(3,4,5)P_3 (i.e. the different composition in fatty acyl chains) extracted from any biological samples. It is also possible to quantify PtdIns, PtdInsP and PtdInsP_2 by this method but, unfortunately, it is still impossible to distinguish between the PtdInsP and the PtdInsP_2 isomers because of similar molecular weights and charges.

3.2. Localization

It is possible to localize PIs by imaging using PI-binding domains (Fig. 1, **top right**). These domains can either be used as recombinant proteins or be overexpressed as fluorescent-tag fusions. Recombinant proteins (generally GST tagged) are used on fixed and permeabilized cells, and are then detected using an anti-tag antibody and a secondary antibody coupled to a fluorophore. This two steps

approach using antibodies can be bypassed by directly labeling the PI-binding domain with a fluorophore or by adding a fluorescent tag (GFP or mCherry for example). Another approach is to use antibodies specifically directed against PIs. Since lipids cannot be fixed, caution should be taken during the fixation and permeabilization procedures, as described by Hammond et al. [60]. In the case of overexpression of PI-binding domains, the major drawback is that it cannot be applied to tissues or clinical samples. Moreover, the overexpression of PI-binding proteins may prevent endogenous proteins to interact with their cognate PIs, thereby competing with their endogenous target proteins and interfering with downstream signaling. As a consequence, this approach is often used to block the effect of a specific PI or to localize newly synthesized pools of a PI following a specific stimulus.

4. Phosphoinositide-metabolizing enzymes and pathologies

As illustrated in Table 1 and Fig. 1 (**bottom panel**), loss or gain of function mutations in many PI-metabolizing enzymes are involved in human pathologies. Some genetic diseases such as muscular dystrophy or Charcot-Marie-Tooth myotubular neuropathy are due to mutations in PtdIns3P/PtdIns(3,5)P_2 3-phosphatases of the myotubularins family [61]. Lowe syndrome or Francois-Neetens speckled corneal dystrophy are due to mutations in genes coding for the PtdIns(4,5)P_2 5-phosphatase OCRL and the 5-kinase PIKfyve, respectively. Moreover, the involvement of class I PI3Ks and the PtdIns(3,4,5)P_3 3-phosphatase PTEN in cancer is well documented [62,63] and new molecules modulating this pathway are now available in clinic, as commented below.

5. Targeting PI3K in cancer and thrombosis

PI3K activity associated with a viral oncoprotein was a major discovery by L. Cantley and colleagues in the late 80s [64,65]. Thirty years later, inhibitors of PI3K start to be used in clinic. Indeed, idelalisib, a selective inhibitor of class I PI3Kδ, has just been approved by the “Food and Drug Administration” (FDA) in the US for the treatment of chronic lymphocytic leukemia (CLL) and indolent non-Hodgkin lymphoma (NHL). Inhibitors of class I PI3Kα, which is often mutated in cancer, have entered clinical trials, as well pan Class I PI3K inhibitors. Some result also suggest a potential therapeutic application for Class III PI3K inhibitors in cancer therapy [66]. Moreover, selective inhibitors of PI3Kβ are under development to target platelets in the prevention of arterial thrombosis.

5.1. Class I PI3K and cancer

5.1.1. PI3Kα

PI3Kα (*PIK3CA*) is ubiquitous and plays a major role in cell proliferation and survival as well as insulin receptor signaling. It is now a validated therapeutic target in oncology because gain of function mutations are frequently found in solid cancers in humans [67]. Experimental studies using cell lines and genetically modified mice have demonstrated that two frequently found activating mutations (E545K and H1047R) are sufficient to induce an increase in the level of PtdIns(3,4,5)P_3 and to transform cells [68]. In addition, the presence of these mutations sensitize cells to PI3Kα and mTORC1 pathway inhibitors. Independently of gain-of-function mutations, PI3Kα is activated by many oncogenes and loss of function mutations in the PTEN phosphatase lead to an over-activation of oncogenic signaling pathway.

Some selective PI3Kα inhibitors have entered clinical trials for the treatment of solid cancers with an activating mutation of this kinase. The effect of these inhibitors as monotherapy are relatively limited but their combination with other drugs used in chemotherapy or specifically targeting Poly (ADP-ribose) polymerase (PARP) could yield very interesting results (L. Cantley, personal communication, October 2014). PI3Kα inhibitors could also be useful in the treatment of rare hereditary pathologies associated with somatic mutations of *PIK3CA* (overgrowth syndromes [69]). Finally, under certain conditions, pan-class I PI3K inhibitors could avoid compensation mechanism by another isoform from this class of lipid kinases [70].

5.1.2. PI3Kδ

PI3Kδ is primarily expressed in leukocytes where it plays a key role downstream of antigen receptor in B-cells (BCR) [71]. BCR signaling uses tyrosine phosphorylation of ITAM motifs-based mechanisms (Immunoreceptor Tyrosine-based Activation Motifs) of the intracytoplasmic portion of CD79 to form multiprotein complexes. Syk and Btk tyrosine kinases as well as PI3Kδ are key elements of BCR signaling. PI3Kδ also plays an important role

Table 1
Phosphoinositides and pathophysiology.

Diseases	Genes (protein)	Modifications	Ref.
Lowe syndrome	OCRL	Mutation	[87]
Dent disease	OCRL	Mutation	[88]
Lethal contractural syndrome type 3	PIP5K1C (PtdIns(4)P-5-Kinase 1 Gamma)	Mutation	[89]
Centronuclear X-linked myopathy	MTM1	Mutation	[90]
	MTMR14		
Charcot-Marie-Tooth disease	MTMR2	Mutations	[90]
	MTMR5		
	MTMR13		
	FIG4		
François-Neetens mouchetée fleck corneal dystrophia	PIP5K3 (PIKfyve)	Mutation	[91]
Cowden syndrome/Cancer	PTEN	Mutation	[92]
Cancer	PIK3CA (Classe I PI3K alpha)	p110α mutation, amplification	[93]
Ataxia-oculomotor apraxia 3	PIK3R5 (PI3K p101 subunit)	Mutation	[94]
Agammaglobulinemia	PIK3R1 (PI3K subunit p85 α)	Mutation leading to gene deletion	[95]
Activated PI3K-delta syndrome	(PIK3CD) PI3K p110δ subunit	Activating mutation	[96]
Megalencephaly capillary malformation	PIK3R2 (p85β sub-unit PI3K)/PIK3CA (p110α subunit PI3K)	Mutation	[97]
Cancer (AML, ALL)	INPP5D (SHIP1)	Mutation	[98]
Type 2 diabetes	INPPL1 (SHIP2)	16 bp deletion	[99]
Opsismodysplasia.	INPPL1 (SHIP2)	Mutation	[100]
Morm and Joubert syndromes	INPP5E	Mutation	[101]
Down syndrome/Parkinson disease	SYNJ1 (Synaptojanin 1)	Amplification	[102]
Segmental overgrowth syndrome	PIK3CA (Class I PI3K alpha)	Mutation	[69]

downstream of cytokines/chemokines and adhesion receptors, which strongly contributes to the regulation of proliferation, differentiation, migration and survival of B cells. CLL, the most common leukemia in western Europe, is characterized by an accumulation of B cells (CD5 +) in blood, bone marrow and secondary lymphoid organs. Chronic activation of BCR signaling plays a major role in the pathophysiology and progression of this hematologic malignancy and also in B cells indolent NHL. It is uncommon to observe mutations in genes coding for class I PI3Ks in CLL and indolent NHL. Similarly, the incidence of loss of function mutations in the gene encoding the PTEN phosphatase is low in these pathologies (except for the mantle NHL). However, many studies have shown that *ex vivo* inhibition of PI3Kδ affects the proliferation and survival of CLL patients cells [72]. The first clinical trials with selective PI3Kδ inhibitor (CAL-101 or idelalisib) in relapsing patients showed very encouraging and sustained response with a quick exit of malignant B cells from lymphoid organs accompanied by a transitional hyperlymphocytosis [73,74]. It is important to note that stopping treatment causes a reappearance of the pathology. PI3Kδ inhibition decreases BCR signaling but also the production of chemokines and the response of malignant B cells to chemokines, thus affecting their migration and anchorage to the protective niche provided by the lymphoid tissues. The exit of these cells from the niche reduces the proliferation and survival signals resulting in their progressive death by apoptosis. When idelalisib is associated with molecules such as rituximab (anti-CD20 used to treat these diseases), the destruction of these cells is accelerated. Side effects of idelalisib appeared tolerable to consider a long-term treatment. In France, idelalisib has obtained a temporary authorization for the treatment of relapsed CLL and for refractory follicular NHL with the molecule used as monotherapy or in combination.

In the future, it is conceivable that PI3Kδ inhibitors will also be used in the treatment of some immune diseases linked to hyperactivation of PI3Kδ [75] and for the treatment of non-hematological solid tumors [76].

5.2. PI3Kβ and arterial thrombosis

Blood platelets play a key role in haemostasis and thrombosis. They express all class I PI3K isoforms, but the class I PI3Kβ plays the most important role in this model [77]. A selective inhibitor of PI3Kβ (TGX-221) showed an *ex vivo* antithrombotic potential in arterial flow condition and in *in vivo* experimental thrombosis rat models [78]. The use of mice expressing an inactive p110β or mice deleted of p110β selectively in megakaryocytes and platelets has demonstrated the role of the PI3K downstream of different seven-transmembrane domain receptors (thrombin, thromboxane A2 or ADP receptors), ITAM receptors (collagen receptor GPVI) and integrins (αIIbβ3 and α2β1) [79–81]. One of the amplification loops of platelet activation involves ADP (secreted by platelets at the beginning of activation) and its purinergic receptor P2Y12 (coupled to Gi). The β/γ subunits of Gi interact with p110β, which potentiates PI3Kβ activation. This amplification loop, characteristic of platelets, could explain the predominant role of PI3Kβ this model. PtdIns(3,4,5)P_3 production contributes to the recruitment and activation of several PH domain proteins such as Akt, Btk and PLCγ2. With these mouse models, it has been clearly shown that the inhibition of PI3Kβ has an antithrombotic effect without affecting primary haemostasis and without increasing the bleeding risk [82]. A Phase I clinical trial done with a new selective PI3Kβ inhibitor (AZD6482) also shows no increasing risk of bleeding and indicates a good tolerability of the compound in humans [83,84]. E*x-vivo* experiments confirm the earlier results and underline the importance of this type of inhibitor in the prevention of arterial thrombosis. However, we have recently shown that in pathological arterial flow conditions (during arterial stenosis or during partially occlusive thrombus formation), PI3Kβ inhibition causes thrombus fragmentation with a potential risk of distal embolization which may occlude downstream microvessels [85,86]. In summary, targeting PI3Kβ for the prevention of arterial occlusive thrombosis has a number of benefits (limited bleeding risk, bearable side effects, rapid and reversible effect on arterial thrombosis). It will be, however, essential to determine whether the released thrombus fragments in certain conditions are potentially dangerous or are likely to be dislocated without causing downstream ischemic events.

6. Conclusion

PIs are a family of lipids that strongly contributes to the assembly and the spatiotemporal organization of multi-protein complexes. They are critical to coordinate the maintenance of cellular territories integrity, the organization of signaling pathways, the regulation of intracellular trafficking, the dynamics of cytoskeleton and the cell polarity. A set of specific kinases and phosphatases precisely controls the production and interconversion of the different PIs. A loss of this strict control (due to mutations or modulation of the expression of some of the PI-metabolizing enzymes) leads to pathologies. It is therefore important to characterize the regulatory mechanisms of these kinases and phosphatases and continue the analysis of the role of the different PIs. The recent emergence of class I PI3K inhibitors in clinic illustrates how advances in the understanding of lipid signaling mechanisms can improve the management of some diseases.

Competing interests

The authors declare that they have no competing financial interests.

Acknowledgment

This work was supported by grants from the Agence Nationale de la Recherche (ANR) (ANR-13-BSV2-0004-01), Association pour la Recherche contre le Cancer (ARC), Inserm, la ligue contre le cancer and the Fondation pour la Recherche Médicale. BP is a senior member of the Institut Universitaire de France.

References

[1] Y. Sun, N. Thapa, A.C. Hedman, R.A. Anderson, Phosphatidylinositol 4,5-bisphosphate: targeted production and signaling, BioEssays News Rev. Mol. Cell. Dev. Biol. 35 (2013) 513–522.
[2] R.S. Salamon, J.M. Backer, Phosphatidylinositol-3,4,5-trisphosphate: tool of choice for class I PI 3-kinases, BioEssays News Rev. Mol. Cell. Dev. Biol. 35 (2013) 602–611.
[3] K.O. Schink, C. Raiborg, H. Stenmark, Phosphatidylinositol 3-phosphate, a lipid that regulates membrane dynamics, protein sorting and cell signalling, BioEssays News Rev. Mol. Cell. Dev. Biol. 35 (2013) 900–912.
[4] M.A. De Matteis, C. Wilson, G. D'Angelo, Phosphatidylinositol-4-phosphate: the Golgi and beyond, BioEssays News Rev. Mol. Cell. Dev. Biol. 35 (2013) 612–622.
[5] A. Gassama-Diagne, B. Payrastre, Phosphoinositide signaling pathways: promising role as builders of epithelial cell polarity, Int. Rev. Cell Mol. Biol. 273 (2009) 313–343.
[6] M. Falasca, et al., The role of phosphoinositide 3-kinase C2alpha in insulin signaling, J. Biol. Chem. 282 (2007) 28226–28236.
[7] C. Valet, et al., Essential role of class II PI3K-C2alpha in platelet membrane morphology, Blood 126 (2015) 1128–1137.
[8] I. Ivetac, et al., The type Ialpha inositol polyphosphate 4-phosphatase generates and terminates phosphoinositide 3-kinase signals on endosomes and the plasma membrane, Mol. Biol. Cell 16 (2005) 2218–2233.
[9] J.E. Slessareva, S.M. Routt, B. Temple, V.A. Bankaitis, H.G. Dohlman, Activation of the phosphatidylinositol 3-kinase Vps34 by a G protein alpha subunit at the endosome, Cell 126 (2006) 191–203.
[10] A. Kihara, T. Noda, N. Ishihara, Y. Ohsumi, Two distinct Vps34

phosphatidylinositol 3-kinase complexes function in autophagy and carboxypeptidase Y sorting in Saccharomyces cerevisiae, J. Cell Biol. 152 (2001) 519–530.
[11] L. Tawk, et al., Phosphatidylinositol 3-phosphate, an essential lipid in Plasmodium, localizes to the food vacuole membrane and the apicoplast, Eukaryot. Cell 9 (2010) 1519–1530.
[12] G. Chicanne, et al., A novel mass assay to quantify the bioactive lipid PtdIns3P in various biological samples, Biochem. J. 447 (2012) 17–23.
[13] T. Proikas-Cezanne, Z. Takacs, P. Donnes, O. Kohlbacher, WIPI proteins: essential PtdIns3P effectors at the nascent autophagosome, J. Cell Sci. 128 (2015) 207–217.
[14] V. Dominguez, et al., Class II phosphoinositide 3-kinase regulates exocytosis of insulin granules in pancreatic beta cells, J. Biol. Chem. 286 (2011) 4216–4225.
[15] C. Ellson, K. Davidson, K. Anderson, L.R. Stephens, P.T. Hawkins, PtdIns3P binding to the PX domain of p40phox is a physiological signal in NADPH oxidase activation, EMBO J. 25 (2006) 4468–4478.
[16] A.P. Sagona, et al., PtdIns(3)P controls cytokinesis through KIF13A-mediated recruitment of FYVE-CENT to the midbody, Nat. Cell Biol. 12 (2010) 362–371.
[17] D. Lu, et al., Phosphatidylinositol 4-kinase IIalpha is palmitoylated by Golgi-localized palmitoyltransferases in cholesterol-dependent manner, J. Biol. Chem. 287 (2012) 21856–21865.
[18] Y.J. Wei, et al., Type II phosphatidylinositol 4-kinase beta is a cytosolic and peripheral membrane protein that is recruited to the plasma membrane and activated by Rac-GTP, J. Biol. Chem. 277 (2002) 46586–46593.
[19] A. Godi, et al., ARF mediates recruitment of PtdIns-4-OH kinase-beta and stimulates synthesis of PtdIns(4,5)P2 on the Golgi complex, Nat. Cell Biol. 1 (1999) 280–287.
[20] A. Hausser, et al., Phospho-specific binding of 14-3-3 proteins to phosphatidylinositol 4-kinase III beta protects from dephosphorylation and stabilizes lipid kinase activity, J. Cell Sci. 119 (2006) 3613–3621.
[21] A. Blagoveshchenskaya, et al., Integration of Golgi trafficking and growth factor signaling by the lipid phosphatase SAC1, J. Cell Biol. 180 (2008) 803–812.
[22] M. de Saint-Jean, et al., Osh4p exchanges sterols for phosphatidylinositol 4-phosphate between lipid bilayers, J. Cell Biol. 195 (2011) 965–978.
[23] G. D'Angelo, M. Vicinanza, A. Di Campli, M.A. De Matteis, The multiple roles of PtdIns(4)P – not just the precursor of PtdIns(4,5)P2, J. Cell Sci. 121 (2008) 1955–1963.
[24] L. Demmel, et al., The clathrin adaptor Gga2p is a phosphatidylinositol 4-phosphate effector at the Golgi exit, Mol. Biol. Cell 19 (2008) 1991–2002.
[25] E. Mizuno-Yamasaki, M. Medkova, J. Coleman, P. Novick, Phosphatidylinositol 4-phosphate controls both membrane recruitment and a regulatory switch of the Rab GEF Sec2p, Dev. Cell 18 (2010) 828–840.
[26] J. Viaud, F. Boal, H. Tronchere, F. Gaits-Iacovoni, B. Payrastre, Phosphatidylinositol 5-phosphate: a nuclear stress lipid and a tuner of membranes and cytoskeleton dynamics, BioEssays news Rev. Mol. Cell. Dev. Biol. 36 (2014) 260–272.
[27] D. Sarkes, L.E. Rameh, A novel HPLC-based approach makes possible the spatial characterization of cellular PtdIns5P and other phosphoinositides, Biochem. J. 428 (2010) 375–384.
[28] O. Gozani, et al., The PHD finger of the chromatin-associated protein ING2 functions as a nuclear phosphoinositide receptor, Cell 114 (2003) 99–111.
[29] K. Niebuhr, et al., Conversion of PtdIns(4,5)P(2) into PtdIns(5)P by the S.flexneri effector IpgD reorganizes host cell morphology, EMBO J. 21 (2002) 5069–5078.
[30] C. Pendaries, et al., PtdIns5P activates the host cell PI3-kinase/Akt pathway during Shigella flexneri infection, EMBO J. 25 (2006) 1024–1034.
[31] D. Ramel, et al., Shigella flexneri infection generates the lipid PI5P to alter endocytosis and prevent termination of EGFR signaling, Sci. Signal. 4 (2011) ra61.
[32] F. Boal, et al., TOM1 is a PI5P effector involved in the regulation of endosomal maturation, J. Cell Sci. 128 (2015) 815–827.
[33] A. Puhar, H. Tronchere, B. Payrastre, G.T. Nhieu, P.J.A. Sansonetti, Shigella effector dampens inflammation by regulating epithelial release of danger signal ATP through production of the lipid mediator PtdIns5P, Immunity 39 (2013) 1121–1131.
[34] G. Guittard, et al., Cutting edge: Dok-1 and Dok-2 adaptor molecules are regulated by phosphatidylinositol 5-phosphate production in T cells, J. Immunol. 182 (2009) 3974–3978.
[35] D. Sbrissa, O.C. Ikonomov, J. Strakova, A. Shisheva, Role for a novel signaling intermediate, phosphatidylinositol 5-phosphate, in insulin-regulated F-actin stress fiber breakdown and GLUT4 translocation, Endocrinology 145 (2004) 4853–4865.
[36] J. Viaud, et al., Phosphatidylinositol 5-phosphate regulates invasion through binding and activation of Tiam1, Nat. Commun. 5 (2014) 4080.
[37] M. Vicinanza, et al., PI(5)P regulates autophagosome biogenesis, Mol. Cell 57 (2015) 219–234.
[38] J. Xie, C. Erneux, I. Pirson, How does SHIP1/2 balance PtdIns(3,4)P2 and does it signal independently of its phosphatase activity? BioEssays News Rev. Mol. Cell. Dev. Biol. 35 (2013) 733–743.
[39] Y. Posor, et al., Spatiotemporal control of endocytosis by phosphatidylinositol-3,4-bisphosphate, Nature 499 (2013) 233–237.
[40] H. Li, A.J. Marshall, Phosphatidylinositol (3,4) bisphosphate-specific phosphatases and effector proteins: a distinct branch of PI3K signaling, Cell. Signal. 27 (2015) 1789–1798.
[41] S. Wullschleger, D.H. Wasserman, A. Gray, K. Sakamoto, D.R. Alessi, Role of TAPP1 and TAPP2 adaptor binding to PtdIns(3,4)P2 in regulating insulin sensitivity defined by knock-in analysis, Biochem. J. 434 (2011) 265–274.
[42] E. Boucrot, et al., Endophilin marks and controls a clathrin-independent endocytic pathway, Nature 517 (2015) 460–465.
[43] M. Krause, et al., Lamellipodin, an Ena/VASP ligand, is implicated in the regulation of lamellipodial dynamics, Dev. Cell 7 (2004) 571–583.
[44] T. Oikawa, T. Itoh, T. Takenawa, Sequential signals toward podosome formation in NIH-src cells, J. Cell Biol. 182 (2008) 157–169.
[45] A.J. McCartney, Y. Zhang, L.S. Weisman, Phosphatidylinositol 3,5-bisphosphate: low abundance, high significance, BioEssays News Rev. Mol. Cell. Dev. Biol. 36 (2014) 52–64.
[46] D. Sbrissa, O.C. Ikonomov, A. Shisheva, Phosphatidylinositol 3-phosphate-interacting domains in PIKfyve. Binding specificity and role in PIKfyve. Endomenbrane localization, J. Biol. Chem. 277 (2002) 6073–6079.
[47] K. Hnia, I. Vaccari, A. Bolino, J. Laporte, Myotubularin phosphoinositide phosphatases: cellular functions and disease pathophysiology, Trends Mol. Med. 18 (2012) 317–327.
[48] J. de Lartigue, et al., PIKfyve regulation of endosome-linked pathways, Traffic 10 (2009) 883–893.
[49] Y. Zhang, et al., Loss of Vac14, a regulator of the signaling lipid phosphatidylinositol 3,5-bisphosphate, results in neurodegeneration in mice, Proc. Natl. Acad. Sci. U. S. A. 104 (2007) 17518–17523.
[50] A.C. Rutherford, et al., The mammalian phosphatidylinositol 3-phosphate 5-kinase (PIKfyve) regulates endosome-to-TGN retrograde transport, J. Cell Sci. 119 (2006) 3944–3957.
[51] M. Thumm, et al., It takes two to tango: PROPPINs use two phosphoinositide-binding sites, Autophagy 9 (2013) 106–107.
[52] R. Krick, et al., Structural and functional characterization of the two phosphoinositide binding sites of PROPPINs, a beta-propeller protein family, Proc. Natl. Acad. Sci. U. S. A. 109 (2012) E2042–E2049.
[53] K.M. Vasudevan, L.A. Garraway, AKT signaling in physiology and disease, Curr. Top. Microbiol. Immunol. 347 (2010) 105–133.
[54] J. Viaud, F. Gaits-Iacovoni, B. Payrastre, Regulation of the DH-PH tandem of guanine nucleotide exchange factor for Rho GTPases by phosphoinositides, Adv. Biol. Regul. 52 (2012) 303–314.
[55] A. Gassama-Diagne, et al., Phosphatidylinositol-3,4,5-trisphosphate regulates the formation of the basolateral plasma membrane in epithelial cells, Nat. cell Biol. 8 (2006) 963–970.
[56] M.A. Lemmon, K.M. Ferguson, C.S. Abrams, Pleckstrin homology domains and the cytoskeleton, FEBS Lett. 513 (2002) 71–76.
[57] B. Payrastre, Phosphoinositides: lipid kinases and phosphatases, Methods Mol. Biol. 273 (2004) 201–212.
[58] J.B. Morris, K.A. Hinchliffe, A. Ciruela, A.J. Letcher, R.F. Irvine, Thrombin stimulation of platelets causes an increase in phosphatidylinositol 5-phosphate revealed by mass assay, FEBS Lett. 475 (2000) 57–60.
[59] J. Clark, et al., Quantification of PtdInsP3 molecular species in cells and tissues by mass spectrometry, Nat. Methods 8 (2011) 267–272.
[60] G.R. Hammond, G. Schiavo, R.F. Irvine, Immunocytochemical techniques reveal multiple, distinct cellular pools of PtdIns4P and PtdIns(4,5)P(2), Biochem. J. 422 (2009) 23–35.
[61] Hélène Tronchère, Alessandra Bolino, Jocelyn Laporte, Bernard Payrastre, Myotubularins and associated neuromuscular diseases, Clin. Lipidol. 7 (2012) 151–162.
[62] D.A. Fruman, C. Rommel, PI3K and cancer: lessons, challenges and opportunities, Nat. Rev. Drug Discov. 13 (2014) 140–156.
[63] S.J. Leevers, B. Vanhaesebroeck, M.D. Waterfield, Signalling through phosphoinositide 3-kinases: the lipids take centre stage, Curr. Opin. Cell Biol. 11 (1999) 219–225.
[64] M. Whitman, C.P. Downes, M. Keeler, T. Keller, L. Cantley, Type I phosphatidylinositol kinase makes a novel inositol phospholipid, phosphatidylinositol-3-phosphate, Nature 332 (1988) 644–646.
[65] L.C. Cantley, The phosphoinositide 3-kinase pathway, Science 296 (2002) 1655–1657.
[66] B. Pasquier, SAR405, a PIK3C3/Vps34 inhibitor that prevents autophagy and synergizes with MTOR inhibition in tumor cells, Autophagy 11 (2015) 725–726.
[67] Y. Samuels, et al., High frequency of mutations of the PIK3CA gene in human cancers, Science 304 (2004) 554.
[68] L. Zhao, P.K. Vogt, Helical domain and kinase domain mutations in p110alpha of phosphatidylinositol 3-kinase induce gain of function by different mechanisms, Proc. Natl. Acad. Sci. U. S. A. 105 (2008) 2652–2657.
[69] G. Mirzaa, R. Conway, J.M. Graham Jr., W.B. Dobyns, in: R.A. Pagon, et al. (Eds.), GeneReviews(R), 1993 (Seattle (WA).
[70] D.W. Cescon, C. Gorrini, T.W. Mak, Breaking up is hard to do: PI3K isoforms on the rebound, Cancer Cell 27 (2015) 5–7.
[71] S.T. Jou, et al., Essential, nonredundant role for the phosphoinositide 3-kinase p110delta in signaling by the B-cell receptor complex, Mol. Cell. Biol. 22 (2002) 8580–8591.
[72] D.A. Fruman, C. Rommel, PI3Kdelta inhibitors in cancer: rationale and serendipity merge in the clinic, Cancer Discov. 1 (2011) 562–572.
[73] A.K. Gopal, et al., PI3Kdelta inhibition by idelalisib in patients with relapsed indolent lymphoma, N. Engl. J. Med. 370 (2014) 1008–1018.
[74] R.R. Furman, et al., Idelalisib and rituximab in relapsed chronic lymphocytic

leukemia, N. Engl. J. Med. 370 (2014) 997–1007.
[75] C.M. Walsh, D.A. Fruman, Too much of a good thing: immunodeficiency due to hyperactive PI3K signaling, J. Clin. Invest. 124 (2014) 3688–3690.
[76] K. Ali, et al., Inactivation of PI(3)K p110delta breaks regulatory T-cell-mediated immune tolerance to cancer, Nature 510 (2014) 407–411.
[77] M.P. Gratacap, et al., Regulation and roles of PI3Kbeta, a major actor in platelet signaling and functions, Adv. Enzyme Regul. 51 (2011) 106–116.
[78] S.P. Jackson, et al., PI 3-kinase p110beta: a new target for antithrombotic therapy, Nat. Med. 11 (2005) 507–514.
[79] I. Canobbio, et al., Genetic evidence for a predominant role of PI3Kbeta catalytic activity in ITAM- and integrin-mediated signaling in platelets, Blood 114 (2009) 2193–2196.
[80] V. Martin, et al., Deletion of the p110beta isoform of phosphoinositide 3-kinase in platelets reveals its central role in Akt activation and thrombus formation in vitro and in vivo, Blood 115 (2010) 2008–2013.
[81] A. Consonni, et al., Role and regulation of phosphatidylinositol 3-kinase beta in platelet integrin alpha2beta1 signaling, Blood 119 (2012) 847–856.
[82] S.P. Jackson, S.M. Schoenwaelder, Antithrombotic phosphoinositide 3-kinase beta inhibitors in humans: a 'shear' delight!, J. Thromb. Haemost. JTH 10 (2012) 2123–2126.
[83] S. Nylander, et al., Human target validation of phosphoinositide 3-kinase (PI3K)beta: effects on platelets and insulin sensitivity, using AZD6482 a novel PI3Kbeta inhibitor, J. Thromb. Haemost. JTH 10 (2012) 2127–2136.
[84] S. Nylander, F. Wagberg, M. Andersson, T. Skarby, D. Gustafsson, Exploration of efficacy and bleeding with combined phosphoinositide 3-kinase beta inhibition and aspirin in man, J. Thromb. Haemost 13 (2015) 1494–1502.
[85] P.A. Laurent, et al., Platelet PI3Kbeta and GSK3 regulate thrombus stability at a high shear rate, Blood 125 (2015) 881–888.
[86] M. Torti, PI3Kbeta inhibition: all that glitters is not gold, Blood 125 (2015) 750–751.
[87] O. Attree, et al., The Lowe's oculocerebrorenal syndrome gene encodes a protein highly homologous to inositol polyphosphate-5-phosphatase, Nature 358 (1992) 239–242.
[88] R.R. Hoopes Jr., et al., Dent Disease with mutations in OCRL1, Am. J. Hum. Genet. 76 (2005) 260–267.
[89] G. Narkis, et al., Lethal contractural syndrome type 3 (LCCS3) is caused by a mutation in PIP5K1C, which encodes PIPKI gamma of the phophatidylinsitol pathway, Am. J. Hum. Genet. 81 (2007) 530–539.
[90] L. Amoasii, K. Hnia, J. Laporte, Myotubularin phosphoinositide phosphatases in human diseases, Curr. Top. Microbiol. Immunol. 362 (2012) 209–233.
[91] S. Li, et al., Mutations in PIP5K3 are associated with Francois-Neetens mouchetee fleck corneal dystrophy, Am. J. Hum. Genet. 77 (2005) 54–63.
[92] C.A. Worby, J.E. Dixon, Pten. Annu. Rev. Biochem. 83 (2014) 641–669.
[93] J.E. Burke, R.L. Williams, Synergy in activating class I PI3Ks, Trends Biochem. Sci. 40 (2015) 88–100.
[94] N. Al Tassan, et al., A missense mutation in PIK3R5 gene in a family with ataxia and oculomotor apraxia, Hum. Mutat. 33 (2012) 351–354.
[95] M.E. Conley, et al., Agammaglobulinemia and absent B lineage cells in a patient lacking the p85alpha subunit of PI3K, J. Exp. Med. 209 (2012) 463–470.
[96] I. Angulo, et al., Phosphoinositide 3-kinase delta gene mutation predisposes to respiratory infection and airway damage, Science 342 (2013) 866–871.
[97] J.B. Riviere, et al., De novo germline and postzygotic mutations in AKT3, PIK3R2 and PIK3CA cause a spectrum of related megalencephaly syndromes, Nat. Genet. 44 (2012) 934–940.
[98] S. Fernandes, S. Iyer, W.G. Kerr, Role of SHIP1 in cancer and mucosal inflammation, Ann. N. Y. Acad. Sci. 1280 (2013) 6–10.
[99] A. Suwa, T. Kurama, T. Shimokawa, SHIP2 and its involvement in various diseases, Expert Opin. Ther. Targets 14 (2010) 727–737.
[100] E.C. Chai, R.R. Singaraja, Opsismodysplasia: implications of mutations in the developmental gene INPPL1, Clin. Genet. 83 (2013) 527–529.
[101] M. Jacoby, et al., INPP5E mutations cause primary cilium signaling defects, ciliary instability and ciliopathies in human and mouse, Nat. Genet. 41 (2009) 1027–1031.
[102] E.L. Clayton, S. Minogue, M.G. Waugh, Phosphatidylinositol 4-kinases and PI4P metabolism in the nervous system: roles in psychiatric and neurological diseases, Mol. Neurobiol. 47 (2013) 361–372.

Annexe n°2

Inactivation of the class II PI3K-C2β potentiates insulin signaling and sensitivity.

Samira Alliouachene[1], Benoit Bilanges[2], Gaetan Chicanne[3], Karen E Anderson[4], Wayne Pearce[2], Khaled Ali[2], Colin Valet[3], York Posor[2], Pei Ching Low[2], Claire Chaussade[2], Cheryl L Scudamore[5], Rachel S Salamon[6], Jonathan M Backer[6], Len Stephens[4], Phill T Hawkins[4], Bernard Payrastre[3], Bart Vanhaesebroeck[7]

[1] UCL Cancer Institute, University College London, 72 Huntley street, London WC1E 6DD, UK. Electronic address: s.alliouachene@ucl.ac.uk

[2] UCL Cancer Institute, University College London, 72 Huntley street, London WC1E 6DD, UK.

[3] Inserm U1048, I2MC and Universite Paul Sabatier, 31432, Toulouse Cedex 04, France

[4] Inositide Laboratory, The Babraham Institute, Cambridge CB22 3AT, UK.

[5] Mary Lyon Centre, MRC Harwell, Harwell Science and Innovation Campus, Harwell OX11 0RD, UK.

[6] Department of molecular pharmacology, Albert Einstein College of Medecine, Bronx, NY 10461, USA.

[7] UCL Cancer Institute, University College London, 72 Huntley street, London WC1E 6DD, UK. Electronic address: bart.vanh@ucl.ac.uk

Article in Cell reports 2016; 13: 1881-94

Article

Cell Reports

Inactivation of the Class II PI3K-C2β Potentiates Insulin Signaling and Sensitivity

Graphical Abstract

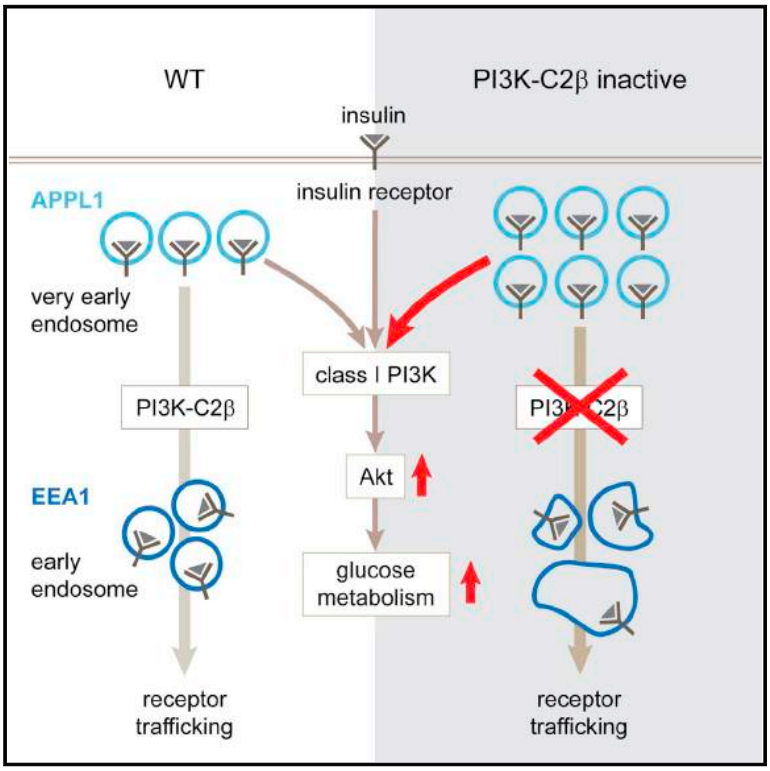

Authors

Samira Alliouachene, Benoit Bilanges, Gaëtan Chicanne, ..., Phill T. Hawkins, Bernard Payrastre, Bart Vanhaesebroeck

Correspondence

s.alliouachene@ucl.ac.uk (S.A.), bart.vanh@ucl.ac.uk (B.V.)

In Brief

Organismal roles of class II PI3Ks are unclear. Alliouachene et al. show that inactivation of the class II PI3K-C2β in mice, by regulating insulin receptor trafficking, enhances insulin sensitivity and protects against high-fat-diet-induced liver steatosis. The results suggest that PI3K-C2β is a potential drug target for insulin sensitization.

Highlights

- PI3K-C2β kinase-dead mice are viable with enhanced glucose tolerance
- PI3K-C2β inactivation sensitizes to insulin and protects from liver steatosis
- PI3K-C2β inactivation selectively enhances insulin/Akt signaling in metabolic tissues
- PI3K-C2β activity regulates very early endosomal compartments in hepatocytes

Alliouachene et al., 2015, Cell Reports *13*, 1881–1894
December 1, 2015 ©2015 The Authors
http://dx.doi.org/10.1016/j.celrep.2015.10.052

Cell Reports
Article

Inactivation of the Class II PI3K-C2β Potentiates Insulin Signaling and Sensitivity

Samira Alliouachene,[1,*] Benoit Bilanges,[1] Gaëtan Chicanne,[2] Karen E. Anderson,[3] Wayne Pearce,[1] Khaled Ali,[1,6] Colin Valet,[2] York Posor,[1] Pei Ching Low,[1] Claire Chaussade,[1,7] Cheryl L. Scudamore,[4] Rachel S. Salamon,[5] Jonathan M. Backer,[5] Len Stephens,[3] Phill T. Hawkins,[3] Bernard Payrastre,[2] and Bart Vanhaesebroeck[1,*]
[1]UCL Cancer Institute, University College London, 72 Huntley Street, London WC1E 6DD, UK
[2]Inserm/UPS UMR 1048, Institut des Maladies Métaboliques et Cardiovasculaires, 1 Avenue Jean Poulhès BP 84225, 31432 Toulouse Cedex 4, France
[3]Inositide Laboratory, The Babraham Institute, Cambridge CB22 3AT, UK
[4]Mary Lyon Centre, MRC Harwell, Harwell Science and Innovation Campus, Harwell OX11 0RD, UK
[5]Department of Molecular Pharmacology, Albert Einstein College of Medicine, Bronx, NY 10461, USA
[6]Present address: Amgen Inc., 1120 Veterans Boulevard, South San Francisco, CA 94080, USA
[7]Present address: Galderma R&D, BP87, 06902 Sophia Antipolis Cedex, France
*Correspondence: s.alliouachene@ucl.ac.uk (S.A.), bart.vanh@ucl.ac.uk (B.V.)
http://dx.doi.org/10.1016/j.celrep.2015.10.052

SUMMARY

In contrast to the class I phosphoinositide 3-kinases (PI3Ks), the organismal roles of the kinase activity of the class II PI3Ks are less clear. Here, we report that class II PI3K-C2β kinase-dead mice are viable and healthy but display an unanticipated enhanced insulin sensitivity and glucose tolerance, as well as protection against high-fat-diet-induced liver steatosis. Despite having a broad tissue distribution, systemic PI3K-C2β inhibition selectively enhances insulin signaling only in metabolic tissues. In a primary hepatocyte model, basal PI3P lipid levels are reduced by 60% upon PI3K-C2β inhibition. This results in an expansion of the very early APPL1-positive endosomal compartment and altered insulin receptor trafficking, correlating with an amplification of insulin-induced, class I PI3K-dependent Akt signaling, without impacting MAPK activity. These data reveal PI3K-C2β as a critical regulator of endosomal trafficking, specifically in insulin signaling, and identify PI3K-C2β as a potential drug target for insulin sensitization.

INTRODUCTION

PI3Ks, a family of lipid kinases that are activated by growth factors, hormones, and cytokines play key roles in cell growth, proliferation, and differentiation (Jean and Kiger, 2014; Vanhaesebroeck et al., 2010). Mammals have eight isoforms of PI3K, divided into three classes of which the class I PI3Ks have been most extensively studied. Through their non-redundant roles in plasma membrane receptor signaling, these PI3Ks have been implicated in overgrowth, cancer, metabolic disease, and inflammation (Jean and Kiger, 2014; Vanhaesebroeck et al., 2010). Class I PI3Ks convert the phosphatidylinositol(4,5)bisphosphate [PI(4,5)P_2] lipid at the plasma membrane to PI(3,4,5)P_3, also known as PIP_3. PIP_3 and its metabolite PI(3,4)P_2 bind and modulate the activity of pleckstrin homology (PH) domain-containing effectors such as protein kinases (including Akt and Btk), adaptor proteins, and regulators of small GTPases. Among the four class I PI3Ks isoforms (p110α, β, γ, and δ), p110α has been identified as the most important isoform in systemic or hepatic insulin signaling (Foukas et al., 2006; Knight et al., 2006; Sopasakis et al., 2010), although within the hypothalamus both p110α and p110β are required for normal energy homeostasis (Al-Qassab et al., 2009; Tups et al., 2010).

The class II (PI3K-C2α, -C2β, and -C2γ) and III (vps34) PI3K isoforms are thought to mainly convert PI to PI3P on endosomal and autophagic membranes, resulting in the recruitment and activation of effector proteins containing FYVE or PX lipid-binding domains. Class II PI3Ks might also convert PI(4)P to PI(3,4)P_2 (Nigorikawa et al., 2014; Posor et al., 2013). Class II PI3Ks have been reported to be activated by a wide range of agonists, such as growth factors, G protein-coupled receptors, and adhesion molecules (reviewed in Falasca and Maffucci, 2012; Jean and Kiger, 2014; Vanhaesebroeck et al., 2010). However, the molecular details of how class II PI3Ks couple to this multitude of upstream receptors remain unclear.

Previous cell-based studies have implicated a role for class II PI3Ks in the regulation of a broad variety of biological activities, including glucose transport, neurosecretory granule release, insulin secretion, endocytosis and muscle cell contraction (PI3K-C2α), cell migration and K^+ channel activation (PI3K-C2β), and cell growth and survival (PI3K-C2α and PI3K-C2β) (Falasca and Maffucci, 2012; Jean and Kiger, 2014). The organismal roles of the class II/III PI3Ks remain less clear, with homozygous deletion of PI3K-C2α or vps34 being embryonic lethal (Franco et al., 2014; Yoshioka et al., 2012; Zhou et al., 2011) and mice homozygous deletion of PI3K-C2β being viable without reported phenotypes (Harada et al., 2005). PI3K-C2α gene knockout (KO) studies have implicated this PI3K isoform in angiogenesis (Yoshioka et al., 2012) and in the generation of the primary cilium

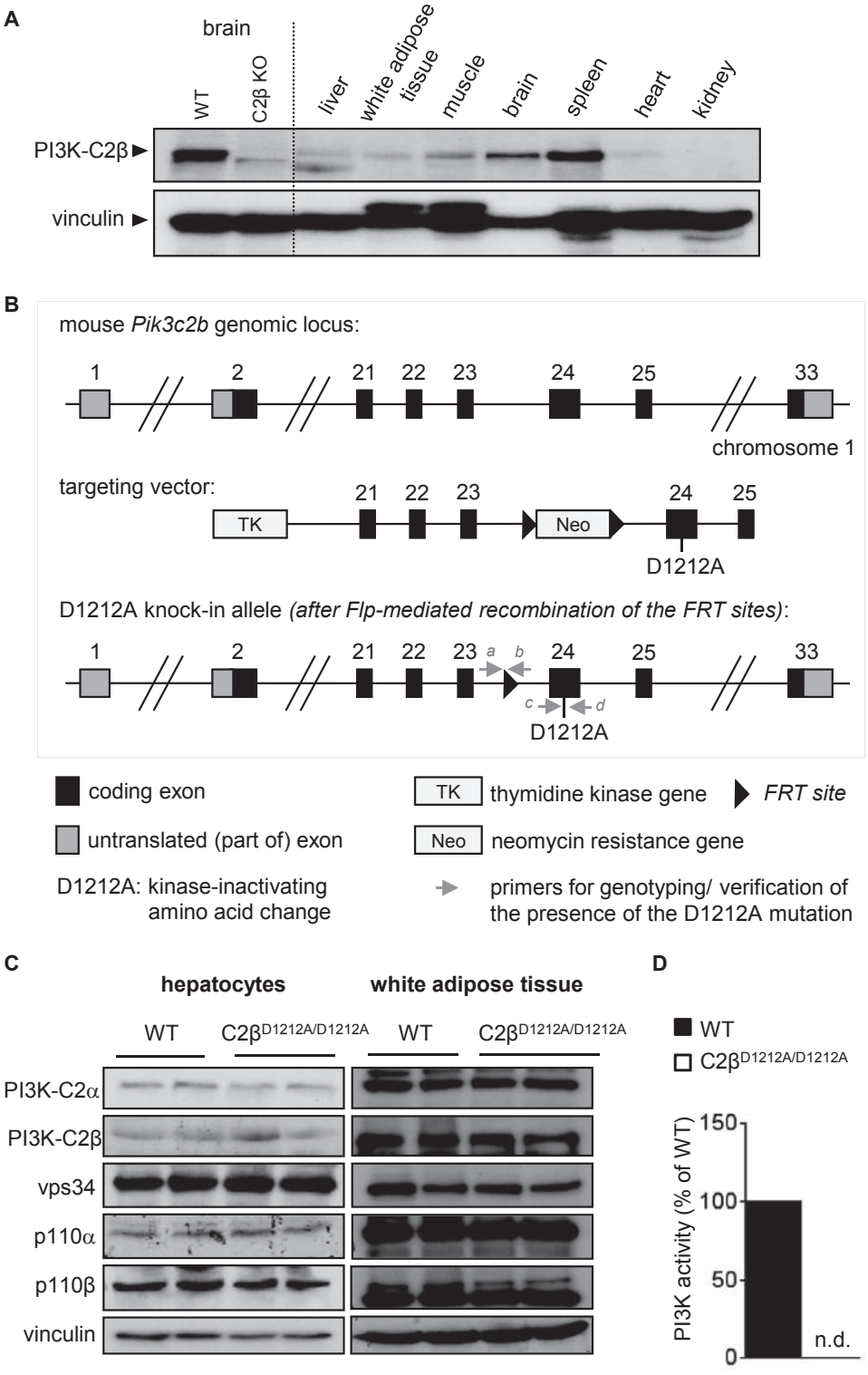

Figure 1. Generation and Characterization of PI3K-C2β^{D1212A} KI Mice

(A) Expression of PI3K-C2β protein in mouse tissues. Brain lysates from PI3K-C2β KO mice (Harada et al., 2005) were included as controls. 100 μg of protein was loaded per lane.

(B) Gene targeting strategy to generate the constitutive D1212A knockin mutation in the *Pik3c2b* gene. The D1212A mutation was introduced in the DFG motif in exon 24 of the *Pik3c2b* gene. The FRT-flanked cassette encoding *Pgk Neo* selection marker was removed in vivo by breeding onto ACTB-Flp mice.

(legend continued on next page)

(Franco et al., 2014). Mice homozygous for a gene-trap PI3K-C2α allele, which encodes a PI3K-C2α protein with reduced activity, are viable but develop chronic renal failure (Harris et al., 2011).

All class II/III PI3K mutant mice reported to date were created by gene targeting approaches that remove the protein of interest but do not allow the discrimination between scaffold- and kinase-dependent functions of these enzymes (Vanhaesebroeck et al., 2005). In the present study, we have therefore generated mice in which endogenous PI3K-C2β is converted to a kinase-dead protein, thereby mimicking the impact of systemically administered small molecule kinase inhibitors of PI3K-C2β. Given previous evidence from cell-based studies that class II PI3K is involved in insulin action, as shown for PI3K-C2α (Brown et al., 1999; Dominguez et al., 2011; Falasca et al., 2007; Leibiger et al., 2010; Soos et al., 2001; Ursø et al., 1999), we focused our initial characterization of the PI3K-C2β kinase-dead mice on systemic glucose homeostasis. Our data reveal a role for PI3K-C2β in the control of insulin receptor trafficking and glucose metabolism in metabolic tissues and identify this kinase as a component in the regulation of insulin signal transduction.

RESULTS

Generation of PI3K-C2β Kinase-Dead Knockin Mice

There are currently no published data available on the tissue distribution of the PI3K-C2β protein in mice. As shown in Figure 1A, PI3K-C2β protein expression was broad and varied widely across different mouse tissues, in line with PI3K-C2β mRNA profiling studies in human tissues (Ho et al., 1997 in which PI3K-C2β is referred to as T105). Tissue distribution did therefore not provide any clear indication for a possible in vivo role of PI3K-C2β.

In order to assess the organismal role of the kinase activity of PI3K-C2β, we generated a germline knockin (KI) mouse line in which the genomic DNA encoding the aspartic acid residue on position 1212 (D1212) in the conserved ATP-binding DFG motif of PI3K-C2β was mutated to alanine (further referred to as D1212A; Figure 1B). This gene targeting strategy is expected to give rise to expression of an intact PI3K-C2β protein carrying the kinase-inactivating D1212A mutation. We previously used this strategy to constitutively inactivate class I PI3K isoforms, thereby uncovering non-redundant functions for these kinases (Vanhaesebroeck et al., 2005). Mice homozygous for the PI3K-C2β KI allele (further referred to as C2β$^{D1212A/D1212A}$ mice) were born at a normal Mendelian ratio, with no impact on organismal growth (Figure S1) or fertility. The overall histopathology of 38 tissues from these mice was investigated and, up to 20 months of age, did not show any abnormalities (Table S1). Expression of the mutant PI3K-C2β protein and the other, non-targeted, PI3K isoforms (Figure 1C) was similar in C2β$^{D1212A/D1212A}$ and wild-type (WT) mice, whereas the lipid kinase activity of PI3K-C2β was fully lost (Figure 1D).

Improved Glucose Homeostasis and Insulin Sensitivity in C2β$^{D1212A/D1212A}$ Mice

As part of a metabolic characterization of PI3K mutant mice, we subjected C2β$^{D1212A/D1212A}$ mice to standard metabolic analysis. Six- to 8-week-old C2β$^{D1212A/D1212A}$ mice had unaltered blood glucose levels under both randomly fed and fasted conditions (Figure 2A); however, the levels of circulating insulin were reduced under fed but not under fasted conditions (Figure 2B). When subjected to glucose or insulin tolerance tests, overnight fasted C2β$^{D1212A/D1212A}$ mice showed enhanced glucose tolerance (Figure 2C), due to an increased insulin hypoglycemic response (Figure 2D). Under randomly fed conditions, WT and C2β$^{D1212A/D1212A}$ mice had similar levels of circulating leptin, adiponectin, triglycerides, free fatty acids, and cholesterol, with similar food intake and energy expenditure (Table S2). Taken together, these data reveal that PI3K-C2β negatively regulates insulin sensitivity and glucose metabolism in vivo. Interestingly, this metabolic phenotype was observed despite the low expression of PI3K-C2β in metabolic tissues relative to other tissues, such as the spleen or brain (Figure 1A).

PI3K-C2β Inactivation Leads to Enhanced Insulin-Stimulated Akt Signaling Selectively in Metabolic Tissues

We next investigated the impact of PI3K-C2β inactivation on insulin signaling in mice and in explanted hepatocytes. Upon insulin stimulation, the insulin receptor (IR) at the plasma membrane engages with the intracellular insulin receptor substrate (IRS) adaptor protein that recruits several cytosolic signaling proteins. These include the p85 subunit of the class I PI3Ks (leading to PIP_3 production and activation of Akt) and the adaptor protein Grb2 that, through its association with the SOS guanine nucleotide exchange factors, activates the Ras/MAPK pathway.

Compared to WT mice, stimulation of C2β$^{D1212A/D1212A}$ mice with insulin in vivo led to enhanced Akt phosphorylation in metabolic tissues (liver, muscle, and white adipose tissue; Figure 3A). Remarkably, PI3K-C2β inactivation did not lead to an increase in insulin-induced Akt signaling in the spleen (Figure 3A), despite high expression of PI3K-C2β in this tissue compared to metabolic tissues (Figure 1A).

We next carried out a kinetic assessment of insulin signaling in cultured primary hepatocytes isolated from WT and C2β$^{D1212A/D1212A}$ mice. Also in hepatocytes, insulin-stimulated Akt signaling was enhanced and prolonged upon PI3K-C2β inactivation (Figure 3B), with no impact on MAPK signaling (Figure 3B). Interestingly, EGF- or IGF-1-induced phosphorylation of Akt was not affected by PI3K-C2β inactivation in hepatocytes (Figures S2A and S2B).

(C) PI3K isoform expression in WT and C2β$^{D1212A/D1212A}$ mice. Homogenates of cultured hepatocytes or white adipose tissue were resolved by SDS-PAGE and immunoblotted using the indicated antibodies. Each lane represents a tissue/hepatocyte culture derived from an individual mouse. 150 and 100 μg of protein was loaded per lane for hepatocytes and white adipose tissue, respectively.
(D) Lipid kinase activity associated with PI3K-C2β in WT and C2β$^{D1212A/D1212A}$ mice. Brain homogenates were immunoprecipitated using an antibody to PI3K-C2β, followed by an in vitro lipid kinase assay using PI as a substrate. n.d., not detected.

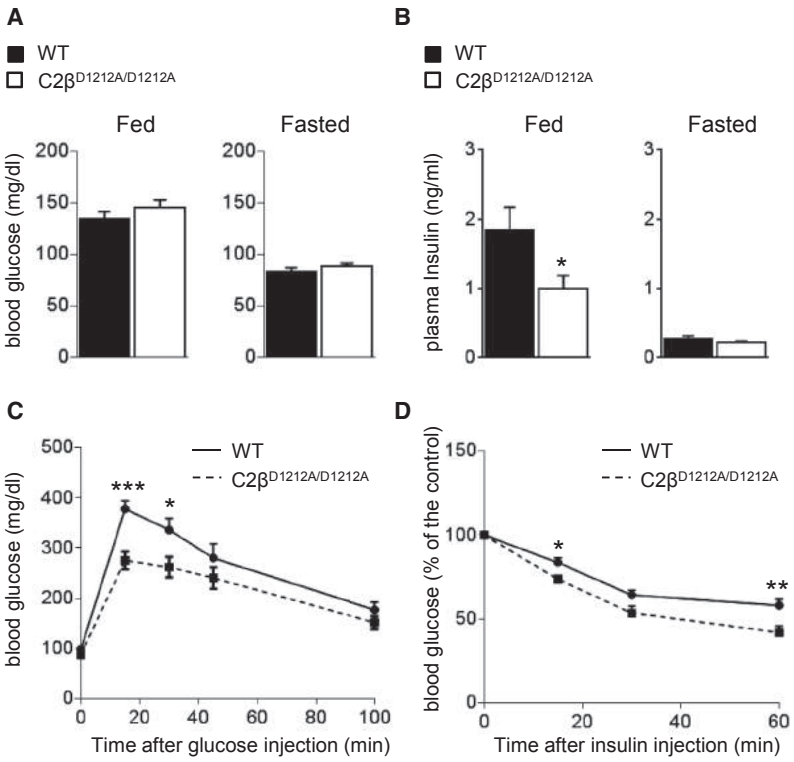

Figure 2. Enhanced Glucose Tolerance and Insulin Sensitivity in C2β$^{D1212A/D1212A}$ Mice

(A) Blood glucose levels under randomly fed and fasted conditions.

(B) Plasma insulin levels under randomly fed and fasted conditions.

(C) Glucose tolerance test after intraperitoneal injection of 2 g/kg of glucose in mice after overnight starvation.

(D) Insulin tolerance test after intraperitoneal injection of 0.75 U/kg of insulin in mice after overnight starvation. Glucose levels are expressed relative to the levels in mice of the same genotype before injection of insulin.

For all experiments shown, ten or more mice/genotype were used. Data represent mean ± SEM. *$p < 0.05$, **$p \leq 0.01$, ***$p \leq 0.001$.

PI3K-C2β Inactivation Leads to Enhanced Insulin-Stimulated Class I PI3K Signaling

Akt is activated by PIP_3 that is produced by class I PI3Ks. In line with the enhanced activation of Akt upon PI3K-C2β inactivation (Figure 3B), insulin-stimulated PIP_3 levels were increased to a higher extent in C2β$^{D1212A/D1212A}$ hepatocytes as compared to WT cells (Figure 4A). Treatment of WT and C2β$^{D1212A/D1212A}$ hepatocytes with GDC-0941, a class I PI3K-selective inhibitor, blocked insulin-stimulated Akt activation (Figure 4B). These data indicate that PI3K-C2β inactivation in hepatocytes leads to an early and transient enhancement of class I PI3K activation upon insulin stimulation, resulting in enhanced activation of Akt.

PI3K-C2β Inactivation Does Not Affect the Early Stages of Starvation-Induced Autophagy but Induces Defects in Endosomal Trafficking and Expansion of the APPL1 Early Endosomal Compartment

We next set out to uncover the underlying mechanism of this temporarily enhanced insulin-induced Akt signaling, using primary mouse hepatocytes as a cell-based model. A mass assay to quantitate PI3P levels (Chicanne et al., 2012) revealed a 60% reduction in the level of total PI3P in unstimulated hepatocytes upon inactivation of PI3K-C2β (Figure 5A). PI3P levels were unaffected by insulin stimulation in both WT and C2β$^{D1212A/D1212A}$ hepatocytes (Figure 5A). Interestingly, PI3K-C2β inactivation did not affect the PI3P levels in mouse embryonic fibroblasts or splenocytes (Figure 5A), despite the latter expressing high levels of PI3K-C2β protein (Figure 1A).

We next assessed the subcellular distribution of PI3P in fixed hepatocytes using a GST-2xFYVE^{HRS} probe (Gillooly et al., 2000). In line with the PI3P quantitation by mass assay, unstimulated C2β$^{D1212A/D1212A}$ cells had a clear decrease in the number of the PI3P-positive vesicles. However, there was no significant difference in the size (Figure 5B; Figure S3A) or subcellular distribution (Figure 5B) of these vesicles upon PI3K-C2β inactivation.

Key processes in which PI3P has been implicated include autophagy and endocytosis (Raiborg et al., 2013). WT and C2β$^{D1212A/D1212A}$ hepatocytes did not show differences at the early stage of starvation-induced autophagy, as assessed by immunofluorescence (IF) staining for autophagic markers (LC3 and the PI3P-binding proteins WIPI-1 and WIPI-2; Figure S3B), indicating that PI3K-C2β does not regulate the starvation-induced autophagic PI3P pool in these cells. However, a very mild decrease in the number of WIPI-1 punctae was observed under non-starved conditions in C2β$^{D1212A/D1212A}$ hepatocytes, compared to WT cells (Figure S3B), without any apparent impact on LC3 punctae. This suggests that PI3K-C2β may contribute to a small proportion of the PI3P pool that controls basal autophagy (i.e., the macroautophagic activity of cells in medium containing amino acids and growth factors).

PI3P has previously been reported to be important for the conversion of very early APPL1-positive endosomes into EEA1-positive endosomes (Zoncu et al., 2009). In accordance with the observed reduction in PI3P in unstimulated conditions, the number, but not the overall size, of the APPL1-positive punctae was increased in C2β$^{D1212A/D1212A}$ hepatocytes, compared to WT cells (Figure 5C; Figure S3A). In addition, due to the "expansion" of this endosomal compartment in C2β$^{D1212A/D1212A}$ hepatocytes, the distribution of the APPL1-positive vesicles was less restricted to the cell periphery, but instead the vesicles seemed more dispersed toward the cytoplasm (Figure 5C, inset). Under these conditions, EEA1-positive early endosomes and Rab7-positive late endosomes were found to be irregularly shaped in C2β$^{D1212A/D1212A}$ hepatocytes, and in the case of EEA1 endosomes also enlarged, whereas their numbers were unchanged (Figure S4). Upon insulin stimulation, C2β$^{D1212A/D1212A}$ hepatocytes resulted in a further increase in the number of APPL1-positive vesicles, with a less clear impact in WT cells (Figure 5C).

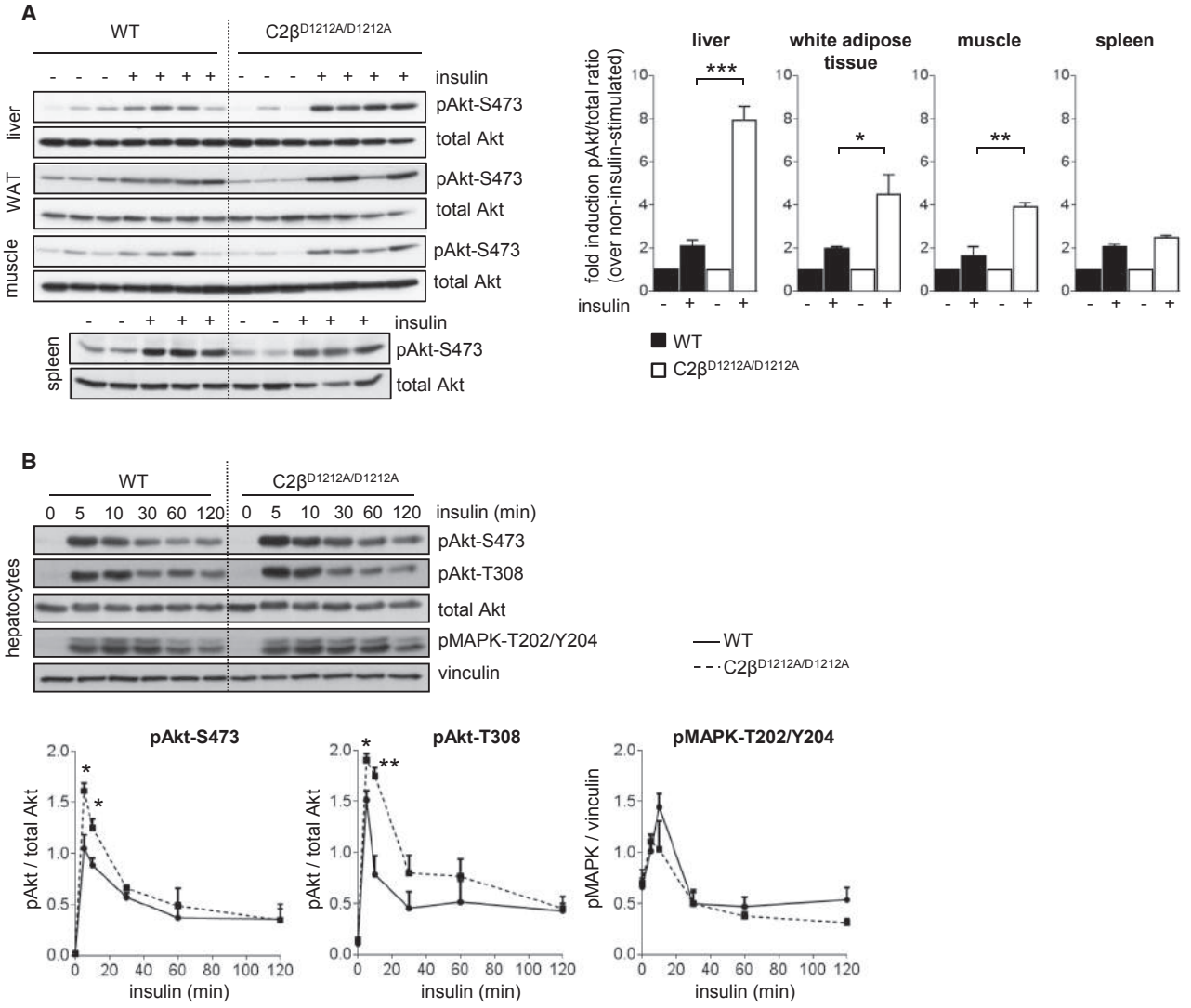

Figure 3. PI3K-C2β Inactivation Leads to Enhanced Insulin-Stimulated Akt Signaling Selectively in Metabolic Tissues

(A) Tissue homogenates, isolated from overnight starved mice, 30 min after intraperitoneal injection of 0.75 U/kg insulin or PBS, were analyzed by SDS-PAGE and immunoblotting using the indicated antibodies. Each lane represents an individual mouse. Quantification of the signals in tissues of three to four mice/genotype is shown. WAT, white adipose tissue.

(B) Cultured hepatocytes were starved overnight and stimulated for the indicated time points with 100 nM insulin, followed by SDS-PAGE analysis and immunoblotting using the indicated antibodies. Quantification of data from hepatocyte cell cultures derived from three individual mice/genotype is shown.

Data represent mean ± SEM. *$p < 0.05$, **$p \leq 0.01$, ***$p \leq 0.001$.

Taken together, these data suggest a defect in endosomal trafficking upon PI3K-C2β inactivation in hepatocytes, starting at the level of the very early APPL1 compartment, which could affect its maturation into EEA1-positive endosomes.

PI3K-C2β Inactivation Increases IR Levels and Delays IR Trafficking

PI3P depletion in cultured mammalian cell lines (COS7, HeLa), and the ensuing expansion of the very early APPL1 compartment, has been shown to result in an accumulation of the EGF receptor (EGFR) in this compartment (Zoncu et al., 2009) from which endocytosed cell surface receptors can continue to signal (Platta and Stenmark, 2011). We therefore assessed the impact of PI3K-C2β inactivation on the expression and function of the IR, EGFR, and transferrin receptors in primary hepatocytes.

Total cell extracts of unstimulated C2β$^{D1212A/D1212A}$ hepatocytes showed increased expression of IR protein compared to WT (Figure 6A), with no changes in the levels of IR mRNA (Figure S5) or EGFR and transferrin receptor protein levels (Figure 6A). To assess whether this increase in total IR levels was due to higher levels of IR at the cell surface or an accumulation in intracellular compartments, we analyzed the subcellular distribution of the IR in WT and C2β$^{D1212A/D1212A}$ hepatocytes. When incubated with labeled insulin at 4°C, WT, and C2β$^{D1212A/D1212A}$

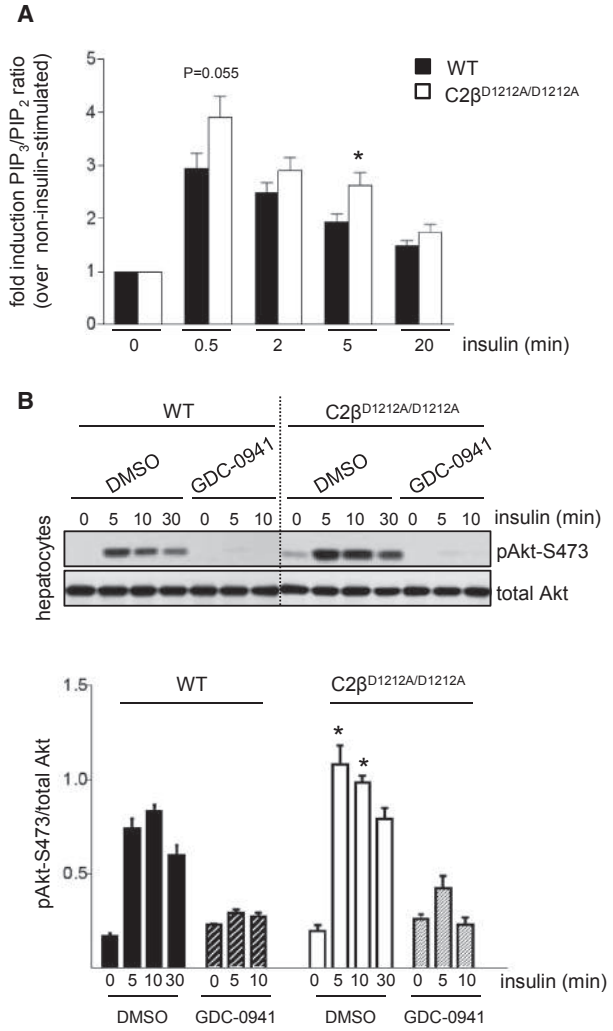

Figure 4. PI3K-C2β Inactivation Leads to Enhanced Insulin-Stimulated Class I PI3K Signaling

(A) Hepatocytes were starved overnight and stimulated with 100 nM insulin for the indicated time points, followed by analysis of total cellular PIP_3 levels by mass spectrometry. The mean ± SEM of four independent experiments is shown. Hepatocyte cultures from three mice/genotype were used in three of the experiments and three WT and two KI mice for the fourth experiment.

(B) Hepatocytes were starved overnight and treated with 500 nM GDC-0941 for 30 min before stimulation with insulin for different time points, followed by analysis of pAkt-S473 levels. A quantification of hepatocyte cell cultures from three independent mice/genotype is shown.

Data represent mean ± SEM. *$p < 0.05$, **$p \leq 0.01$, ***$p \leq 0.001$.

hepatocytes showed a similar binding capacity of insulin (Figure 6B), indicative of similar levels of IR at the cell surface. Insulin-induced tyrosine phosphorylation of IR was unaffected by PI3K-C2β inactivation (Figure 6C; Figure S6). Insulin-induced tyrosine phosphorylation of IRS1 and IRS2 was variable, and, although a tendency for an increase was observed for IRS1 in $C2\beta^{D1212A/D1212A}$ mice, this was not statistically significant (Figure 6C; Figure S6). Taken together, these data suggest that the overall increase in the total levels of IR observed upon PI3K-C2β inactivation (Figure 6A) is due to an increase in the pool of *intracellular* IR that is not available for insulin binding at the plasma membrane.

Despite the unchanged levels of IR at the plasma membrane, insulin uptake at 37°C was reduced by 20% in $C2\beta^{D1212A/D1212A}$ hepatocytes, especially at the 10- and 30-min time points (Figure 6D), suggesting a delay in IR trafficking early after insulin stimulation upon PI3K-C2β inactivation. This was also suggested by subcellular fractionation of $C2\beta^{D1212A/D1212A}$ hepatocytes whereby the IR was found to become temporarily (i.e., 10 min after insulin stimulation) enriched in an APPL1-positive light microsomal cell fraction (Figure 6E). Upon insulin stimulation, the IR is known to mainly recycle and not to undergo acute degradation (Gorden et al., 1989; Knutson, 1991). Indeed, in WT hepatocytes, IR degradation occurred over several hours upon insulin stimulation (Figure 6F). In $C2\beta^{D1212A/D1212A}$ cells, the total levels of IR normalized to WT levels in 6–7 hr (Figure 6F), suggesting a "reset" of total IR levels by ligand-induced repeated endocytic cycling, possibly as a consequence of a small fraction of the IR pool being trafficked along the degradative route in each endocytic cycle. In contrast to the IR, PI3K-C2β inactivation did not affect transferrin uptake (Figure S7).

Taken together, these data indicate that PI3K-C2β inactivation does not alter IR levels at the plasma membrane but affects IR trafficking, correlating with a temporary amplification of insulin-stimulated class I PI3K/Akt signaling.

$C2\beta^{D1212A/D1212A}$ Mice Are Protected against High-Fat-Diet-Induced Steatosis

To investigate the role of PI3K-C2β in a pathophysiological context, WT and $C2\beta^{D1212A/D1212A}$ mice were subjected to a high-fat diet for 16 weeks. Whereas PI3K-C2β inactivation did not affect body-weight increase (Figure 7A), $C2\beta^{D1212A/D1212A}$ mice showed a significant reduction in liver weight gain (Figure 7B), a significant protection against liver steatosis (Figure 7C) as well as reduced levels of neutral lipids (as documented by oil red O staining) and triglycerides in the liver (Figure 7D). $C2\beta^{D1212A/D1212A}$ mice were also less insulin-resistant than WT mice (Figure 7E). Taken together, our data highlight an important role of PI3K-C2β in insulin signaling and glucose metabolism, especially in the liver.

DISCUSSION

A New Model for Studying the In Vivo Role of the Kinase Activity of PI3K-C2β

No selective class II PI3K inhibitors are available. In order to assess the role of the kinase activity of the PI3K-C2β isoform of class II PI3Ks, we have created a mouse model in which this PI3K isoform has been rendered inactive by introduction of a germline KI mutation in the conserved DFG motif of the ATP-binding site. We previously used this strategy to uncover biological roles of the class I PI3Ks (Ali et al., 2004; Foukas et al., 2006; Graupera et al., 2008; Guillermet-Guibert et al., 2008; Okkenhaug et al., 2002). In contrast to PI3K gene deletion, such a KI strategy inactivates the PI3K in an inhibitor-like fashion, preserves the molecular balance of the expression of PI3K isoforms, minimizes compensatory effects, and, therefore, allows

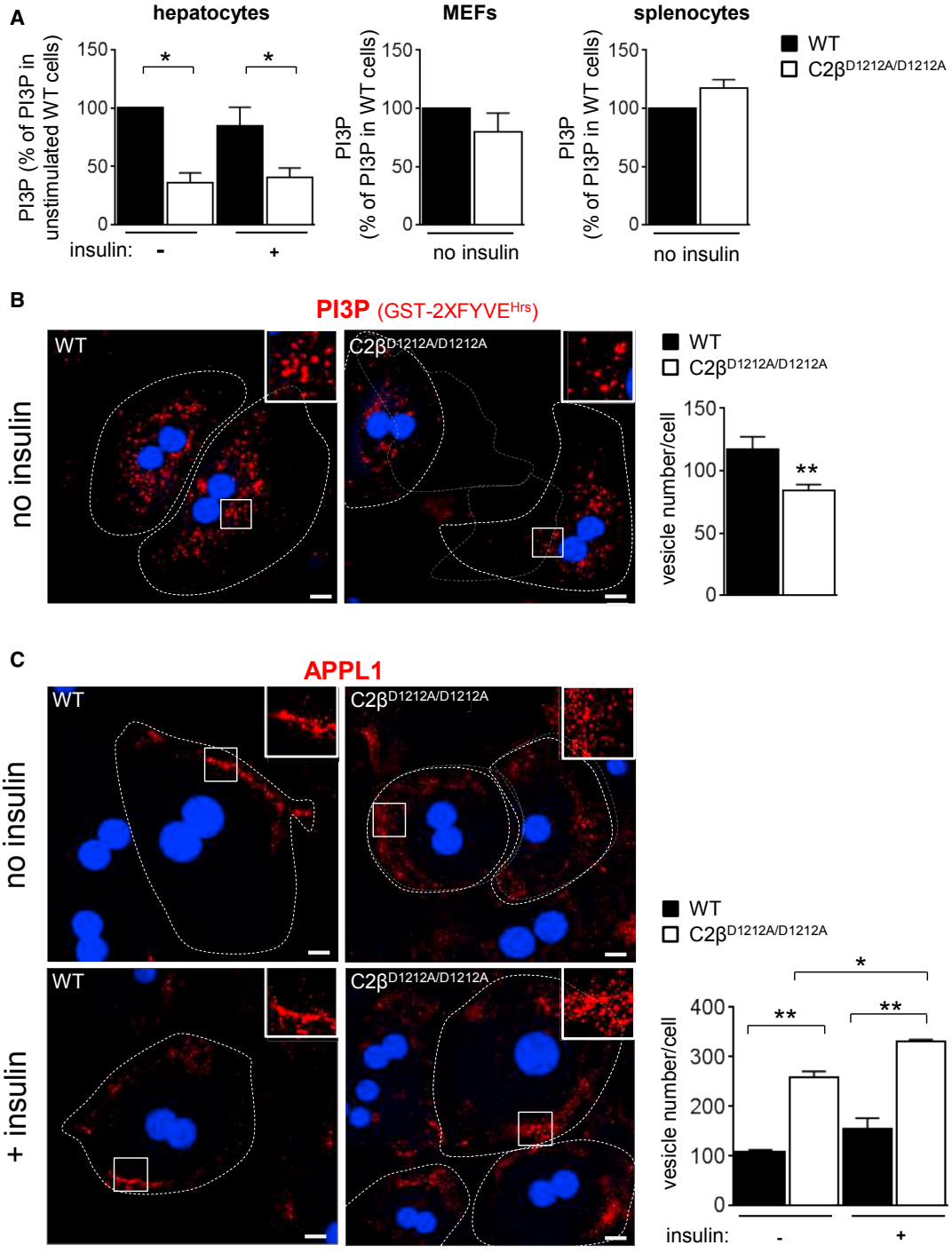

Figure 5. PI3K-C2β Inactivation Induces Endosomal Trafficking Defects and Expansion of the Very Early APPL1 Endosomal Compartment

(A) Analysis of total cellular PI3P levels in different cell types/tissues. Hepatocytes and MEFs were starved overnight, and hepatocytes were stimulated with or without insulin (100nM) for 10 min. Splenocytes were collected from mice after overnight starvation. Cell cultures from five mice/genotype were used for all tissues, except for MEF (three WT/six C2β$^{D1212A/D1212A}$).

(B) Analysis of endogenous PI3P in fixed overnight starved hepatocytes by staining using a GST-2xFYVE^{HRS} probe.

(C) Analysis of APPL1 staining in overnight starved hepatocytes stimulated with or without insulin (100nM) for 10 min.

(B and C) DAPI-stained nuclei are shown in blue. The inset shows a higher magnification (300×) of FYVE- and APPL1-positive vesicles. Quantification using Metamorph software was performed on three to five independent hepatocyte cell cultures/genotype. Scale bar, 20 μm.

Data represent mean ± SEM. *$p < 0.05$, **$p \leq 0.01$, ***$p \leq 0.001$.

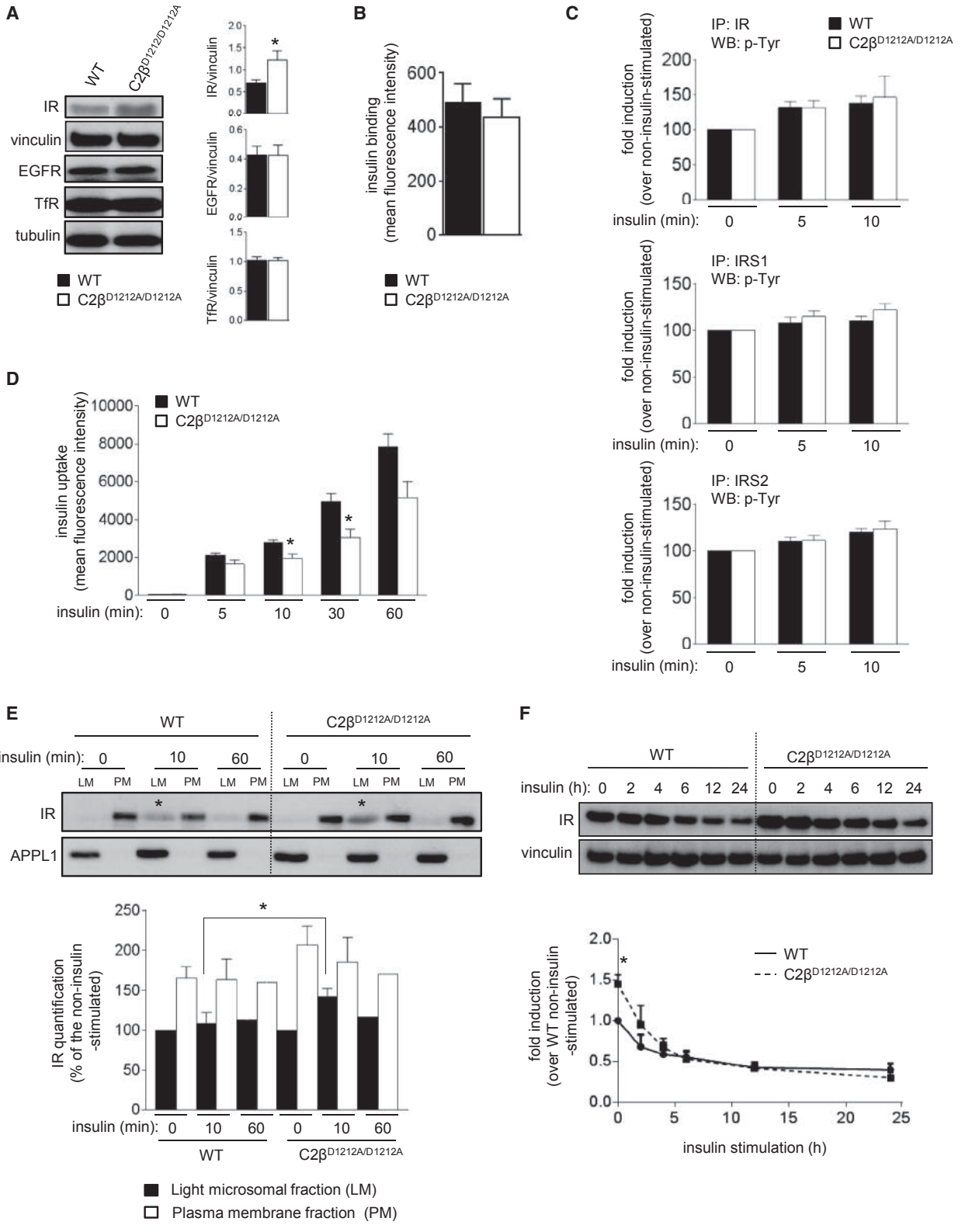

(legend on next page)

assessment of the role of the catalytic activity rather than possible scaffolding functions of the targeted PI3K.

PI3K-C2β Inactivation Increases Insulin Sensitivity and Glucose Metabolism

Our study uncovered that kinase inactivation of PI3K-C2β in mice enhances insulin sensitivity and protects against high-fat-diet-induced hepatic steatosis. These findings were unexpected, for several reasons. First, previous studies in cell lines had mainly implicated PI3K-C2α, and not PI3K-C2β, in insulin signaling (Brown et al., 1999; Falasca et al., 2007; Leibiger et al., 2010; Soos et al., 2001; Ursø et al., 1999) and insulin secretion (Dominguez et al., 2011), although in most of these studies, the role of PI3K-C2β was not assessed. Second, it was remarkable to observe that inactivation of a kinase leads to *improved* insulin signaling and metabolic sensitization. Last, and still unexplained, is the apparent exclusive action of PI3K-C2β downstream of insulin, and its restriction to Akt signaling and metabolic tissues (discussed in more detail below).

Although we focused our experiments on hepatocytes, it is likely that the adipose tissue and muscle are also functionally involved in the global metabolic improvement seen in PI3K-C2β KI mice, as we also observed clearly enhanced insulin-induced Akt activation in these tissues. Based on the notion that insulin and activation of Akt are known to induce lipid storage in the liver (Leavens and Birnbaum, 2011), sustained hepatic Akt activation could be expected to lead to an increase in steatosis. This is also supported by observations in transgenic mice that express membrane-bound (and therefore constitutively active) Akt in the liver (Ono et al., 2003) or in mice with liver-specific deletion of PTEN (Horie et al., 2004), which also show enhanced steatosis. While it is challenging to link short-term signaling (minutes to hours) to long-term biological effects (4 months in the case of high-fat diet), it is important to mention that, in contrast to the *constitutive* over-activation of Akt in the mutant mice mentioned above, $C2\beta^{D1212A/D1212A}$ mice only display a *transient* over-activation of Akt upon insulin stimulation. Moreover, it is very likely that the systemic enhancement in insulin sensitivity, with increased Akt activity in muscle and adipose tissue in addition to the liver, leads to an overall improved metabolism of $C2\beta^{D1212A/D1212A}$ mice, which reduces the development of hepatic steatosis as a consequence.

Together with the observation that no abnormalities were observed in an in-depth histopathological analysis of adult $C2\beta^{D1212A/D1212A}$ mice, our data identify PI3K-C2β as a potential drug target for insulin sensitization in the treatment of insulin resistance in type 2 diabetes or non-alcoholic fatty liver disease.

PI3K-C2β Is a Major Endosomal Producer of Basal PI3P in Hepatocytes

One previous study has implicated PI3K-C2β in PI3P production, namely, in the PI3P synthesis induced by lysophosphatidic acid in HeLa and SKOV-3 cell lines (Maffucci et al., 2005). Our study shows that PI3K-C2β is required for a large fraction (60%) of the basal PI3P in hepatocytes and therefore demonstrates that class II PI3Ks can significantly contribute to PI3P pools in vivo in the liver. Interestingly, the reduction in PI3P upon PI3K-C2β inactivation selectively impacted on endosomal trafficking but did not affect the formation of starvation-induced early autophagic vacuoles in these cells, indicating that PI3K-C2β mainly controls the endosomal PI3P pool in hepatocytes. It is possible that vps34 or class II PI3K isoforms other than PI3K-C2β (Devereaux et al., 2013) generate the autophagic PI3P pool in the liver.

PI3K-C2β Inactivation Results in an "APPL1 Expansion Signature"

IF analysis of intracellular vesicles revealed that PI3K-C2β inactivation led to an expansion of the very early APPL1-positive endosomal compartment in hepatocytes, under basal and insulin-stimulated conditions. We show in this study that PI3K-C2β is linked to the regulation of intracellular vesicular trafficking.

APPL1 is a scaffolding protein with multiple functional domains, including a Bin1/amphiphysin/rvs167 (BAR) domain, a PH domain, a phosphotyrosine binding (PTB) domain, and a CC motif (Deepa and Dong, 2009). APPL1 interacts with various receptors (such as the IR, TrkA, and the adiponectin receptor), signaling and scaffolding proteins (including Akt, IRS, and the OCRL inositol polyphosphate 5-phosphatase), and vesicular trafficking proteins (such as GTP-bound Rab5) (Deepa and Dong, 2009; Ryu et al., 2014). Our findings are in line with a cell-based study that highlighted a critical role for PI3P in the maturation of the APPL1-positive very early endosomes to

Figure 6. Impact of PI3K-C2β Inactivation on IR Levels and Trafficking in Hepatocytes

(A) Expression levels of IR, EGF, and transferrin receptor in total cell extracts. Homogenates of hepatocytes were analyzed by SDS-PAGE and immunoblotting using indicated antibodies. Quantification of three to five independent hepatocyte cultures/genotype is shown.

(B) Insulin binding capacity of hepatocytes. Quantification of three independent hepatocyte cultures/genotype is shown.

(C) Cultured hepatocytes were serum-starved overnight and stimulated for the indicated times with 100 nM insulin, followed by immunoprecipitation using the indicated antibodies. The immune complexes were analyzed by western blot and probed with the indicated antibodies. The bar charts represent the quantification of western blots from four to five independent experiments, shown in Figure S6 as follows: time point 0: averages of experiments a–e (apart from IRS1, average of experiments a–d); time point 5 min: averages of experiments b–e; time point 10 min: averages of experiments a–c.

(D) Insulin uptake in hepatocytes. Quantification of five independent hepatocyte cultures/genotype is shown.

(E) Distribution of IR and APPL1 in subcellular fractions of hepatocytes. Hepatocytes were starved overnight and stimulated with insulin for the indicated time points, followed fractionation of lysates in light microsome (LM) and plasma membrane (PM) fractions by ultracentrifugation, followed by SDS-PAGE analysis and immunoblotting with antibodies to the indicated proteins. A representative experiment is shown. The star indicates the different levels of IR in the APPL1-positive fraction in WT and $C2\beta^{D1212A/D1212A}$ cells stimulated for 10 min with insulin. Three independent hepatocyte cell cultures/genotype were used.

(F) Insulin-stimulated IR degradation in hepatocytes. Cells were starved overnight, stimulated with insulin for the indicated time points, followed by SDS-PAGE analysis and immunoblotting using antibodies to IR. Three independent hepatocyte cell cultures/genotype were used.

Data represent mean ± SEM. $^{*}p < 0.05$, $^{**}p \leq 0.01$, $^{***}p \leq 0.001$.

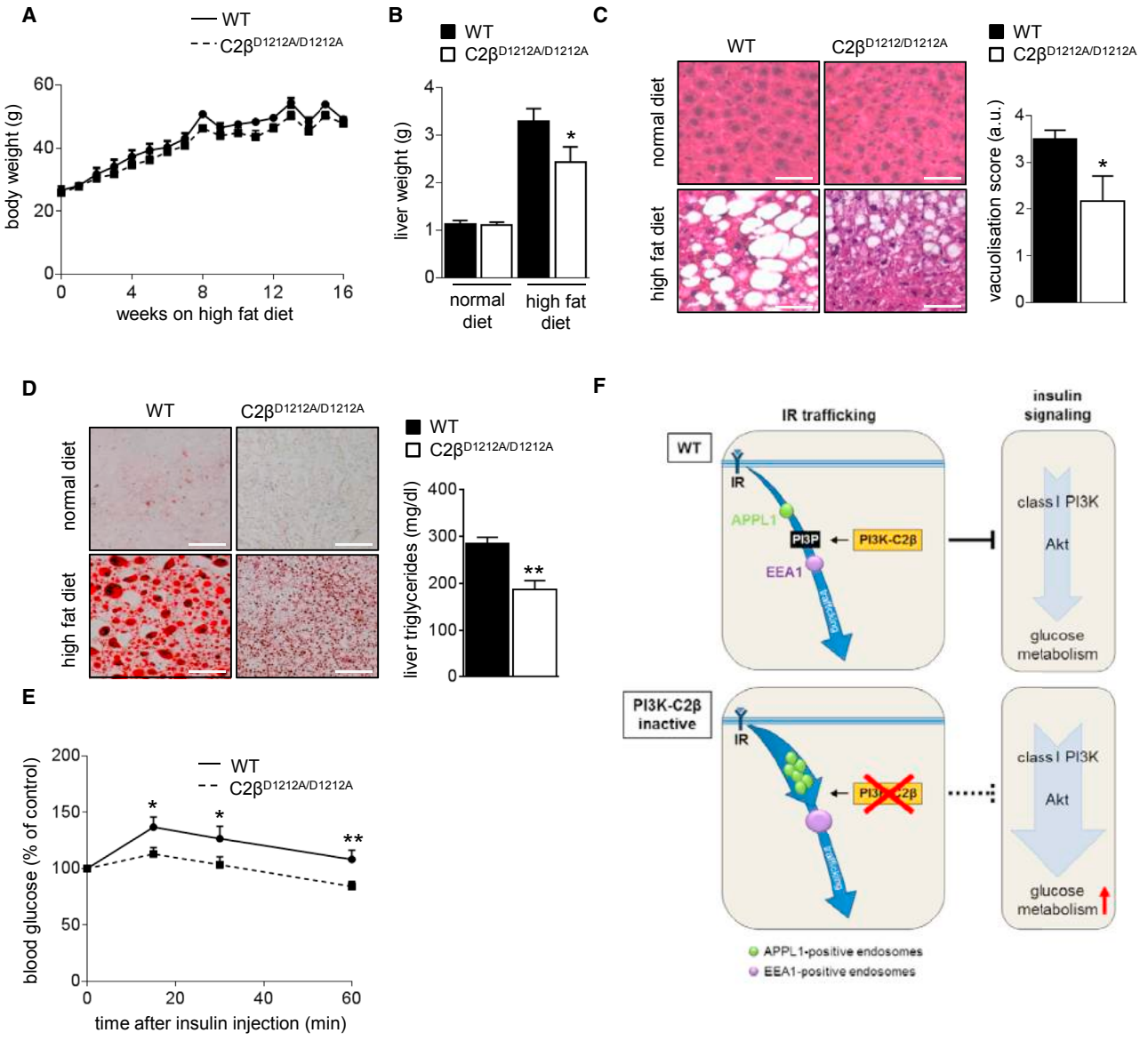

Figure 7. C2β$^{D1212A/D1212A}$ Mice Are Protected against High-Fat-Diet-Induced Steatosis

(A) Body weight of mice during 16 weeks of high-fat diet.

(B) Liver weight after 16 weeks of high-fat diet. Five to ten livers/genotype were used of mice on a normal (control) or high-fat diet.

(C) Liver histology. H&E staining of liver sections of mice after 16 weeks of high-fat diet. Quantification of vacuolization of seven livers/genotype is shown on the right. a.u., arbitrary units. Scale bar, 50 μm.

(D) Oil red O staining and liver triglyceride levels. Oil red O staining of liver sections after 16 weeks of normal or high-fat diet. Ten mice/genotype. Scale bar, 50 μm.

(E) Insulin tolerance test after intraperitoneal injection of 0.75 U/kg of insulin in overnight starved mice. Ten mice/genotype.

(F) Model of the role of PI3K-C2β in PI3P production in hepatocytes and its impact on IR trafficking through endosomal compartments. In WT cells, PI3K-C2β generates a large fraction of the PI3P that controls the maturation of the very early APPL1-positive endosomes into early EEA1-positive endosomes. In WT mice, this attenuates IR signaling by enabling the transit of IR through endosomal compartments, either toward recycling or degradation. Inactivation of PI3K-C2β leads to a decrease in endosomal PI3P, which could delay the maturation of the very early APPL1-positive endosomes into early EEA1-positive endosomes. This leads to an accumulation of APPL1-positive endosomes and temporarily affects IR trafficking, correlating with an increased and more sustained Akt signaling in metabolic tissues. This increase in Akt signaling enhances insulin sensitivity and glucose metabolism in cells and mice with inactive PI3K-C2β.

Data represent mean ± SEM. *$p < 0.05$, **$p \leq 0.01$, ***$p \leq 0.001$.

EEA1-positive early endosomes (Zoncu et al., 2009). These authors showed that PI3P depletion in the Rab5-positive compartment (by introduction of PI3P-specific phosphatases) led to an accumulation of the EGFR in an expanded very early APPL1-positive endosomal compartment upon EGF stimulation, resulting in enhanced downstream signaling (Zoncu et al., 2009). Our

study uncovers a similar APPL1-based mechanism for IR trafficking, correlating with enhanced insulin-stimulated Akt activation. Further support for a role for APPL1 in insulin action comes from observations made by APPL1 KO/overexpression in mice. For example, APPL1 KO mice show the opposite metabolic phenotype to C2β$^{D1212A/D1212A}$ mice, being insulin-resistant and glucose-intolerant with decreased insulin-stimulated Akt signaling in the liver, muscle, and adipose tissue (Ryu et al., 2014). Conversely, APPL1 overexpression in the liver increases Akt activation and alleviates insulin resistance in obese mice (Cheng et al., 2009).

PI3K-C2β Inactivation Enhances Insulin Signaling in Metabolic Tissues

Under basal conditions, C2β$^{D1212A/D1212A}$ hepatocytes had substantially lower levels of total cellular PI3P than WT cells. Insulin stimulation of these cells did not alter PI3P levels in either genotype but did increase PIP_3 levels, as expected. Interestingly, insulin stimulation led to a higher PIP_3 increase in C2β$^{D1212A/D1212A}$ hepatocytes compared to WT cells.

These data are consistent with a model (Figure 7F) whereby, in hepatocytes, PI3K-C2β is responsible for the *constitutive* production of a large fraction of the PI3P required for the basal endosomal flux. Under basal conditions, C2β$^{D1212A/D1212A}$ hepatocytes had an ~2-fold increase in overall IR levels over WT cells, without higher IR expression at the cell surface, pointing to the existence of an intracellular pool of IR. At present, the exact subcellular location of this IR pool is unknown. Given that the APPL1-positive compartment is expanded, it is possible that the IR is stuck as a consequence of a "traffic jam" in its endocytic flux.

Upon insulin stimulation, there was no difference in tyrosine phosphorylation of the IR, in line with unaltered IR levels at the cell surface. However, as insulin-mediated Akt signaling was temporarily enhanced upon PI3K-C2β inactivation, it is possible that the ligand-bound IR signals longer as a result of its slower endocytosis due to the "traffic jam" in the APPL1 compartment. A similar phenomenon was previously shown for the EGFR and its downstream signaling upon expansion of the APPL1 compartment due to PI3P reduction (Zoncu et al., 2009). Upon prolonged (6–7 hr) exposure to insulin, the higher overall IR levels in C2β$^{D1212A/D1212A}$ hepatocytes were found to return to that seen in WT cells, possibly due to insulin-induced repeated endocytic cycling whereby a small fraction of the activated IR pool is trafficked along the degradative route in each endocytic cycle.

Supportive of our model that IR traffic is delayed in the APPL1 compartment is the recent report showing that APPL1 can bind both IR and IRS and facilitate the insulin-stimulated interaction between IR and IRS (Ryu et al., 2014). The capacity of IR/IRS/Akt/APPL1 to dynamically interact, in a subcellular compartment controlled by PI3P, is likely to be key in explaining the selective metabolic impact of PI3K-C2β inactivation.

Unfortunately, we were not able to visualize endogenous IR, PIP_3, or phospho-Akt by IF using an extensive range of homemade or commercially available antibodies. IF analyses using fluorescently labeled insulin on primary hepatocytes, both on fixed cells or by live imaging, were also not successful. We therefore do not know the exact subcellular location of increased PIP_3 production and Akt activation upon PI3K-C2β inactivation.

Selective Role of PI3K-C2β in Insulin-Stimulated Akt Activation in Metabolic Tissues

One of the most surprising findings of our work is the apparent exclusive action of PI3K-C2β downstream of insulin, and its restriction to Akt signaling and metabolic tissues. Our data clearly show that a reduction in PI3P, as a consequence of PI3K-C2β inactivation, and the ensuing block in endosomal traffic enhances cell signaling in a very specific manner. At the organismal level, PI3K-C2β inactivation induced an increase in insulin-stimulated Akt signaling specifically in insulin target tissues (liver, muscle, and adipose tissue) but not in the spleen where PI3K-C2β is expressed highly. PI3K-C2β inactivation did also not affect the basal levels of PI3P in splenocytes or MEFs. Further studies conducted on hepatocytes showed additional specificity of PI3K-C2β action. First, at the receptor level, PI3K-C2β inactivation led to increased IR protein expression in these cells, without altering the levels of the receptors for EGF or transferrin and modulated the intracellular trafficking of the IR but not that of the transferrin receptor. Second, at the ligand level, PI3K-C2β inactivation increased insulin-induced Akt signaling in hepatocytes, without altering EGF- or IGF-mediated Akt signaling. Last, but not least, at the downstream signaling level, PI3K-C2β inactivation in hepatocytes led to an increased insulin-stimulated Akt activation without affecting MAPK signaling.

At present, we do not have a clear explanation for these observations. The absolute expression levels of the PI3K-C2β protein in different tissues are unlikely to be key in this phenomenon, given that PI3K-C2β expression is high in the spleen compared to liver. PI3P turnover in different tissues may depend on tissue-specific activities of the PI3Ks and other PI kinases but also of lipid phosphatases. It is also possible that such specificity could be provided by the scaffolding properties of APPL1, allowing this protein to interact with tissue- and receptor-specific binding partners, creating tissue-/ligand-/signaling-selective protein hubs. It is of interest to note that, despite the broad tissue distribution of APPL1, numerous studies have described APPL1 as an important player specifically in metabolic tissues and in particular in insulin signaling (Cheng et al., 2014). In line with our observations, other studies have documented that alterations in APPL1 expression can differentially affect signaling depending on the stimulus. For example, APPL1 KO in MEFs was found to reduce Akt activation induced by Hepatocyte Growth Factor, but not by EGF, insulin, or serum (Tan et al., 2010). Likewise, APPL1 knockdown in zebrafish led to a decrease in growth factor-induced Akt signaling with no impact on MAPK (Schenck et al., 2008). These data suggest that APPL1 endosomes can serve as signaling platforms for selective recruitment and activation of signaling components.

Conclusions

Taken together, our study reports on the creation of the class II PI3K knockin mice to model systemic PI3K-C2β kinase inactivation and identifies this isoform of PI3K as a drug target for the treatment of insulin resistance in type 2 diabetes or non-alcoholic fatty liver diseases.

EXPERIMENTAL PROCEDURES

Mice

All experiments were performed on 6- to 12-week-old male C57BL/6J mice, unless otherwise specified. Mice were kept on standard chow diet (20% protein, 75% carbohydrate, 5% fat) on a 12-hr light-dark cycle (lights on at 7 a.m.) with free access to water in individually ventilated cages and cared for according to United Kingdom Animals (Scientific Procedures) Act (1986). For high-fat-diet experiments, mice were maintained on diet 824053 from Special Diet Services (20% protein, 35% carbohydrate, and 45% fat) for 16 weeks.

Creation of C2β^{D1212A} Mice and PCR Genotyping

Mouse gene targeting was performed by Artemis in C57BL/6NT embryonic stem cells. Mice were backcrossed on the C57BL/6J strain (Charles River Laboratories) for greater than ten generations, and mice used for experiments were on mixed C57BL/6J × C57BL/6NT background, with WT littermates used as controls. The sequences of the primers used for genotyping are as follows: forward primer (*a* in Figure 1B): 1614-29 KI: CACTGCAGGAAGT GTGAAGC; antisense primer (*b* in Figure 1B): 1614-30 KI: GTGGACA GAAAGGCTGATGC, with expected fragments of 235 (WT) and 398 (KI) bp. PCR conditions were as follows: 95°C for 5 min, 34 cycles of (95°C 30 s, 65°C 30 s, 72°C 1 min) and 72°C for 10 min. The presence of the D1212A mutation was verified by sequencing of a PCR fragment generated using forward primer 1743-25 ivm: GCTTTGGTATATGATGAAAGG (*c* in Figure 1B) and antisense primer 1743-26 ivm: GTCTTCTGGTCTCCAGAAGC (*d* in Figure 1B) using the PCR conditions described above. PCRs were performed using Titanium Taq polymerase (Clontech) on a ThermalCycler (MJ Research).

Hepatocyte and Mouse Embryonic Fibroblast Isolation and Culture

Primary mouse hepatocytes were isolated from 8- to 12-week-old mice as described, with minor changes (Guidotti et al., 2003). Briefly, primary hepatocytes were isolated by a two-step perfusion protocol using collagenase I (Sigma) and seeded on collagen-coated plates in complete medium (William's E GlutaMAX medium containing 0.1% BSA, 1% penicillin/streptomycin, 25 nM dexamethasone [Sigma], and 100 nM insulin) in the presence of 10% (v/v) fetal bovine serum (FBS). After 4 hr incubation at 37°C to allow cell adhesion, the medium was replaced either by starvation medium (complete medium without insulin) or complete medium (for autophagy studies), and cells were further incubated at 37°C overnight.

For signaling studies, fluorescence-activated cell sorting (FACS) analysis, immunofluorescence, lipid analysis, and cell fractionation, culture medium was removed and replaced by fresh starvation medium containing insulin (100 nM), EGF (200 nM), or IGF-1 (3.9 nM) for the indicated times. In some experiments, GDC-0941 (500 nM) was added at 30 min before cell stimulation.

For autophagy studies, complete medium was removed and cultures were washed twice with amino-acid- and serum-free medium (EBSS; Invitrogen), and cells were maintained in EBSS for 30 min. Control, non-starved cells were washed in complete medium instead of EBBS.

Mouse embryonic fibroblasts (MEFs) were isolated from intercrosses of mice heterozygous for the PI3K-C2β^{D1212A} allele as described (Foukas et al., 2006).

Antibodies and Reagents

All antibodies were against mouse proteins as follows: APPL1, EEA1, Rab7, GST, pAkt-S473, pAkt-T308 Akt, p42/44 pMAPK-T202/pY204, Akt, p110α, insulin receptor, vps34 (Cell Signaling Technology); PI3K-C2α, PI3K-C2β (BD Biosciences); p110β, ptyr99 (Santa Cruz Biotechnology); vinculin, α-tubulin, EGFR (Sigma); transferrin receptor (Abcam); and LC3 (2G6; Nanotools). Antibodies to WIPI-1 and WIPI-2 were kindly provided by Sharon Tooze (London Research Institute). In-house-made antibodies to IRS1 and IRS2 were provided by Dominic Withers (Imperial College London). Fluorescein isothiocyanate (FITC)-insulin (bovine) was from Sigma, and FITC-transferrin (human) was from Molecular Probes. Unless otherwise mentioned, PBS (Sigma) was Ca^{2+} and Mg^{2+} free. All culture media for primary cell culture were from Invitrogen. A plasmid expressing GST-2xFYVE^{HRS} (Gillooly et al., 2000) was kindly provided by Harald Stenmark, Norway. Recombinant GST protein was purified from *E. coli* BL21 (DE3) cells according to the manufacturer's instructions. All buffers used during purification of the GST-fusion steps were EDTA free, and the recombinant protein was dialyzed against HEPES buffer (pH 7.4) containing 10 μM $ZnCl_2$. Agonists used were insulin (human [Actrapid] and bovine [Sigma] for in vivo and in vitro experiments, respectively), EGF (human; PeproTech), or IGF-1 (human; PeproTech). GDC-0941 was from Axon-Medchem.

Statistical Analysis

All data are shown as mean ± SEM. Data sets were compared for statistical significance using a two-tailed Student's t test. All statistical analyses were generated using Excel software and statistical significance indicated as $^*p < 0.05$, $^{**}p \leq 0.01$, $^{***}p \leq 0.001$.

SUPPLEMENTAL INFORMATION

Supplemental Information includes Supplemental Experimental Procedures, seven figures, and two tables and can be found with this article online at http://dx.doi.org/10.1016/j.celrep.2015.10.052.

AUTHOR CONTRIBUTIONS

S.A., B.B., G.C., K.E.A., W.P., K.A., C.V., P.C.L., Y.P., C.C., and R.S.S. performed experiments and data analyses with input from B.P., J.M.B., L.S., P.T.H., and B.V.; C.L.S. analyzed and interpreted histopathology. S.A., B.B., and B.V. wrote the paper.

ACKNOWLEDGMENTS

We thank M. Falasca (Curtin University, Australia) and G. Tibolla (University of Milan, Italy) for providing tissues from PI3K-C2β KO mice, D. Ciantar for help with microscopy (UCL, UK), C. Woelk (Southampton University, UK) and S. Castillo (UCL, UK) for help with statistics, Harald Stenmark (University of Oslo, Norway), S. Tooze (London Research Institute, UK), D. Withers (Imperial College London, UK), L. Foukas (UCL, UK), and R. Chin and A. Toker (Harvard, Boston) for advice and providing reagents, staff at TaconicArtemis (Cologne, Germany) for the mouse gene targeting, and M. Whitehead for critical input in interpretation of the data and writing of the manuscript. Fellowships were from EU Marie Curie (PIEF-GA-2009-252916) and EMBO (ALTF 753-2010) for S.A., from EMBO (ALTF 1227-2014) for Y.P., from EU Marie Curie (PIIF-GA-2009-252846) for C.C. and from EU Marie Curie (PIIF-GA-2013-330716) for P.C.L. Work in the laboratory of B.V. was supported by the UK BBSRC (BB/I007806/1), Cancer Research UK (C23338/A15965), the Ludwig Institute for Cancer Research and the National Institute for Health Research (NIHR) UCL Hospitals Biomedical Research Centre. Work in the laboratory of J.M.B. was supported by NIH DK 20541 and the Albert Einstein Diabetes Research and Training Center Animal Physiology Core. Work in the laboratory of B.P. was supported by Inserm and the Fondation pour la recherche médicale. Work in the laboratory of L.S. and P.T.H. was supported by the UK BBSRC (BB/J004456/1 and BB/I003916/1). B.V., L.S., and P.T.H. are consultants to Karus Therapeutics (Oxford, UK).

Received: December 11, 2014
Revised: August 25, 2015
Accepted: October 15, 2015
Published: November 19, 2015

REFERENCES

Al-Qassab, H., Smith, M.A., Irvine, E.E., Guillermet-Guibert, J., Claret, M., Choudhury, A.I., Selman, C., Piipari, K., Clements, M., Lingard, S., et al. (2009). Dominant role of the p110beta isoform of PI3K over p110alpha in energy homeostasis regulation by POMC and AgRP neurons. Cell Metab. *10*, 343–354.

Ali, K., Bilancio, A., Thomas, M., Pearce, W., Gilfillan, A.M., Tkaczyk, C., Kuehn, N., Gray, A., Giddings, J., Peskett, E., et al. (2004). Essential role for the p110delta phosphoinositide 3-kinase in the allergic response. Nature *431*, 1007–1011.

Brown, R.A., Domin, J., Arcaro, A., Waterfield, M.D., and Shepherd, P.R. (1999). Insulin activates the alpha isoform of class II phosphoinositide 3-kinase. J. Biol. Chem. *274*, 14529–14532.

Cheng, K.K., Iglesias, M.A., Lam, K.S., Wang, Y., Sweeney, G., Zhu, W., Vanhoutte, P.M., Kraegen, E.W., and Xu, A. (2009). APPL1 potentiates insulin-mediated inhibition of hepatic glucose production and alleviates diabetes via Akt activation in mice. Cell Metab. *9*, 417–427.

Cheng, K.K., Lam, K.S., Wang, B., and Xu, A. (2014). Signaling mechanisms underlying the insulin-sensitizing effects of adiponectin. Best Pract. Res. Clin. Endocrinol. Metab. *28*, 3–13.

Chicanne, G., Severin, S., Boscheron, C., Terrisse, A.D., Gratacap, M.P., Gaits-Iacovoni, F., Tronchère, H., and Payrastre, B. (2012). A novel mass assay to quantify the bioactive lipid PtdIns3P in various biological samples. Biochem. J. *447*, 17–23.

Deepa, S.S., and Dong, L.Q. (2009). APPL1: role in adiponectin signaling and beyond. Am. J. Physiol. Endocrinol. Metab. *296*, E22–E36.

Devereaux, K., Dall'Armi, C., Alcazar-Roman, A., Ogasawara, Y., Zhou, X., Wang, F., Yamamoto, A., De Camilli, P., and Di Paolo, G. (2013). Regulation of mammalian autophagy by class II and III PI 3-kinases through PI3P synthesis. PLoS ONE *8*, e76405.

Dominguez, V., Raimondi, C., Somanath, S., Bugliani, M., Loder, M.K., Edling, C.E., Divecha, N., da Silva-Xavier, G., Marselli, L., Persaud, S.J., et al. (2011). Class II phosphoinositide 3-kinase regulates exocytosis of insulin granules in pancreatic beta cells. J. Biol. Chem. *286*, 4216–4225.

Falasca, M., and Maffucci, T. (2012). Regulation and cellular functions of class II phosphoinositide 3-kinases. Biochem. J. *443*, 587–601.

Falasca, M., Hughes, W.E., Dominguez, V., Sala, G., Fostira, F., Fang, M.Q., Cazzolli, R., Shepherd, P.R., James, D.E., and Maffucci, T. (2007). The role of phosphoinositide 3-kinase C2alpha in insulin signaling. J. Biol. Chem. *282*, 28226–28236.

Foukas, L.C., Claret, M., Pearce, W., Okkenhaug, K., Meek, S., Peskett, E., Sancho, S., Smith, A.J., Withers, D.J., and Vanhaesebroeck, B. (2006). Critical role for the p110alpha phosphoinositide-3-OH kinase in growth and metabolic regulation. Nature *441*, 366–370.

Franco, I., Gulluni, F., Campa, C.C., Costa, C., Margaria, J.P., Ciraolo, E., Martini, M., Monteyne, D., De Luca, E., Germena, G., et al. (2014). PI3K class II α controls spatially restricted endosomal PtdIns3P and Rab11 activation to promote primary cilium function. Dev. Cell *28*, 647–658.

Gillooly, D.J., Morrow, I.C., Lindsay, M., Gould, R., Bryant, N.J., Gaullier, J.M., Parton, R.G., and Stenmark, H. (2000). Localization of phosphatidylinositol 3-phosphate in yeast and mammalian cells. EMBO J. *19*, 4577–4588.

Gorden, P., Arakaki, R., Collier, E., and Carpentier, J.L. (1989). Biosynthesis and regulation of the insulin receptor. Yale J. Biol. Med. *62*, 521–531.

Graupera, M., Guillermet-Guibert, J., Foukas, L.C., Phng, L.K., Cain, R.J., Salpekar, A., Pearce, W., Meek, S., Millan, J., Cutillas, P.R., et al. (2008). Angiogenesis selectively requires the p110alpha isoform of PI3K to control endothelial cell migration. Nature *453*, 662–666.

Guidotti, J.E., Bregerie, O., Robert, A., Debey, P., Brechot, C., and Desdouets, C. (2003). Liver cell polyploidization: a pivotal role for binuclear hepatocytes. J. Biol. Chem. *278*, 19095–19101.

Guillermet-Guibert, J., Bjorklof, K., Salpekar, A., Gonella, C., Ramadani, F., Bilancio, A., Meek, S., Smith, A.J., Okkenhaug, K., and Vanhaesebroeck, B. (2008). The p110beta isoform of phosphoinositide 3-kinase signals downstream of G protein-coupled receptors and is functionally redundant with p110gamma. Proc. Natl. Acad. Sci. USA *105*, 8292–8297.

Harada, K., Truong, A.B., Cai, T., and Khavari, P.A. (2005). The class II phosphoinositide 3-kinase C2beta is not essential for epidermal differentiation. Mol. Cell. Biol. *25*, 11122–11130.

Harris, D.P., Vogel, P., Wims, M., Moberg, K., Humphries, J., Jhaver, K.G., DaCosta, C.M., Shadoan, M.K., Xu, N., Hansen, G.M., et al. (2011). Requirement for class II phosphoinositide 3-kinase C2alpha in maintenance of glomerular structure and function. Mol. Cell. Biol. *31*, 63–80.

Ho, L.K., Liu, D., Rozycka, M., Brown, R.A., and Fry, M.J. (1997). Identification of four novel human phosphoinositide 3-kinases defines a multi-isoform subfamily. Biochem. Biophys. Res. Commun. *235*, 130–137.

Horie, Y., Suzuki, A., Kataoka, E., Sasaki, T., Hamada, K., Sasaki, J., Mizuno, K., Hasegawa, G., Kishimoto, H., Iizuka, M., et al. (2004). Hepatocyte-specific Pten deficiency results in steatohepatitis and hepatocellular carcinomas. J. Clin. Invest. *113*, 1774–1783.

Jean, S., and Kiger, A.A. (2014). Classes of phosphoinositide 3-kinases at a glance. J. Cell Sci. *127*, 923–928.

Knight, Z.A., Gonzalez, B., Feldman, M.E., Zunder, E.R., Goldenberg, D.D., Williams, O., Loewith, R., Stokoe, D., Balla, A., Toth, B., et al. (2006). A pharmacological map of the PI3-K family defines a role for p110alpha in insulin signaling. Cell *125*, 733–747.

Knutson, V.P. (1991). Cellular trafficking and processing of the insulin receptor. FASEB J. *5*, 2130–2138.

Leavens, K.F., and Birnbaum, M.J. (2011). Insulin signaling to hepatic lipid metabolism in health and disease. Crit. Rev. Biochem. Mol. Biol. *46*, 200–215.

Leibiger, B., Moede, T., Uhles, S., Barker, C.J., Creveaux, M., Domin, J., Berggren, P.O., and Leibiger, I.B. (2010). Insulin-feedback via PI3K-C2alpha activated PKBalpha/Akt1 is required for glucose-stimulated insulin secretion. FASEB J. *24*, 1824–1837.

Maffucci, T., Cooke, F.T., Foster, F.M., Traer, C.J., Fry, M.J., and Falasca, M. (2005). Class II phosphoinositide 3-kinase defines a novel signaling pathway in cell migration. J. Cell Biol. *169*, 789–799.

Nigorikawa, K., Hazeki, K., Guo, Y., and Hazeki, O. (2014). Involvement of class II phosphoinositide 3-kinase α-isoform in antigen-induced degranulation in RBL-2H3 cells. PLoS ONE *9*, e111698.

Okkenhaug, K., Bilancio, A., Farjot, G., Priddle, H., Sancho, S., Peskett, E., Pearce, W., Meek, S.E., Salpekar, A., Waterfield, M.D., et al. (2002). Impaired B and T cell antigen receptor signaling in p110delta PI 3-kinase mutant mice. Science *297*, 1031–1034.

Ono, H., Shimano, H., Katagiri, H., Yahagi, N., Sakoda, H., Onishi, Y., Anai, M., Ogihara, T., Fujishiro, M., Viana, A.Y., et al. (2003). Hepatic Akt activation induces marked hypoglycemia, hepatomegaly, and hypertriglyceridemia with sterol regulatory element binding protein involvement. Diabetes *52*, 2905–2913.

Platta, H.W., and Stenmark, H. (2011). Endocytosis and signaling. Curr. Opin. Cell Biol. *23*, 393–403.

Posor, Y., Eichhorn-Gruenig, M., Puchkov, D., Schöneberg, J., Ullrich, A., Lampe, A., Müller, R., Zarbakhsh, S., Gulluni, F., Hirsch, E., et al. (2013). Spatiotemporal control of endocytosis by phosphatidylinositol-3,4-bisphosphate. Nature *499*, 233–237.

Raiborg, C., Schink, K.O., and Stenmark, H. (2013). Class III phosphatidylinositol 3-kinase and its catalytic product PtdIns3P in regulation of endocytic membrane traffic. FEBS J. *280*, 2730–2742.

Ryu, J., Galan, A.K., Xin, X., Dong, F., Abdul-Ghani, M.A., Zhou, L., Wang, C., Li, C., Holmes, B.M., Sloane, L.B., et al. (2014). APPL1 potentiates insulin sensitivity by facilitating the binding of IRS1/2 to the insulin receptor. Cell Rep. *7*, 1227–1238.

Schenck, A., Goto-Silva, L., Collinet, C., Rhinn, M., Giner, A., Habermann, B., Brand, M., and Zerial, M. (2008). The endosomal protein Appl1 mediates Akt substrate specificity and cell survival in vertebrate development. Cell *133*, 486–497.

Soos, M.A., Jensen, J., Brown, R.A., O'Rahilly, S., Shepherd, P.R., and Whitehead, J.P. (2001). Class II phosphoinositide 3-kinase is activated by insulin but not by contraction in skeletal muscle. Arch. Biochem. Biophys. *396*, 244–248.

Sopasakis, V.R., Liu, P., Suzuki, R., Kondo, T., Winnay, J., Tran, T.T., Asano, T., Smyth, G., Sajan, M.P., Farese, R.V., et al. (2010). Specific roles of the p110alpha isoform of phosphatidylinsositol 3-kinase in hepatic insulin signaling and metabolic regulation. Cell Metab. *11*, 220–230.

Tan, Y., You, H., Wu, C., Altomare, D.A., and Testa, J.R. (2010). Appl1 is dispensable for mouse development, and loss of Appl1 has growth

factor-selective effects on Akt signaling in murine embryonic fibroblasts. J. Biol. Chem. *285*, 6377–6389.

Tups, A., Anderson, G.M., Rizwan, M., Augustine, R.A., Chaussade, C., Shepherd, P.R., and Grattan, D.R. (2010). Both p110alpha and p110beta isoforms of phosphatidylinositol 3-OH-kinase are required for insulin signalling in the hypothalamus. J. Neuroendocrinol. *22*, 534–542.

Ursø, B., Brown, R.A., O'Rahilly, S., Shepherd, P.R., and Siddle, K. (1999). The alpha-isoform of class II phosphoinositide 3-kinase is more effectively activated by insulin receptors than IGF receptors, and activation requires receptor NPEY motifs. FEBS Lett. *460*, 423–426.

Vanhaesebroeck, B., Ali, K., Bilancio, A., Geering, B., and Foukas, L.C. (2005). Signalling by PI3K isoforms: insights from gene-targeted mice. Trends Biochem. Sci. *30*, 194–204.

Vanhaesebroeck, B., Guillermet-Guibert, J., Graupera, M., and Bilanges, B. (2010). The emerging mechanisms of isoform-specific PI3K signalling. Nat. Rev. Mol. Cell Biol. *11*, 329–341.

Yoshioka, K., Yoshida, K., Cui, H., Wakayama, T., Takuwa, N., Okamoto, Y., Du, W., Qi, X., Asanuma, K., Sugihara, K., et al. (2012). Endothelial PI3K-C2α, a class II PI3K, has an essential role in angiogenesis and vascular barrier function. Nat. Med. *18*, 1560–1569.

Zhou, X., Takatoh, J., and Wang, F. (2011). The mammalian class 3 PI3K (PIK3C3) is required for early embryogenesis and cell proliferation. PLoS ONE *6*, e16358.

Zoncu, R., Perera, R.M., Balkin, D.M., Pirruccello, M., Toomre, D., and De Camilli, P. (2009). A phosphoinositide switch controls the maturation and signaling properties of APPL endosomes. Cell *136*, 1110–1121.

Annexe n°3

Membrane grease eases platelet production.

Sang H Min[1], Charles S Abrams[1]

[1] University of Pennsylvania, USA.

Inside *Blood* Commentaries 2015 Aug 27; 126: 1055-6

formation of new blood vessels. Exosome-educated stromal cells showed an enhanced capacity to support CLL cell survival. Finally, promotion of tumor growth/dissemination was demonstrated using a cotransfer in vivo model (CLL cells with exosomes). These initial data demonstrate a protumorigenic effect of CLL-derived exosomes when tumor cells engage the microenvironment to proliferate and promote angiogenesis. Taken together, the authors conclude that CLL exosomes actively promote disease progression by subverting the function of stromal cells that reside in the TME which acquire features of proinflammatory CAFs (see figure). Clearly, future studies will need to examine the coevolution of tumor cells and the reprogrammed stroma including characterizing the role CAFs play in regulating cancer hallmark capabilities.

This work by Paggetti et al establishes the tumorigenic importance of CLL-derived exosomes, including the transfer of their molecular cargo to other TME cells. This contributes to increasing evidence that the ability of tumor cells to induce CAFs is a universal feature of progression in both solid[8] and blood[7,10] cancers. These data also provide incentive for detailed mechanistic investigation of the role exosomes play in pathogenic signaling processes[6] and regulating the understudied CLL-TME. Examining the contribution of exosomes and their content in predicting response (biomarkers) to different therapeutic agents including newly targeted kinase inhibitors will be of interest. Paggetti et al show that CLL-derived exosomes act as decoys for the therapeutic antibody rituximab (anti-CD20) that highlights a potential drug escape mechanism in the TME. Continued research on TME regulation of tumor progression will provide insight into disease pathogenesis and also the exciting prospect of identifying novel targeted therapies designed to re-educate the TME to have antitumorigenic effects.

Conflict-of-interest disclosure: The authors declare no competing financial interests. ■

REFERENCES

1. Paggetti J, Haderk F, Seiffert M, et al. Exosomes released by chronic lymphocytic leukemia cells induce the transition of stromal cells into cancer-associated fibroblasts. *Blood.* 2015;126(9):1106-1117.

2. Scott DW, Gascoyne RD. The tumour microenvironment in B cell lymphomas. *Nat Rev Cancer.* 2014;14(8):517-534.

3. Webber J, Yeung V, Clayton A. Extracellular vesicles as modulators of the cancer microenvironment. *Semin Cell Dev Biol.* 2015;40:27-34.

4. Ghosh AK, Secreto C, Boysen J, et al. The novel receptor tyrosine kinase Axl is constitutively active in B-cell chronic lymphocytic leukemia and acts as a docking site of nonreceptor kinases: implications for therapy. *Blood.* 2011;117(6):1928-1937.

5. Moussay E, Wang K, Cho JH, et al. MicroRNA as biomarkers and regulators in B-cell chronic lymphocytic leukemia. *Proc Natl Acad Sci USA.* 2011;108(16):6573-6578.

6. Yeh YY, Ozer HG, Lehman AM, et al. Characterization of CLL exosomes reveals a distinct microRNA signature and enhanced secretion by activation of BCR signaling. *Blood.* 2015;125(21):3297-3305.

7. Lutzny G, Kocher T, Schmidt-Supprian M, et al. Protein kinase c-β-dependent activation of NF-κB in stromal cells is indispensable for the survival of chronic lymphocytic leukemia B cells in vivo. *Cancer Cell.* 2013;23(1):77-92.

8. Öhlund D, Elyada E, Tuveson D. Fibroblast heterogeneity in the cancer wound. *J Exp Med.* 2014;211(8):1503-1523.

9. Ruan J, Hyjek E, Kermani P, et al. Magnitude of stromal hemangiogenesis correlates with histologic subtype of non-Hodgkin's lymphoma. *Clin Cancer Res.* 2006;12(19):5622-5631.

10. Frassanito MA, Rao L, Moschetta M, et al. Bone marrow fibroblasts parallel multiple myeloma progression in patients and mice: in vitro and in vivo studies. *Leukemia.* 2014;28(4):904-916.

DOI 10.1182/blood-2015-07-655233

● ● ● PLATELETS AND THROMBOPOIESIS

Comment on Valet et al, page 1128

Membrane grease eases platelet maturation

Sang H. Min and Charles S. Abrams UNIVERSITY OF PENNSYLVANIA

In this issue of *Blood*, Valet et al[1] report a novel regulatory role of class II phosphoinositide 3-kinase (PI3K)-C2α in the morphology and remodeling of platelet membranes and its implications in platelet maturation and arterial thrombosis.

In 1906, James Homer Wright first postulated that platelets are produced in the bone marrow from megakaryocytes.[2] Our megakaryocytes collectively generate and release ~1 million platelets per second (10 billion platelets per day) into the bloodstream through a sequence of remodeling events. Megakaryocytes first undergo a series of maturation processes whereby they increase their overall size as they develop highly tortuous membrane invaginations that are called the invaginated membrane system (previously known as the demarcation membrane system).[3] Megakaryocytes use this extensive membrane reservoir to form long and thin cytoplasmic extensions to produce intermediate platelet structures called proplatelets.[4] Once released into the bloodstream, proplatelets undergo further remodeling steps that allow membrane fragmentation and generation of mature platelets. Proplatelet formation and maturation are heavily dependent on the membrane and cytoplasmic skeletal machinery, which include microtubule, actin, and spectrin.[5,6] Although microtubules and actin function as engines to power platelet formation and elongation, spectrin is necessary for the ultimate shape changes that occur when proplatelets mature

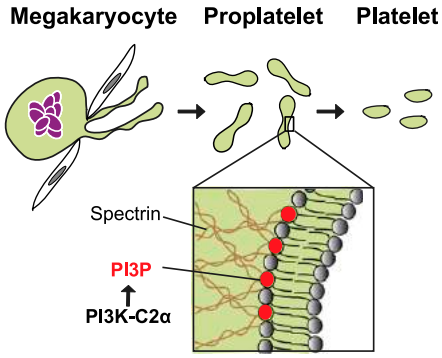

Membrane remodeling by class II PI3K-C2α is essential for platelet maturation. Megakaryocytes initiate platelet production by extending and releasing intermediate platelet structures called proplatelets into the bloodstream. Released proplatelets undergo a series of remodeling steps to generate mature platelets. Valet et al show that PI3K-C2α generates a distinct pool of PI3P in resting platelets that may modulate membrane elasticity and remodeling by reorganizing membrane skeletal proteins such as spectrin.

into platelets. However, the signaling molecules that are regulating and triggering these processes are not well understood.

PI3Ks are one family of lipid kinases that are involved in the complex synthesis of phosphoinositides.[7] In platelets, PI3Ks play critical signaling roles during the platelet plug formation.[8] For instance, class I PI3K synthesize phosphatidylinositol 3,4,5 trisphosphate, which recruits downstream effector proteins that are essential for the activation of the key platelet adhesion integrin receptor, αIIbβ3. In contrast, class II and class III PI3K isoforms are thought to synthesize the phosphoinositides phosphatidylinositol 3-phosphate (PI3P) and phosphatidylinositol 3,4 bisphosphate, which are involved in the regulation of endosomal trafficking and cell migration in other cell types. However, the precise roles of class II and class III PI3K isoforms and their lipid products in platelets remain elusive.

In a recent publication, Mountford et al showed that class II PI3K-C2α is a novel regulator of the internal membrane structures of megakaryocytes and platelets.[9] Using knockdown mouse models, the authors showed that PI3K-C2α deficiency in platelets disrupted the membrane structure of the invaginated membrane system in megakaryocytes and the open canalicular system in platelets by a mechanism that was independent of phosphoinositide production. The authors further showed that these membrane abnormalities were associated with defective platelet adhesion and stable thrombus formation. However, the mechanism by which PI3K-C2α regulates the membrane structures in megakaryocytes and in platelets was not investigated.

In this issue of *Blood*, Valet et al provide an important clue on how PI3K-C2α may regulate the membrane structures in platelets and in megakaryocytes.[1] Using heterozygous PI3K-C2α kinase-inactive knockin mouse models, Valet et al demonstrate that class II PI3K-C2α is essential for the synthesis of PI3P in platelets under basal but not stimulated conditions. Importantly, this distinct constitutive pool of PI3P is necessary for the remodeling of platelet membrane morphology during the maturation of proplatelets into platelets. The PI3K-C2α inactive megakaryocytes form an underdeveloped invaginated membrane system, and their platelets also develop aberrant and tortuous invaginations of the plasma membrane. Interestingly, mice with inactive PI3K-C2α accumulate barbell-shaped proplatelets in the bloodstream despite a normal platelet count. Moreover, these platelets have a more rigid plasma membrane and impaired filopodium formation upon stimulation. It is remarkable that these membrane defects were associated with a reduced recruitment of membrane skeletal proteins such as spectrin and myosin and membrane receptors such as GPIIb and GPIb. Finally, PI3K-C2α–inactive mice did not have prolonged bleeding times, but they showed delayed arterial thrombus formation when compared with control mice.

These illuminating findings by Valet et al demonstrate important biochemical and physiological roles of class II PI3K-C2α in platelets. In contrast to a recent publication where PI3K-C2α was found to be unnecessary for the intracellular pool of PI3P,[9] Valet et al provide evidence that class II PI3K-C2α contributes to the maintenance of the basal, but not the agonist-induced, pool of PI3P in platelets. Although a sudden change in the concentration of phosphoinositides has been known to be critical for diverse cellular processes, the physiological role of the housekeeping (basal) pool of phosphoinositides within the cell membrane has been more elusive. Thus, these findings highlight the potentially important functional roles of the housekeeping pools of phosphoinositides.

This study also reveals a previously unknown physiological role of PI3K-C2α in membrane remodeling and has implications for platelet maturation as well as thrombus formation. The authors propose that PI3K-C2α generates a PI3P pool that may modulate membrane elasticity by reorganizing the membrane skeletal proteins (see figure). However, PI3P has been shown to localize predominantly on the early endosomal membranes and not on the plasma membrane. Thus, how does a phospholipid on an internal membrane reorganize events on the cellular membrane? At the very least, further analysis of the precise localization of PI3P pools in platelets will be required to understand these events.

In conclusion, the work by Valet et al sheds light on the novel role and mechanism of class II PI3K-C2α on the membrane morphology and reorganization in platelets. Further research will be essential to understand the signaling mechanisms regulating the complex process of platelet production and maturation.

Conflict-of-interest disclosure: The authors declare no competing financial interests. ■

REFERENCES

1. Valet C, Chicanne G, Severac C, et al. Essential role of class II PI3K-C2α in platelet membrane morphology. *Blood.* 2015;126(9):1128-1137.

2. Wright JH. Die Entstehung der Blutplättchen. *Virchows Arch.* 1906;186(1):55-63.

3. Behnke O. An electron microscope study of the megacaryocyte of the rat bone marrow. I. The development of the demarcation membrane system and the platelet surface coat. *J Ultrastruct Res.* 1968;24(5):412-433.

4. Machlus KR, Italiano JE Jr. The incredible journey: from megakaryocyte development to platelet formation. *J Cell Biol.* 2013;201(6):785-796.

5. Patel-Hett S, Wang H, Begonja AJ, et al. The spectrin-based membrane skeleton stabilizes mouse megakaryocyte membrane systems and is essential for proplatelet and platelet formation. *Blood.* 2011;118(6):1641-1652.

6. Thon JN, Montalvo A, Patel-Hett S, et al. Cytoskeletal mechanics of proplatelet maturation and platelet release. *J Cell Biol.* 2010;191(4):861-874.

7. Cantley LC. The phosphoinositide 3-kinase pathway. *Science.* 2002;296(5573):1655-1657.

8. Min SH, Abrams CS. Regulation of platelet plug formation by phosphoinositide metabolism. *Blood.* 2013;122(8):1358-1365.

9. Mountford JK, Petitjean C, Putra HW, et al. The class II PI 3-kinase, PI3KC2α, links platelet internal membrane structure to shear-dependent adhesive function. *Nat Commun.* 2015;6:6535.

DOI 10.1182/blood-2015-07-655241